

WATER RESEARCH COMMISSION

THE APPLICABILITY OF HYDRODYNAMIC RESERVOIR MODELS FOR WATER QUALITY MANAGEMENT OF STRATIFIED WATER BODIES IN SOUTH AFRICA:

APPLICATION OF *DYRESM* AND *CE-QUAL-W2*

Compiled by:

A J Bath, K O de Smidt, A H M Görgens

E J Larsen

Report to the Water Research Commission

by

Ninham Shand (Pty) Ltd (Consulting Engineers)

NSI Project No. 6207

WRC Report No. 304/2/97
ISBN 1 86845 344 8

EXECUTIVE SUMMARY

BACKGROUND AND OBJECTIVES

Water quality is an increasingly important consideration in the management and planning of river systems in South Africa. A number of factors have resulted in the overall deterioration in quality of the surface water resources in the country. These factors include river regulation, increased return flows from point and nonpoint sources, and the processes which take place within water bodies and reservoirs. The interaction of processes and driving forces which determine the water quality patterns in reservoirs is complex; consequently there has been a growing awareness of the need for a greater range in decision support tools for water quality management and planning in South Africa. In response to this need, the Water Research Commission appointed Ninham Shand Pty Ltd in association with the Department of Civil Engineering, University of Cape Town, in 1990 to conduct an investigation into the applicability of hydrodynamic reservoir models for water quality management of stratified water bodies in South Africa. The research had the following objectives:

- *Investigation of the predictive abilities of selected existing hydrodynamic reservoir models by verification on selected water bodies in South Africa for which water quality depth profile data and associated hydrometeorological records were available.*
- *Adaptation of the selected models for application under South African conditions.*
- *Application of the selected models to specific water quality management and planning problems in South African reservoirs.*

In total, four models were implemented using a data base created from scratch for four water bodies. The work carried out was successful in that at least two models were identified which were capable of simulating the water quality and hydrodynamics in a number of reservoirs; these being *CE-QUAL-W2* and *DYRESM*¹. These two models were supplied to the research team in experimental form and required adaptation and modification to provide improved simulation for South African conditions. The effort required to create the data bases as well as modification of the models prevented the research team from satisfying the third aim completely, namely, the use of the models for management and planning purposes. This project is an extension of the original contract conducted by Ninham Shand Inc. to demonstrate the use of the models for management purposes. This report contains the results of the extension of the original contract.

The original aims of the extended contract include:

- *Investigate the possible improvements in water quality of selected reservoirs as a result of destratification using aeration techniques (using the data sets for Roodeplaats, Hartbeespoort and Inanda Dams).*
- *Determine the change in water quality of selected reservoirs as a result in changes in the external*

¹ A third promising model, MINLAKE, was studied by the UCT team of Ms A Venter and Prof. G Marais, with technical support by Dr A Görgens of the NS team.

nutrient loading from point and nonpoint sources (using the Inanda Dam data set).

- *Determine the influence on reservoir quality of hypolimnetic releases (Inanda Dam) and compensation releases from upstream reservoirs (Vaal Barrage).*
- *Determine the optimum location for domestic and industrial abstraction points in reservoirs which show gradients in water quality along their length (using the Vaal Barrage, Laing Dam and Inanda Dam data sets).*
- *Provide information on site-specific water quality management decisions, such as the use of diversion canal systems, and their beneficial influence on water quality (using the Vaal Barrage data set).*

Later extensions to this original brief included the use of *CE-QUAL-W2* to examine the possible water quality gradients in a future reservoir, and detailed analysis of the calibration and predictive capabilities of the model using the data set for Roodeplaat Dam.

GENERAL COMMENTS ON THE MODELS AND THEIR REQUIREMENTS

The two models selected for the extended contract were *DYRESM* and *CE-QUAL-W2*. Relevant literature, software and documentation was supplied by the respective custodians of the two models. A great deal of supporting software development took place during the study to enhance both the input and the output sides of the models, with a strong emphasis on interactive computer graphical display.

DYRESM-1D is a one-dimensional hydrodynamic reservoir simulation model for the prediction of the daily vertical temperature and salinity distribution in small to medium size lakes and reservoirs, developed at the University of Western Australia. The model uses a one-dimensional Lagrangian layer structure which allows for varying layer thickness and the model design is based on parameterisations of the individual processes that contribute to the hydrodynamics of a water body.

DYRESM-2D is a *quasi* two-dimensional, laterally averaged, hydrodynamic reservoir simulation model and uses a Lagrangian layer structure in which each layer is divided into 'parcels'. These parcels are only changed when layers are combined or split, or when parcels become too large or too small.

Key features of the current versions of the *DYRESM* models and supporting software include:

- (1) simulation of density, temperature and salinity profiles,
- (2) applicability to water bodies with multiple off-takes,
- (3) simulation of bubble plume dynamics as generated by any given aerator design,
- (4) ability to simulate extended time periods (months or years),
- (5) user friendly input requirements and graphical and plotting utilities for output.

CE-QUAL-W2 is a two-dimensional, laterally averaged, fixed grid, hydrodynamic and water quality simulation model which uses horizontal layers and vertical columns to delineate each computational cell. The model has been under continuous development by the US Army Corps of Engineers since 1975 and used in a number of countries for the water quality assessment of reservoirs, rivers and estuaries. Key features of the model and supporting software, as modified in this project, include:

- (1) simulation of 21 water quality constituents in addition to water temperature and water movement,
- (2) flexible design of the model allowing the application to water bodies of complex physical form,
- (3) applicability to water bodies with multiple branches, withdrawals, releases and abstractions,
- (4) ability to simulate extended time periods (months or years),
- (5) user friendly input requirements and graphical and plotting utilities for output.

In line with their mechanistic nature, these type of reservoir models require:

- Hydrometeorological input data of a *daily* time resolution to represent the reservoir driving forces.
- A number of water quality depth profiles in the water body of interest for calibration and/or verification of the models.
- Certain physical and water quality process representations in the models are represented by coefficients or parameters of a site-specific nature.
- Spatial information on the dimensions, volume, morphology and outlet configuration of the reservoir basin and its embankment.

METHODS

No field work or field gathering of data was undertaken and all modelling data bases were assembled from the original data sets as part of the first contract. For application purposes, the models were matched to reservoirs both in terms of their particular data needs and in terms of their appropriateness to deal with a likely water quality management challenge. Table EX1 gives an overview of the model applications, as well as information about the models themselves. The study was carried out by calibrating or verifying the hydrodynamic models using the data sets for six reservoirs (namely: Inanda, Roodeplaat, Hartbeespoort, Laing, Rooipoort Dams as well as the Vaal Barrage). These reservoirs were selected because of their water quality characteristics, available data set, and the existence of water quality problems. The calibrated/verified models were then used to provide information on a number of management and planning options for each of the reservoirs. The information derived from the models was then discussed with end users.

Table EX1: Models tested and calibrated using data bases for South African water bodies

| Model: | Dimensional representation | Variables simulated | Water bodies calibrated |
|------------|----------------------------|--|---|
| DYRESM | one-dimensional | water temperature, TDS, and hydrodynamics | Roodeplaat, Hartbeespoort and Inanda Dams |
| MINLAKE | one-dimensional | Full eutrophication related variables | Roodeplaat and Hartbeespoort Dams |
| CE-QUAL-W2 | multi-dimensional | Water temperature, TDS, PO ₄ , algal biomass, SS, DO, and hydrodynamics | Vaal Barrage and Inanda Dam |
| WASP | multi-dimensional | Hydrodynamics and volume balance | Roodeplaat Dam and Vaal Barrage |

GENERAL CONCLUSIONS

CAPABILITIES OF *DYRESM* AND *CE-QUAL-W2*

For one or more of the reservoirs selected in this study, the models provided acceptable simulation of one or more of the following processes: reservoir volume balance, thermal stratification, hydrodynamic mixing, non-conservative constituents (including: nutrients, oxygen regime and algal biomass), conservative constituents, and sediment-water interactions. The combination of predictive ability and model structure allowed the evaluation of a range of reservoir management options, such as: destratification by bubble plume aeration, selective abstraction, control of reservoir operating level, hypolimnetic releases, freshening options, and changes to reservoir input loading.

RESERVOIR CASE STUDIES

***DYRESM-1D* application: Inanda, Hartbeespoort and Roodeplaat Dams**

The model was used to perform preliminary bubble plume aeration system designs for both reservoir destratification and maintenance of mixed conditions in the water bodies. These designs were tested and refined using the following scenarios:

- (1) Destratification of a strongly stratified dam over a three to four week period.
- (2) Continuation of mixed conditions after initial destratification.
- (3) Prevention of the onset of stratification at the beginning of spring and maintenance of mixed conditions throughout the summer season.

The above investigation included an analysis of the effects of the following factors on the efficiency and effectiveness of the bubbler designs:

- (1) First and second efficiency peak design associated with one or two whole bubble plumes forming between the bubble source and the water surface.
- (2) Independent vs interacting plumes, influenced by the spacing between bubble sources.
- (3) Number of typical compressors required to ensure desired mixing within acceptable time period.
- (4) Optimisation of energy requirements by intermittent bubbler operation in maintenance mode.
- (5) Reservoir depth (Hartbeespoort Dam).

In the case of Inanda Dam, the model was used to assess the probable causes for failure of previous attempts by DWAF to destratify the dam.

***DYRESM-2D* application: Inanda Dam**

The model was used to perform the following analyses:

- (1) Preliminary comparison of *DYRESM-1D* and *DYRESM-2D* simulations of Inanda Dam.
- (2) Comparison of observed versus simulated profiles along the length of the reservoir.
- (3) Destratification of a strongly stratified dam over a three to four week period.
- (4) Prevention of the onset of stratification at the beginning of spring and maintenance of mixed conditions throughout the summer season.

CE-QUAL-W2 application: Inanda Dam

The model was used to examine: selective abstraction, algal-phosphorous dynamics, sediment release characteristics, phosphorus budget, hydrodynamic mixing, variable water level, and hypolimnetic releases. The simulations showed that four factors influence the water quality of Inanda: the quality of the inflow, density of the inflow, morphology of the reservoir basin, and contaminant release from sediments. In response, Inanda has: pronounced stratification, high algal growth, a large anaerobic hypolimnion (making up ± 44 percent of the volume at full supply level), and contaminant release into the hypolimnion from the reservoir sediments. To make the model conducive to multiple scenario testing (i.e. a short model run-time), a reduced segment/layer configuration was investigated and gave acceptable results. Preliminary scenario analysis shows that a reduction in algal biomass (1) in the withdrawal water could be achieved through selective withdrawal at the offtake, and (2) in-dam could be achieved through phosphorus control in the upstream catchment. Hydrodynamic studies show the beneficial influence of flood entrainment which introduces aerated water into the hypolimnion during the summer high runoff period.

CE-QUAL-W2 application: Vaal Barrage

The model was used to examine the influence of: low salinity (freshening) releases from the Vaal Dam on the salinity of the Vaal Barrage, modification of the freshening release patterns, and the diversion of Vaal Dam water into the middle reaches of the Barrage. The simulation shows that the salinity of the Barrage can be controlled using releases from the Vaal Dam. The salinity can be readily controlled between 500 and 600 mg/l at the cost of releasing water from Vaal Dam. The diversion canal option provides an improved salinity in the lower Barrage, particularly when Zuikerbosch treatment works withdraws higher salinity return flow in the upper reaches of the Barrage.

CE-QUAL-W2 application: Roodeplaat Dam

The model was used to (1) calibrate and verify the temperature simulation of Roodeplaat Dam using the *DYRESM* input data set, (2) compare the predictive capabilities of *DYRESM* with *CE-QUAL-W2* to simulate the temperature stratification of Roodeplaat, and (3) examine the predictive capabilities of *CE-QUAL-W2* to simulate the vertical dissolved oxygen patterns in Roodeplaat. The model provides a consistent and acceptable simulation of the vertical water temperature profile over a period of 800 days with minimal discrepancy between simulated and measured data. The simulation showed that a first good estimate of the vertical dissolved oxygen profile can be achieved using surface aeration and sediment demand as the governing processes.

CE-QUAL-W2 application: Rooipoort Dam

As part of the Olifants-Sand River Transfer Study, information was required on the water quality of a proposed dam to be built on the Olifants River at Rooipoort. These information requirements were: a prediction of the stratification and water quality patterns of the reservoir (for the preliminary design of the water treatment works), and the identification of an optimum location point for the offtake structure. The model was successfully used to show that: (1) during drought periods the salinity of the reservoir may exceed domestic limits and thus require blending, (2) sediment release of iron and manganese could influence water treatment at the end of the summer, (3) the offtake tower should be positioned at the inflow to the main basin to benefit from the local mixing conditions, and (4) possible water quality impacts when water is released for

the downstream environment.

CE-QUAL-W2 application: Laing Dam

The model was used to examine the thermal and chemical stratification patterns of Laing Dam, and determine the influence of low salinity transfers from Wriggleswade Dam on the quality of Laing Dam. The model provided an acceptable simulation of the hydrodynamics and salinity of Laing Dam. The diversion of low salinity water from Wriggleswade Dam is predicted to freshen Laing Dam and control the TDS of the reservoir.

RESERVOIR DATA SETS

The six reservoir case studies provided insights into the data requirements for: model configuration, time varying input data, and model calibration. The available hydrometeorological data sets were generally found to be adequate for the configuration and calibration of the models. Specific issues relating to the data for each dam studied, are described in the text.

ROLE OF HYDRODYNAMIC MODELS IN THE MANAGEMENT OF WATER QUALITY

Internationally, mathematical modelling has become an accepted part of the process of establishing and evaluating alternative scenarios for water quality management and decision making purposes. These models have been used in the design phase of reservoir construction to preempt water quality problems, in the operation of reservoirs and the development of operating rules, destratification systems and the evaluation of management strategies, and to manage the chemical process interactions taking place within a water body. The widespread use of models is in recognition that:

- (1) Each and every water body has a unique water quality character and response, and empirical 'rule-of-thumb' methods have certain limitations.
- (2) Reservoirs exhibit comparatively complex interactions between physical, chemical and biological processes can be explored using models.
- (3) The response of a reservoir to a given management practice is difficult to predict reliably without a detailed understanding of the governing processes and driving forces and that modelling can provide refinement of particular management practices to suit local conditions.
- (4) Reservoir modelling is relatively cheap in comparison to the cost of implementing a management option, the cost of water and wastewater treatment, and the cost of water paid by consumers.
- (5) Reservoir modelling exposes monitoring and data collection inadequacies.

In South Africa, in the past, great emphasis has been put on the management of water quantity resulting in the development of *system operating rules*. It is now being recognised that the decision making process must be enhanced to address the management of both water quality and water quantity. This study clearly shows how hydrodynamic reservoir models can be used to provide information which can be used in the management of water quality. Recommendations are given below regarding the use of models in the management process.

GENERAL RECOMMENDATIONS

The general conclusions given above confirm that this project has succeeded in its goal to explore the "applicability of hydrodynamic reservoir models for water quality management in stratified water bodies in South Africa". Time and budget constraints meant that certain research tasks could not be explored exhaustively. It is therefore recommended that further research be undertaken to complete the tasks described in the following sections.

RECOMMENDATIONS: SPECIFIC TO THE RESERVOIRS

It is recommended that both *CE-QUAL-W2* and *DYRESM* be used by the various organizations responsible for water quality management to provide the following decision support:

Management information for Inanda Dam:

- Evaluate changes in the water quality of Inanda Dam in response to changes in the contaminant loading from the upstream catchment. An example would include the use of the model to investigate the influence of phosphorus control in the upper catchment on algal growth within Inanda.
- Define operating rules for abstractions, timed releases, selective abstraction, and operation of the reservoir water level.
- Evaluate, design and operate a reservoir destratification installation.
- Examine the role of sediment nutrient release on water quality and identify management practices which can be used to control the impact of sediment release on the overlying water column.

Management information for the Vaal Barrage:

- Develop operating rules for the release of freshening water from Vaal Dam.
- Provide detailed water quality information for water quality impact assessment studies. An example includes the effect of mine dewatering on the salinity of the Barrage.
- Provide information on the optimum design and operation of a diversion canal which routes Vaal Dam water into the middle reaches of the Barrage.
- Develop contingency plans for the Vaal Barrage in the event of accidental spillage of contaminants from the adjacent catchment.

Management information for Roodeplaat Dam:

- Evaluate, design and operate a bubble plume aeration system for the destratification of the reservoir.
- Evaluate the impact of point and nonpoint sources, as well as internal nutrient cycling on the water quality of Roodeplaat Dam.
- Develop operating rules to manage the water quality in the reservoir, and quality supplied to downstream water users.

Management information for Laing Dam:

- Develop operating rules regarding the release of water from Wiggleswade Dam.
- Evaluate the benefits on the water quality of using hypolimnetic releases, timed releases, aeration and

destratification methods.

Management information for Hartbeespoort Dam:

- Evaluate changes in the water quality of Hartbeespoort Dam in response to changes in the contaminant loading from the upstream catchment and internal sediment releases.
- Evaluate, design and operate a bubble plume aeration system for the destratification of the reservoir.

Management information for other reservoirs:

- Develop operating rules for the release of water from reservoirs where downstream users have stringent water quality requirements.
- Evaluate the stratification patterns in reservoirs where the dam wall may be raised to increase the storage capacity. This has particular importance in reservoirs which show minimal chemical stratification. Raising the dam wall could result in the onset of anaerobic conditions and resultant deterioration in water quality.
- Prediction of water quality patterns in future reservoirs which are still at the planning stage of development.

RECOMMENDATIONS: SPECIFIC TO THE MODELS

CE-QUAL-W2

- The existing post-processor (*POST2*) was developed by NSI and used in this study to calibrate, verify and interpret the output produced by the model. It is recommended that the post-processor be modified to provide a more interactive *user interface* for the production and interpretation of information.
- The creation of input data sets for the model is time consuming. The development of an *information manager* would simplify the formatting, processing and verification of the input data sets.
- The linking of the *information manager*, model and *user interface* will result in the development of a Decision Support System for *CE-QUAL-W2* which will transform the model into an even more powerful tool for the management of water quality in reservoirs.

DYRESM

- Further investigation into the relationship between total dissolved salts (TDS in mg/l) and NaCl concentration (ppm) is required in order that the density function within the model can be amended for South African conditions, i.e. to use TDS in place of NaCl concentration.
- The NSI developed *DYPLOT* programs, which are capable of producing, viewing and plotting both profiles and two-dimensional model output data should be enhanced to be able to display isoline plots and additional time series information, such as bubbler configuration, air flow rate and mechanical efficiency.

RECOMMENDATIONS: SPECIFIC TO THE DATA SETS

On a national basis, a short list of reservoirs should be compiled where detailed water quality management

is expected in the near future and that a monitoring strategy be devised to accommodate the primary input requirements of hydrodynamic models. Such a monitoring strategy should include the collection of the data listed below.

Meteorological data: Hydrodynamic models require a variety of input data which includes: cloud cover, solar radiation, wind speed, dew point and air temperature. Wind speed is of major importance in the hydrodynamic modelling of reservoirs. Attention should be given to the placement of wind measuring stations so that data can be recorded at a height of 10 metre, and measurements can be taken both over water and over land.

In-reservoir water quality (profile) data: Variables which should be given high priority include:

- water temperature
- dissolved oxygen
- TDS or conductivity
- phosphorus (soluble, and total)
- nitrogen species (nitrate and ammonia)
- chlorophyll-a, algal biomass, numbers, and dominant algal species
- suspended solids, turbidity, secchi depth, and particle fall velocities
- bacteriological constituents such as *E.coli*

These variables should be measured at discrete intervals throughout the depth profile. However, as a minimum requirement, samples should be collected at the surface, mid-depth (metalimnion), and hypolimnion at weekly to quarterly intervals of time, depending on the season. The sampling of profiles should be positioned along the length of the reservoir so that longitudinal gradients in water quality can be evaluated.

The monitoring system used by Umgeni Water in Inanda Dam represents a near ideal design. It is recommended that additional samples should be collected on a routine basis to ascertain the release of nutrients from the bottom reservoir sediments, sampling of vertical profiles for phosphorus, suspended solids, and metals (iron and manganese), and sampling for algae in the surface layers.

In the Vaal Barrage, the existing monitoring program provides data on the longitudinal and vertical gradients in water quality. Additional sampling will be required on suspended solids to provide information on the dynamics of soluble orthophosphate within the water body, and calibration of the flow gauging weirs on the tributaries.

In Roodeplaat Dam, the data set for the period 1980 to 1984 provided detailed information on the water quality of the inflows and in-reservoir response. However, the existing monitoring of the reservoir should include samples collected from the metalimnion and hypolimnion.

In Laing Dam, the monitoring of the inflow on the Buffalo River should be weekly, and meteorological data should be recorded in proximity to the reservoir to account for local climatic conditions.

For **Hartbeespoort Dam**, the accuracy of the reservoir inflow/outflow recording should be improved and weekly water quality profiling should take place at several points in the reservoir basin. Meteorological data should be recorded in proximity to the reservoir to account for local climatic conditions and wind data should be measured at more than one location to take account of seasonal wind effects.

Water quality of inflowing streams: Key requirements are daily to weekly measurements of:

- water temperature
- TDS or conductivity
- nutrients
- suspended solids
- bacteriological constituents such as *E.coli*

Data storage: The establishment of a databank at an appropriate institution, linked to the Computer Centre for Water Research (CCWR), should form part of the monitoring strategy.

RECOMMENDATIONS: SPECIFIC TO WATER QUALITY MANAGEMENT

General In South Africa, mathematical modelling should become an accepted part of the process of establishing and evaluating alternative scenarios for water quality management and decision making purposes. The models should be used in:

- (1) The design phase of reservoir construction to identify potential water quality problems.
- (2) The operation of reservoirs to develop operating rules and destratification systems, and evaluate management strategies.
- (3) The management of chemical process interactions taking place within a water body.
- (4) To assess future management options and thereby preempt possible changes in quality.

To incorporate hydrodynamic models into the water quality management process will require:

- Training of personnel responsible for water quality management of reservoirs.
- Development of a decision support system to make the models more "user-friendly".
- Using the models in case studies to develop a South African "Guide" for reservoir management.

Bubble plume destratification system design

The following general rules should be applied when a bubble plume destratification system design is undertaken:

- i) The second efficiency peak associated with the forming of two whole plumes should be aimed for in most cases.
- ii) If possible the aerator layout should ensure independent bubble plumes by spacing the sources at a distance of at least 20 percent of the full supply level depth of the reservoir.
- iii) Although designs should be undertaken for a reservoir depth measured from full supply level, other reservoir depths should be taken into account when performing the design.
- iv) Maximum operating efficiency and effectiveness, both during destratification and maintenance of mixed conditions, should be strived for in the design and operation of a bubbler system.

- v) The minimisation of energy requirements should be integral to the design process in order to ensure minimum operating costs. This is achieved by ensuring maximum operating efficiency and effectiveness, while using the minimum number of compressors required and intermittent bubbler operation if appropriate.
- vi) A design should combine the ability to operate effectively as both a strong destratification dismantling system and a prevention system capable of maintaining the reservoir in a mixed state efficiently. This requires the design of two aerator lines in most cases.

The use of *state of the art* bubbler design (Schladow, 1991) in combination with optimisation by hydrodynamic simulation and the practical realisation of design parameters in the field, are indispensable in the successful implementation of a bubble plume destratification system.

RECOMMENDATIONS: FURTHER RESEARCH

- **Development of a guide for reservoir management:** A field of local research which has not been adequately addressed includes the development of management methods for large bulk supply impoundments. In South Africa, bulk supply impoundments play a vital role in the water supply infrastructure because of the variable hydrology and high demand. Unfortunately, the importance of impoundments has not been matched with an adequate development of procedures to manage water quality. Existing impoundment management has largely involved the use of "trial and error" approaches which have had varying degrees of success. This study shows that effective management of an impoundment requires:
 - The ability to select an appropriate reservoir management practice which controls water quality (and reduces water treatment costs) but is both cost effective and has the least influence on the water yield of the system.
 - The ability to define and test long-term operating policies. Locally, impoundments show distinct trends in quality which directly influence water treatment and water use. To manage water quality over extended time horizons requires the testing of a number of management practices which are capable of addressing short and long term variability in reservoir quality.
 - the ability to select management strategies and practices for multiple impoundment systems with their complex configuration of water bodies, return flows, abstractions and control structures.

In the light of the urgent need to develop water and sanitation services, it is essential that the nation's water resource management policy addresses all aspects of the supply infrastructure, including impoundments.

- **DSS: Development of a Decision Support System for *CE-QUAL-W2* to allow efficient:**
 - handling of the input data sets (ie information and data manager)

- EX12 -

- configuration and operation of the model
 - interpretation and assessment of the output information (ie user interface).
-
- The current version of *DYRESM* should be implemented on a data set for a reservoir with a significant salinity component in order to test this aspect of the model's capabilities.
 - The quasi two-dimensional *DYRESM-2D* model should be re-applied to Inanda Dam once the problems associated with the inflow downflow stack and the use of interacting bubble plumes have been addressed.
 - Further research using the *DYRESM-WQ* model which incorporates the simulation of the water quality components of a reservoir should be undertaken using South African data sets, when the model becomes available. Apart from the benefit of the availability of an additional tool for the prediction of the biological and chemical aspects of water quality, which has been shown by the Centre for Water Research to give good results, the use of *DYRESM-WQ* would enable an investigation of the effects of the use of bubble plume destratification on the biological and chemical components of reservoir water quality in South Africa.

List of Contents

| | |
|----------------------------|--|
| EXECUTIVE SUMMARY | |
| LIST OF CONTENTS | |
| ACKNOWLEDGEMENTS | |
| ABBREVIATIONS AND UNITS | |
| TERMINOLOGY | |
| LIST OF FIGURES AND TABLES | |

| | | |
|-----------|---|--------------|
| 1. | INTRODUCTION | Page: |
| 1.1 | WATER QUALITY RESPONSE OF SOUTH AFRICAN RESERVOIRS | 1.1 |
| 1.2 | WATER QUALITY MANAGEMENT IN SOUTH AFRICA | 1.5 |
| 1.3 | RESERVOIR MANAGEMENT | 1.6 |
| 1.4 | RESERVOIR MODELS | 1.9 |
| 1.5 | WATER QUALITY BASED DECISION SUPPORT SYSTEMS | 1.11 |
| 1.6 | ROLE OF MODELS IN RESERVOIR MANAGEMENT INFORMATION SYSTEMS | 1.13 |
| 1.7 | BACKGROUND TO THE STUDY | 1.16 |
| 1.8 | DETAILED AIMS OF THE STUDY | 1.17 |
| 1.9 | REPORT FORMAT | 1.21 |
| 1.10 | GENERAL COMMENT | 1.21 |
| 1.11 | REFERENCES | 1.22 |
| 2. | DYRESM APPLICATIONS | |
| 2.1 | INTRODUCTION | 2.3 |
| 2.1.1 | Reservoir Applications | 2.3 |
| 2.1.2 | Description of Models | 2.4 |
| 2.1.3 | Bubble Plume Aerator Design | 2.8 |
| 2.1.4 | Julian Days | 2.11 |
| 2.2 | APPLICATION OF <i>DYRESM-1D</i> AND <i>DYRESM-2D</i> TO SIMULATE THE HYDRODYNAMICS AND DESTRATIFICATION OF INANDA DAM | 2.12 |
| 2.2.1 | Introduction | 2.12 |
| 2.2.2 | <i>DYRESM-1D</i> Model Application | 2.12 |
| 2.2.3 | <i>DYRESM-2D</i> Model Application | 2.42 |
| 2.2.4 | Comparison of the Current Bubbler Design with that of Previous Destratification Attempts | 2.69 |
| 2.3 | APPLICATION OF <i>DYRESM-1D</i> TO SIMULATE THE HYDRODYNAMICS AND DESTRATIFICATION OF HARTBEESPOORT DAM | 2.77 |
| 2.3.1 | Introduction | 2.77 |
| 2.3.2 | Model input data | 2.77 |
| 2.3.3 | Model 'calibration' | 2.81 |
| 2.3.4 | Bubble plume aerator design | 2.101 |
| 2.3.5 | Bubble plume destratification - Simulation results | 2.104 |
| 2.3.6 | Bubble plume destratification - Conclusions | 2.121 |
| 2.4 | APPLICATION OF <i>DYRESM-1D</i> TO SIMULATE THE HYDRODYNAMICS AND DESTRATIFICATION OF ROODEPLAAT DAM | 2.122 |
| 2.4.1 | Introduction | 2.122 |
| 2.4.2 | Bubble plume aerator design | 2.122 |
| 2.4.3 | Bubble plume destratification - Simulation results | 2.125 |
| 2.4.4 | Bubble plume destratification - Conclusions | 2.151 |

| | | |
|-----|---|-------|
| 2.5 | DYPLOT : <i>DYRESM</i> OUTPUT VISUALISATION SOFTWARE | 2.152 |
| 2.6 | CONCLUSIONS : <i>DYRESM</i> APPLICATIONS | 2.154 |
| 2.7 | RECOMMENDATIONS : <i>DYRESM</i> APPLICATIONS | 2.159 |
| 2.8 | REFERENCES : <i>DYRESM</i> APPLICATIONS | 2.162 |
| 3. | <i>CE-QUAL-W2</i> APPLICATIONS | |
| 3.1 | INTRODUCTION | |
| | 3.1.1 Reservoir applications | 3.2 |
| | 3.1.2 Model description | 3.3 |
| | 3.1.3 References | 3.5 |
| 3.2 | APPLICATION OF <i>CE-QUAL-W2</i> TO SIMULATE THE WATER QUALITY AND HYDRODYNAMIC BEHAVIOUR OF INANDA DAM. | |
| | 3.2.1 Introduction | 3.6 |
| | 3.2.2 Model configuration | 3.10 |
| | 3.2.3 Model calibration | 3.12 |
| | 3.2.4 Model application | 3.20 |
| | 3.2.5 Conclusion | 3.36 |
| | 3.2.6 Recommendations | 3.37 |
| | 3.2.7 References | 3.39 |
| 3.3 | APPLICATION OF <i>CE-QUAL-W2</i> TO SIMULATE THE SALINITY AND HYDRODYNAMICS OF THE VAAL BARRAGE. | |
| | 3.3.1 Introduction | 3.43 |
| | 3.3.2 Model Input | 3.45 |
| | 3.3.3 Model Configuration | 3.46 |
| | 3.3.4 Model calibration | 3.47 |
| | 3.3.5 Salinity characteristics during the freshening release | 3.49 |
| | 3.3.6 Description of scenarios | 3.54 |
| | 3.3.7 Results of scenario testing | 3.54 |
| | 3.3.8 Conclusions | 3.62 |
| | 3.3.9 Recommendations | 3.63 |
| | 3.3.10 References | 3.63 |
| 3.4 | APPLICATION OF <i>CE-QUAL-W2</i> USING THE ROODEPLAAT DAM DATA SET TO EVALUATE THE SIMULATION OF THERMAL AND CHEMICAL STRATIFICATION. | |
| | 3.4.1 Introduction | 3.65 |
| | 3.4.2 Data compilation | 3.67 |
| | 3.4.3 Model application and calibration | 3.73 |
| | 3.4.4 Results and conclusions | 3.85 |
| | 3.4.5 Recommendations | 3.87 |
| | 3.4.6 References | 3.88 |
| 3.5 | APPLICATION OF <i>CE-QUAL-W2</i> TO ESTIMATE THE WATER QUALITY RESPONSE OF A PROPOSED RESERVOIR IN THE OLIFANTS RIVER AT ROOIPOORT. | |
| | 3.5.1 Introduction | 3.89 |
| | 3.5.2 Compilation of data set | 3.90 |
| | 3.5.3 Model configuration | 3.92 |
| | 3.5.4 Results | 3.94 |
| | 3.5.5 Conclusions | 3.98 |
| | 3.5.6 Acknowledgment | 3.101 |
| | 3.5.7 References | 3.102 |

| | | |
|------------|---|-------|
| 3.6 | APPLICATION OF <i>CE-QUAL-W2</i> TO LAING DAM TO EVALUATE THE MANAGEMENT IMPLICATIONS OF DIVERSIONS FROM WRIGGLESWADE DAM. | |
| 3.6.1 | Introduction | 3.103 |
| 3.6.2 | Input data compilation | 3.104 |
| 3.6.3 | Model verification | 3.106 |
| 3.6.4 | Wriggleswade diversion scenarios | 3.114 |
| 3.6.5 | Conclusions | 3.119 |
| 3.6.6 | References | 3.121 |
| 4. | GENERAL CONCLUSIONS | |
| 4.1 | INTRODUCTION | 4.1 |
| 4.2 | CAPABILITIES AND FEATURES OF <i>DYRESM</i> AND <i>CE-QUAL-W2</i> | 4.1 |
| 4.3 | RESERVOIR CASE STUDIES | 4.2 |
| 4.4 | RESERVOIR DATA SETS | 4.8 |
| 4.5 | ROLE OF HYDRODYNAMIC MODELS IN WATER QUALITY MANAGEMENT | 4.9 |
| 5. | GENERAL RECOMMENDATIONS | |
| 5.1 | INTRODUCTION | 5.1 |
| 5.2 | SPECIFIC TO THE MODELS | 5.1 |
| 5.3 | SPECIFIC TO THE RESERVOIRS | 5.2 |
| 5.4 | SPECIFIC TO THE DATA SETS | 5.4 |
| 5.5 | SPECIFIC TO WATER QUALITY MANAGEMENT | 5.5 |
| 5.6 | RECOMMENDATIONS FOR FURTHER RESEARCH | 5.7 |

ACKNOWLEDGEMENTS

The research described in this report emanated from a project funded by the Water Research Commission titled:

*The applicability of hydrodynamic reservoir models for water quality management of stratified water bodies in South Africa:
Application of DYRESM and CE-QUAL-W2.*

The Steering Committee for this project consisted of the following:

| | |
|---------------------|--|
| Mr H M du Plessis | Water Research Commission (Chairman) |
| Mr H Maaren | Water Research Commission |
| Mrs A M du Toit | Water Research Commission (Secretary) |
| Mr G Quibell | IWQS, Department of Water Affairs and Forestry |
| Dr J Howard | Umgeni Water |
| Mr J N Rossouw | Watertek, CSIR |
| Dr C Viljoen | Rand Water |
| Prof. G v R Marais | University of Cape Town |
| Prof. A H M Görgens | University of Stellenbosch |

The financing of the project by the Water Research Commission and the contribution by the members of the Steering Committee are gratefully acknowledged.

The authors wish to express their gratitude to the individuals and organisations mentioned below who provided valuable input to this project.

- Mr G Quibell
- Dr J Howard and staff of Umgeni Water
- Dr C Viljoen and staff of the Rand Water
- Dr J Patterson, Centre for Water Research, University of Western Australia
- Mr T Cole, US Army Corps of Engineers, Waterways Experimental Station, Vicksburg, MS, USA for his support and valuable assistance in the application of *CE-QUAL-W2*.
- Mrs Swart and staff of the Weather Bureau, Pretoria
- Mr J Schutte and staff of the Directorate of Hydrology (DWAF)
- Regional and operational staff of the Department of Water Affairs and Forestry
- Mr N van Wyk for permission to publish results on the Rooipoort Dam water quality study.
- The CCWR for computer support.

ABBREVIATIONS AND UNITS

| | |
|-------|--|
| WRC | Water Research Commission |
| DWAF | Department of Water Affairs & Forestry, Pretoria |
| IWQS | Institute for Water Quality Studies (former HRJ) |
| UW | Umgenti Water |
| RW | Rand Water |
| ISCOR | Iron and Steel Corporation |
| ESKOM | Electricity Supply Commission |
| CCWR | Computer Centre for Water Research |

| | |
|-----------|--|
| NTU | Nephelometric turbidity units |
| SS | Suspended solids (units mg/l) |
| EC | Electrical conductivity (units mS/m) |
| TDS | Total dissolved solids (units mg/l) |
| Phosphate | Soluble orthophosphate (units mg-P/l) |
| DO | Dissolved oxygen (units mg/l) |
| SOD | Sediment oxygen demand (units: mg/m ² /day) |
| MIS | Management Information System |
| DSS | Decision Support System |
| FSL | Reservoir Full Supply Level |
| FSC | Reservoir Full Supply Capacity |

| | | |
|---------|----|-----------|
| Length: | m | metre |
| | km | kilometre |

| | | |
|---------|----------------|-------------|
| Volume: | m ³ | cubic metre |
| | l | litre |

| | |
|-------|---|
| Flow: | Cubic metre per second (m ³ /s), cumec |
|-------|---|

| | | |
|-------|---|--------|
| Time: | s | second |
|-------|---|--------|

| | | |
|----------------|------|---------------------|
| Concentration: | µg/l | microgram per litre |
| | mg/l | milligram per litre |

| | | |
|-----------|-----------------|----------------------------|
| Energy: | kWh | kilowatt hours |
| Units: | 10 ⁶ | million (M) |
| Elevation | masl | metre above mean sea level |

TERMINOLOGY

Adsorption refers to the attachment of molecules or ions to a substrate.

Aerobic the requirement of molecular oxygen for respiration, or where there is oxygen available.

Anaerobic refers to conditions where there is insufficient oxygen available, or when oxygen is not required for respiration.

Assimilative capacity is the ability of aquatic systems to dilute, disperse, and degrade certain contaminants without having a detrimental influence on the users of the water.

Benthic is inhabiting the bottom of a water body.

Chlorophyll is the green pigment in plants and algae which is part of the process of photosynthesis which captures sunlight energy and converts it into chemical energy in the form of carbohydrates. Chlorophyll is used as a measure of the amount of algae in water.

Diffuse pollution source is equivalent to nonpoint pollutant source.

Desorption refers to the detachment of molecules or ions from a substrate.

Domestic water use is the use of water for drinking, washing, bathing, cooking, etc.

Epilimnion refers to the upper layer in a water body, which during the summer is warmer and mixed by wind action.

Eutrophic refers to water, particularly in lakes and reservoirs, which is high in nutrients and hence has excessive plant and algal growth therefore rendering the water less fit for use.

Fitness for use is the suitability of the quality of the water for one of the following five recognised water uses: domestic use, agricultural use, industrial use, recreational use and water for the natural environment.

Hypolimnion refers to the bottom zone of a water body.

Isopleth plot refers to the graphical presentation of reservoir data using a depth versus time plot.

Isothermal refers to the same water temperature throughout the vertical profile.

Macrophyte refers to macroscopic (large) forms of aquatic vegetation and includes certain species of algae, mosses and ferns as well as aquatic vascular plants.

Mesotrophic is a term applied to freshwater bodies which contain moderate amounts of plant nutrients and are therefore of moderate productivity.

Metalimnion refers to the layer situated between the epilimnion and hypolimnion, and represents the layer with maximum rate of change of temperature and dissolved oxygen with respect to depth.

Nonpoint sources are distributed or dispersed discharges and export of contaminants derived from surface and subsurface drainage as well as atmospheric sources.

Oligotrophic is the term applied to freshwater bodies which contain low amounts of plant nutrients resulting in low productivity.

Overtturn refers to the destratification of a water body resulting in vertical mixing of the surface and bottom layers.

Oxycline is the plane of maximum rate of change in oxygen concentration with respect to depth.

Point source refers to the discharge of contaminants from known discrete sources. For example, effluent discharge pipe from a wastewater treatment works.

Salinity refers to the salt content of water.

Stratification refers to the heating of the upper layers faster than the lower layers giving rise to a distinct vertical gradient.

Sediment oxygen demand (SOD) refers to the uptake of oxygen by the reservoir bottom sediments causing the development of anaerobic conditions in the hypolimnion.

Thermocline is the plane of maximum rate of change in water temperature with respect to depth.

Vertical profile plots are used to show the variation with depth at a specific point in a water body.

LIST OF FIGURES

| Figure number: | Description: | Page: |
|----------------|---|-------|
| 1.1 | Structure of generic management information system (from Pegram, 1995) | 1.13 |
| 1.2 | Generalised procedure for the management of reservoirs highlighting the role played by mathematical models (modified from Walmsley & Butty, 1980) | 1.16 |
| 2.1.1 | Schematic of bubble plume discharging into a density gradient, with two internal detrainment levels and surface detrainment | 2.9 |
| 2.1.2 | Theoretical mechanical efficiency as a function of stratification parameter, C , for different values of source strength parameter, M | 2.9 |
| 2.2.2.1 | Observed profiles at Stations 51 to 55 (Julian day 90011 to 90186) | 2.14 |
| 2.2.2.2 | Observed profiles at Stations 51 to 55 (Julian day 90193 to 90298) | 2.15 |
| 2.2.2.3 | Location of Inanda Dam profiling stations | 2.16 |
| 2.2.2.4 | Observed profiles at Station 51, initial and 0.8x wind simulations | 2.17 |
| 2.2.2.5 | Observed profiles at Station 51, initial and 0.8x wind simulations (cont.) | 2.18 |
| 2.2.2.6 | Station 51, average of Stations 51-54 and 0.8x wind simulation | 2.19 |
| 2.2.2.7 | Station 51, average of Stations 51-54 and 0.8x wind simulation (cont.) | 2.20 |
| 2.2.2.8 | Station 51 observed profiles, 0.8x wind simulation and bubbler scenario 7 | 2.26 |
| 2.2.2.9 | Inflow, inflow temperature and observed, simulated and bubbler 7 profiles | 2.27 |
| 2.2.2.10 | Station 51 observed profiles, 0.8x wind simulation & bubbler scenarios 7 & 8 | 2.28 |
| 2.2.2.11 | Station 51 observed profiles, 0.8x wind simulation and bubbler scenario 10 | 2.29 |
| 2.2.2.12 (A) | Daily mechanical efficiency of bubbler scenarios 7 & 10 | 2.30 |
| 2.2.2.12 (B) | 10 Day moving average mechanical efficiency of bubbler scenarios 7 & 10 | 2.30 |
| 2.2.2.13 | Station 51 observed profiles and bubbler scenarios 7 and 11 | 2.32 |
| 2.2.2.14 | Station 51 observed profiles and bubbler scenarios 7 and 11 (cont.) | 2.33 |
| 2.2.2.15 | 0.8x Wind simulation and scenario 11 type maintenance bubbler | 2.34 |
| 2.2.2.16 | Station 51 observed profiles and bubbler scenarios 11 and 12 | 2.36 |
| 2.2.2.17 | Station 51 observed profiles and bubbler scenarios 11 and 12 (cont.) | 2.37 |
| 2.2.2.18 | Station 51 observed profiles and bubbler scenarios 11 and 13 | 2.38 |
| 2.2.2.19 | Station 51 observed profiles and bubbler scenarios 11 and 13 (cont.) | 2.39 |
| 2.2.2.20(A) | Mechanical efficiency and operating frequency of bubbler scenario 12 | 2.40 |
| 2.2.2.20(B) | Mechanical efficiency and operating frequency of bubbler scenario 13 | 2.40 |
| 2.2.3.1 | Station 51, average of Stations 51-54, 0.8x wind 1D & 2D simulations | 2.45 |
| 2.2.3.2 | Station 51, average of Stations 51-54, 0.8x wind 1D & 2D simulations (cont.) | 2.46 |
| 2.2.3.3 | Average of Stations 51-54 and 0.8 x wind 2D simulation | 2.47 |
| 2.2.3.4 | Average of Stations 51-54 and 0.8 x wind 2D simulation (cont.) | 2.48 |
| 2.2.3.5 | Station 51 to 55 observed profiles and 0.8 x wind 2D simulation | 2.49 |
| 2.2.3.6 | Station 51 to 55 observed profiles and 0.8 x wind 2D simulation (cont.) | 2.50 |
| 2.2.3.7 | Station 51 to 55 observed profiles and 0.8 x wind 2D simulation (cont.) | 2.51 |
| 2.2.3.8 | Station 51 to 55 observed profiles and 0.8 x wind 2D simulation (cont.) | 2.52 |
| 2.2.3.9 | Station 51 to 55 observed profiles and 0.8 x wind 2D simulation (cont.) | 2.53 |
| 2.2.3.10 | Station 51 to 55 observed profiles and 0.8 x wind 2D simulation (cont.) | 2.54 |
| 2.2.3.11 | Station 51 to 55 observed profiles and 0.8 x wind 2D simulation (cont.) | 2.55 |
| 2.2.3.12 | Station 51 to 55 observed profiles and 0.8 x wind 2D simulation (cont.) | 2.56 |
| 2.2.3.13 | Station 51 to 55 observed profiles and 0.8 x wind 2D simulation (cont.) | 2.57 |

LIST OF FIGURES (continued)

| Figure number: | Description: | Page: |
|----------------|---|-------|
| 2.2.3.14 | Inflow, inflow temperature and profiles of average of Stations 51-54 and 2D simulation | 2.58 |
| 2.2.3.15 | 0,8 x Wind 2D simulation and bubbler scenario 11 | 2.60 |
| 2.2.3.16 | 0,8 x Wind 2D simulation and bubbler scenario 11 (cont.) | 2.61 |
| 2.2.3.17 | 0,8 x Wind 2D simulation and bubbler scenario 11 (cont.) | 2.62 |
| 2.2.3.18 | 0,8 x Wind 2D simulation and bubbler scenario 11 (cont.) | 2.63 |
| 2.2.3.19 | 0,8 x Wind 2D simulation and bubbler scenario 11 (cont.) | 2.64 |
| 2.2.3.20 | 0,8 x Wind 2D simulation and bubbler scenario 11 (cont.) | 2.65 |
| 2.2.3.21 | Average 2D simulation profiles and scenario 11 type maintenance bubbler | 2.66 |
| 2.2.3.22 | 0,8 x Wind 2D simulation and scenario 11 type maintenance bubbler | 2.67 |
| 2.2.3.23 | 0,8 x Wind 2D simulation and scenario 11 type maintenance bubbler (cont.) | 2.68 |
| 2.2.4.1 | Design details of the original aerators used at Inanda Dam showing the aerator line and aerator head layout | 2.71 |
| 2.2.4.2 | Design, layout and location details of the revised aerators used at Inanda Dam | 2.73 |
| 2.2.4.3 | 1992 Station 51 observed profiles and 1990 1D and 2D simulated profiles | 2.74 |
| 2.2.4.4 | 1D simulation, bubbler scenario 11 and experimental bubbler scenarios 2a and 2b | 2.76 |
| 2.3.1 (A) | Comparison of inflow factors | 2.82 |
| 2.3.1 (B) | Comparison of inflow factors (continued) | 2.83 |
| 2.3.1 (C) | Comparison of inflow factors (continued) | 2.84 |
| 2.3.1 (D) | Comparison of inflow factors (continued) | 2.85 |
| 2.3.1 (E) | Comparison of inflow factors (continued) | 2.86 |
| 2.3.1 (F) | Comparison of inflow factors (continued) | 2.87 |
| 2.3.2 (A) | Comparison of wind factors | 2.88 |
| 2.3.2 (B) | Comparison of wind factors (continued) | 2.89 |
| 2.3.2 (C) | Comparison of wind factors (continued) | 2.90 |
| 2.3.3 (A) | Combination of sensitivity tests vs "base case" | 2.94 |
| 2.3.3 (B) | Combination of sensitivity tests vs "base case" (continued) | 2.95 |
| 2.3.3 (C) | Combination of sensitivity tests vs "base case" (continued) | 2.96 |
| 2.3.4 (A) | Comparison of "base case" and "final case" | 2.98 |
| 2.3.4 (B) | Comparison of "base case" and "final case" (continued) | 2.99 |
| 2.3.4 (C) | Comparison of "base case" and "final case" (continued) | 2.100 |
| 2.3.5 | Bubble plume scenarios 1A, 3A and 5A - first peak case | 2.106 |
| 2.3.6 | Bubble plume scenarios 2A, 4A and 6A - second peak case | 2.107 |
| 2.3.7 | Design based on a weak stratification: first (1A) vs second (2A) peak cases | 2.108 |
| 2.3.8 | Design based on an intermediate stratification: first (3A) vs second (4A) peak cases | 2.109 |
| 2.3.9 | Design based on a strong stratification: first (5A) vs second (6A) peak cases | 2.110 |
| 2.3.10 | Comparison of effectiveness of independent and interacting plumes at destratification | 2.112 |
| 2.3.11 | Drawn down reservoir - maintenance: Designs for drawn down case vs full dam case | 2.113 |

LIST OF FIGURES (continued)

| Figure number: | Description: | Page: |
|----------------|---|-------|
| 2.3.12 | Full reservoir - maintenance: Designs for drawn down case vs full dam case | 2.114 |
| 2.3.13 | Full reservoir - destratification: Designs for drawn down case vs full dam case | 2.116 |
| 2.3.14 | Full reservoir - maintenance: Comparison of bubbler designs with differing total air flow rates (Q_T) | 2.117 |
| 2.3.15 | Full reservoir - maintenance: Comparison of bubbler designs with differing air flow rates per source (Q_0) | 2.119 |
| 2.3.16 | Example of the effect of a disturbance caused by a sudden large inflow | 2.120 |
| 2.4.1 | Observed and simulated depth-temperature profiles for Roodeplaat Dam | 2.123 |
| 2.4.2 | Comparison of effectiveness of first and second peak cases at destratification | 2.128 |
| 2.4.3 | Mechanical efficiency of first and second peak cases during destratification | 2.129 |
| 2.4.4 | Comparison of effectiveness at destratification of bubbler scenarios based on strong and weak stratification | 2.131 |
| 2.4.5 | Comparison of effectiveness of independent and interacting plumes at destratification | 2.132 |
| 2.4.6 | Mechanical efficiency of independent and interacting plumes during destratification | 2.133 |
| 2.4.7 | Comparison of first and second peak cases during maintenance | 2.135 |
| 2.4.8 | Mechanical efficiencies of first and second peak cases during maintenance | 2.136 |
| 2.4.9 | Comparison of bubbler optimisation cases during maintenance | 2.138 |
| 2.4.10 | Mechanical efficiencies of bubbler optimisation cases during maintenance | 2.139 |
| 2.4.11 | Factors determining optimal use of bubbler | 2.141 |
| 2.4.12 | Comparison of effectiveness of weak (3B, 4B) and intermediate (5B, 6B) stratification scenarios during maintenance | 2.142 |
| 2.4.13 | Mechanical efficiencies of weak (4B) and intermediate (6B) stratification scenarios during maintenance | 2.143 |
| 2.4.14 | Comparison of independent (3D) and interacting plumes (3E) for the first peak case during maintenance | 2.145 |
| 2.4.15 | Comparison of independent (4D) and interacting plumes (4E) for the second peak case during maintenance | 2.146 |
| 2.4.16 | Mechanical efficiencies of independent (4D) and interacting (4E) plumes during maintenance | 2.147 |
| 2.4.17 | Comparison of the combined bubbler run (2A & 4B) with the destratification run only (2A) | 2.149 |
| 2.4.18 | Comparison of the combined bubbler run (2A & 4B) with the maintenance run only (4B) | 2.150 |
| 3.2.1 | Location map of Inanda Dam with water quality monitoring points. | 3.8 |
| 3.2.2 | Inset A: 23 segment configuration. Note: Segments 1 and 25 are upstream and downstream boundary segments. Inset B: 6 segment configuration. Note: Segments 1 and 8 are upstream and downstream boundary segments. | 3.11 |
| 3.2.3 | Two dimensional plots for the 23 and 6 segment reservoir configurations. | 3.13 |
| 3.2.4 | Simulated and measured water elevations. | 3.14 |
| 3.2.5 | Simulated and measured surface water temperature. | 3.14 |
| 3.2.6 | Simulated and measured suspended solids concentration. | 3.16 |

LIST OF FIGURES (continued)

| Figure number: | Description: | Page: |
|----------------|---|-------|
| 3.2.7 | Simulated and measured hypolimnion phosphorus concentration. | 3.16 |
| 3.2.8 | Simulated and measured dissolved oxygen profiles. | 3.17 |
| 3.2.9 | Dissolved oxygen 2-D plots for selected days during the simulation period. | 3.18 |
| 3.2.10 | Simulated and measured surface phosphorus concentration. | 3.19 |
| 3.2.11 | Simulated and measured algal biomass. | 3.19 |
| 3.2.12 | Simulated and measured ammonia and nitrate concentration in the surface layer and hypolimnion. | 3.21 |
| 3.2.13 | Isopleth (depth vs time) plot: iron concentration. | 3.22 |
| 3.2.14 | Isopleth (depth vs time) plot: algal biomass | 3.23 |
| 3.2.15 | Isopleth (depth vs time) plot: ammonia concentration. | 3.24 |
| 3.2.16 | Isopleth (depth vs time) plot: dissolved oxygen concentration. | 3.25 |
| 3.2.17 | Isopleth (depth vs time) plot: phosphorus concentration. | 3.27 |
| 3.2.18 | Isopleth (depth vs time) plot: phosphorus concentration with sediment release of 0.05 mg/m ² /day. | 3.28 |
| 3.2.19 | Algal biomass at the dam wall basin, with normal and reduced phosphorus loading. | 3.30 |
| 3.2.20 | 2-D plots showing the distribution of phosphorus with vertical and longitudinal concentration gradients. | 3.32 |
| 3.2.21 | 2-D plot showing the penetration of flood waters into the metalimnion of Inanda Dam: Julian Day 123. | 3.33 |
| 3.2.22 | 2-D plot showing the penetration of flood waters into the hypolimnion of Inanda Dam: Julian Day 88. | 3.33 |
| 3.2.23 | Influence of scour release entrainment on the dissolved oxygen concentration: Julian Day 116. | 3.34 |
| 3.2.24 | Isopleth plot: dissolved oxygen with scour releases causing entrainment of water during high inflow period. | 3.35 |
| 3.2.25 | Isopleth plot: ammonia with releases from the hypolimnion. | 3.35 |
| 3.2.26 | Simulated and measured water temperature: vertical profiles | 3.41 |
| 3.2.27 | Simulated and measured water temperature: 2-D plots | 3.42 |
| 3.3.1 | Location map of the Vaal Barrage showing the main tributaries, abstractions and gauging weirs. | 3.44 |
| 3.3.2 | Simulated and measured surface water temperature. | 3.48 |
| 3.3.3 | Simulated and measured water elevation. | 3.48 |
| 3.3.4 | Measured tributary inflows to the Barrage | 3.50 |
| 3.3.5 | Measured Barrage inflow at Lethabo Weir and spillage from the Vaal Barrage. | 3.50 |
| 3.3.6 | Measured and simulated EC for segments along the length of the Barrage. | 3.51 |
| 3.3.7 | 2-D plot of the simulated conductivity of the Barrage during the release period (Day 204 onward). | 3.52 |
| 3.3.8 | 2-D plots of the vertical & horizontal movement of water in Vaal Barrage. | 3.55 |
| 3.3.9 | Insets A, B and C showing the hydrograph and EC during the release period. Insets D, E & F show the modified release hydrograph and simulated EC response of the Barrage. | 3.56 |
| 3.3.10 | Simulated EC response of the Barrage to reduced releases (zero, 75% and 50% reduction), and increased releases (50% and 100%). | 3.58 |
| 3.3.11 | Location map showing the two hypothetical diversion canal options investigated using CE-QUAL-W2. | 3.60 |

LIST OF FIGURES (continued)

| Figure number: | Description: | Page: |
|----------------|---|-------|
| 3.3.12 | Simulated EC response of the Barrage to the diversion canal options. Normal release, Canal option A (20 km long) with maximum transfer of 8 cumec, and Canal option B (14 km long) with maximum transfer of 4 cumec. | 3.61 |
| 3.4.1 | Segment layout for Roodeplaat Dam | 3.66 |
| 3.4.2 | Roodeplaat Dam: inflow data: Pienaars River | 3.69 |
| 3.4.3 | Roodeplaat Dam: inflow data: Hartbeesspruit | 3.70 |
| 3.4.4 | Roodeplaat Dam: inflow data: Edendalespruit | 3.71 |
| 3.4.5 | Roodeplaat Dam: spillage and releases | 3.72 |
| 3.4.6 | Roodeplaat Dam: meteorological data | 3.74 |
| 3.4.7 | Roodeplaat Dam: measured and simulated storage capacity vs water elevation | 3.76 |
| 3.4.8 | Roodeplaat Dam: measured and simulated storage capacity | 3.76 |
| 3.4.9 | Roodeplaat Dam: measured and simulated water temperature | 3.77 |
| 3.4.10 | Roodeplaat Dam: measured and simulated water temperature | 3.78 |
| 3.4.11 | Roodeplaat Dam: measured and simulated water temperature: 2-D plot | 3.79 |
| 3.4.12 | Roodeplaat Dam: measured and simulated water temperature: 2-D plot | 3.80 |
| 3.4.13 | Roodeplaat Dam: measured and simulated water temperature profile | 3.81 |
| 3.4.14 | Roodeplaat Dam: measured and simulated water temperature profile | 3.82 |
| 3.4.15 | Roodeplaat Dam: measured and simulated water temperature profile | 3.83 |
| 3.4.16 | Roodeplaat Dam: measured and simulated water temperature profile | 3.84 |
| 3.4.17 | Roodeplaat Dam: Simulated and measured dissolved oxygen profiles | 3.86 |
| 3.5.1 | Location map of the Olifants River | 3.91 |
| 3.5.2 | Reservoir configuration: Rooipoort Dam site | 3.93 |
| 3.5.3 | Influence of wind velocity on reservoir mixing conditions | 3.96 |
| 3.5.4 | Influence on high flow entering the reservoir during draw down | 3.97 |
| 3.5.5 | Behaviour of high salinity inflows | 3.98 |
| 3.5.6 | Isopleth plots for TDS, DO and temperature for the dam wall at Segment 27: Scenario 1: High storage level, low runoff entering reservoir | 3.99 |
| 3.5.7 | Isopleth plots for TDS, DO and temperature for the dam wall at Segment 27: Scenario 4: Low storage level, high runoff entering reservoir | 3.100 |
| 3.6.1 | Vertical temperature profiles in the middle of the dam (Segment 11) and at the dam wall (Segment 16), for observations February to July. | 3.108 |
| 3.6.2 | Two-dimensional plots of TDS for the flood of 25 July 1983. | 3.109 |
| 3.6.3 | Vertical temperature profiles in the middle of the dam (Segment 11) and at the dam wall (Segment 16), for observations August to December | 3.110 |
| 3.6.4 | Historical simulated and observed vertical TDS profiles at the dam wall, from February to July. | 3.111 |
| 3.6.5 | Historical simulated and observed vertical TDS profiles at the dam wall, from August to December | 3.111 |
| 3.6.6 | TDS concentration in Laing Dam during a Scenario 2 diversion from Wiggleswade into Laing during January 1983. | 3.116 |
| 3.6.7 | Vertical temperature and TDS profiles at the dam wall, from February to December 1983, under 3 cumec diversions from Wiggleswade & 1.17 cumec abstractions (Scenario 2). | 3.117 |
| 3.6.8 | Sequence of 2-D TDS plots during a 3 month Scenario 3 diversion from Wiggleswade into Laing from November 1982 to January 1983. | 3.118 |

LIST OF TABLES

| Table number: | Description: | Page: |
|----------------------|--|--------------|
| 1.1 | Reservoir management practices | 1.9 |
| 1.2 | Models tested and calibrated using data bases for South African water bodies | 1.17 |
| 2.2.2.1 | Temperature Profile Characteristics | 2.21 |
| 2.2.2.2 | Bubble Plume Aerator Analysis Results | 2.22 |
| 2.2.2.3 | Operating Conditions for Bubbler Runs | 2.24 |
| 2.3.1 | Wind Conversion Factors | 2.79 |
| 2.3.2 | SECCHI Disk Depths and ET1 Values | 2.92 |
| 2.3.3 | Temperature Profile Characteristics | 2.101 |
| 2.3.4 | Bubble Plume Aerator Analysis Results | 2.102 |
| 2.3.5 | Bubble Plume Destratification System Design Scenarios | 2.103 |
| 2.3.6 | Operating Conditions for Bubbler Runs | 2.104 |
| 2.4.1 | Temperature Profile Characteristics | 2.122 |
| 2.4.2 | Bubble Plume Aerator Analysis Results | 2.124 |
| 2.4.3 | Bubbler Plume Destratification System Design Scenarios | 2.125 |
| 2.4.4 | Bubbler Runs for Destratification | 2.126 |
| 2.4.5 | Bubbler Runs for Maintaining a Mixed Reservoir | 2.134 |
| 2.4.6 | Details of Combination Scenario | 2.148 |
| 2.6.1 | Comparison of Bubbler Designs | 2.158 |
| 3.1 | Four scenarios used in the Rooipoort Dam analysis | 3.89 |

CHAPTER 1

INTRODUCTION

by
A J Bath and A H M Görgens

1.1 WATER QUALITY RESPONSE OF SOUTH AFRICAN RESERVOIRS

Water quality is an increasingly important consideration in the management of river systems in South Africa. A number of factors have contributed to a deterioration in the overall quality of the surface water resources in the country. These factors include river regulation, increased return flow from point and nonpoint sources, and the processes which take place within water bodies such as reservoirs. This section describes some of the main processes influencing the water quality of reservoirs. Subsequent sections describe the management of water quality in reservoirs.

Stratification: Stratification can occur as a result of solute concentrations, suspended solids concentrations, or temperature variation as a result of surface heat exchange taking place across the air-water interface. Surface heat exchange is a function of both short and long wave radiation as well as surface conduction, evaporation and precipitation. In the remainder of the report, stratification will refer to density variations caused by water temperature effects. The term chemical stratification will refer to the density of water brought about by the mass concentration of dissolved salts and suspended solids.

At the beginning of spring, a reservoir is essentially homogeneous. At the onset of warmer weather, the water near the surface warms due to heat exchange from the atmosphere. The warmer water then mixes downwards primarily by wind action. By late summer, the reservoir will attain maximum stratification with three distinct regions. A warm upper layer which has a comparatively constant temperature with depth. This layer becomes generally well mixed due to surface wind action and is called the epilimnion. The temperature then diminishes rapidly with depth in a region called the metalimnion. Below the metalimnion is the cool deeper water in the region called the hypolimnion. As defined by Hutchinson (1957), the thermocline is the plane of maximum rate of change in temperature with respect to depth. During autumn, the cooler weather results in the surface water temperature decreasing giving rise to denser water at the surface and a corresponding convective overturning. The mixed condition results in an isothermal water body which remains in this state during the winter. In South Africa, the combined effect of local climate and morphology results in monomictic water bodies (one mixing period each year) and the stratification of the water body lasts for almost nine months each year.

The variation of water density in a stratified reservoir gives rise to what is known as internal density currents, or stratified flow. A water mass with greater density flowing beneath or over a water mass of lower density will be subject to gravitational effects that are dependent on the differences in the two densities. Withdrawals from a stratified reservoir might also occur in a selective fashion, restricting outflow primarily to certain horizontal layers. Such stratified flows can have an important influence on the water quality in a reservoir. Bosman (1983) presented an example of density currents in Darlington Dam, in the Southern Cape, where a bottom density current was responsible for transporting flood waters through to the outlet point. This report describes the density currents which are shown to have an influence on the water quality of Inanda Dam, refer to Section 3.2.

A primary water quality concern related to stratification is associated with the isolation of the hypolimnion from the atmospheric oxygen exchange in the epilimnion. Biotic activity and sedimentary chemical exchange often lead to deoxygenation of the deeper layers in the reservoir. Such near-anaerobic conditions may result in:

- Release of compounds of iron and manganese that increase the cost of treatment,
- Release of orthophosphate (phosphate) from sediments, which increase the total nutrient loading of the reservoir and may aid algal blooms (termed internal cycling), and
- Loss of diversity (and abundance) of vertebrates and invertebrates in the hypolimnion.

The main objective for simulating the stratification and stratified flow in reservoirs is to determine the influence of temperature and hydrodynamics on water quality processes, with a view to formulating corrective or management actions. Chemical and biological substances are dispersed within a reservoir by advection, convection and turbulent diffusion. In addition, such substances are also acted upon by various chemical, biological and physical processes which occur both in the reservoir sediments and water column.

Eutrophication: may be defined as the increased supply of nutrients, over or above the basic supply from the natural environment, or from its former state. Eutrophication manifests itself in excessive growth of aquatic plants, both attached and planktonic, to levels that interfere with desirable water uses (Thomann & Mueller, 1987). The growth of aquatic plants results from many causes. One of the main stimulants is an excess concentration of plant nutrients such as phosphorus and nitrogen. In recent years, eutrophication in water bodies has increased due to discharge of nutrients from municipal and industrial sources, as well as return flows from agricultural and urban areas. The increased production of aquatic plants has several consequences regarding water use, these include:

1. Aesthetic and recreational interference caused by algal mats, odours and discolouration of the water.

2. Diurnal variation in dissolved oxygen can result in low concentrations at night which may cause fish kills.
3. Phytoplankton and weeds settle to the bottom of the water body and create an increased sediment oxygen demand which in turn results in low dissolved oxygen in the hypolimnion.
4. Phytoplankton can clog water treatment works filters and result in reduced time between backwashing. A number of algal species produce extracellular products which impart taste and odours in treated potable water. Where pre-chlorination is practised, trihalomethanes and other potentially carcinogenic compounds may be produced.
5. Extensive growth of aquatic macrophytes interfere with navigation and aeration of the water body.
6. Certain species of algae have been identified as producing toxins which may cause the death of livestock when ingested in large quantities and are thought to be carcinogenic when ingested in small quantities over extended periods of time (Quibell, 1995).

Eutrophication can thus be further defined as the input of organic and inorganic nutrients into a water body which stimulates the growth of algae resulting in the interference with desirable water uses, including domestic supply, agriculture, recreation and functioning of aquatic ecosystems. The condition of the water body is described in terms of its trophic state and three designations are used: *oligotrophic* (clear, low productivity lakes), *mesotrophic* (intermediate productivity lakes), and *eutrophic* (high productivity lakes relative to a basic natural level).

The level of eutrophication due to excessive amounts of phytoplankton can be measured using cell counts, dry algal biomass, and chlorophyll-a. In South Africa, it has been shown that all three methods are generally required to identify and quantify algal problems in eutrophic water bodies. In many local reservoirs, the nutrients may be supplied to the water body either from external point and nonpoint sources, or by the release of nutrients from the sediments as well as mineralization and decay (referred to as internal nutrient cycling).

Micropollutant contamination: A water quality issue which is receiving increasing attention among industrial nations is pollution by metals and by man-made organic compounds, such as pesticides. A number of health related incidents involving humans and animals have occurred where there has been inadequate control of these micropollutants. In South Africa, a survey of raw water intakes to various purification works showed that highly toxic heavy metals are generally not detected. However, the metals associated with clay particles and humic acids such as iron, aluminium and manganese are found in a number of reservoirs (DWAF, 1991). In a number of South African reservoirs which show anoxic conditions, the sediments release iron and manganese which can have a direct influence on domestic users as well as on the downstream natural environment.

Microbiological contamination: Water contaminated by faecal matter is the medium for the spread of diseases such as dysentery, cholera and typhoid. Microbiological data are important for assessing the fitness for use of the water body for domestic use and recreation. In South Africa, studies have shown that the development of informal settlements with poor sanitation have resulted in increased presence of microbiological contaminants in rivers and reservoirs (DWAF, 1993).

Erosion and sedimentation: Average sediment yields for South African catchments range from 10 to 1000 tonne/km²/year giving rise to high turbidity and sedimentation problems. In some parts of the country, erosion has been attributed to the impact of human development, particularly relating to agriculture. Erosion has affected the agricultural sector through soil loss, but also affected reservoirs through loss of storage, sedimentation during floods, high turbidity, increasing treatment costs, and aesthetic problems for recreational users.

Salinisation: In South Africa, salinisation has become a widespread problem which has two main sources: natural and anthropogenic (man-made). Natural salinisation arises in catchments where the geology and soils contain large quantities of mineral salts which undergo dissolution and transport during periods of leaching and runoff. Man-made salinisation is a result of point and nonpoint sources. Point discharges occur from industrial, mining and domestic sources. Nonpoint sources are of major concern in South Africa because of the long term influence on surface water resources. Nonpoint sources include: agricultural return flow, urban runoff, mining activities, and atmospheric deposition. In the Vaal Dam, the total dissolved salts concentration of the outflow has risen from less than 100 mg/l during the 1950's to a present value of over 150 mg/l. Studies have shown that increased salinisation of the catchment occurs during flood events when nonpoint sources are the dominant source entering the reservoir (DWAF, 1991).

Reservoir Operation: In addition to the above factors, the quality of South African reservoirs is also influenced by the mode of operation of the water body. This has been observed where

- (1) water is transferred between catchments resulting in dramatic changes in quality of the recipient reservoir,
- (2) compensation releases are made from upstream water bodies resulting in disruptive changes in water quality downstream, and
- (3) release of bottom water has an adverse influence on the downstream users. Studies have been undertaken to determine and minimize the impact of system operation on water users (NSI, 1993).

1.2 WATER QUALITY MANAGEMENT IN SOUTH AFRICA

In a number of countries, the management of water quality has focussed on two aspects (1) the maintenance of water quality in some original, or pristine, condition, and (2) the maintenance of water quality in such a condition that it remains fit for recognised users.

In South Africa, the Department of Water Affairs and Forestry is responsible for ensuring that adequate water supplies of acceptable quality are available for all recognised uses. The recognised uses, as defined in the Water Act, 1956 (Act 54 of 1956) include: domestic, agricultural, industrial, and recreation. Therefore, the overall water quality management aim of the Department is the maintenance of the *fitness for use* of South Africa water resources on a sustained basis. The *fitness for use* concept implies the evaluation of water quality in terms of the needs of users. Published water quality guidelines have been produced to assist in the interpretation of user requirements (DWAF, 1993).

Uniform effluent standards were applied until recently to control pollution of surface water resources. To counter the continuing deterioration in water quality the Department changed to the receiving water quality objectives approach for non-hazardous substances, and to the pollution prevention approach for hazardous substances. The receiving water quality objectives approach focuses on the fundamental water quality management goal, namely *fitness for use*. The receiving water quality management objective approach involves (1) defining the water quality objectives in the receiving waters, and (2) control of point and nonpoint sources of contamination to comply with the water quality objectives. The receiving water quality objective approach accepts that receiving waters are capable of assimilating contaminants without having a detrimental influence on the users of the water. In general the receiving water quality objective approach involves:

- the identification of water users,
- the definition of water quality objectives for particular contaminants in a water body, and
- control of the point and nonpoint sources so that the objectives are satisfied.

The receiving water quality objectives approach has several advantages over the uniform effluent standard approach in that:

- the resource is managed based on the water quality requirements of users,
- both point and nonpoint sources of contaminants are considered, and
- the assimilative capacity of the water body is treated as part of the resource and managed for the benefit for all water users.

A manual of practice has been produced which addresses the impacts of effluent discharges on the receiving water bodies, and provides detailed information on the current management principles, policies and approaches (DWAF, 1995).

1.3 RESERVOIR MANAGEMENT

To improve the water quality of a reservoir, three approaches may be adopted. Firstly, to reduce the loading of contaminants entering a reservoir through control of sources and delivery from the upstream catchment. Secondly, to control of contaminant transport through river systems, and thirdly, to manage the reservoir to bring about an improvement in water quality (termed *in-situ* management practises). The reduction in contaminant source load is the most desirable long term management option but requires (1) a detailed study of the sources of contaminants in the upstream catchment (Walmsley & Butty, 1980), (2) study of the transport and fate of contaminants, and (3) a feasibility analysis to examine the practicality of catchment management options (Raman, 1985).

Catchment management practises have primarily focused on: the control of point and nonpoint sources, land use management, development of wetlands, and use of riparian strips. The *in-situ* reservoir management practises primarily focus on the effects of the problem but are capable of producing a rapid improvement in water quality over the short term (UW, 1993). In addition, catchment management programs are unable to control the water quality of reservoirs influenced by internal cycling of nutrients from bottom sediments (Raman, 1985). Examples of *in-situ* reservoir management practices include:

1. Abstraction of raw water from a particular layer (also termed: selective withdrawal)
2. Scour releases of deoxygenated water from the lower layers (hypolimnion) of the reservoirs.
3. Control of reservoir water level to improve vertical mixing and reduce the residence time.
4. Aeration of the hypolimnion to reduce the release of contaminants from sediments.
5. Destratification of the reservoir to reduce the build-up of constituents in the lower layers.
6. Deactivation and sealing of the reservoir sediments to reduce the release of contaminants.
7. Diversion of poor quality water around the reservoir.
8. Harvesting of invasive plant species to reduce the quantity of plant material in the reservoir.
9. Bio-manipulation of the species composition and abundance within the reservoir.

Reservoir management practices

Selective abstraction (drawoff): is used in reservoirs where vertical gradients exist in the water quality of the water body. The objective is to drawoff water at a specific depth which coincides with the quality requirements of the users. For example, in Inanda Dam, where water of poor quality is situated in the surface and bottom layers it is necessary to drawoff water from the metalimnion region to avoid algae in the surface layer, and iron and manganese in the bottom layer (UW, 1993). This reservoir management practice requires (1) a multi-level offtake structure, (2) operational control to adjust the offtake depth to account for water level fluctuations, and (3) detailed information on the

vertical gradients in water quality. This practice primarily benefits the abstractor, but may have little influence on the overall quality of the water body.

Hypolimnetic releases: To reduce the build-up of nutrients and metals in the lower layers of a reservoir, scour releases can be effective in improving the quality of the reservoir (Walmsley & Butty, 1980; Hansen *et al.*, 1987). This management option requires the availability of a bottom outlet structure and also the availability of sufficient reservoir storage capacity¹. Documented information is available on the use of this option in overseas reservoirs. Locally, this approach is more often used to scour sediment from the reservoir and occurs during flood events when the reservoir is spilling. The water released through the scour outlet can contain sufficient sediment, nutrients (particularly ammonia), organic compounds, and metals to have a severe influence on downstream users of the river (Bath & Timm, 1994). Therefore, the use of scour releases should coincide with periods of high runoff to dilute and reduce the downstream impact.

Reservoir operating level: It has been found that operating the water body at a reduced water level can in some cases result in improved water quality (Raman, 1985; NSI, 1989; NSI, 1994). This finding has been attributed to (1) reduced stratification associated with a reduced mean water depth, (2) decreased storage capacity, (3) decreased volume of the hypolimnion, (4) decreased residence time of the reservoir, and (5) sediment oxidation and inhibition of nutrient release (Walmsley & Butty, 1980). The combination of these factors results in improved vertical mixing of oxygenated water into the lower layers. This results in the reduced concentrations of metals and nutrients in the hypolimnion. This management option may cause water supply problems for a reservoir (and associated supply area).

Dilution and flushing of a reservoir: This option involves the replacement of contaminant-rich reservoir water with contaminant-poor water from some other source. In South Africa, high runoff during the summer results in considerable natural flushing of many reservoirs thereby alleviating some water quality problems (Walmsley & Butty, 1980), but regulated dilution occurs in the Vaal Barrage (from Vaal Dam) and in saline multi-reservoir systems such as the Great Fish/Sundays Rivers.

Hypolimnetic aeration: In reservoirs which exhibit an anaerobic hypolimnion, units have been installed which introduce air into the hypolimnion. The introduction of air causes: (1) a reduction in the release of metals and nutrients from the sediments, (2) reduction in algal biomass, and (3)

¹ The combination of high variability of the South African hydrology and high demand for water may restrict the practical use of management options which require the release of water from a reservoir to bring about an improvement in water quality. In many systems, release of water from upstream impoundments is part of the system operation. In these cases bottom releases should be encouraged.

improved conditions for aquatic organisms (Walmsley & Butty, 1980). Such a management approach however requires information on the oxygen demand imposed by the sediments, and reservoir mixing conditions (Hansen *et al.*, 1987).

Bubble plume destratification: Considerable research has been carried out using bubble plume aeration systems to bring about destratification and vertical mixing of reservoirs (Hansen *et al.*, 1987). In essence, the system consists of air compressors and aerator pipelines with diffusers. The pipes are usually located in the main basin of the reservoir and the air flow creates air bubble plumes which cause entrainment and vertical mixing of the water body. Recent research in Australia (Schladow, 1992), and local research in South Africa (Görgens *et al.*, 1993) show the importance of detailed computer-aided design of the system prior to installation to determine capital and running costs. Chapter 2 describes the use of *DYRESM* to derive information on the destratification requirements of selected local reservoirs.

Mechanical destratification: This involves the cycling of water from the upper oxygenated layers into the lower layers using pumps and jets. The approach is similar to that used in the bubble plume method (Hansen *et al.*, 1987), but tends to be more costly.

Management of reservoir bottom sediments: Overseas, small impoundments in need of rehabilitation have been lined with plastic sheets to prevent the release of nutrients from the bottom sediments. In some cases, clays, metal oxides, and alum have been used to line the reservoir bottom and reduce the rate of nutrient release. Dredging and removal of nutrient-rich sediments has been used to reduce the release into the overlying water column (Walmsley & Butty, 1980; Hansen *et al.*, 1987).

Harvesting: In some eutrophic reservoirs, the prolific growth of aquatic weeds has been controlled by mechanical harvesting of both floating, submerged and attached macrophytes.

Chemical control: Noxious blooms of planktonic algae and macrophyte growth can reach such proportions that all water users are affected. Chemicals are used locally and internationally to control the growth of aquatic plants. This management option has generally been reserved for highly eutrophic water bodies where other management options have been ineffective (Walmsley & Butty, 1980).

Biological control: A variety of methods have been used both locally and internationally to control algal growth. These include the use of pathogens, fish, plankton and protozoans as well as bio-manipulation (Raman, 1985).

Summary: Hanson *et al.* (1987) provide a comprehensive review of lake management techniques used in the United States of America. The document examines the effectiveness and cost of some one hundred management methods. Table 1.1 shows some general examples of the management methods used to control water quality problems in reservoirs. The literature shows that the management approaches described above have, in particular cases, been effective in producing improvement in the water quality. However, studies have shown that the development of a reservoir management plan requires an extensive analysis and modelling of the prototype before an appropriate management practice can be implemented. The following sections describe the development of reservoir models and the use of models in decision support systems to aid water quality management.

Table 1.1: Reservoir management practices

| Water quality problem | <i>In-situ</i> reservoir practice to improve water quality |
|--------------------------------------|--|
| Eutrophication | prevention of stratification and destratification hypolimnetic aeration hypolimnetic and timed releases compensation and freshening releases chemical control of algae selective drawoff harvesting of plant material bio-manipulation and chemical addition sealing of bottom sediments |
| Salinity | dilution releases from other reservoirs timed releases control of operating level selective drawoff and diversion of saline baseflow |
| Sedimentation | diversion of high turbidity water scour releases & timed releases |
| Microbiological contamination | selective drawoff location of drawoff point timed drawoff |

1.4 RESERVOIR MODELS

In 1925, the Streeter-Phelps Equation (also commonly known as the oxygen sag equation) was developed in response to the need to describe and characterise the oxygen regime in the Ohio River, in the USA. The equation was subsequently studied to derive more detailed information on the role of natural processes. It became apparent that the simple equation was incapable of providing information on the more complex interactions taking place in aquatic systems. The advent of computational hardware and analytical methods provided the opportunity to simulate more complex aquatic systems. This in turn provided the opportunity for managers of water resources to examine a wide range of management options.

One of the first prominent models was the Delaware Estuary model (Thomann, 1963), developed for the Federal Water Pollution Control Administration. The Delaware Estuary model incorporated a modified version of the Streeter-Phelps equation for the simulation of multiple compartments. The model was developed to evaluate multiple point source waste loads along the estuary and spatially variable properties of the water body. The model provided the means of rapid assessment of alternative strategies for the control of water pollution. The pollution was assessed in terms of the impact of discharges on the dissolved oxygen concentration of the estuary. Orlob (1992) states that this was one of the first decision support tools in the field of water quality management.

Up to the middle 1980's, numerous mathematical models were developed for riverine systems, lakes, reservoirs, estuaries and coastal systems. A large number of these models were developed for academic and research purposes to provide detailed descriptions of the aquatic systems. However, only a few models were capable of providing information which could be used directly in the management of water quality.

Early empirical modelling of the eutrophication of lakes used a simple (zero-dimensional) nutrient budget that showed the rate of change in the trophic status of an impoundment (Vollenweider, 1969). More detailed description of the processes taking place within water bodies was carried out by Chen & Orlob (1971). This work resulted in the development of the one-dimensional model LAKECO (Chen *et al.*, 1975). More comprehensive and intricate mathematical models of the biological processes were developed, examples of which include CLEAN, and CLEANER (Park *et al.*, 1974). Studies of the eutrophication of the Great Lakes resulted in the extension of the one-dimensional descriptions into two-dimensional and multi-dimensional models. This in turn required the simulation of advection, wind mixing, and thermal stratification. Wind induced mixing of Lake Ontario was studied and yielded two- and three-dimensional models (Simons, 1973). These models were also coupled to water quality models to describe the fate of nutrients and algae (Orlob, 1992).

In the early 1970's, water quality modelling of lakes and reservoirs received a new injection of interest by the need to evaluate the impact of water storage and stratification of impoundments on the downstream riverine ecosystems (Orlob, 1992). Particular attention focused on the heat exchange processes at the air-water interface. These studies resulted in the development of a number of one-dimensional hydrodynamic descriptions of reservoirs which also included simulation of the dissolved oxygen regime (Huber *et al.*, 1972; Markofsky & Harleman, 1973). The Corps of Engineers, Waterways Experimental Station produced a one-dimensional reservoir water quality model, *CE-QUAL-R1*. Stefan & Ford (1975) extended upon the earlier heat exchange formulations and developed a total energy integration approach for medium sized lakes. Their model provided successful simulation of the annual thermal cycle in such water bodies. The Minnesota Lake

Temperature Model (MLTM) provided a foundation for the assessment of stratification and eutrophication phenomena in impoundments. *DYRESM* was originally developed by Imberger *et al.* (1978) for lakes influenced by saline inflows, and also uses a total energy budget approach to produce a one-dimensional Lagrangian description of the thermal and salinity patterns in impoundments. *DYRESM* has since undergone continuous development to include (1) bubble-plume destratification options, (2) a quasi two-dimensional description of a reservoir, and (3) the simulation of a variety of water quality variables (this version is yet to be distributed).

The latest version of *CE-QUAL-W2* is a multi-dimensional laterally averaged, hydrodynamic and water quality simulation model. The model is based on the assumption that the water body is homogenous across the lateral width. Therefore, the model is suited to relatively long and narrow water bodies that show water quality gradients in the longitudinal and vertical directions. The model has been developed for use on rivers, lakes, reservoirs and estuaries. Modifications were made to the model to improve the structure of the code and decrease the data storage requirements. The latest enhancements to the model include: dynamic adjustment of the timestep, selective withdrawal algorithm, higher order transport scheme, and improved volume balance and mass balance algorithms (Cole & Buchak, 1993).

1.5 WATER QUALITY BASED DECISION SUPPORT SYSTEMS

In the early 1960's, when mathematical modelling of water quality was in its embryonic form, models were generally used, and developed for research purposes and provided little information for decision makers. In recent years, advances in computer hardware technology coupled with increasingly complex problems in water quality management have stimulated greater use of mathematical models as tools to assist decision makers. Even though these models are designed to enhance the decision support process, the quantity of information they require for implementation on a particular problem, and the copious output they are capable of producing seemed at times to restrict their acceptance by those in a decision making role. To enhance the use of models in a decision making role, it has been accepted that there should be an integrated assemblage of models, data, interpretative routines, and other relevant information that processes input data, run the models, and displays the results in an easy to interpret form. Such an assemblage of software makes up a decision support system (DSS).

Loucks *et al.* (1982) stated that the concept of decision support for water quality management includes more than just the simulation capability, it should make the decision support tools acceptable to decision makers. In the South African context, decision makers function at several levels with respect to the decision support system. In the past, the role of the modeller was to interpret results

and translate these into summaries, graphs or other forms that the water quality manager, planner, designer or policy maker could use. In recent times, with the availability of the personal computer, the decision maker at any of these levels may prefer to make interpretation of model output, or to set up the model to resolve a specific problem. This requires not only a suitable platform from which to run the model but also model run times which are short enough to ensure almost immediate turn around. Unfortunately, most of the models are sufficiently demanding in terms of hardware that the model run times do not allow immediate production of results. In such a case, the decision support system can be designed so that the model is run in batch process outside the DSS shell and imports the results in file form. Within the DSS, the results can be interpreted through a user interface that allows selection and comparison of results. If the model has a comparatively short run time, it could be used within the DSS interactively. In South Africa, DSS have been developed for water quality management of catchments and reservoirs, but incorporate only zero-dimensional models (Grobler, 1986).

Orlob (1992) states that the general layout of the DSS includes at least three elements: an information manager, a set of analytical tools, and a user interface. The information manager is used to receive, identify and store data and information in a data base. These data may be used during the preprocessing phase in the setting up of the model, or later for postprocessing and interpreting the results. Analytical tools, such as mathematical models and statistical routines, are the core of the decision support system. As mentioned earlier, distinction must be made between the tools that can be run interactively and those that must be run off-line, with the results imported through a user interface for interpretation. When the models are run interactively they should produce results in a time frame which does not impede the decision making process. Where models are run off-line, the output files from the model would be stored in the information manager for later perusal and interpretation. The user interface allows the user to select specific files, edit data, determine model parameters and coefficients and display graphical or tabular data, and as is described in later chapters (refer to Chapters 2 and 3).

In the United States, the latest interactive computer graphics allow simple, rapid methods to interpret results for decision makers. Loucks *et al.* (1985) developed a water quality management plan for the Ave River Basin in Northern Portugal which employed user-friendly, menu driven programs for interactive decision making. Arnold & Orlob (1989) developed a DSS for a water quality management plan for the estuarine environment of the Santa Ana River in Southern California. The DSS incorporated interactive design of the models, selection of boundary conditions and coefficients, hydrodynamic and water quality simulation, graphical display of results, and iterative cost evaluation. A similar approach was used to develop a DSS for the South Delta Water Agency in California to facilitate design and operation of a system of tidal barriers to control water levels and

quality in the Sacramento-San Joaquin Delta (Orlob, 1992). Information displayed includes locations of water quality monitoring points, records of historical observations at these points, and the configuration of models used to simulate the estuary hydrodynamics and water quality. For decision making, the DSS allowed a visual comparative assessment of the performance of alternative management schemes with supporting graphics, statistics, and animated displays.

Orlob (1992) states that mathematical modelling has become an accepted part of the process of establishing and evaluating alternative scenarios for water quality management and decision making purposes. These models have been used in the design phase of reservoir construction to preempt water quality problems, in the operation of reservoirs to develop operating rules and evaluate management strategies, and to manage the chemical process interactions taking place within a water body. Therefore, it is shown that the decision making process has been greatly enhanced through the models, but the inappropriate use of models can lead to limitations in the value of the information produced. The following section describes the use of reservoir models in the decision support process for the management of reservoir water quality.

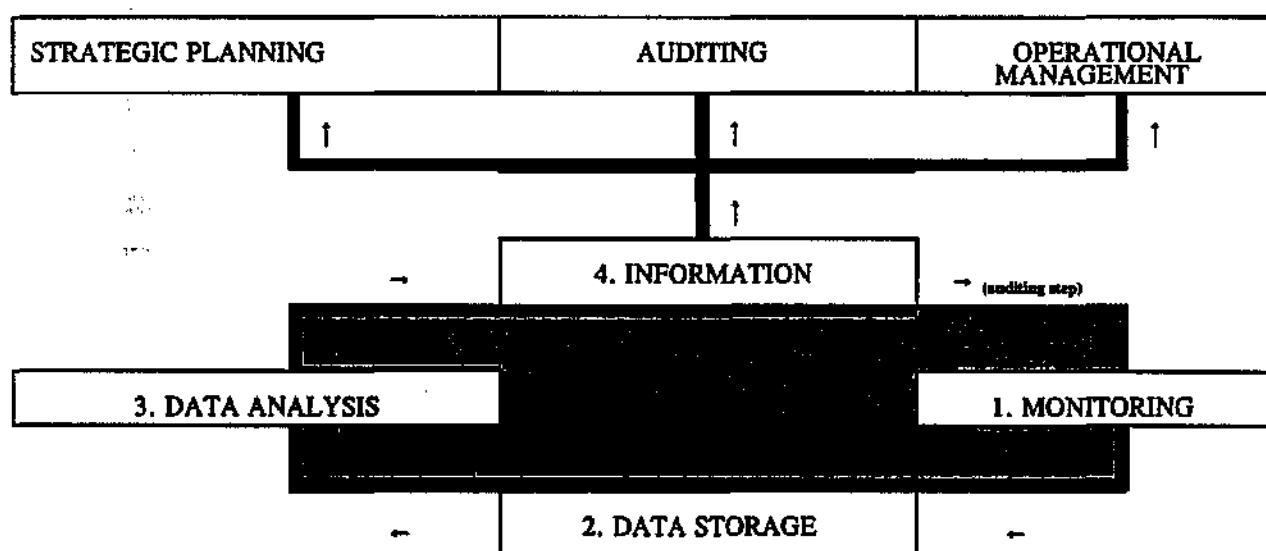


Figure 1.1 Structure of a generic management information system (from Pegram, 1995).

1.6 ROLE OF MODELS IN RESERVOIR MANAGEMENT INFORMATION SYSTEMS

This section describes the structure of the management information system (MIS) and the role played by reservoir models in the production of information. Figure 1.1 shows the structure of a generic MIS (Pegram, 1995). The components of the MIS include: (1) the collection of data using a water quality monitoring program, (2) data screening and storage, (3) the analysis, processing and interpretation of data using models and other numerical methods, and (4) the production of information. The information produced by the MIS is divided into three main groups.

- ***Strategic information:*** This involves identification of receiving water quality objectives and management approaches based on the existing and expected conditions within the catchment. Examples include the assessment of: phosphorus detergent ban, phosphorus point and nonpoint source control, reservoir operation, and impact of future land use changes within a catchment.
- ***Auditing information:*** This involves the evaluation of whether the implemented management approaches are achieving the specified management objective, and to also anticipate potential problems in the catchment. Examples include the auditing of: effluents, rivers and reservoirs to verify that their quality complies with the prescribed standards and water quality objectives.
- ***Operational information:*** This involves the "fine-tuning" of the management approaches to comply with the water quality objectives. Examples include providing information on the use of: freshening releases to control the quality in a recipient water body, operation of wastewater and water treatment facilities, and operation of reservoirs.

Using the above description of a generic MIS, it is necessary to examine how reservoir models contribute to the data analysis and information sections shown in Figure 1.1.

Figure 1.2 shows a simple procedure in which water quality models are used in the analysis of data and production of information. The procedure consists of four basic steps, these include: monitoring and problem identification, determination of management approach, detailed design and implementation, and monitoring and performance (see Figure 1.2). The main components of the procedure include the following.

- ***Monitoring and problem identification:*** The first part of the management process involves the identification of the water quality problems. This is achieved by comparing the water quality requirements of the various water users with the existing water quality data for the reservoir. Traditionally, a problem was identified when the water quality did not meet the user requirement. However, the current trend is to use models to identify water quality problems through the extension of the measured data set and description of the governing processes thereby providing more detailed assessment of the original data set. In South Africa, reservoir models are being used to assess the fate of contaminants and determine the assimilative capacity of reservoirs.

- ***Determination of the general management issues:*** The second step involves the identification of management approaches which will be required to control the existing water quality problems, or methods which may be required in the future to manage the water quality. Reservoir models are widely used to provide information on the interaction of reservoir processes and also to review possible management approaches.
- ***Detailed Design and implementation:*** The third step involves the detailed evaluation of management approaches, and the implementation of a management plan. Reservoir models have long been used in the evaluation of reservoir management approaches and quantifying the benefits in terms of improvement in water quality. In South Africa, reservoir models are being used to provide both strategic and operational information. The strategic information is used to identify future problems and the operational information is used to control the existing water quality problems (NSI, 1993; NSI, 1994; Bath & Timm, 1994).
- ***Monitoring and performance:*** The last step involves the routine monitoring of a reservoir. The data are used to assess the performance of the management plan, and also to identify where adjustment of the plan is required to compensate for changes in the response of the reservoir. Models are used overseas to fine-tune (and audit) monitoring programs. This is of particular importance in reservoirs which experience considerable variability in inflow discharge and water storage level.

Reservoir models have therefore become widely used in water quality management providing information on a wide selection of management issues. Some of the key reasons for the wide spread use is that:

- Each reservoir has a unique water quality character.
- Reservoirs exhibit complex interactions between processes.
- The response of a reservoir to a given management option is not easy to predict without a detailed understanding of the governing processes and driving forces.
- Reservoir modelling is cheap when compared with the cost of implementing a management option, cost of water treatment, and the cost implications for users.
- The predictive capability of models is being enhanced as a result of ongoing model development.

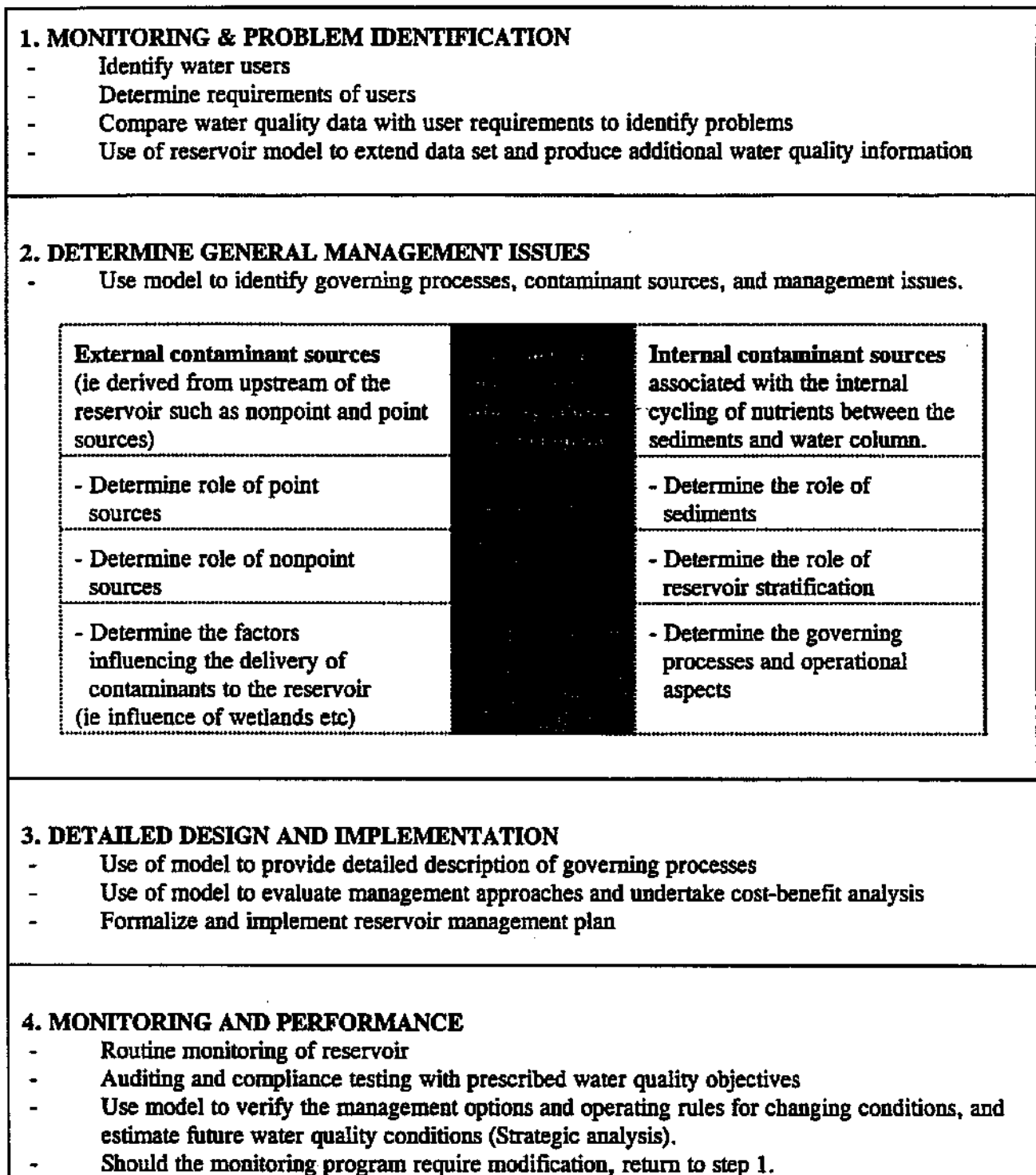


Figure 1.2 Generalised procedure for the management of reservoirs, highlighting the role of mathematical models (modified from Walmsley & Butty, 1980).

1.7 BACKGROUND TO THE STUDY

In January 1990, the Water Research Commission appointed Ninham Shand Pty Ltd and the Department of Civil Engineering, University of Cape Town, to conduct a collaborative investigation into the applicability of hydrodynamic reservoir models for water quality management of stratified

water bodies in South Africa. The objectives of that study included (1) investigate the predictive ability of selected hydrodynamic reservoir models by verification on chosen water bodies in South Africa, (2) adaptation of the models for application under South African conditions, and (3) use of the models to resolve specific water quality management and planning problems in local reservoirs.

In total, four models were implemented using a data base created from scratch for four water bodies. Table 1.2 shows the models and reservoirs studied as part of that investigation. The work carried out under the original contract was successful in that at least two models were identified which were capable of simulating the water quality and hydrodynamics in a number of reservoirs; these models being *CE-QUAL-W2* and *DYRESM*². The two models were made available to the research team in experimental form and required adaptation and modification to provide improved simulations for South African conditions. The extensive effort required to create the data bases, as well as modification and calibration of the models prevented the research team from satisfying the third aim completely, namely, the use of the models for management and planning purposes. This project is an extension of the original contract to demonstrate the use of the models for management purposes. This report contains the results of the extension of the original contract.

Table 1.2 Models tested and calibrated using data bases for South African water bodies

| Model: | Dimensional representation | Variables simulated | Water bodies calibrated |
|------------|----------------------------|--|---|
| DYRESM | one-dimensional | water temperature, TDS, and hydrodynamics | Roodeplaat, Hartbeespoort and Inanda Dams |
| MINLAKE | one-dimensional | Full eutrophication related variables | Roodeplaat and Hartbeespoort Dams |
| CE-QUAL-W2 | multi-dimensional | Water temperature, TDS, PO ₄ , algal biomass, SS, DO, and hydrodynamics | Vaal Barrage and Inanda Dam |
| WASP | multi-dimensional | Hydrodynamics and volume balance | Roodeplaat Dam and Vaal Barrage |

1.8 DETAILED AIMS OF THE STUDY

The objective of this study is to demonstrate the use of *DYRESM* and *CE-QUAL-W2* in providing information which can be used for water quality management and planning. Thereby this study will permit the completion of the work in terms of the original objectives. Examples of the applications

² A third promising model, MINLAKE, was studied by the UCT team of Professor GvR Marais and Ms A Venter. Further work on the application of MINLAKE involved: (1) the modification of the model to simulate the water quality of Roodeplaat Dam, (2) assessment of model sensitivity to reduced data input, and (3) application of the model to another reservoir (Lake Riley in the USA). The findings of this study appear in a separate report to the WRC.

include:

- Investigate the possible improvements in water quality of selected reservoirs as a result of destratification using aeration techniques.
- Determine the change in water quality of selected reservoirs as a result of changes in the external nutrient loading from point and nonpoint sources.
- Determine the influence on reservoir water quality of hypolimnetic releases and compensation releases from upstream reservoirs.
- Determine the optimum location for domestic and industrial abstraction points in reservoirs which show gradients in water quality along their length.
- Provide information on site-specific water quality problems, these include the use of diversion canal systems, and their beneficial influence on water quality.

In the original contract, it was proposed that *DYRESM* and *CE-QUAL-W2* would be used to simulate the water quality of a number of selected water bodies. *DYRESM* would be used with the Hartbeespoort and Inanda Dam data sets to:

- Evaluate the influence of destratification of Hartbeespoort Dam on the stratification regime using bubble plume aeration.
- Determine the influence of destratification options on the stratification regime of Inanda Dam.

CE-QUAL-W2 would be used to simulate the water quality of the Vaal Barrage and Inanda Dam to:

- Obtain information on the optimum release strategies from the Vaal Dam to obtain the best mixing conditions and quality in the Barrage, and middle Vaal River.
- Evaluate the influence on the water quality (salinity) of the Vaal Barrage of diverting Vaal Dam water directly into the middle reaches of the Vaal Barrage.
- Determine the influence of "catchment" and "in-situ" based management options on the water quality response of Inanda Dam.

At the inception of the study, the original proposal was modified by the steering committee to provide more detail on each of the model applications. The revised terms of reference, which formed the basis for the study, is described below.

DYRESM is used to simulate the hydrodynamics of:

- (1) Inanda, Roodeplaat and Hartbeespoort Dams using the one-dimensional (1-D) version of the model, and
- (2) Inanda Dam using the two-dimensional (2-D) version. In summary, **DYRESM** is used to investigate a number of management options described below.

Roodeplaat Dam

- Evaluate the influence of destratification of Roodeplaat Dam on the temperature regime using bubble plume aeration. The latest version of **DYRESM** has been developed with the option to simulate and evaluate destratification methods. These applications permit the evaluation of various bubble plume aeration design configurations. **DYRESM** has been configured for Roodeplaat Dam using the data set constructed from the raw data supplied by the Department of Water Affairs and Forestry, and the Weather Bureau. Recommendations are made regarding future water quality and hydrometeorological monitoring requirements.

Hartbeespoort Dam

- Errors have been identified in the hydrological data for Hartbeespoort Dam. Further analysis of the data is required to refine the volume balance of the reservoir before application of **DYRESM** can proceed. **DYRESM** is used to provide preliminary information on thermal stratification as well as vertical mixing characteristics of the reservoir.

Inanda Dam

- Evaluate the influence of destratification options on the water quality of Inanda Dam. The one-dimensional version of **DYRESM** is configured for Inanda Dam using the data set constructed from the raw data supplied by Umgeni Water, Department of Water Affairs, and the Weather Bureau. The 1-D version is used to provide preliminary information on the stratification and heat exchange characteristics of the reservoir. The 2-D version is used to investigate the optimum design and location for the aeration point taking account of local conditions. Particular attention is focused on the use of the model to determine why the existing aeration system has been unsuccessful in destratifying the water body in the main basin.

CE-QUAL-W2 is used to provide the following water quality management information:

Vaal Barrage

- The water quality of the Vaal Barrage and middle reaches of the Vaal River are managed using water releases from the Vaal Dam. The volume, discharge rate and timing of such

releases have a direct influence on the water quality of the Barrage. The model is used to examine the influence of different release scenarios on the water quality (salinity) of the Barrage.

- At present, a blending option guide of 600 mg-TDS/l is used in the operation of the releases during the winter. The model is used to explore the releases required to achieve a hypothetical TDS blending option of 500 mg/l-TDS.
- A diversion canal is being considered which transfers low salinity water from Lethabo Weir (downstream of Vaal Dam) into the Barrage at the confluence with the Klip River. The canal will bypass the Zuikerbosch treatment works abstraction point thereby reducing the volume of low salinity water withdrawn by the works. Simulations are performed to provide information on the influence of the canal on salinity gradients within the water body.

Preliminary information is also obtained on the future monitoring needs within the Barrage and associated inflows.

Inanda Dam

- The model is used to provide information on the time varying water quality of Inanda Dam in terms of the variables: chlorophyll-a, suspended solids, phosphorus and iron. Such information would be of value in the operation of the Wiggins water treatment works. Attention is also focussed on the possible influence of reservoir draw-down on water quality.
- Evaluate the possible influence of a number of management options on the water quality of Inanda Dam. The "*catchment*" based management options include reduced phosphorus input loading brought about by reduction in point source loading. The "*in-situ*" management options include the use of hypolimnetic releases, and timed releases from the reservoir.
- Water quality monitoring needs for Inanda Dam.

Roodeplaat Dam

- To compare output from both models, *CE-QUAL-W2* is calibrated using the Roodeplaat Dam data. A comparison is made of the temperature/stratification output data from both models.

Rooipoort Dam

- The model is used to determine the thermal and chemical stratification which can be expected in the reservoir which may be built on the Olifants River, in the Northern Transvaal.

Laing Dam

- As part of the Amatole System Analysis, *CE-QUAL-W2* is used to examine the existing water quality status of Laing Dam, and determine the possible influence of catchment transfers from Wriggleswade Dam on the salinity of the reservoir.

General Approach The study was carried out by calibrating and testing the hydrodynamic models using the above mentioned data sets. The information derived from the models was then discussed with a number of the steering committee members and other individuals who were involved with the management of the water bodies. The various individuals and organizations who participated in this study are listed in the Acknowledgements.

1.9 REPORT FORMAT

The report is divided into five chapters:

Chapter 2 describes the application of *DYRESM*. Simulations are carried out using the data sets for Roodeplaat Dam, Hartbeespoort Dam, and Inanda Dam. In each application information is provided on the use of bubble plume aeration for the destratification of the water bodies.

Chapter 3 describes the application of *CE-QUAL-W2*. Simulations are carried out using the data sets for Inanda Dam, the Vaal Barrage, Roodeplaat Dam, Rooipoort (proposed) Dam, and Laing Dam. The applications are used to provide information on the water quality response of the reservoirs, addressing such issues as eutrophication, salinisation, stratification, and water quality projections for a future reservoir.

Chapter 4 describes the main conclusions and *Chapter 5* describes the recommendations of the study.

1.10 GENERAL COMMENT

The project was executed as a two year contract on a fixed budget. As the relevant sections of the report show, the application and calibration of the models as well as evaluation of scenarios was found to be time consuming. In almost all of the applications, the results showed that the development of a management approach for a reservoir requires detailed analysis, and in some cases field trials and testing. Therefore, it was accepted that the study should demonstrate the worth of hydrodynamic modelling, but not strive to develop detailed management plans.

1.11 REFERENCES

Arnold, U., & Orlob, G.T. (1989)

Decision support system for estuarine water quality management. *J. Water Res. Plng. and Mgmt. ASCE*. 115 (6), 775-792.

Bath, A.J. & Timm, T.D. (1994)

Hydrodynamic simulations of water quality in reservoirs of Southern Africa. *ICOLD proceedings*, 18th congress, Durban, 625-633.

Bosman H.H. (1983)

Flood water behaviour of Lake Mentz, Hydrological Research Institute, Department of Water Affairs and Forestry, Pretoria, Internal report.

Chen, C.W. & Orlob, G.T. (1971)

Ecological simulation for aquatic environments. Office of water resources research, Department of the Interior, August.

Chen, C.W., Lorenzen, M., & Smith, D.J. (1975)

A comprehensive water quality-ecologic model for Lake Ontario. Great Lakes Environmental Research Laboratory, National Oceanic and Atmospheric Admin. Washington, D.C.

Cole, T.M. & Buchak, E.M. (1993)

CE-QUAL-W2: A two-dimensional, laterally averaged, hydrodynamic and water quality model. User Manual, Environmental Laboratory, US Army Corps of Engineers, Waterways Experimental Station, Vicksburg, MS, Instruction report number ITL-93, September 1993.

DWAF (1991)

Water quality management policies and strategies in the RSA. Department of Water Affairs and Forestry, Government Printers, April 1991.

DWAF (1993)

South African water quality guidelines. Volumes 1 to 4, Department of Water Affairs and Forestry, Government Printers, Pretoria.

Grobler, D.C. (1986)

Assessment of the impact of eutrophication control measures on South African Reservoirs. Ecol. Modelling. 31, 237-247.

Hanson, M.J., Riley, M.J. & Stefan, H.G. (1987)

An introduction to mathematical modeling of lake processes for management decisions. Report compiled for the Legislative Commission on Minnesota Resources State of Minnesota by the University of Minnesota St. Anthony Falls Hydraulic laboratory.

Huber, W.C., Harleman, D.R.F. & Ryan, P.J. (1972)

Temperature prediction in stratified reservoirs. J. Hydr. Div. ASCE. 98 (4), 649-666.

Hutchinson, G.E. (1957)

A treatise on limnology. I. Geography, physics and chemistry. 1015 pp. Wiley, New York.

Imberger, J., Patterson, J., Herbert, B. & Loh, L. (1978)

Dynamics of reservoirs of medium size. J. Hydr. Div. ASCE, 104 (4), 725-743.

Imberger, J., Patterson, J.C. (1981)

A dynamic reservoir simulation model - *DYRESM* : 5, Transport Models for Inland and Coastal Waters, Academic Press, New York, 310-361.

Loucks, D.P., French, P.N., & Taylor, M.R. (1982)

Water resources and environmental planning using interactive graphics. Water Supply Mgmt. 6 (2) 303-320.

Loucks, D.P., Taylor, M.R. & French, P.N. (1985)

Interactive data management for resource planning and analysis. Water Resources Res. 21 (2) 131-142.

Markofsky, J. & Harleman, D.R.F. (1973)

Prediction of water quality in stratified reservoirs. J. Hydr. Div. ASCE, 99 (5), 729-745.

NSI (1989)

Laing Dam: Application of a hydrodynamic model for planning purposes. Report number 1521/4705 to the Department of Water Affairs & Forestry by Ninham Shand Inc.

NSI (1993)

Water Quality Assessment. Amatole System Analysis Report Series, Report by Ninham Shand Inc. for the Directorate of Project Planning of the Department of Water Affairs and Forestry, Pretoria.

NSI (1994)

Water quality situation statement. Algoa System Analysis Study Report Series, Report by Ninham Shand Inc. for Project Planning of the Department of Water Affairs and Forestry.

Orlob, G.T. (1992)

Water quality modelling for decision making. J. Water Res. Plan. & Man. ASCE, 118 (3) 295-307

Park, R.A., Scavia, D. & Clersi, N. (1974)

CLEANER, the Lake George model. Contribution 184, US International Biological Program, Rensselaer Polytechnic Insts., Troy, N.Y.

Pegram, G.C. (1995)

Water Quality Monitoring. Technical Report Series of the Mgeni Catchment Water Quality Management Plan. Report for Umgeni Water and DWAF by Ninham Shand Inc.

Quibell, G. (1995)

Personal communication, Institute for Water Quality Studies, Department of Water Affairs and Forestry, Pretoria.

Raman, R.K. (1985)

Controlling algae in water supply impoundments. Journal of the American Water Works Association, August 1985.

Schladow, S.G. (1991)

A design methodology for bubble plume destratification systems. Environmental Hydraulics, 1, 167-172.

Simons, T.J. (1973)

Development of three-dimensional numerical models of the Great Lakes. Science Series 12, Canada Centre for Inland Waters, Burlington Ontario, Canada.

Stefan, H. & Ford, D.E. (1973)

Temperature dynamics in dimictic lakes. J. Hydr. Div. ASCE, 101 (1) 97-114.

Thomann, R.V. (1963)

Mathematical model for dissolved oxygen. J. Sanitary. Engrg. Div. ASCE, 89 (5) 1-30.

Thomann, R.V. & Mueller, J.A. (1987)

Principles of surface water quality modeling and control. Harper and Row, New York.

UW (1992)

Impact of artificial destratification by aeration on Inanda Dam, Natal, South Africa. Water Quality Department, Scientific Services, Umgeni Water, Report Number WQP 6/92.

UW (1993)

Raw water quality of Inanda Dam, Implications for treatment facilities and sludge handling at Wiggins Water Works, Water Quality Planning Section, Umgeni Water, Report number WQP 2/93.

Van der Merwe, W. & Grobler, D.C. (1990)

Water quality management in the RSA: preparing for the future. Water SA, 16, 1, 49-53.

Vollenweider, R.A. (1969)

Möglichkeiten und grenzen elementarer modelle der stoffbilanz von seen. Archiv. Hydrobiologie, 66 (1), 1-36.

Water Act (1956)

Statutes of the Republic of South Africa - Water, 1201-1400.

CHAPTER 2

DYRESM APPLICATIONS

by

K O de Smidt, E J Larsen and A H M Görgens

| | <u>Contents</u> | <u>Page:</u> |
|------------|--|---------------------|
| 2.1 | INTRODUCTION | 2.3 |
| 2.1.1 | Reservoir Applications | 2.3 |
| 2.1.2 | Description of Models | 2.4 |
| 2.1.3 | Bubble Plume Aerator Design | 2.8 |
| 2.1.4 | Julian Days | 2.11 |
| 2.2 | APPLICATION OF <i>DYRESM-1D</i> AND <i>DYRESM-2D</i> TO SIMULATE THE HYDRODYNAMICS AND DESTRATIFICATION OF INANDA DAM | 2.12 |
| 2.2.1 | Introduction | 2.12 |
| 2.2.2 | <i>DYRESM-1D</i> Model Application | 2.12 |
| | Model input data | 2.12 |
| | Model 'calibration' | 2.13 |
| | Bubble plume aerator design | 2.21 |
| | Bubble plume destratification - Simulation results | 2.23 |
| | Bubble plume destratification - Conclusions | 2.41 |
| 2.2.3 | <i>DYRESM-2D</i> Model Application | 2.42 |
| | Model software | 2.42 |
| | Model input data | 2.43 |
| | Simulation results | 2.43 |
| 2.2.4 | Comparison of the Current Bubbler Design with that of Previous Destratification Attempts | 2.69 |
| | Background | 2.69 |
| | Analysis of previous bubbler configurations | 2.69 |
| | Bubbler effectiveness - Observed and simulated results | 2.72 |

| | | |
|------------|--|--------------|
| 2.3 | APPLICATION OF <i>DYRESM-1D</i> TO SIMULATE THE HYDRODYNAMICS AND DESTRATIFICATION OF HARTBEESPOORT DAM | 2.77 |
| 2.3.1 | Introduction | 2.77 |
| 2.3.2 | Model input data | 2.77 |
| 2.3.3 | Model 'calibration' | 2.81 |
| 2.3.4 | Bubble plume aerator design | 2.101 |
| 2.3.5 | Bubble plume destratification - Simulation results | 2.104 |
| | Strength of design stratification | 2.105 |
| | First vs second peak case | 2.105 |
| | Independent vs interacting plumes | 2.111 |
| | Reservoir depth | 2.111 |
| | Destratification of a full reservoir (hypothetical case) | 2.115 |
| | Maintenance of a full reservoir (hypothetical case) | 2.115 |
| | Effect of a disturbance | 2.118 |
| | Bubbler system operational costs | 2.118 |
| 2.3.6 | Bubble plume destratification - Conclusions | 2.121 |
| 2.4 | APPLICATION OF <i>DYRESM-1D</i> TO SIMULATE THE HYDRODYNAMICS AND DESTRATIFICATION OF ROODEPLAAT DAM | 2.122 |
| 2.4.1 | Introduction | 2.122 |
| 2.4.2 | Bubble plume aerator design | 2.122 |
| 2.4.3 | Bubble plume destratification - Simulation results | 2.125 |
| | Destratification of an already strongly stratified reservoir | 2.126 |
| | Maintenance of a mixed reservoir | 2.130 |
| | Combination of destratification and maintenance | 2.144 |
| | Bubbler system operational costs | 2.151 |
| 2.4.4 | Bubble plume destratification - Conclusions | 2.151 |
| 2.5 | DYPLOT : <i>DYRESM</i> OUTPUT VISUALISATION SOFTWARE | 2.152 |
| 2.6 | CONCLUSIONS : <i>DYRESM</i> APPLICATIONS | 2.154 |
| 2.7 | RECOMMENDATIONS : <i>DYRESM</i> APPLICATIONS | 2.159 |
| 2.8 | REFERENCES : <i>DYRESM</i> APPLICATIONS | 2.162 |

SECTION 2.1

INTRODUCTION : *DYRESM* APPLICATIONS

by

K O de Smidt and A H M Görgens

2.1.1 Reservoir Applications

The application of *DYRESM* to three reservoirs was undertaken in order to demonstrate the use of the model for the simulation of thermal hydrodynamics, and the evaluation and optimisation of bubble plume destratification systems for a range of water bodies.

The three reservoirs analysed were Inanda, Hartbeespoort and Roodeplaat Dams. Hydrodynamic simulation research was previously undertaken for these impoundments and is reported on by Görgens *et al.* (1993). The reader is referred to this document as a background to the work presented in Chapter 2.

The *DYRESM-1D* model was used to perform initial and further refined designs of bubble plume destratification and maintenance systems for the three reservoirs. In particular the following with regard to the reservoir analyses was undertaken:

- 1) Extensive investigation into the Hartbeespoort input dataset in order to determine the source of mass balance anomalies.
- 2) An investigation of bubbler system mechanical efficiencies under varying conditions in Roodeplaat Dam.
- 3) An evaluation of the possible reasons for failure of the previous attempts at bubble plume destratification of Inanda Dam.

The *DYRESM-2D* model was applied to Inanda Dam, which has been shown to display hydrodynamic two-dimensionality, in order to investigate the usefulness of the quasi two-dimensional model and DYPlot software in the visualisation of the hydrodynamics of the reservoir.

2.1.2 Description of Models

DYRESM-1D is a one-dimensional hydrodynamic reservoir simulation model for the prediction of the vertical temperature and salinity distribution in small to medium size lakes and reservoirs. The model uses a one-dimensional Lagrangian layer structure which allows for varying layer thickness and the model design is based on parameterisations of the individual processes that contribute to the hydrodynamics of a water body. The processes included in the basic *DYRESM* model are:

- Surface heat, mass and momentum exchanges
- Surface mixed layer deepening
- Inflow
- Outflow
- Mixing in the hypolimnion

A more detailed description of the *DYRESM-1D* model is given in Görgens *et al.* (1993) and is therefore not repeated here.

DYRESM-2D is a quasi two-dimensional hydrodynamic reservoir simulation model (Hocking and Patterson, 1991). It represents the reservoir being modelled by a two-dimensional 'wedge' similar to that used by *CE-QUAL-W2* (see Chapter 3), however, *DYRESM-2D* uses a Lagrangian layer structure in which each layer is divided into 'parcels'. These parcels are only changed when layers are combined or split, or when parcels become too large or too small. This approach reduces the computation time required when compared with models which use a fixed grid such as *CE-QUAL-W2*.

This basic *DYRESM* model structure has formed the background to a number of specialist developments and applications. These include the following (Patterson, pers comm, 1995):

Large Lake version: A version for application in a limited sense to large lakes, in which Coriolis influences are important. In this version, simulations of the profile averaged over the inertial period were calculated by modifying the shear production algorithm to account for rotational effects. This model also incorporated a bottom mixed layer with the energy production arising from a bottom current. This was specifically for application in Lake Erie, but was also incorporated into the dissolved oxygen version of the model.

Dissolved oxygen (DO): A version of the model which incorporated a simple dissolved oxygen budget was developed for Lake Erie, as a first step to demonstrate the validity of the *DYRESM* hydrodynamic module for water quality models in general. Briefly, the model incorporated equilibrium productivity-light intensity (P-I) relationships, and fixed respiration and sediment demand. The oxygen model was totally driven by the dynamics: the DO distribution in the upper mixed layer was determined by integrating the P-I curve over the exponentially decaying light field. This is an extreme simplification, but one which, in some circumstances, may be appropriate for a first model; specifically, when the response time of the phytoplankton to changing light is short compared to the circulation time. Alternatively, if attenuation depth is much greater than the mixed layer depth, the cells are circulating in an essentially constant light environment, and equilibrium productivity relationships are again relevant. *(The above simplification may well not be adequate for the correct simulation of DO in South African water bodies.)*

Ice and snow cover: To simulate cold northern lakes, ice and snow models were added to the basic model, together with an expanded density-temperature algorithm with pressure effects, to account for the effects near 4°C. These models were based on the assumption that the heat transfer through the cover was quasi-steady: the temperature field in the ice and snow adjusted on a time scale faster than the changes to the boundary conditions, in this case the meteorological forcing. This was shown to be appropriate for all but very thick ice, and the difficulties associated with the moving boundaries at the ice-water interface were avoided. The model included the effects of partial ice cover by applying the surface forcing to only the open fraction of the surface.

Solar pond models: A version of the model for simulating salt gradient solar ponds has been developed. This involved the incorporation of an algorithm to simulate the double diffusive instabilities which may arise, and a much finer Lagrangian layer specification. This model has been applied successfully to solar ponds in Israel and Australia. A control system for managing the ponds, based on the simulation model, has also been designed.

Destratification models: To simulate the effect of bubble plume aerators, a version of the model has been constructed which includes an algorithm which models the effect of a bubble plume as a single buoyant plume of a density which is the mean density of the air-water mixture. A simulation of Myponga Reservoir in South Australia showed that this simple model was, in certain circumstances, successful. The assumption that a single aerator plume behaves as a simple buoyant plume with the mean density is effectively assuming that the bubbles are infinitely small; for the case of large bubbles, the fixed entrainment rate

associated with buoyant plumes must be modified. For the case of a number of closely spaced aerator outlets, the model switches to a line source plume algorithm, rather than a number of separate single plume models. This model has been extensively used for the design of aerator systems and management practices.

The model has also been used to simulate a number of other lakes and reservoirs without significant change to the model structure, although in all cases the simulations have guided further development of various aspects of the model. These simulations include the following lakes and reservoirs:

- Babine Lake, Canada
- Burrumbidgee Reservoir, New South Wales, Australia
- Canning Reservoir, Western Australia
- Chaffey Reservoir, New South Wales
- Char Lake, Canada
- Darwin River Reservoir, Northern Territories, Australia
- Eklutna Lake, United States of America
- Glennies Creek Reservoir, New South Wales, Australia
- Harding Reservoir, Western Australia
- Harris Reservoir, Western Australia
- Kootenay Lake, Canada
- Lake Argyle, Western Australia
- Lake Constance, Germany
- Lake Erie, Canada
- Lake Geneva, Switzerland
- Lake Le Roux (Van der Kloof Dam), South Africa
- Lake Lugano, Italy
- Lake Mendota, USA
- Manton River Reservoir, Northern Territories, Australia
- Mt Bold, Southern Australia
- Myponga Reservoir, Southern Australia
- Wellington Reservoir, Western Australia

The results of these simulations depend to a high degree on the quality of the input data. With high quality data excellent simulations may be achieved.

The model has been widely distributed both within Australia and overseas for use in teaching, research and industry in a wide variety of applications.

These applications include the use of the model for reservoir management and the design of destratification systems by, amongst others, the following organisations:

Engineering and Water Supply, Southern Australia
Department of Water Resources, New South Wales, Australia
Sydney Water Board, New South Wales, Australia
Rural Water Commission, Victoria, Australia
Murray Darling Basin Commission, Australia
Power and Water Authority, Northern Territories, Australia
Mt Isa Mines, Australia
Ward and Associates, Vancouver, Canada
Ninham Shand, South Africa

In particular *DYRESM* has been used to design physical bubbler systems for, amongst others, the following reservoirs:

Lake Burbury, Tasmania, Australia
Glennies Creek Reservoir, New South Wales, Australia
Avon Reservoir, New South Wales, Australia
Nepean Reservoir, New South Wales, Australia
Sugarloaf Reservoir, Victoria, Australia
Upper Yarra Reservoir, Victoria, Australia
Myponga Reservoir, Southern Australia
Harding Reservoir, Western Australia
Lan Tarn Reservoir, Taiwan
Hollywood Reservoir, California, USA

Cognisance should be taken of the fact that the *DYRESM* models are non-calibratory by design, in that they do not require calibration of model constants, coefficients, etc. Application of the models might, however, require adjustment of the hydrometeorological input data to take account of the differences between measured and actual values due to gauge location, local topographical or meteorological effects and the accuracy of measuring techniques. Such adjustments are only justified within rational and plausible limits.

It should also be remembered that errors in the predicted profile in the lowest region of the reservoir are of reduced significance due to the lower volumes involved, however, this region is of significance for nutrient release and uptake.

2.1.3 Bubble Plume Aerator Design

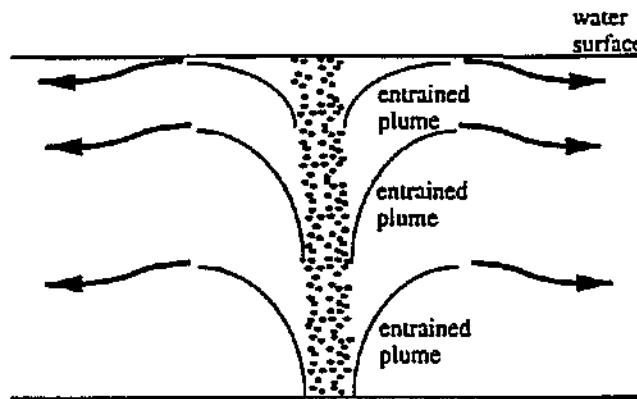
It is important at this point to discuss the two cases for which reservoir destratification is required. Firstly, there is the case of the destratification of an already strongly stratified water body in which a relatively large air flow rate is required to remove the stratification over a period of a few weeks. In the second case, the bubbler is used to prevent the onset of stratification and maintain the reservoir in a mixed state, which requires a smaller air flow rate. In the practical implementation of a bubble plume destratification system, however, both air flow rates are often required. For example, should the compressor system be out of action for whatever reason for a long enough period, strong stratification may result, requiring an air flow rate greater than that available from a prevention/maintenance system alone, to destratify the reservoir.

The bubbler design philosophy as laid out by Schladow (1991) was used to calculate the required air flow rates and bubble plume configurations. The first step was to determine the degree of stratification that would have to be broken down. This was done by calculating the equivalent linear stratification that has the same potential energy as a typical stratified observed field profile. For this purpose a few profiles were chosen for each dam for which a bubbler analysis was undertaken, with the purpose of obtaining a range of probable equivalent linear stratifications. The next step was to calculate the difference in potential energy between the stratified temperature profiles and their corresponding uniform temperature (mixed) profiles. The isothermal work required to destratify a stratified profile is proportional to the above potential energy difference and the constant of proportionality is equal to the inverse of the mechanical efficiency of the bubbler system.

Schladow (1991) shows that the mechanical efficiency of a bubbler system is related to:

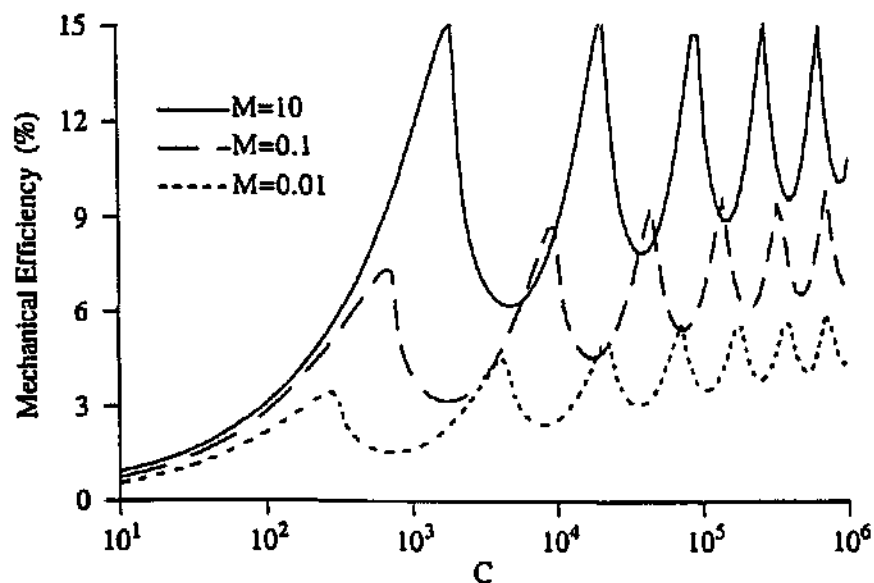
- Air flow rate through each bubble source
- Total pressure head at the bubble source (water head plus atmospheric pressure head)
- Equivalent linear stratification

Schladow (1991) also shows that efficiency peaks exist that are related to the number of whole plumes that form between the bubble source and the water surface (see Figures 2.1.1 and 2.1.2). It is recommended that, since the efficiency drops off dramatically for single plumes with an air flow rate that could carry the plume further than the available depth, the "second efficiency peak" associated with an optimal case with only two whole plumes forming, should be strived for in bubbler design.



Schematic of bubble plume discharging into a density gradient, with two internal detrainment levels and surface detrainment

Figure 2.1.1



Theoretical mechanical efficiency as a function of stratification parameter, C , for different values of source strength parameter, M

Figure 2.1.2

The three design variables that determine the characteristics of the bubbler plume aeration system and hence its efficiency are:

- Total air flow rate for the system.
- Number of bubble plume sources (this variable then in turn determines the air flow rate per bubble plume source).
- Distance between sources (which then determines the total length of the bubbler system and also determines whether or not the bubble plumes will interact or operate independently).

Other variables such as plume source orifice size, number and layout are also important in the final design of a bubbler system, but are not significant in a theoretical design. Schladow's nomograms were then used to determine the desired air flow rate per bubble plume source and associated mechanical efficiency for the various equivalent linear stratifications. The mechanical efficiency in each case was then used to determine the isothermal work required for destratification which in turn yielded the total air flow rate required to destratify within a given time period. This time period is typically taken as 3 weeks but is dependant on a number of factors. The total air flow rate divided by the air flow rate per bubble plume source then yielded the number of bubble plume sources required. The recommended plume spacing is 0,2 times the water depth in order to avoid plume interaction, however, a large number of required plume sources may necessitate unacceptable aerator lengths. It should also be pointed out that interacting plumes can enhance bubble plume efficiency in certain circumstances.

Since an aerator design is significantly influenced by water depth it follows that an aerator designed for a water depth (from surface to bubbler) measured from Full Supply Level (FSL) will not necessarily perform efficiently when the water level in the dam drops to that representing say 50% or 25% of the Full Supply Capacity (FSC) of the reservoir. It is therefore possible that at least two dam water level scenarios should be designed for and that the consequences of using only one of the designs should be checked, preferably by simulation.

The object of a bubble plume aeration system is to destratify or prevent the onset of stratification of a water body. In so doing the bubbler attempts to create and maintain mixed conditions, i.e. a uniform profile, within the reservoir. The resultant very weakly stratified profiles cause the mechanical efficiency of even a 'maintenance' mode bubbler to drop to low levels.

Operating the bubbler system in so-called optimisation mode allows the bubbler to be switched on when the temperature difference between the top and bottom levels of the reservoir profile is greater than a specified difference, and to be switched off when the top to bottom temperature difference is less than a second specified difference. This optimisation of the bubbler operation can enable significant cost saving in terms of the operational costs of the bubbler system's compressors.

Cognisance should be taken of the fact that the prevention of stratification and/or the destratification of a water body does not imply that an improvement in water quality will definitely be realised. For example, the advantage of the oxygenation of the hypolimnion by maintaining a mixed water body and the resultant reduction in sediment nutrient uptake, may be offset by the mixing of nutrients throughout the water column or the creation of a temperature regime that results in negative implications for water quality. Further research into the impact of the prevention of stratification on the water quality of various water bodies is needed to further quantify the economical justification of bubble plume destratification.

2.1.4 Julian Days

The *DYRESM* models use the Julian day method to describe time, both for input to, and output from, the models. A Julian day is simply made up of a year number and a day number counted from 1 January. In leap years a particular date may have a different Julian day number due to the addition of 29 February.

As an example:

1 April 1983 = Julian day 83091

1 April 1984 = Julian day 84092

In order to facilitate the determination of which season, month and period within a month a particular Julian day falls, a fold out conversion table is enclosed as the very last page of this report.

SECTION 2.2

APPLICATION OF *DYRESM-1D* AND *DYRESM-2D* TO SIMULATE THE HYDRODYNAMICS AND DESTRATIFICATION OF INANDA DAM

by

K O de Smidt and A H M Görgens

2.2.1 Introduction

Previous work undertaken on Inanda Dam using *CE-QUAL-W2* was described in a previous report (Görgens *et al.*, 1993). This section describes the application of both *DYRESM-1D* and *DYRESM-2D* to Inanda Dam and includes the initial design and refinement of a bubble plume destratification and maintenance system.

The usefulness of the quasi two-dimensional model and DYPlot software in the visualisation of the hydrodynamics of Inanda Dam, along with an evaluation of the possible reasons for failure of the previous attempts at bubble plume destratification is presented.

2.2.2 *DYRESM-1D* Model Application

Model input data

The data set used in the *DYRESM* simulation of Inanda Dam was taken from a data set prepared for the application of *CE-QUAL-W2* described by Görgens *et al.* (1993) (see Section 3). This data set was converted for use in the *DYRESM* model via a set of computer programs written for this purpose. The data set available from the previous work covered the period from 11 January 1990 to 31 December 1990 (355 days).

Although since the preparation of the above data set an additional three years of new data has become available, the working up of this data into a complete data set for use in the hydrodynamic models was beyond the scope of this project.

Data specific to *DYRESM* and not available in the *CE-QUAL-W2* data set was obtained from, inter alia, the Department of Water Affairs and Forestry's 1990 Report, entitled: "Inanda Dam : Capacity Determination", data supplied by Umgeni Water and appropriate mapping.

A total of 39 temperature profiles at five sites along the length of the impoundment were available for the modelling period. These observed profiles are shown in Figures 2.2.2.1 and 2.2.2.2. See Figure 2.2.2.3 for the location of the profiling stations.

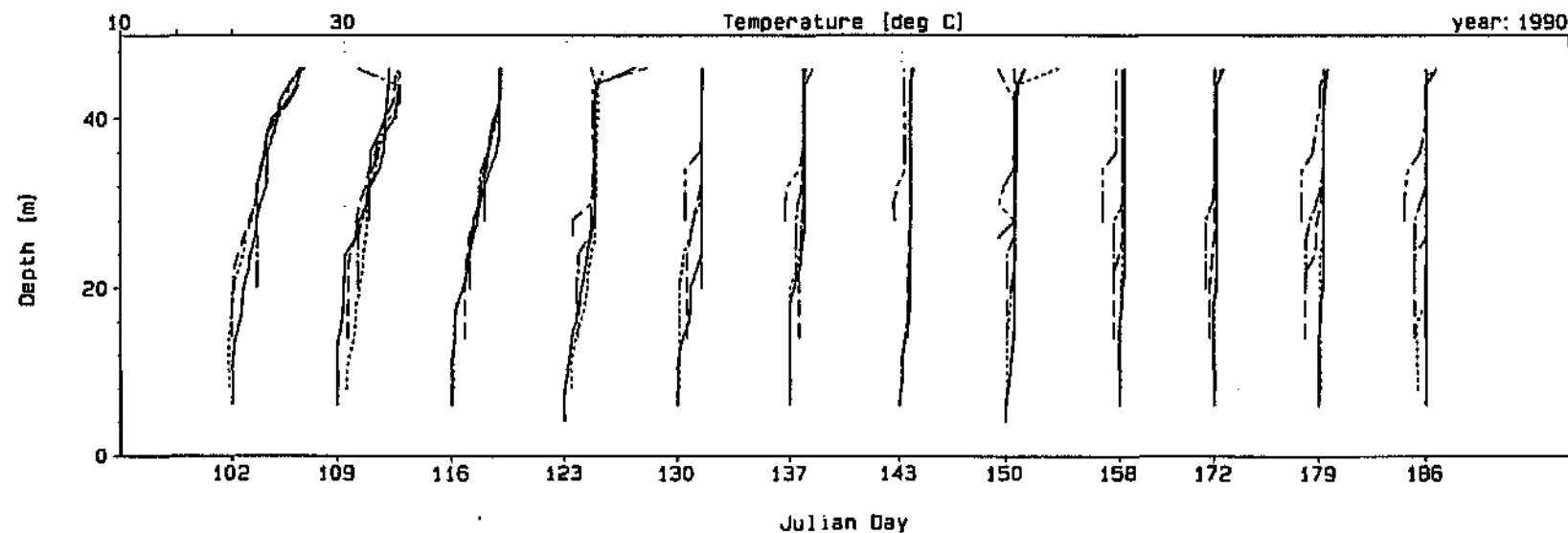
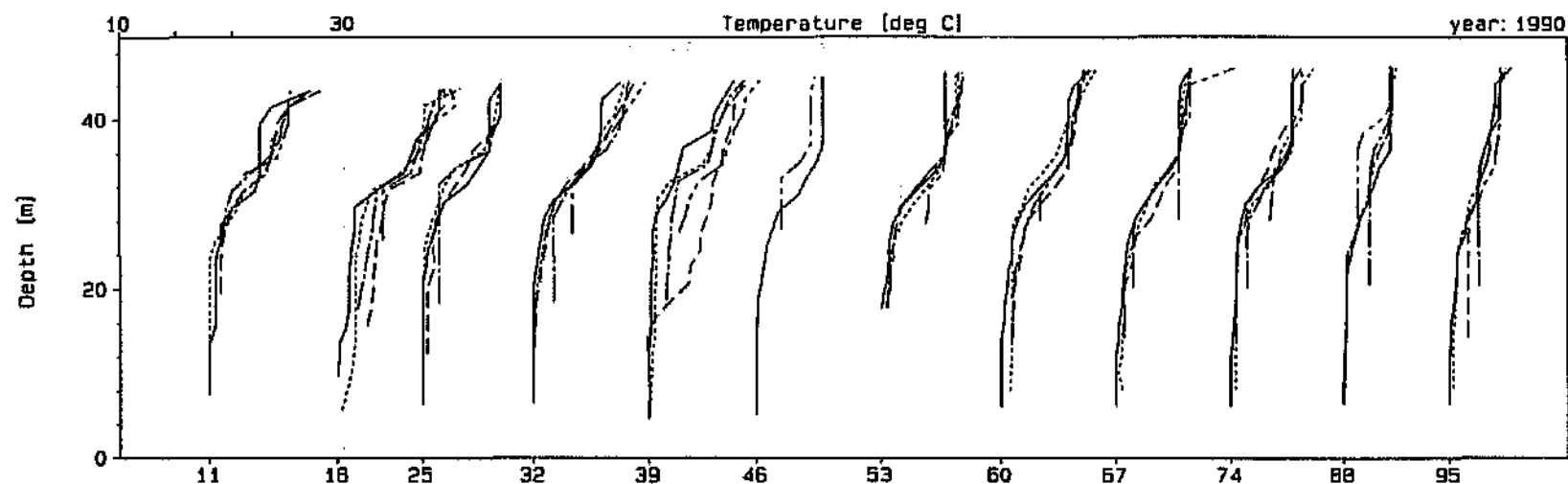
The first and last available profiles were for 11 January 1990 (Julian day 90011) and 25 October 1990 (Julian day 90298) respectively, giving a profiled modelling period of 288 days that starts with stratified summer conditions, includes autumn overturn (mixing), winter mixed conditions and ends shortly after the onset of stratification at the beginning of the following summer.

Model 'calibration'

An initial model run using the data as taken from the *CE-QUAL-W2* data set was undertaken which yielded reasonable results but showed a simulated mixed layer and thermocline that was too deep, indicating that wind speeds may be too high. A first 'calibration' run in order to attempt to improve the fit between the simulated and observed profiles was undertaken using a wind factor of 0,8. Figures 2.2.2.4 and 2.2.2.5 show the *DYRESM* simulated temperature profiles for the initial run and first 'calibration' run (0,8 wind factor), versus the observed field temperature profiles at Station 51 (dam wall) for the period from 11 January 1990 to 25 October 1990. In most instances *DYRESM* has simulated the observed profiles fairly well, however, an improvement in fit was achieved by reducing the wind speed. This may be due to a wind sheltering effect in some parts of the water body.

In particular a comparison of the profiles for Julian days 90060 and 90067 shows an exceptionally good fit. The shape of the simulated profiles fits that of the observed profiles very well between Julian day 90018 and 90046, however the temperature prediction is approximately $\pm 2-3$ °C higher on average. This difference could be due to a number of reasons such as consistent errors in; (1) observed profile temperature measurement (unlikely), (2) inflow temperature timeseries (generated from intermittent sampling), (3) certain hydrometeorological data. The input data that effects only the surface layers is unlikely to cause this difference, however, since the simulated profile shapes are quite accurate.

When the simulated profiles (0,8 wind factor) are plotted against the average of the observed profiles at Stations 51 to 54 (Figures 2.2.2.6 and 2.2.2.7) it becomes apparent that an average one-dimensional profile is to some extent inadequate for describing the hydrodynamics of Inanda Dam and that a two-dimensional approach is desirable.



Profile Legend: — Station 51 Station 52 ---- Station 53 ——— Station 54 -.-.- Station 55



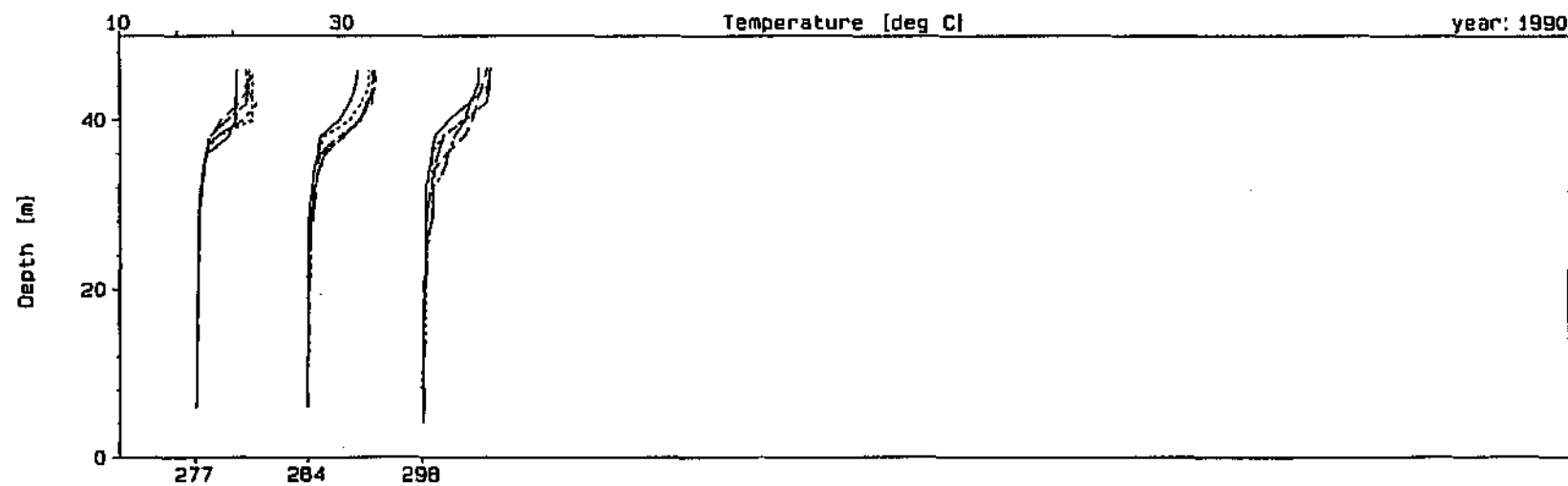
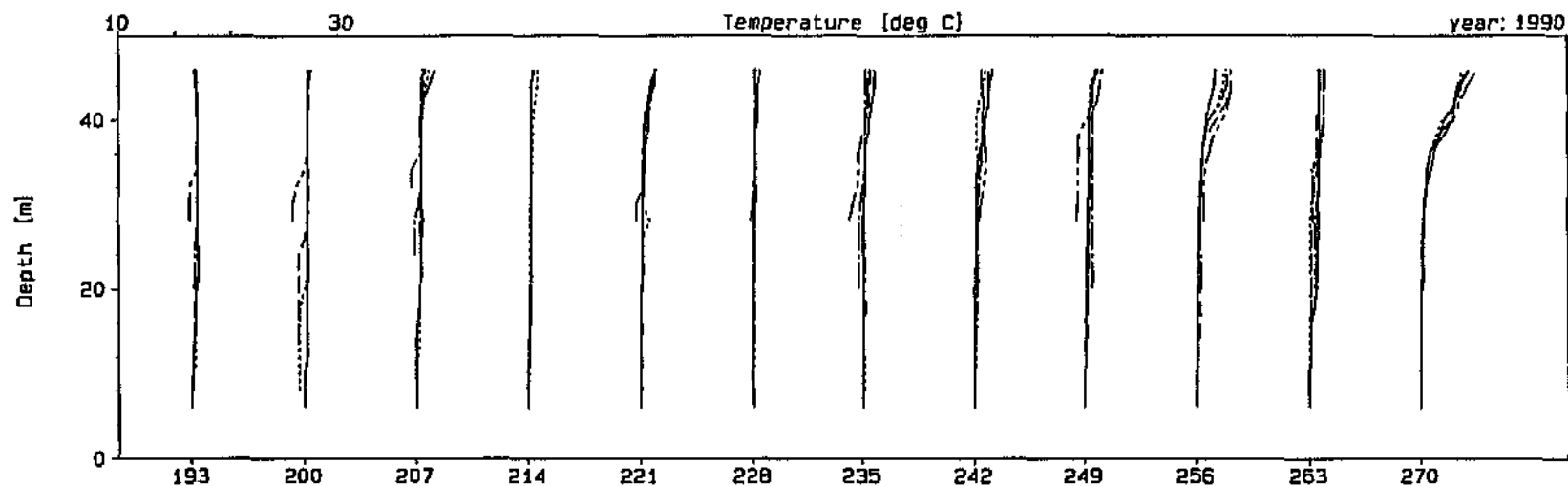
Observed profiles at Stations 51 to 55 (Julian day 90011 to 90186)

Figure 2.2.2.1

DYPLOT10 : DYRESM-10

Dam : Inanda Dam

Plot Date : 24 Oct 94, 21:49



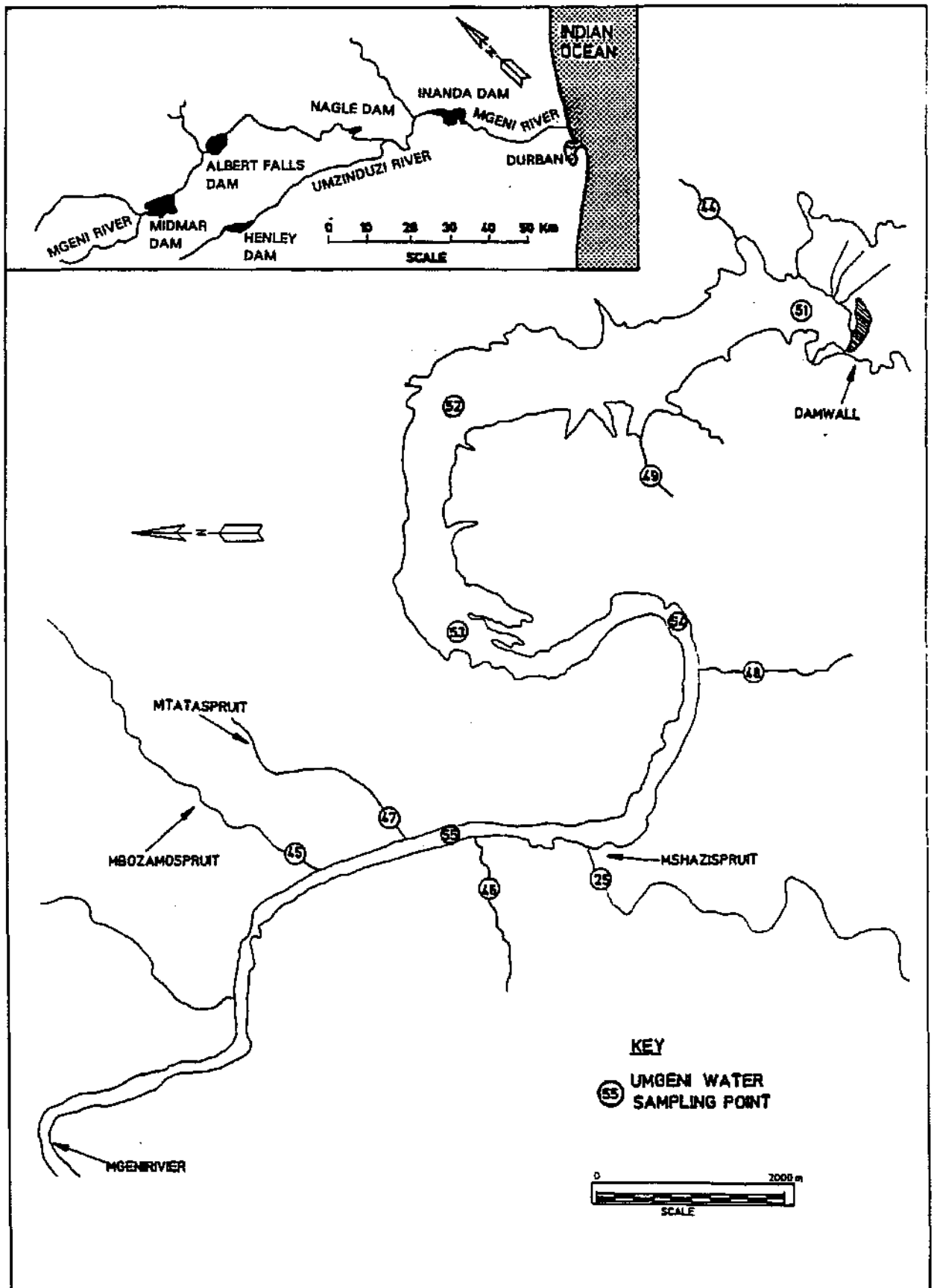
Julian Day

Profile Legend: — Station 51 Station 52 --- Station 53 — Station 54 — Station 55



Observed profiles at Stations 51 to 55 (Julian day 90193 to 90298)

Figure 2.2.2.2



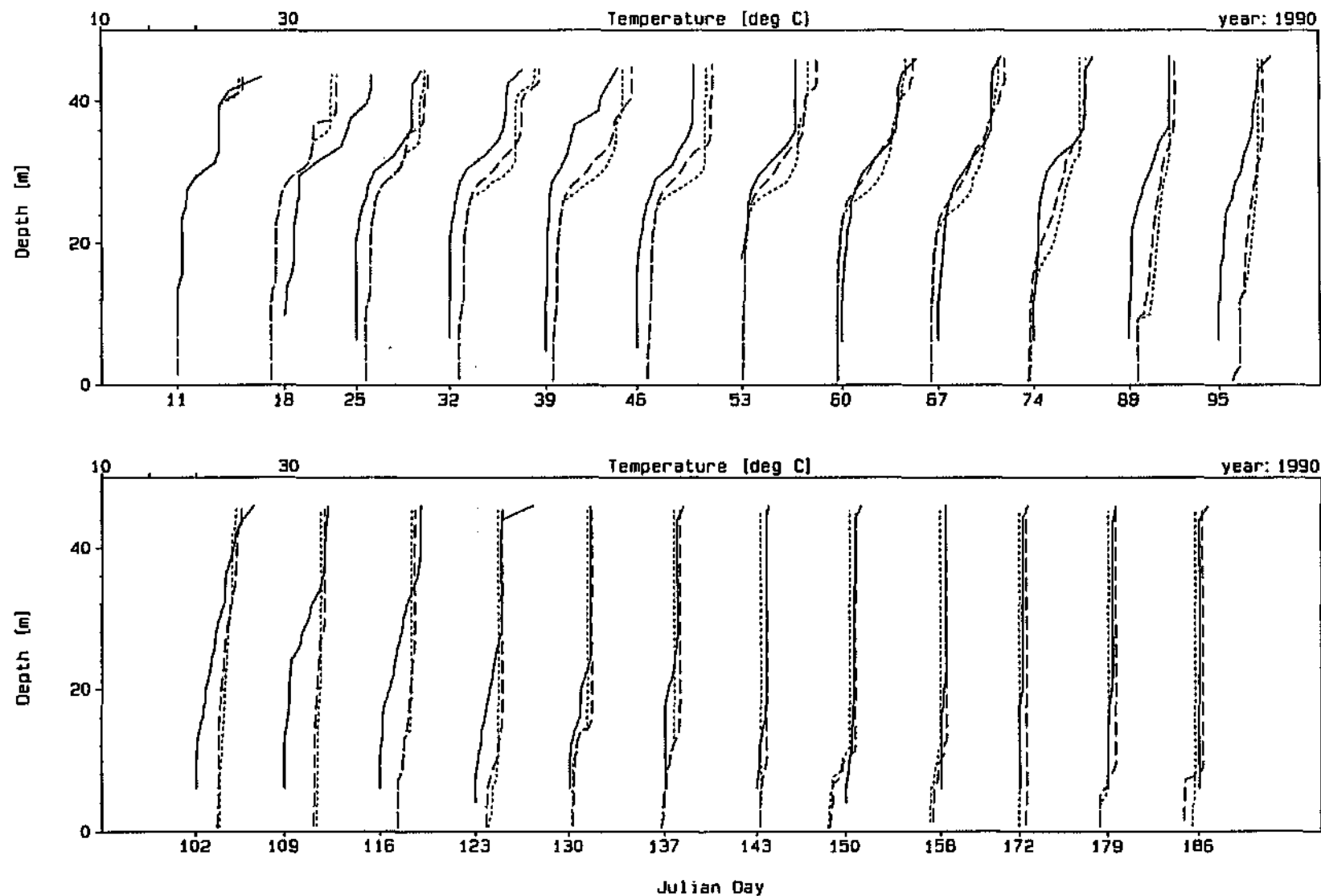
Location of Inanda Dam profiling stations

Figure 2.2.2.3

DYPLOT1D : DYRESM-1D

Dam : Inanda Dam

Plot Date : 25 Oct 94, 09:39

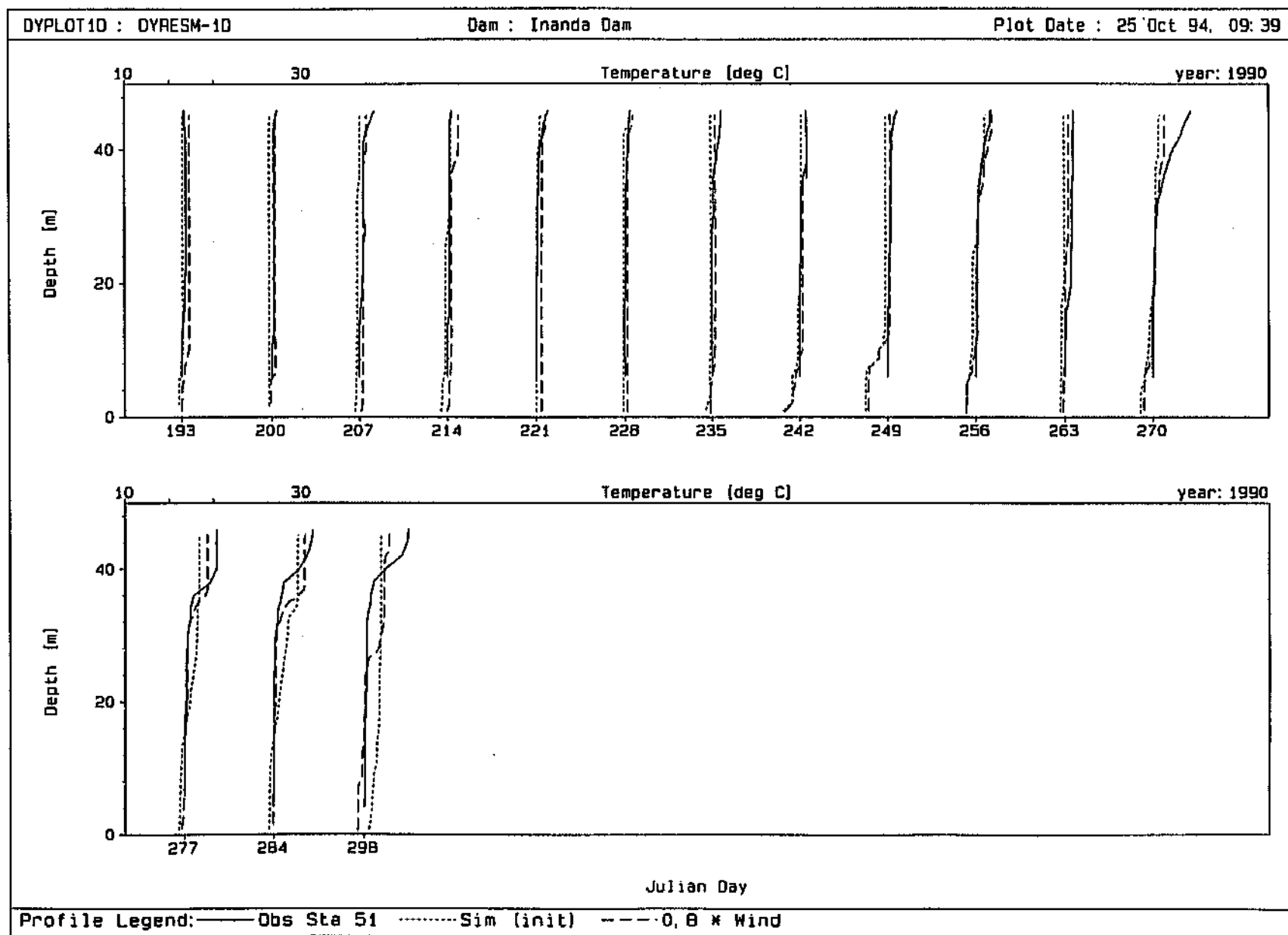


Profile Legend: — Obs Sta 51 Sim (init) --- 0.8 * Wind



Observed profiles at Station 51, initial and 0,8 x wind simulations

Figure 2.2.2.4



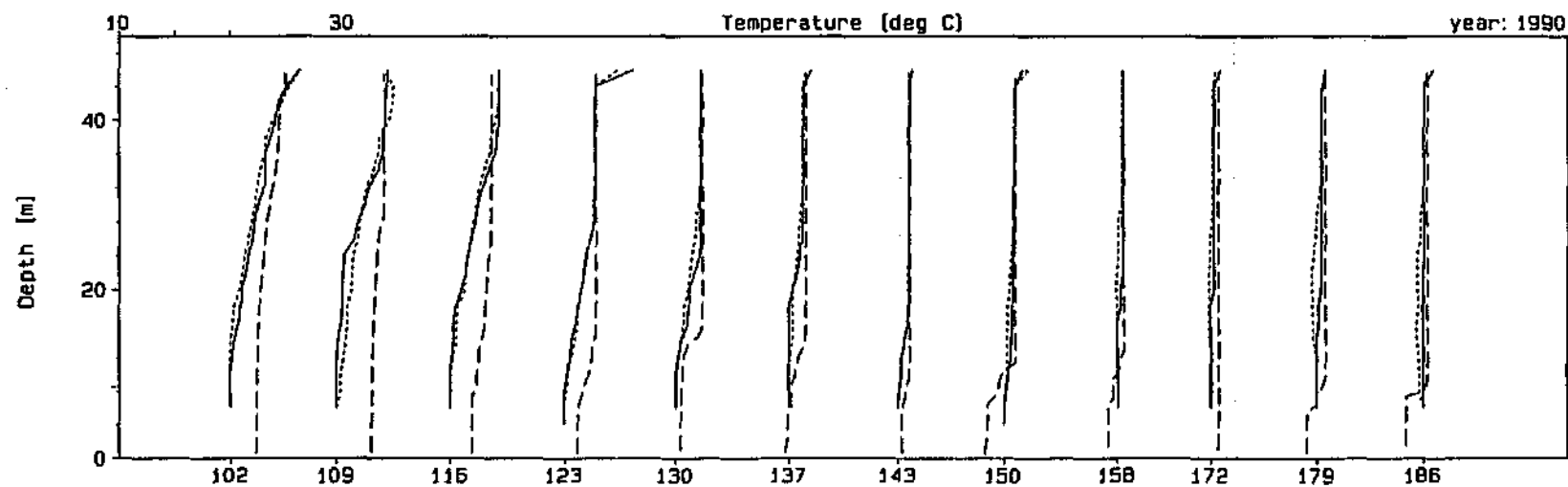
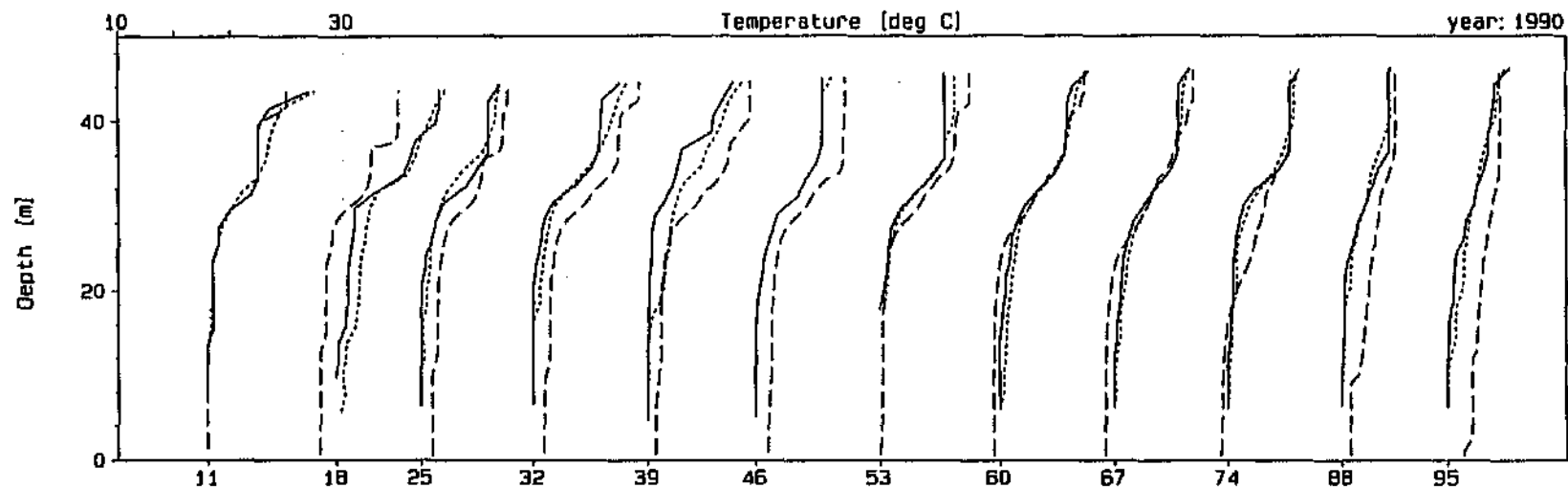
Observed profiles at Station 51, initial and 0,8 x wind simulations (cont.)

Figure 2.2.2.5

DYPLOT1D : DYRESM-1D

Dam : Inanda Dam

Plot Date : 25 Oct 94, 09:42



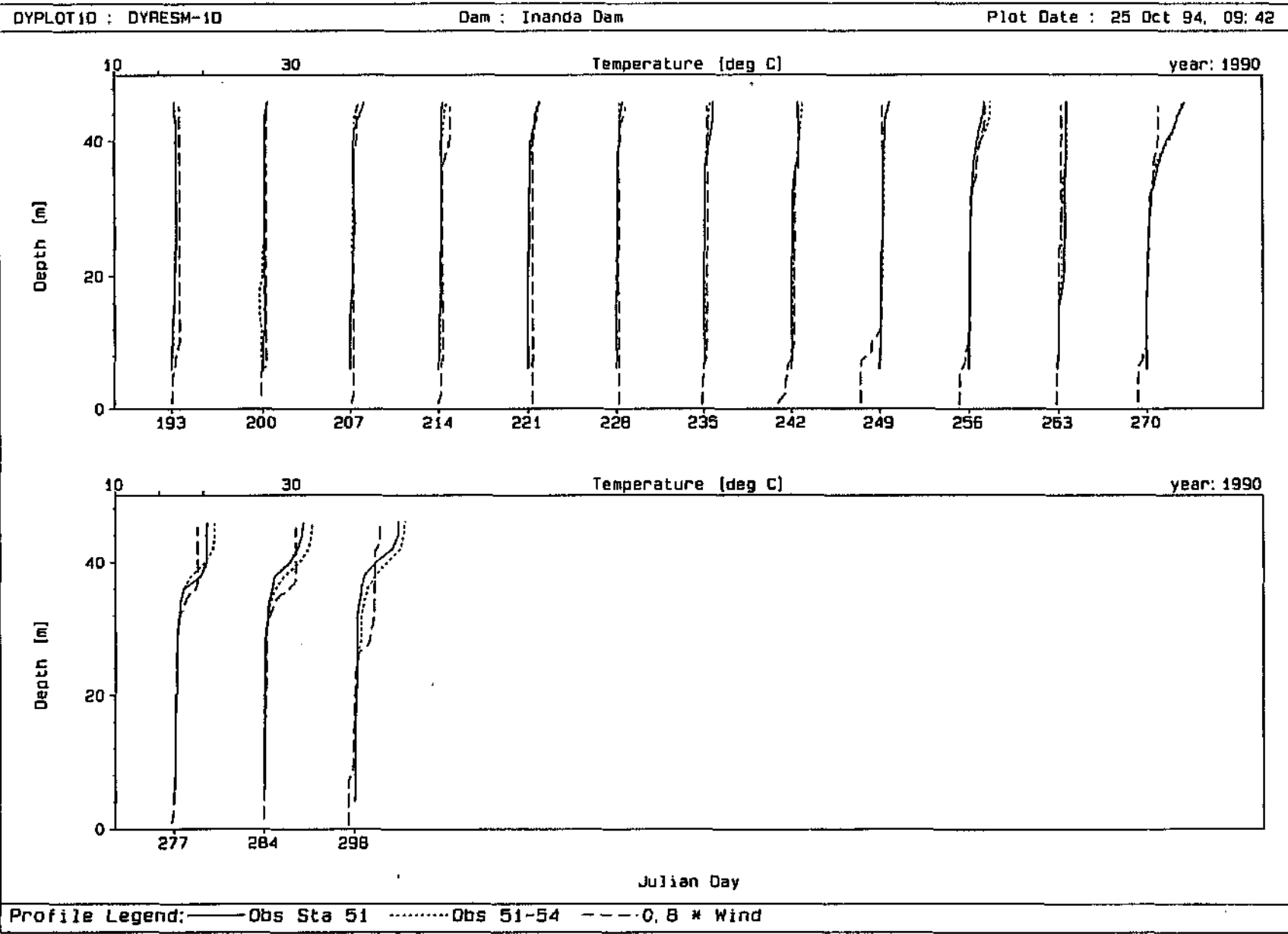
Julian Day

Profile Legend: — Obs Sta 51 Obs 51-54 --- 0.8 x Wind



Station 51, average of Stations 51-54 and 0,8 x wind simulation

Figure 2.2.2.6



Station 51, average of Stations 51-54 and 0,8 x wind simulation (cont.)

Figure 2.2.2.7

The model simulates the temperature of the surface mixed layer adequately for Julian days 90088 to 90123 but over estimates the hypolimnion temperature and shows more mixed profiles. Adjustment of the hydrometeorological data may improve the fit in this region. The winter mixed profile temperatures for the period from Julian day 90130 to 90263 are simulated quite well. At the onset of stratification towards the end of 1990 the simulated profiles tend to indicate the need for a greater wind sheltering effect, which would result in a warmer shallower surface mixed layer. Seasonal wind factors may be required in further 'calibration' attempts.

It was decided that in order to focus attention on the management of stratified water bodies, in this case by bubble plume destratification, further work would be done using the present Inanda Dam data set, as adjusted. The initial data set with a wind speed adjustment factor of 0,8 was therefore adopted for the bubble plume destratification modelling described in Section 2.2.2.4 below.

Bubble plume aerator design

It is important to stress that this analysis is not to be viewed as a full design of a bubbler system for Inanda Dam but rather as a demonstration of the feasibility of a bubbler required for adequate destratification of the dam.

Observed temperature profiles for Julian day 90046, 90067 and 90137 and simulated temperature profiles for Julian day 90137 and 90365 were chosen as a typical range of strongly and weakly stratified profiles. The profiles were converted to equivalent linear stratifications by calculating the potential energy of the water body relative to the bottom of the reservoir and finding a linear stratification with the same potential energy. In a similar manner the change in potential energy from stratified to mixed conditions was calculated. These calculations were made using a spreadsheet specifically developed for these purposes. The results are presented in Table 2.2.2.1 below.

TABLE 2.2.2.1 : TEMPERATURE PROFILE CHARACTERISTICS

| Profile | Julian Day of Temperature Profile | Time of the Year | Degree of stratification (°C/m) | PE _{initial} - PE _{final} (GJoules) |
|---------|-----------------------------------|------------------|---------------------------------|---|
| 1 | 90046 (observed) | Middle February | 0,131 | 11,7 |
| 2 | 90067 (observed) | Early March | 0,128 | 13,1 |
| 3 | 90137 (observed) | Middle May | 0,044 | 1,8 |
| 4 | 90137 (simulated) | Middle May | 0,046 | 0,3 |
| 5 | 90365 (simulated) | End December | 0,138 | 15,9 |

The first, second and fifth profiles described in Table 2.2.2.1 represent 'strong' stratification requiring a bubbler configuration capable of destratifying an already stratified water body. The third and fourth profiles display 'weak' stratification and are similar to profiles that a 'maintenance' bubbler system should be able to destratify.

Based on reservoir basin cross-sections taken from the 1990 capacity determination (DWAf, 1990) a bubbler level of RL 105,0 m was chosen for the design. Given the FSL of RL 147,0 and assuming an atmospheric pressure head of 10,2 m of water, the total pressure head at the level of the bubbler was taken to be 52,2 m of water. Using the first and second efficiency peak concept, associated with the development of one and two whole bubble plumes between the plume source and water surface respectively, both total and per source air flow rates were determined for the range of profiles described above. Table 2.2.2.2 shows a summary of the more pertinent results.

TABLE 2.2.2.2 : BUBBLE PLUME AERATOR ANALYSIS RESULTS

| Scenario | Total Head (m) | dT/dz (°C/m) | No. Plumes | μ (%) | Q_s (l/s) | dPE (GJ) | Time (days) | Q_t (l/s) | N_s | Source Spacing (m) | Aerator Length (m) |
|----------|----------------|--------------|------------|-----------|-------------|----------|-------------|-------------|-------|--------------------|--------------------|
| 1 | 52,2 | 0,131 | 1 | 8,0 | 15,14 | 13,1 | 21 | 625,1 | 41,3 | 8,0 | 330,3 |
| 2 | 52,2 | 0,131 | 2 | 5,5 | 2,27 | 13,1 | 21 | 909,2 | 400,4 | 2,0 | 800,8 |
| 3 | 52,2 | 0,140 | 1 | 8,0 | 16,65 | 15,9 | 21 | 758,7 | 45,6 | 8,0 | 364,5 |
| 4 | 52,2 | 0,140 | 2 | 8,0 | 7,57 | 15,9 | 21 | 758,7 | 100,2 | 8,0 | 801,9 |
| 5 | 52,2 | 0,050 | 1 | 6,0 | 4,54 | 1,8 | 21 | 114,5 | 25,2 | 8,0 | 201,7 |
| 6 | 52,2 | 0,050 | 2 | 4,0 | 0,76 | 1,8 | 21 | 171,8 | 226,9 | 2,0 | 453,9 |
| 7 | 52,2 | 0,131 | 1 | 8,0 | 15,19 | 13,1 | 28 | 471,0 | 31,0 | 8,0 | 248,0 |
| 8 | 52,2 | 0,131 | 1 | 8,0 | 14,95 | 13,1 | 21 | 628,0 | 42,0 | 8,0 | 336,0 |
| 9 | 52,2 | 0,050 | 2 | 4,0 | 1,00 | 1,8 | 12 | 314,0 | 314,0 | 2,0 | 628,0 |
| 10 | 52,2 | 0,050 | 2 | 4,0 | 1,00 | 5,0 | 21 | 471,0 | 471,0 | 2,0 | 942,0 |

where: dT/dz = equivalent linear stratification
 μ = mechanical efficiency (greater efficiency being desirable)
 Q_s = air flow rate per source
dPE = difference in potential energy between the stratified and mixed profile
 Q_t = total air flow rate for the bubbler system
 N_s = total number of bubble plume sources

It is of interest to note that the calculated design mechanical efficiencies range between 4% and 8%, which although low, is offset by the ease and cost of installation, operation and maintenance when compared to mechanical mixing methods.

Although the above table shows a significant range in bubble plume aerator configurations, cognisance should be taken of the fact that air flow rates are only available in discreet steps due to the availability of compressor capacities. It has become apparent from enquiries in the marketplace that multiple 157 l/s compressors (55 kW) would most likely be the most appropriate for typical South African impoundments. In particular, two 157 l/s compressors were used at Inanda Dam in the previous bubble plume destratification attempts and would most probably be available for any further tests emanating from the current research. Scenarios 1 to 6 above show the theoretical aerator configuration for the given destratification case, while scenarios 7 to 10 are for Q_c values for multiples of 157 l/s and whole source numbers.

The above scenarios show that up to six compressors would be required for air flow rates up to 910 l/s. At a typical capital cost of R 80 000 per compressor, this requirement is clearly very costly and more favourable options need to be sought by optimisation. It was therefore decided to test the effect of using bubble plume scenarios 7 to 10 above and various slight variations and combinations thereof in the Inanda Dam *DYRESM-ID* model.

Bubble plume destratification - Simulation results

A Summary of the specific operating conditions used for the *DYRESM* Inanda Dam bubbler runs are given in Table 2.2.2.3. The Table includes design parameters such as efficiency peak, plume spacing and consequently whether the bubbler has interacting or independent plumes, the number of 157 l/s compressors used and the time period over which the bubbler system was operational and whether this operation was continuous or intermittent.

TABLE 2.2.2.3 : OPERATING CONDITIONS FOR BUBBLER RUNS

| Scenario Number | Specific Operating Conditions | | | | | |
|-----------------|---|---------------------------------|-----------------------------------|-------------------|---|--|
| | First or Second Peak Case | Independent/ Interacting Plumes | Plume Spacing/ Aerator Length (m) | No of Compressors | Bubbler Mode | Bubbler Operating Period |
| 7 | 1 | Independent | 8 / 248 | 3 | Continuous | 90012 - 90101 (12 Jan 1990 - 10 April 1990) (90 days) |
| 8 | 1 | Independent | 8 / 336 | 4 | Continuous | 90012 - 90101 (12 Jan 1990 - 10 April 1990) (90 days) |
| 9 | 2 | Interacting | 2 / 628 | 2 | - | - |
| 10 | 2 | Interacting | 2 / 942 | 3 | Continuous | 90012 - 90101 (12 Jan 1990 - 10 April 1990) (90 days) |
| 11 | Combination of scenarios : 7 for destratification, and | | | | Continuous | 90012 - 90039 (12 Jan 1990 - 8 Feb 1990) |
| | 9 for maintenance | | | | Continuous | 90040 - 90298 9 Feb 1990 - 24 Sept 1990) |
| 12 | Combination of scenarios : 7 for destratification, and | | | | Continuous | 90012 - 90039 (12 Jan 1990 - 8 Feb 1990) |
| | 9 for maintenance | | | | Intermittent operation for temp differences between 2°C and 4°C | 90040 - 90151 (9 Feb 1990 - 30 May 1990) and 90244 - 90365 (31 Aug 1990 - 30 Dec 1990) |
| 13 | As for scenario 12 except that range is from 1°C to 3°C | | | | Optimisation | Temperature dependant |

Figure 2.2.2.8 shows the results for scenario 7 (strong destratification) with the bubbler in operation from Julian day 90012 to 90101, a period of 90 days. The effect of the 'destratification' bubbler (dashed line) can be clearly seen in that the bubbler simulation profile for Julian day 90039 shows a largely mixed reservoir when compared with both the observed profiles (Station 51 measurements shown as solid line) and simulated profiles (dotted line) without bubble plume operation. This scenario can therefore be seen to be capable of almost completely mixing a strongly stratified Inanda Dam within a period of a few weeks. Also, when a significant disturbance is seen to occur, such as that associated with the large inflow in the region of Julian day 90088 which inserts into the middle of the reservoir causing increased stratification, the bubbler system is capable of remixing the reservoir quite well (see Figure 2.2.2.9).

Figure 2.2.2.10 shows both bubbler scenario 7 and 8 results in which the faster and more complete destratification by Julian day 90039 due to the larger total air flow rate of scenario 8 (chain line) can be clearly seen. It is also interesting to note that after initial destratification the additional total air flow rate associated with scenario 8 has little effect. It is suggested that this is largely due to the reduced efficiency of bubble plumes that form less than one whole plume in a weakly stratified water column.

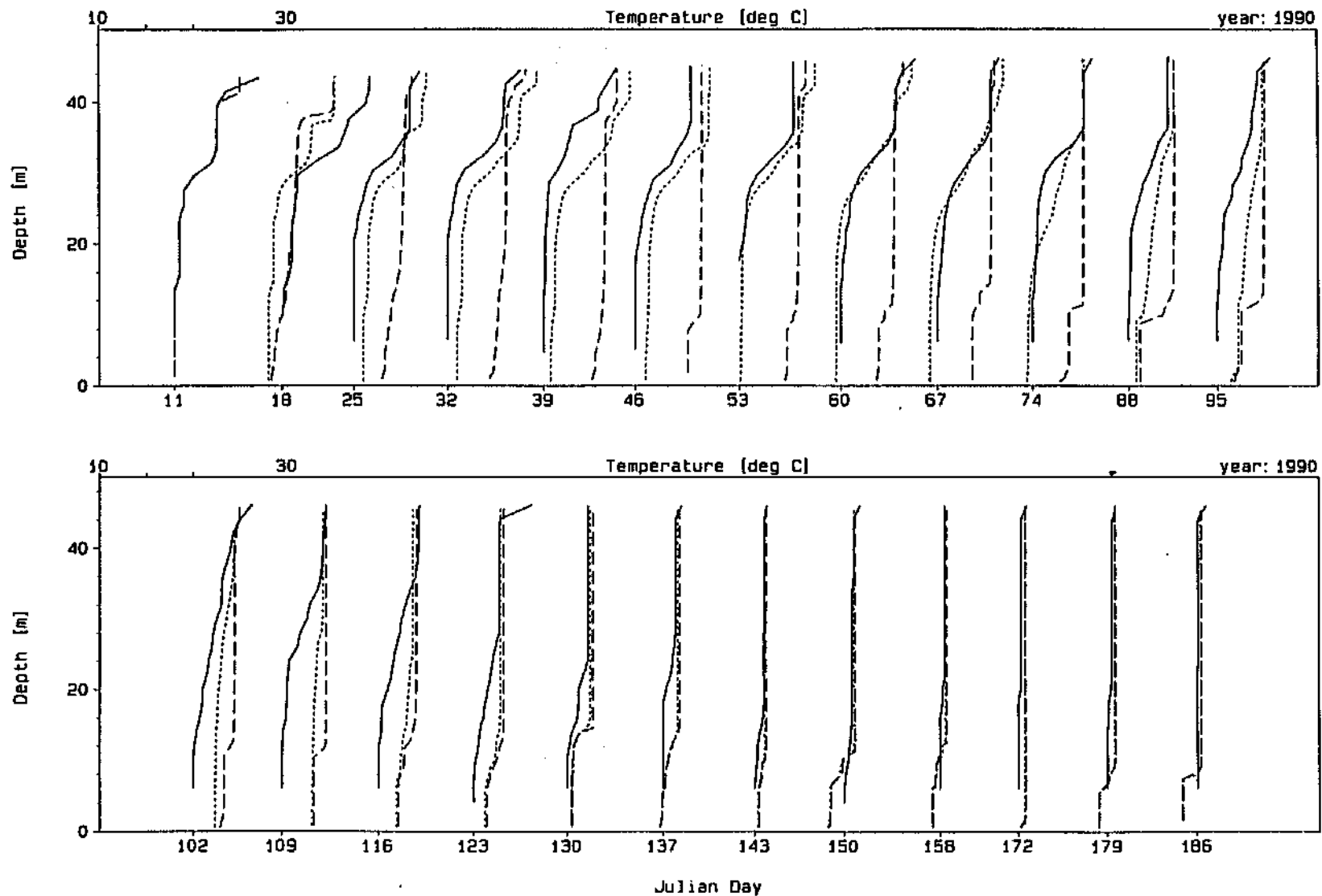
The simulated profiles for the scenario 10 case which was designed as a 'maintenance' type bubbler (dashed line) are presented in Figure 2.2.2.11. In this instance the low air flow rate per bubble plume source seemed to merely raise the thermocline and mix the hypolimnion initially. The bubbler system did, however, achieve an almost completely mixed reservoir by Julian Day 90074 and responded better to the inflow disturbance in the region of Julian day 90088 by producing a more mixed profile on Julian day 90095.

Figure 2.2.2.12 (A) and Figure 2.2.2.12 (B) show the daily and 10 day moving average mechanical efficiency respectively of the scenario 7 and 10 bubbler systems. It is clear that the greatest efficiency is achieved by the single plume scenario 7 bubbler while it is operating on a stratification profile close to that for which it was designed. In accordance with the design theory (see Figure 2.1.2), this scenario's efficiency falls dramatically when operating on a less stratified profile and continues dropping as the water body is destratified. Some local peaks are observed, however, and can be attributed to disturbances that bring the temperature profile closer to the bubbler's design profile (see Figure 2.2.2.9).

DYPLOT10 : DYRESM-10

Dam : Inanda Dam

Plot Date : 25 Oct 94, 10: 20

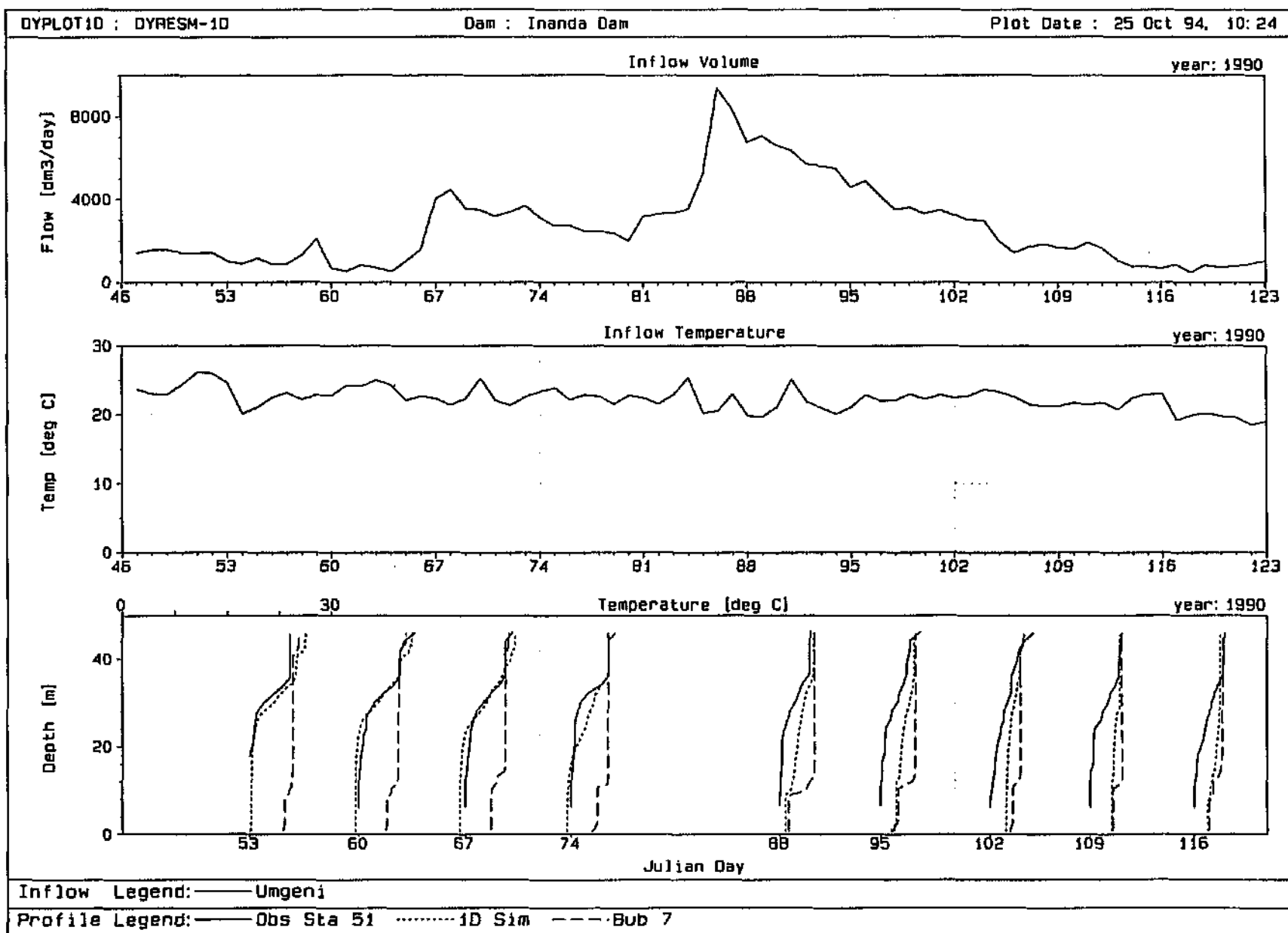


Profile Legend: — Obs Sta 51 1D Sim ---- Bub 7



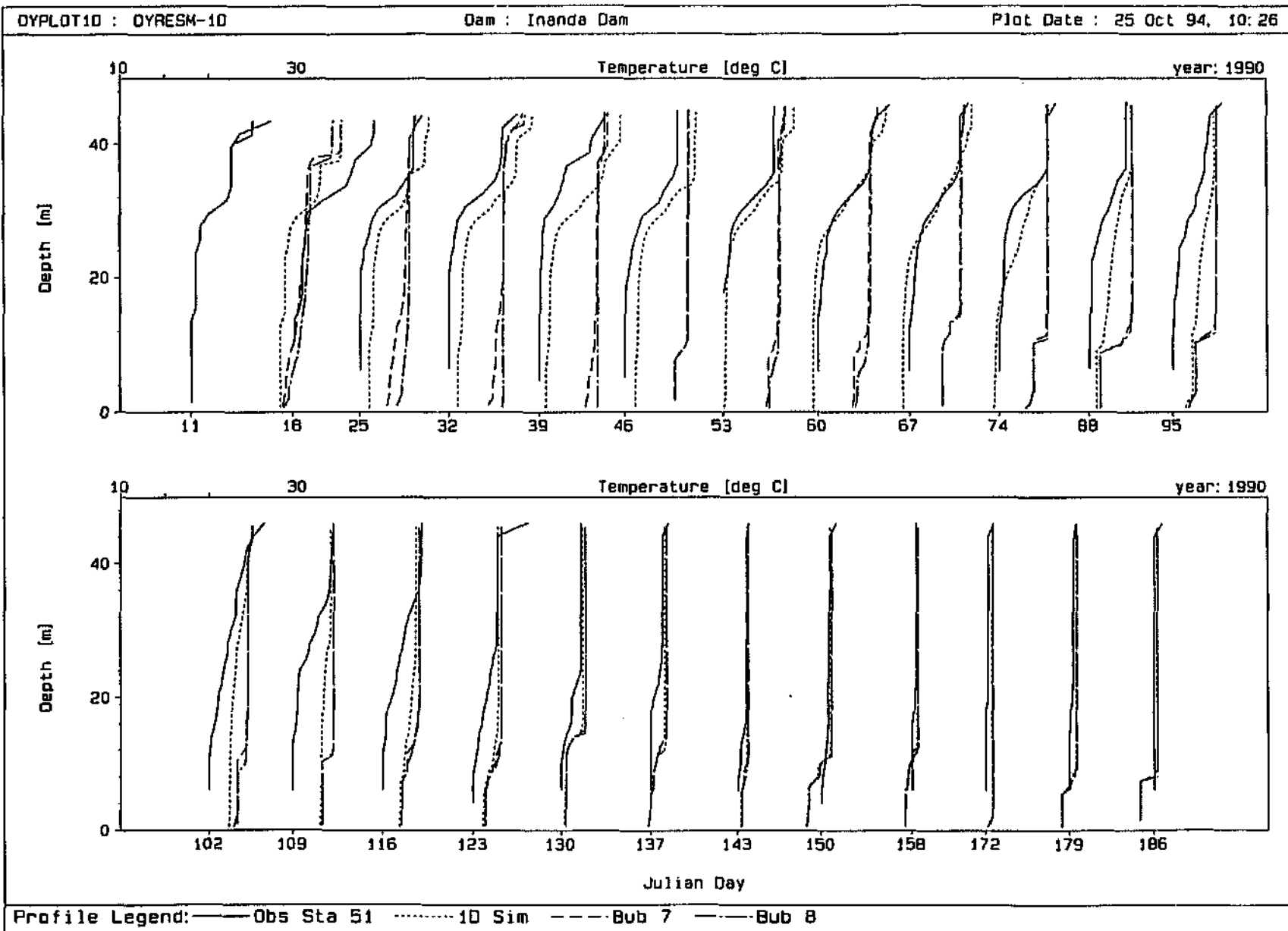
Station 51 observed profiles, 0,8 x wind simulation and bubbler scenario 7

Figure 2.2.2.8



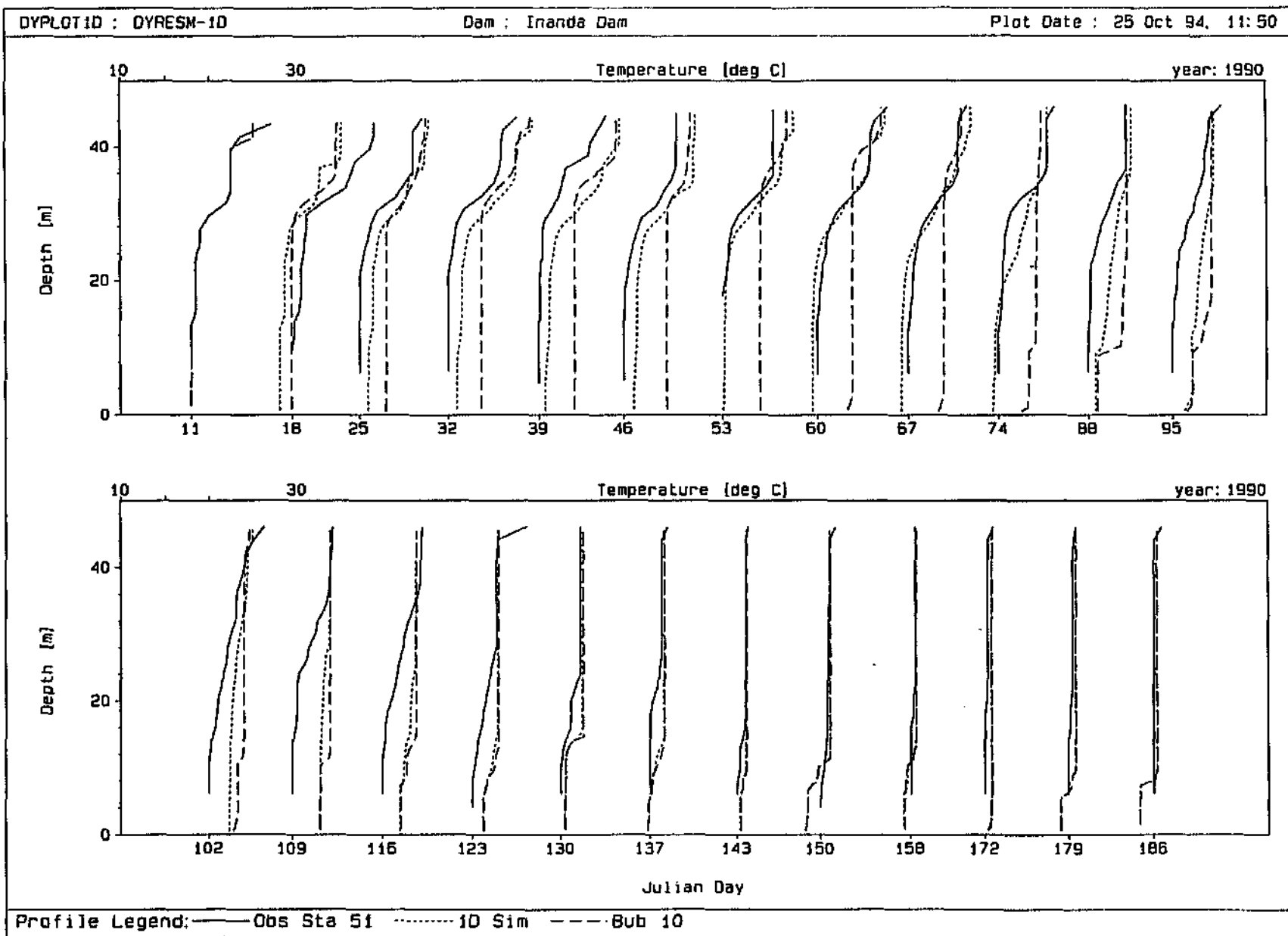
Inflow, inflow temperature and observed, simulated and bubbler 7 profiles

Figure 2.2.2.9



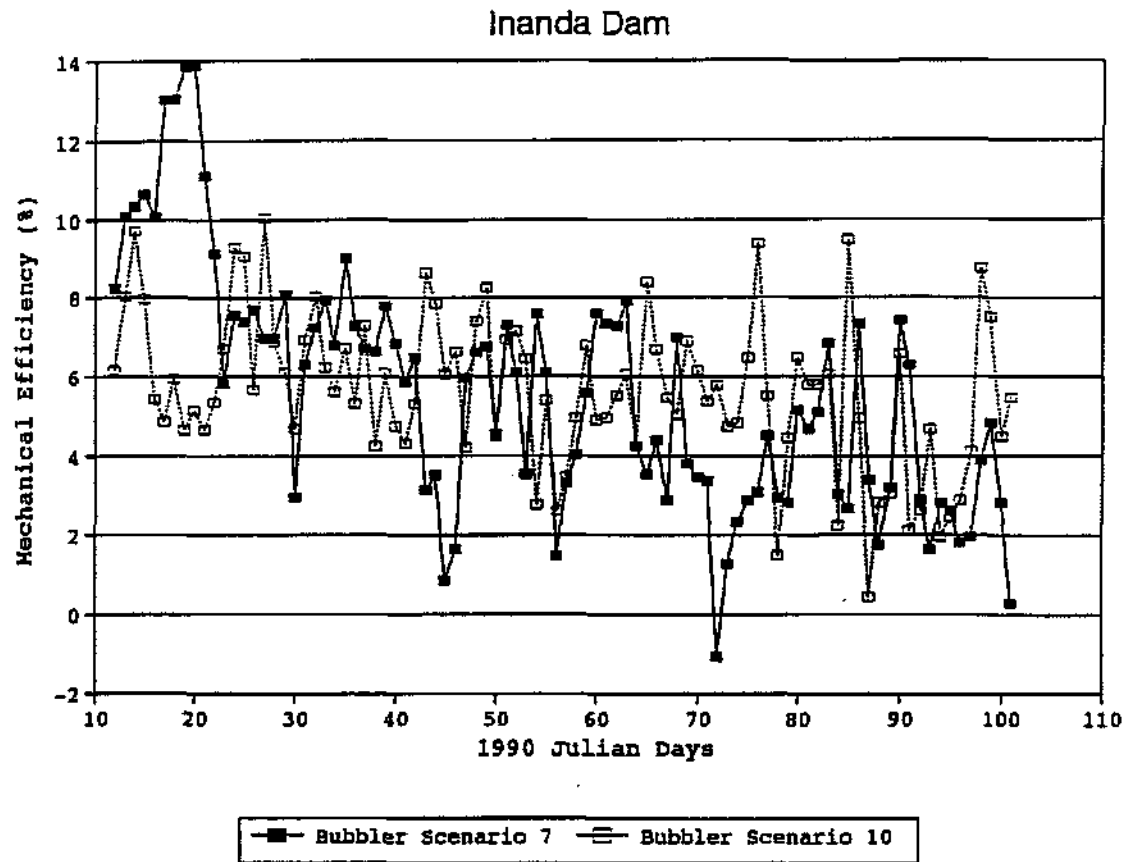
Station 51 observed profiles, 0,8 x wind simulation and bubbler scenarios 7 and 8

Figure 2.2.2.10



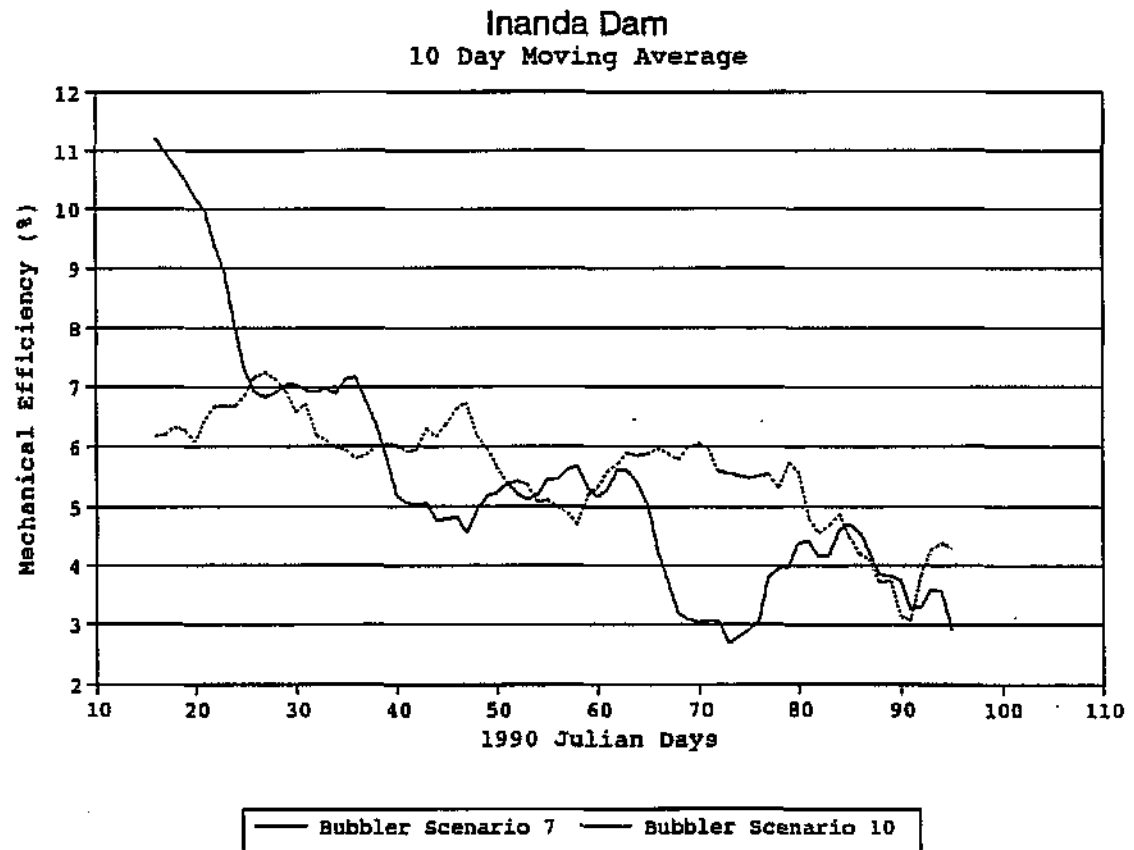
Station 51 observed profiles, 0,8 x wind simulation and bubbler scenario 10

Figure 2.2.2.11



Daily mechanical efficiency of bubbler scenarios 7 and 10

Figure 2.2.2.12 (A)



10 Day moving average mechanical efficiency of bubbler scenarios 7 and 10

Figure 2.2.2.12 (B)

A point is reached after which the 'maintenance' design of the scenario 10 bubbler is generally more efficient and less subject to very low efficiencies. This identifies the need for two bubbler systems, viz. a destratification and a maintenance system, to be available for the ongoing destratification of a water body, and a mechanism for the determination of the most appropriate point at which to switch between systems. The dropping of the efficiency of both bubbler scenarios to very low levels is seen to coincide with weakly stratified profiles (less than 2°C top to bottom temperature difference), due to the destratification/prevention work of the bubbler, and indicates the need for bubbler optimisation by intermittent use or the use of a very weak 'maintenance' mode, which in this case may be achieved by the use of only one compressor during these periods.

Since the capital and running costs of the continuous use of an additional compressor, over and above the two already available at Inanda Dam, is high, the effect of using a combination of scenario 7 (from Julian day 90012 to 90039) and scenario 9 (a two compressor system in operation from Julian day 90040 to 90298) was tested. *Let us call this model run scenario 11.* This run was undertaken assuming interacting plumes due to the excessive overall aerator length associated with ensuring independent plumes.

The results given in Figures 2.2.2.13 and 2.2.2.14 (observed profiles at Station 51 shown as solid line and bubbler scenarios 7 and 11 shown as dotted and dashed lines respectively) show that the scenario 11 bubbler configuration is capable of sufficiently destratifying the reservoir (from a strongly stratified profile to a mixed one) and of maintaining the reservoir in a relatively mixed state throughout the summer period. It is also interesting to note that the onset of stratification (from Julian day 90263) in the middle of September is largely prevented by the 314 l/s, 314 plume source system.

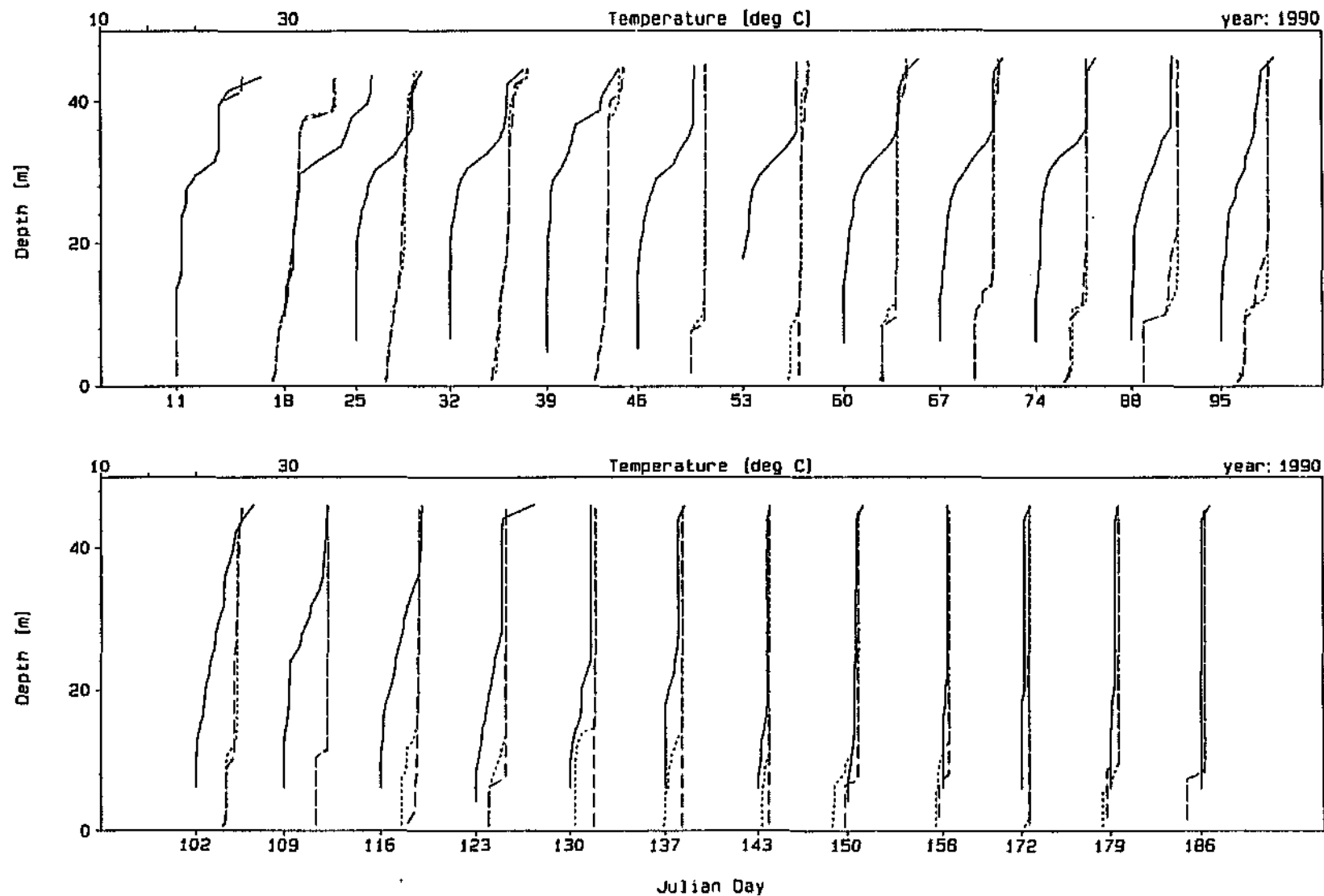
At this point it is important to be reminded that the ultimate purpose of the design and operation of a bubble plume aeration system is the avoidance of stratification by maintaining the reservoir in a mixed condition all year round.

Figure 2.2.2.15 shows how a two compressor maintenance bubbler system, similar to scenario 11, effectively prevents the onset of stratification in the spring and summer in the later part of 1990 when compared with the no-bubbler case. The necessity of running a three compressor system at Inanda Dam may therefore be limited to cases where strong stratification arises due to malfunction of the maintenance bubbler system or extreme hydrometeorological conditions.

DYPLOT10 : DYRESM-10

Dam : Inanda Dam

Plot Date : 25 Oct 94, 11:53



Profile Legend: — Obs Sta 51 Bub 7 --- Bub 11



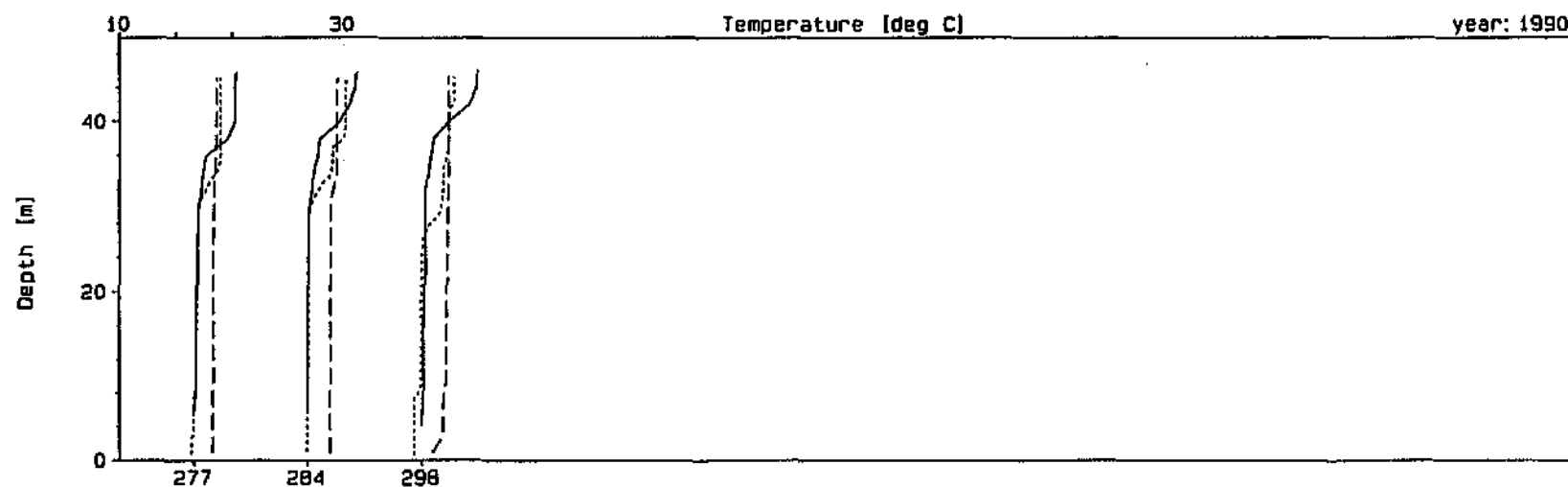
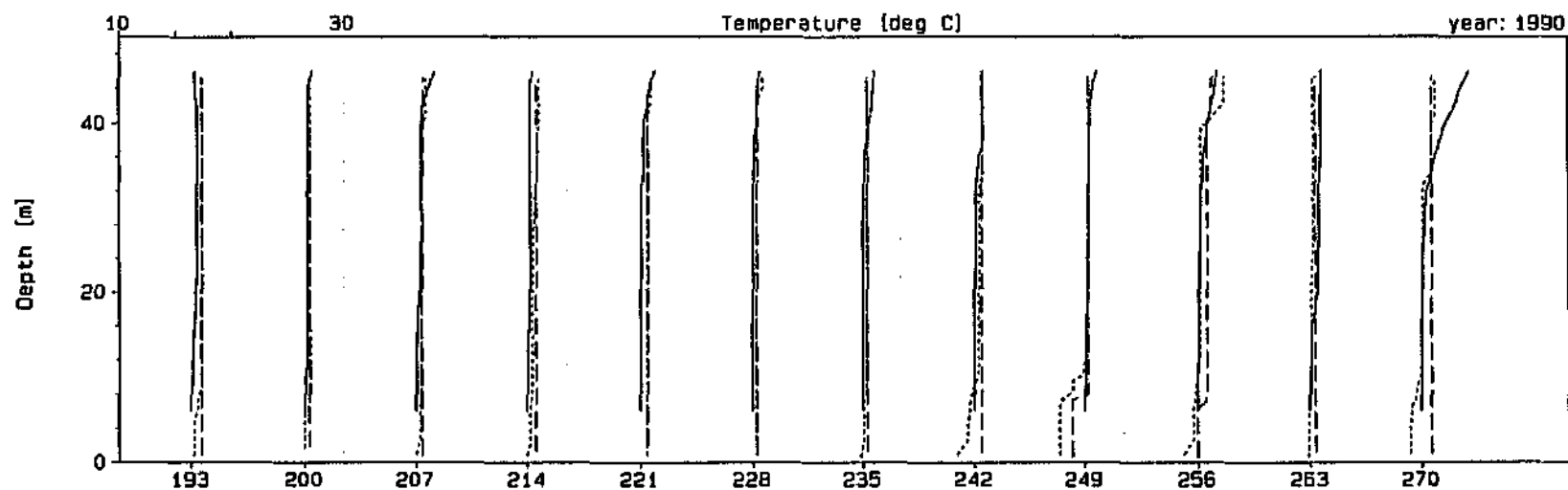
Station 51 observed profiles and bubbler scenarios 7 and 11

Figure 2.2.2.13

DYPLOTID : DYRESM-10

Dam : Inanda Dam

Plot Date : 25 Oct 94, 11:53



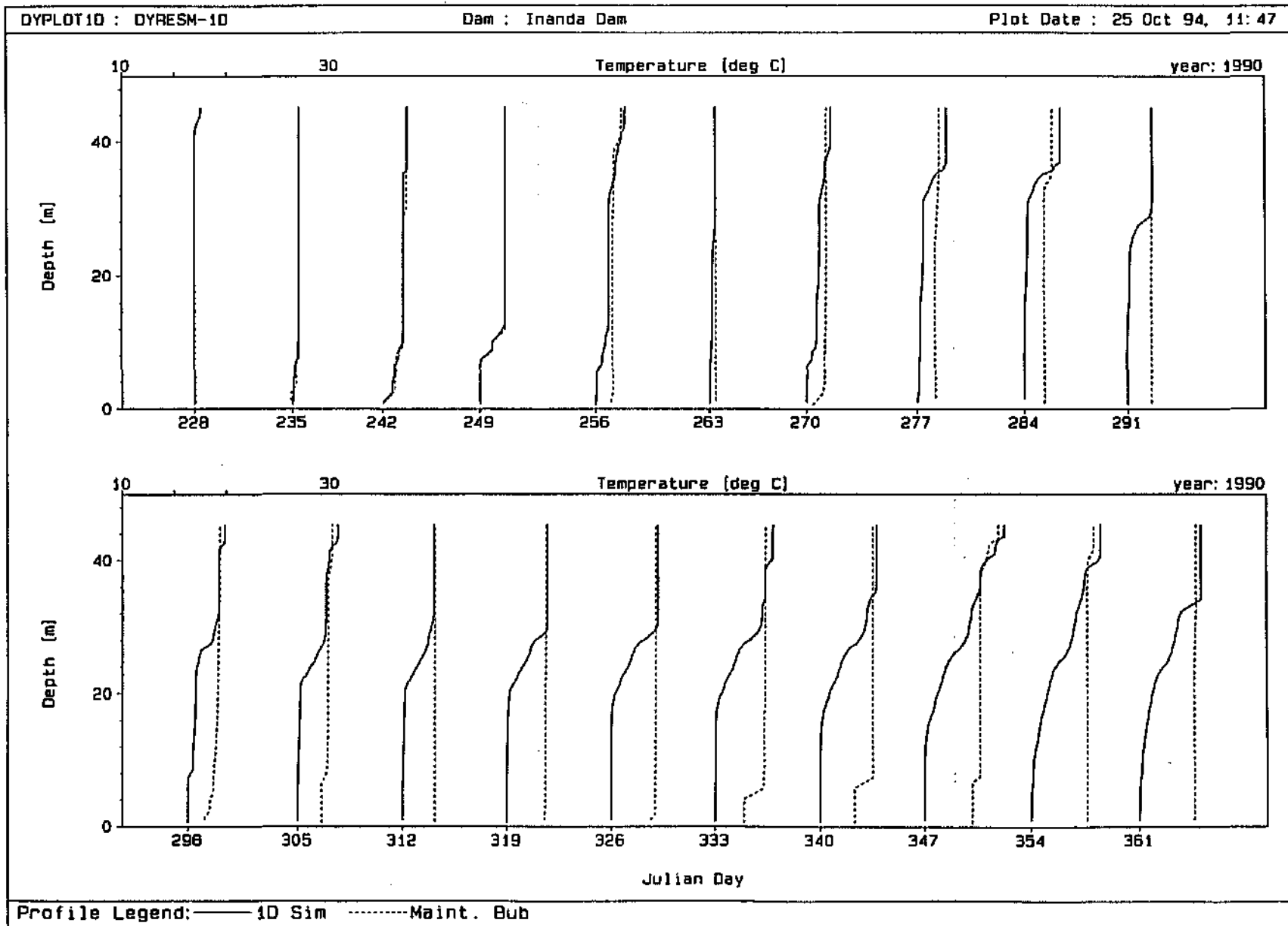
Julian Day

Profile Legend: — Obs Sta 51 Bub 7 --- Bub 11



Station 51 observed profiles and bubbler scenarios 7 and 11 (cont.)

Figure 2.2.2.14



0,8 x Wind simulation and scenario 11 type maintenance bubbler

Figure 2.2.2.15

The running and maintenance costs of a bubbler system must, however, be considered when contemplating the benefits of destratification. Typically, the cost of electricity supply to Inanda Dam is in the order of R4250/month for one 55 kW, 157 l/s compressor. For a continuous nine month period the cost of running two compressors could be in the region of R 77 000. When compared with water treatment costs of approximately R 200 000 per season to remove geosmin produced from blue-green algae using activated carbon (Howard, pers comm, 1994) it can be seen that significant savings may be achieved if the prevention of stratification by bubble plume aeration improves water quality.

In order to investigate whether or not there would be scope for cost saving associated with an intermittent use of the bubbler system two model runs were undertaken using the *DYRESM* bubbler optimisation option. In this case the bubbler is turned on when the surface to bottom water temperature difference reaches a given value and the system is in turn switched off when the temperature difference falls to a second given value.

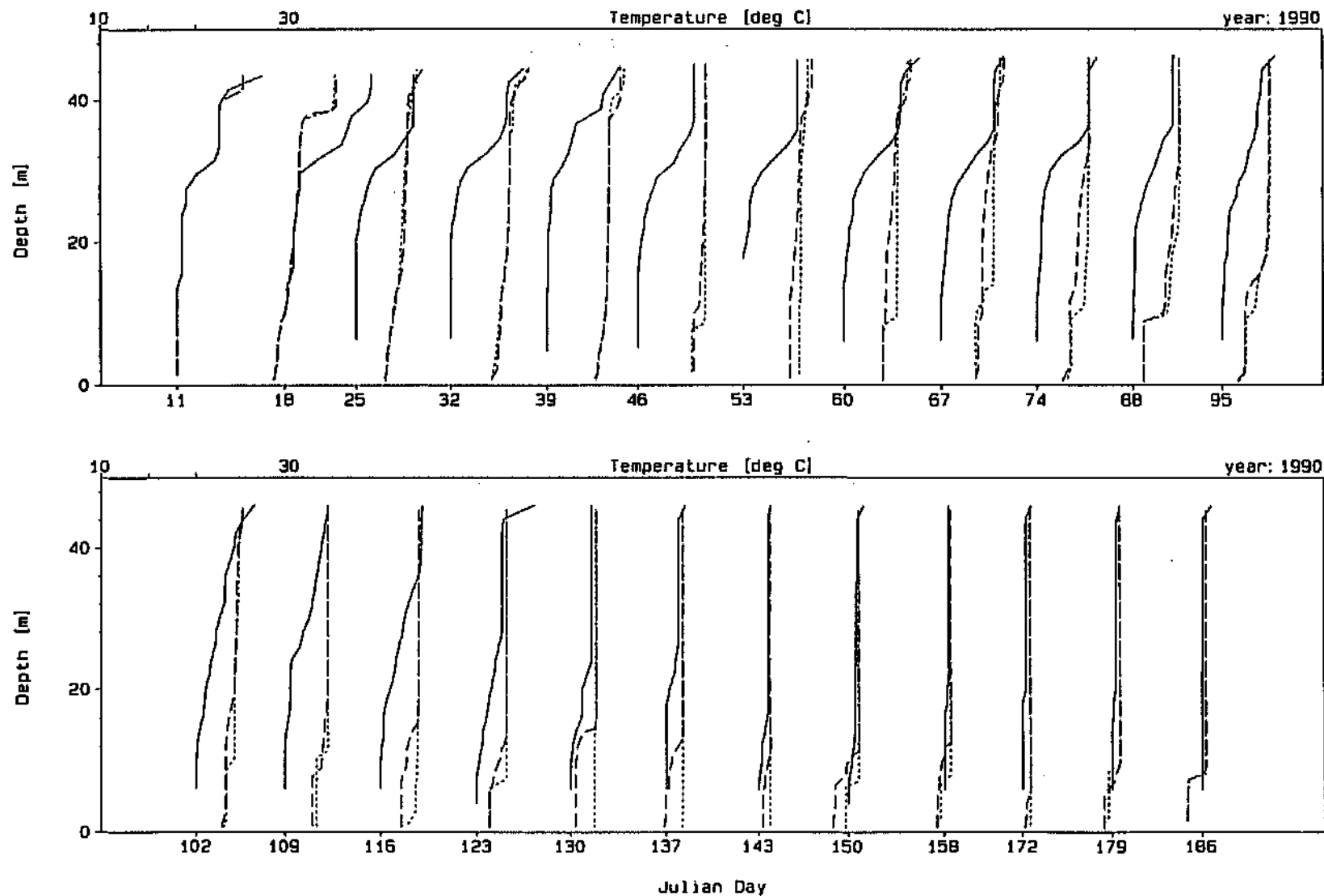
In the first simulation (*scenario 12*) bubbler scenario 7 was used with independent plumes from Julian day 90012 to 90039 and then bubbler scenario 9 was used with interacting plumes and optimisation on/off temperatures of 4 °C and 2 °C respectively for the periods Julian day 90040 to 90151 and 90244 to 90365. The bubbler was completely inactive for the winter period from Julian day 90152 to 90243 (June to August, inclusive). Figures 2.2.2.16 and 2.2.2.17 show the effect of this type of bubbler operation (solid lines representing the Station 51 observed profiles, dotted lines showing scenario 11 and dashed lines scenario 12). The reduction in bubbler operation time can be seen to have had an effect on the degree of reservoir mixing (see Julian day 90130), however, the dam remained in a relatively mixed condition when compared with the no bubbler case (see Figure 2.2.2.4). Figure 2.2.2.20 (A) shows both the mechanical efficiency and the frequency of bubble plume operation for the scenario 12 model run. A considerable saving in the bubbler system running costs would have been achieved when compared to the continuous aeration of scenario 11.

In the second intermittent operation simulation (*scenario 13*) only the bubbler optimisation on/off temperatures of 3 °C and 1,5 °C respectively differed from bubbler scenario 12. Figures 2.2.2.18 and 2.2.2.19 show the effect of this bubbler operation (solid lines representing the Station 51 observed profiles, dotted lines showing scenario 11 and dashed lines scenario 13). Although the degree of reservoir mixing remained relatively similar to that of scenario 12, Figure 2.2.2.20 (B) shows that the frequency of bubble plume operation increased dramatically.

DYPLOT1D : DYRESM-1D

Dam : Inanda Dam

Plot Date : 25 Oct 94, 11:55



Profile Legend: — Obs Sta 51 Bub 11 ---- Bub 12



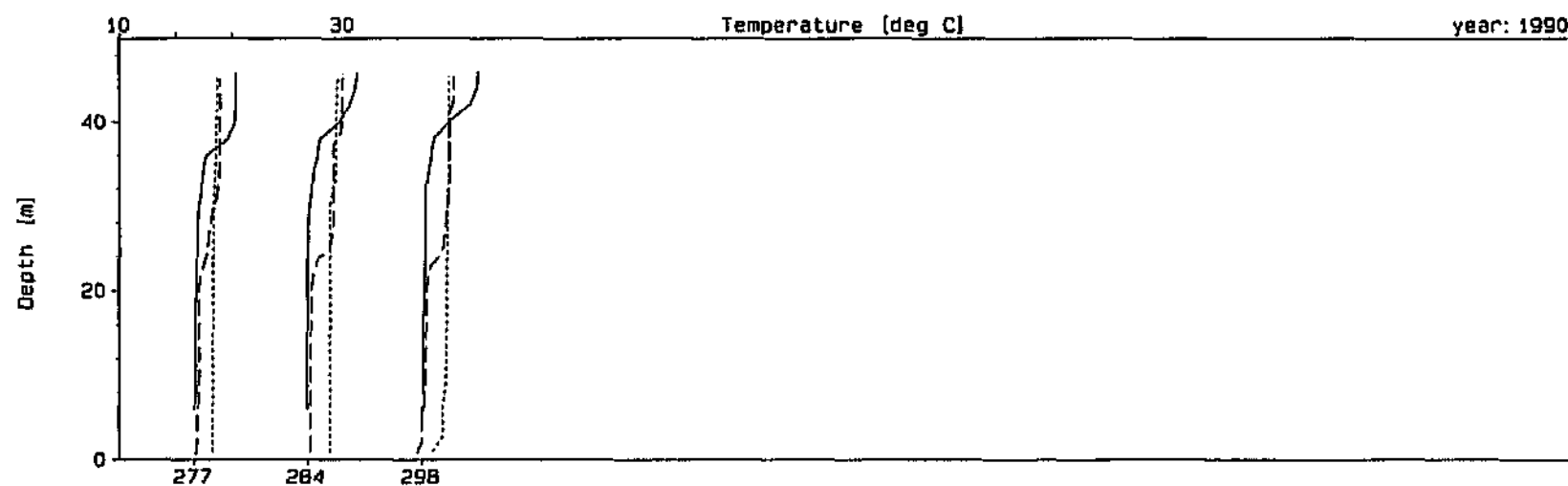
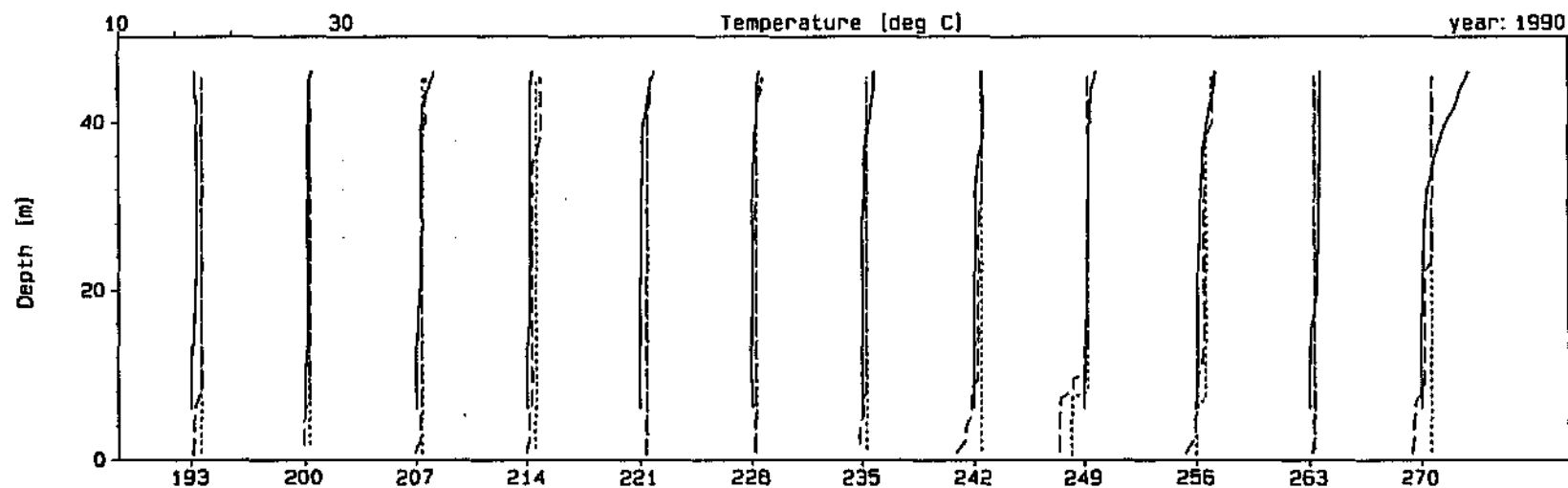
Station 51 observed profiles and bubbler scenarios 11 and 12

Figure 2.2.2.16

DYLOT1D : DYRESM-10

Dam : Inanda Dam

Plot Date : 25 Oct 94, 11:55



Julian Day

Profile Legend: — Obs Sta 51 Bub 11 --- Bub 12



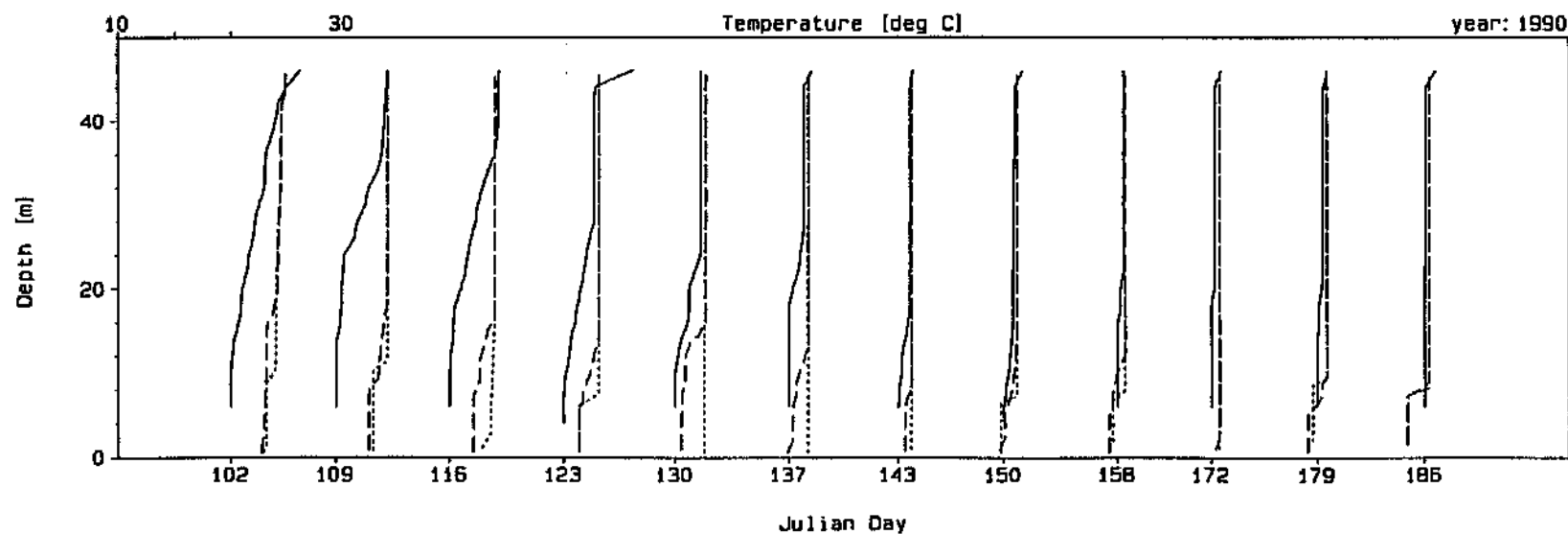
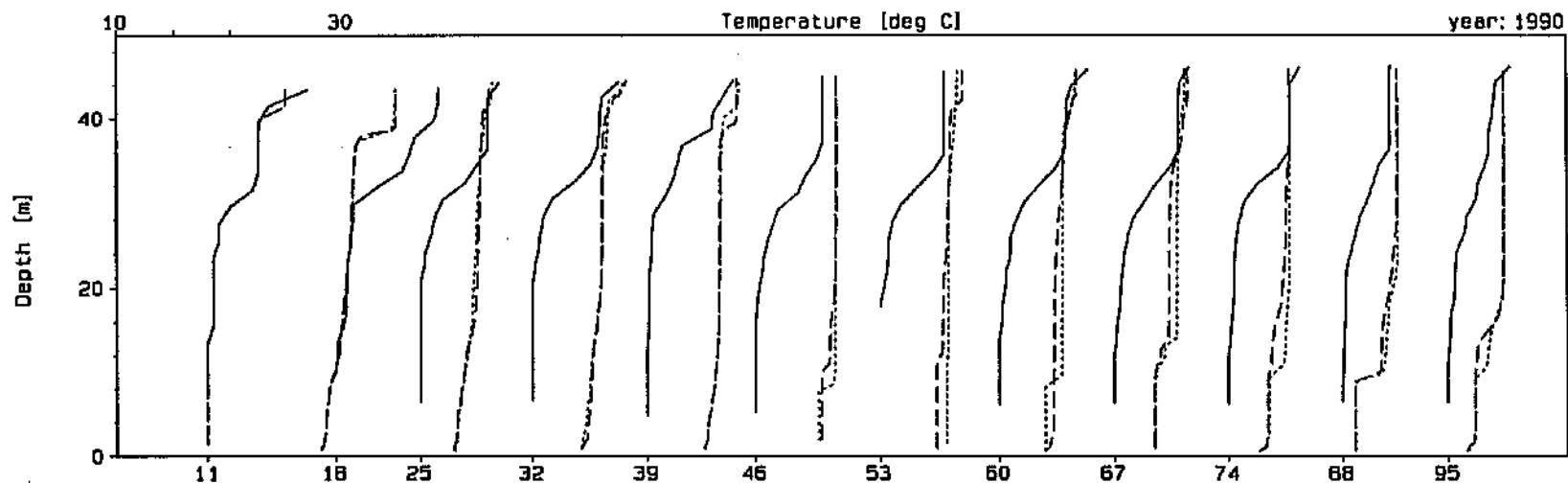
Station 51 observed profiles and bubbler scenarios 11 and 12 (cont.)

Figure 2.2.2.17

DYPlot10 : DYRESM-10

Dam : Inanda Dam

Plot Date : 25 Oct 94, 11:56

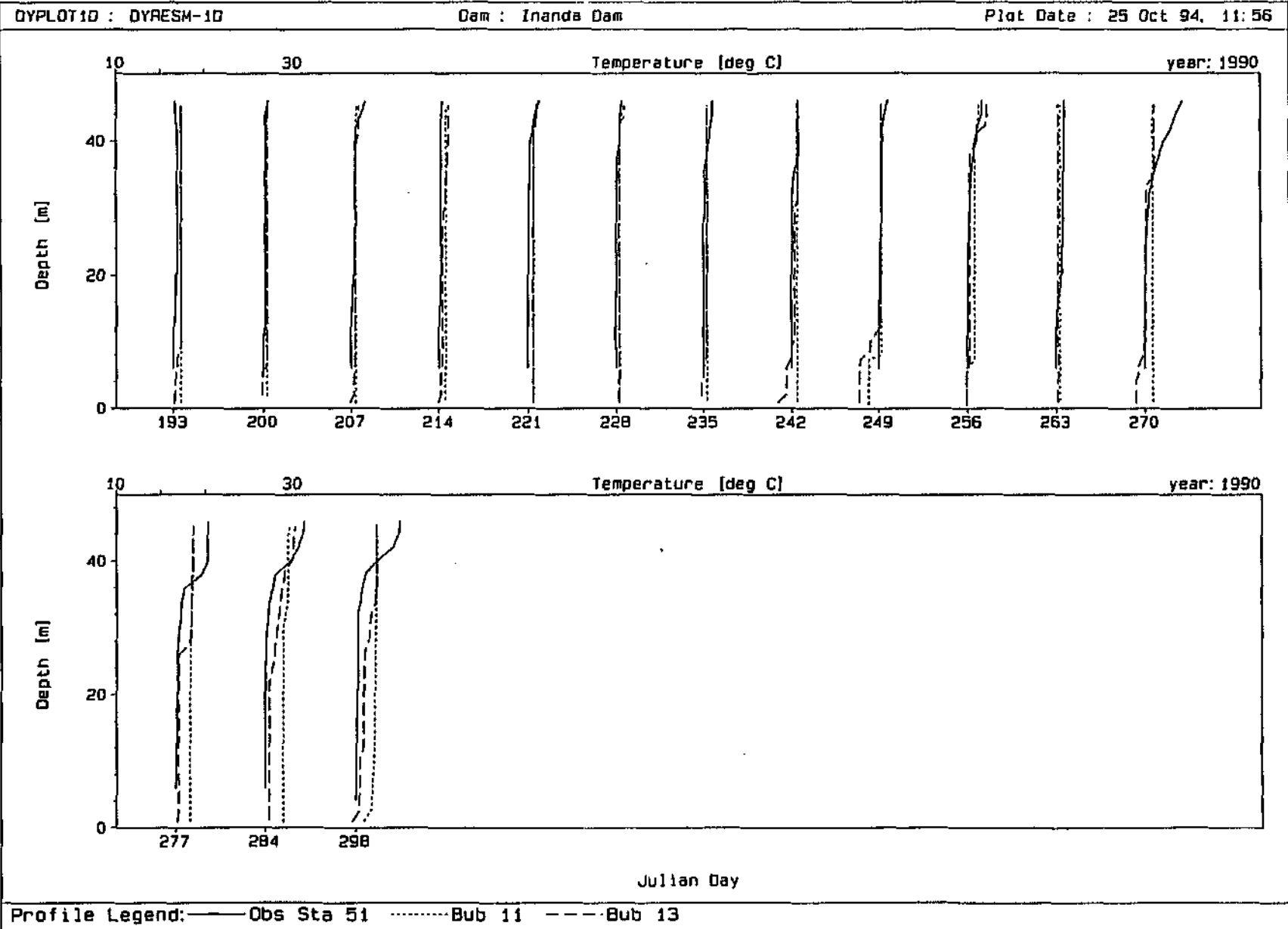


Profile Legend: — Obs Sta 51 - - - - - Bub 11 - - - - - Bub 13



Station 51 observed profiles and bubbler scenarios 11 and 13

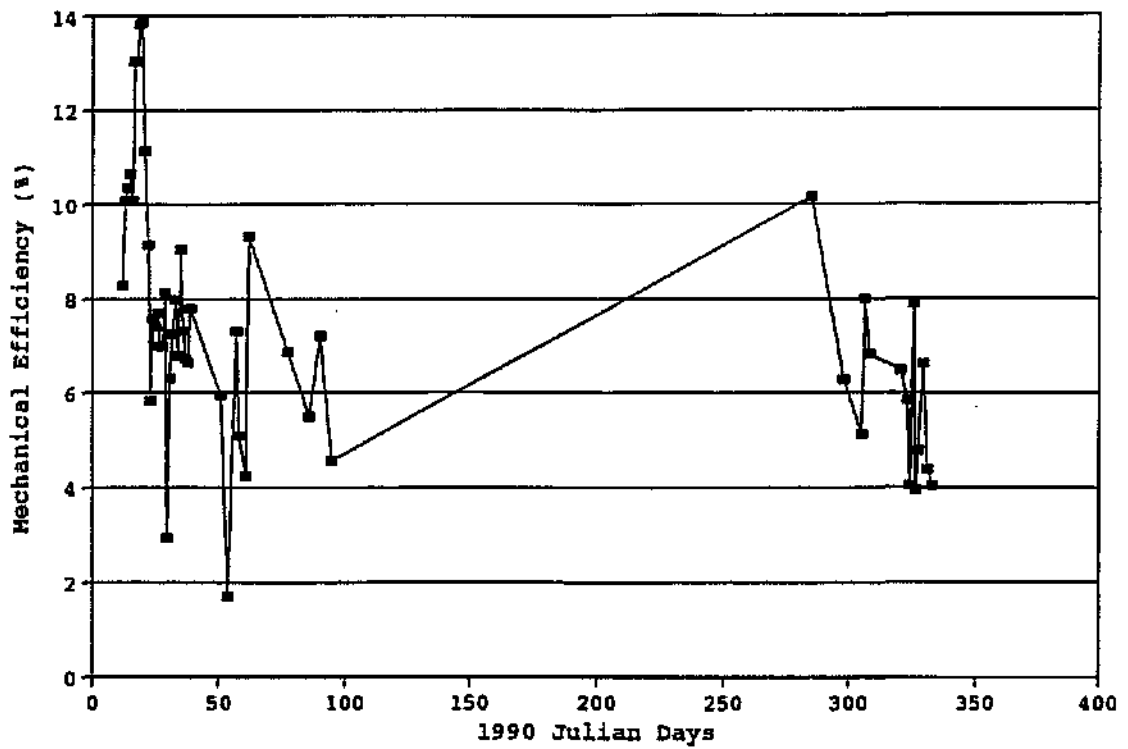
Figure 2.2.2.18



Station 51 observed profiles and bubbler scenarios 11 and 13 (cont.)

Figure 2.2.2.19

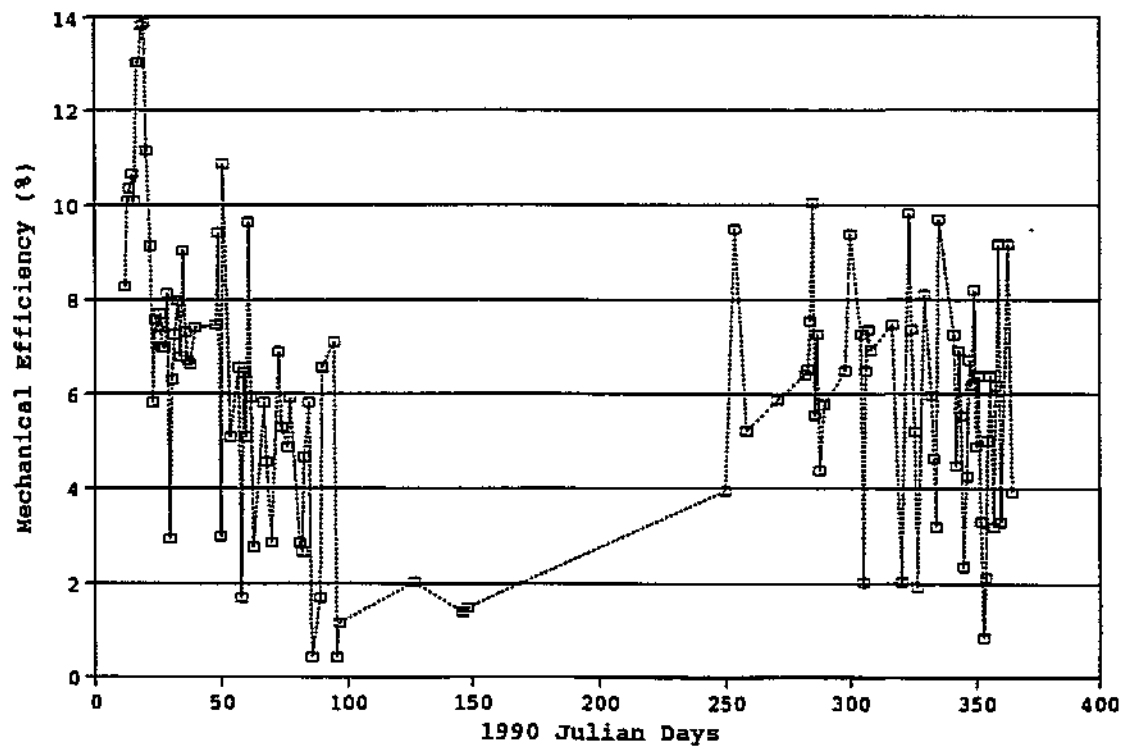
Inanda Dam
Bubbler Scenario 12



Mechanical efficiency and operating frequency of bubbler scenario 12

Figure 2.2.2.20 (A)

Inanda Dam
Bubbler Scenario 13



Mechanical efficiency and operating frequency of bubbler scenario 13

Figure 2.2.2.20 (B)

Bubble plume destratification - Conclusions

The bubbler simulations indicate that a bubbler system incorporating three 157 l/s compressors and a 250 m aerator line, is theoretically capable of destratifying a strongly stratified Inanda Dam.

The need for two bubbler systems, viz. a destratification and a maintenance system, has been identified. Furthermore, if a 'maintenance' type bubbler is used to maintain mixed conditions only two compressors and a 630 m aerator line are required, provided that strong stratification is not induced by extreme conditions or bubbler malfunction. The maintenance bubbler is also seen to be capable of the prevention of the onset of stratification, which serves as a reminder that the ultimate purpose of the design and operation of a bubble plume aeration system is the avoidance of stratification by maintaining the reservoir in a mixed condition all year round.

The results in the above section also highlight the need for an in-depth hydrodynamic reservoir simulation analysis to accompany the theoretical design of a bubble plume destratification system. Design testing and optimisation by undertaking simulations can yield significant capital savings and running cost savings (due to intermittent use) as opposed to designs based purely on the above theory.

2.2.3 *DYRESM-2D* Model Application

Model software

The *DYRESM-2D* model was made available to Ninham Shand Inc. by the Centre for Water Research (CWR), University of Western Australia, in a pre-final release form with the understanding that close links with the developers be maintained for support and feedback during its application.

Several significant problems have arisen in the application of *DYRESM-2D* during the course of this research project. These problems have been largely resolved through electronic mail correspondence with the authors of the model at the CWR, via the Computing Centre for Water Research (CCWR), and a new version of the model was received and compiled. At present, however, the model has certain aspects that are either disabled or do not function correctly. These include the inability to record bubbler efficiencies, the inability to specify interacting bubble plumes and the disabling of particular aspects of the inflow downflow stack, which in turn prevents visualisation of the migration and insertion into the water body of underflows.

The two-dimensional graphical output of the model showing a schematic long-section of the water body with the parcel temperatures displayed, has been found to be cumbersome and inflexible. The *DYRESM-2D* model also only outputs the one-dimensional laterally averaged reservoir profiles and does not allow for profiles at different locations along the length of the impoundment to be viewed. To overcome these disadvantages which restrict the visualisation and resultant increased understanding of the hydrodynamic and destratification processes at work within the reservoir to some degree, the DYLOT software program was enhanced during the course of this project and used to present the two-dimensional model output shown below. DYLOT is discussed in further detail in Section 2.5.

Ongoing liaison is taking place with the CWR concerning suggested improvements to the model's software input and output interface.

Due to the added complexity involved in the quasi two-dimensional model, computational run-times are significantly increased over those of the one-dimensional model. Run-times in excess of five hours on a 66 MHz 486DX2 personal computer have been found to occur regularly when the bubbler is operational for several months.

These run-times could be significantly reduced by using a personal computer with a PENTIUM processor or by obtaining a version of the model that will run on the Computing Centre for Water Research (CCWR) UNIX workstation. However, the increased computational speed that the CCWR computer can provide is to some extent offset by the need to download very large output files over relatively slow links for local post-processing.

Model input data

The data input requirements of the model are in fact identical to those of *DYRESM-1D*, allowing existing data sets to be used in the model. This once again serves to highlight the quasi two-dimensional nature of the model in which the one-dimensional input data is used to determine a two-dimensional 'wedge' shaped water body. No cognisance is taken of the longitudinal profile of the reservoir or lake, nor the orientation of longitudinal segments, as is the case with true two-dimensional models such as *CE-QUAL-W2*. As is the case for the one-dimensional model, no real calibration of the model is required, since all the algorithms are process based.

Simulation results

The new recompiled version of the *DYRESM-2D* model was successfully applied to the Inanda Dam data set and a number of model runs performed.

***DYRESM-2D* versus *DYRESM-1D* comparison:**

Figures 2.2.3.1 and 2.2.3.2 show that in certain instances the average profile describing the two-dimensional (2D) simulation (0,8 wind factor) better approximates the observed profiles for Station 51 and the average observed profiles for Stations 51 to 54, when compared with the one-dimensional (1D) simulation (0,8 wind factor), however, the improvement is somewhat marginal and cannot be isolated to the epi- or hypolimnion, or the shape and location of the thermocline. It is of particular interest though, that the fit obtained between the 2D simulation (0,8 wind factor) and the average observed profiles for Stations 51 to 54 is reasonably good (see Figures 2.2.3.3 and 2.2.3.4) which confirms the somewhat two-dimensional nature, in terms of hydrodynamics, of this impoundment.

Two-dimensional comparison of the observed versus simulated hydrodynamics:

Figures 2.2.3.5 to 2.2.3.13 show the *DYRESM-2D* output and the profile data for Stations 51 to 54 for selected days within the simulation period. In general it can be seen that the 2D simulation matches the observed data fairly well in terms of temperature (with the exception of Julian day 90018) and the level of the thermocline. In most instances the simulation shows a more profound longitudinal uniformity than was observed.

In particular the cold plunging inflow noted in the observed profiles of Julian days 90179 and 90186 (see Figures 2.2.3.11 and 2.2.3.14) are not visually reproduced in the model. This is most likely due to the disabled inflow downflow stack, however, the resultant average profile temperature remains correct and the simulated profile indicates that insertion has in fact taken place at the bottom of the water body (see Figures 2.2.3.3 and 2.2.3.4).

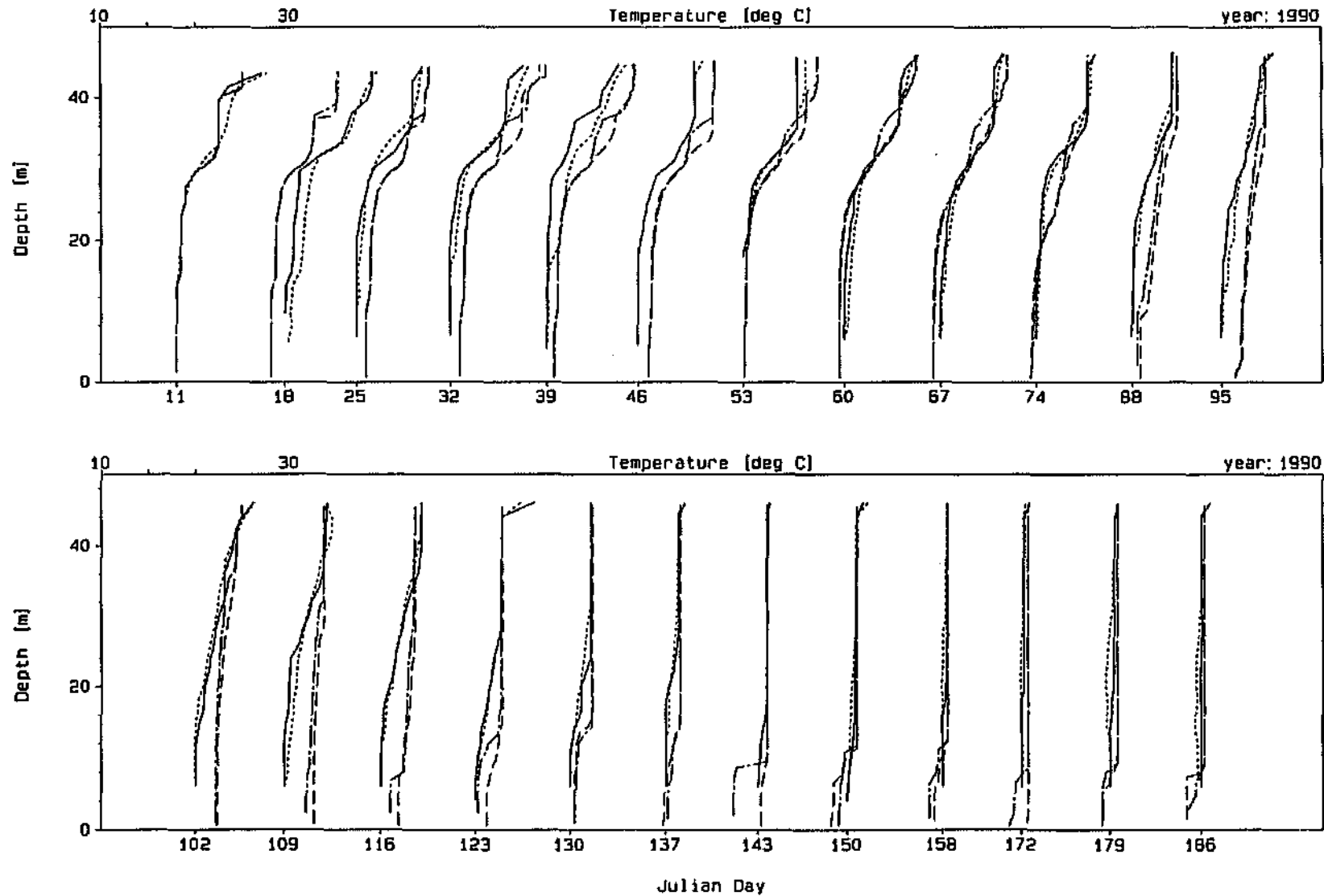
Figure 2.2.3.12 indicates that by Julian day 90256 a significant amount of water of temperature 18,5 to 20 °C had flowed over the surface of the reservoir. Similarly in the case of Julian day 90270, water of temperature between 20 and 21,5 °C was observed in the top four metres of the reservoir, while the simulation only shows water of those temperatures beginning to enter the reservoir on those days.

Since stratification due to radiation effects is relatively mild at this particular time of year it appears that the anomaly results from the inflow temperature being incorrect (see Figure 2.2.3.14). It is with an example like this that the usefulness of the quasi two-dimensional model in the conceptualisation of the processes driving the hydrodynamics of an impoundment, and the usefulness of the DYPLOT software in the visualisation thereof, becomes apparent.

DYPLOT10 : DYRESM-10

Dam : Inanda Dam

Plot Date : 25 Oct 94, 15:20



Profile Legend: — Obs 51 Obs 51-54 ---- 1D Sim -.-.- 2D Sim



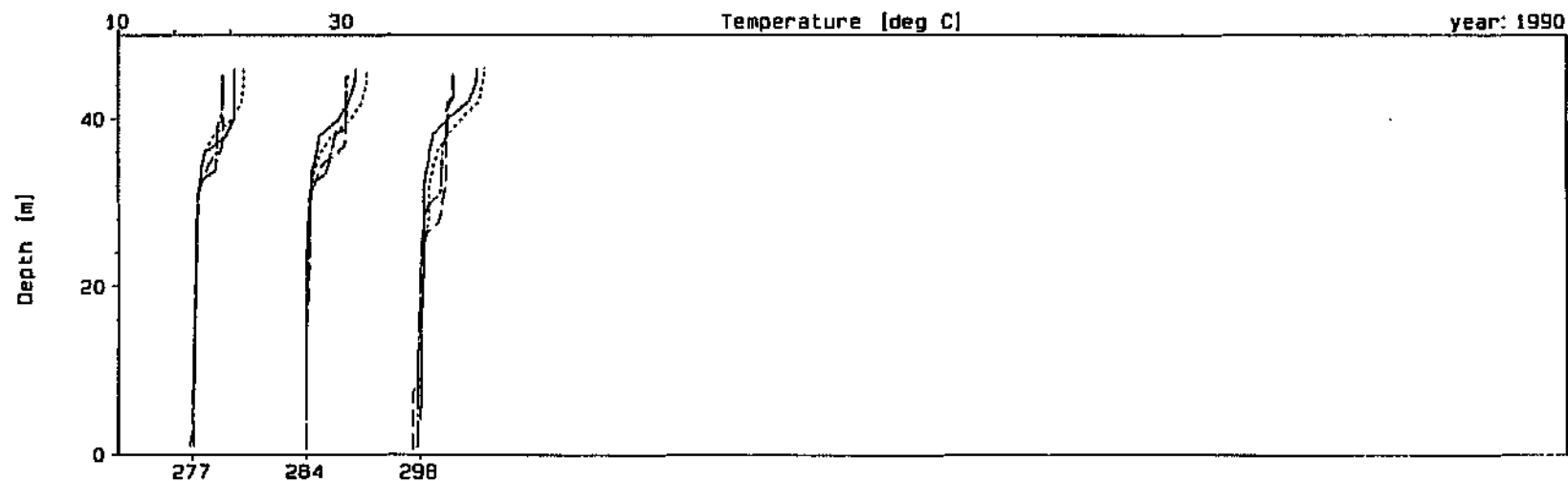
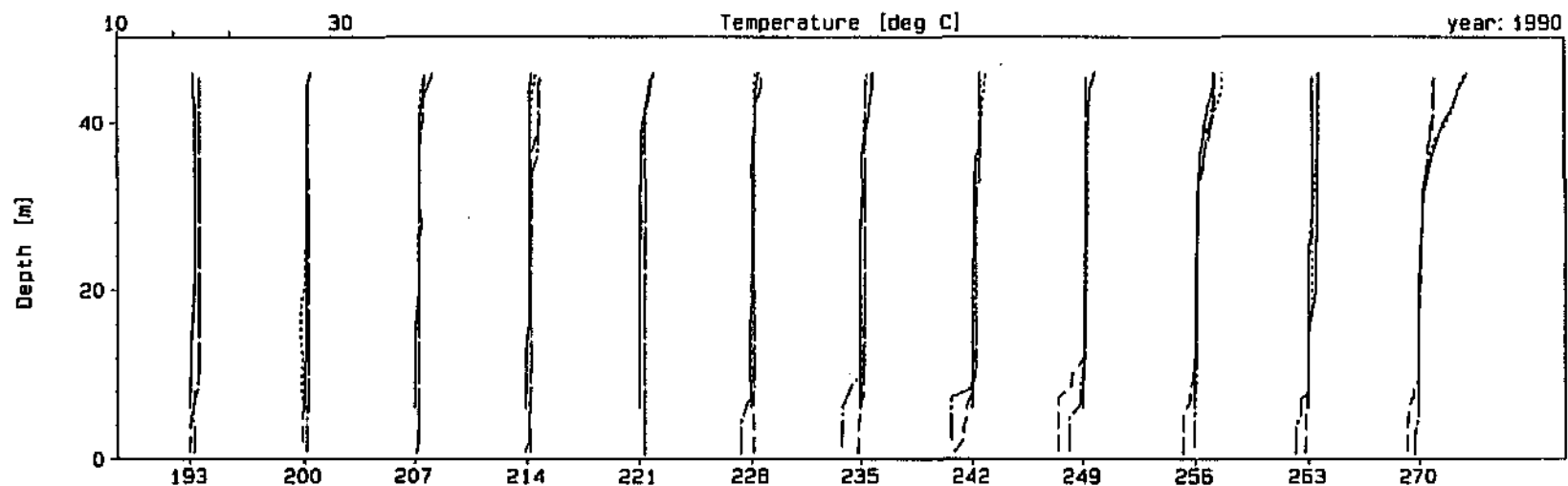
Station 51, average of Stations 51-54, 0,8 x wind 1D and 2D simulations

Figure 2.2.3.1

DYPLOT1D : DYRESM-1D

Dam : Inanda Dam

Plot Date : 25 Oct 94, 15:20



Julian Day

Profile Legend: — Obs 51 Obs 51-54 --- 1D Sim — 2D Sim



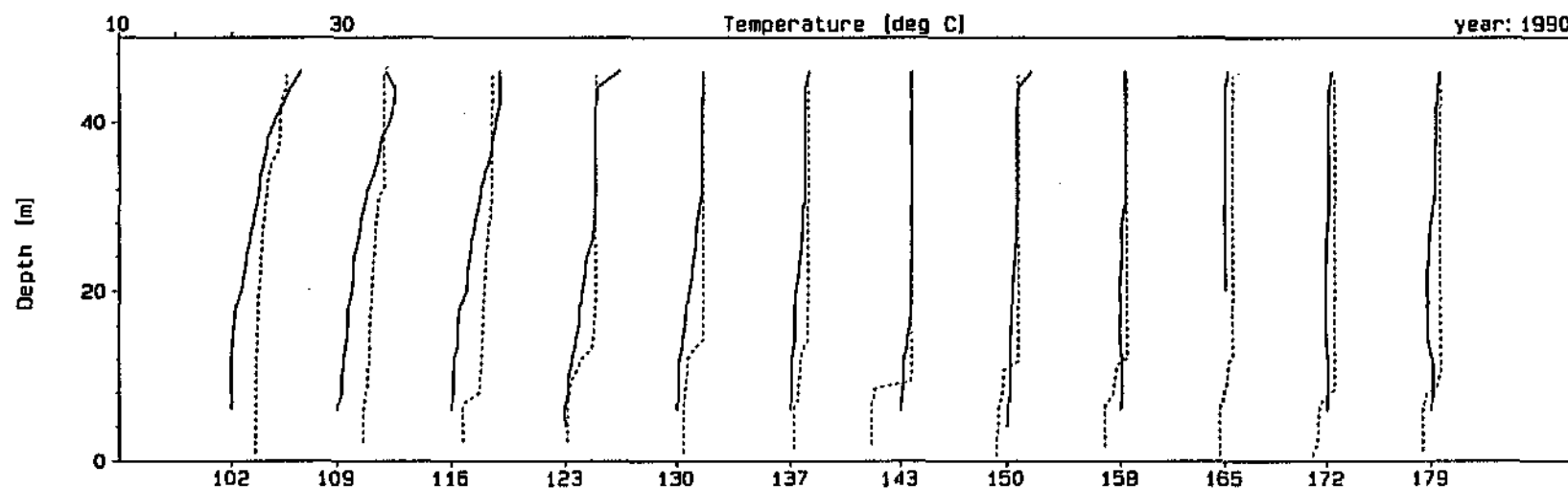
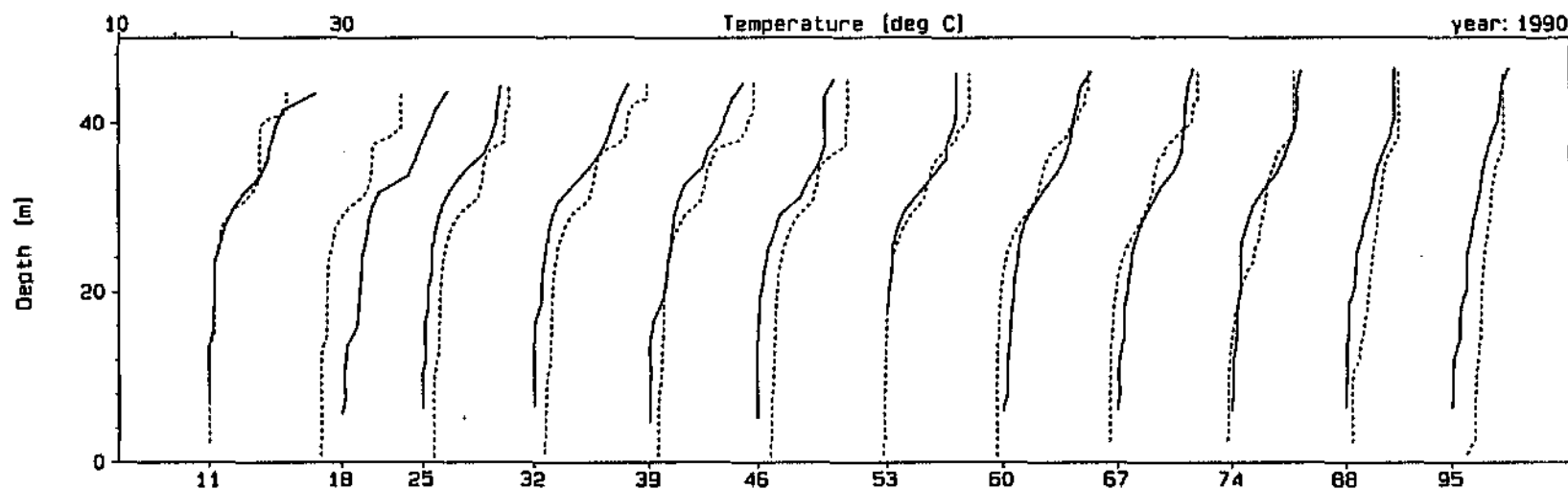
Station 51, average of Stations 51-54, 0,8 x wind 1D and 2D simulations (cont.)

Figure 2.2.3.2

DYPLOT10 : DYRESM-10

Dam : Inanda Dam

Plot Date : 25 Oct 94. 15: 21



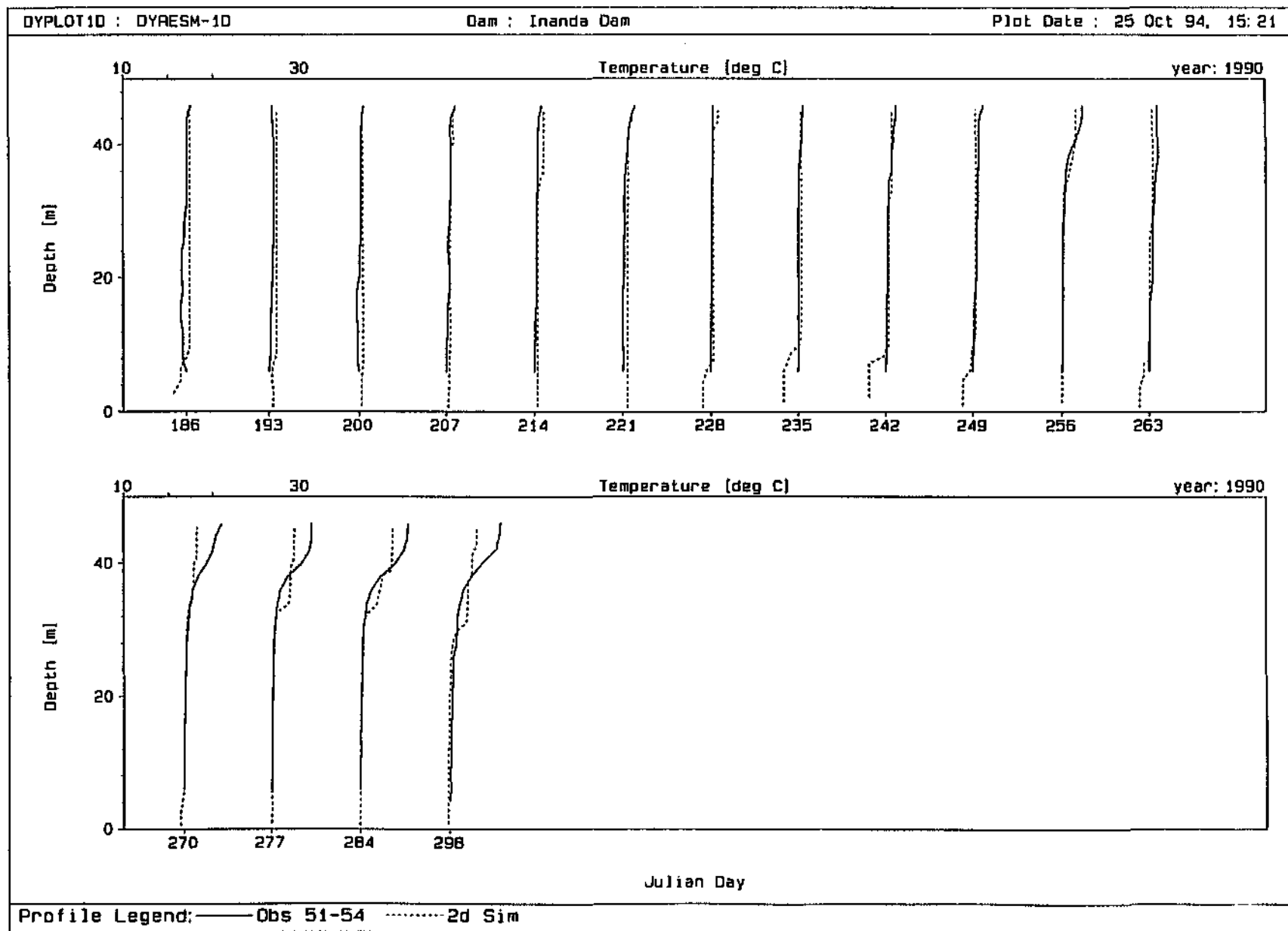
Julian Day

Profile Legend: — Obs 51-54 - - - 2d Sim



Average of Stations 51-54 and 0,8 x wind 2D simulation

Figure 2.2.3.3



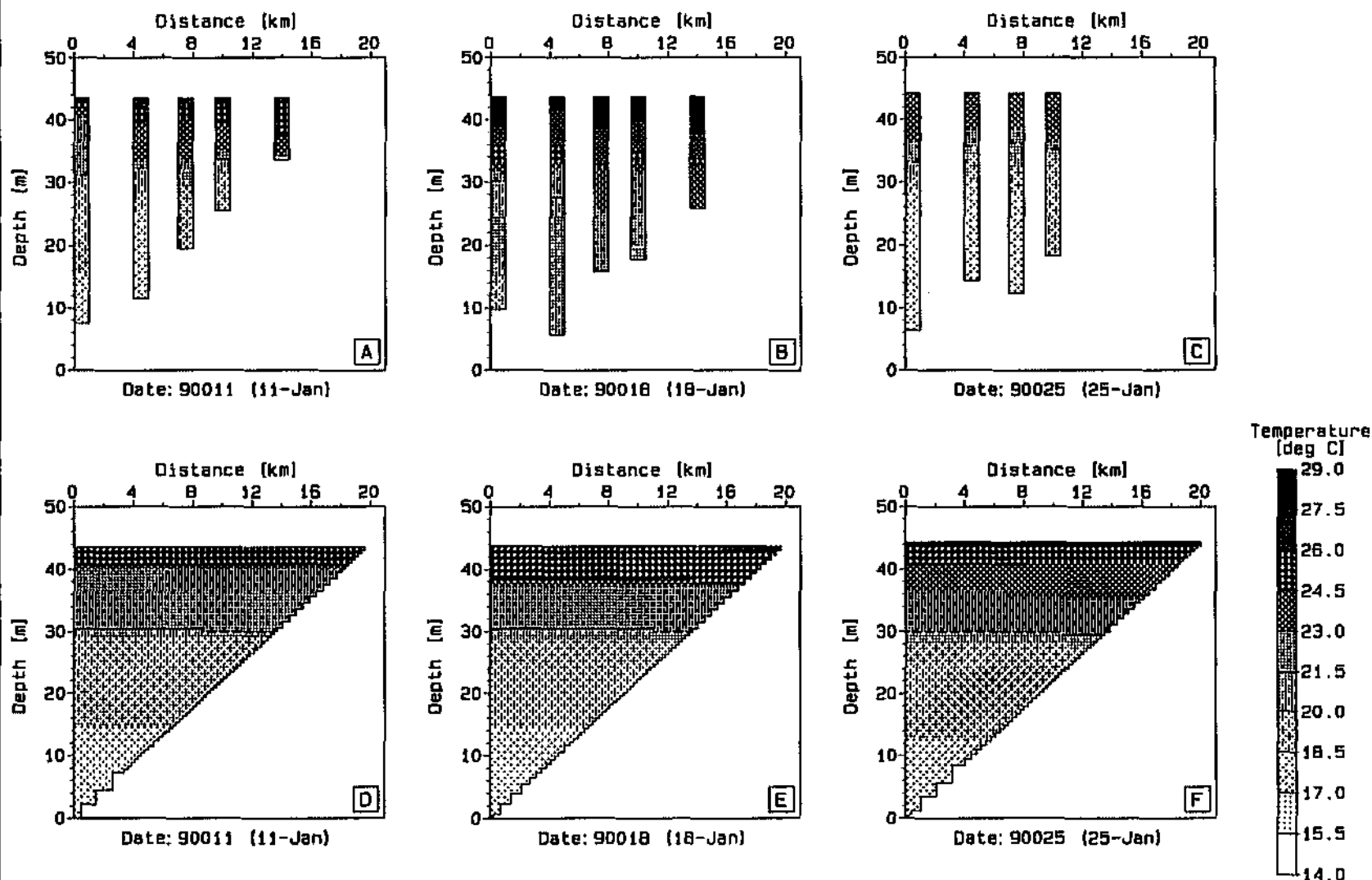
Average of Stations 51-54 and 0,8 x wind 2D simulation (cont.)

Figure 2.2.3.4

DYDROT : DYRESM-20

Dam : Inanda Dam

Plot Date : 29 May 95, 11:19



LEGEND: A, B, C : INANDA (INANDA.F2D)

D, E, F : T0841801 (T0841801.S2D)



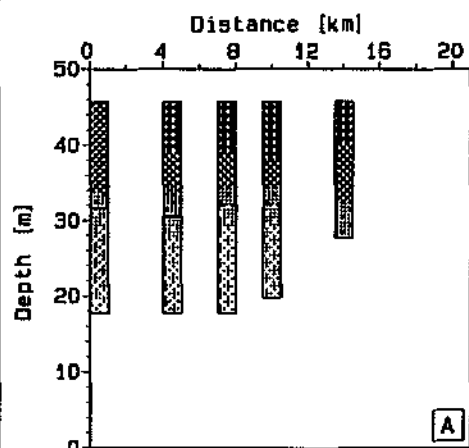
Station 51 to 55 observed profiles and 0,8 x wind 2D simulation

Figure 2.2.3.5

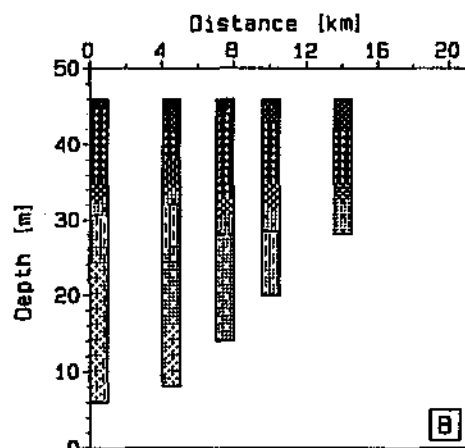
DYPLOT : DYRESM-2D

Dam : Inanda Dam

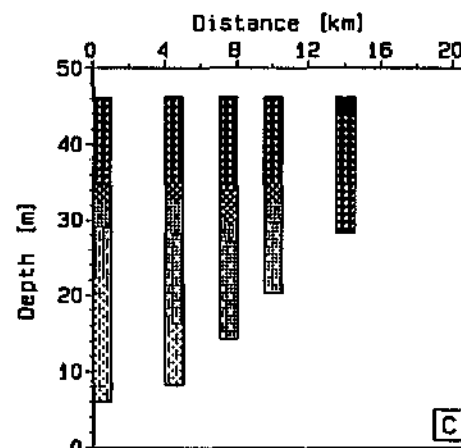
Plot Date : 29 May 95, 11:20



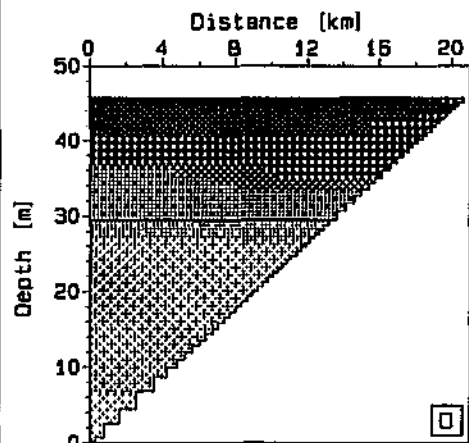
Date: 90053 (22-Feb)



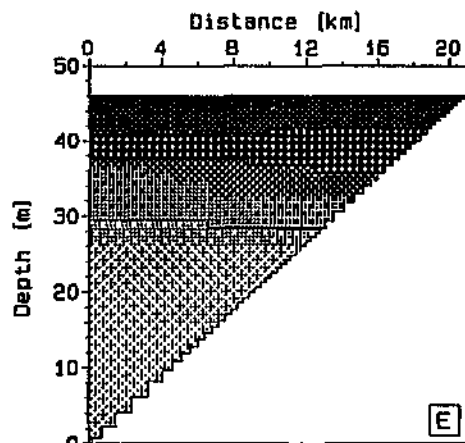
Date: 90060 (1-Mar)



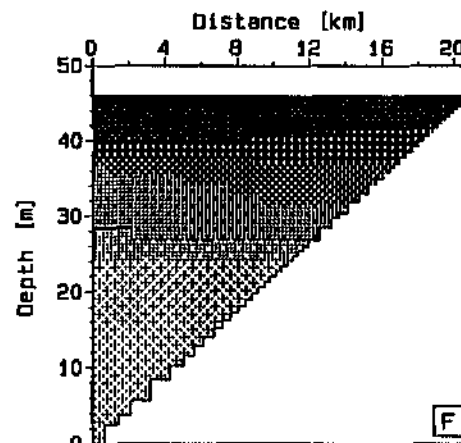
Date: 90067 (8-Mar)



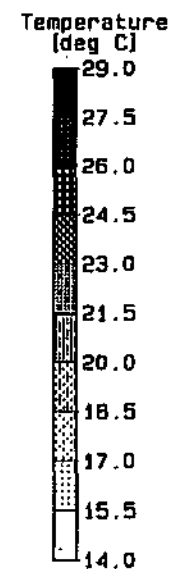
Date: 90053 (22-Feb)



Date: 90060 (1-Mar)



Date: 90067 (8-Mar)



LEGEND: A, B, C : INANDA (INANDA.F2D)

D, E, F : T0841801 (T0841801.S2D)



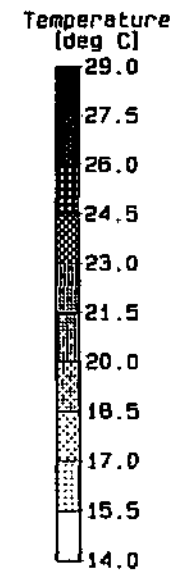
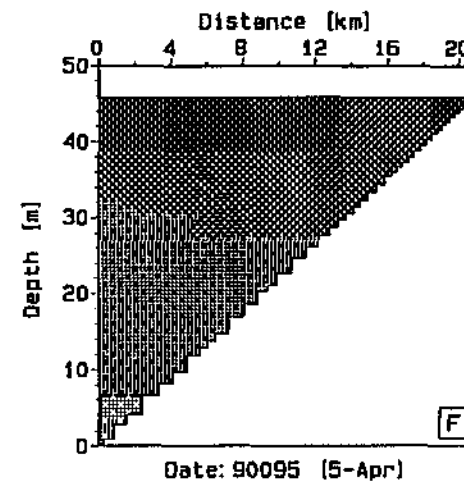
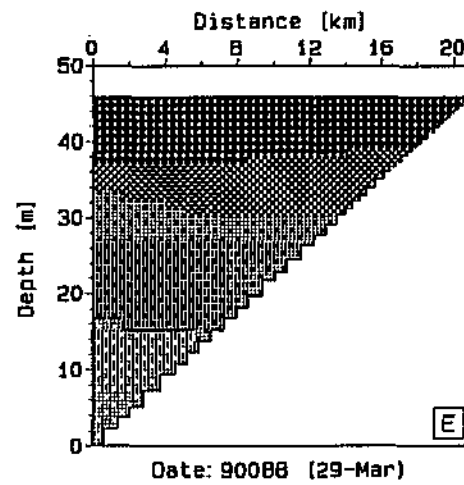
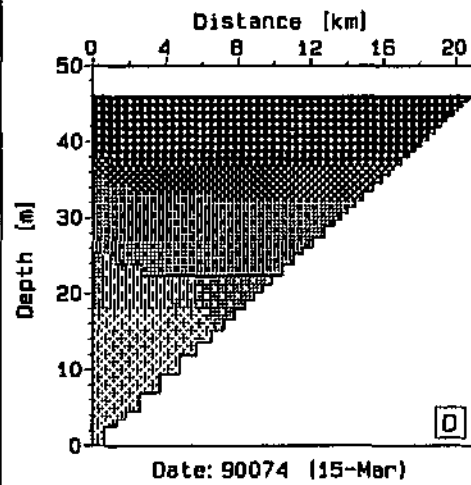
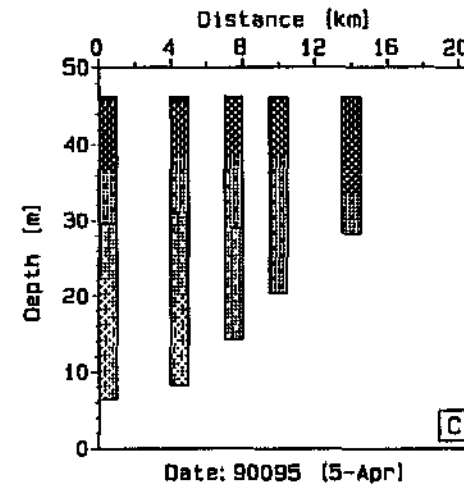
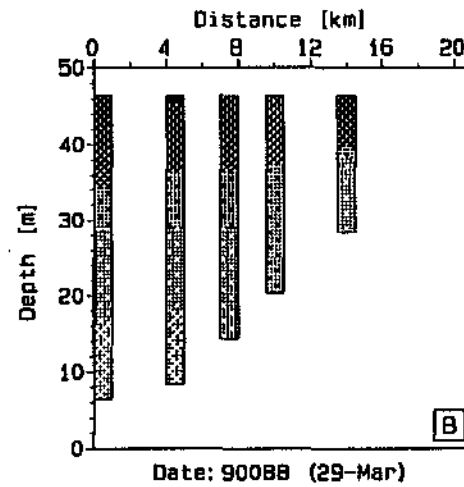
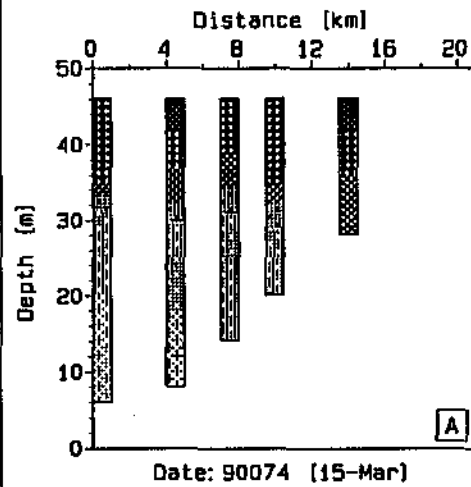
Station 51 to 55 observed profiles and 0,8 x wind 2D simulation (cont.)

Figure 2.2.3.6

DYPLOT : DYRESM-2D

Dam : Inanda Dam

Plot Date : 29 May 95, 11:21



LEGEND: A, B, C : INANDA (INANDA.F2D)

D, E, F : T0841801 (T0841801.S2D)



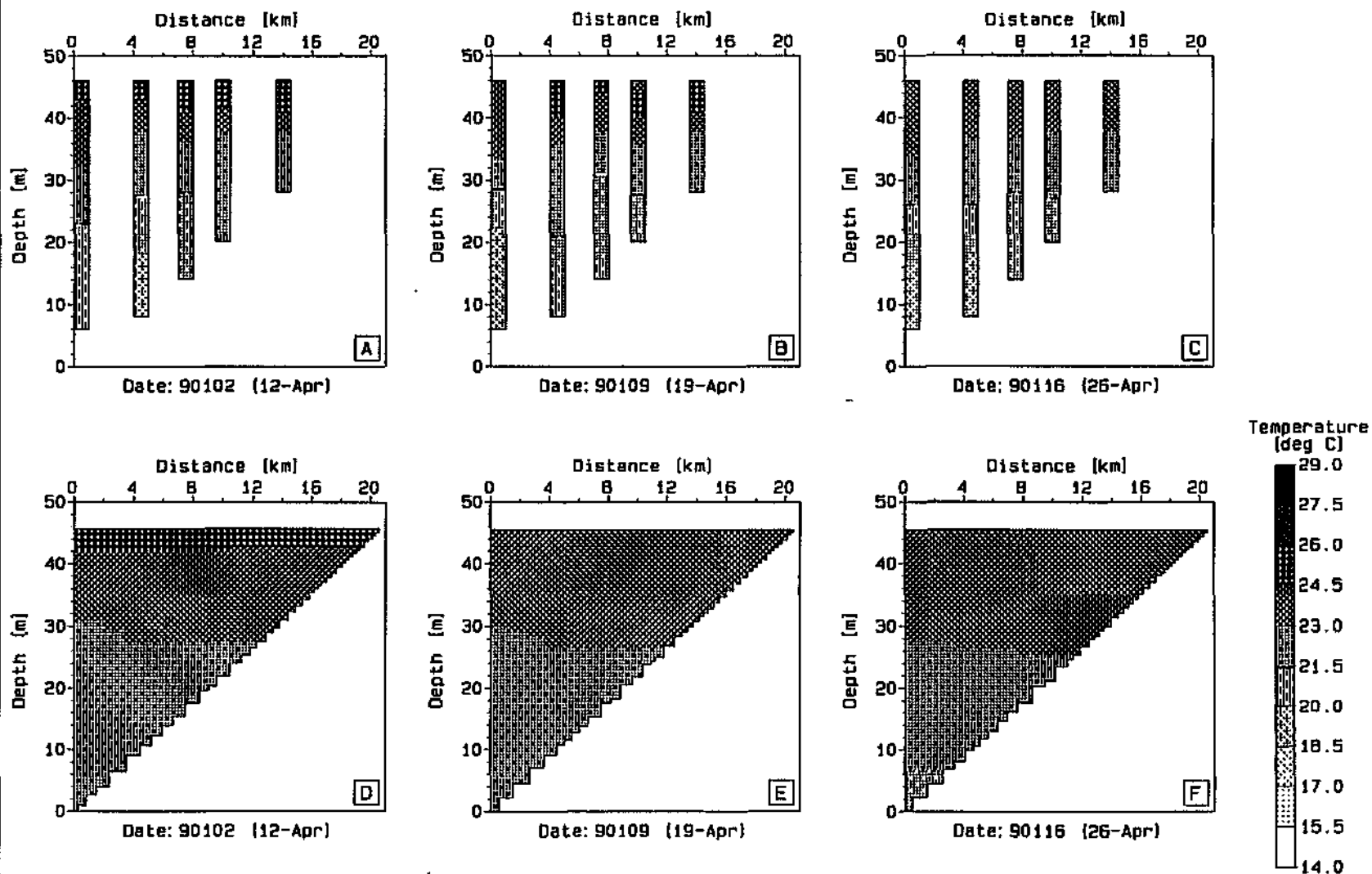
Station 51 to 55 observed profiles and 0,8 x wind 2D simulation (cont.)

Figure 2.2.3.7

DYPLOT : DYRESM-2D

Dam : Inanda Dam

Plot Date : 29 May 95, 11:22



LEGEND: A, B, C : INANDA (INANDA.F2D)

D, E, F : T0841801 (T0841801.S2D)



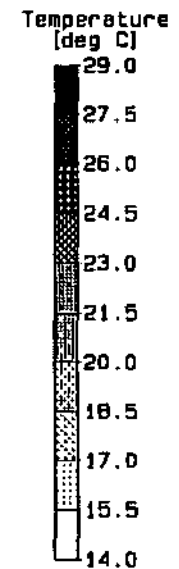
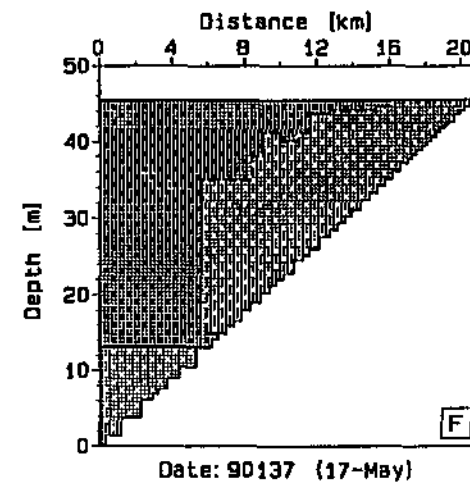
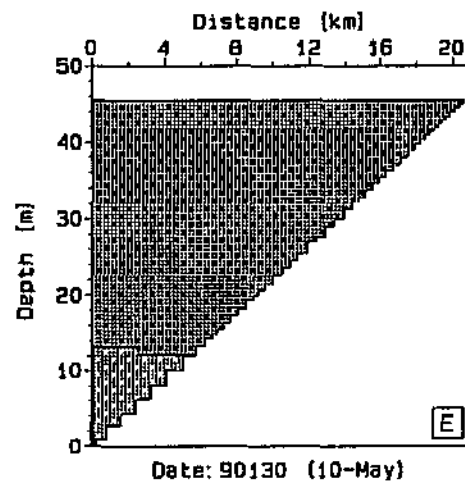
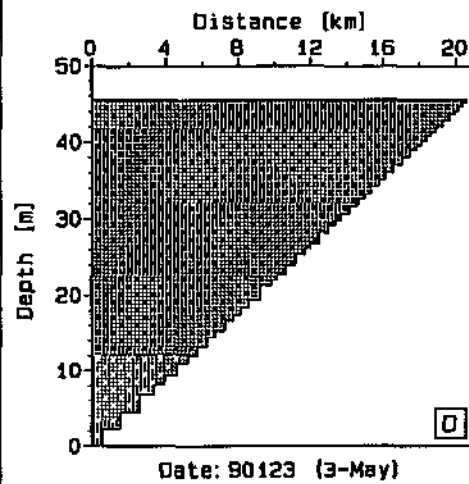
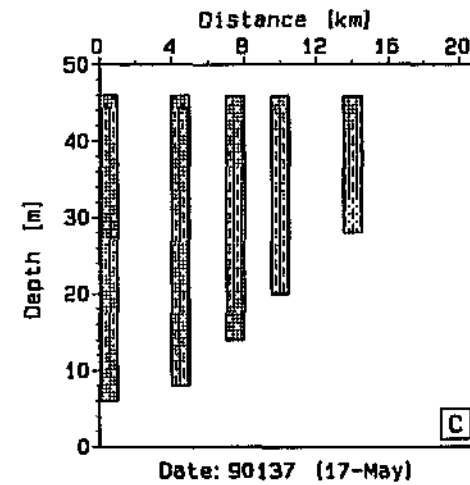
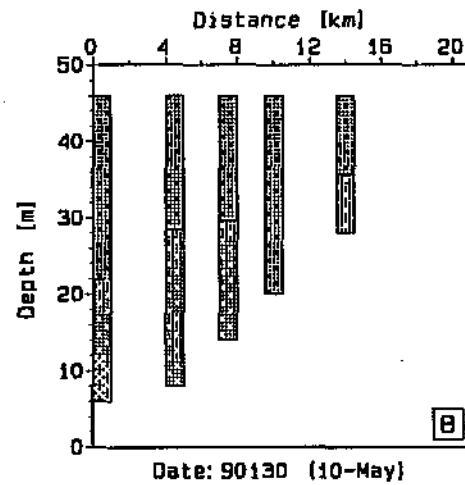
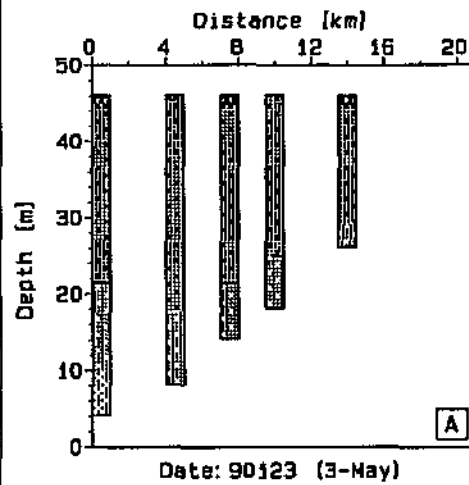
Station 51 to 55 observed profiles and 0,8 x wing 2D simulation (cont.)

Figure 2.2.3.8

DYPLOT : DYRESM-2D

Dam : Inanda Dam

Plot Date : 29 May 95, 11:23



LEGEND: A, B, C : INANDA (INANDA.F2D)

D, E, F : T0841801 (T0841801.S2D)



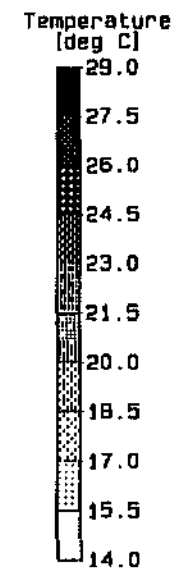
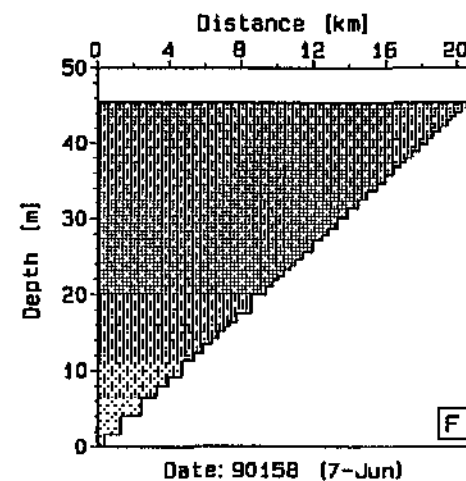
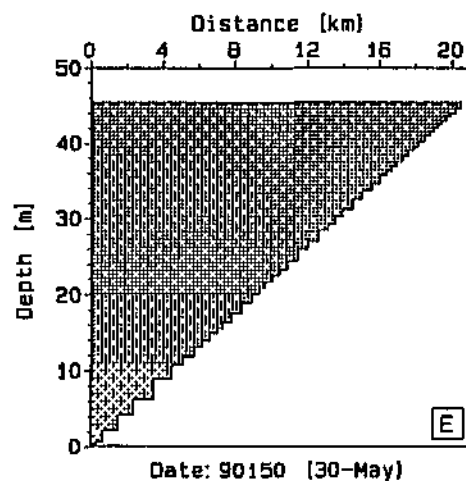
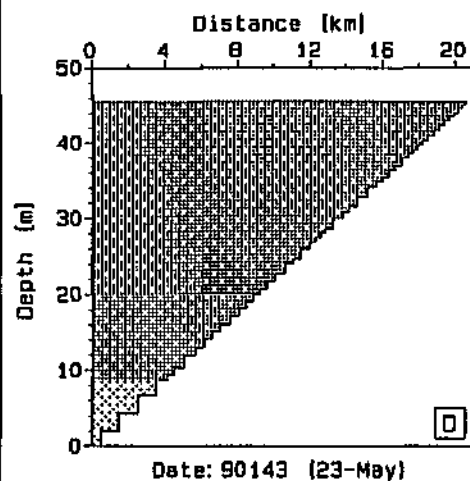
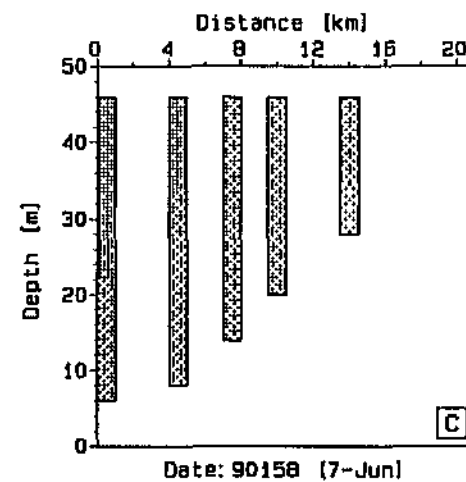
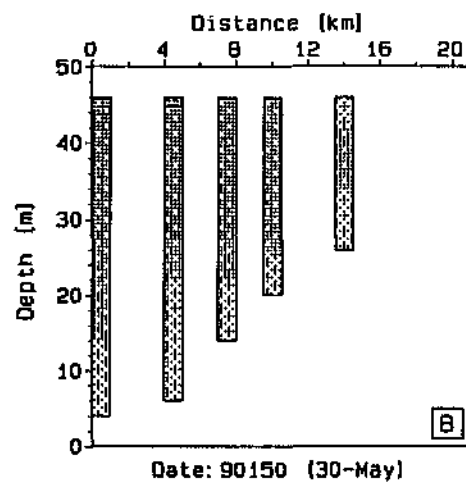
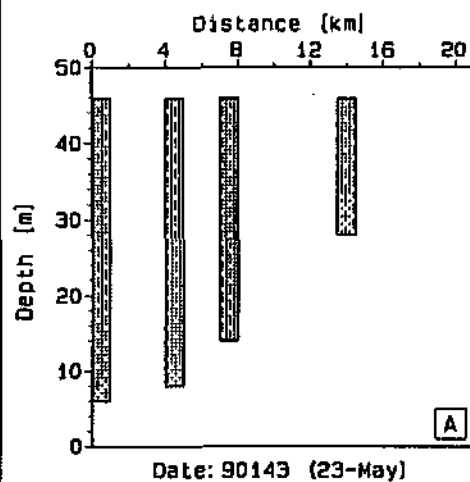
Station 51 to 55 observed profiles and 0,8 x wind 2D simulation (cont.)

Figure 2.2.3.9

DYDLOT : DYRESM-2D

Dam : Inanda Dam

Plot Date : 29 May 95, 11:24



LEGEND: A, B, C : INANDA [INANDA.F20]

D, E, F : T0841801 [T0841801.S20]



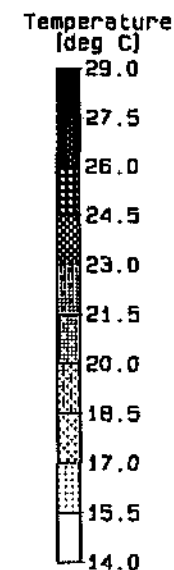
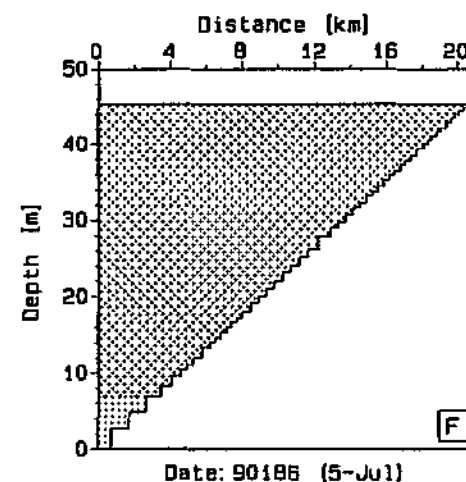
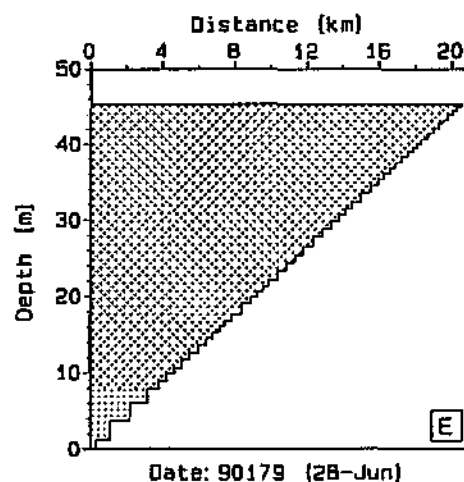
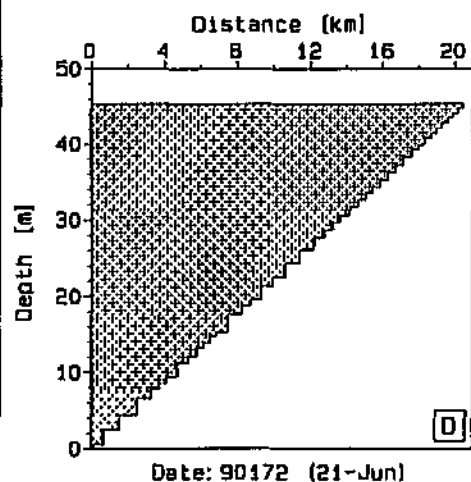
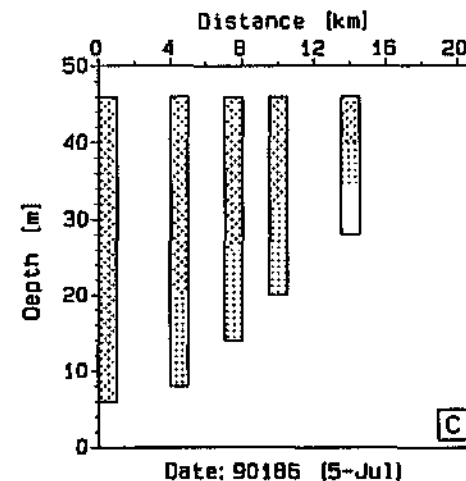
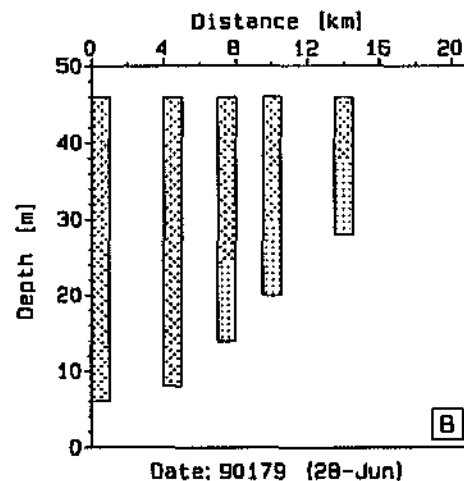
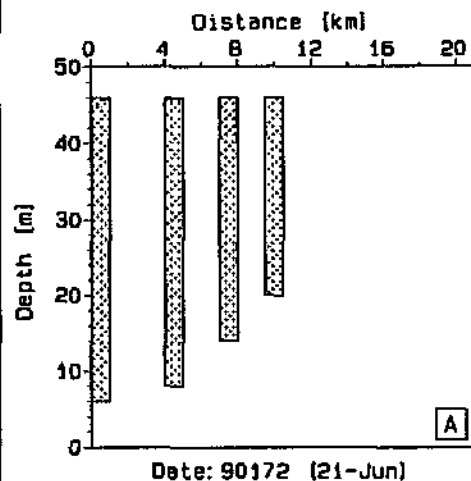
Station 51 to 55 observed profiles and 0,8 x wind 2D simulation (cont.)

Figure 2.2.3.10

DYDLOT : DYRESM-2D

Dam : Inanda Dam

Plot Date : 29 May 95, 11:26



LEGEND: A, B, C : INANDA (INANDA.F2D)

D, E, F : TOB41801 (TOB41801.S2D)



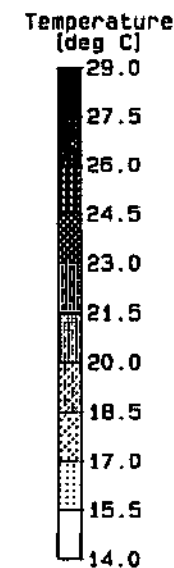
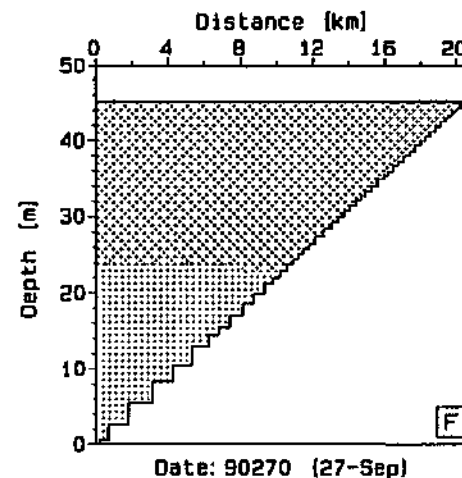
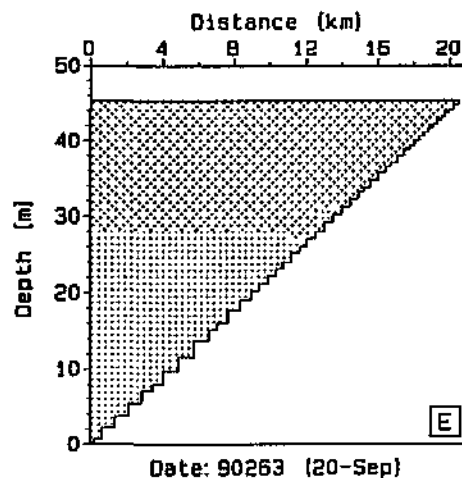
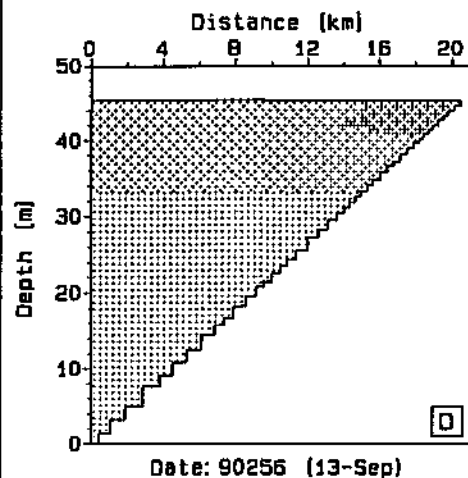
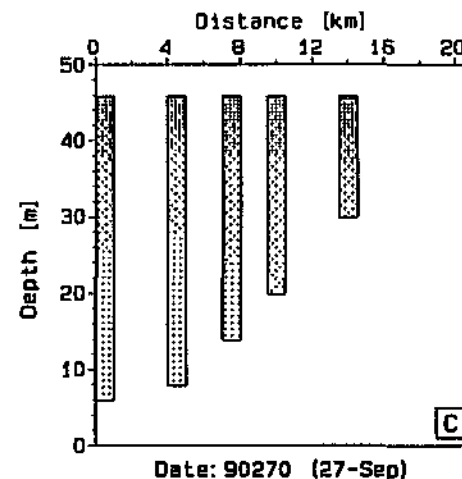
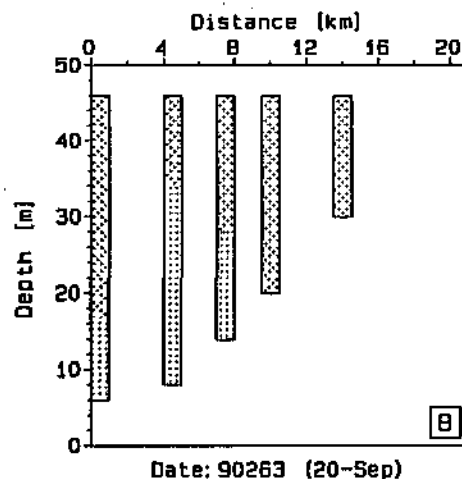
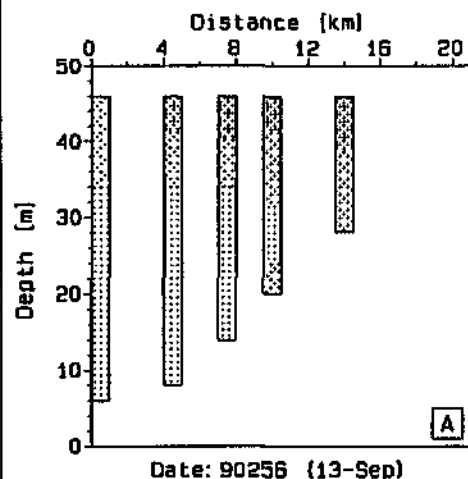
Station 51 to 55 observed profiles and 0,8 x wind 2D simulation (cont.)

Figure 2.2.3.11

DYDROT : DYRESM-20

Dam : Inanda Dam

Plot Date : 29 May 95, 11:27



LEGEND: A, B, C : INANDA (INANDA.F2D)

D, E, F : T0841801 (T0841801.S2D)



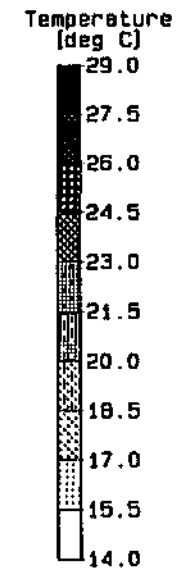
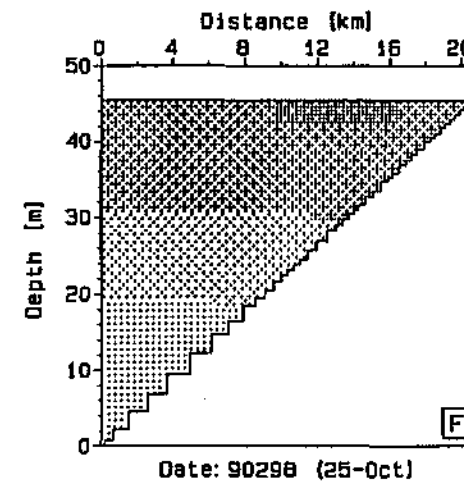
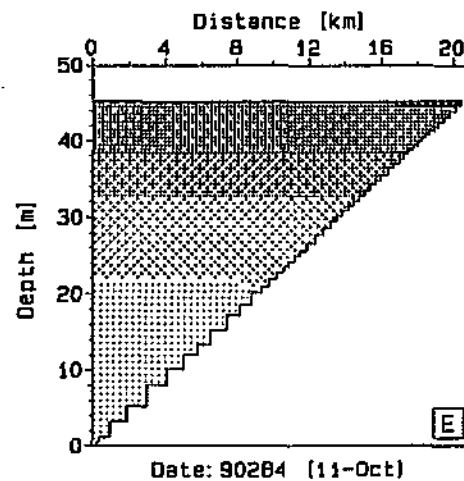
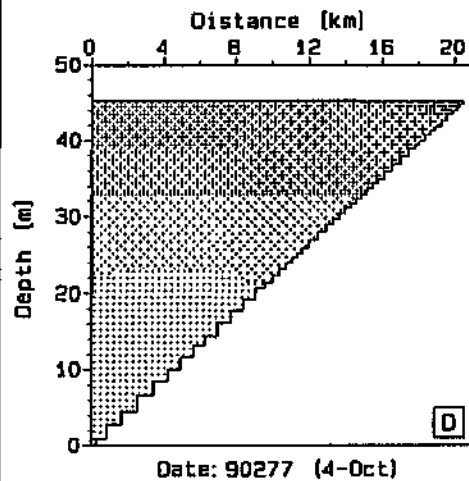
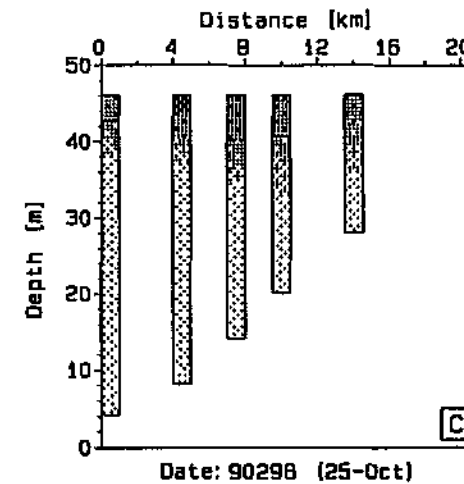
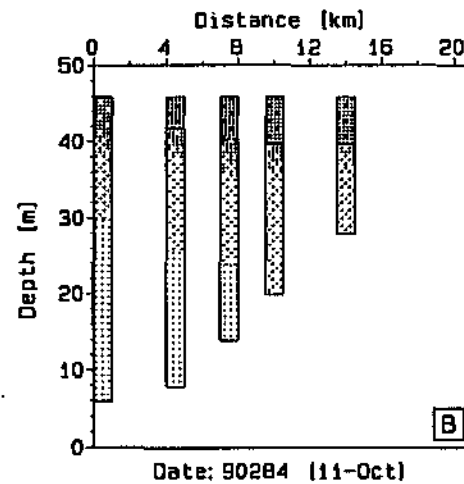
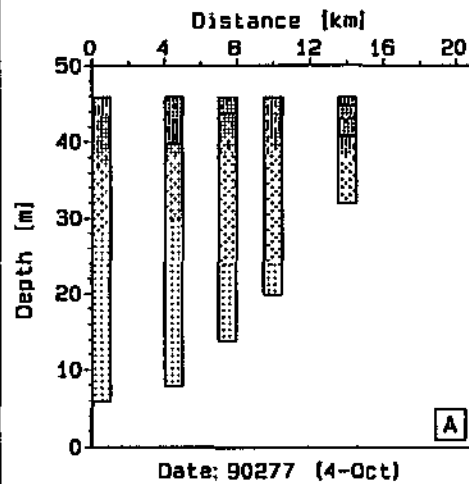
Station 51 to 55 observed profiles and 0,8 x wind 2D simulation (cont.)

Figure 2.2.3.12

DYPLOT : DYRESM-20

Dam : Inanda Dam

Plot Date : 29 May 96, 11:33



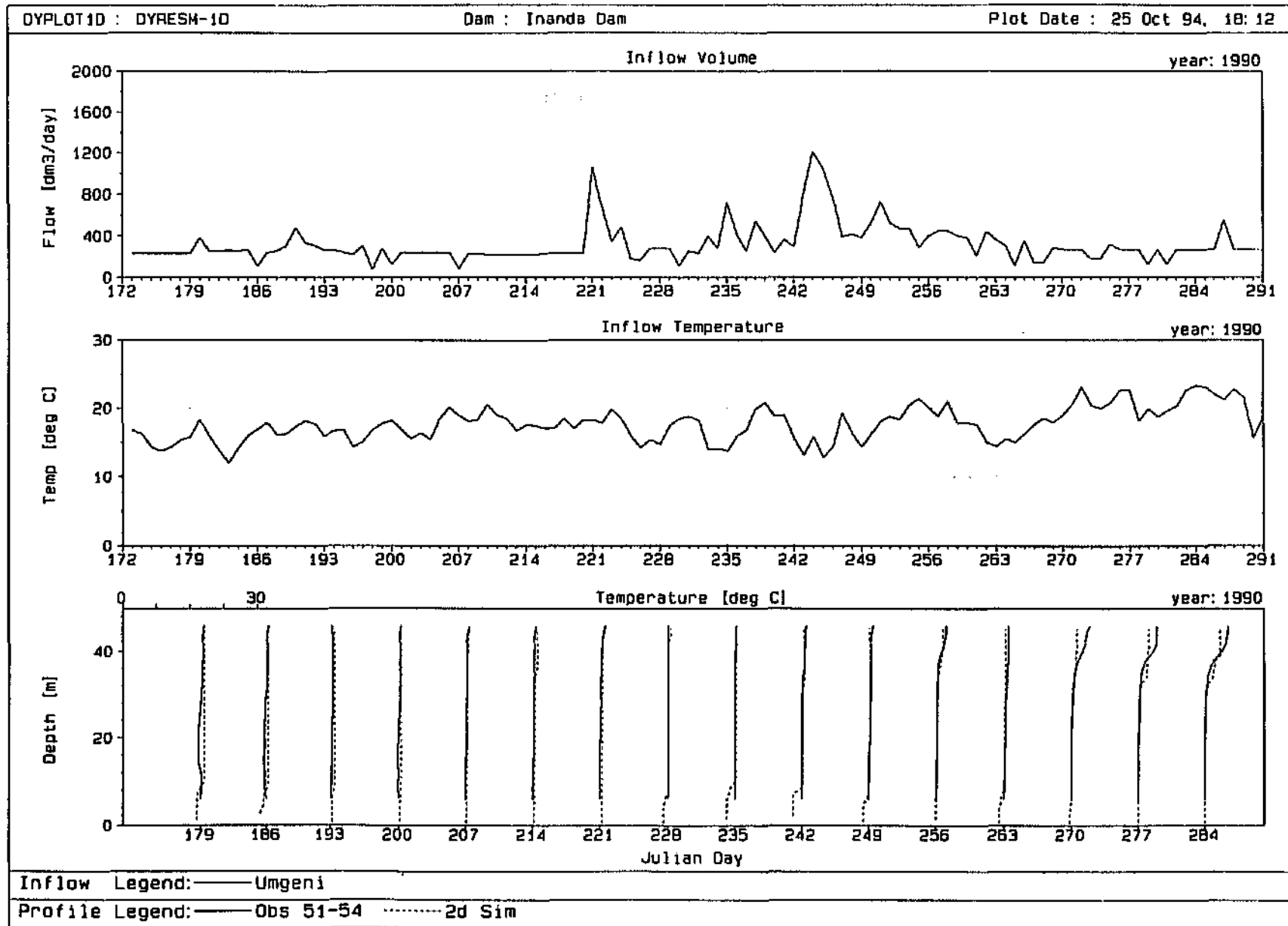
LEGEND: A, B, C : INANDA (INANDA.F2D)

D, E, F : T0841801 (T0841801.S2D)



Station 51 to 55 observed profiles and 0,8 x wind 2D simulation (cont.)

Figure 2.2.3.13



Inflow, inflow temperature and profiles of average of Stations 51-54 and 2D simulation Figure 2.2.3.14

DYRESM-2D bubbler simulations: A simulation using bubbler scenario 11 (see Section 2.2.2.4) was undertaken and the DYPLOT rendition of the 2D output showing the destratification process in progress is shown in Figures 2.2.3.15 to 2.2.3.20. These figures show both the no-bubbler case and the scenario 11 bubbler case for comparison purposes. Figure 2.2.2.13 shows the corresponding 1D profiles.

The vertical and longitudinal mixing initiated by the bubble plumes is clearly evident, as is the detrainment and subsequent mixing at the thermocline and at the reservoir surface. It is of interest to note the efficiency of the longitudinal mixing which allows the vertical mixing caused by the bubbler system over a relatively short length of the reservoir to result in the mixing of practically the entire water body.

Figures 2.2.3.5 to 2.2.3.13 show, however, that the *DYRESM-2D* model may be optimistic with respect to the degree and efficiency of longitudinal mixing when compared with the observed data. This observation may indicate that the longitudinal mixing initiated by a physical bubbler system in Inanda Dam may not be quite as successful as indicated by the model simulations.

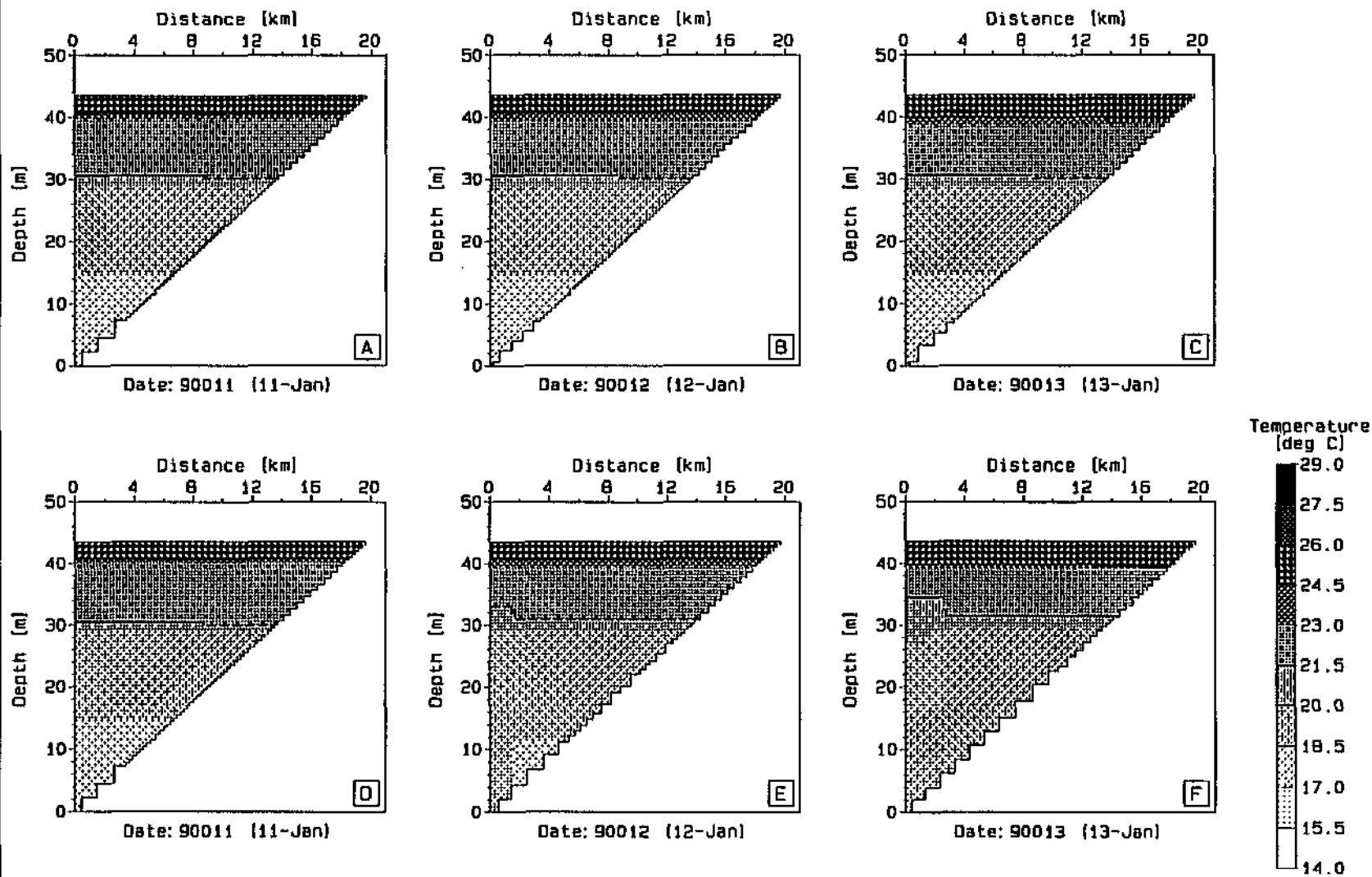
In order to test the ability of the scenario 11 bubbler system to prevent the onset of stratification using *DYRESM-2D*, a model run was undertaken with the bubbler on in 'maintenance' mode from the beginning of September (Julian day 90244). Figure 2.2.3.21 shows the average 2D profiles for the period from Julian day 90228 (middle of August) to the end of 1990.

The 314 l/s, 314 plume source, two compressor bubbler system is clearly seen to be capable of practically maintaining Inanda Dam in a mixed state through Spring and early Summer. Figures 2.2.3.22 and 2.2.3.23 show the 2D output of the model and also clearly indicate the mixed reservoir state as a result of the bubbler operation compared to the significant stratification experienced under natural conditions.

DYPLOT : DYRESM-20

Dam : Inanda Dam

Plot Date : 29 May 95, 11:59



LEGEND: A, B, C : T0841801 (T0841801.S2D)

D, E, F : T0781834 (T0781834.S2D)



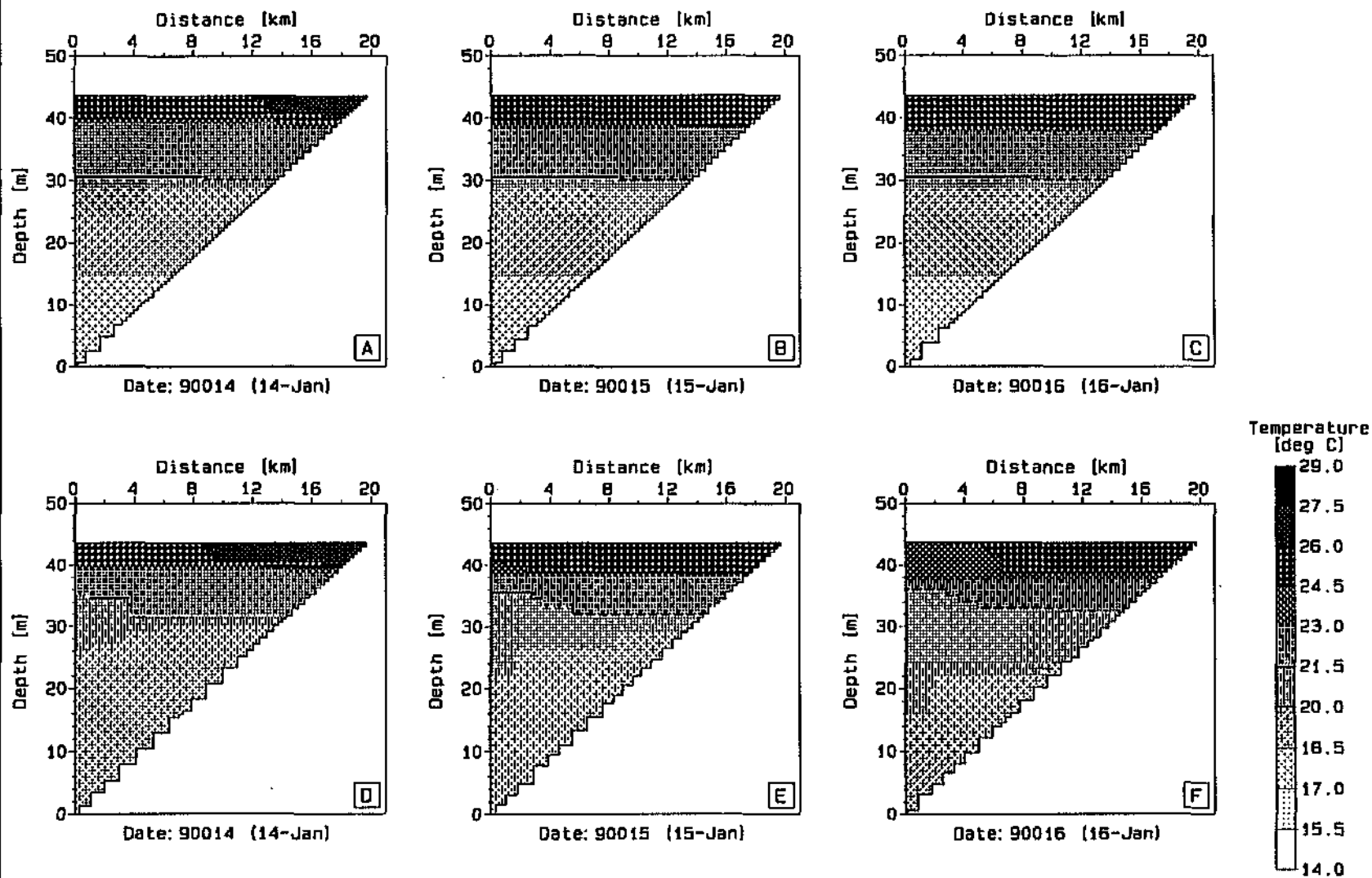
0,8 x Wind simulation and bubbler scenario 11

Figure 2.2.3.15

DYPLOT : DYRESM-20

Dam : Inanda Dam

Plot Date : 29 May 95, 12:00



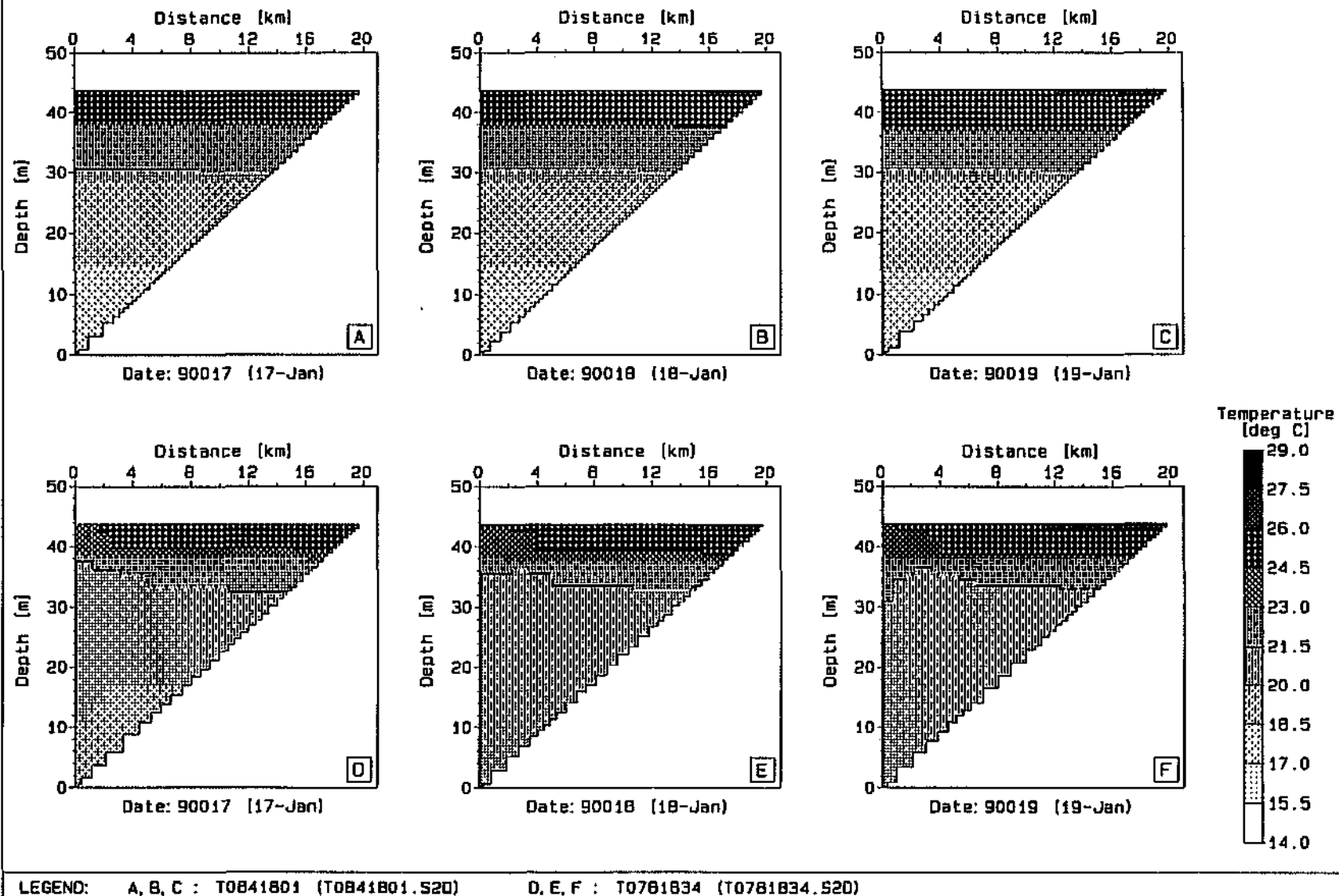
LEGEND: A, B, C : T0841801 (T0841801.S20)

D, E, F : T0781834 (T0781834.S20)



0,8 x Wind simulation and bubbler scenario 11 (cont.)

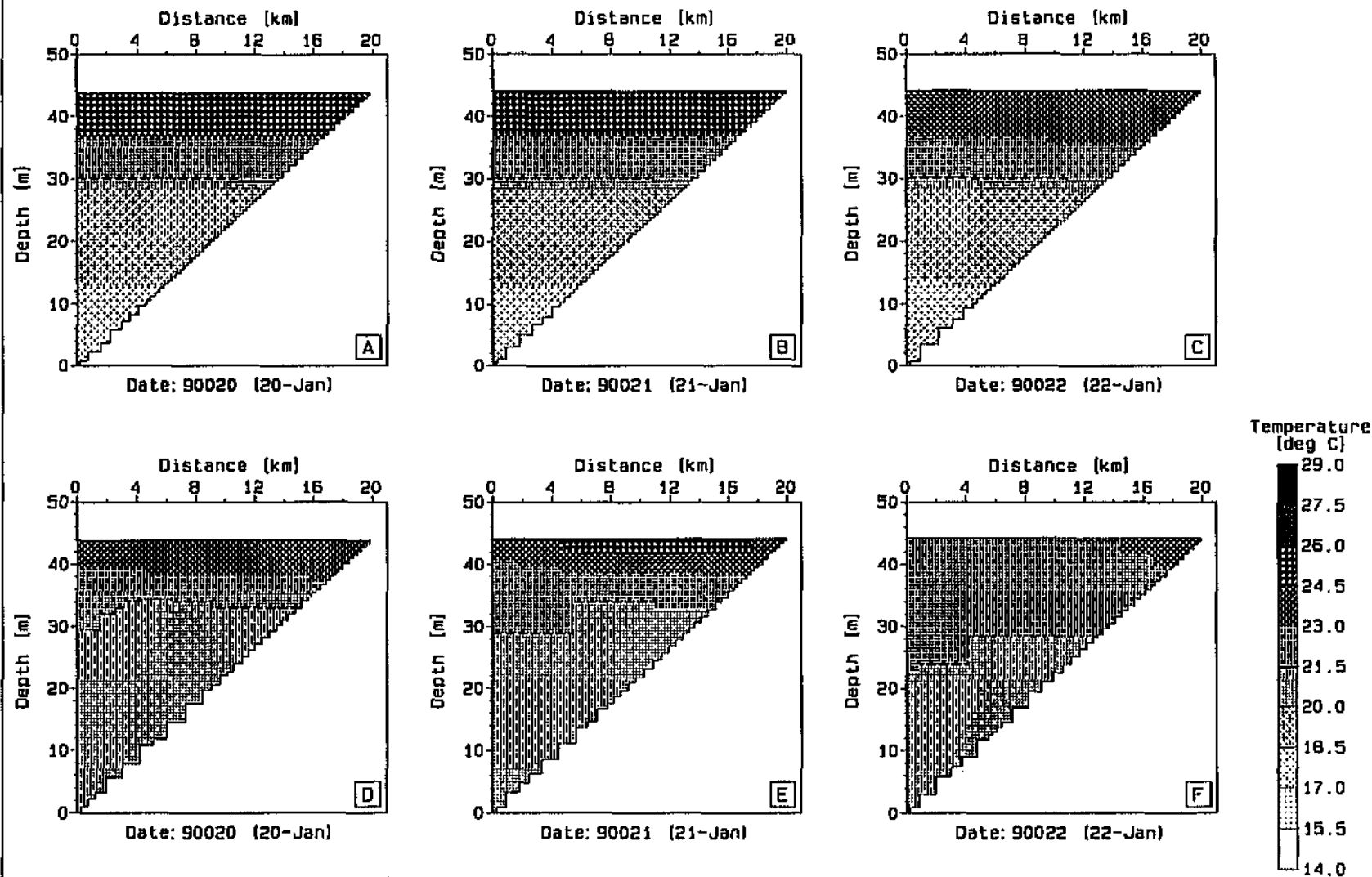
Figure 2.2.3.16



DYPlot : DYRESM-2D

Dam : Inanda Dam

Plot Date : 29 May 95, 12:01



LEGEND: A, B, C : T0B41B01 (T0B41B01.S20)

D, E, F : T07B1B34 (T07B1B34.S20)



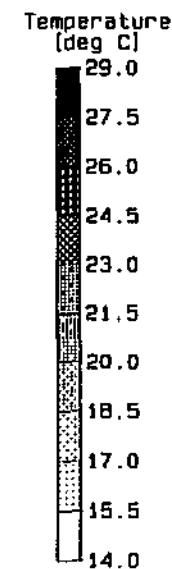
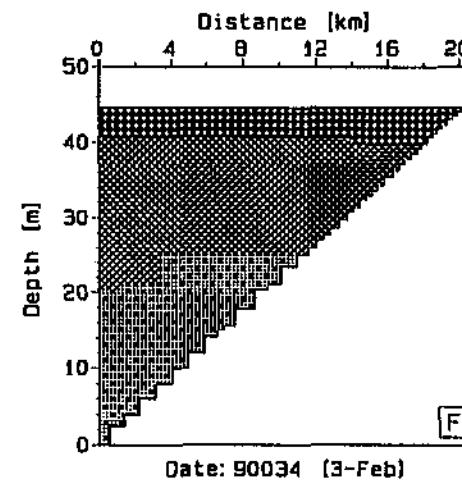
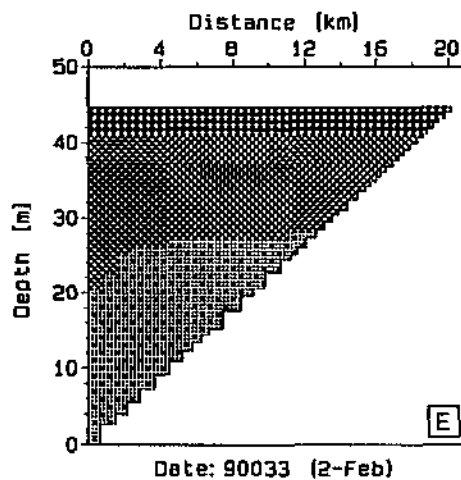
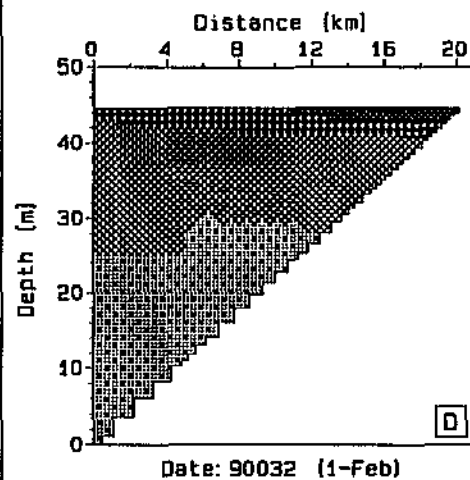
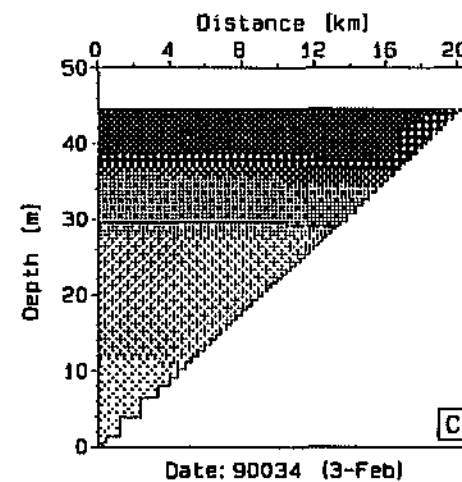
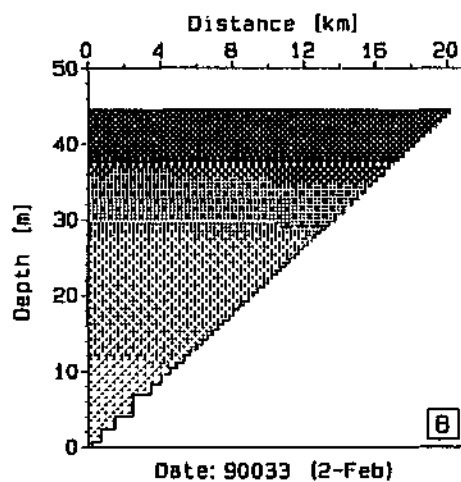
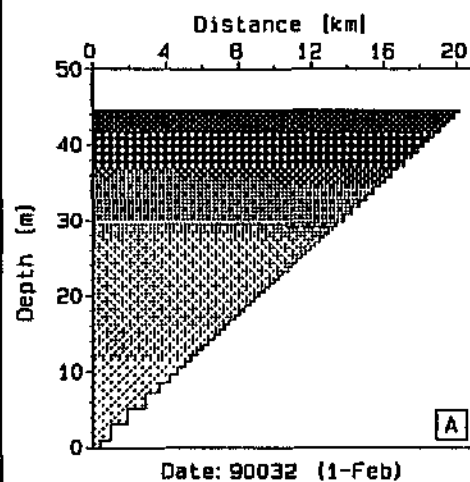
0,8 x Wind simulation and bubbler scenario 11 (cont.)

Figure 2.2.3.18

DYDLOT : DYRESM-2D

Dam : Inanda Dam

Plot Date : 29 May 95, 12:02



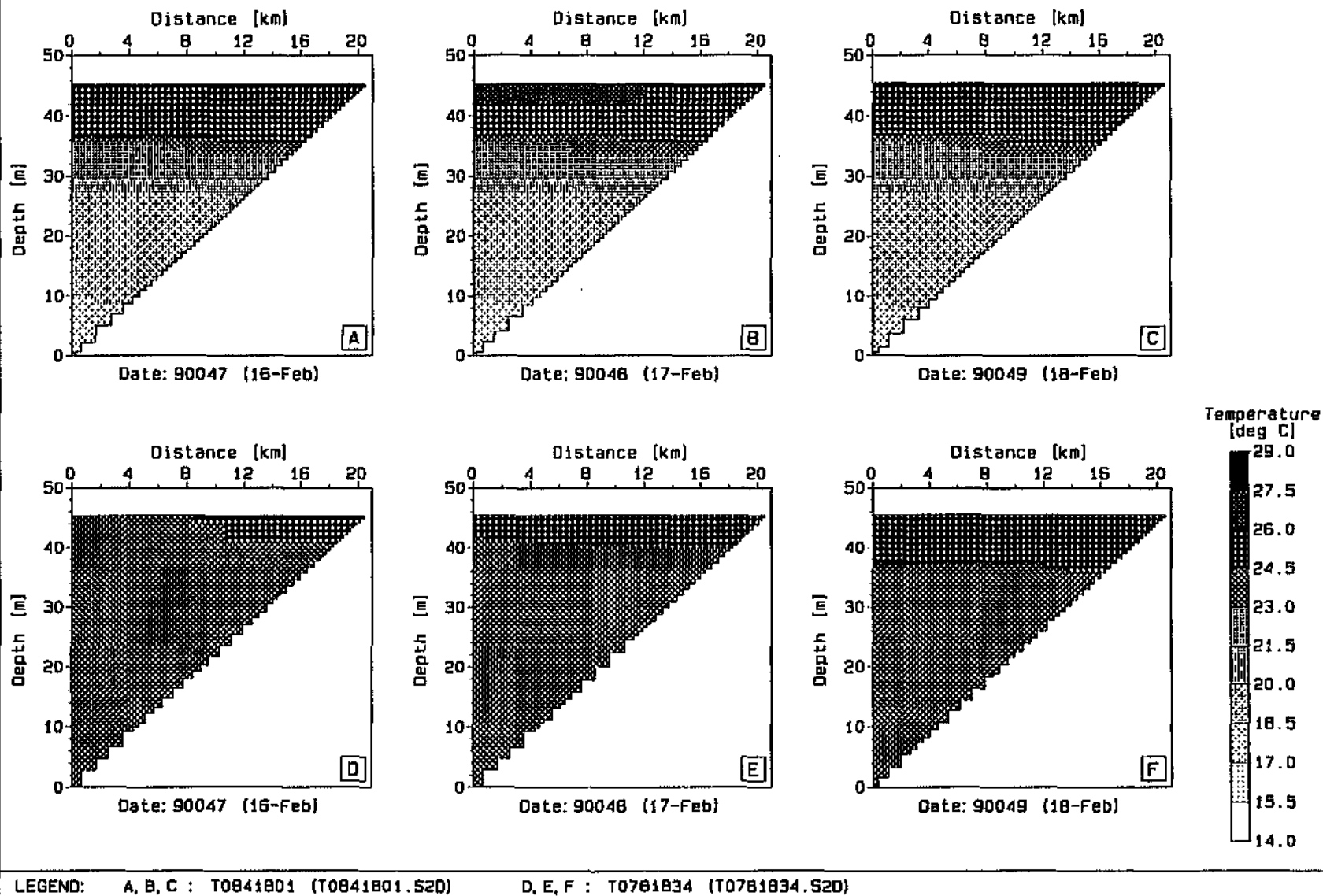
LEGEND: A, B, C : T0841801 (T0841801.S2D)

D, E, F : T0781834 (T0781834.S2D)



0,8 x Wind simulation and bubbler scenario 11 (cont.)

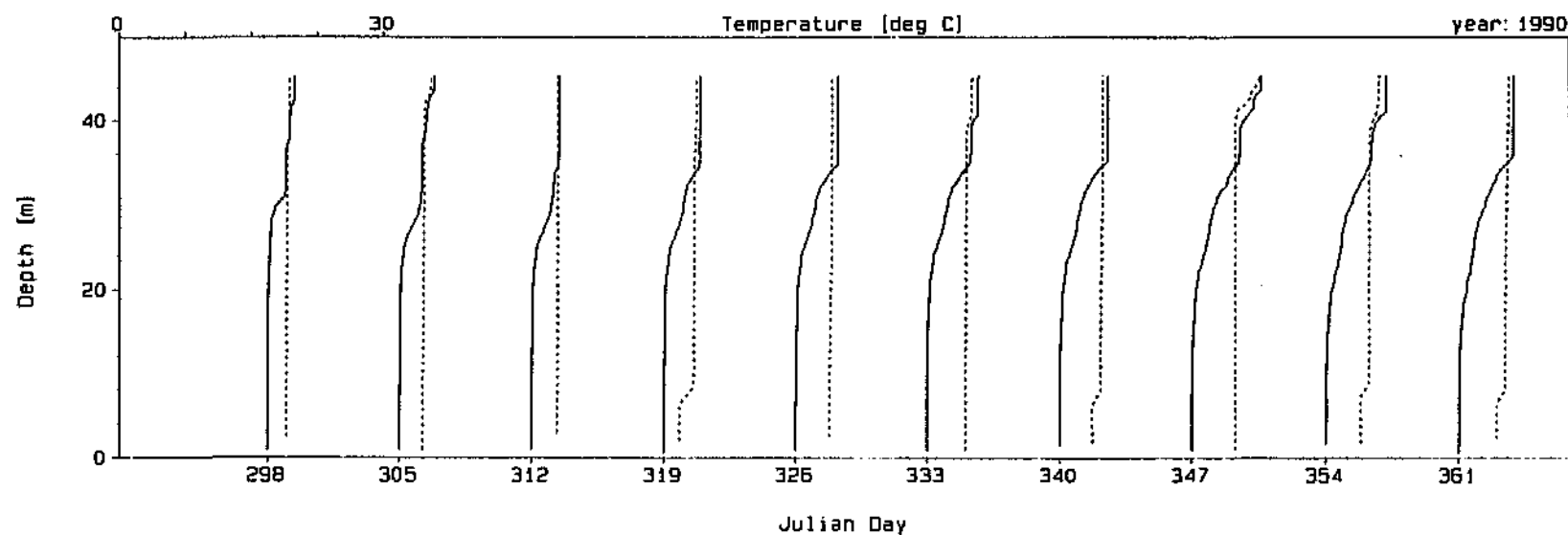
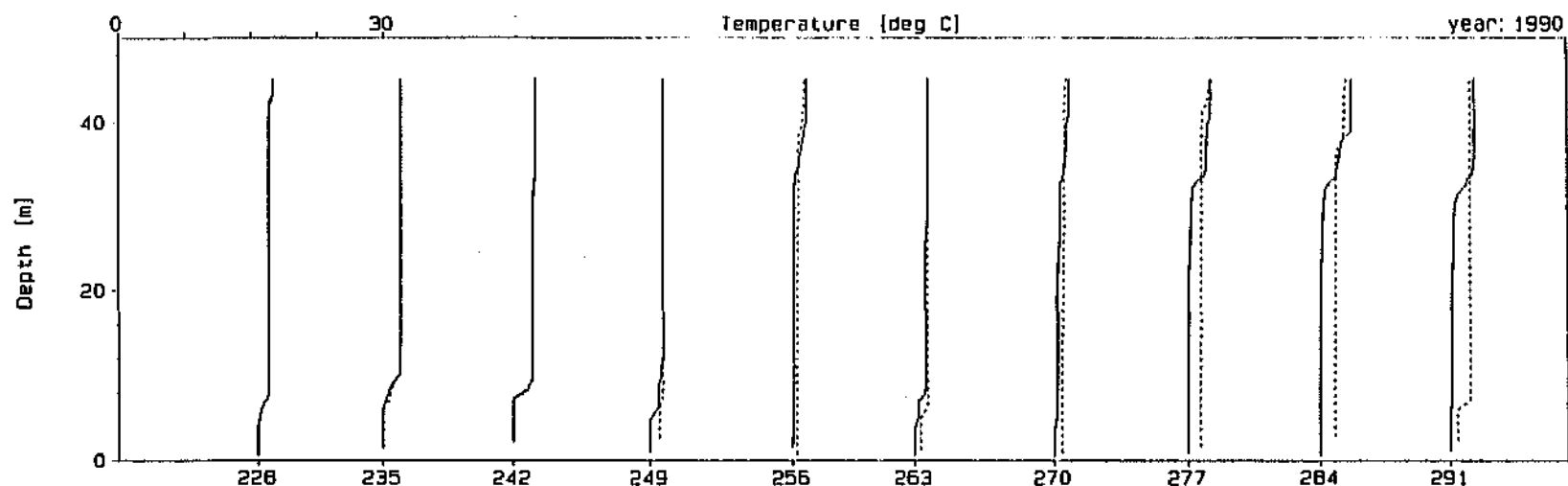
Figure 2.2.3.19



DYPlot1D : DYRESM-1D

Dam : Inanda Dam

Plot Date : 24 Oct 94, 10:11



Profile Legend: — 2D Sim Maint. Bub



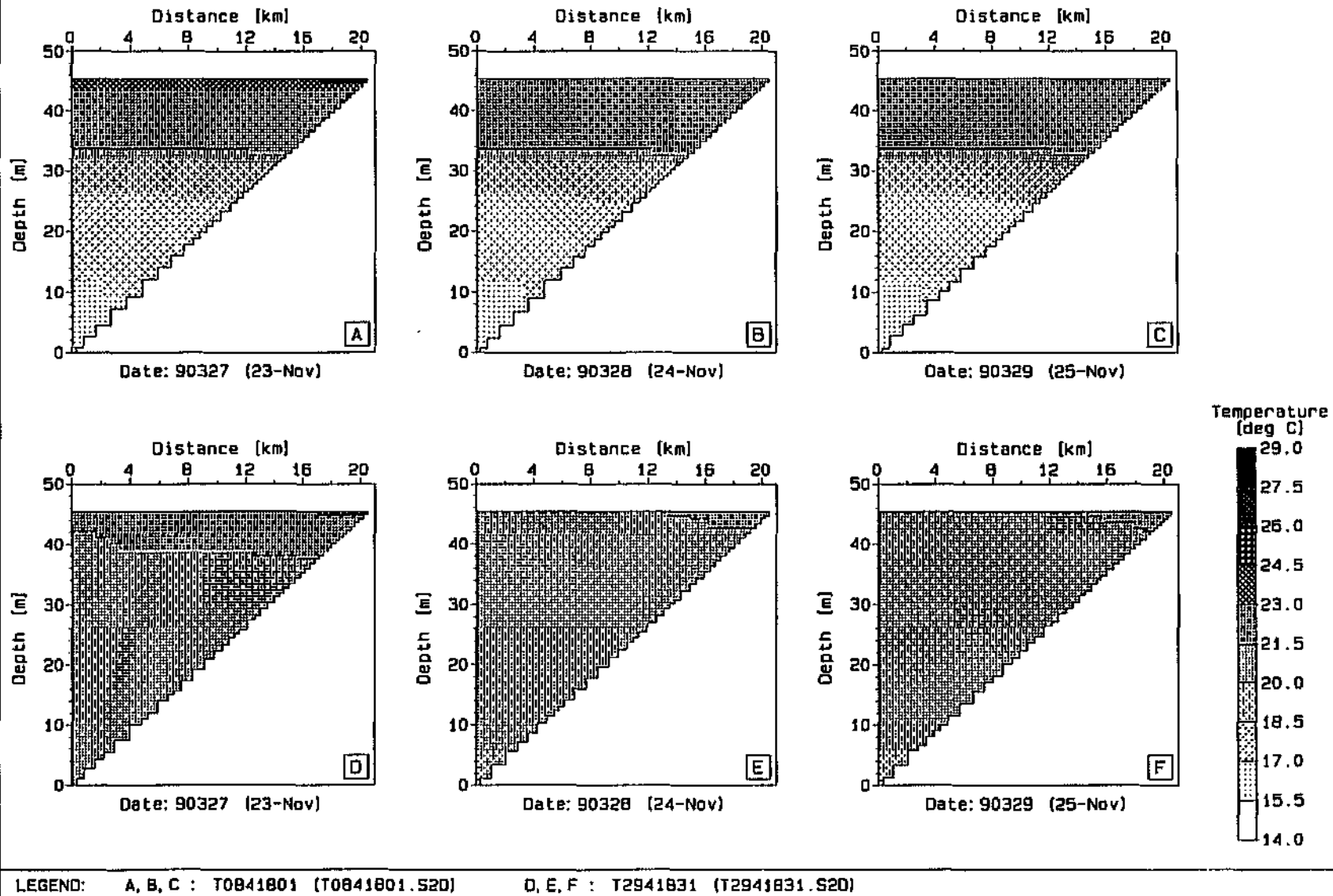
Average 2D simulation profiles and scenario 11 type maintenance bubbler

Figure 2.2.3.21

DY PLOT : DYRESM-2D

Dam : Inanda Dam

Plot Date : 29 May 95, 12:16



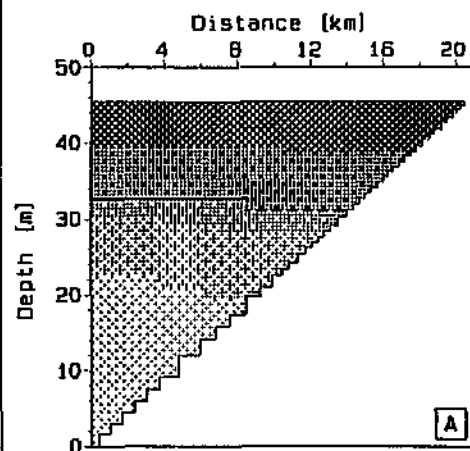
0,8 x Wind simulation and scenario 11 maintenance bubbler

Figure 2.2.3.22

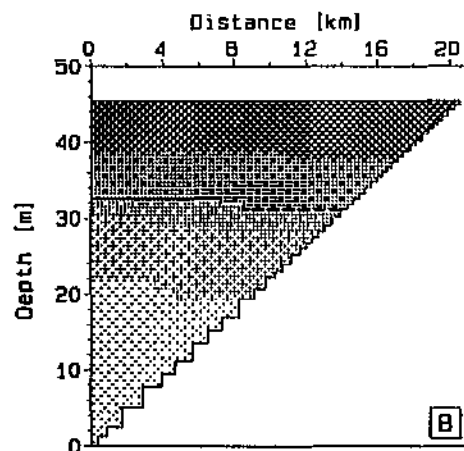
DYPlot : DYRESM-20

Dam : Inanda Dam

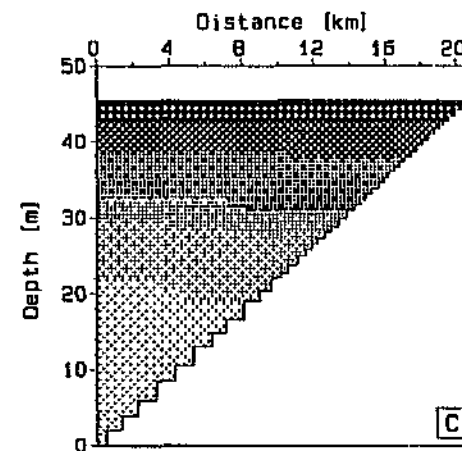
Plot Date : 29 May 95, 12:24



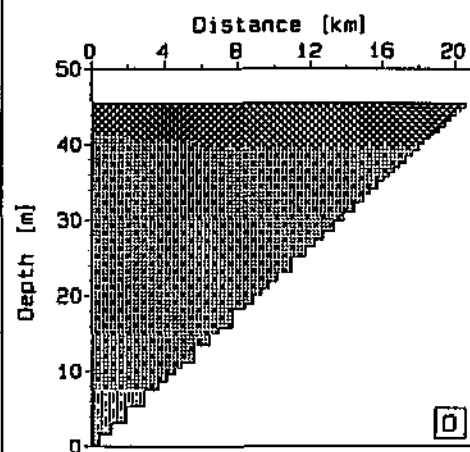
Date: 90354 (20-Dec)



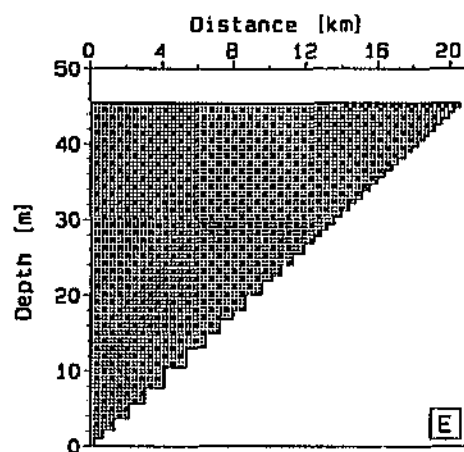
Date: 90355 (21-Dec)



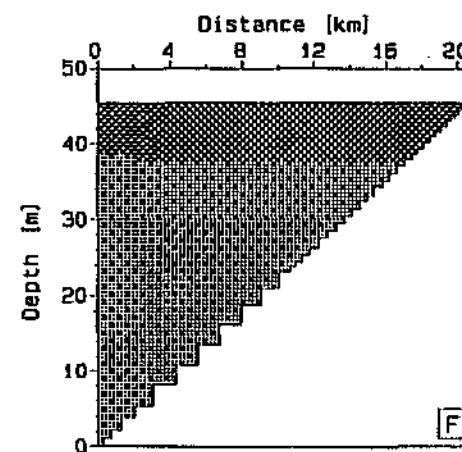
Date: 90356 (22-Dec)



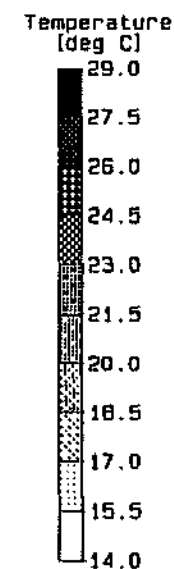
Date: 90354 (20-Dec)



Date: 90355 (21-Dec)



Date: 90356 (22-Dec)



LEGEND: A, B, C : T0841801 (T0841801.S2D)

D, E, F : T2941831 (T2941831.S2D)



0,8 x Wind simulation and scenario 11 maintenance bubbler (cont.)

Figure 2.2.3.23

2.2.4 Comparison of the Current Bubbler Design with that of Previous Destratification Attempts

Background

Thirion and Chutter (1993) describe in detail the two previous attempts to destratify Inanda Dam. The original design was used with the objective of preventing the reservoir becoming stratified. Several problems arose in the operation of the bubbler system during the period August to November 1991 including compressor cutouts and oscillation of the aerator lines. The operation of the bubbler completely failed to prevent the onset of stratification of the water body. After this attempt had failed to provide the desired effect a revised design was undertaken.

This revised bubbler system was operated from late March to the middle of May 1992 with the objective of destratifying an already stratified reservoir. Although the thermocline and oxycline of the reservoir were lowered during the period of operation of the bubbler system (the impoundment naturally starts to gradually destratify between March and May) the desired effect of destratification of the already stratified water body was not achieved. Installation problems associated with the revised bubbler had resulted in part of the aerator producing uneven bubble plumes.

Analysis of previous bubbler configurations

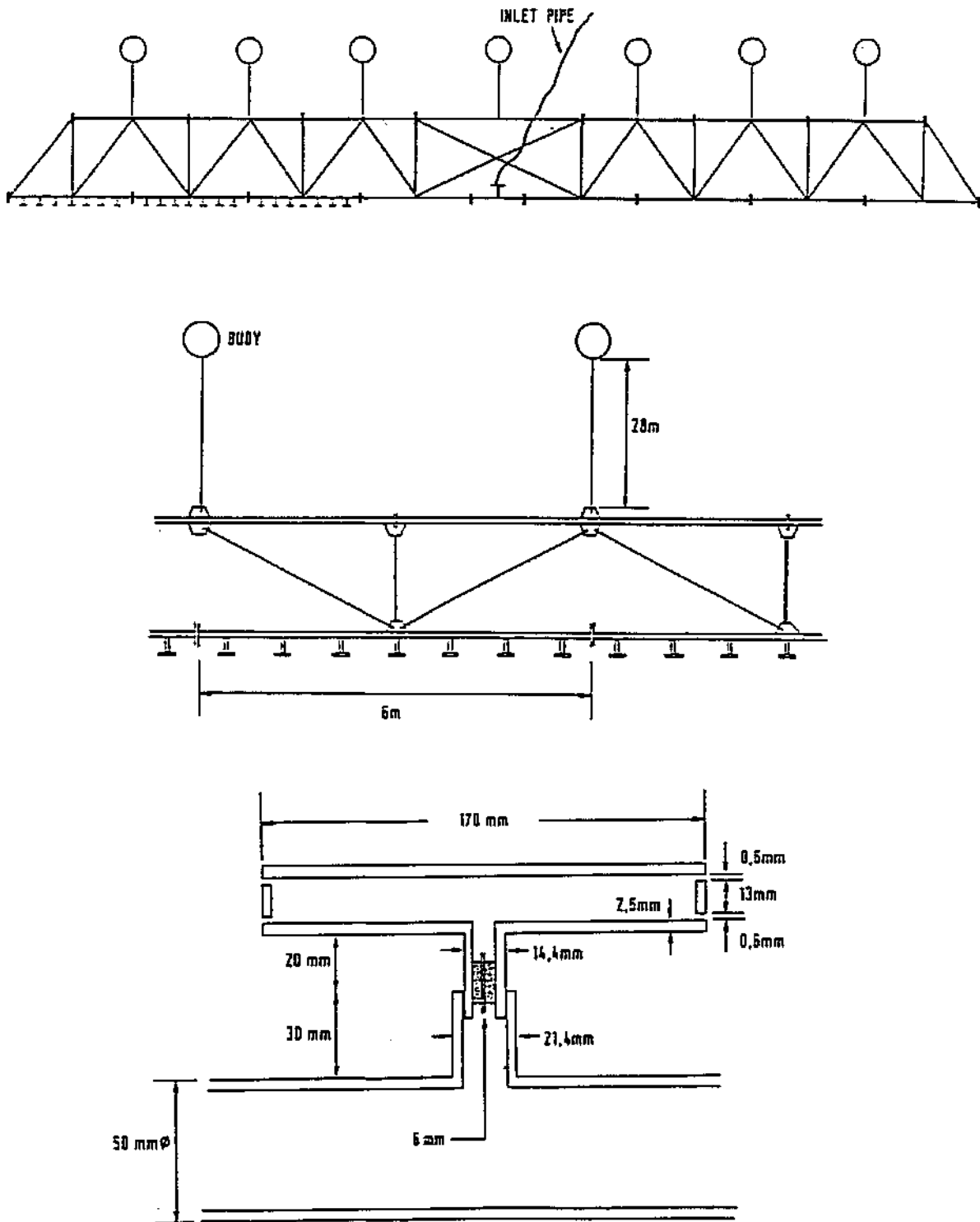
An analysis of the design and possible reasons for failure, in the light of current research, of the original and revised bubbler systems previously used at Inanda Dam follows.

Original design: The original design comprised of two 157 l/s compressors capable of supplying the maximum air flow rate at the bottom of the reservoir, and two aerator lines each 24 m long and each with 42 aerator 'heads'. This resulted in a head spacing of only approximately 0,86 m. The resultant air flow rate per head was approximately 3,74 l/s. The two aerator lines were installed side by side and suspended 18 m above the reservoir bottom. The aerator head layout, as shown in Figure 2.2.4.1, would also have resulted in large, erratic bubbles.

It is the opinion of the authors that the original bubble plume stratification prevention attempt failed for, inter alia, the following reasons:

- 1) The aerator head layout did not cause a proper bubble plume, for which a fine mass of bubbles is required. The large, erratic bubbles would have entrained little water as they rose to the surface, therefore not providing the mixing necessary for the prevention of stratification.
- 2) Although the total air flow rate of 314 l/s has been shown to be adequate for the prevention of the onset of stratification (see Figures 2.2.2.15 and 2.2.3.21), the number of bubble plume sources was too low, and the corresponding air flow rate per bubble plume source of 3,74 l/s was too high, for a 'maintenance' bubbler operation (see Table 2.2.2.2 and Section 2.2.2.4).
- 3) The height at which the aerator lines were suspended caused the bubbler system to operate on only 60% of the available water column, i.e. the aerators were too high off the bottom of the reservoir.
- 4) The arrangement of the aerator lines side by side would have reduced the mixing efficiency of the bubbler system.
- 5) The head spacing used would have caused significant interaction between plumes, had they formed properly, which would have reduced their efficiency to some extent. Robertson *et al.* (1991) found that in general interacting plumes are less efficient than independent plumes (see Section 2.4.3).

Revised design: The revised design used the same two compressors as used by the original design with a completely redesigned aerator. The new aerator comprised of two lines each 50 m long and each with 167 aerator nozzles. This resulted in a plume spacing of only 300 mm and a theoretical air flow rate per plume of approximately 0,94 l/s. The two aerator lines were installed end to end approximately 5 m above the reservoir bottom. The aerator nozzles used were plastic horticultural micro-jets with a 0,8 mm nozzle opening. Figure 2.2.4.2 shows the layout of the revised aerator system.



**Design details of the original aerators used at Inanda Dam
showing the aerator line and aerator head layout**

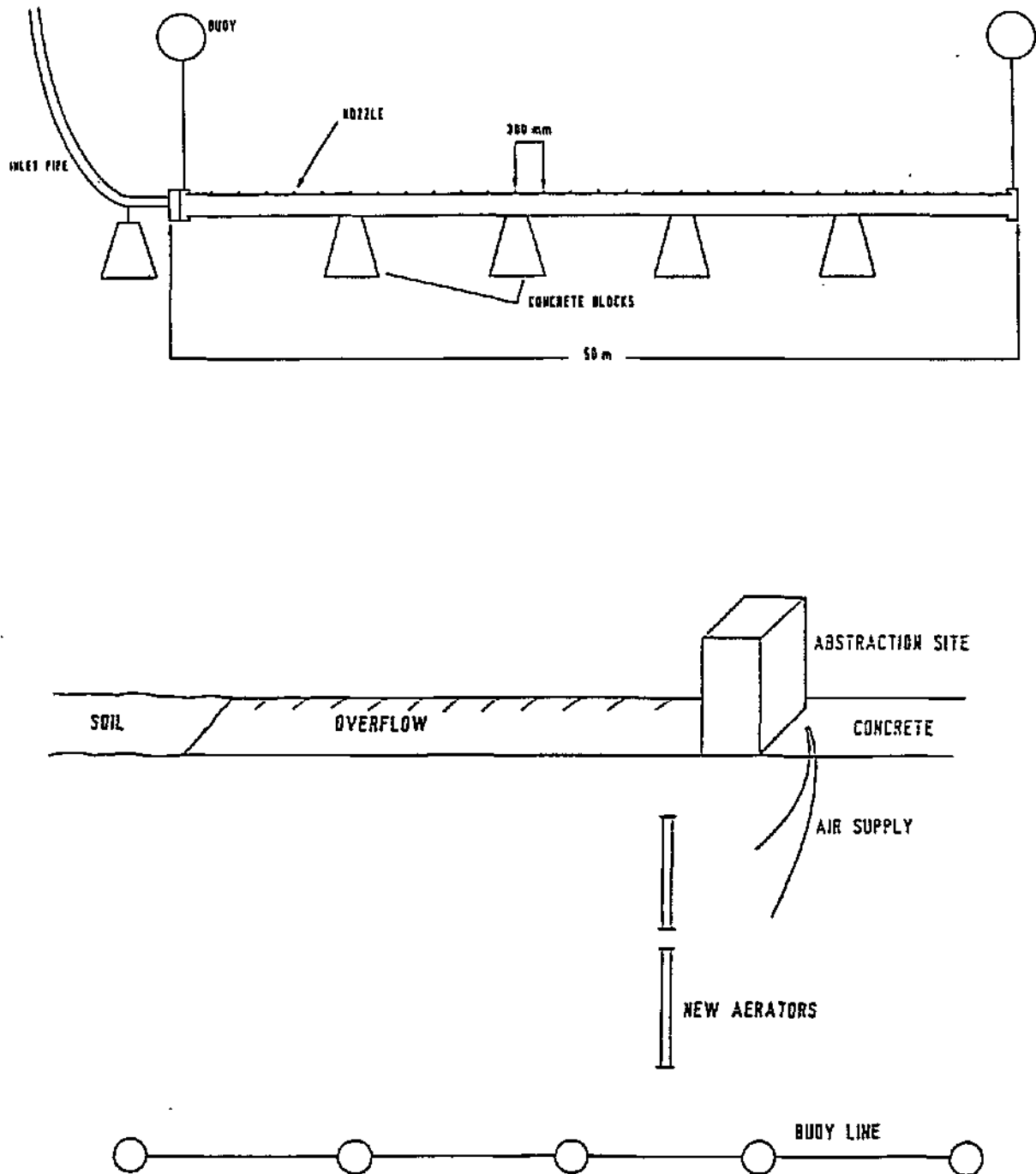
Figure 2.2.4.1

It is the opinion of the authors that the revised design bubble plume destratification attempt failed for, inter alia, the following reasons:

- 1) The total air flow rate of 314 l/s was inadequate for the destratification of the impoundment. Also the number of bubble plume sources was too high, and the corresponding air flow rate per bubble plume source of 0,94 l/s was too low, for the purposes of destratifying the already stratified water body (see Table 2.2.2.2 and Section 2.2.2.4).
- 2) An analysis of the probable hydraulics of the revised aerator system using the theory of compressible flow through a converging nozzle (Daugherty and Franzini, 1981) resulted in the conclusion that the realised air flow rate may have been as little as one third of the expected air flow rate. The resultant total air flow rate of approximately 105 l/s and air flow rate per plume source of approximately 0,31 l/s would have been even less likely to destratify an already stratified Inanda Dam than the desired air flow rate.
- 3) The plume spacing used would have caused severe interaction between plumes which, although increasing their height of rise before detrainment, would have reduced their entrainment capability and mechanical efficiency significantly (Robertson *et al.*, 1991 and Section 2.4.3).

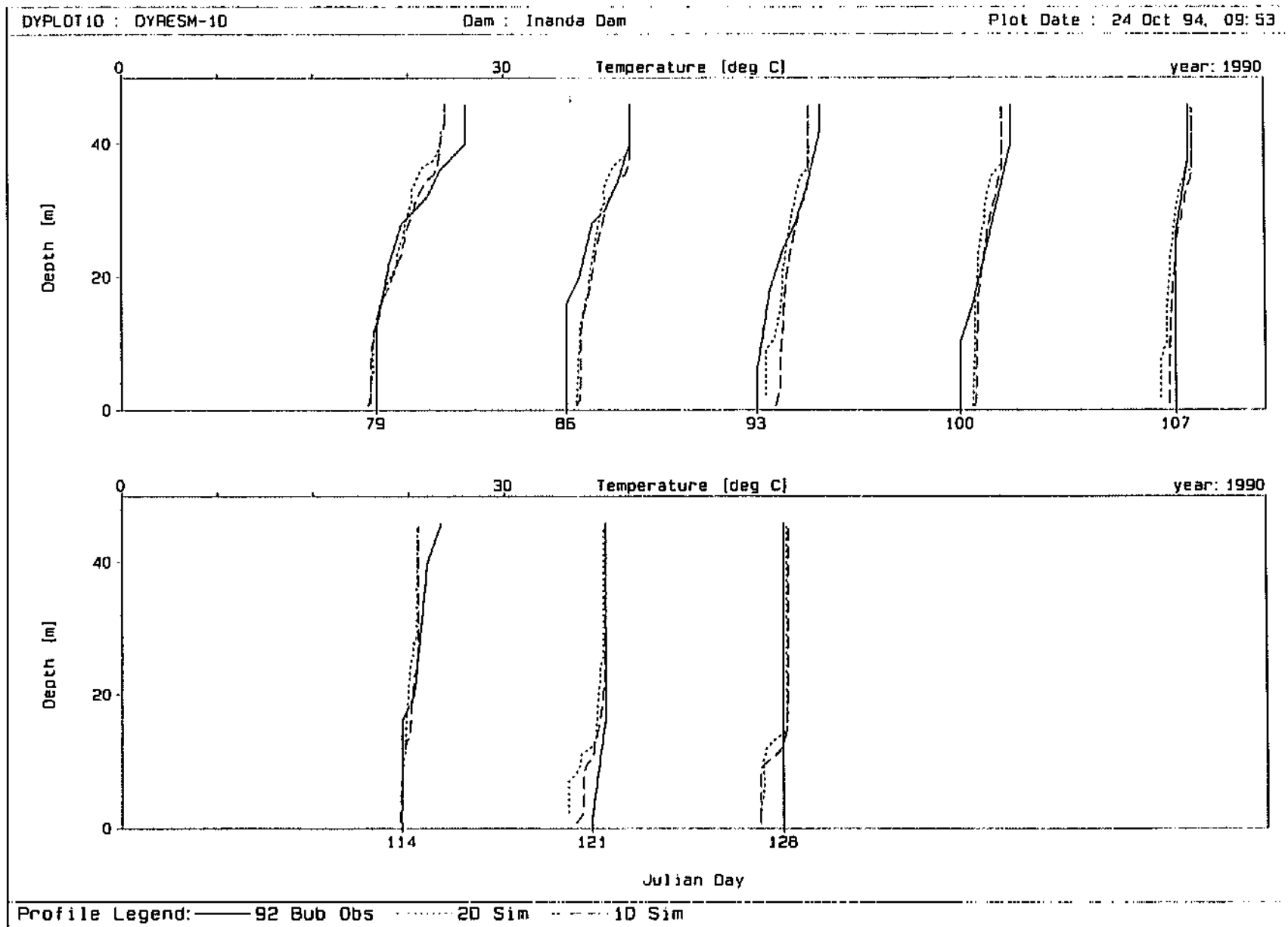
Bubbler effectiveness - Observed and simulated results

The revised bubbler system was operational from approximately Julian day 92085 to Julian day 92135. Temperature profiles were extracted at weekly intervals from Station 51 temperature isopleth information presented by Thirion and Chutter (1993). These 1992 profiles are shown together with the corresponding 1D and 2D simulated 1990 profiles in Figure 2.2.4.3. Although not for the same year, it can be clearly seen that the observed profiles and the simulated profiles are significantly similar, indicating that the bubbler had little effect on the typical stratification of Inanda Dam at this stage in the year.



**Design, layout and location details of the revised aerators
used at Inanda Dam**

Figure 2.2.4.2



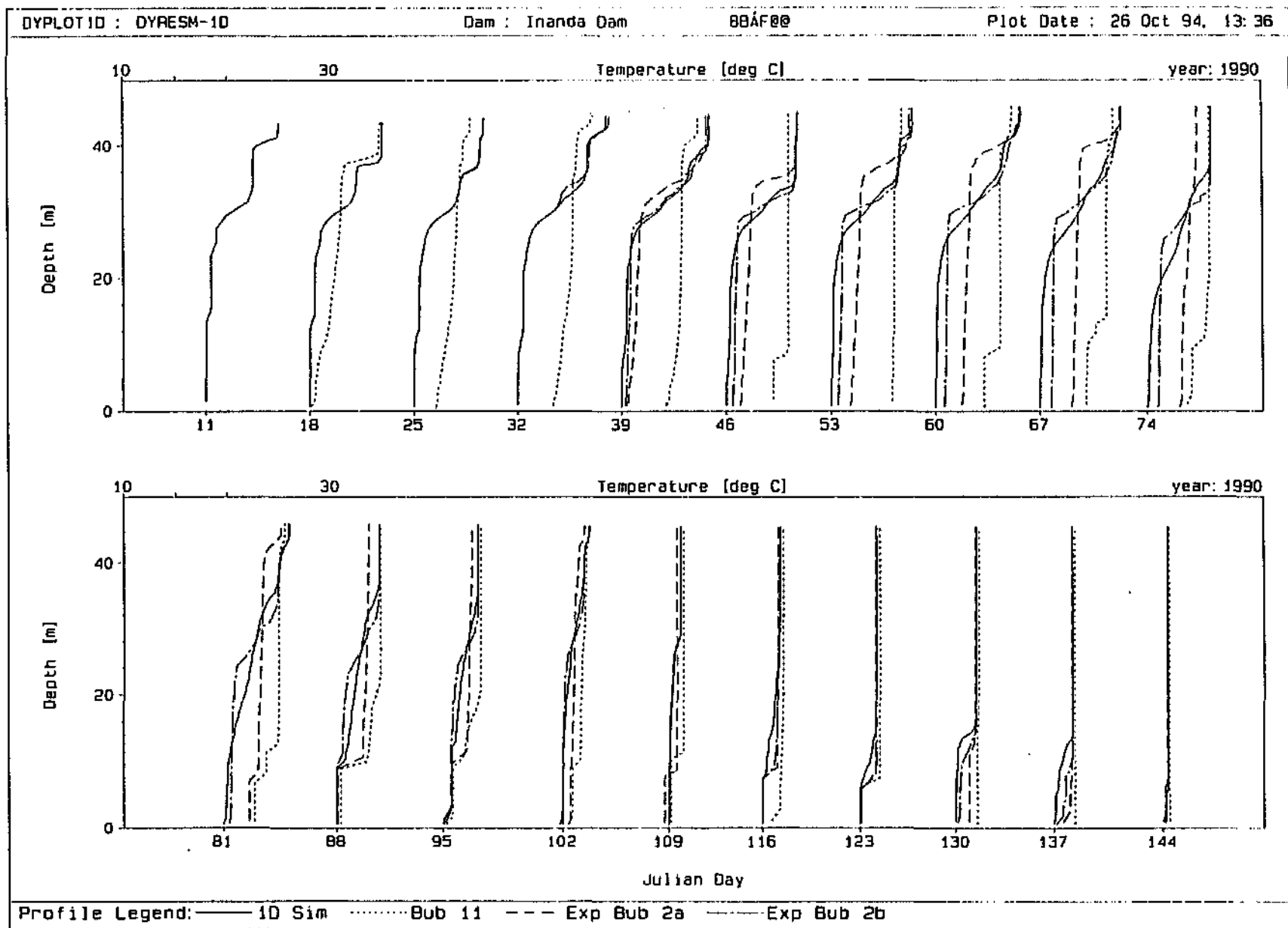
1992 Station 51 observed profiles and 1990 1D and 2D simulated profiles

Figure 2.2.4.3

In order to compare the predicted effectiveness of the revised design bubbler with that of the bubbler design using the Schladow (1991) methodology with *DYRESM* simulation refinements, 1D model runs were undertaken using a 100 m long aerator with 334 plume sources spaced 300 mm apart. These runs were made with the interacting plumes simulation option switched on. Two scenarios were analysed, viz. experimental bubbler scenario 2a with a total air flow rate of 314 l/s and experimental bubbler scenario 2b with a total air flow rate of 105 l/s (see Section 2.2.4.2 above).

Figure 2.2.4.4 shows the comparative results in which the experimental bubblers were operational from Julian day 90033 to Julian day 90134. Bubbler scenario 11 represents a combination destratification/maintenance bubbler system (see Section 2.2.2.4) with a 471 l/s, 31 plume source aerator (bubbler scenario 7) operational from the start of the analysis to Julian day 90039 and a 314 l/s, 314 plume source aerator (bubbler scenario 9) operational from Julian day 90040 to the end of the simulation period.

It is interesting to note that the 105 l/s experimental bubbler scenario 2b shows very little improvement over the no-bubbler simulated profiles, possibly confirming the reduced resultant air flow rate theory. The 314 l/s experimental bubbler 2a can be seen to largely destratify the impoundment within approximately 42 days (6 weeks) while the scenario 11 bubbler significantly destratifies the reservoir within approximately two weeks.



1D simulation, bubbler scenario 11 and experimental bubbler scenarios 2a and 2b

Figure 2.2.4.4

SECTION 2.3

APPLICATION OF *DYRESM-ID* TO SIMULATE THE HYDRODYNAMICS AND DESTRATIFICATION OF HARTBEESPOORT DAM

by

E J Larsen and K O de Smidt

2.3.1 Introduction

Previous work undertaken on the application of *DYRESM-ID* to Hartbeespoort Dam was described in a previous report (Görgens *et al.*, 1993). This section reports on further work undertaken on Hartbeespoort Dam based on this previous research. Extensive investigation into the input data set, to resolve anomalies and achieve a base data set as representative as possible of conditions at the dam, was undertaken. Once a final 'calibration' was decided on, the bubble plume destratification routine within *DYRESM-ID* was applied to the dam.

2.3.2 Model input data

The model input data set used by Görgens *et al.* (1992) was taken from a data set prepared for MINLAKE application, and was converted for *DYRESM* input via a set of computer programs written for this purpose. The data available covered the period from 4 January 1984 to 31 December 1986.

Problems with the mass balance of the reservoir were experienced in the 1992 study, and further investigation into the matter was recommended in the final report on that work (Görgens *et al.*, 1993). Only preliminary model runs were undertaken in the light of the uncertainty about the data.

Further work on the Hartbeespoort Dam data set and simulations were undertaken during 1993 and 1994. The first stage of this further work consisted of a thorough check of the data set used in the previous study. The aspects of the data set that were checked were the depth-temperature profiles, wind data, inflow and outflow data.

Observed Depth-temperature Profiles

It did not prove possible to obtain the original measured profile data in order to check the *DYRESM* input against the original data. However, the observed depth-temperature profiles used in the preliminary *DYRESM* simulations of 1992 were checked against those used for the MINLAKE simulations and were found to be the same.

Wind Data

From the preliminary runs carried out previously, the wind appeared to be causing more mixing in the dam than the measured profiles indicated. It was found that a height conversion factor had been inadvertently applied to the *DYRESM* wind data twice, which resulted in the wind being stronger than it should be, and supports the observations made earlier concerning over-mixing. The *DYRESM* wind data was replaced with unadjusted wind data from the original raw wind-run records for a nearby wind station (Oberon). Any adjustments required for height, or surface type (overland or overwater) would be made in the "management" of a particular run within *DYRESM*.

This problem highlighted the need to set up and work with a base set of data which consists of the unadjusted measured field data. This will allow data sets to be easily transferred and result in maximum use of such data, which are costly to collect and process.

The factors used to adjust the wind data for height and surface over which it is measured were also investigated. The wind data at Oberon was measured over land at 1,8 m above ground level. *DYRESM* requires wind speed at 10 m above the water surface. Various mathematical relationships were investigated, and the relevant factors to apply a height conversion followed by a surface type conversion are shown in Table 2.3.1.

Another aspect that was considered was the effect of wind direction on the application of the different conversion factors. The Oberon wind station is situated very close to the edge of the dam. Therefore if the predominant wind direction in a particular season blows from the dam surface towards the wind station, it will only travel over a very short section of land

before being measured, and its speed may more accurately reflect that of an "over water" case. In such an instance, it would only be necessary to apply the height conversion factor to the wind data during that season. We believe that this situation may exist at Hartbeespoort, and so tried such a seasonal wind adjustment. This was done by adjusting the values manually in a spreadsheet, as there is no facility within *DYRESM* to factor the wind data on a seasonal basis within a particular run. This is further described in the following section.

TABLE 2.3.1 WIND CONVERSION FACTORS

| FROM | CONVERSION FACTOR | TO | CONVERSION FACTOR | TO | OVERALL CONVERSION FACTOR |
|--|--|---|---|--|---------------------------|
| Observed wind speed at 1,8 m over land | x 1,78 (height conversion over land using Logarithmic law) | Intermediate wind speed at 10 m over land | x 1,43 (land to water conversion at 10 m) | Required wind speed at 10 m over water | x 2,55 |

Inflow to Reservoir

The Hartbeespoort Dam has a catchment area of 4112 km². The inflow to the dam is measured by flow gauges A2H012 on the Crocodile River (2251 km², or 62% of the total catchment area) and A2H013 on the Magalies River (1171 km², or 28% of the total catchment area). There is an ungauged incremental catchment of 390 km², or 10% of the total catchment area.

As a first step, the processed daily flow data for these flow gauges was obtained from DWAF. The 1992 *DYRESM* inflow data stored in the *.INF file was checked against the new flow data acquired from DWAF. Differences between +6% and -12% were found in the daily flow values in some months. A new *.INF file was created using the latest DWAF data for the inflow to replace the data transferred from the MINLAKE data set. A slight improvement was noticeable when comparing simulations from the two data sets, but the mass balance remained a problem.

A hydrological study of the Crocodile River Catchment was undertaken for DWAF recently (DWAF, March 1992). It was reported in this study that gauge A2H012 was under-reading by an estimated 9% (pg 66, Section 5.2). It was recommended in this report that the

discharge table be re-evaluated and the flow record be re-calculated (pg 102, Section 6.2, point 1), but such a study was not carried out as part of that particular study.

The estimation of a 9% under-reading is adequate for water resource modelling purposes, but is not sufficiently accurate for a daily model such as *DYRESM*. However it is outside the scope of this study to re-rate the gauge, so a factor of 1,1 (approximated to a 10% increase) was adopted for the Crocodile River .

In addition, the report indicated that the return flows from water obtained from the Vaal catchment through treated effluent discharge from towns and industries was a significant characteristic of the hydrology of the catchment. Inflows recorded in the DWAF report (Table 2.16, pg 40) show that all flows except one (from Pelindaba) are accounted for in the two gauges. The contribution from Pelindaba is estimated to be approximately $0,4 \times 10^6 \text{ m}^3$ on average per annum for the period 1984 to 1986, and did not appear to be significant enough to adjust the inflow.

A factor of 1,1 was applied to the inflows for each gauge to allow for the 10% ungauged catchment area.

Conclusion: The factors which were seen to be rational ones to be adopted for the *DYRESM* inflows were as follows:

| | |
|------------------------|---|
| A2H012 Crocodile River | $1,1 \text{ (gauge readings)} \times 1,1 \text{ (ungauged catchment)} = 1,21$ |
| A2H013 Magalies River | $1,1 \text{ (ungauged catchment)}$ |

The results of *DYRESM* simulations using these factors are discussed in Section 2.3.3.

Outflow

Outflow from the dam is measured by three separate gauges, namely A2H081, A2H082 and A2H083. Data for these gauges was obtained from DWAF and was compared with the outflow data in the *DYRESM* *.OUT file. Differences of between +4% and -2% were found in some periods. The specific periods were identified, replaced with the DWAF data and simulations were run with the amended outflow data. No significant difference was found and therefore the original outflow data, as transferred from MINLAKE, was retained for further simulations.

2.3.3 Model 'calibration'

A "base case" simulation was decided on in the following manner:

- The unadjusted wind data and inflow data, as described in the previous section, were adopted as the basic input data for the model.
- The inflow factors as described in the previous section were adopted. A plot of the simulated profiles for these factors combined with the basic, unadjusted wind data is shown in Figure 2.3.1 (A to F). The measured field profiles are shown as a solid line, the simulation using unadjusted flow data is shown as dotted, and the simulation using adjusted flows is shown as a dashed line.

An improvement in mass balance was seen in the earlier portion of the record, but significant mass balance problems still exist in the latter portion. Since it is outside the scope of this study to re-rate the flow gauges to correct the mass balance problem completely, it was decided to concentrate on the first portion of the data set, up to Julian day 85148 (28 May 1985), for the purposes of the remaining simulations. Where plots are given in the document from this point onwards, only those portions deemed to adequately illustrate the point are shown, in order to reduce the numbers of plots.

- Various wind adjustment factors were tried in the model. Simulation results for the conversion factors given in Table 2.3.1 plotted against the measured profile data and a simulation with no wind adjustment are presented in Figure 2.3.2 (A to C). The various simulations shown on the plots are as follows:

measured profile data

unadjusted wind data (wind factor of 1,0)

wind factor of 1,43 (land to water conversion at 10 m)

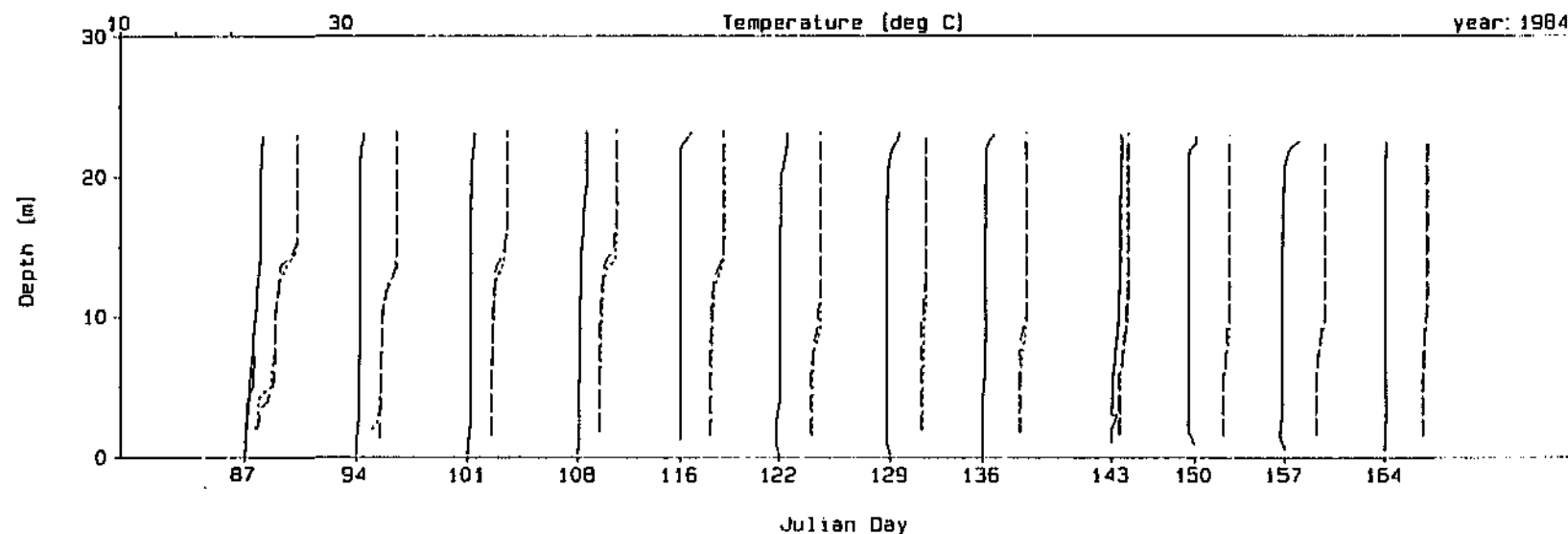
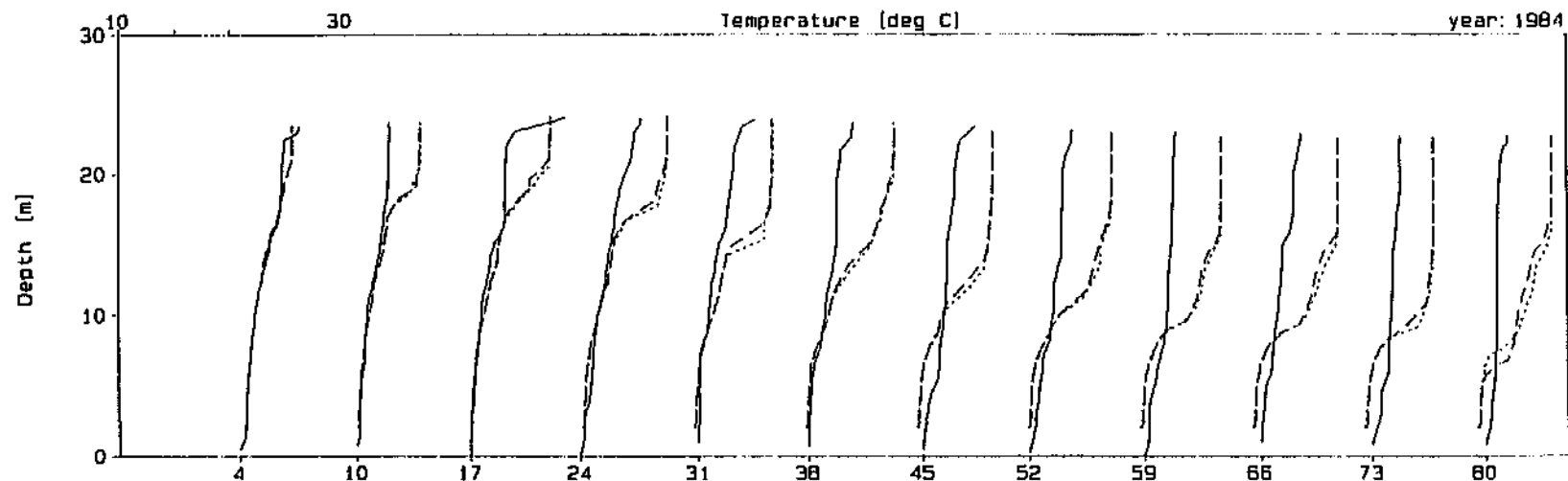
wind factor of 1,78 (height conversion over land)

wind factor of 2,55 (height conversion x surface type conversion)

DYDLOT 10 : DYRESM-1D

Dam : Hartbeespoort Dam

Plot Date : 25 Oct 94, 09:26

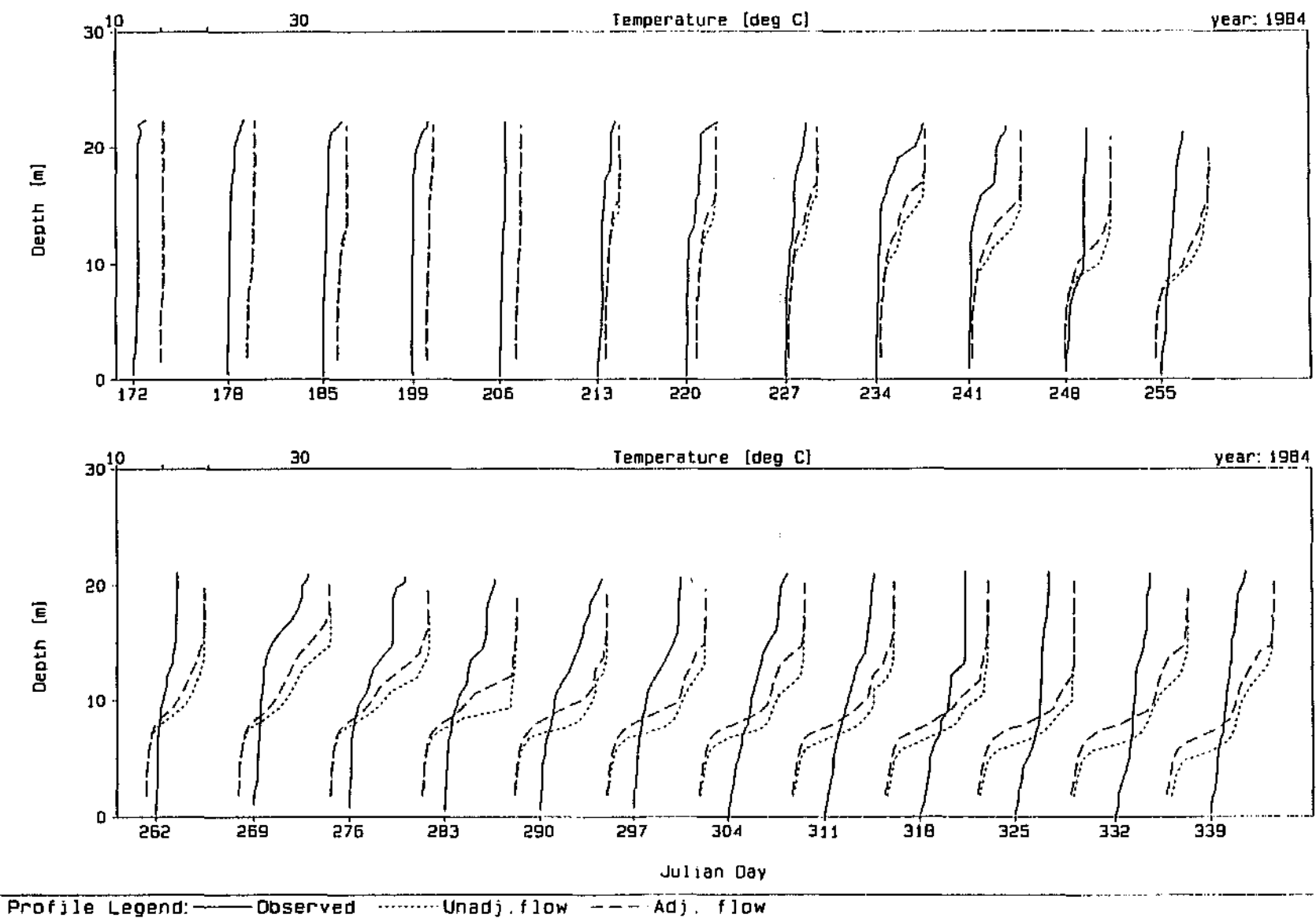


Profile Legend: ——— Observed Unadj. flow --- Adj. flow



Comparison of inflow factors

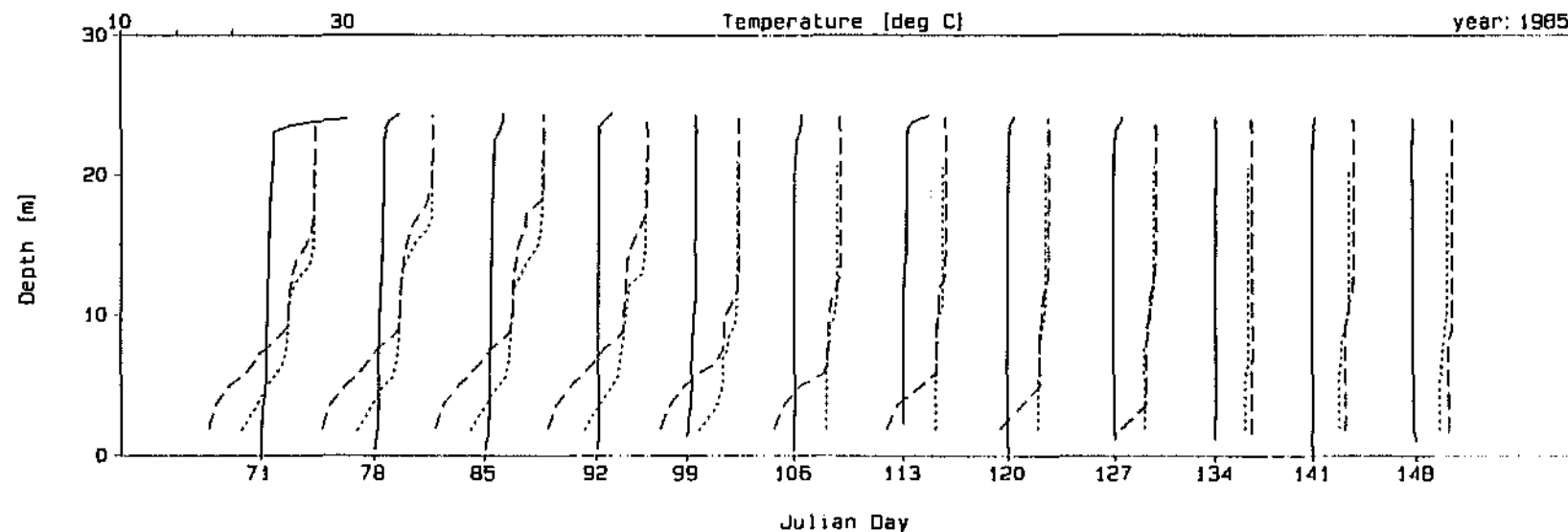
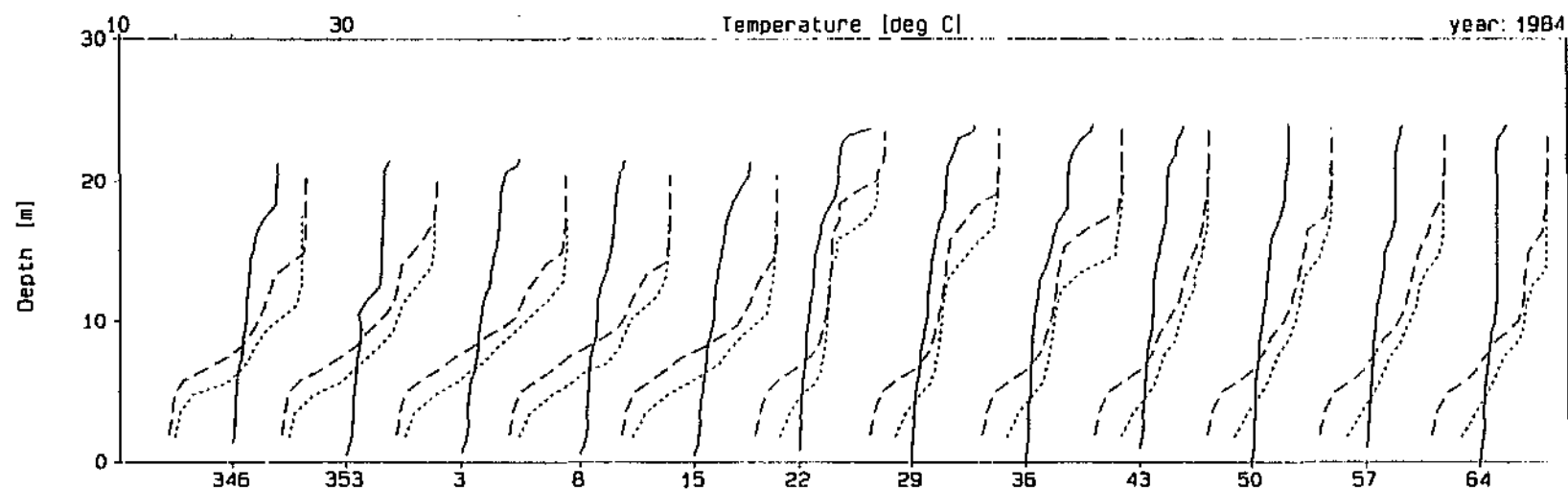
Figure 2.3.1 (A)



DYPlot 10 : DYRESM-10

Dam : Hartbeespoort Dam

Plot Date : 25 Oct 94, 09:26



Profile Legend: — Observed Unadj. flow --- Adj. flow



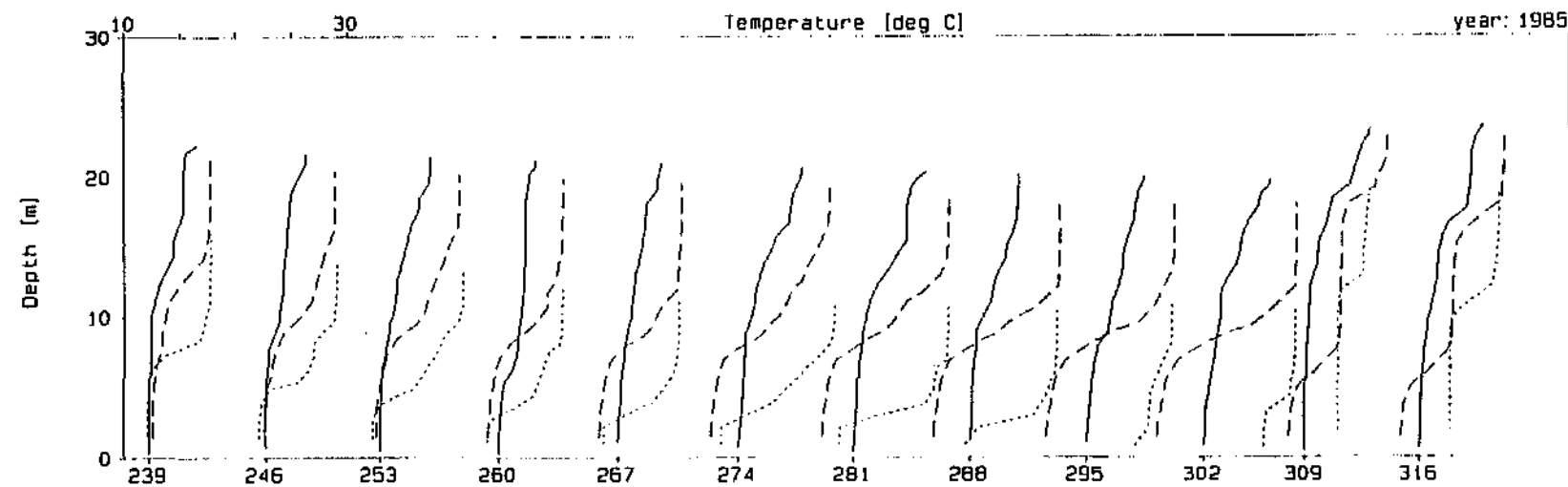
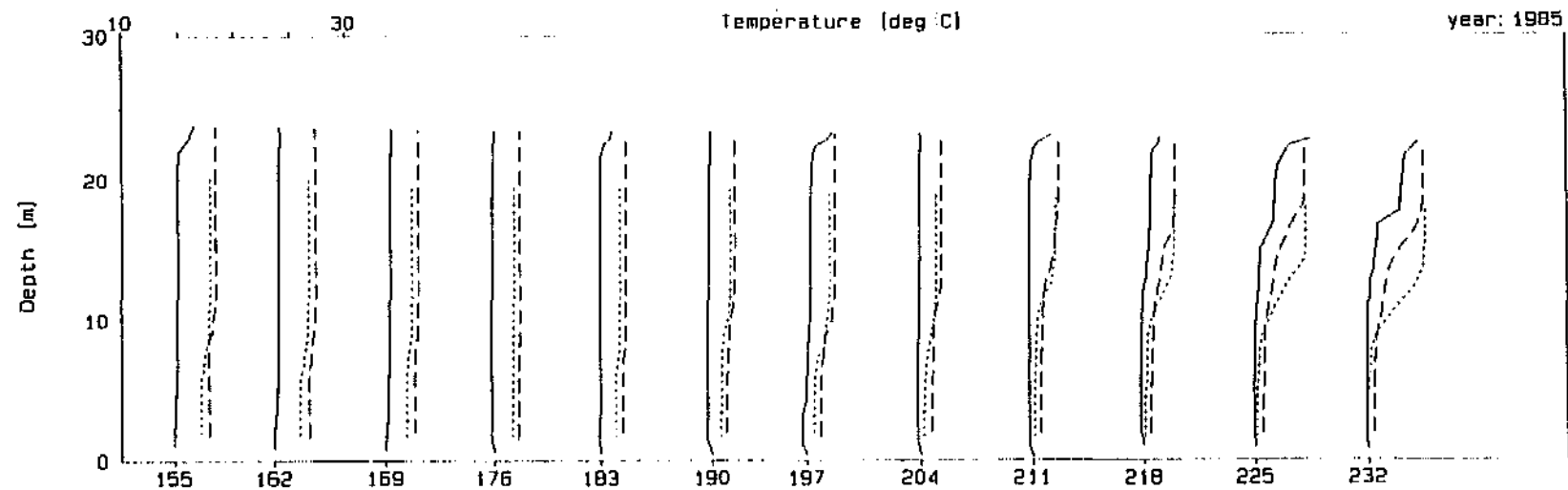
Comparison of inflow factors (continued)

Figure 2.3.1 (C)

DYDLOTID : DYRESM-10

Dam : Hartbeespoort Dam

Plot Date : 8 Feb 95, 16:33



Profile Legend: --- Observed --- Unadj. flow --- Adj. flow



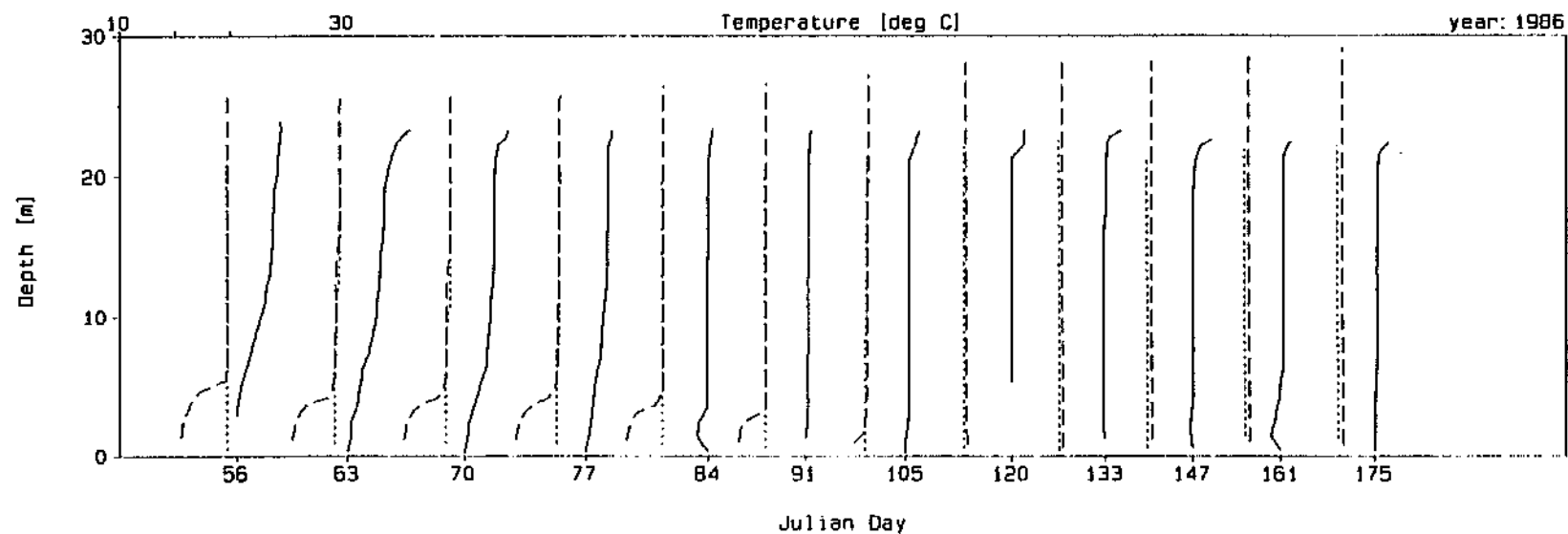
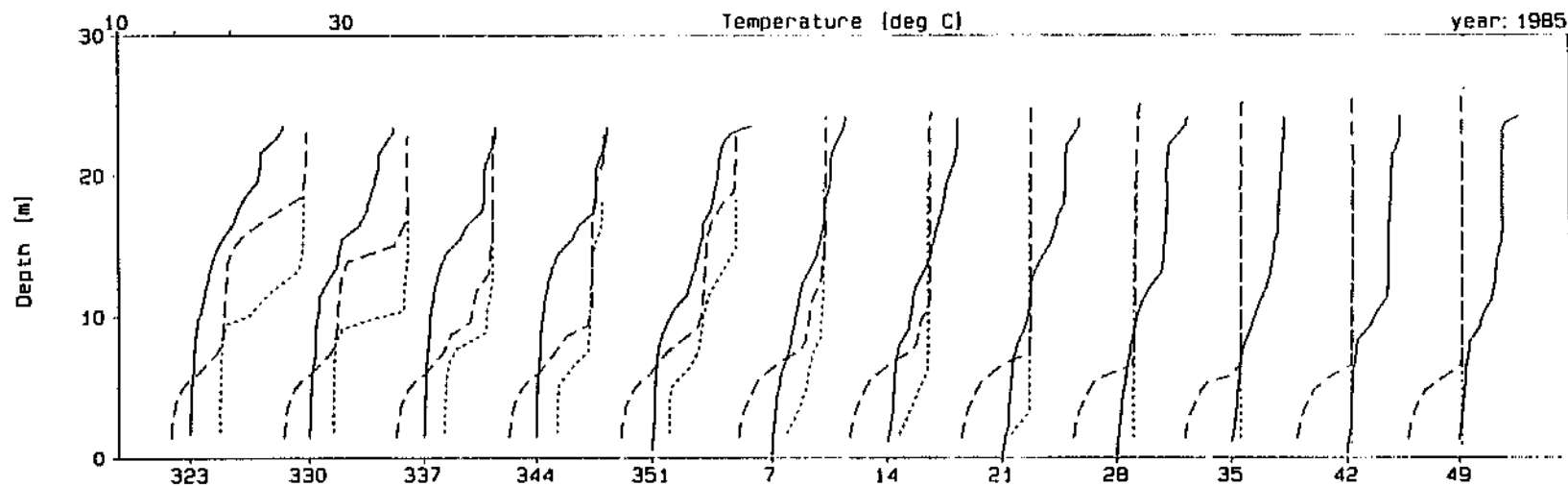
Comparison of inflow factors (continued)

Figure 2.3.1 (D)

DYDLOT 10 : DYRESM-10

Dam : Hartbeespoort Dam

Plot Date : 25 Oct 94, 09:27



Profile Legend: — Observed - - - Unadj. flow . . . Adj. flow



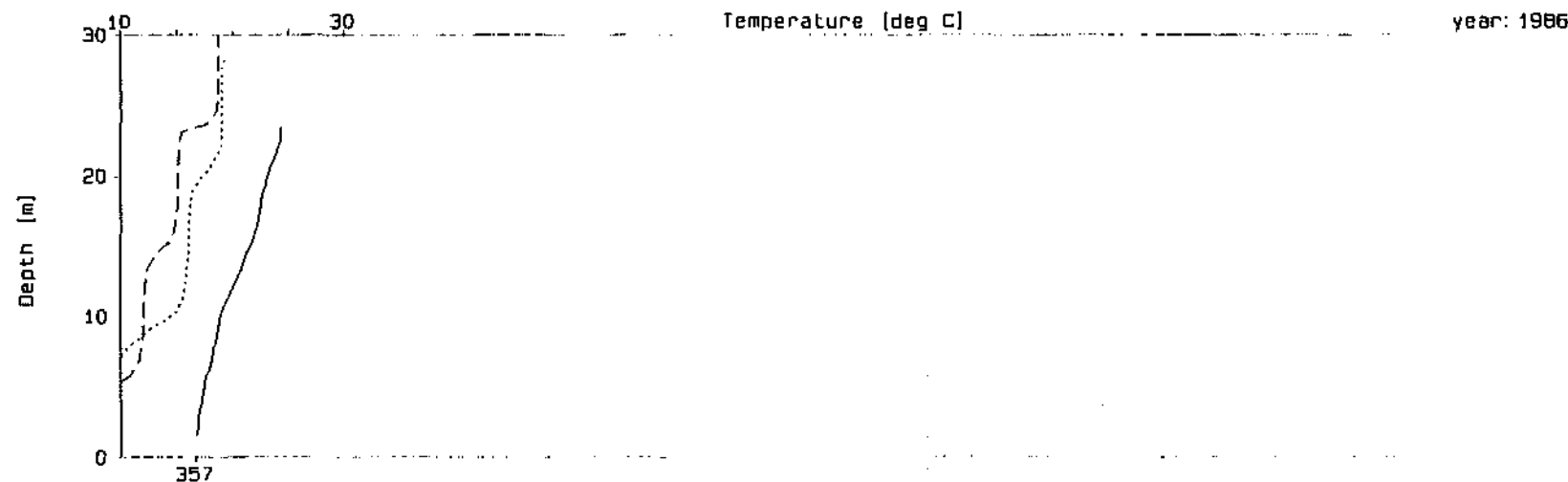
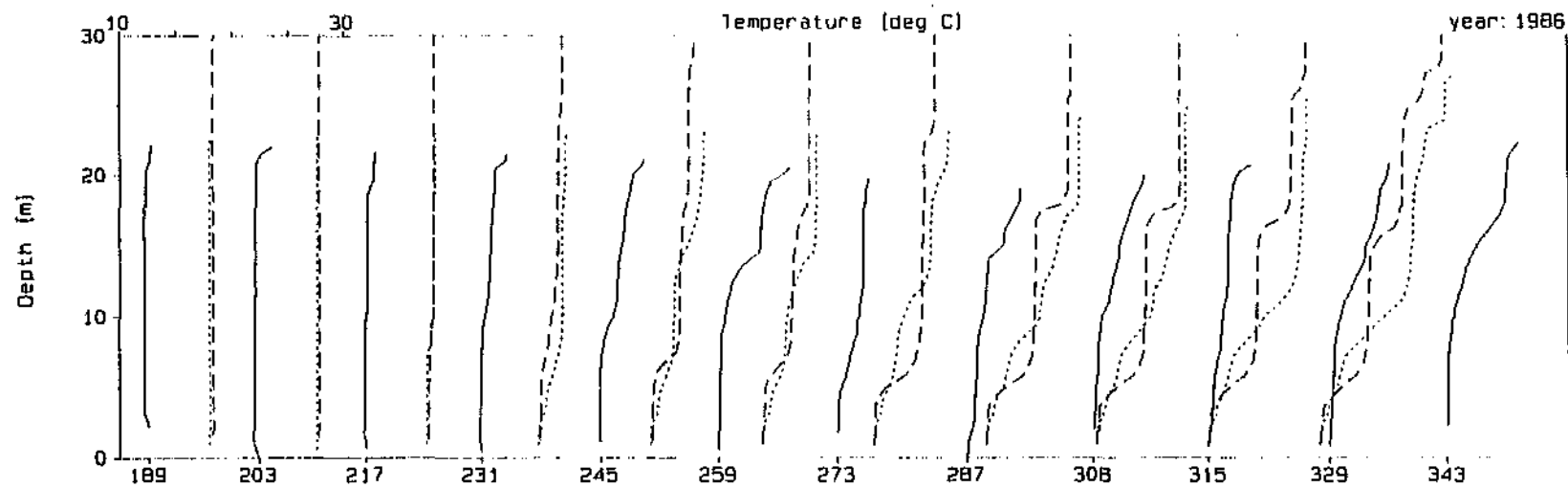
Comparison of inflow factors (continued)

Figure 2.3.1 (E)

DYPLOT10 : DYRESM-10

Dam : Hartbeespoort Dam

Plot Date : 8 Feb 95, 16:34



Profile Legend: --- Observed --- Unadj. flow

Julian Day

Adj. flow



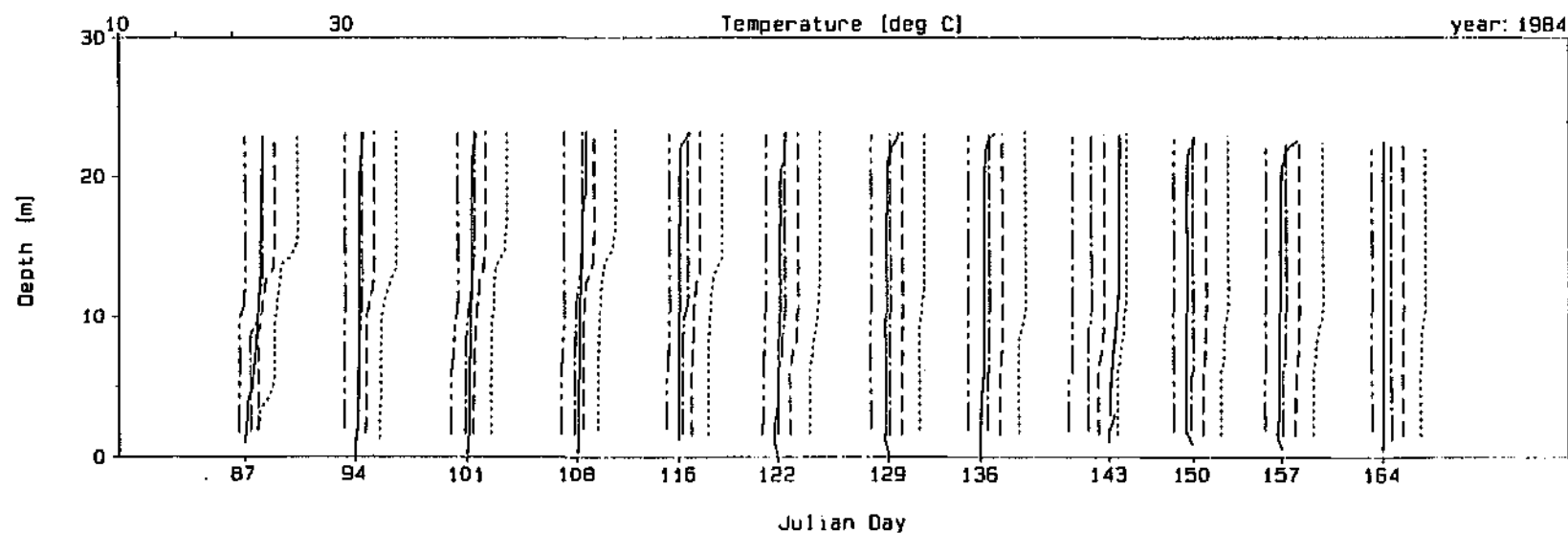
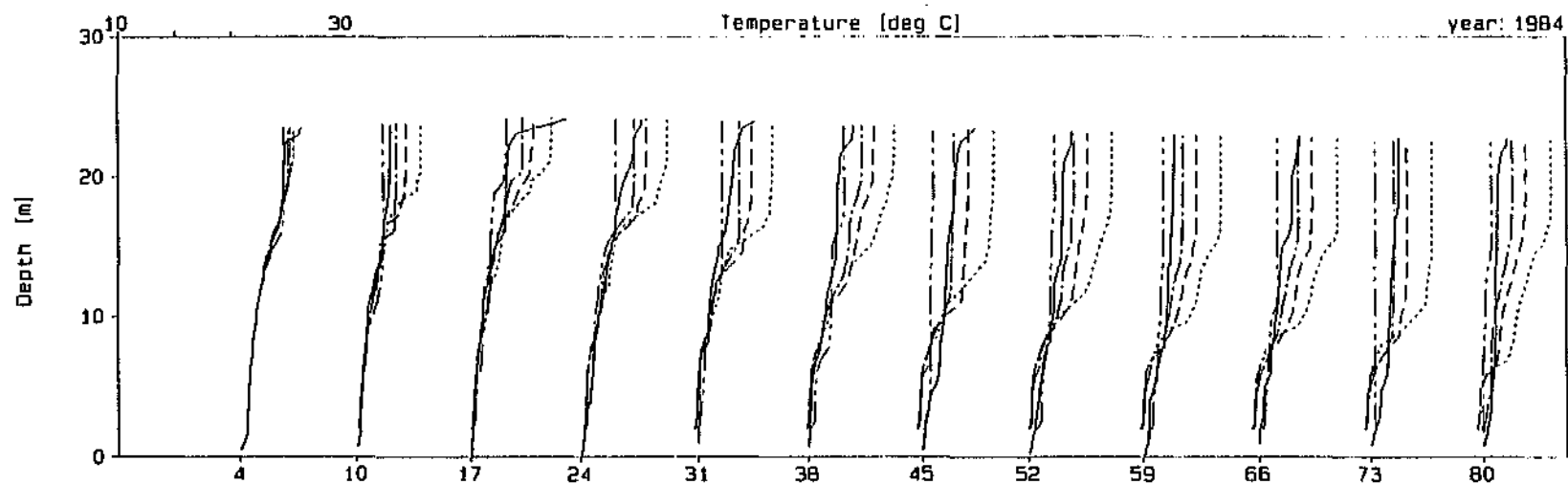
Comparison of inflow factors (continued)

Figure 2.3.1 (F)

DYPLOT10 : DYRESM-10

Dam : Hartbeespoort Dam

Plot Date : 25 Oct 94, 09:42

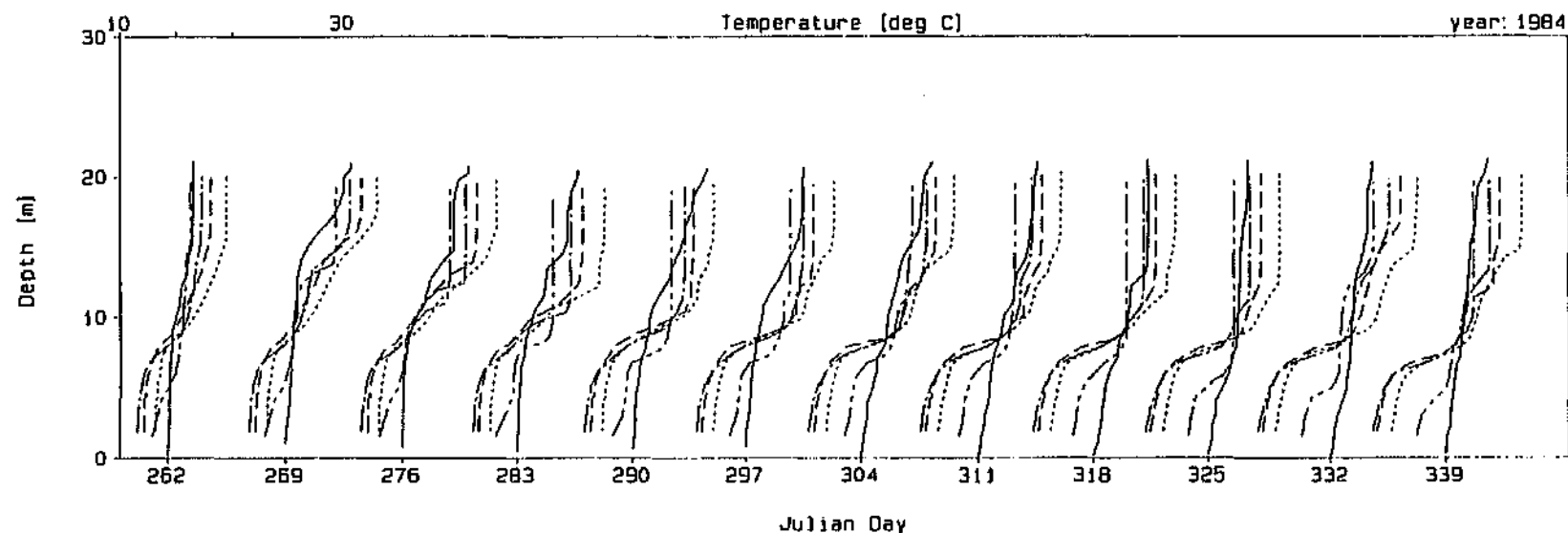
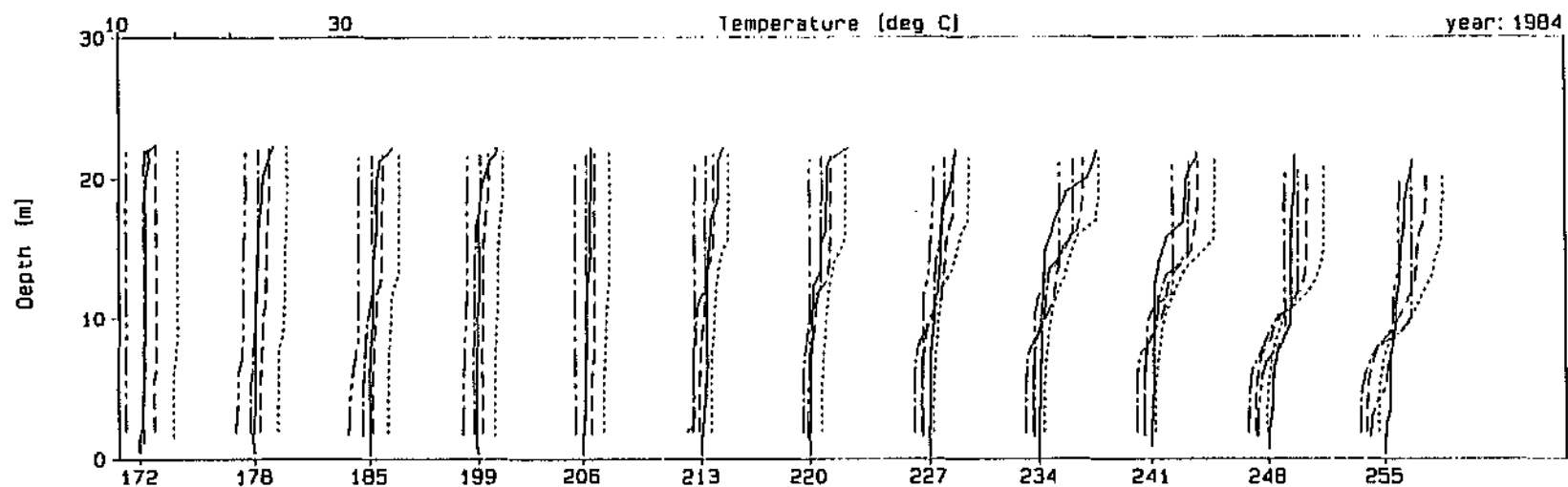


Profile Legend: ——— Observed - - - - - Wind x1,00 - - - - - Wind x1,43 - - - - - Wind x1,78 - - - - - Wind x2,55



Comparison of wind factors

Figure 2.3.2 (A)



Profile Legend: — Observed - - - Wind x1.00 - - - Wind x1.43 - - - Wind x1.78 - - - Wind x2.55



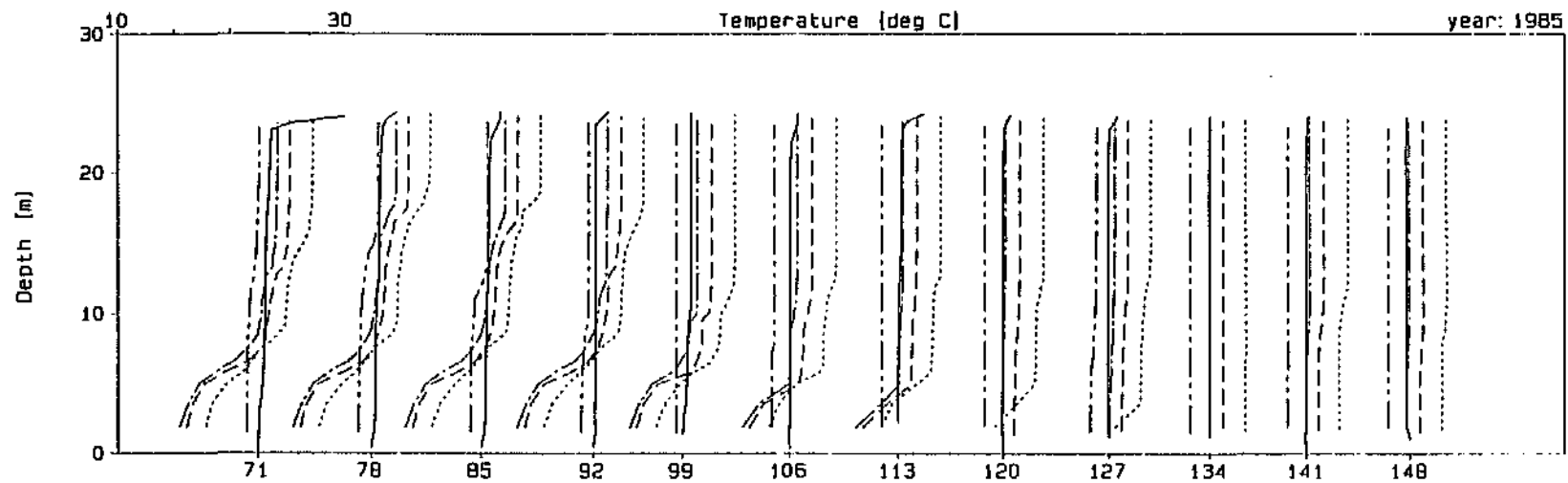
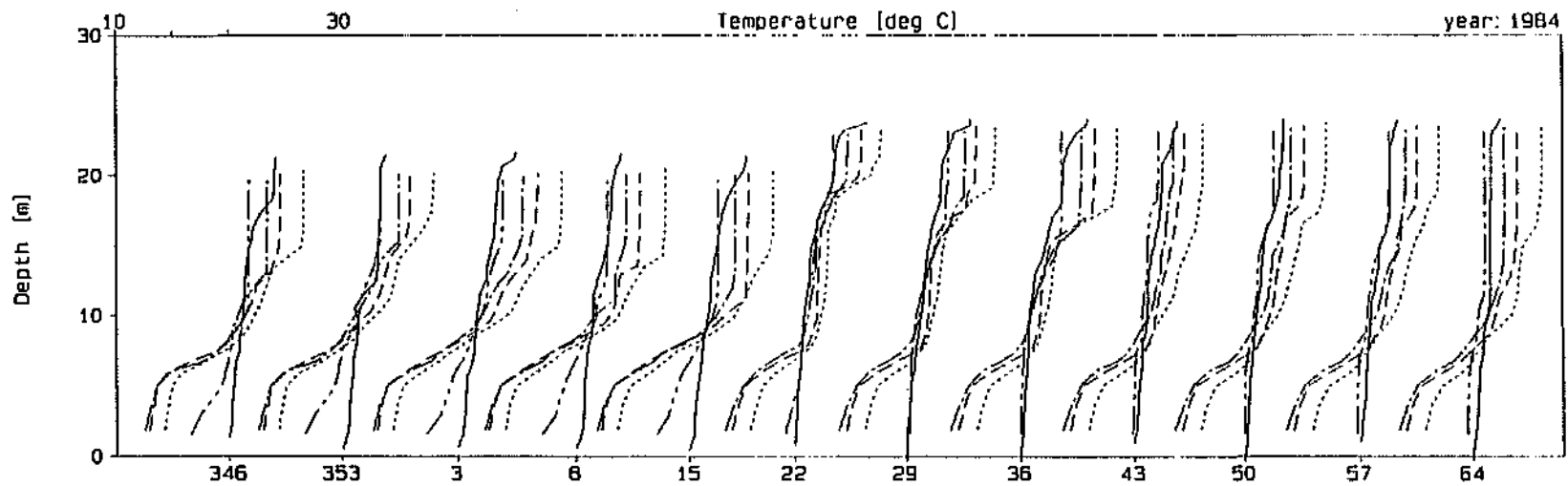
Comparison of wind factors (continued)

Figure 2.3.2 (B)

DYPlot10 : DYRESM-10

Dam : Hartbeespoort Dam

Plot Date : 25 Oct 94, 09:42



Profile Legend: — Observed - - - Wind x1.00 - - - Wind x1.43 - - - Wind x1.78 - - - Wind x2.55



Comparison of wind factors (continued)

Figure 2.3.2 (C)

Figure 2.3.2 shows that during mixed periods (eg. 84087 to 84206), the 1,78 factor seems to show the best fit. At other times, for example during a more stratified period such as shown by profile 84332, a higher factor seems better, although 2,55 seems a little high. It was decided to adopt the wind factor of 1,78 as the "base case", and to test the effect of seasonal wind factors as part of the sensitivity checking of the model.

Various sensitivity checks were carried out to investigate the response of the model simulations to changes in the various input parameters and input data. These are listed below and described in more detail thereafter:

- light extinction exponent (ET1) / secchi disk depth
- width of basin at full supply level
- seasonally different wind factors
- reduced outflow volumes
- inflow temperature
- short wave radiation
- salinity of inflow
- air temperature
- various combinations of the above.

Light extinction exponent (ET1) / secchi disk depth: The conversion of secchi disk depths to light extinction exponent (ET1) used is shown below.

$$\begin{aligned}\text{Light extinction exponent ET1} &= (1,44 \text{ to } 2,3) / \text{secchi disk depth} \\ &= 1,7 / \text{secchi disk depth}\end{aligned}$$

It allows a range of between 1,44 and 2,3 and an average of 1,7 for the factor which is divided by the secchi disk depth in metres. One measured secchi disk depth of 2,7 m was readily available for Hartbeespoort Dam for this period, and the value used for the basic data set was the average ET1 of $1,7 / 2,7 = 0,63$. Two different simulations were done using the minimum and maximum values of $1,44 / 2,7 = 0,53$ and $2,3 / 2,7 = 0,85$. The "base case" factors for inflow (1,21 and 1,1) and wind (1,78) were used for the simulations.

The lower ET1 value tended to give a deeper mixed layer, while the higher ET1 value generally gave a better fit, especially in the summer months.

Other secchi disc measurements for Hartbeespoort Dam were obtained from the literature (Walmsley and Bruwer, 1980). The secchi disk and ET1 values are presented in Table 2.3.2.

TABLE 2.3.2: SECCHI DISK DEPTHS AND ET1 VALUES (Walmsley and Bruwer, 1980)

| | MEAN | MAXIMUM | MINIMUM |
|-----------------------|------|---------|---------|
| ET1 | 0,67 | 1,94 | 0,37 |
| Secchi disk depth (m) | 0,99 | 2,50 | 0,01 |

The available secchi disk measurement of 2,7 m used in the base data set is higher than the maximum of 2,5 m from the reference, but the ET1 value of 0,63 corresponds well with the published mean of 0,67.

Width of basin at full supply level: The value used for the width of the basin at full supply level in the base data set was 1 km. Three other values for the width were selected and simulations run with base case inflow and wind factors. These were:

- an estimated minimum width of 0,5 km,
- an estimated average width of 2 km
- a maximum width of 12 km (NTWR, 1985).

The wider width tended to give a better fit because it provides a less sharply defined thermocline.

Seasonally different wind factors: As discussed previously, it became apparent that different wind adjustment factors may be required for different seasons. The wind data in the *DYRESM *.MET* file was edited to apply a factor of 1,78 from April to August (day 091 to 243), and a factor of 2,27 from September to March (day 244 to 090). The simulation using the seasonal wind data was found to give a significantly better fit than that with a constant wind factor, and the slightly reduced factor of 2,27 resulted in a simulated profile closer to the observed profile than the combined factor of 2,55 from Table 2.3.1.

Outflow volumes: The outflow volume was reduced by 10 % by applying a factor of 0,9 in the *DYRESM* run, as a test of sensitivity to this data. The reduced outflow from the reservoir improved the mass balance, but there did not seem to be much sensitivity in terms of an improved fit overall.

Inflow temperature: The temperature of the inflow was adjusted up and down by 3 °C, which is approximately 10 % of the order of magnitude of temperatures experienced. It was found that the cooler temperatures improved the shape of the profiles over the summer period by forming a less definite thermocline.

Short wave radiation: The short wave radiation data in the *.MET file was varied up and down by 10 %. The increased values resulted in generally warmer simulated profiles, and the decreased values in generally cooler profiles, particularly in the upper portions. This adjustment also appeared to have a seasonal aspect to it, as the decreased values improved the fit in summer, but not elsewhere.

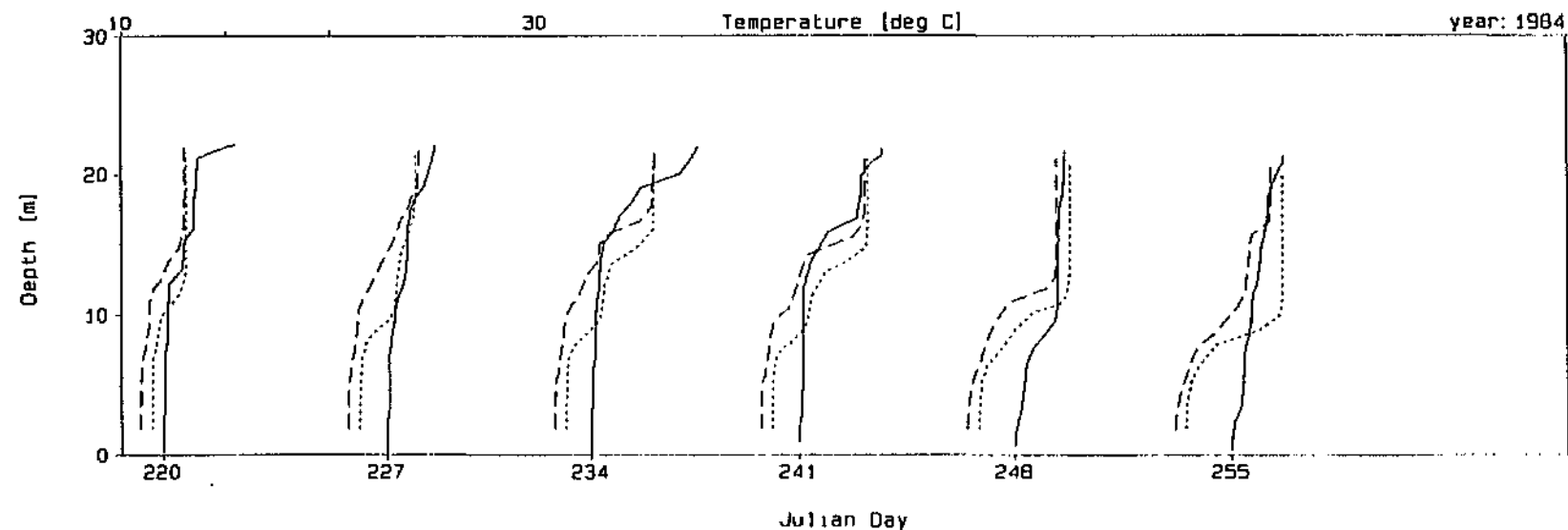
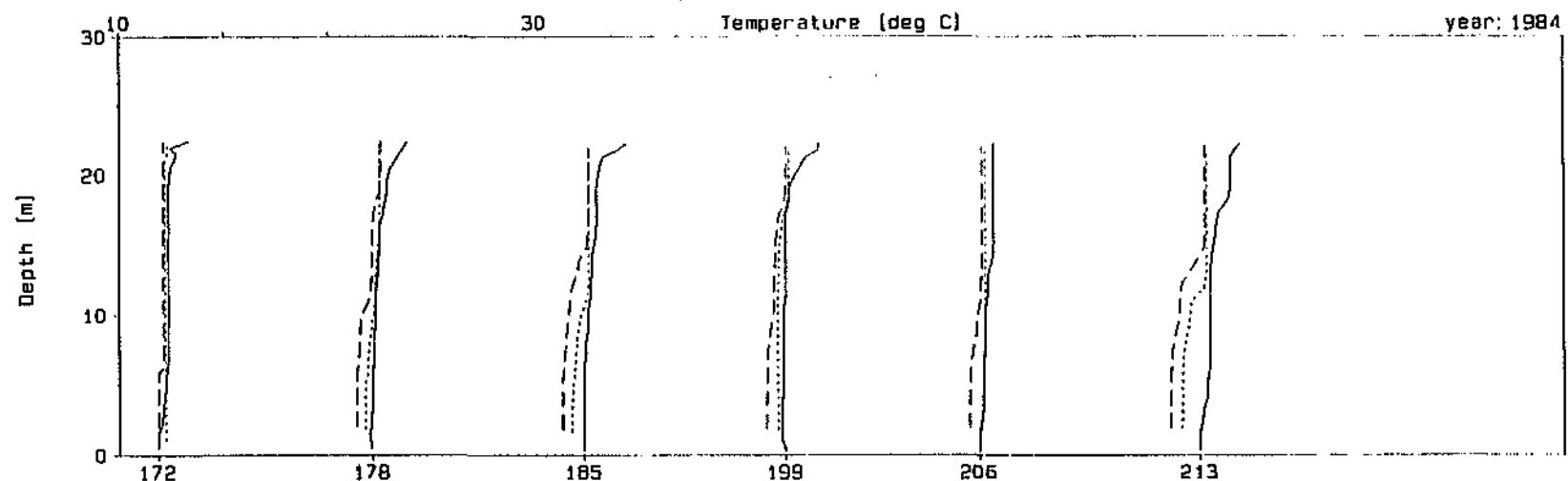
Salinity of inflow: The salinity of the inflow was varied by 10 %. The resultant simulations showed very little change from the original. The temperature of the profile was lower when the higher salinity was used, and higher when the lower salinity was used.

Air temperature: The air temperature in the *.MET file was both increased and decreased by 10 %. The range of air temperatures in the data set was from 3,89 °C to 28,39 °C and therefore a 3 °C variation was deemed appropriate. The simulations with decreased temperatures tended to improve the fit in summer, although a decrease of 1 or 2 °C may be more successful. The increased air temperature did not provide any improvement.

Combinations of the above: A combination of the above sensitivity tests was chosen as follows:

- ET1 = 0,85 (maximum) (*.FIZ file)
- Dam width at FSL = 3 km (*.TAB file)
- Outflow x 0,95 (in *DYRESM* run)
- Inflow temperature cooler by 2 °C (*.INF)
- Seasonal wind factors.

Figure 2.3.3 (A to C) shows the simulation (dashed line) plotted against the measured profiles (solid line) and the base case (dotted line). The figure shows all measured profiles from Julian day 84172 to 84339, and then from 85071 to 85148. Generally the selected combination did not improve the fit, except for a few isolated profiles. It seems that there is a degree of overcompensation from the selection of factors.

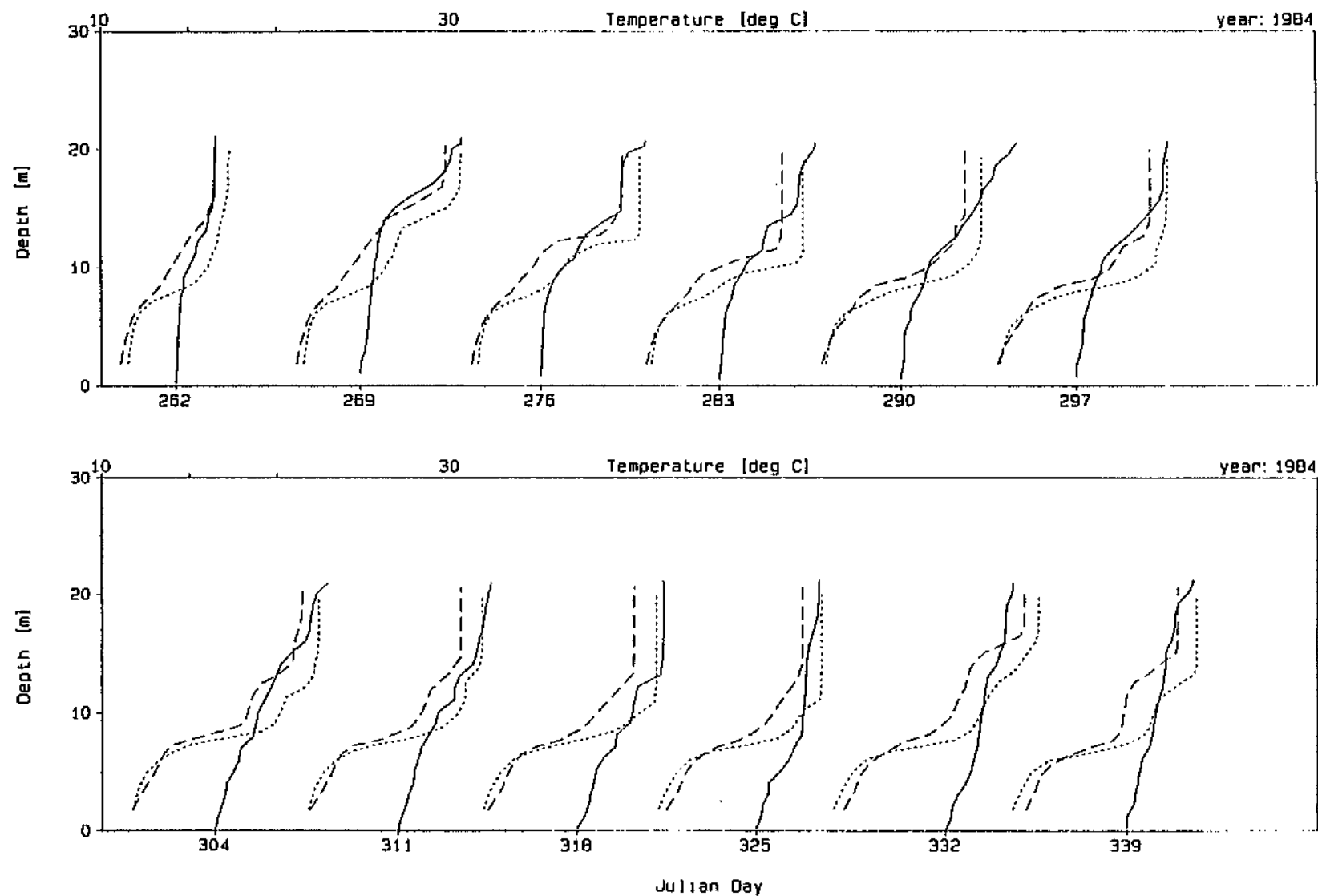


Profile Legend: — Observed Base Case --- Combined



Combination of sensitivity tests vs "base case"

Figure 2.3.3 (A)



Profile Legend: — Observed Base Case --- Combined



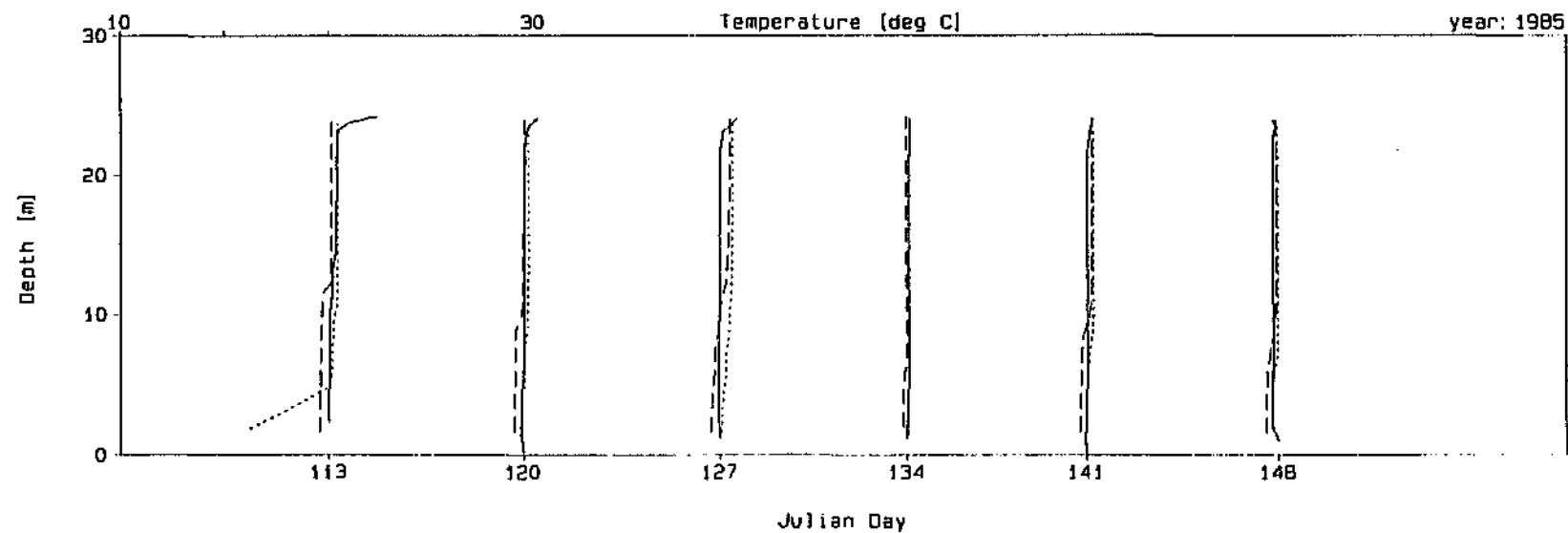
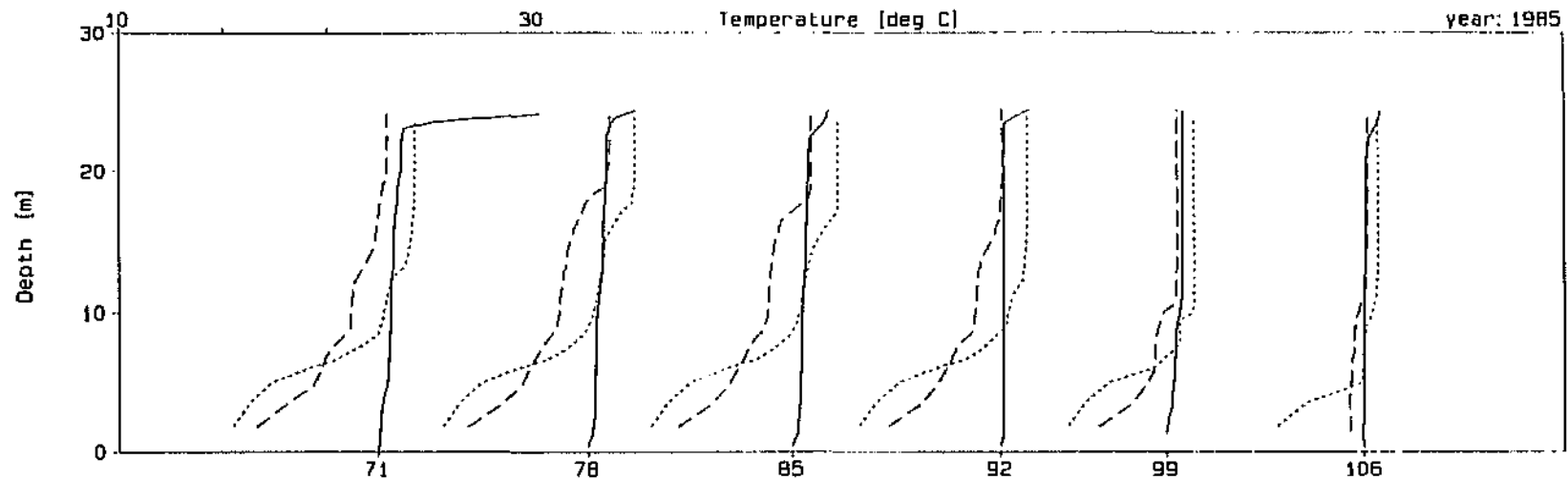
Combination of sensitivity tests vs "base case" (continued)

Figure 2.3.3 (B)

DYPLOT1D : DYRESM-1D

Dam : Hartbeespoort Dam

Plot Date : 25 Oct 94, 10:03



Profile Legend: — Observed Base Case --- Combined



Combination of sensitivity tests vs "base case" (continued)

Figure 2.3.3 (C)

Various other combinations were tried and no significant improvement was found. In the end it was decided to leave the base data set unchanged, except for the following:

- use the seasonal wind factors
- cooler summer inflow temperatures (-2°C from September (day 245) to the end of March (day 090)).

The above simulation was chosen as a "final case" and is shown (dashed line) plotted against the "base case" (dotted line) in Figure 2.3.4 (A to C).

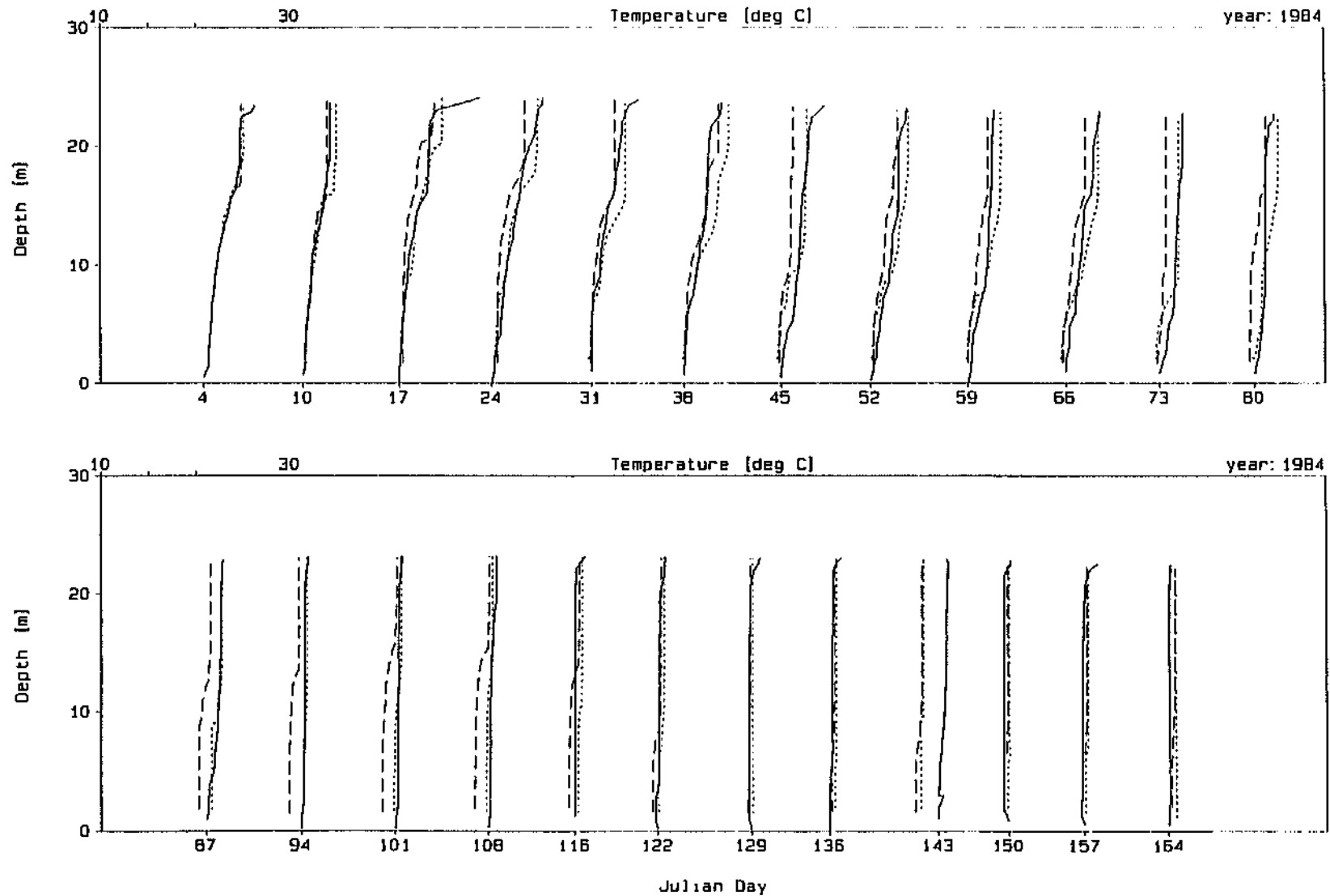
Conclusion

The model was most sensitive to changes in wind data, including changes made on a seasonal basis. The one other factor to which the model showed a relatively high degree of sensitivity was inflow temperature. The model showed relatively little sensitivity to changes of the order of 10% for the remaining input variables.

DYPLOT1D : DYRESM-1D

Dam : Hartbeespoort Dam

Plot Date : 25 Oct 94, 10:06



Profile Legend: — Observed Base Case --- Final Case



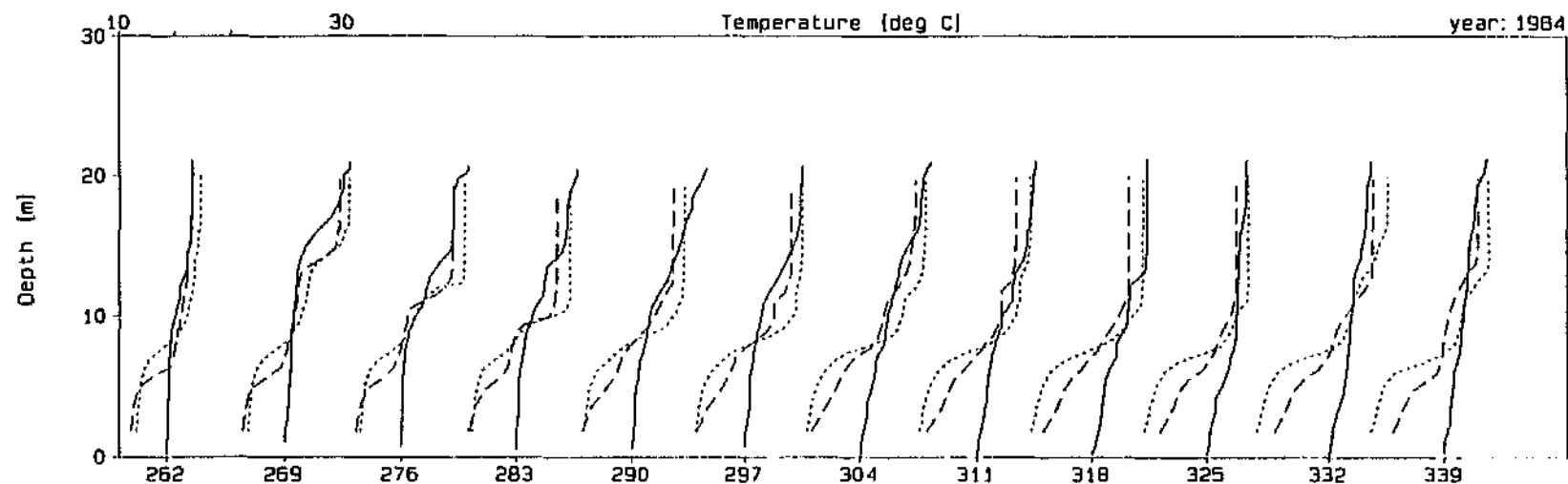
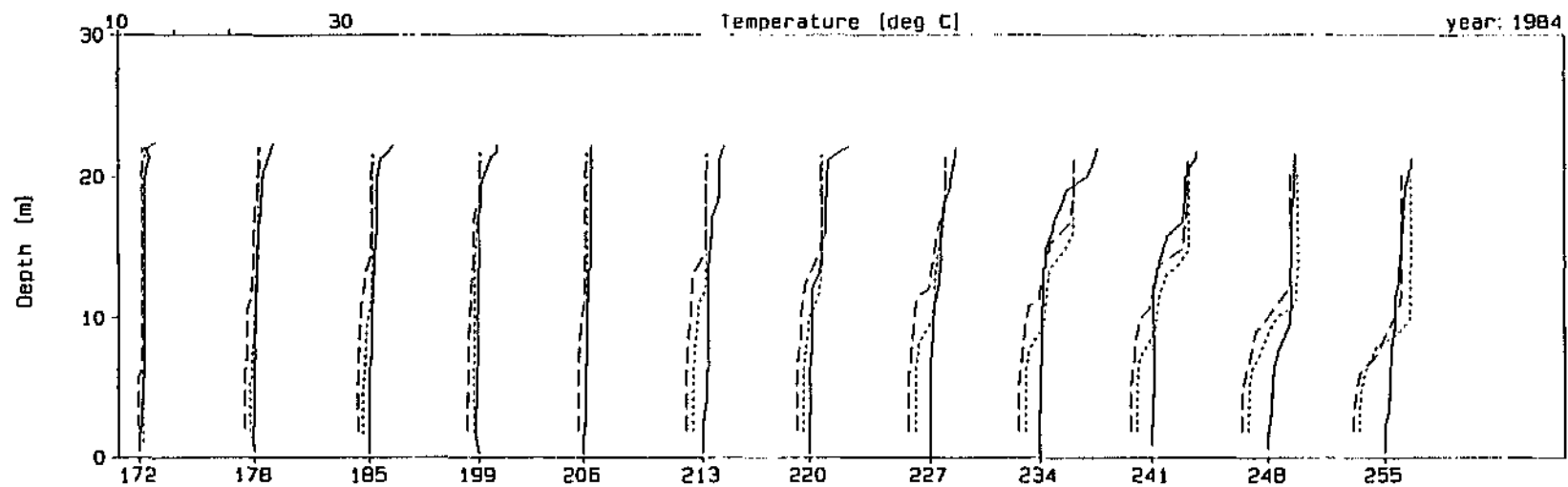
Comparison of "base case" and "final case"

Figure 2.3.4 (A)

DYPLOT10 : DYRESM-10

Dam : Hartbeespoort Dam

Plot Date : 25 Oct 94, 10:06



Julian Day

Profile Legend: — Observed Base Case --- Final Case



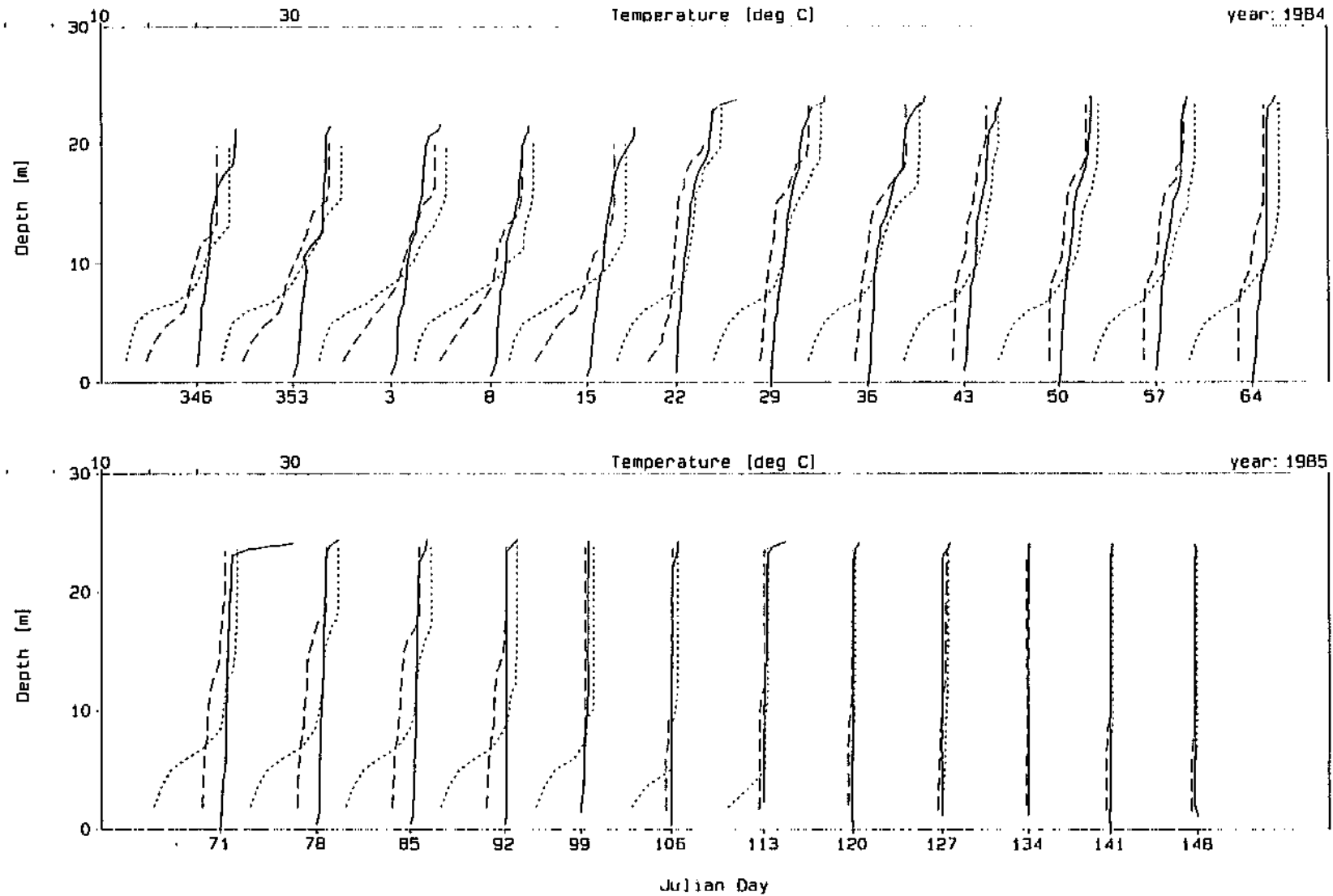
comparison of "base case" and "final case" (continued)

Figure 2.3.4 (B)

DYDPL01D DYRESM-1D

Dam : Hartbeespoort Dam

Plot Date : 25 Oct 94, 10:07



Profile Legend: — Observed Base Case - - - Final Case



Comparison of "base case" and "final case" (continued)

Figure 2.3.4 (C)

2.3.4 Bubble plume aerator design

Despite the remaining concerns with the quality of the data set for Hartbeespoort Dam, we believe that the profiles and their variation are typical for this type of impoundment. Therefore we decided to use the "final" simulation to further test and demonstrate the application of the bubble plume destratification routine. As before, the analysis should not be viewed as a full design of a bubbler system for Hartbeespoort Dam but rather as a demonstration of the feasibility of a bubbler required for adequate destratification in a typical reservoir in the summer rainfall region.

The bubbler design philosophy described in Section 2.1.3 of this report is followed here. Three Julian days with varying levels of stratification were chosen from the "final" simulated profiles. The equivalent linear stratifications that have the same potential energy as these profiles were calculated, and are shown in Table 2.3.3 below.

TABLE 2.3.3 : TEMPERATURE PROFILE CHARACTERISTICS

| Julian Day of Temperature Profile | Degree of stratification | | $PE_{\text{initial}} - PE_{\text{final}}$ (GJoules) |
|--------------------------------------|--------------------------|----------------|--|
| | (°C/m) | Description | |
| 84038 (simulated) - 7 February 1984 | 0,16 | 'weak' | 1,1 |
| 84241 (simulated) - 28 August 1984 | 0,26 | 'intermediate' | 0,7 |
| 84290 (simulated) - 16 October 1984 | 0,50 | 'strong' | 0,5 |

The last profile described in Table 2.3.3 represents 'strong' stratification requiring a bubbler configuration capable of destratifying an already stratified water body. The first and second profiles display 'weak' and 'intermediate' stratifications respectively and are typical of profiles that a 'maintenance' bubbler system should be able to destratify.

It was decided that bubbler configurations for stratification of the entire range from 0,16 °C/m to 0,5 °C/m would be tested to enable the design of a bubbler system that can both destratify an already strongly stratified reservoir, and prevent the onset of stratification and maintain a mixed state.

The total pressure head at the level of the bubbler was taken to be 38,9 m of water, made up of the 30 m FSL head and an atmospheric pressure head of 8,9 m of water. Using the first and second efficiency peak concept, associated with the development of one and two

whole bubble plumes between the plume source and water surface respectively, both total and per source air flow rates were determined for the range of profiles described above. Table 2.3.4 shows a summary of the more pertinent results of these calculations.

During the period modelled, the dam varied between 19,05 m and 24,43 m in depth, with an average of approximately 23 m. This corresponds to approximately 20 % to 40 % of full supply capacity. Therefore, although the overall design of the bubbler should be for FSC, the modelled results will correspond to a lower reservoir height. The effect of using a reservoir depth of 20 m was also investigated. As shown in Table 2.3.4, the effect of decreasing the depth was to decrease the air flow per source (Q_s), and increase the total air flow rate (Q_t).

TABLE 2.3.4 : BUBBLE PLUME AERATOR ANALYSIS RESULTS

| Scenario | Total Head (m) | dT/dz (°C/m) | No. Plumes | μ (%) | Q_s (l/s) | dPE (GJ) | Time (days) | Calc. Q_t (l/s) | N_t | Source Spacing (m) | Aerator Length (m) |
|----------|----------------|--------------|------------|-----------|-------------|----------|-------------|-------------------|-------|--------------------|--------------------|
| 1 | 38,9 | 0,160 | 1 | 6,3 | 4,2 | 1,1 | 21 | 89,0 | 21,2 | 6,0 | 127,0 |
| 2 | 38,9 | 0,160 | 2 | 4,3 | 0,50 | 1,1 | 21 | 130,3 | 258,4 | 6,0 | 1550,5 |
| 3 | 38,9 | 0,260 | 1 | 8,0 | 10,93 | 0,7 | 21 | 44,6 | 4,1 | 6,0 | 24,5 |
| 4 | 38,9 | 0,260 | 2 | 5,0 | 1,26 | 0,7 | 21 | 71,3 | 56,6 | 6,0 | 339,4 |
| 5 | 38,9 | 0,503 | 1 | 9,5 | 25,22 | 0,5 | 21 | 26,8 | 1,1 | 6,0 | 6,4 |
| 6 | 38,9 | 0,503 | 2 | 6,5 | 2,52 | 0,5 | 21 | 39,2 | 15,5 | 6,0 | 93,2 |
| 7 | 28,9 | 0,160 | 1 | 6,3 | 2,32 | 1,1 | 21 | 133,5 | 57,5 | 6,0 | 345,3 |
| 8 | 28,9 | 0,160 | 2 | 4,3 | 0,28 | 1,1 | 21 | 195,6 | 702,6 | 6,0 | 4215,9 |
| 9 | 28,9 | 0,260 | 1 | 8,0 | 6,03 | 0,7 | 21 | 66,9 | 11,1 | 6,0 | 66,6 |
| 10 | 28,9 | 0,260 | 2 | 5,0 | 0,70 | 0,7 | 21 | 107,1 | 153,8 | 6,0 | 922,9 |
| 11 | 28,9 | 0,503 | 1 | 9,5 | 13,92 | 0,5 | 21 | 40,2 | 2,9 | 6,0 | 17,3 |
| 12 | 28,9 | 0,503 | 2 | 6,5 | 1,39 | 0,5 | 21 | 58,8 | 42,3 | 6,0 | 253,5 |

where: dT/dz = equivalent linear stratification
 μ = mechanical efficiency (greater efficiency being desirable)
 Q_s = air flow rate per source
dPE = difference in potential energy between the stratified and mixed profile
 Q_t = total air flow rate for the bubbler system (as calculated)
 N_t = total number of bubble plume sources

Based on the above table, several bubbler scenarios were designed using an actual delivery total air flow rate of 157 l/s per compressor. Since it is only possible to provide additional total air flow rate in increments as provided by whole compressors (in this case 157 l/s), the actual designs of the bubblers differ slightly from the calculated values in Table 2.3.4. The design values are shown in Table 2.3.5.

The scenarios chosen for bubbler simulations are:

Scenarios 1 to 6: For the FSL design, one compressor unit capable of delivering a total air flow rate of 157 l/s was used with air flow rates per source as close as possible to those shown in Table 2.3.4.

Scenarios 7 to 12: Four bubbler simulations were originally chosen from scenarios 7 to 12 for the decreased reservoir level. As will be evident later, only two of these (scenarios 10 and 12) are reported on further in this report.

For each of these scenarios the appropriate number of bubble sources was calculated. Where practical, the lengths of the bubble plume systems were calculated based on the number of sources and the rule-of-thumb that the diameter of a bubble plume increases at the rate of 0,2 times the height of rise, assuming non-interacting plumes. Where this assumption resulted in impractical bubbler lengths, a spacing of 2 m was chosen assuming interacting plumes. The scenarios selected are summarised in Table 2.3.5.

TABLE 2.3.5 : BUBBLE PLUME DESTRATIFICATION SYSTEM DESIGN SCENARIOS

| Design Scenario | | Based on full reservoir (30m depth) | | | | | | (20m depth) | | | |
|--|-------------|-------------------------------------|------|----------------|------|----------|------|-------------|------|--------|----------|
| | | 1 | 2 | 3 | 4 | 5 | 6 | 7 | 8 | 10 | 12 |
| First or second peak case* | | 1st | 2nd | 1st | 2nd | 1st | 2nd | 1st | 2nd | 2nd | 2nd |
| Degree of stratification* | (°C/m) | 0,16 | 0,16 | 0,26 | 0,26 | 0,50 | 0,50 | - | 0,16 | 0,26 | 0,50 |
| | Description | 'weak' | | 'intermediate' | | 'strong' | | 'weak' | | 'int.' | 'strong' |
| Total design air flow rate Q_t (l/s) | | 157 | 157 | 157 | 157 | 157 | 157 | 314 | 314 | 157 | 157 |
| Individual bubble source air flow rate Q_b (l/s)** | | 4,24 | 0,5 | 10,47 | 1,26 | 26,23 | 2,53 | 0,5 | 0,28 | 0,70 | 1,39 |
| Number of bubble sources | | 37 | 314 | 15 | 125 | 6 | 62 | 628 | 1121 | 224 | 113 |
| Length of bubbler system (m) | | 222 | 1884 | 90 | 750 | 36 | 372 | 1256 | 2242 | 896 | 678 |
| Number of compressors | | 1 | 1 | 1 | 1 | 1 | 1 | 2 | 2 | 1 | 1 |

* indicates values that were obtained directly from Table 2.3.4

** indicates values that were calculated to be as close as possible to those in Table 2.3.4

2.3.5 Bubble plume destratification - Simulation results

Details of the specific operating conditions used for the chosen scenarios are given in Table 2.3.6, for example whether the bubbler has interacting or independent plumes, and the time period over which the bubbler operated.

TABLE 2.3.6 : OPERATING CONDITIONS FOR BUBBLER RUNS

| Base Scenario | Case | Specific Operating Conditions | | | |
|---------------|------|---------------------------------------|----------------|----------------------|--|
| | | Independent/ interacting plumes | Spacing (m) | No of compressors | Bubbler operating period |
| 1 | A | independent | 6 | 1 | 84270 (26 September 1984) to 84340 (5 December 1984) |
| 2 | A | independent | 6 | 1 | 84270 (26 September 1984) to 85064 (4 March 1985) |
| | B | independent | 6 | 1 | 84005 (5 January 1984) to 85150 (30 May 1985) |
| | C | interacting | 2 | 1 | 85001 (1 January 1985) to 85090 (31 March 1985) |
| | D | interacting | 2 | 2 | 85001 (1 January 1985) to 85090 (31 March 1985) |
| 3 | A | independent | 6 | 1 | 84270 (26 September 1984) to 84340 (5 December 1984) |
| 4 | A | independent | 6 | 1 | 84270 (26 September 1984) to 84340 (5 December 1984) |
| | D | interacting | 2 | 1 | 84173 (21 May 1984) to 85090 (31 March 1985) |
| 5 | A | independent | 6 | 1 | 84270 (26 September 1984) to 84340 (5 December 1984) |
| 6 | A | independent | 6 | 1 | 84270 (26 September 1984) to 84340 (5 December 1984) |
| | D | independent | 6 | 2 | 85024 (24 January 1985) to 85058 (27 February 1985) (5 weeks) |
| | E | interacting | 2 | 2 | 85001 (1 January 1985) to 85090 (31 March 1985) |
| 10 | D | interacting | 2 | 1 | 84173 (21 May 1984) to 85090 (31 March 1985) |
| 12 | D | independent | 6 | 2 | 85024 (24 January 1985)to 85058 (27 February 1985) |

The results of the above bubbler runs are discussed below.

Strength of design stratification

Figure 3.2.5 shows the results of bubbler runs for the first peak case (scenarios 1A, 3A and 5A) plotted against the measured field data (solid line) and the "final case" (dotted line). As detailed in Table 2.3.6, the bubbler operated from Julian day 84270 to 84340 (26 September 1984 to 5 December 1984), a period of 10 weeks. The effect of the bubbler can be seen in that the bubbler simulation profiles indicate a more mixed reservoir when compared with both simulated and observed profiles without bubble plume operation.

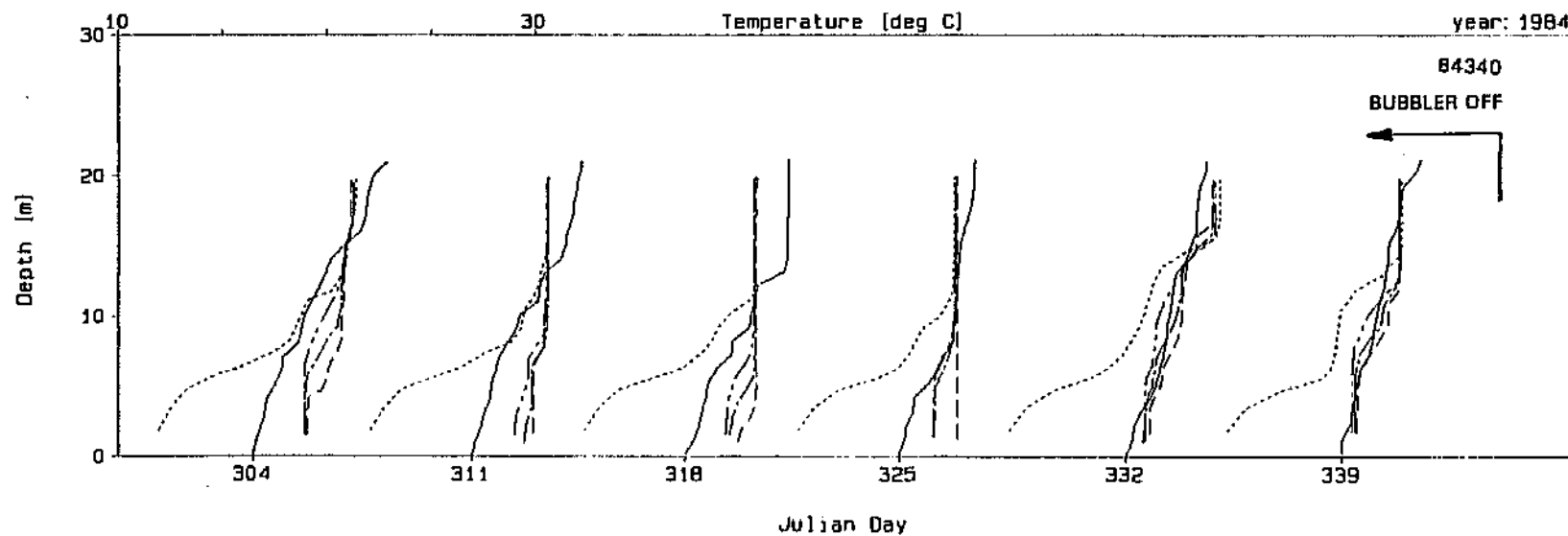
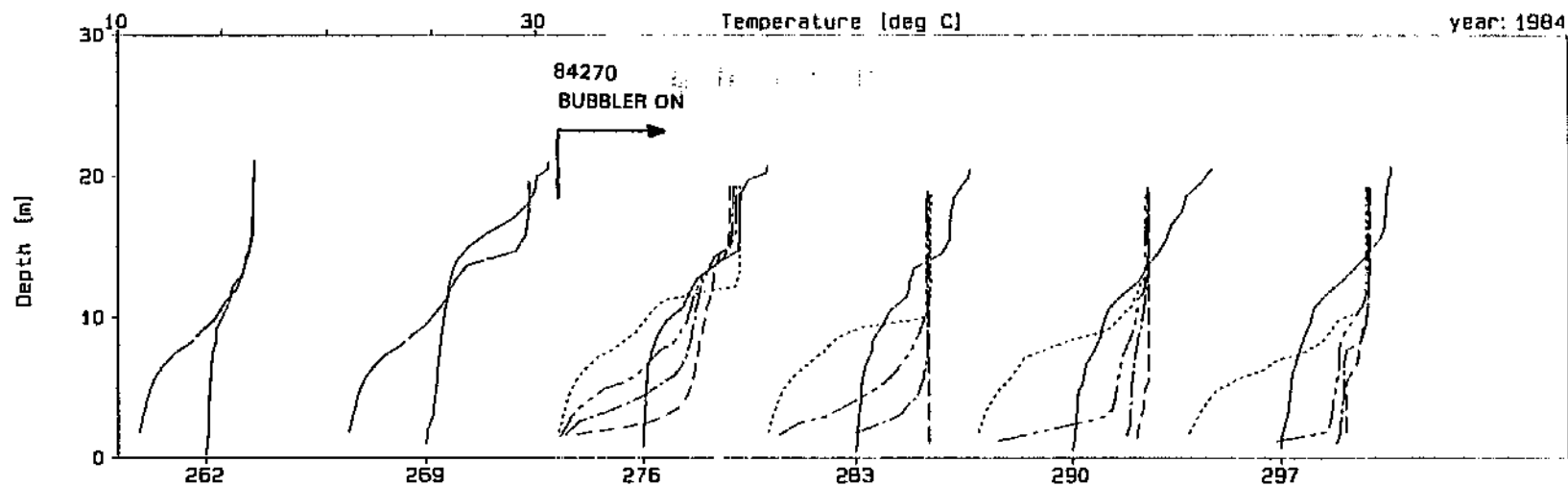
The scenario based on the design for a weak stratification (scenario 1A) performs best at destratifying the reservoir (refer to profiles 84276 and 84283), as well as maintaining the mixed state (profiles 84318-84339). Scenario 1A has the lowest air flow rate per source of the three scenarios being compared ($Q_0=4,24$ l/s).

The above observation contrasts with that shown in Figure 2.3.6 which shows the results for the second peak case (scenarios 2A, 4A and 6A). Here the design based on the strong stratification (scenario 6A) performs best initially (refer to profile 84276). Once the stratification is broken down, the design based on the intermediate stratification (scenario 4A) becomes the most effective for a short while (see profile 84297), and finally the design based on the weak stratification (scenario 2A) becomes slightly more effective (profiles 84304, 84325-84339). Scenario 6A has the highest air flow rate per source of the three scenarios being compared ($Q_0=2,53$ l/s), while scenario 4A has an intermediate Q_0 of 1,26 l/s, and scenario 2A has the lowest Q_0 of 0,5 l/s.

First vs second peak case

Figures 2.3.7, 2.3.8 and 2.3.9 show comparisons of simulation results of first and second peak cases for designs based on a range of stratification strengths. These are:

- weak stratification : scenarios 1A and 2A (first and second peak respectively),
- intermediate stratification : scenarios 3A and 4A (first and second peak respectively),
and
- strong stratification : scenarios 5A and 6A (first and second peak respectively).

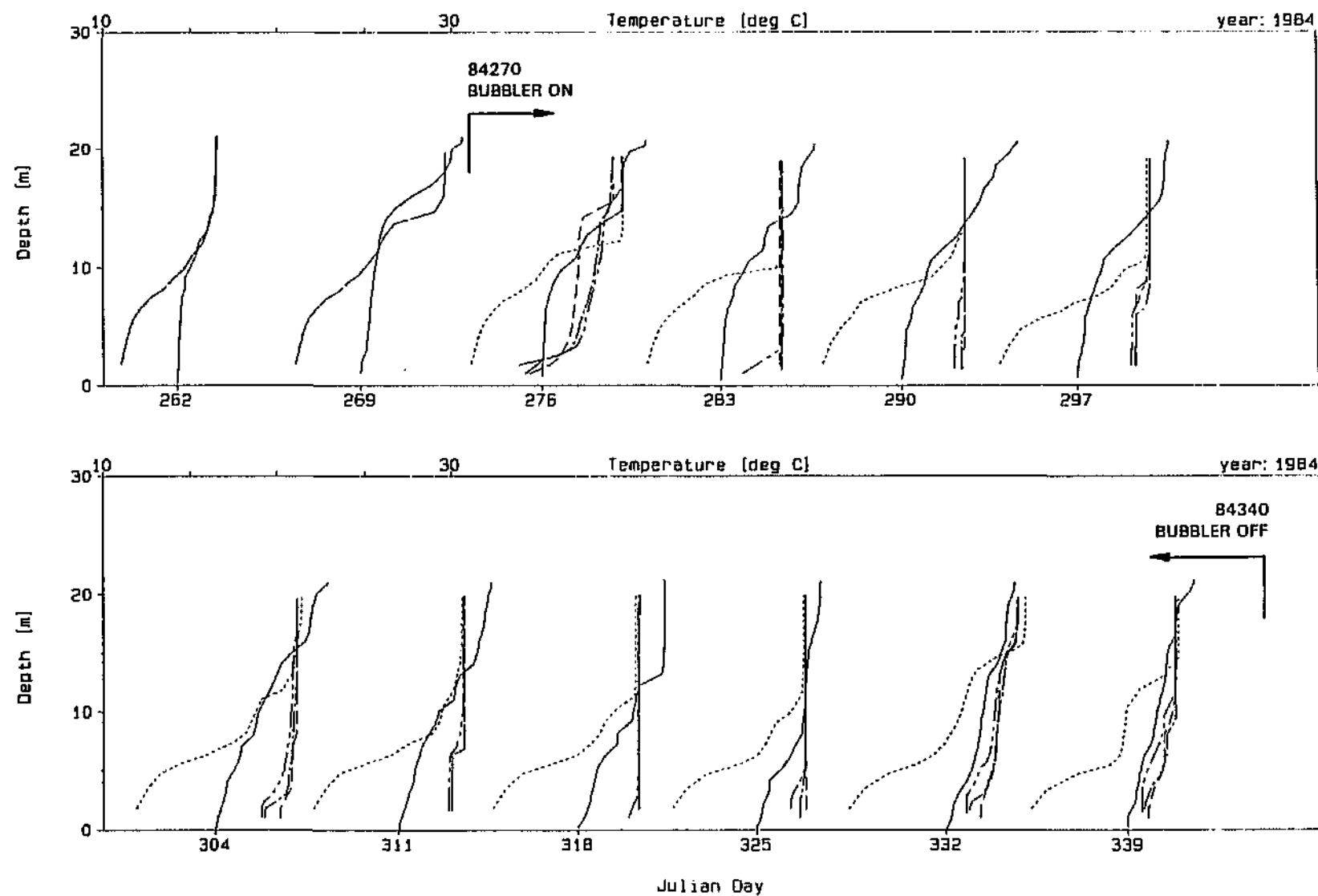


Profile Legend: — Observed Final Case --- 1A: weak --- 3A: interm. --- 5A: strong



Bubble plume scenarios 1A, 3A and 5A - first peak case

Figure 2.3.5

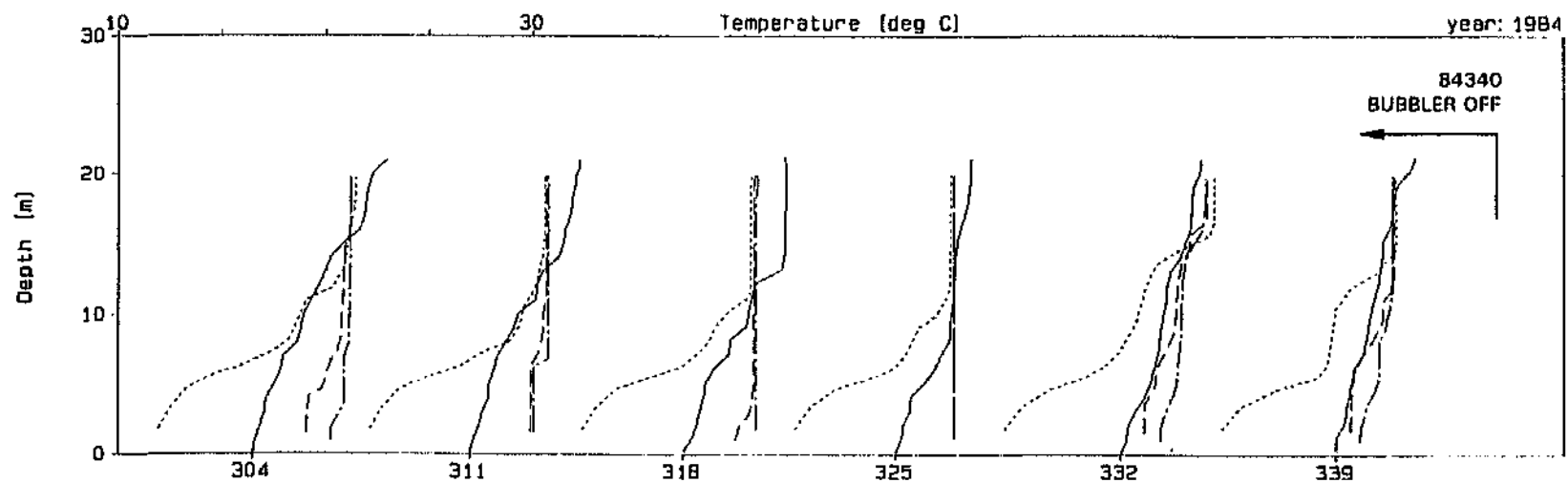


Profile Legend: — Observed Final Case --- 2A: weak -.- 4A: interm. - - - 6A: strong



Bubble plume scenarios 2A, 4A and 6A - second peak case

Figure 2.3.6

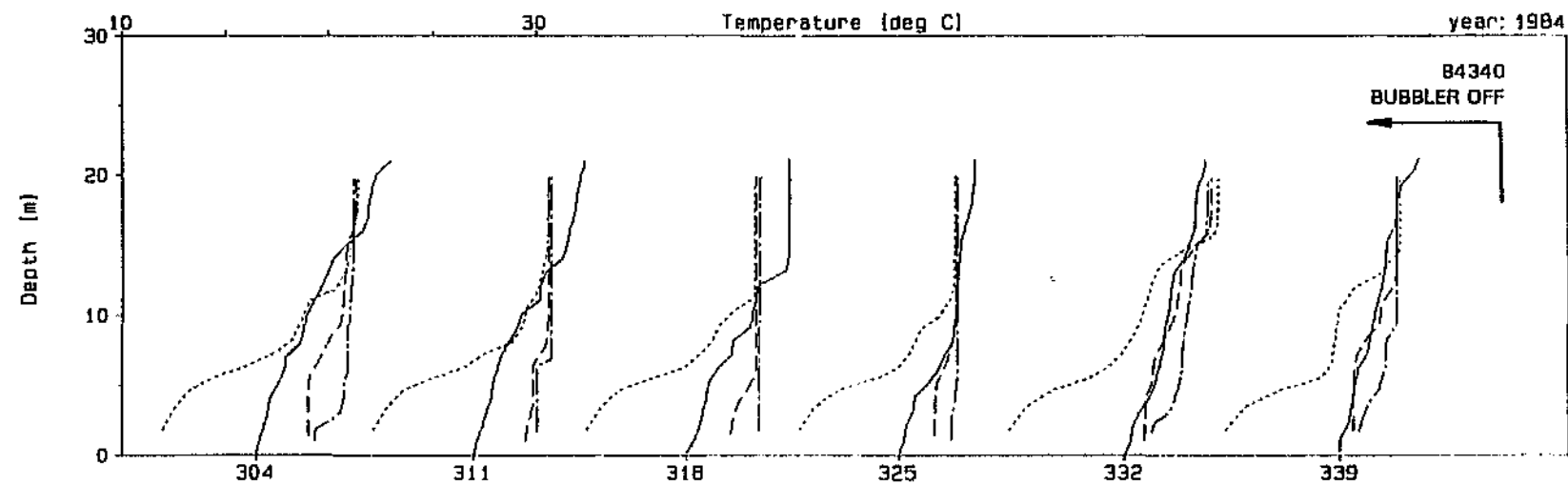
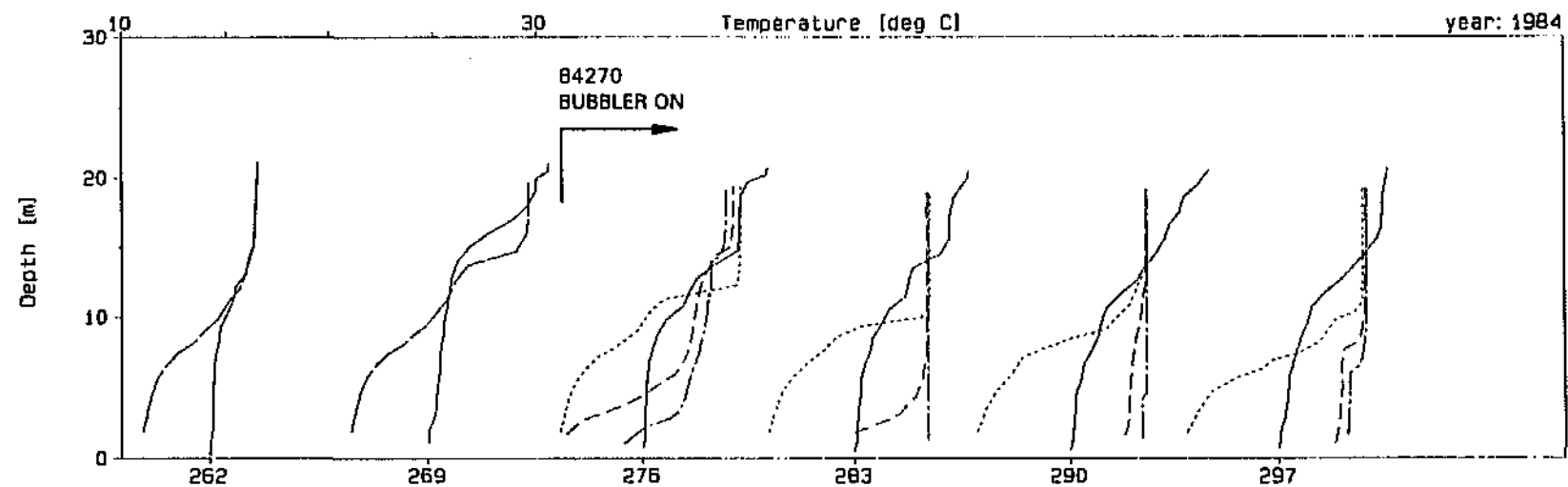


Profile Legend: — Observed Final Case - - - 1A: 1st pk — 2A: 2nd pk



Design based on a weak stratification: first (1A) vs second (2A) peak cases

Figure 2.3.7



Julian Day

Profile Legend: — Observed Final Case --- 3A: 1st pk -.- 4A: 2nd pk



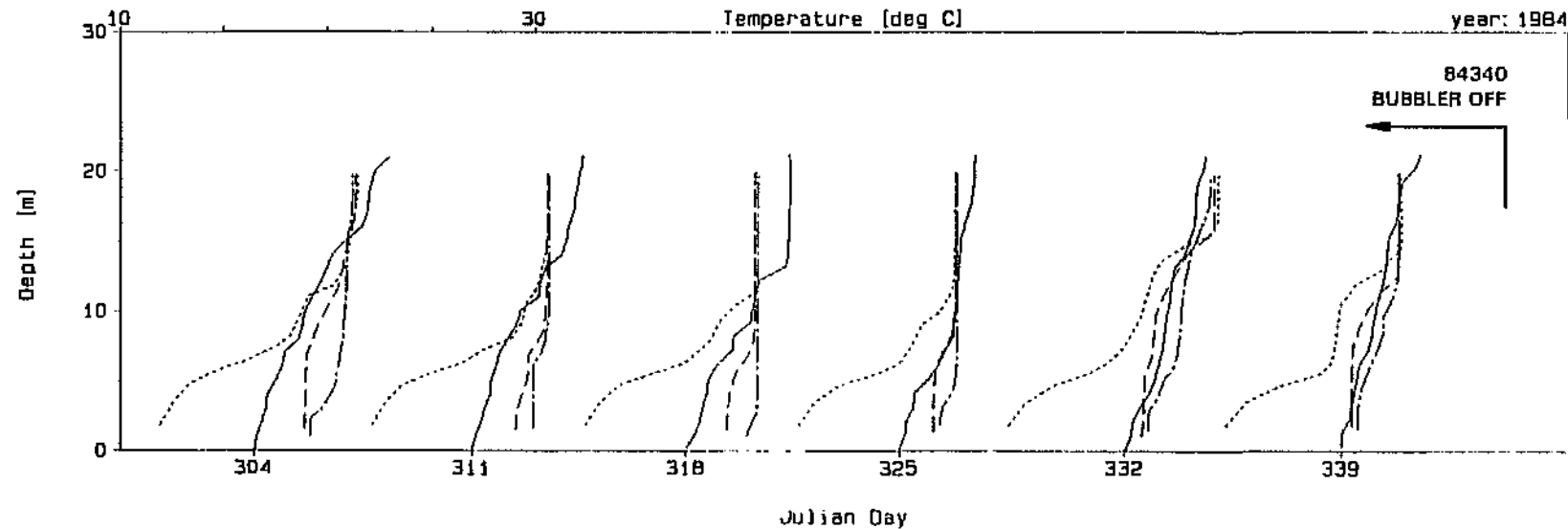
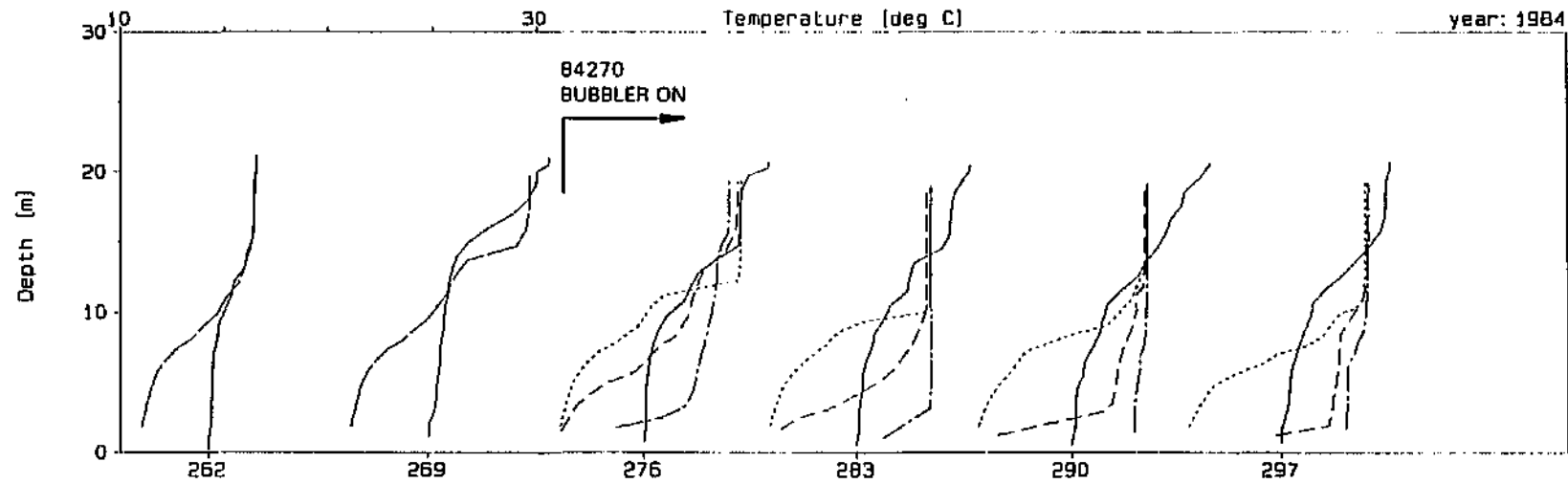
Design based on an intermediate stratification: first (3A) vs second (4A) peak cases

Figure 2.3.8

DyPlotID : DYRESM-1D

Dam : Hartbeespoort Dam

Plot Date : 29 Mar 95, 15: 48



Profile Legend: — Observed Final Case --- 5A: 1st pk -.- 5A: 2nd pk



Design based on a strong stratification: first (5A) vs second (6A) peak cases

Figure 2.3.9

With reference to Figure 2.3.7, the first peak case for the design based on the weak scenario is initially more effective (profile 84276) while the existing stratification in the reservoir is being broken down. Once the reservoir is in a reasonably mixed state (84283 onwards), the second peak case is slightly more effective.

Figure 2.3.8 shows the results for the designs based on the intermediate stratification. The second peak case (scenario 4A) is more effective than the first peak case at both breaking down the existing stratification (profile 84276) and maintaining a mixed condition. A similar result is shown in Figure 2.3.9 for the designs based on the strong stratification.

Independent vs interacting plumes

One example of a comparison between independent and interacting plumes is given in Figure 2.3.10. This figure shows the results with the bubbler operating continuously from Julian day 84005 to 85150. When comparing the two, the independent plume case (scenario 2B) is more effective at maintaining the reservoir in a mixed condition than the interacting plume case (scenario 2C).

Reservoir depth

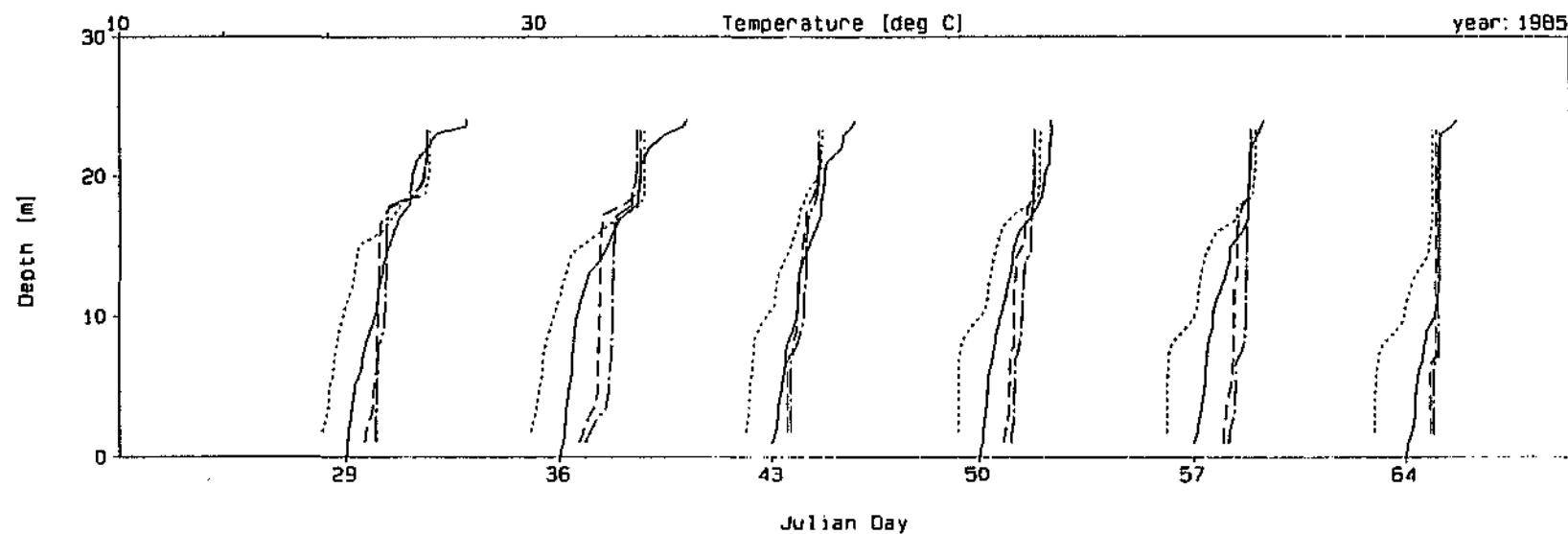
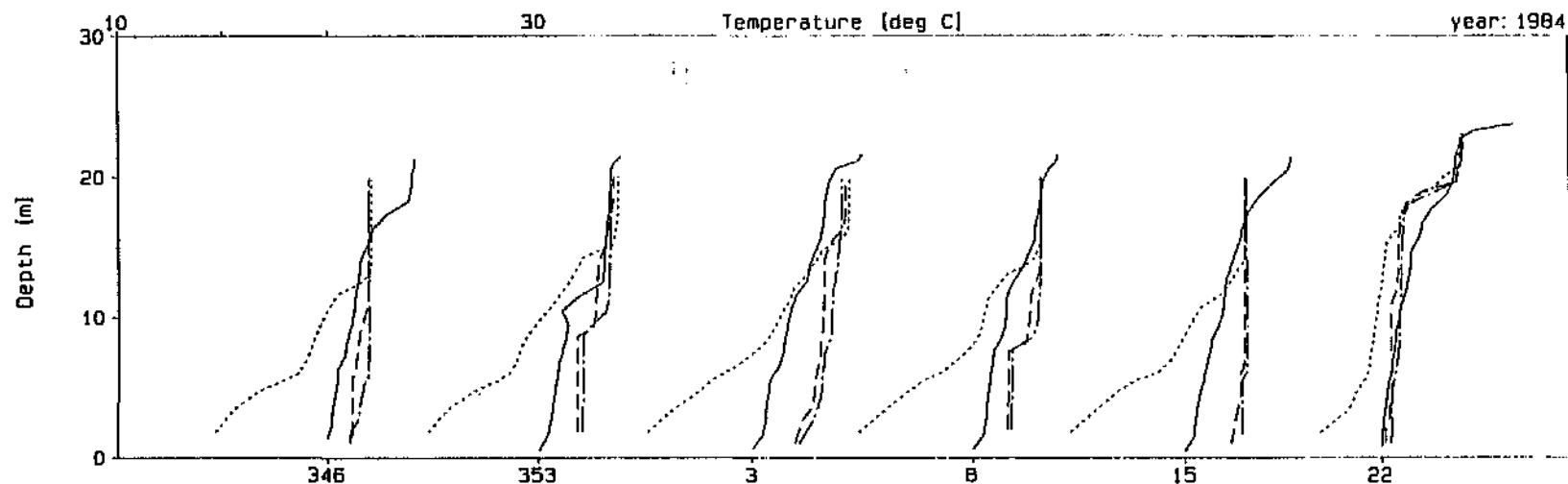
As mentioned previously, the available observed data for Hartbeespoort Dam covers a period where the water level is drawn down to a depth of approximately 20m, compared to the reservoir depth from FSL of 30m. This corresponds to a volume of only 30% of FSC. A hypothetical case for a full reservoir was obtained by adjusting the observed data in order to provide a scenario to test bubble plume destratification with the reservoir level close to FSL. The bubbler designs used are detailed in Table 2.3.6.

The first test scenario was for the case of attempting to maintain a mixed reservoir. Bubbler designs based on the full dam (scenario 4D) and drawn down dam (scenario 10D) were run using the actual observed data set, which represents the drawn down case, and the hypothetical case for the full reservoir. Plots of the results of these runs are shown in Figure 2.3.11 (drawn down case) and Figure 2.3.12 (full dam case).

DYPLOT10 : DYRESM-10

Dam : Hartbeespoort Dam

Plot Date : 26 Oct 94, 15:16



Profile Legend: — Observed Final Case --- 2C (inter) - - - 2A (indep)



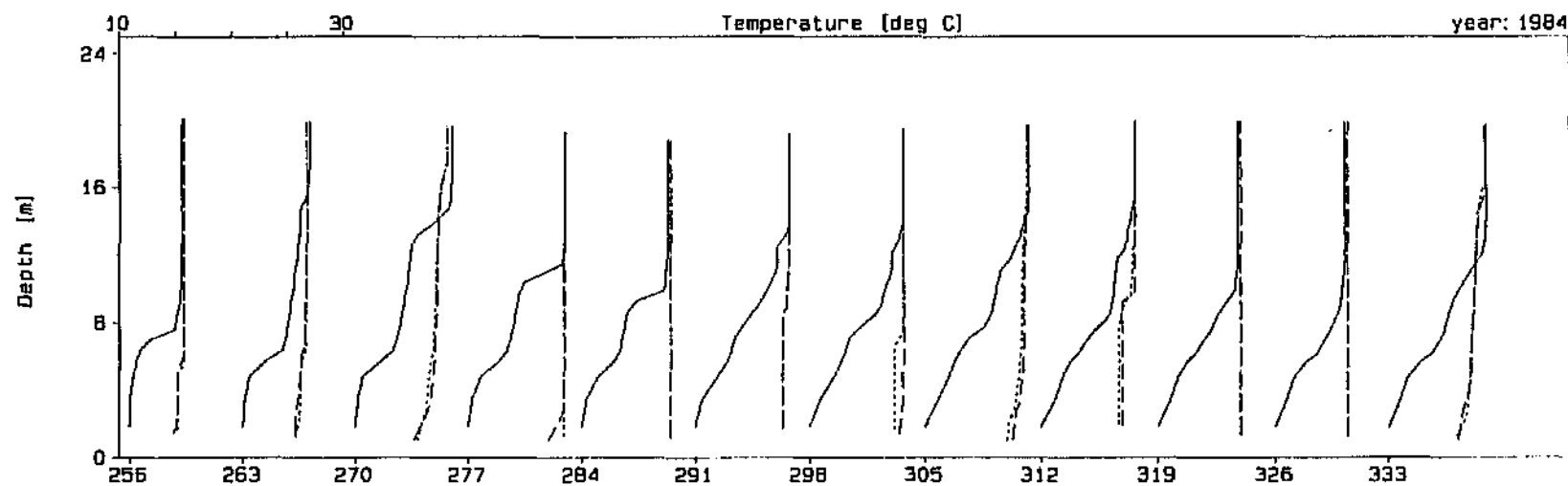
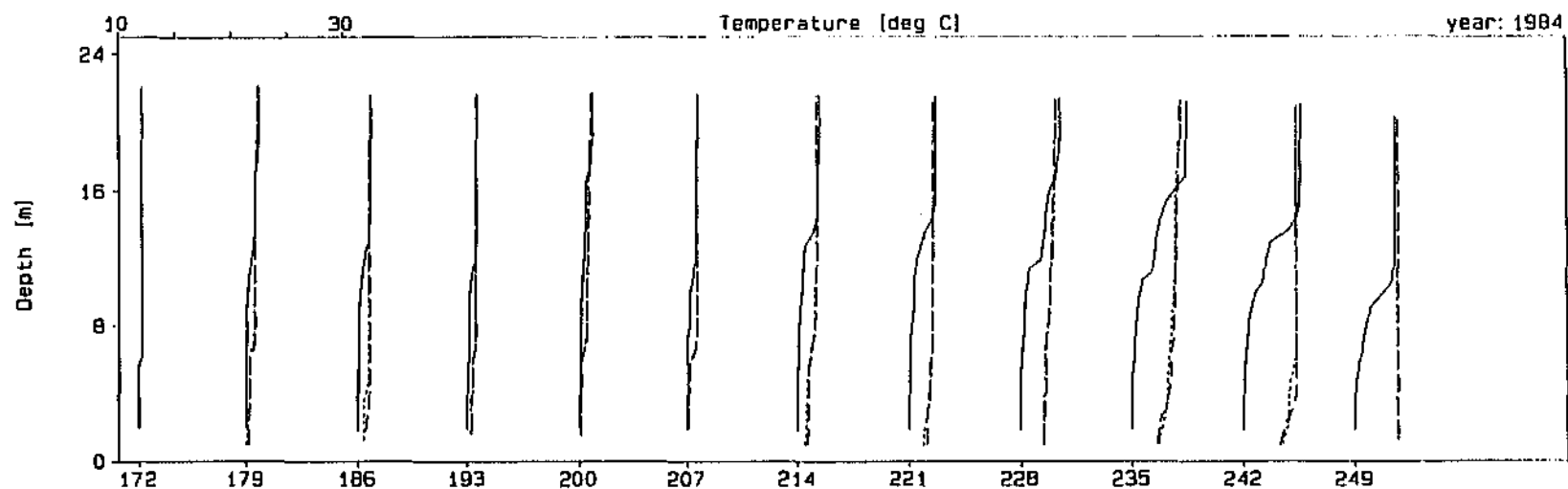
Comparison of effectiveness of independent and interacting plumes at destratification

Figure 2.3.10

DyPlotID : DYRESM-1D

Dam : Hartbeespoort Dam

Plot Date : 30 Mar 95, 16:31



Julian Day

Profile Legend: — Final Case - - - 10D (20m)



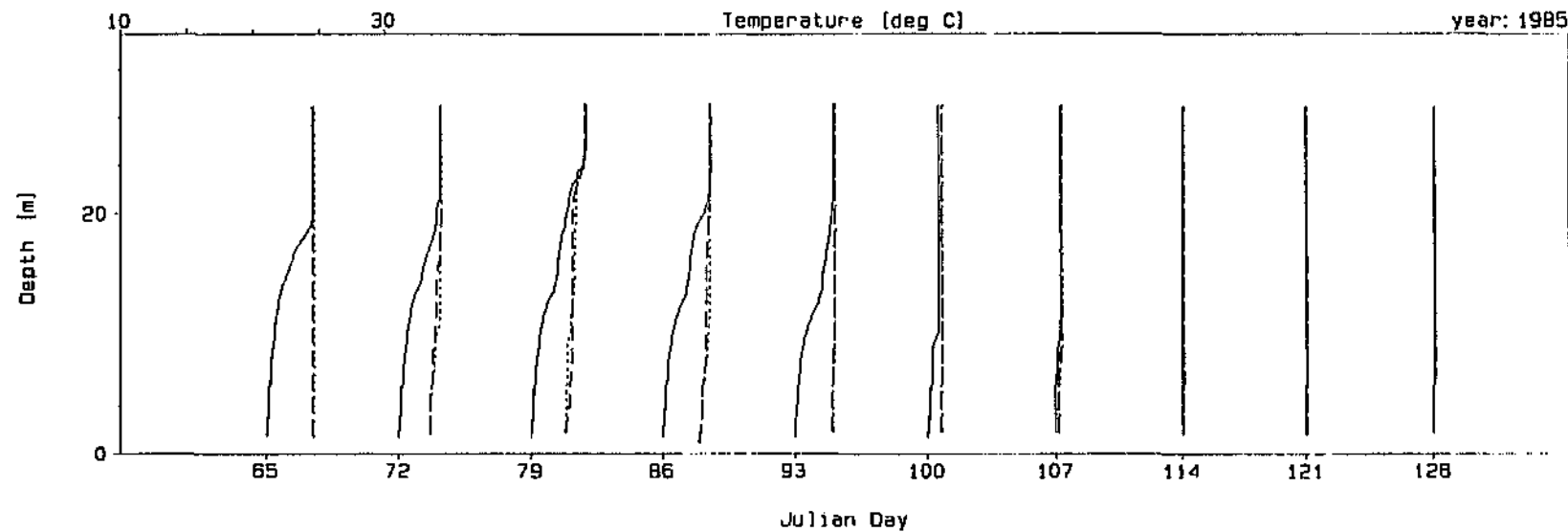
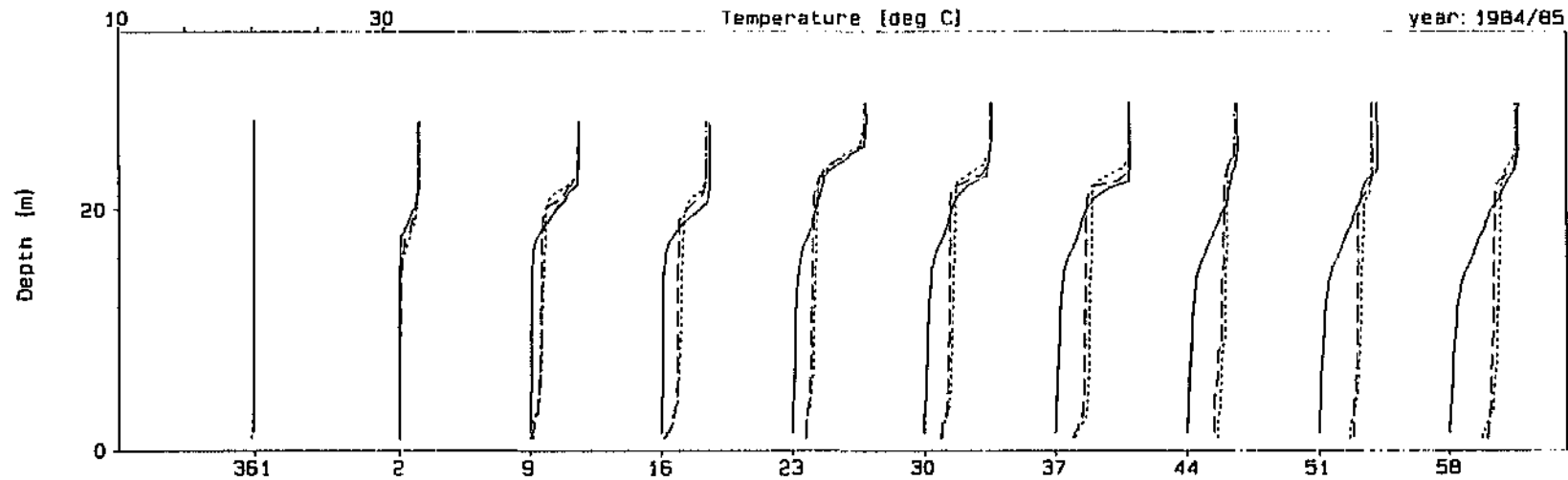
Drawn down reservoir - maintenance: Designs for drawn down case vs full dam case

Figure 2.3.11

DyPlot10 : DYRESM-1D

Dam : Hartbeespoort Dam

Plot Date : 30 Mar 95, 16:33



Profile Legend: — Full Dam 4D (30m) --- 10D (20m)



Full reservoir - maintenance: Designs for drawn down case vs full case

Figure 2.3.12

In both cases, the difference in the two results is very slight, but in each case the design based on the actual reservoir depth performed marginally better *ie.* in Figure 2.3.11, which represents the drawn down case, scenario 10D (the 20 m depth design) was slightly more effective. In Figure 2.3.12, which represents the hypothetical full dam case, scenario 4D (the 30 m depth design) was slightly more effective. Note that scenario 4D has a higher air flow rate per source than scenario 10D.

Destratification of a full reservoir (hypothetical case)

The second test carried out was for the case of the destratification of an already stratified reservoir. Once again, bubbler designs based on the full dam (scenario 6D) and drawn down dam (scenario 12D) were used. Figure 2.3.13 compares the results for the hypothetical full dam case, and shows that the design based on the full reservoir (scenario 6D) is slightly more effective. Once again scenario 6D has a higher air flow rate per source than scenario 12D.

The indication from the above discussion is that the designs with higher air flow rates per source (Q_0) are more effective for the full dam case. This is due to the nature of the area-capacity relationship, which results in a larger volume of water being exposed to the driving forces of stratification in the full dam case.

Destratification of the hypothetical full dam case is achieved within 5 weeks, as shown on Figure 2.3.13. This period may be shortened and the destratification process improved by designing and optimising a bubbler based on a stratified profile from the full dam case, as opposed to using a design based on an observed profile from the drawn down period, as was the case above.

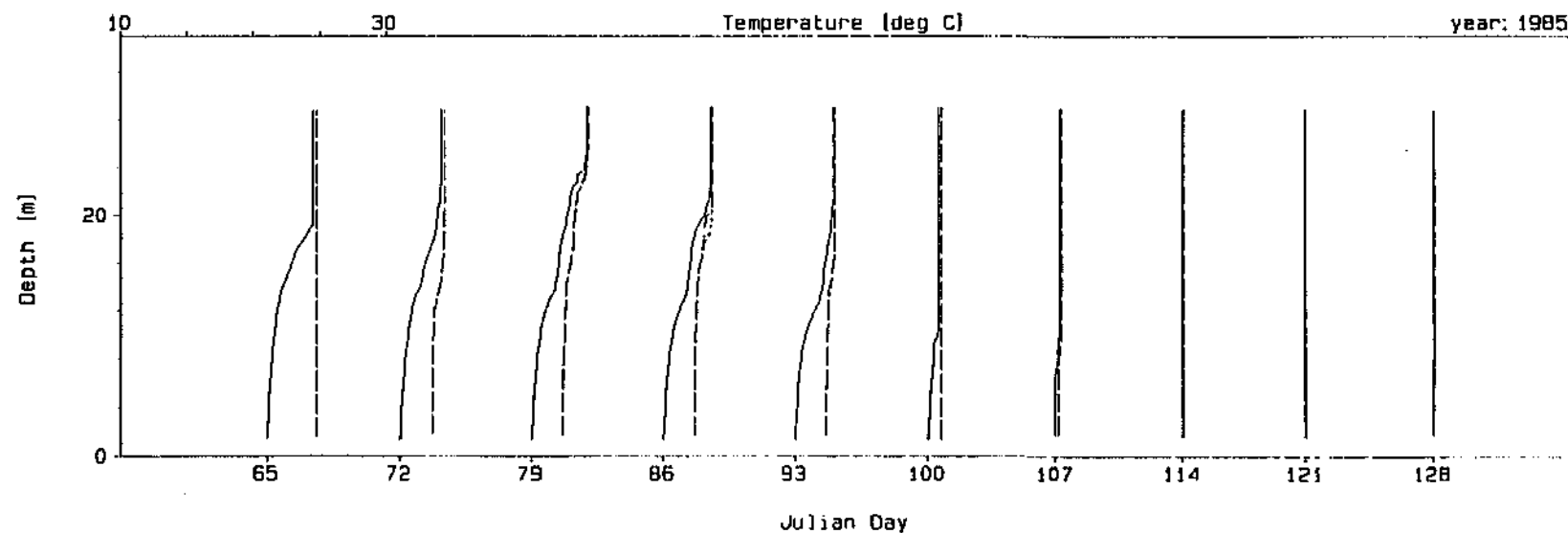
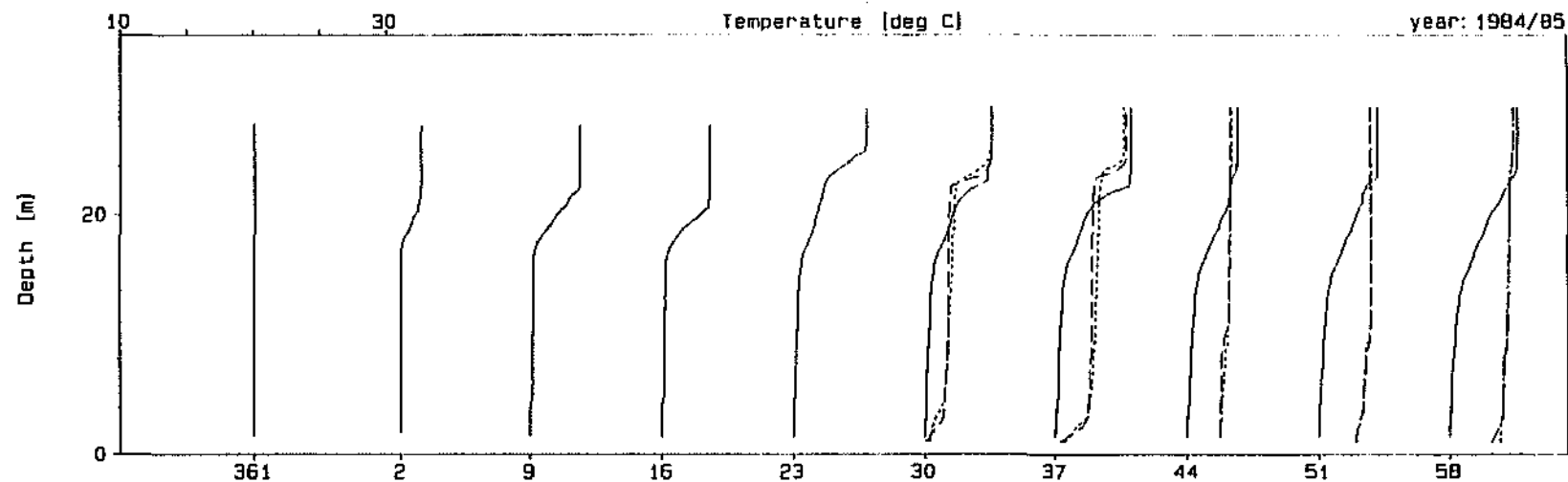
Maintenance of a full reservoir (hypothetical case)

Figure 2.3.14 shows a maintenance situation where a design for the full reservoir case was compared to the effect obtained by doubling the total air flow rate (Q_T) by using two compressors (scenario 2D) instead of one (scenario 2C), and keeping the air flow rate per source (Q_0) the same in both cases. It is evident that the increased total air flow rate provides a significant improvement in the capacity of the bubbler to attempt to maintain the full reservoir in a mixed state.

DyPlot1D : DYRESM-1D

Dam : Hartbeespoort Dam

Plot Date : 30 Mar 95, 11:39



Profile Legend: — Full Dam 6D (30m) --- 12D (20m)



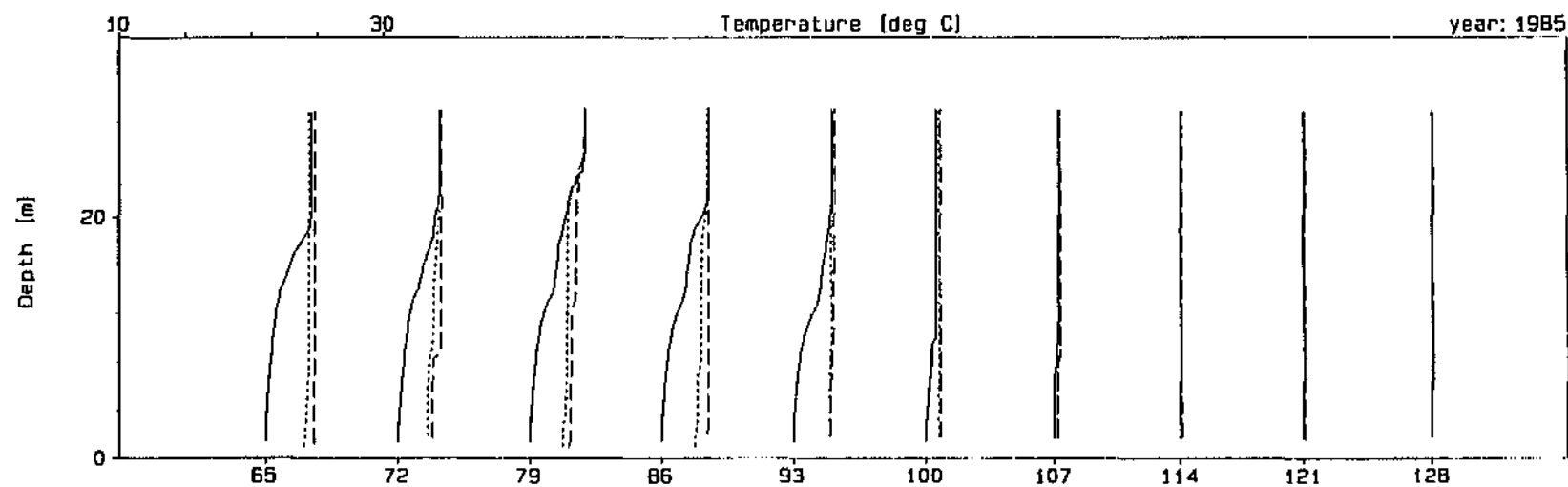
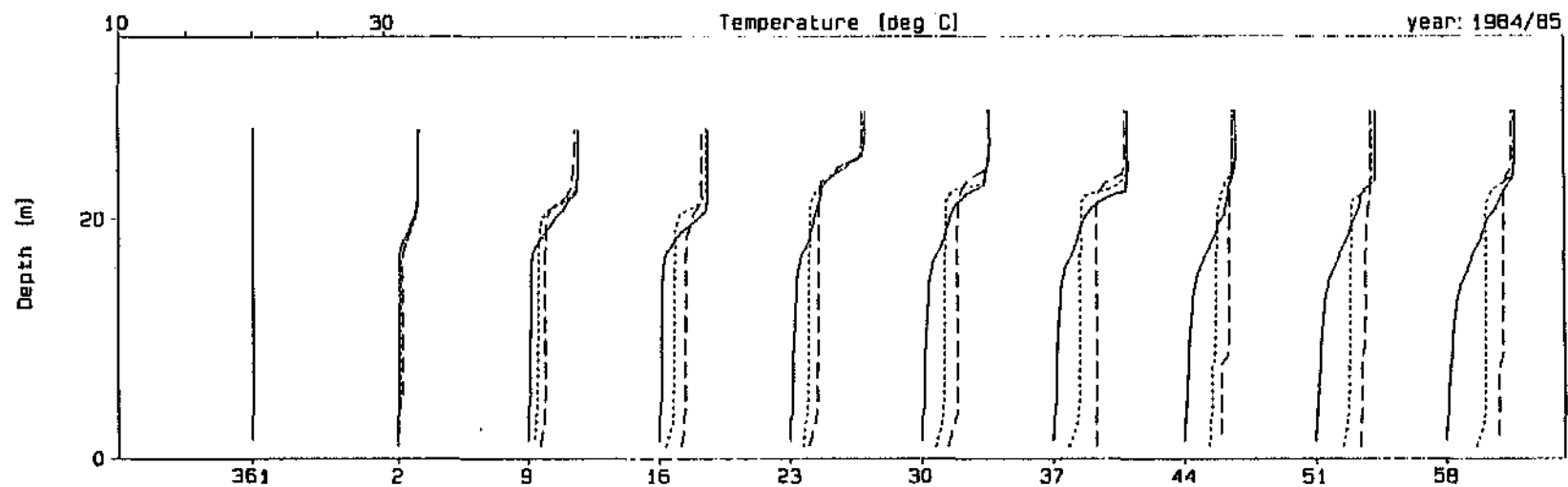
Full reservoir - destratification: Designs for drawn down case vs full dam case

Figure 2.3.13

DyPlot1D : DYRESM-1D

Dam : Hartbeespoort Dam

Plot Date : 30 Mar 95, 11:38



Julian Day

Profile Legend: — Full Dam 2C-1 comp. - - - 2D-2 comp.



FuB reservoir - maintenance: Comparison of bubbler designs with differing total air flow rates (QT)

Figure 2.3.14

The above observation led to a further test using the scenario 6E 'destratification' bubbler in a 'maintenance' mode. The two designs compared have the same total air flow rate but scenario 6E has a higher air flow rate per source. As shown in Figure 2.3.15, the design based on the stronger stratification (6E) was more effective at attempting to maintain a mixed reservoir.

Effect of a disturbance

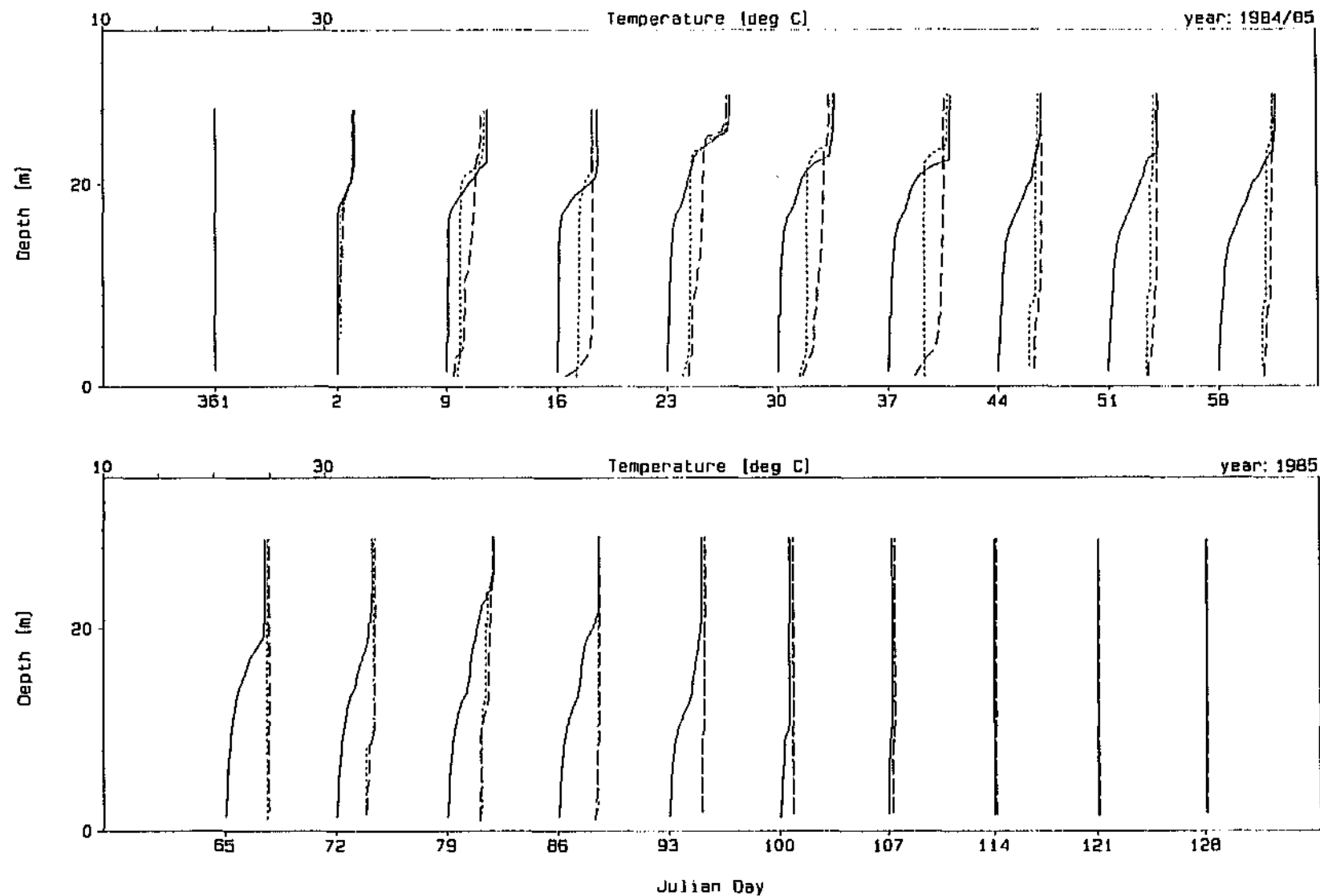
With reference to Figure 2.3.15, there is an increase in reservoir depth between profiles 85016 and 85023, and a corresponding increase in the tendency for stratification to occur. Figure 2.3.16 shows the profiles as before, but also includes the inflow to the reservoir. It shows a sudden large inflow between Julian days 85017 and 85023 that caused the increase in stratification in the reservoir.

The scenario 6E bubbler (destratification design) is seen to react better to the inflow disturbance than bubbler scenario 2D (maintenance design) in that the 6E bubbler remixes the reservoir more effectively. This is because the stratification being broken down is close to that for which the 6E bubbler was designed.

Bubbler system operational costs

The operational costs of the scenarios for the hypothetical full dam case are estimated as follows.

Based on information provided by ESKOM, an electricity cost of 24,18c/kWh for the first 1000 kWh in a month and 13,98c/kWh for the remaining hours was used (Quibell, pers comm, 1984). The commercially available compressors capable of supplying the air flow rate and pressure required have a power rating of 55 kW. The electricity cost to operate one compressor for the first day in any month would be R286,54. For any day thereafter, the cost would be R184,54. The electricity costs for the combination scenario would be:



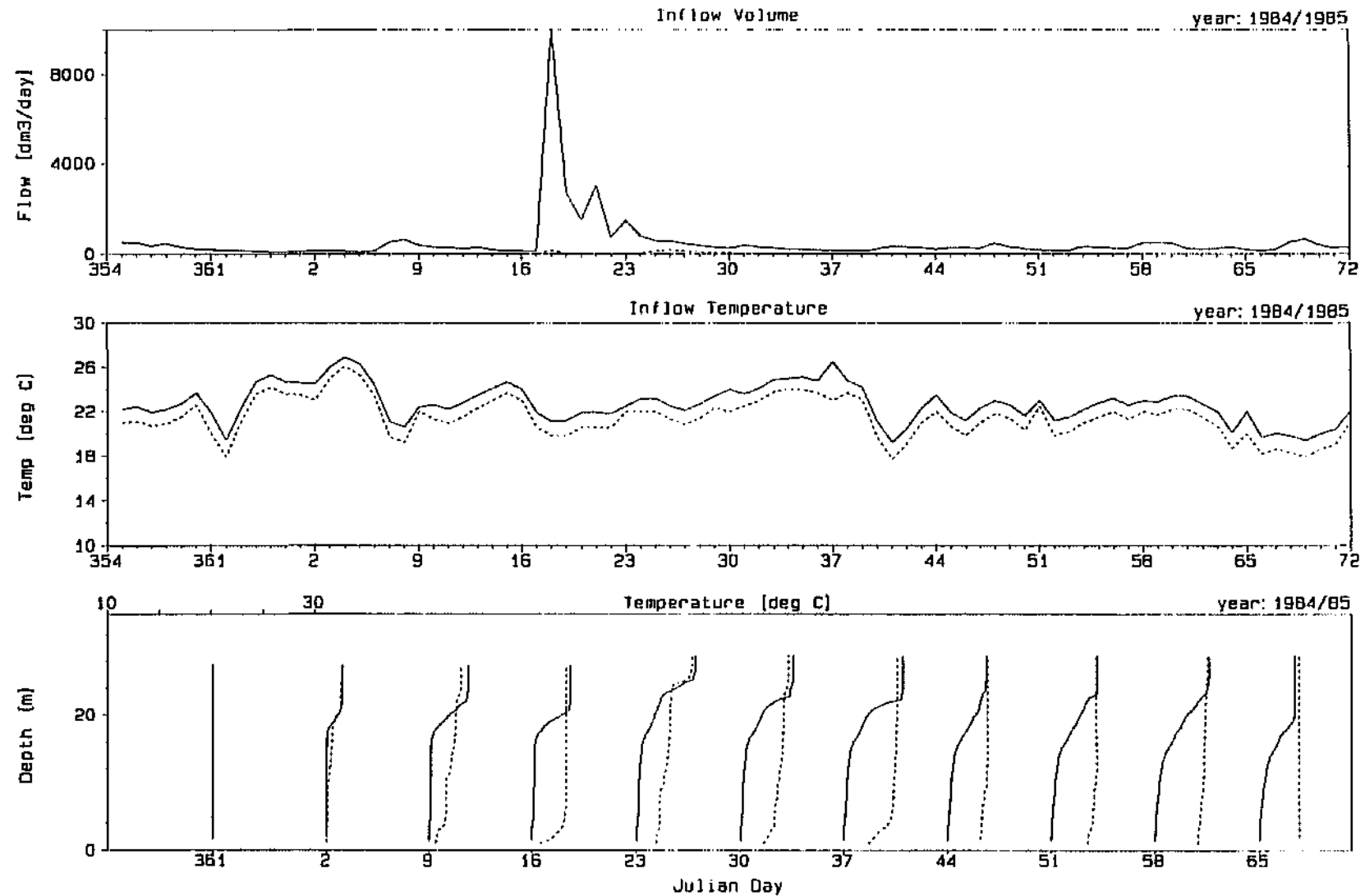
Profile Legend: — Full Dam 2D-maint. --- 6E-destrat



DyPlotID : DYRESM-1D

Dam : Hartbeespoort Dam

Plot Date : 30 Mar 95, 11:41



Inflow Legend: — Crocodile Magalies
 Profile Legend: — Full Dam GE-destrat



Example of the effect of a disturbance caused by a sudden large inflow

Figure 2.3.16

Destratification:

$$21 \text{ days} \times 2 \text{ compressors} = R286,54 + (R184,54 \times (20+21)) = R7\ 850$$

Maintenance:

Approximate monthly electricity cost with bubbler operating full time:

$$30 \text{ days} \times 2 \text{ compressors} = R286,54 + (R184,54 \times (29 + 30)) = R11\ 200$$

If the compressors are kept operating on a continuous basis for seven months of the year (September-March), this would amount to approximately R80 000.

2.3.6 Bubble plume destratification - Conclusions

The scenarios based on the second peak case were generally more effective at both destratification and maintenance than those based on the first peak case. This is because the bubbler efficiencies during operation remained relatively high for a range of degrees of stratification.

Independent plumes were found to be more effective than interacting plumes.

Reservoir depth was found to influence the effectiveness of bubbler designs. The available data set covered a period during which the dam volume was approximately 30% of FSC. The lower reservoir level led to less stratified profiles and consequently a lower air flow rate per source was more effective at destratification.

A hypothetical case for the full reservoir was modelled, and was found to exhibit a greater degree of stratification than the drawn down dam case. The full dam case required higher air flow rates per source to achieve destratification, and a higher total air flow rate for adequate maintenance.

It was interesting to note however that the compressor requirements for ongoing maintenance for the full and drawn down dam cases were the same ($Q_T=314$ l/s or 2 compressors). Therefore operating costs of the maintenance bubbler systems will be similar if operated continuously for 7 months (September to March). It is recommended that further investigation of the bubbler design for a full reservoir be undertaken based on reservoir profiles from the full dam case, in order to optimise the design.

SECTION 2.4

APPLICATION OF *DYRESM-1D* TO SIMULATE THE HYDRODYNAMICS AND DESTRATIFICATION OF ROODEPLAAT DAM

by

E J Larsen and K O de Smidt

2.4.1 Introduction

Previous work undertaken on the application of *DYRESM-1D* to Roodeplaat Dam was described in a previous report (Görgens *et al.*, 1993). No subsequent work has been done on the data set or the calibration of the model. The observed and simulated depth-temperature profiles obtained from that work are shown in Figure 2.4.1. Further work on bubble plume aerator destratification has been undertaken for Roodeplaat Dam and is reported on in this section. In particular, the design has been further refined, and mechanical efficiencies have been investigated.

2.4.2 Bubble plume aerator design

The bubbler design philosophy described in Section 2.1.3 of this report is followed here once again. Three Julian days with varying levels of stratification were chosen from the observed profiles. The equivalent linear stratifications that have the same potential energy as these profiles were calculated, and are shown in Table 2.4.1 below.

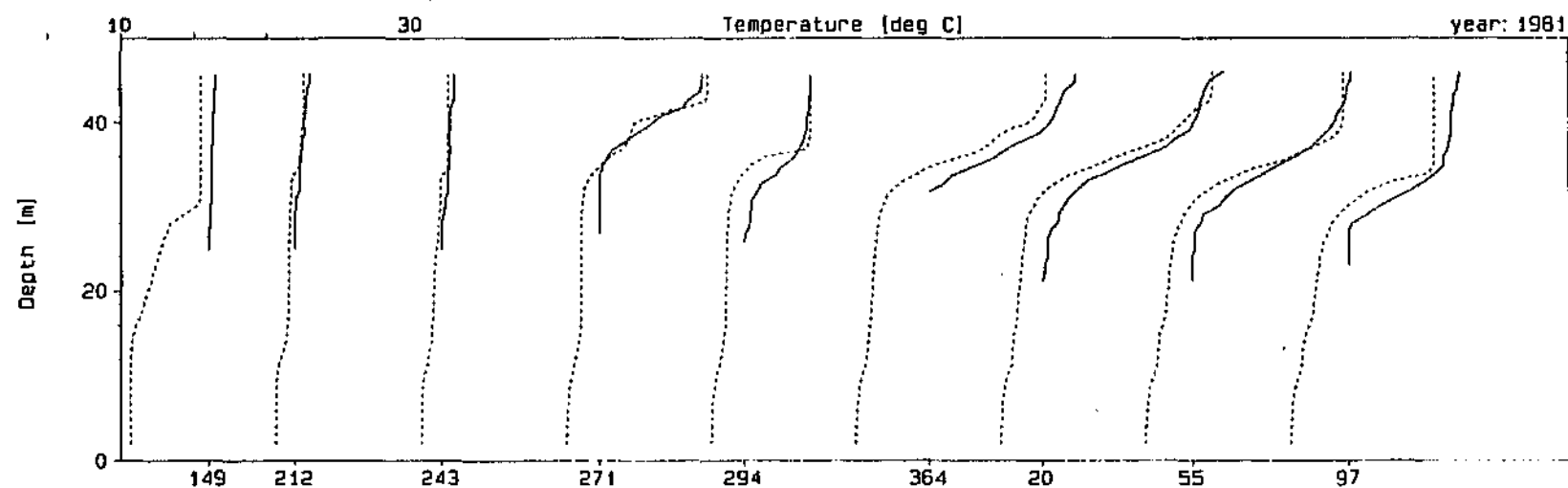
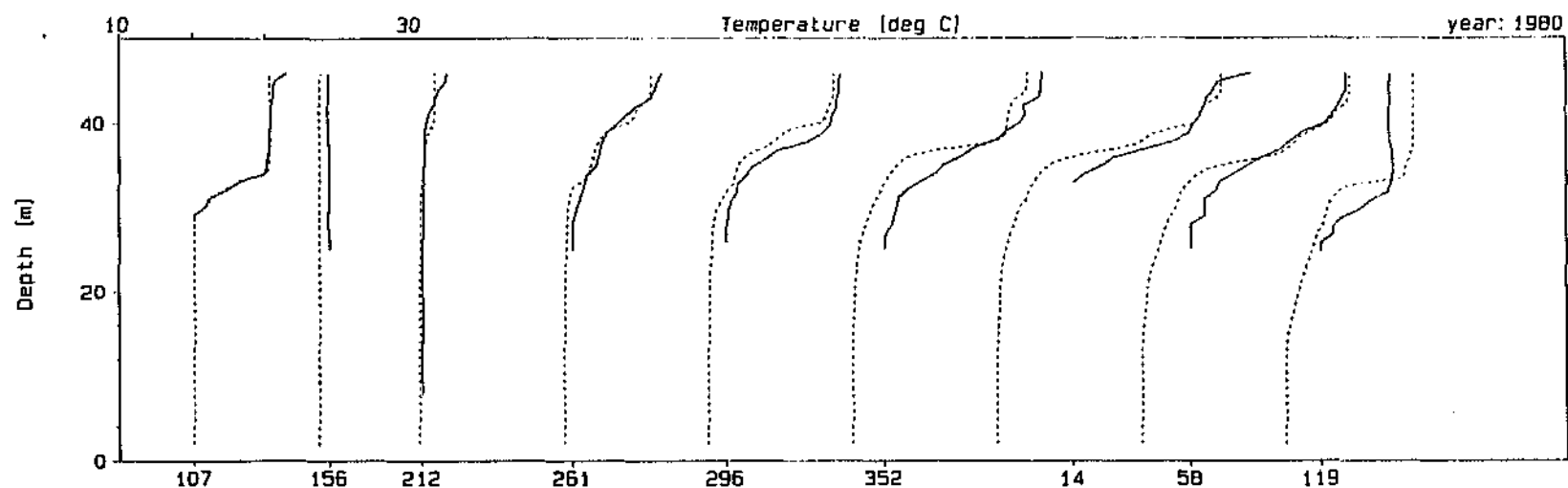
TABLE 2.4.1 : TEMPERATURE PROFILE CHARACTERISTICS

| Julian Day of Temperature Profile | Degree of stratification | | PE _{initial} - PE _{final} (GJoules) |
|--------------------------------------|--------------------------|----------------|--|
| | °C/m | Description | |
| 81014 (14 January 1981) | 0,289 | 'strong' | 7,4 |
| 80261 (17 August 1980) | 0,101 | 'weak' | 1,1 |
| 81271 (28 September 1981) | 0,161 | 'intermediate' | 2,9 |

DYDLOT10 : DYRESM-1D

Dam : Roodeplaat Dam

Plot Date : 25 Oct 94, 14:53



Julian Day

Profile Legend: — Observed Simulated



Observed and Simulated Depth-Temperature Profiles for Roodeplaat Dam

Figure 2.4.1

The first profile described in Table 2.4.1 represents 'strong' stratification requiring a bubbler configuration capable of destratifying an already stratified water body. The second and third profiles display 'weak' and 'intermediate' stratifications respectively and are typical of profiles that a 'maintenance' bubbler system should be able to destratify. It was decided that bubbler configurations for stratification of the entire range from 0,101 °C/m to 0,289 °C/m would be tested to enable the design of a bubbler system that can both destratify an already strongly stratified reservoir, and prevent the onset of stratification and maintain a mixed state.

The total pressure head at the level of the bubbler was taken to be 54,9 m of water, made up of the 46 m FSL head and an atmospheric pressure head of 8,9 m of water. Using the first and second efficiency peak concept, associated with the development of one and two whole bubble plumes between the plume source and water surface respectively, both total and per source air flow rates were determined for the range of profiles described above. Table 2.4.2 shows a summary of the more pertinent results.

TABLE 2.4.2 : BUBBLE PLUME AERATOR ANALYSIS RESULTS

| Scenario | Total Head (m) | dT/dz (°C/m) | No. Plumes | μ (%) | Q_s (l/s) | dPE (GJ) | Time (days) | Calc. Q_t (l/s) | N_s | Source Spacing (m) | Aerator Length (m) |
|----------|----------------|--------------|------------|-----------|-------------|----------|-------------|-------------------|-------|--------------------|--------------------|
| 1 | 54,9 | 0,289 | 1 | 11,0 | 83,78 | 7,4 | 21 | 253,5 | 3,0 | 9,2 | 27,6 |
| 2 | 54,9 | 0,289 | 2 | 8,0 | 8,38 | 7,4 | 21 | 348,6 | 41,6 | 9,2 | 382,7 |
| 3 | 54,9 | 0,101 | 1 | 9,0 | 25,14 | 1,1 | 21 | 46,1 | 1,8 | 9,2 | 16,6 |
| 4 | 54,9 | 0,101 | 2 | 6,5 | 3,35 | 1,1 | 21 | 63,8 | 19,0 | 9,2 | 174,8 |
| 5 | 54,9 | 0,161 | 1 | 10,0 | 50,27 | 2,9 | 21 | 109,3 | 2,2 | 9,2 | 20,2 |
| 6 | 54,9 | 0,161 | 2 | 7,2 | 5,86 | 2,9 | 21 | 151,8 | 25,9 | 9,2 | 238,3 |

where: dT/dz = equivalent linear stratification
 μ = mechanical efficiency (greater efficiency being desirable)
 Q_s = air flow rate per source
dPE = difference in potential energy between the stratified and mixed profile
 Q_t = total air flow rate for the bubbler system (calculated)
 N_s = total number of bubble plume sources

For each of these scenarios the appropriate number of bubble sources was calculated. The lengths of the bubble plume systems for Scenarios 1 to 6 were calculated based on the number of sources and the rule-of-thumb that the diameter of a bubble plume increases at the rate of 0,2 times the height of rise, assuming non-interacting plumes. The actual designs based on the commercially available 157 l/s compressors are shown in Table 2.4.3.

As discussed in Section 2.3.4, the design values in Table 2.3.4 differ slightly from the calculated values in Table 2.4.2 because of the need to provide total air flow rate in increments of whole compressors (in this case increments of 157 l/s).

TABLE 2.4.3 : BUBBLE PLUME DESTRATIFICATION SYSTEM DESIGN SCENARIOS

| Design Scenario | | 1 | 2 | 3 | 4 | 5 | 6 |
|--|-------------|----------|-------|--------|-------|----------------|-------|
| First or second peak case* | | 1st | 2nd | 1st | 2nd | 1st | 2nd |
| Degree of stratification* | (°C/m) | 0,289 | 0,289 | 0,101 | 0,101 | 0,161 | 0,161 |
| | Description | 'strong' | | 'weak' | | 'intermediate' | |
| Total design air flow rate (l/s) | | 314 | 314 | 157 | 157 | 157 | 157 |
| Individual bubble source air flow rate (l/s)** | | 78,50 | 8,49 | 26,20 | 3,34 | 52,33 | 5,81 |
| Number of bubble sources | | 4 | 37 | 6 | 47 | 3 | 27 |
| Length of bubbler system (m) | | 36,8 | 340 | 55,2 | 432 | 27,6 | 248 |
| Number of compressors | | 2 | 2 | 1 | 1 | 1 | 1 |

* indicates values that were obtained directly from Table 2.4.2

** indicates values that were calculated to be as close as possible to those in Table 2.4.2

2.4.3 Bubble plume destratification - Simulation results

Three main types of scenarios were run using the bubbler scenarios in Table 2.4.3:

- Destratification of an already strongly stratified reservoir;
- Maintenance bubbler design to prevent the onset of stratification; and
- Combination of destratification and maintenance.

These are discussed in the three sections that follow. Three specific cases of interest are examined in the first two sections. These are: the first vs second peak cases, the designs for strong and weak stratification, and independent vs interacting plumes. An additional item is discussed in the second section, namely that of optimising the maintenance bubbler. In the third section, the most suitable scenarios from the previous two sections are run in combination.

Destratification of an already strongly stratified reservoir

The scenarios for the strongly stratified profile (Scenarios 1 (1st peak) and 2 (2nd peak) in Table 2.4.3) were used for a bubbler which operated at certain periods where the reservoir was already strongly stratified. Similar operation of the scenarios for the weakly stratified profile (Scenarios 3 (1st peak) and 4 (2nd peak) in Table 2.4.3) were run to enable a comparison between the design for a strong stratification and the design for a weak stratification to be made. The details of the bubbler runs are given in Table 2.4.4.

For each scenario, a number of variations were tried, as denoted by the letter following the scenario number, for example 1A, 3C, etc. The variations in the cases were whether the plumes were interacting or independent, and in the operation time of the bubbler. Cases A and C had independent plumes while case D had interacting plumes. The difference between cases A and C is the period over which the bubbler operates, namely 80353-81016 for case A and 81365-82021 for case C. Cases A and D have the bubbler operating for the same period, the difference being that case A has independent plumes and case D has interacting plumes.

TABLE 2.4.4 : BUBBLER RUNS FOR DESTRAITIFICATION

| Base Scenario | Specific Operating Conditions | | | |
|--|-------------------------------|---|-------------|-------------------------|
| | Case | Time bubbler on | Plumes | How operated |
| 1 (strong stratification, first peak) | A | 80353 - 81016 (19 Dec 1980 - 16 Jan 1981) | Independent | Continuous operation |
| | C | 81365 - 82021 (31 Dec 1981 - 21 Jan 1982) | | |
| | D | 80353 - 81016 (19 Dec 1980 - 16 Jan 1981) | Interacting | |
| 2 (strong stratification, second peak) | A | 80353 - 81016 (19 Dec 1980 - 16 Jan 1981) | Independent | |
| | C | 81365 - 82021 (31 Dec 1981 - 21 Jan 1982) | | |
| | D | 80353 - 81016 (19 Dec 1980 - 16 Jan 1981) | Interacting | |
| 3 (weak stratification, first peak) | A | 80353 - 81016 (19 Dec 1980 - 16 Jan 1981) | Independent | |
| 4 (weak stratification, second peak) | A | 80353 - 81016 (19 Dec 1980 - 16 Jan 1981) | Independent | |

First vs second peak case: The first comparison of the above bubbler simulations was the relative effectiveness of the first peak case compared with the second peak case. In each case, including those for interacting plumes, the second peak case was more effective overall in actual destratification, as detailed below:

Strong, independent, continuous operation from 80353-81016:

2A (2nd peak) more effective than 1A (1st peak);

Strong, independent, continuous operation from 80365-82021:

2C (2nd peak) more effective than 1C (1st peak);

Strong, interacting, continuous operation from 80353-81016:

2D (2nd peak) more effective than 1D (1st peak); and

Weak, independent, continuous operation from 80353-81016:

4A (2nd peak) more effective than 3A (1st peak).

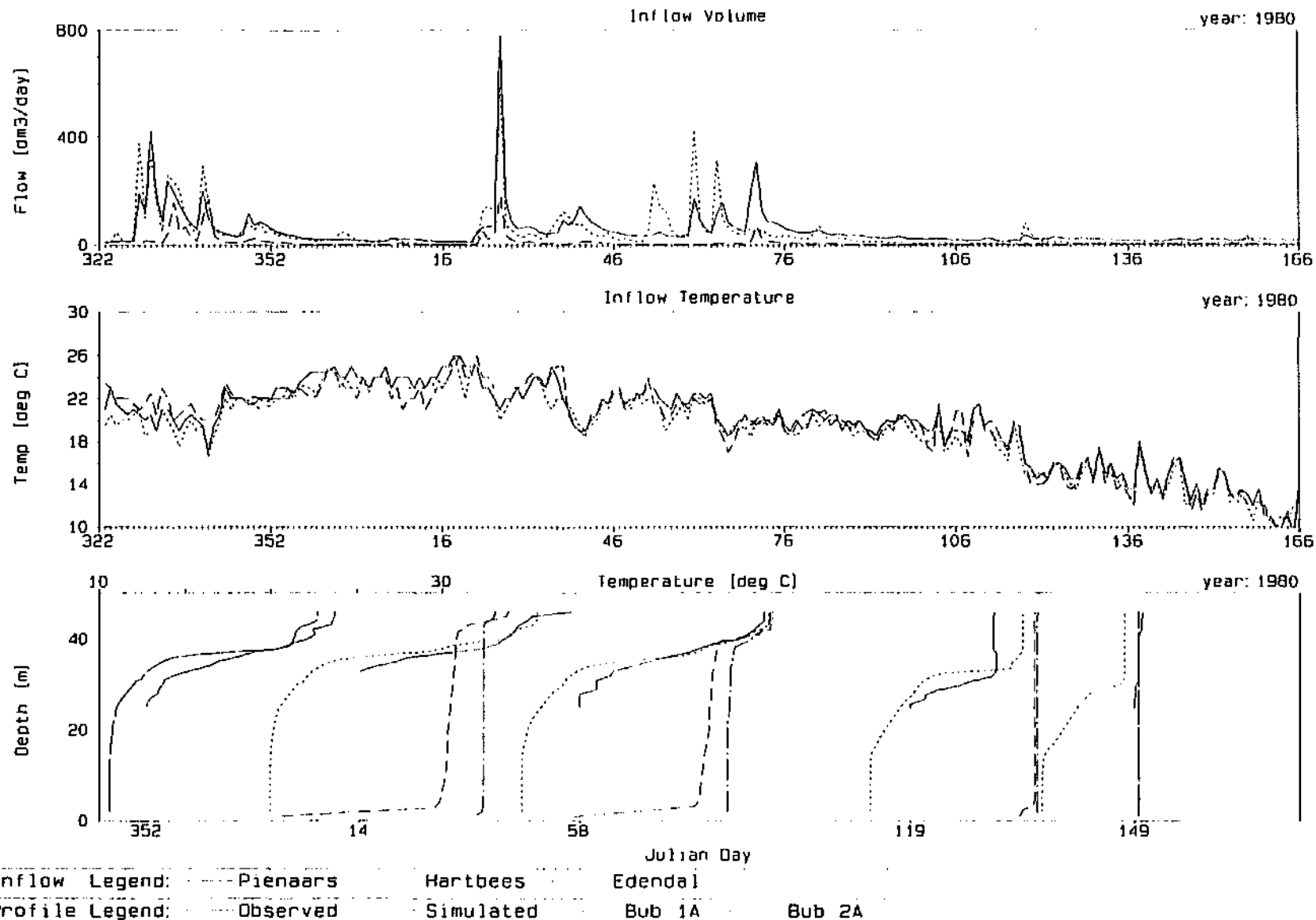
Figure 2.4.2 shows the comparison between 1A and 2A as an example.

A comparison of mechanical efficiencies during runs 1A and 2A, 3A and 4A is shown in Figure 2.4.3. The first peak case (1A and 3A) is more efficient at first, but once the strong stratification has been broken down, the second peak case (2A and 4A) becomes more efficient. For the designs for strong stratification (1A and 2A), the changeover occurs at Julian Day 80356, after the bubbler has been operating for 4 days. For the designs for weak stratification (3A and 4A), the changeover occurs at Julian day 81002, after the bubbler has been operating for 15 days.

DY PLOT 1D : DYRESM-1D

Dam : Roodeplaat Dam

Plot Date : 8 Feb 95, 16: 51

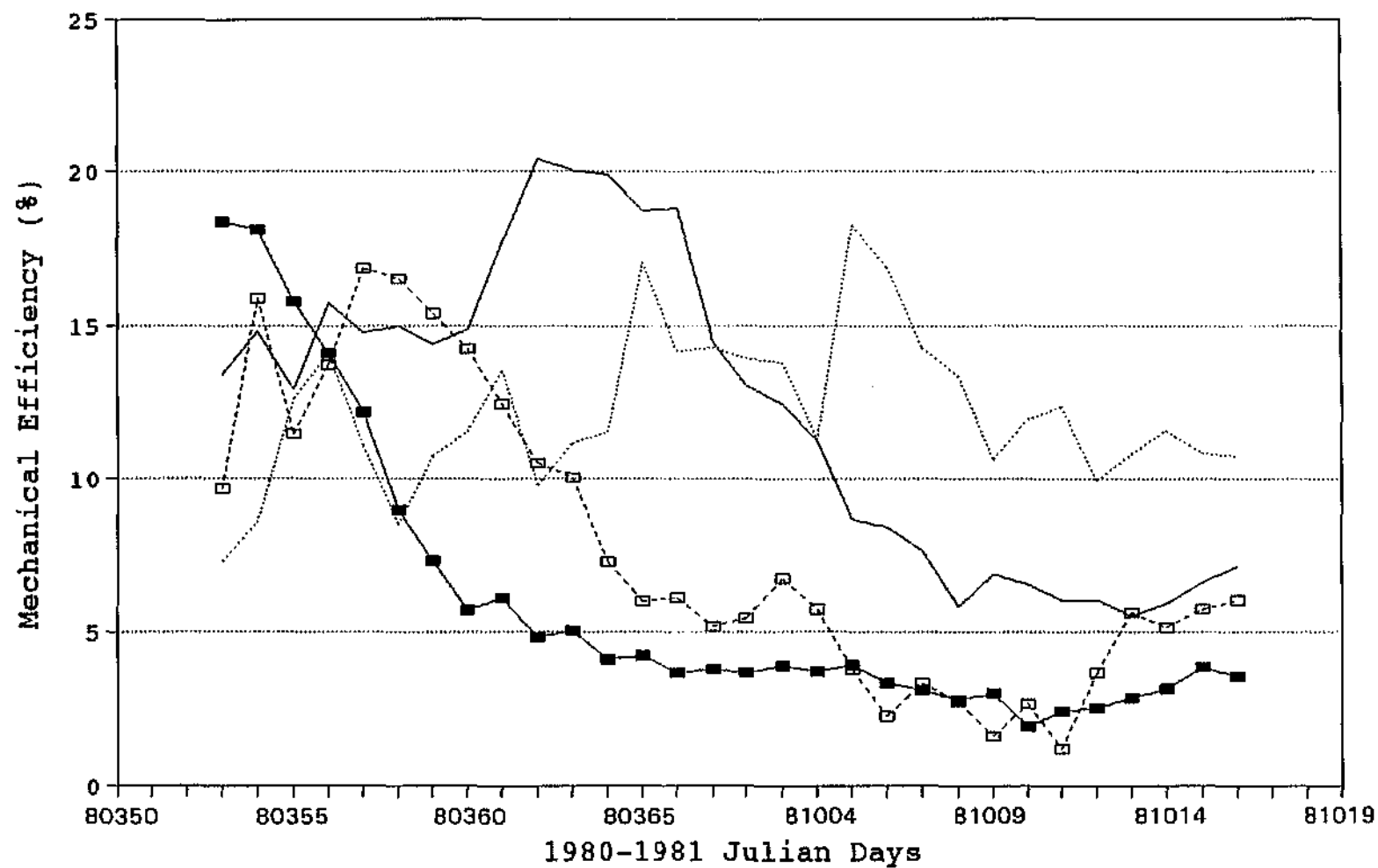


- 2.128 -



Comparison of effectiveness of first and second peak cases at destratification

Figure 2.4.2



—■— 1A (strong, 1st) -□- 2A (strong, 2nd) — 3A (weak, 1st) 4A (weak, 2nd)



Mechanical efficiency of first and second peak cases during destratification

Figure 2.4.3

Designs for strong and weak stratification: The effectiveness of the scenarios based on the strong stratification (1 and 2) compared with those for the weak stratification (3 and 4) was investigated. As expected, the scenarios based on the strongly stratified profile were more effective at destratification, as shown in Figure 2.4.4. Refer also to Figure 2.4.3 to compare the mechanical efficiencies of the two scenarios. The efficiency of the scenarios based on a weak stratification (3A and 4A) are more efficient once the stratification has been broken down to some extent. This reinforces the idea of combining a destratification-type scenario with a maintenance-type scenario in order to maximise the efficiency of the bubbler system.

Independent plumes vs interacting plumes: The cases with independent plumes (1A and 2A) were found to be more effective than the interacting plume cases (1D and 2D), as shown in Figure 2.4.5. Note also, as was mentioned earlier, that the second peak case is more effective than the first peak case, for interacting plumes as well as for independent plumes.

The mechanical efficiencies are shown in Figure 2.4.6. When comparing the independent and interacting plume cases for one scenario, for example 1A vs 1D, initially the independent plume case is more efficient, but after approximately seven days the interacting plume case becomes more efficient. The comparison of 2A and 2D gives a similar result. The indication from the figure is that the second peak cases (2A and 2D) are more efficient overall.

It is important to differentiate between the effectiveness of a bubbler at breaking down the stratification, and the mechanical efficiency of the bubbler itself while it is operating. A bubbler scenario may be effective at breaking down the stratification, but it may do so inefficiently.

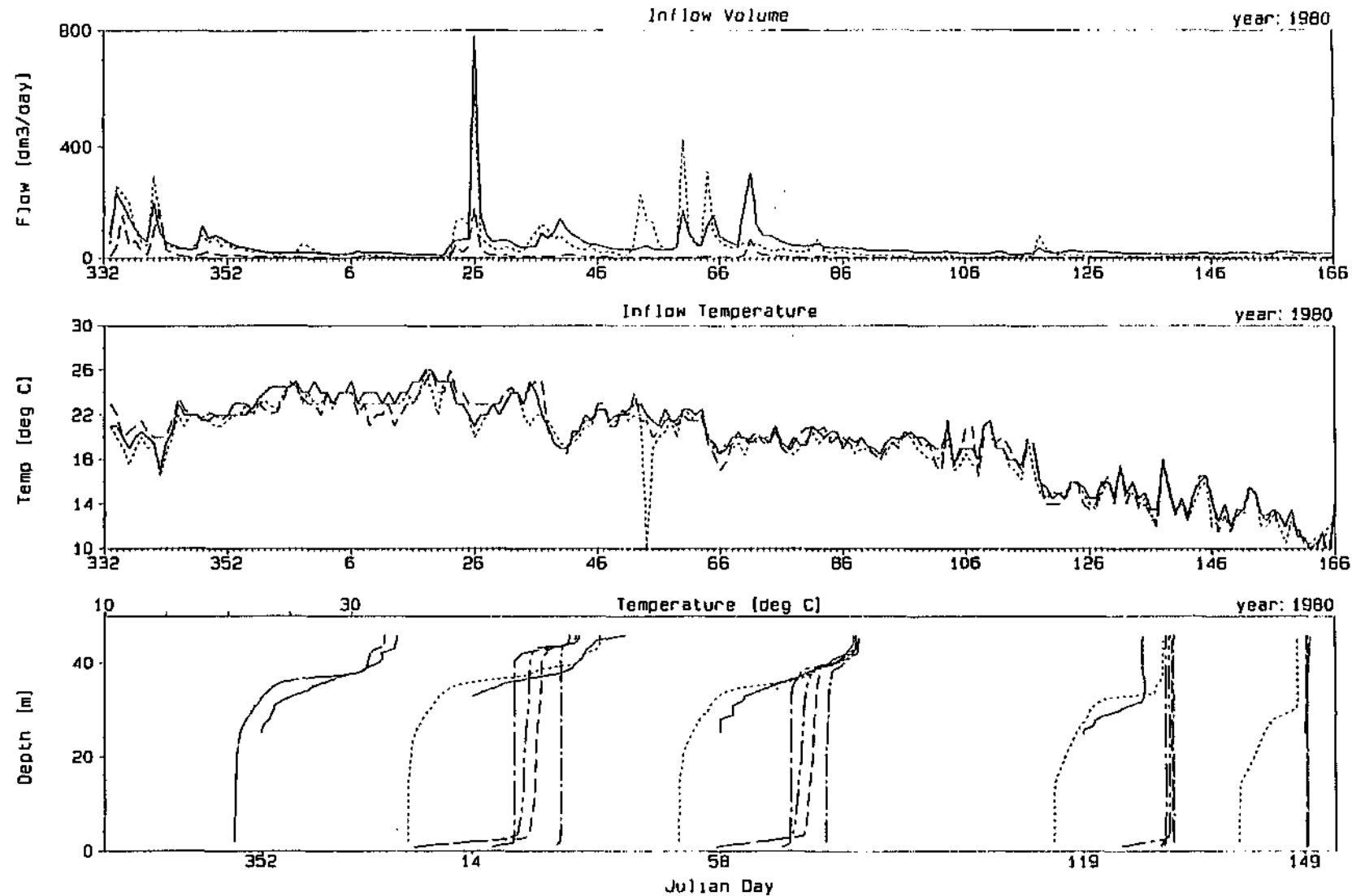
Maintenance of a mixed reservoir

The scenarios for the weak stratification (3 and 4) and the intermediate stratification (5 and 6) were used as maintenance-type bubblers. Firstly both scenarios were run with the bubbler on all the time for the first and second peak cases. Optimisation of the bubbler was then tested by using the optimisation option available in *DYRESM*. This allows the bubbler to be switched on when the temperature difference between the top and bottom levels of the reservoir profile is greater than a specified difference, and to be switched off when the top to bottom temperature difference is less than a second specified difference.

DYPLOT1D : DYRESM-1D

Dam : Rooodeplaas Dam

Plot Date : 25 Oct 94, 15:27



Inflow Legend: — Pienaars Hartbees --- Edendal

Profile Legend: — Observed Simulated --- Bub 1A — Bub 2A --- Bub 3A --- Bub 4A



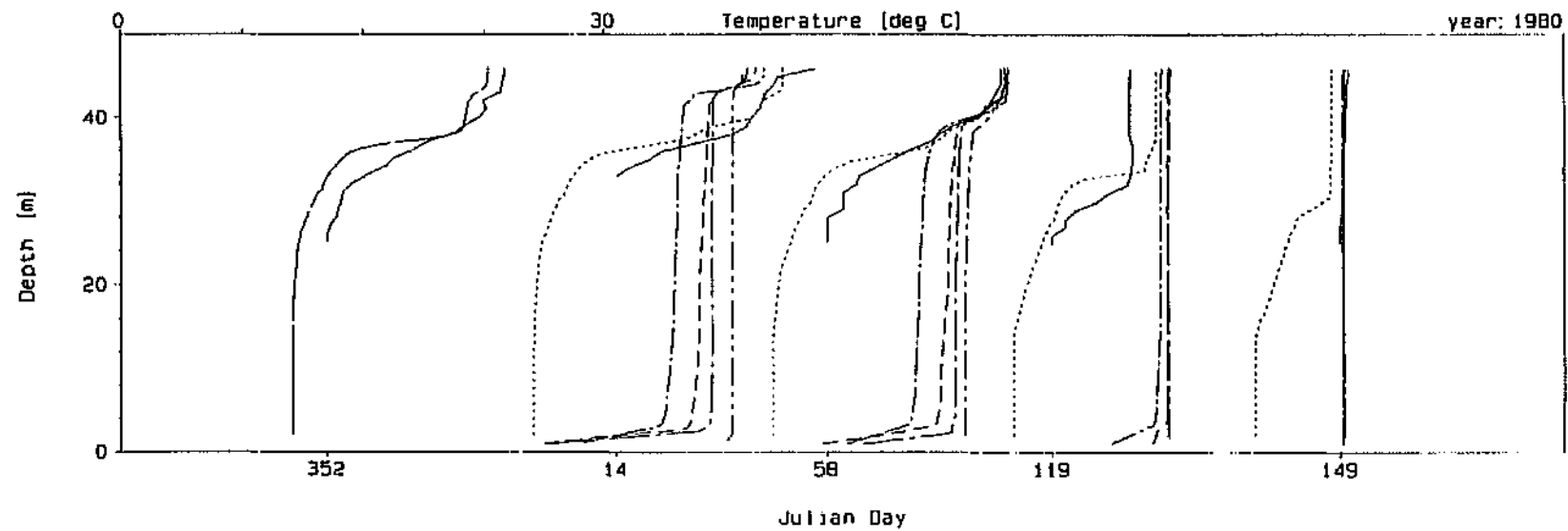
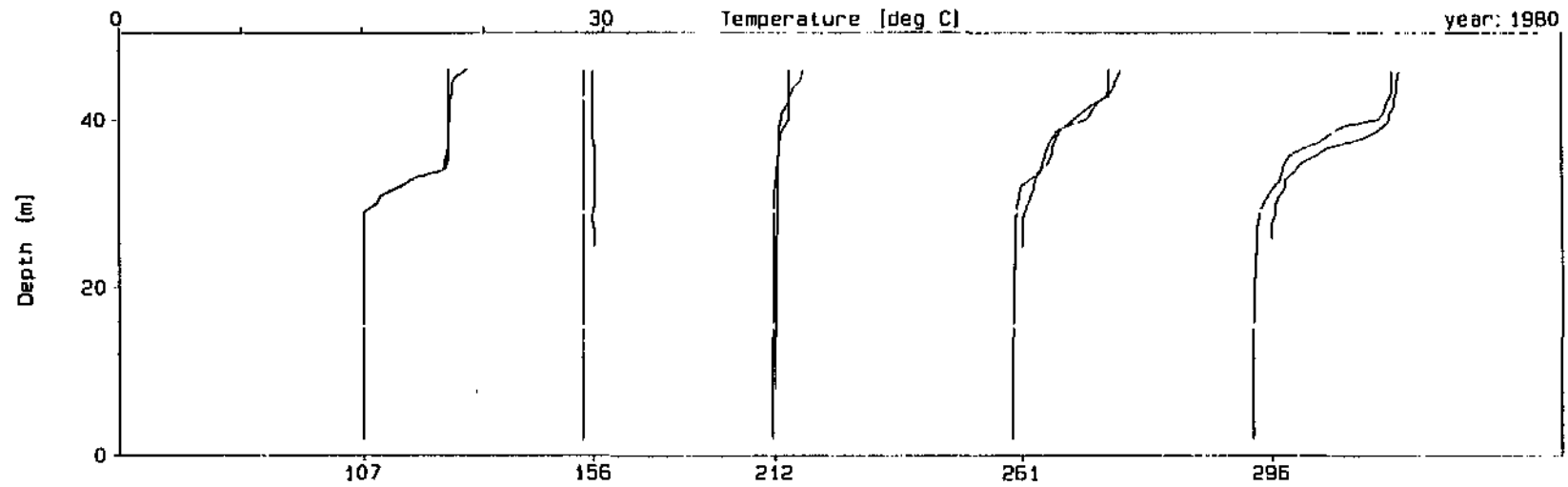
Comparison of effectiveness at destratification of bubbler scenarios based on strong and weak stratification

Figure 2.4.4

DYPLOT1D : DYRESM-1D

Dam : Roodeplaat Dam

Plot Date : 25 Oct 94, 15:39

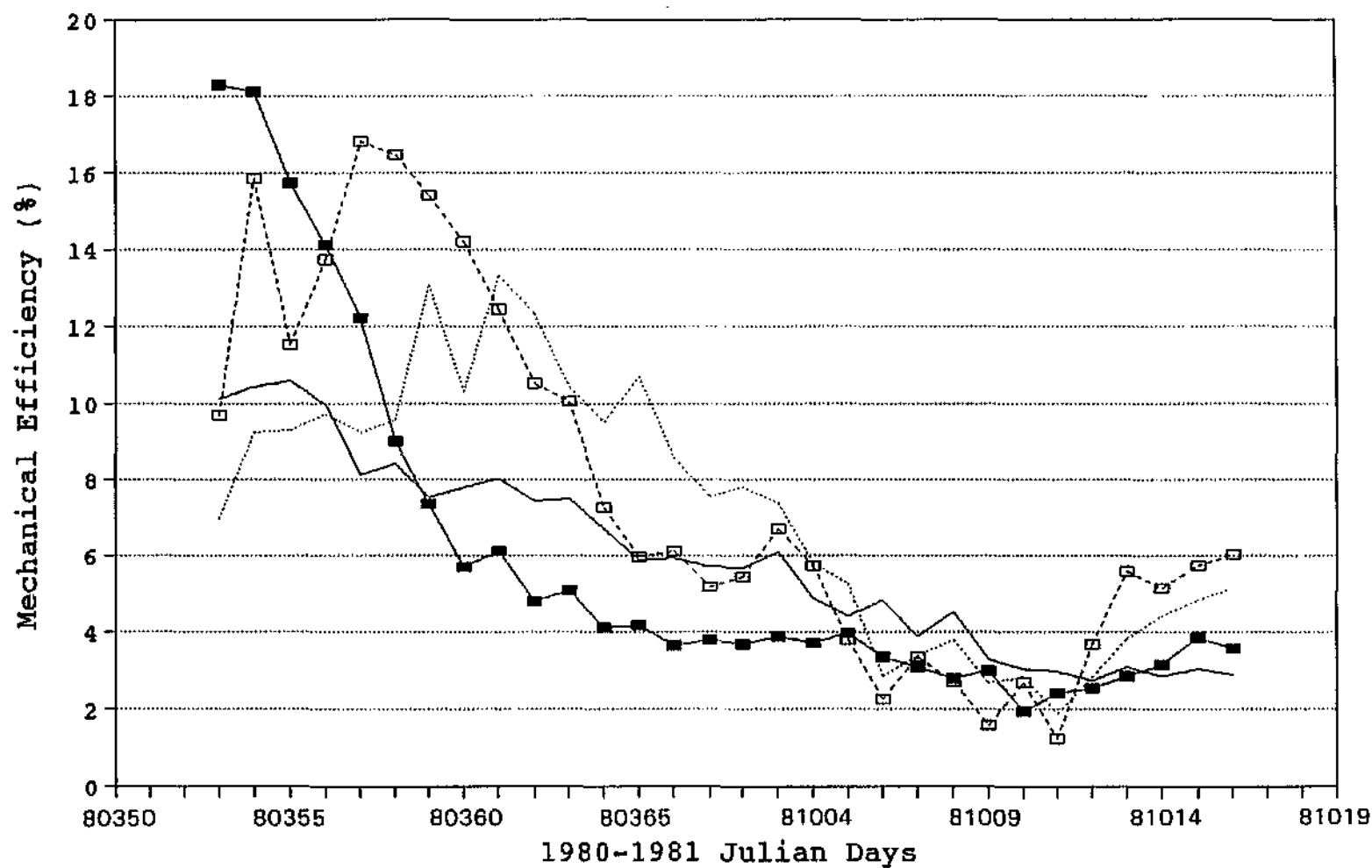


Profile Legend: — Observed - - - Simulated - - - Bub 1A - - - Bub 1D - - - Bub 2A - - - Bub 2D



Comparison of effectiveness of independent and interacting plumes at destratification

Figure 2.4.5



Two different ranges were tested. The bubbler operated for top to bottom temperature differences between 1°C and 3°C for the first case, and for top to bottom temperature differences between 2°C and 4°C for the second case. The first and second peak cases were tested for both of these ranges. Cases with interacting plumes were run with optimisation between 2°C and 4°C. The details of these bubbler runs are summarised in Table 2.4.5.

TABLE 2.4.5 : BUBBLER RUNS FOR MAINTAINING A MIXED RESERVOIR

| Level of Stratification | Scenario | Peak | Details of Specific Bubbler Runs | | | |
|-------------------------|----------|------|---|---|---|---|
| | | | B | C | D | E |
| Weak | 3 | 1st | Independent plumes. Bubbler on all the time. | Independent plumes. | Independent plumes. | Interacting plumes. |
| | 4 | 2nd | | Bubbler optimisation between 1°C and 3°C. | Bubbler optimisation between 2°C and 4°C. | Bubbler optimisation between 2°C and 4°C. |
| Intermediate | 5 | 1st | | | | |
| | 6 | 2nd | | | | |

First vs second peak case: As found previously in the destratification of an already strongly stratified reservoir, the second peak case was found to be more effective at maintaining mixing in all cases, as detailed below:

weak, independent, continuous bubbler operation: 4B (2nd peak) better than 3B (1st peak),

weak, independent, bubbler operating between 1°C and 3°C: 4C (2nd peak) better than 3C (1st peak),

weak, independent, bubbler operating between 2°C and 4°C: 4D (2nd peak) better than 3D (1st peak),

weak, interacting, bubbler operating between 2°C and 4°C: 4E (2nd peak) better than 3E (1st peak),

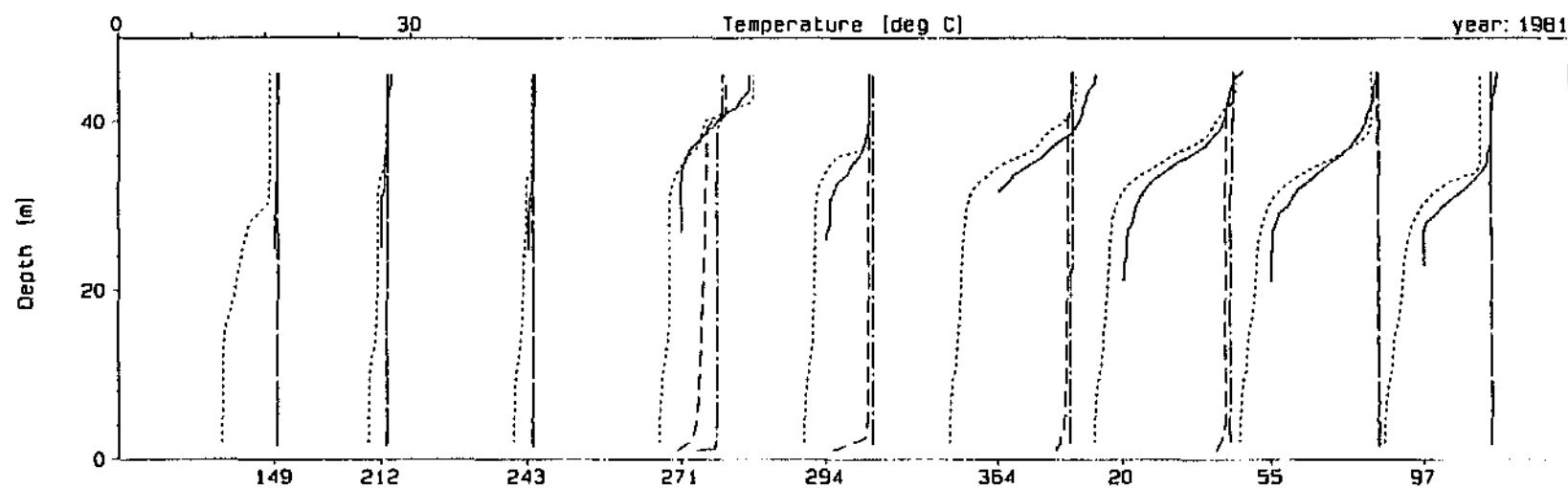
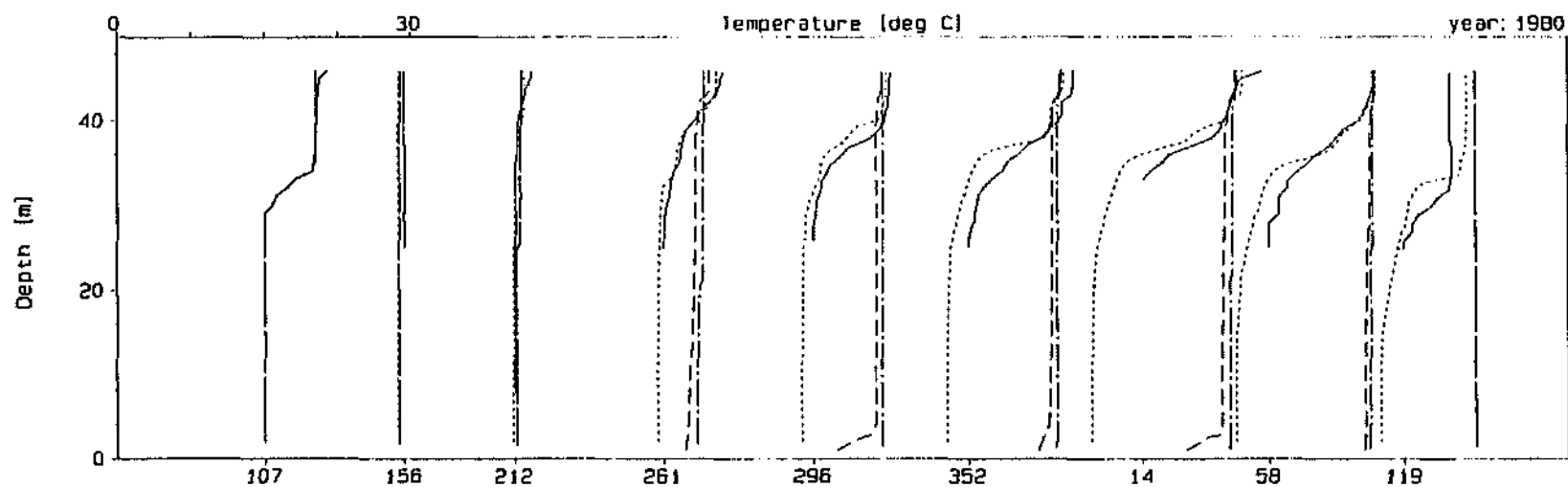
and similarly for the designs based on intermediate stratification, ie. 5 (1st peak) and 6 (2nd peak).

An example of this is given for 4B and 3B in Figure 2.4.7, as all cases were similar. A plot of mechanical efficiencies during the run (Figure 2.4.8) shows that the second peak case is more efficient than the first overall. This differs from the finding in Section 2.4.2.1 where the first peak case was more efficient initially.

DYPLOT1D : DYRESM-1D

Dam : Roodeplaat Dam

Plot Date : 25 Oct 94, 15:41



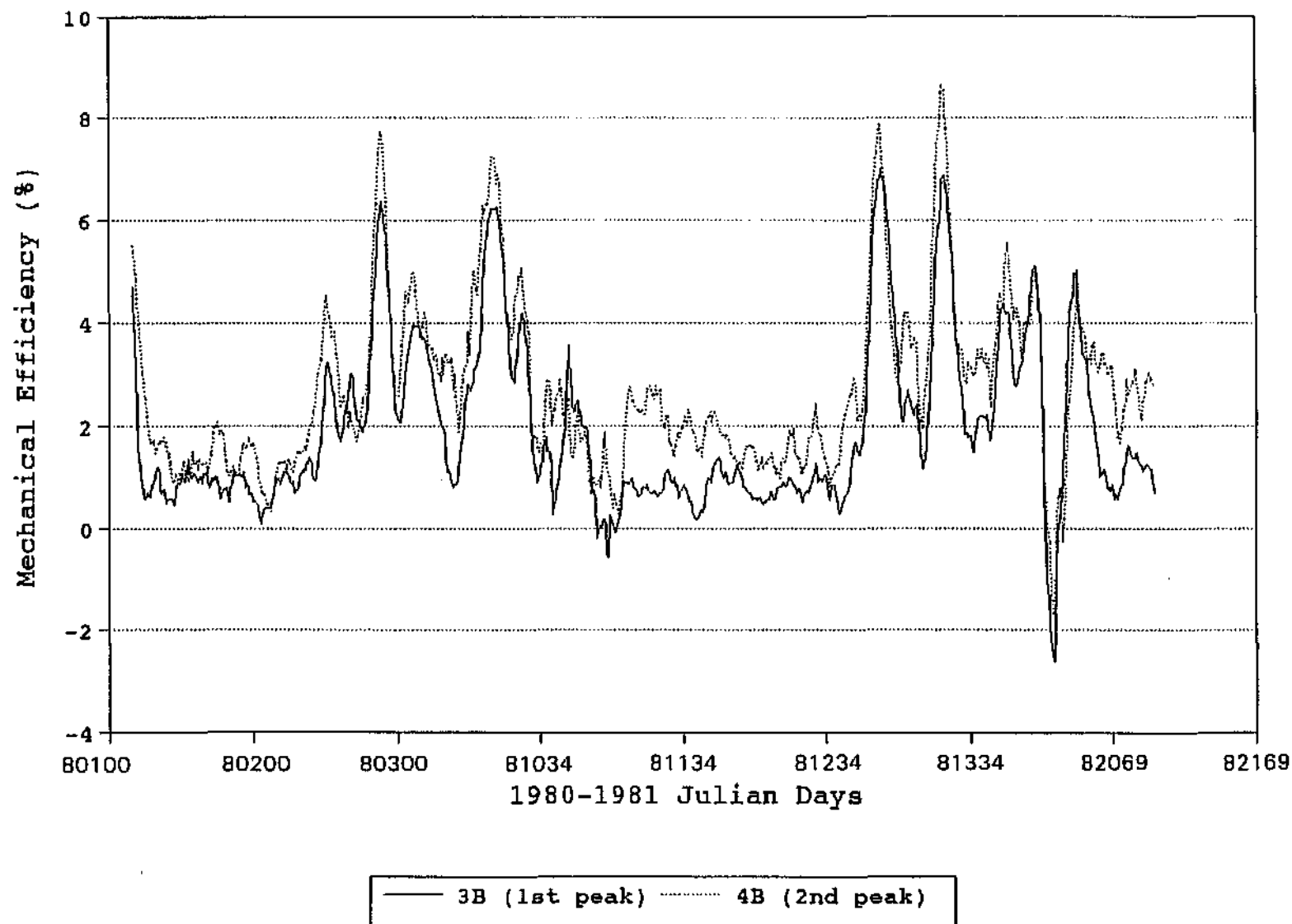
Julian Day

Profile Legend: — Observed Simulated --- Bubbler 3b -.- Bubbler 4b



Comparison of first and second peak cases during maintenance

Figure 2.4.7



Mechanical efficiencies of first and second peak cases during maintenance

Figure 2.4.8

Optimisation: The three different types of bubbler run for Scenario 4 in terms of optimisation are shown in Figure 2.4.9. As expected, the case with the bubbler operating continuously (4B) was the most effective, followed by the case with the bubbler operating between 1°C and 3°C (4C). The least effective was the case with the bubbler operating between 2°C and 4°C (4D). This corresponds to the number of days for which the bubbler operated during the run. In case 4B (continuous operation), the bubbler operated for the full 1355 day period (16 April 1980 to 31 December 1983), while in case 4C (between 1°C and 3°C) it operated for 109 days out of the full period, and in case 4D (between 2°C and 4°C) for 92 days out of the full period. The trend was similar for the other relevant runs, as detailed below:

Weak, 1st peak:

3B (1355 days), 3C (186 days), 3D (134 days);

Intermediate, 1st peak:

5B (1355 days), 5C (246 days), 5D (194 days);

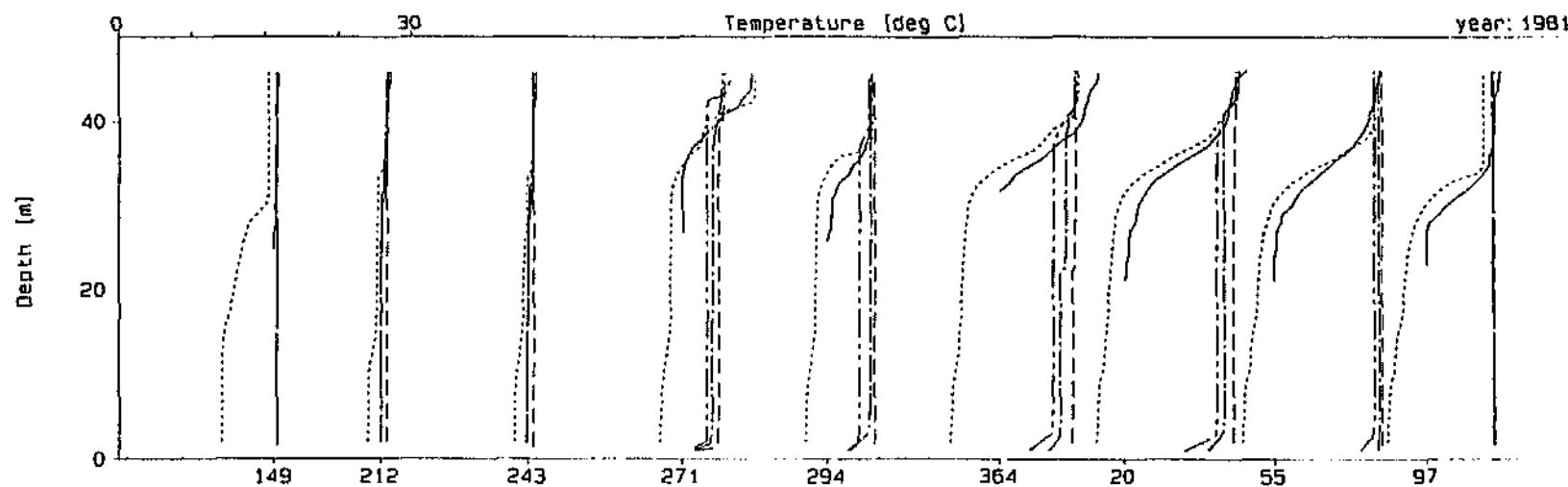
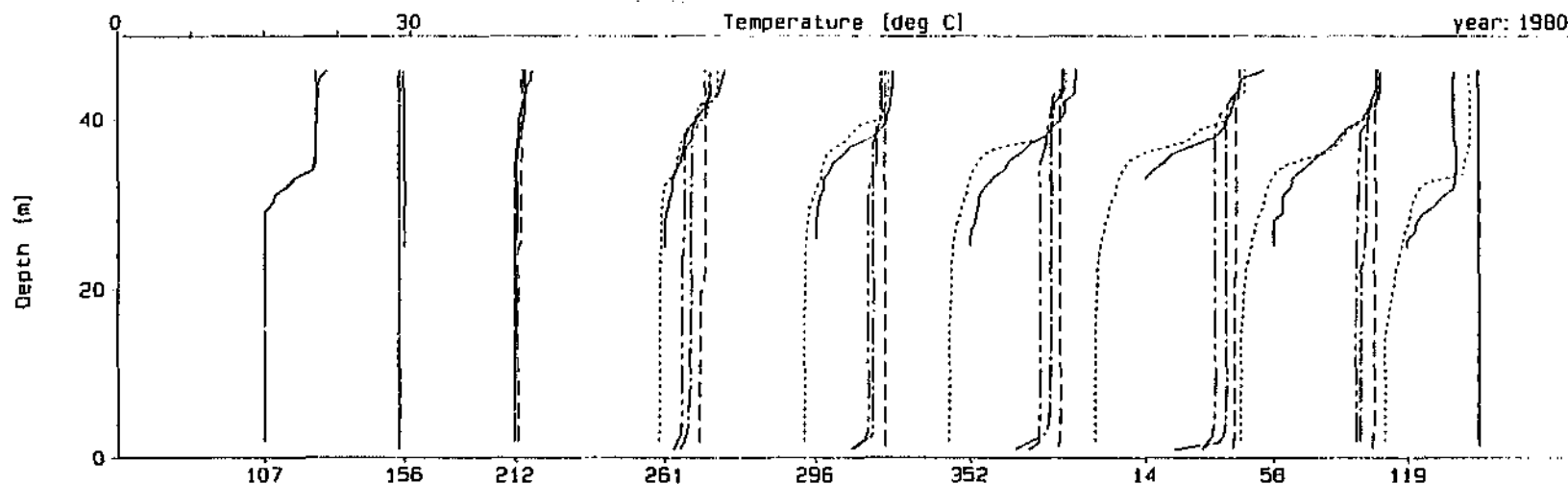
Intermediate, 2nd peak:

6B (1355 days), 6C (116 days) and 6D (88 days).

It can be seen from the profiles in Figure 2.4.9 that complete destratification is not achieved by either of the two optimising cases (for example, profiles 81014, 81271 and 81364). Therefore, although there is some scope for optimisation, some other frequency of bubbler operation between case 4B (bubbler operating continuously) and the optimisation case between 1°C and 3°C (4C) needs to be found that does not allow stratification during the height of summer.

Figure 2.4.10 shows the efficiencies of the bubbler while in operation for the bubbler runs shown in Figure 2.4.9. It is interesting to note that higher efficiencies are associated with reduced bubbler frequency and reduced effectiveness in the prevention of stratification. This is because a more effective scenario does not allow the reservoir to become as stratified as the design was intended for, whereas a less effective scenario allows a more stratified reservoir, which is closer to the design stratification, and is therefore more efficient. This highlights an important principle, namely that efficiency and effectiveness are different. Also that a maintenance bubbler should be designed on a weakly stratified profile so that it can be as efficient as possible most of the time. One must however not design for too weak a stratification, so that if for some reason the reservoir does become more than usually stratified, the maintenance design is still adequate.

DYPlot10 : DYRESM-1D Dam : Roodeplaat Dam Plot Date : 25 Oct 94, 15:44

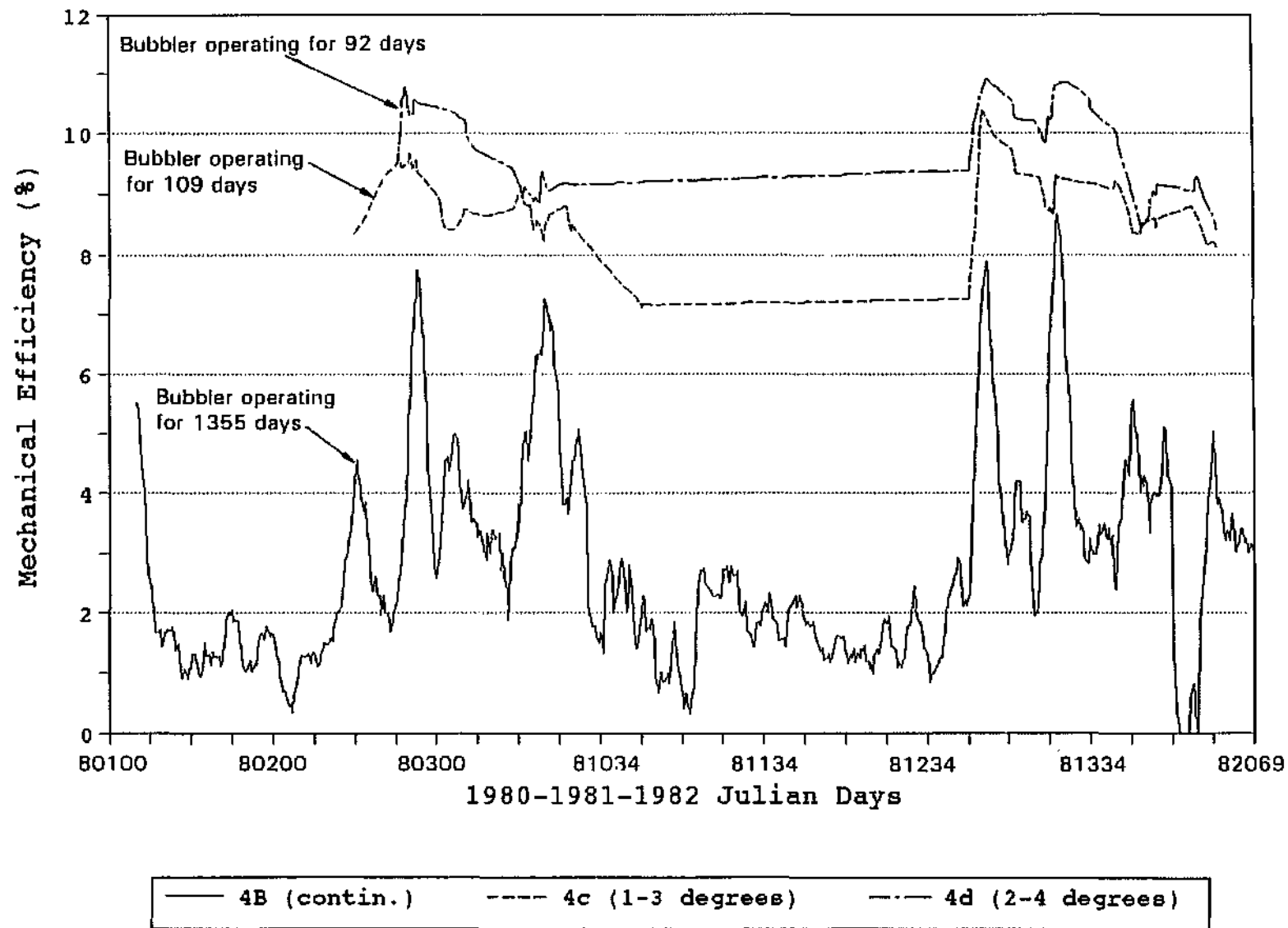


Profile Legend: — Observed Simulated --- Bubbler 4B --- Bubbler 4C --- Bubbler 4D



Comparison of bubbler optimisation cases during maintenance

Figure 2.4.9



Mechanical efficiencies of bubbler optimisation cases during maintenance

Figure 2.4.10

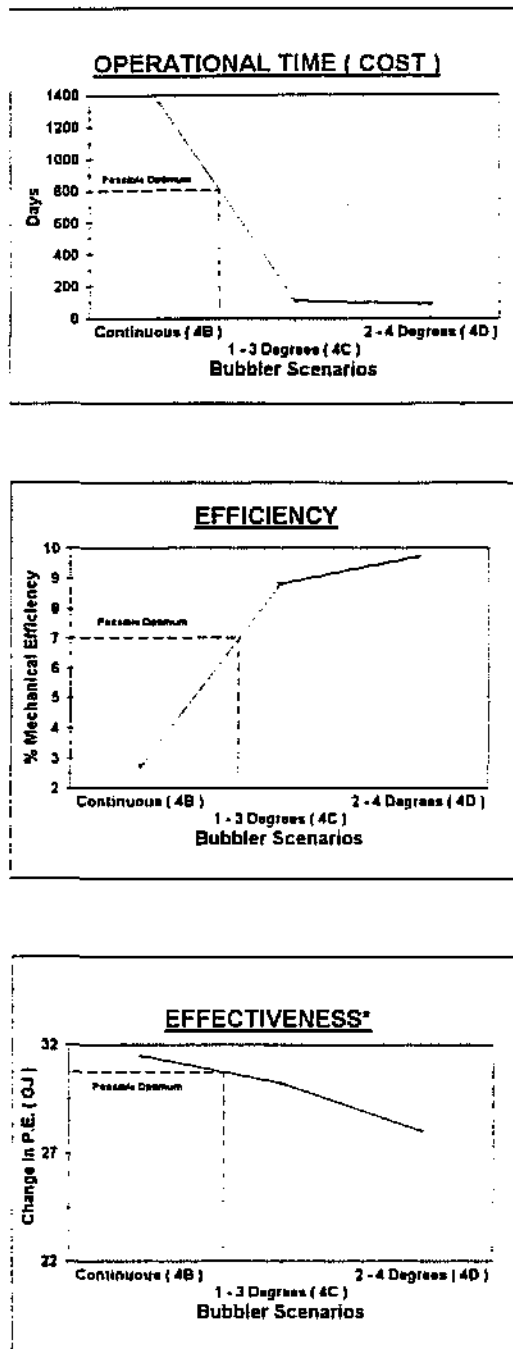
It is clear that three factors must be taken into account when determining the optimal intermittent bubbler case. These are:

- 1) Operational time of the bubbler, which translates to cost (to be minimised).
- 2) Efficiency of the bubbler while in operation (to be maximised).
- 3) Effectiveness of the bubbler in maintaining the reservoir in a mixed state (to be maximised).

Figure 2.4.11 shows these three factors diagrammatically for the bubbler runs shown in Figure 2.4.9, and indicates a possible optimum scenario based on acceptable effectiveness. In the figure, effectiveness is represented by the reduction in potential energy of the bubbler simulation from the original stratified profile for Julian Day 81014.

Designs for weak and intermediate stratification: The maintenance bubbler scenarios designed on a weak stratification (3 (1st peak) and 4, (2nd peak)) were more effective at maintaining a mixed reservoir than those designed on the intermediate stratification (5 (1st peak) and 6 (2nd peak)). This is shown in Figure 2.4.12 for the cases where the bubbler was on all the time (3B, 4B, 5B and 6B), as an example, as the other cases are similar. It is evident from this figure that the most effective case was 4B (weak stratification, 2nd peak), but it is closely followed by 6B (intermediate stratification, 2nd peak). Then comes 3B (weak stratification, 1st peak) and finally 5B (intermediate stratification, 1st peak). Therefore the dominant factor is not the level of stratification on which the scenario is based, but rather the first vs second peak case.

Figure 2.4.13 plots the mechanical efficiencies relating to the two most effective cases (4B and 6B). It shows that the efficiencies are similar. The case based on the weakly stratified profile (4B) is more variable and reaches higher efficiencies than the design for the intermediate stratification (6B). This links in with the observation made previously, that the stronger scenario never allows the reservoir to become stratified enough for its efficiencies to increase, whereas the weak scenario sometimes allows a large enough degree of stratification to occur so that the design level is approached and the bubbler becomes more efficient.

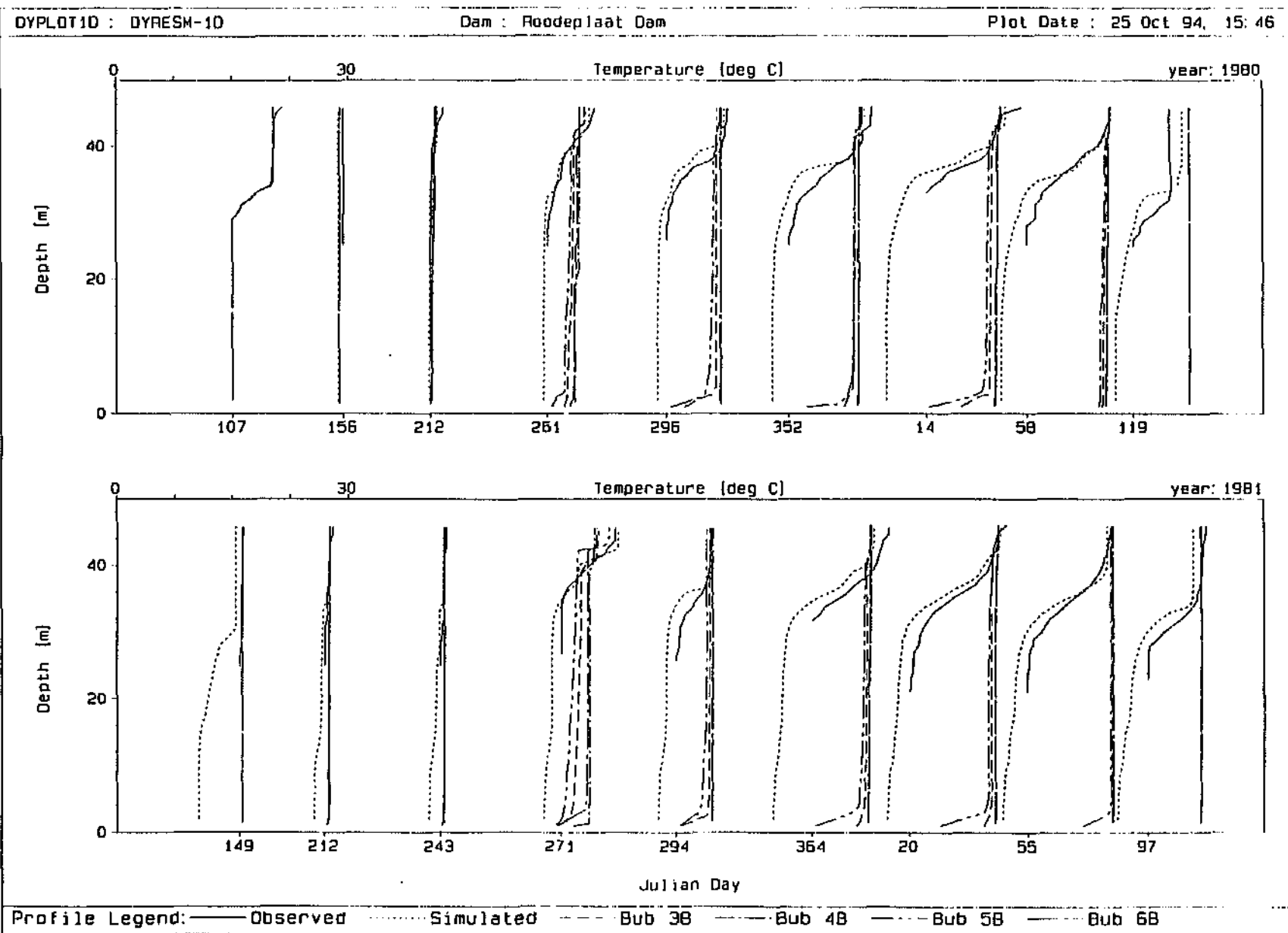


* Note: Effectiveness was taken to be the reduction in potential energy (PE) from stratified profile for Julian Day 81014.



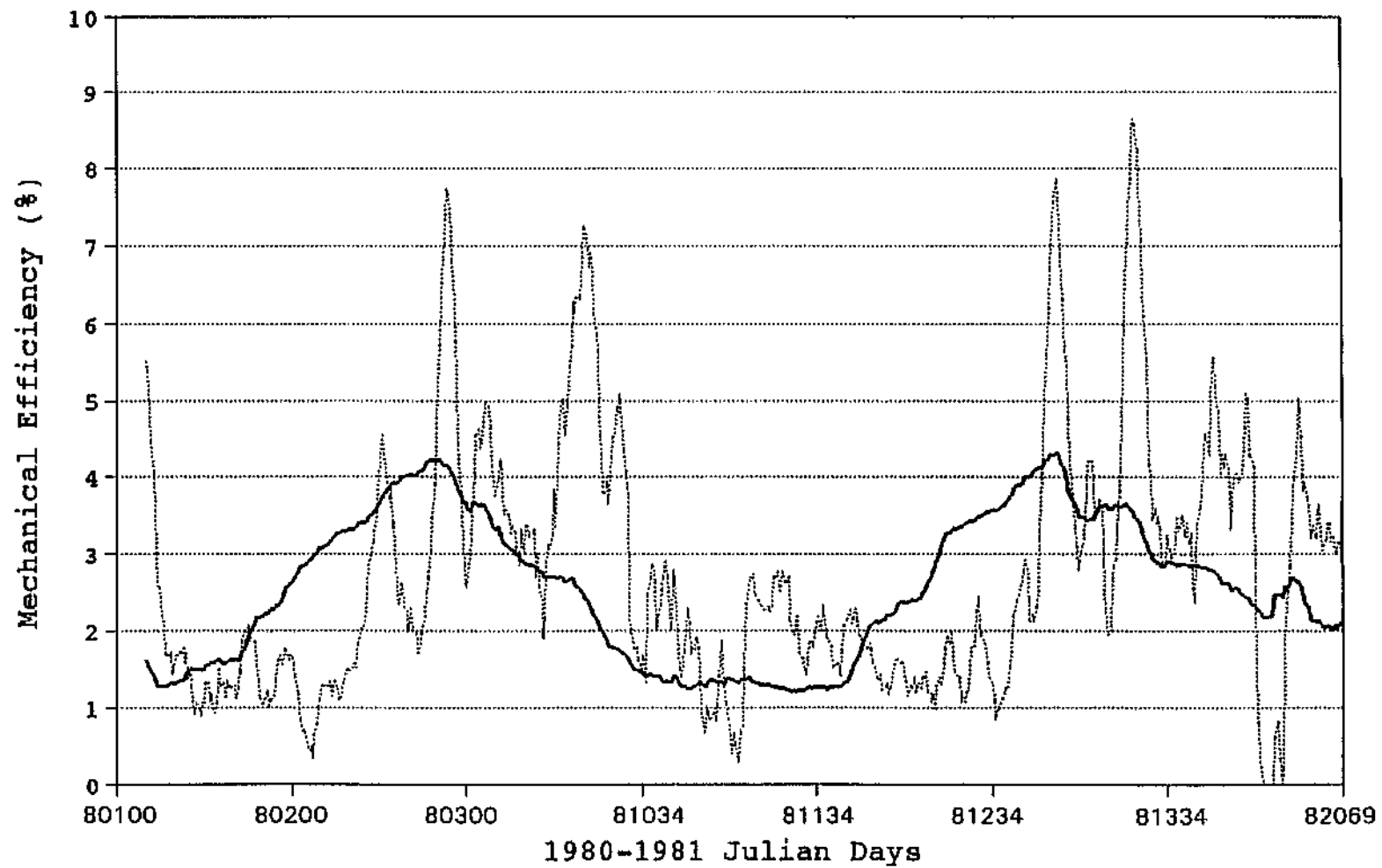
Factors determining optimal use of bubbler

Figure 2.4.11



Comparison of effectiveness of weak (3B, 4B) and intermediate (5B, 6B)
stratification scenarios during maintenance

Figure 2.4.12



..... 4B (weak strat) — 6B (int. strat)

Mechanical efficiencies of weak (4B) and intermediate (6B) stratification scenarios during maintenance

Figure 2.4.13



This is where the scope for optimisation comes in. The aim is to only operate the bubbler at those times when the stratification is close to the design level, so as to ensure it is operating as close to peak efficiency as possible.

Independent plumes vs interacting plumes: Independent plumes (case D for scenarios 3, 4, 5 and 6) were found to be more effective at maintaining a mixed reservoir than interacting plumes (case E for scenarios 3, 4, 5 and 6) in all cases. This finding was reported on by Robertson *et al.* (1991). The difference was greater for the first peak than the second peak cases. An example of the comparison for a first peak case (3D (independent) and 3E (interacting)) is shown in Figure 2.4.14 and that for a second peak case (4D (independent) and 4E (interacting)) is shown in Figure 2.4.15.

Efficiencies of the interacting plume cases were found to always be lower than those for independent plumes, as shown in the example for runs 4D (independent) and 4E (interacting) in Figure 2.4.16. This was also found to be the case by Robertson *et al.* (1991).

Combination of destratification and maintenance

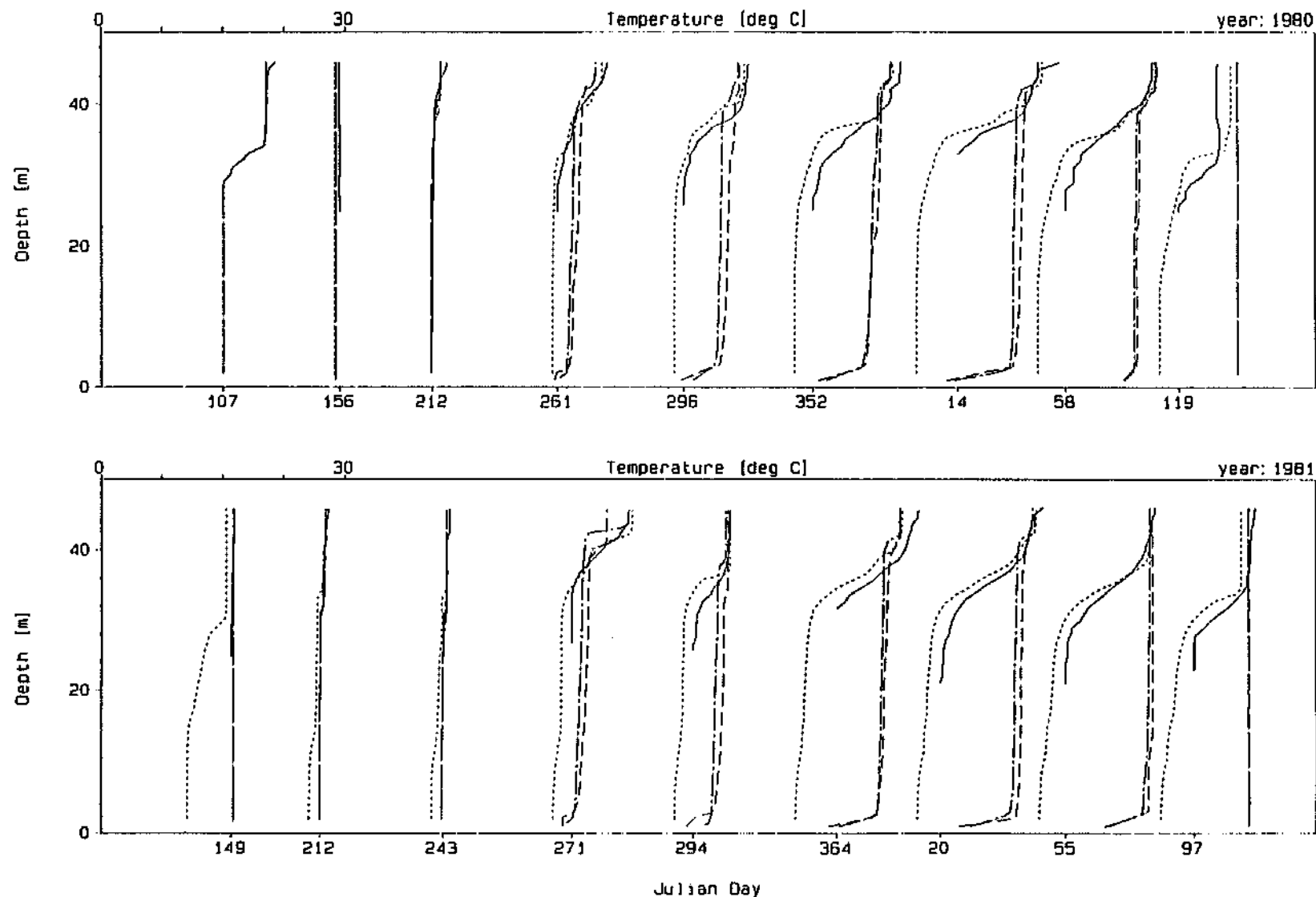
Based on the results of the investigations reported in the preceding two sections on bubbler scenarios for destratification and maintenance, the most suitable scenario from each was chosen and a combination of the two was run. The design for a strong stratification, second peak case with independent plumes (Scenario 2A from Table 2.4.4) was the most effective in 'destratification mode'. The design for a weak stratification, second peak case with independent plumes and continuous bubbler operation (Scenario 4B from Table 2.4.5) was most effective in 'maintenance mode'.

The details of the chosen combination run are given in Table 2.4.6. The reservoir was left 'unbubbled' for the period 80107-80352 to allow the onset of stratification. The destratification bubbler was operated for the period 80353-81012 (26 days), and was immediately followed by the maintenance bubbler which operated continuously for the period 81013-82096 (449 days).

DYPLOT1D : DYRESM-1D

Dam : Roo-de-plaat Dam

Plot Date : 21 Oct 94, 14:26

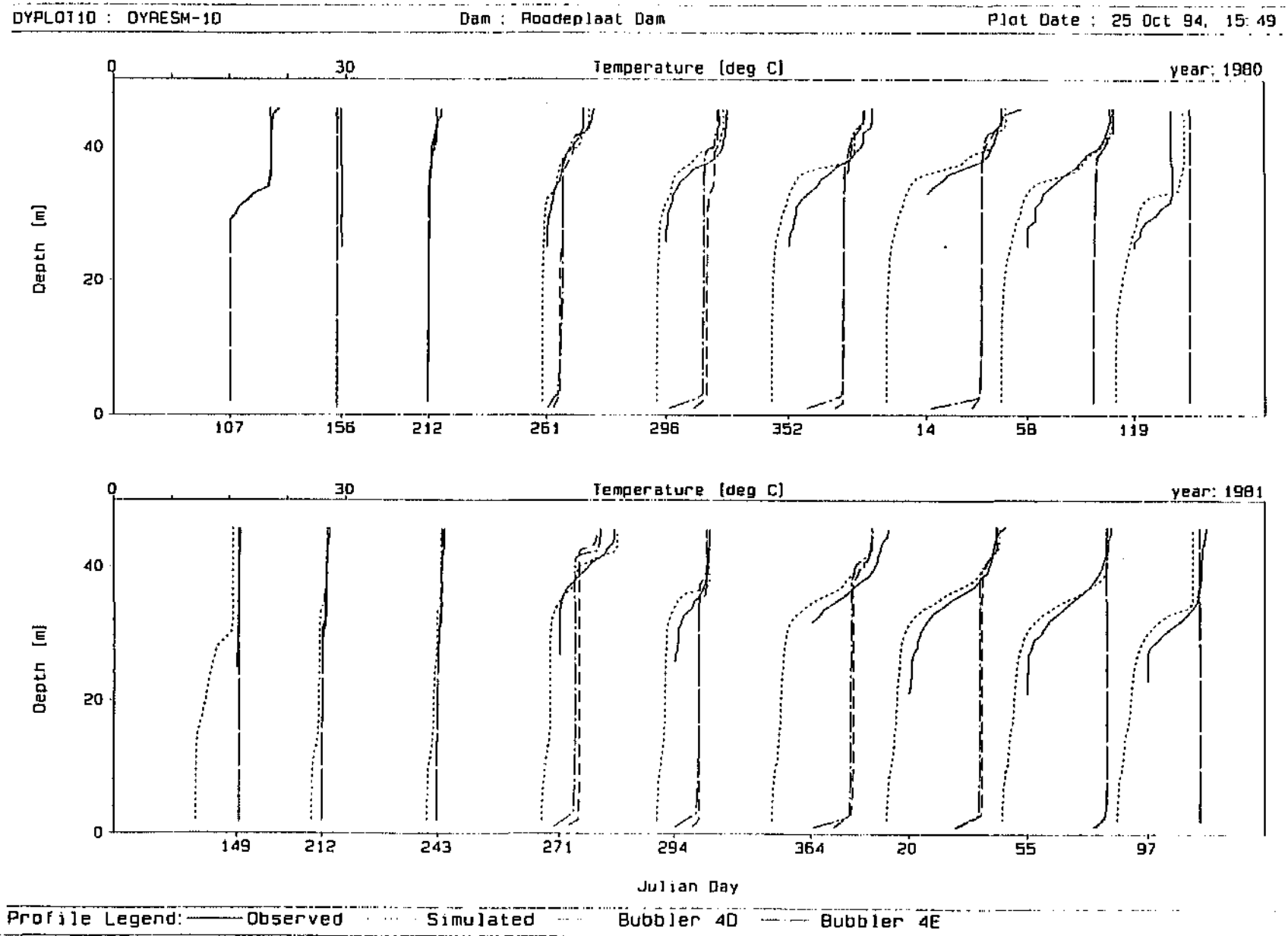


Profile Legend: ——— Observed Simulated --- Bubbler 3d — Bubbler 3e



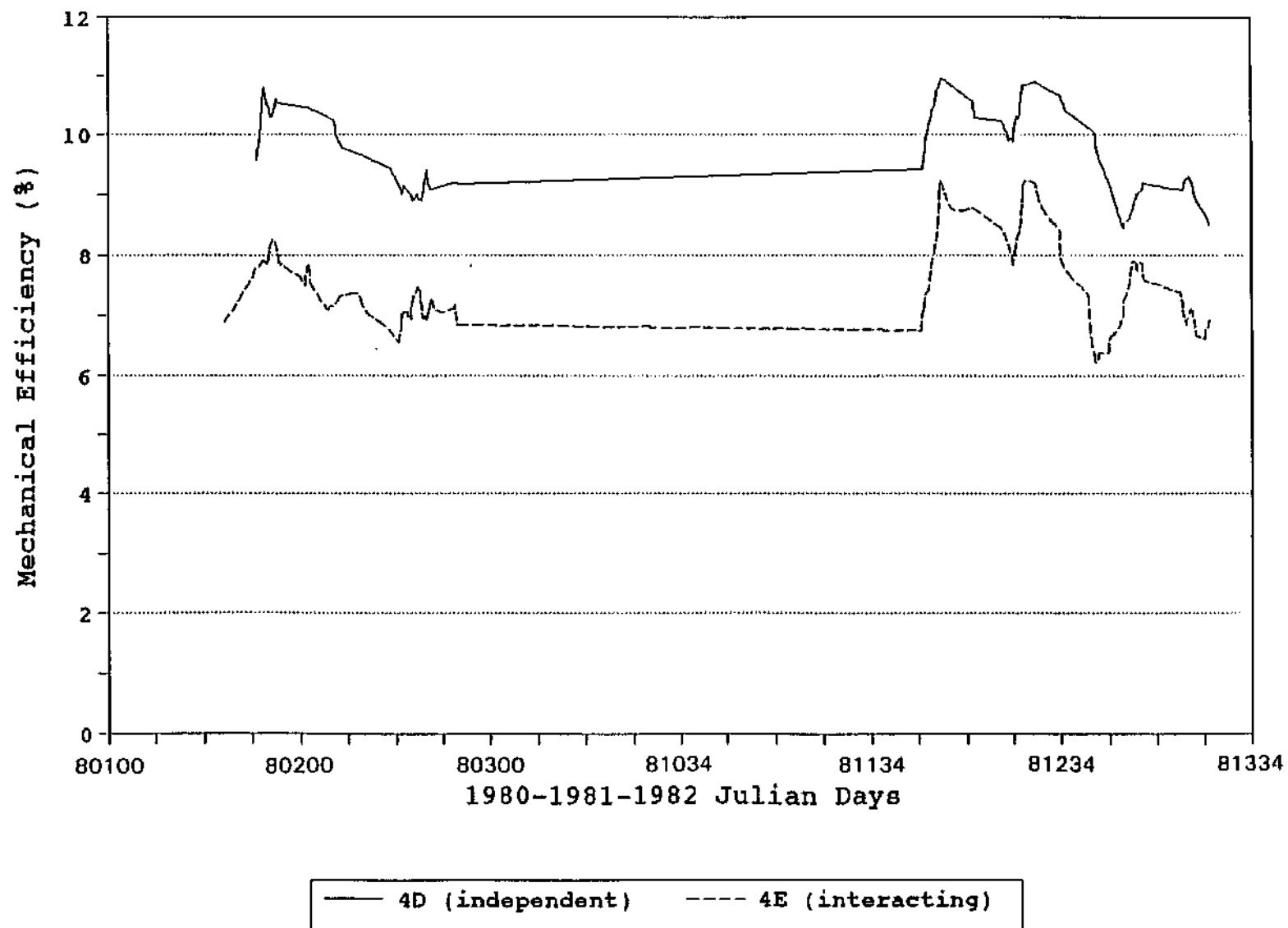
Comparison of Independent (3D) and interacting plumes (3E) for the first peak case during maintenance

Figure 2.4.14



Comparison of independent (4D) and interacting plumes (4E) for the second peak case during maintenance

Figure 2.4.15



- 2.147 -



Mechanical efficiencies of independent (4D) and interacting (4E) plumes during maintenance

Figure 2.4.16

TABLE 2.4.6 : DETAILS OF COMBINATION SCENARIO

| Design Details | Destratification (Scenario 2A from Table 2.4.4) | Maintenance (Scenario 4B from Table 2.4.5) |
|--------------------------------------|---|--|
| Q_u (l/s) | 8.49 | 3.34 |
| Q_d (l/s) | 314 | 157 |
| N_u | 37 | 47 |
| Spacing (m)* | 9.2 | 9.2 |
| Length (m) | 340 | 432 |
| Level of stratification based on | 'strong' | 'weak' |
| Plumes | independent | independent |
| Case | second peak case | second peak case |
| Bubbler operation time (Julian days) | 80353 - 81012 (26 days) (18 December 1980 - 12 January 1981) | 81013 - 82096 (449 days) (13 January 1981 - 6 April 1982) |

Note: No bubbler operates for the period 80107-80352 (246 days)
0.2 x height of rise (46m)

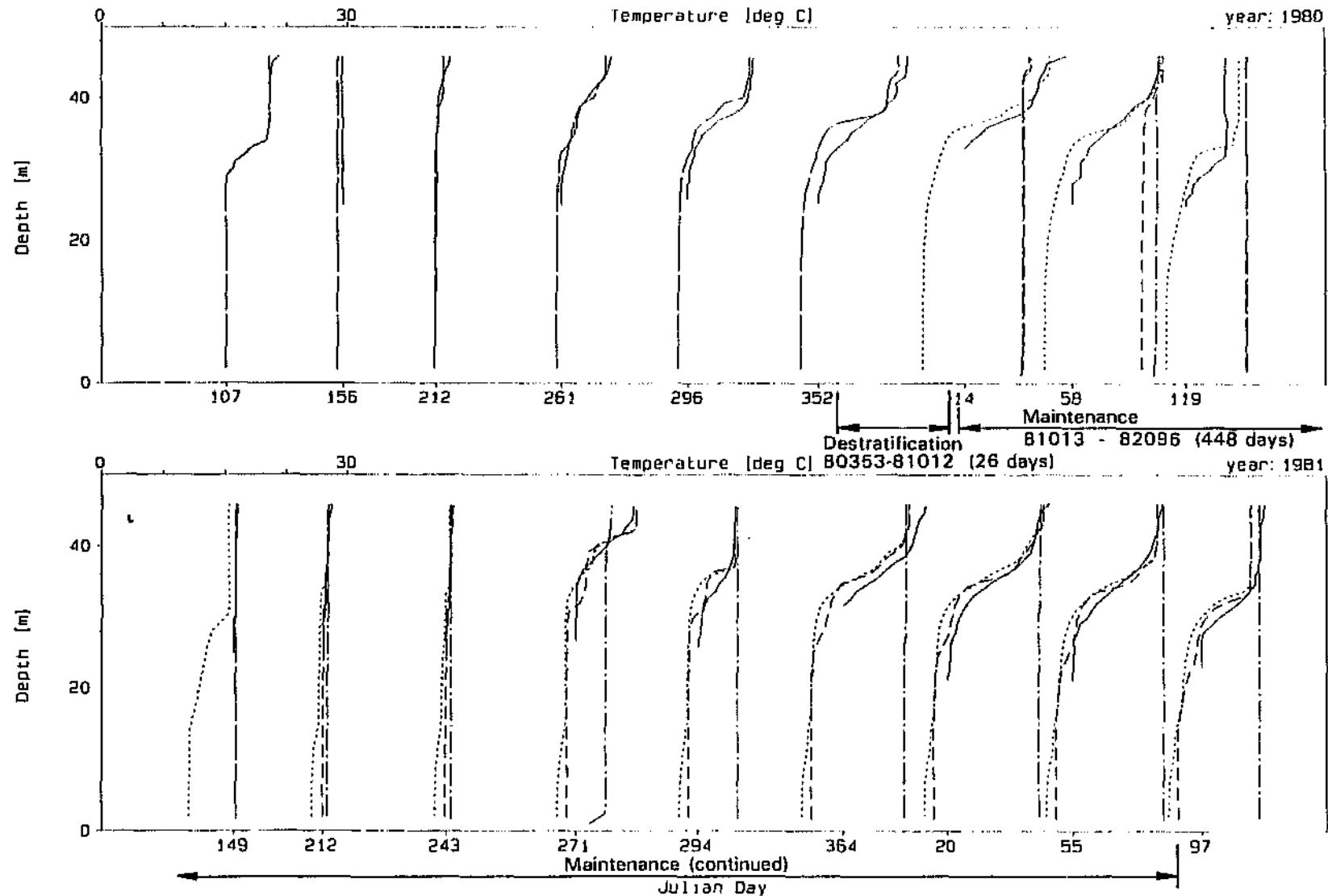
Figure 2.4.17 shows the results of this combination plotted against the results of a simulation with the destratification portion only (case 2A). During the period from 80353 to 81012 when the destratification bubbler operates for both cases, the reservoir is destratified. This is evident from the difference in profiles on Julian days 80353 and 81014. From Julian day 81013, the combination scenario has the maintenance bubbler operating, while the other scenario shown on the figure has no bubbler operating. This difference shows a minor effect until Julian day 81271 when the reservoir begins to stratify again in September 1981. From this date onwards, the maintenance bubbler maintains a mixed reservoir, while the scenario with no bubbler operating stratifies to almost the same extent as the completely 'unbubbled' scenario.

Figure 2.4.18 shows the results of the combination plotted against the results of a simulation with the maintenance scenario (case 4B) operating for the entire period. The case with the maintenance bubbler operating from Julian day 80107 prevents the onset of stratification evident in the 'unbubbled' scenarios at Julian day 80261. It also achieves a greater degree of destratification at Julian day 80014 than the destratification scenario was able to achieve during the 26 days it operated in the combination scenario.

DYPL071D : DYRESM-1D

Dam : Roo-de-plaat Dam

Plot Date : 25 Oct 94, 15:51



Profile Legend: — Observed - - - Simulated - . - Bub 2A - - - Comb-2A&4B



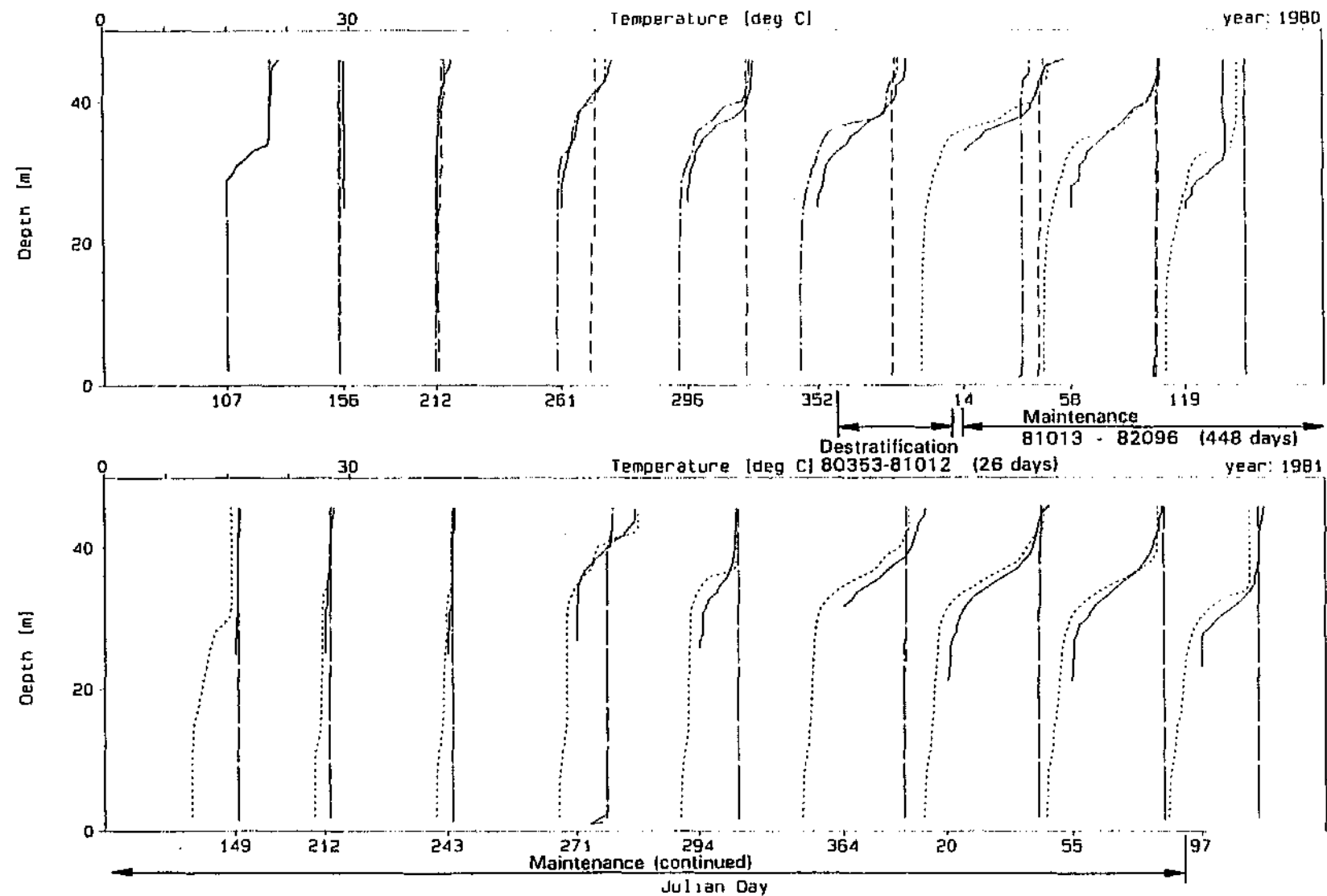
Comparison of the combined bubbler run (2A&4B) with the destratification run only (2A)

Figure 2.4.17

DYPlot1D : DYRESM-1D

Dam : Roo-de-plaat Dam

Plot Date : 25 Oct 94, 15:52



Profile Legend: — Observed ... Simulated --- Bub 4B -.- Comb-2A&4B



Comparison of the combined bubbler run (2A&4B) with the maintenance run only (4B)

Figure 2.4.18

Bubbler system operational costs

Using the same costs as detailed in Section 2.3.5, the electricity costs for the combination scenario would be as follows:

Destratification:

$$26 \text{ days} \times 2 \text{ compressors} = R286,54 + R184,54 \times (26 \times 2 - 1) = R9\ 700$$

Maintenance:

Monthly electricity cost with bubbler operating full time:

$$30 \text{ days} \times 1 \text{ compressor} = R286,54 + R184,54 \times 29 = R5\ 640$$

If the maintenance bubbler is kept operating on a continuous basis for seven months of the year, this would amount to approximately R40 000. If such a bubbler operation resulted in a significant improvement in water quality, significant savings in treatment costs could result. These may far exceed destratification costs (Quibell, 1994). In comparison with the cost of this continuous bubbler operation, intermittent bubbler operation between 1°C and 3°C (Bubbler scenario 4C) would result in an annual cost of approximately R12 000, based on the bubbler operating for 57 days from September to March. Intermittent operation between 2°C and 4°C (Bubbler scenario 4D) would result in an annual cost of approximately R10 000, based on the bubbler operating for 48 days from September to March.

2.4.4 Bubbler Plume Destratification - Conclusions

The bubbler scenario that was most effective at destratification is the design based on the strongly stratified profile, second peak case, with independent plumes (scenario 2A and C). The most successful maintenance scenario was the design based on the weak stratification, second peak (scenario 4). Independent plumes was the preferred option if the bubbler length was practical at that spacing. Optimisation of the bubbler operation requires obtaining a balance between operating time (cost), mechanical efficiency and effectiveness at breaking down the stratification. The advantage of combining two different bubbler designs to deal separately with destratification and maintenance was demonstrated.

SECTION 2.5

DYPLOT : *DYRESM* OUTPUT VISUALISATION SOFTWARE

by

K O de Smidt and A J Greyling

Due to the difficulty of obtaining high quality, high resolution plots via both the one- and two-dimensional *DYRESM* models' plotting facility, and in line with the recommendation in the *DYRESM* chapter of Grgens *et al.* (1993), the DYPLOT program which is capable of viewing and plotting reservoir profiles was converted and enhanced to be able to read directly from the latest *DYRESM* version's output files.

Other enhancements undertaken during the course of this research project include the following:

- 1) The ability to display up to seven profile datasets on a single plot.
- 2) Flexibility in the number of Julian days, profile temperature range, depth range and starting profile.
- 3) The option of specifying the profile interval to display, eg. matching Julian days or regular weekly profiles extracted from daily profile data.
- 4) Automatic, customisable and storable profile legends.
- 5) The ability to display inflow and inflow temperature timeseries along with reservoir profiles correctly spaced relative to time.
- 6) Tabular output of any simulated or observed profile.
- 7) Report ready laser printer plot output.
- 8) Automatically stored parameter file.

It is envisaged that further enhancements to the software should include the ability to plot isoline information, timeseries of outflow and bubbler configuration, air flow rate and mechanical efficiency along with reservoir profiles correctly spaced relative to time. The inclusion of an interface to the WATERMARQUE graphical data visualisation software developed by the DWAF IWQS, would also further enhance the post-processing capabilities of the *DYRESM* models.

The profile plots displayed in the above sections of this report were produced using the latest version of the DYPLOT software, which has now been renamed DYPLOT1D.

Significant progress was also made on a version of DYPLOT to easily view and produce laser printer plots of the two-dimensional *DYRESM-2D* output. The 2D plots displayed in Section 2.2.3 of this report were produced using the latest version of this software, which is now called DYPLOT2D. Features incorporated in DYPLOT2D include:

- 1) The ability to display up to two 2D output datasets for comparison purposes. The datasets may either both be simulated data or one may be observed profiles at several sites along the length of the reservoir.
- 2) The option of animating up to two 2D output datasets in order to enhance the visualisation capabilities of the program and the resultant increased understanding of the hydrodynamic and destratification processes at work within the reservoir.

SECTION 2.6

CONCLUSIONS : *DYRESM* APPLICATIONS

2.6.1 Simulation capabilities and the role of data

- (i) It has been shown that the *DYRESM-1D* reservoir simulation model is capable of acceptably accurate one-dimensional hydrodynamic simulation of typical South African impoundments with relatively minor, plausible adjustment to the available hydrometeorological datasets (usually to the wind data).
- (ii) The quasi two-dimensional *DYRESM-2D* model is capable of simulating the hydrodynamics of a South African hydrodynamically two-dimensional reservoir with reasonable accuracy, given its current limitations. At present, however, the model has certain aspects that are either disabled or do not function correctly. These include the inability to record bubbler efficiencies, the inability to specify interacting bubble plumes and the disabling of particular aspects of the inflow downflow stack, which in turn prevents visualisation of the migration and insertion into the water body of underflows. The *DYRESM-2D* model may also be optimistic with respect to the degree and efficiency of longitudinal mixing when compared with the observed data for Inanda Dam. This observation may indicate that the longitudinal mixing initiated by a physical bubbler system in Inanda Dam may not be quite as successful as indicated by the model simulations.
- (iii) The *DYRESM-2D* model enhances the user and decision maker's capability to conceptualise and visualise the two-dimensional hydrodynamic and destratification processes at work within a reservoir.
- (iv) Since *DYRESM* is a physical process based model it does not require fundamental calibration and therefore, each adjustment made to the input data and parameters to obtain a better fit between the simulated and observed profiles must be justifiable and must represent a possible scenario or encompass feasible data measurement, extrapolation or translation anomalies.

- (v) The necessity of regular, accurate and representative measurement of the various aspects of inflow, outflow, meteorological and observed field profile data has again been highlighted.
- (vi) The sensitivity of the models to wind data indicates the necessity of instituting and maintaining a suitable wind measuring network and database for all dams that are likely to require hydrodynamic analysis in the future.
- (vii) The development and enhancement of the DYLOT1D and DYLOT2D *DYRESM* post-processing software has enhanced the user and decision maker's capability to conceptualise and visualise the one- and two-dimensional hydrodynamic and destratification processes at work within a reservoir.

2.6.2 Destratification modelling : General

- (i) The bubble plume destratification modelling results show that the use of the bubbler routine within *DYRESM* allows the evaluation of existing bubbler systems and the design and optimisation of feasible systems for the destratification and hydrodynamic management of typical South African reservoirs.
- (ii) There is a need for two aerators to be included in the design of a bubbler system, viz. a destratification and a maintenance aerator. The point at which the bubbler operation should be changed from using the destratification aerator to the maintenance aerator should be based on the optimisation of mechanical efficiency. This strategy results in the maximisation of bubbler effectiveness at maintaining mixed conditions, while minimising operational costs.
- (iii) Bubbler designs based on the second efficiency peak are more efficient and effective overall at both destratification and maintenance, due to the changing degree of stratification experienced during bubbler operation. First efficiency peak designs do however show an initial short period of higher efficiency/effectiveness during the breakdown of strong stratification.
- (iv) Independent plumes were found to be more effective than interacting plumes. Ensuring independent plumes sometimes results in impractical aerator lengths, in which case interacting plumes should be used.

- (v) Intermittent bubbler operation results in significant savings in operational cost. Due to a decrease in effectiveness associated with intermittent bubbler operation, an appropriate intermittent operation scenario needs to be determined for each specific dam in order to avoid unacceptable stratification during the height of summer.

2.6.3 Destratification modelling : Specific reservoirs

- (i) Reservoir depth was found to influence the effectiveness of bubbler designs. In the case of Hartbeespoort Dam the full dam case required higher air flow rates per source to achieve destratification, and a higher total air flow rate for adequate maintenance, than for the drawn down dam case.
- (ii) Preliminary comparison of *DYRESM-1D* and *DYRESM-2D* simulations of Inanda Dam showed that the profiles describing the quasi two-dimensional simulation better approximated the observed profiles when compared with the one-dimensional simulation. The preliminary theoretical bubbler design is capable of destratifying a strongly stratified Inanda Dam over a three to four week period in a hydrodynamically two-dimensional environment. Prevention of the onset of stratification at the beginning of spring and maintenance of mixed conditions throughout the summer season is also theoretically possible in the hydrodynamically two-dimensional Inanda Dam.
- (iii) The most significant and most probable causes of the failure of the previous two attempts to destratify and prevent the stratification of Inanda Dam are twofold. Firstly, the wrong number of bubble plume sources and hence the air flow rate per source was used for the desired destratification or stratification prevention objective associated with each attempt. In the case of the revised design the total design air flow rate was also insufficient to efficiently destratify the water body in the available time before natural overturn. Secondly, the aerator layout prevented the forming of proper bubble plumes due to large, erratic bubbles in the original design, and the aerator nozzle hydraulics in the revised design would have resulted in as little as one third of the design air flow rate being achieved. The use of *state of the art* bubbler design (Schladow, 1991) in combination with optimisation by hydrodynamic simulation and the practical realisation of design parameters in the field, are clearly indispensable in the successful implementation of a bubble plume destratification system.

- (iv) The bubble plume aerator designs for destratification and maintenance of mixed conditions for Inanda, Hartbeespoort and Roodeplaat Dams, as determined by the reconnaissance level research performed during this study, are presented in Table 2.6.1 (The Hartbeespoort Dam designs are based on the hypothetical full dam case). It can be seen that in general two 157 l/s compressors (typical compressor suitable for this application) are required for both destratification and maintenance of mixed conditions, with the exception of the destratification of Inanda Dam which requires three compressors and the maintenance of mixed conditions in Roodeplaat Dam which requires only one compressor. Estimated energy operating costs vary between approximately R40 000 and R80 000 per summer for the prevention of the onset of stratification. As shown in the case of Roodeplaat Dam, intermittent bubbler operation results in significant savings in operational cost. However, due to a decrease in effectiveness associated with intermittent bubbler operation, a scenario between continuous and 1-3°C operation is required in order to avoid unacceptable stratification during the height of summer.

TABLE 2.6.1: COMPARISON OF BUBBLER DESIGNS

| RESERVOIR | INANDA | HARTBEESPOORT* | ROODEPLAAT | | |
|--|------------|----------------|------------|---------------|---------------|
| DESTRATIFICATION | | | | | |
| Reference No | 7 | 6D & E | 2A | | |
| Design level of stratification (°C/m) | 0,131 | 0,500 | 0,289 | | |
| No of compressors | 3 | 2 | 2 | | |
| Total air flow rate (l/s) | 471 | 314 | 314 | | |
| Air flow rate per source (l/s) | 15,19 | 2,53 | 8,49 | | |
| Aerator length (m) | 250 | 744 | 340 | | |
| No of days of operation required | 29 | 21 | 26 | | |
| Estimated energy cost | R12 800 | R7 900 | R9 700 | | |
| MAINTENANCE | | | | | |
| Reference No | 9 | 2D | 4B | | |
| Design level of stratification (°C/m) | 0,050 | 0,160 | 0,101 | | |
| No of compressors | 2 | 2 | 1 | | |
| Total air flow rate (l/s) | 314 | 314 | 157 | | |
| Air flow rate per source (l/s) | 1,00 | 0,50 | 3,34 | | |
| Aerator length (m) | 628 | 628 | 432 | | |
| Type of operation | Continuous | Continuous | Continuous | Between 1-3°C | Between 2-4°C |
| No of days of operation required (Sep-Mar) | 212 | 212 | 212 | 57 | 48 |
| Estimated monthly energy cost | R8 500 | R11 200 | R5 640 | varies | varies |
| Estimated energy cost (Sep-Mar) | R59 500 | R78 400 | R40 000 | R12 000 | R10 000 |

Based on hypothetical full dam case

SECTION 2.7

RECOMMENDATIONS : *DYRESM* APPLICATIONS

In order for continued success in hydrodynamic reservoir modelling the following general and *DYRESM* specific recommendations are made :

- 2.7.1 Since the wind speed is of major significance in both of the *DYRESM* models and other hydrodynamic models, careful attention should be given to the placement of wind measuring stations where possible. Periods of wind measurement should be undertaken at a height of 10 metres in order to validate the conversion of wind measured at other heights. Similarly, over water wind speeds should be measured where possible and compared with that measured over land, so that these locational effects may be quantified. It is also recommended that further research be undertaken into the over land to over water and height conversion of wind speeds. Daily wind speed and direction measuring stations and their corresponding databases should be instituted and maintained for all dams that are likely to require hydrodynamic analysis in the future. Moreover, the recorded data should be stored in a digital form that would simplify the extraction of data required by hydrodynamic reservoir models. Preferably more than one wind measurement station should be located at representative sites as close as possible to the water body and a height of 10 m.
- 2.7.2 As far as possible, when hydrometeorological data sets are prepared for the purposes of hydrodynamic modelling, a base set which consists of unadjusted measured field data should be constructed before specific data sets are developed by adjustments such as factoring, conversions, etc. This will allow data sets to be easily transferred which will result in maximum and most accurate use of such data, which are costly to collect and process.
- 2.7.3 When adjustment of measured field data is required, eg. due to locational effects, seasonal effects should be taken into account. This is particularly true for the case of wind speed where seasonal predominant wind direction can result in non-representative wind speed being applied to the water body. Seasonal effects may equally well apply to the adjustment of other hydrometeorological data.

- 2.7.4 The field measurement of profile data should be undertaken at several representative points within water bodies likely to require hydrodynamic analysis. The measurement of profiles should be done from the water surface to the dam bottom, at regular intervals, under all circumstances and Secchi disk depth measurements should always be performed.
- 2.7.5 The current version of *DYRESM* should be implemented on a dataset for a reservoir with a significant salinity component in order to test this aspect of the model's capabilities.
- 2.7.6 Further investigation into the relationship between total dissolved salts (TDS in mg/l) and NaCl concentration (ppm) is required in order that the density function within the model can be amended for South African conditions, ie. to use TDS in place of NaCl concentration.
- 2.7.7 The quasi two-dimensional *DYRESM-2D* model should be re-applied to Inanda Dam once the problems associated with the inflow downflow stack and the use of interacting bubble plumes have been addressed.
- 2.7.8 Further bubble plume destratification field experiments should be undertaken by the Department of Water Affairs and Forestry using refined designs based on the *state of the art* bubbler design methodology and theoretical and simulation research presented in this report and that of Görgens *et al.* (1993). These prototype destratification/stratification prevention attempts would provide a clearer understanding of the potential of bubble plume destratification as a management tool in South African reservoirs than that obtained from the previous attempts undertaken at Inanda Dam.
- 2.7.9 The DY PLOT programs which are capable of producing, viewing and plotting both profiles and two-dimensional model output data should be enhanced to be able to display isoline plots and additional timeseries information, such as bubbler configuration, air flow rate and mechanical efficiency along with reservoir profiles correctly spaced relative to time.
- 2.7.10 Further research using the *DYRESM-WQ* model which incorporates the simulation of the water quality components of a reservoir should be undertaken using South African datasets, when the model becomes available. Apart from the benefit of the

availability of an additional tool for the prediction of the biological and chemical aspects of water quality, which has been shown by the Centre for Water Research to give good results, the use of *DYRESM-WQ* would enable an investigation of the effects of the use of bubble plume destratification on the biological and chemical components of reservoir water quality in South Africa.

2.7.11 The following general rules should be applied when a bubble plume destratification system design is undertaken:

- i) The 2nd efficiency peak associated with the forming of 2 whole plumes should be aimed for in most cases.
- ii) If possible the aerator layout should ensure independent bubble plumes by spacing the sources at a distance of at least 20% of the full supply level depth of the reservoir.
- iii) Although designs should be undertaken for a reservoir depth measured from full supply level, other reservoir depths should be taken into account when performing the design.
- iv) Maximum operating efficiency and effectiveness, both during destratification and maintenance of mixed conditions, should be strived for in the design and operation of a bubbler system.
- v) The minimisation of energy requirements should be integral to the design process in order to ensure minimum operating costs. This is achieved by ensuring maximum operating efficiency and effectiveness, while using the minimum number of compressors required and intermittent bubbler operation if appropriate.
- vi) A design should combine the ability to operate effectively as both a strong destratification dismantling system and a prevention system capable of maintaining the reservoir in a mixed state efficiently. This requires the design of two aerator lines in most cases.

The use of *state of the art* bubbler design (Schladow, 1991) in combination with optimisation by hydrodynamic simulation and the practical realisation of design parameters in the field, are indispensable in the successful implementation of a bubble plume destratification system.

SECTION 2.8

REFERENCES : *DYRESM* APPLICATIONS

- Centre for Water Research, (1992)
"DYRESM 1D user's manual, Ver. 6.75.2 DW", University of Western Australia, Nedlands, Australia.
- Centre for Water Research, (1992)
"2D *DYRESM* supplement to the 1D *DYRESM* user's manual (6.75.2 DW)", University of Western Australia, Nedlands, Australia.
- Daugherty, R.L. and Franzini, J.B. (1981)
"Fluid mechanics with engineering applications", 7th Edition, McGraw Hill, London, 259-261.
- Department of Water Affairs and Forestry (1990)
"Inanda Dam : Capacity Determination", Directorate of Survey Services, Report No. U200-04, Pretoria, South Africa.
- Department of Water Affairs and Forestry (1992)
"Crocodile River (Western Transvaal) Catchment Study : Hydrology of the Upper Crocodile River Sub-system", Report by Stewart, Sviridov & Oliver in association with BKS Inc. to DWA&F (Project Planning), Report No. P A200/00/1492 (Volume 1), Pretoria, South Africa.
- Görgens, A.H.M., Bath, A.J., Venter, A., de Smidt, K. and Marais, G.v.R. (1993)
"The applicability of hydrodynamic reservoir models for water quality management of stratified water bodies in South Africa", Report by Ninham Shand Inc. and the University of Cape Town to the Water Research Commission, Report No. 304/1/93, Pretoria, South Africa, ISBN 1 86845 004 X.
- Hocking, G.C. and Patterson, J.C. (1991)
"Quasi-two-dimensional reservoir simulation model", ASCE Journal of Environmental Engineering, 117(5), 595-613.
- Howard, J.R. (1994)
Umgeni Water, Pietermaritzburg, South Africa, Personal communication.
- Imberger, J., Patterson, J.C., Hebbert, R. and Loh, I. (1978)
"Dynamics of reservoir of medium size", ASCE Journal of Hydraulic Engineering, 104(HY5), 725-743.
- Imberger, J., Patterson, J.C. (1981)
"A dynamic reservoir simulation model - *DYRESM* : 5", Transport Models for Inland and Coastal Waters, Academic Press, New York, 310-361.

- National Institute for Water Research (1985)
"The Limnology of Hartbeespoort Dam", South African National Scientific Programmes Report No. 110, CSIR, Pretoria, South Africa.
- Patterson, J.C. and Imberger, J. (1989)
"Simulation of bubble plume destratification systems in reservoirs", Aquatic Sciences, 51(1), 3-18.
- Patterson, J.C. (1995)
Centre for Water Research, University of Western Australia, Nedlands, Perth, Western Australia, Personal communication.
- Quibell, G. (1994)
Institute for Water Quality Studies, Department of Water Affairs and Forestry, Pretoria, South Africa, Personal communication.
- Riley, M. J. (1988)
"User's manual for the dynamic lake water quality simulation program 'MINLAKE'", St. Anthony Falls Hydraulic Laboratory, University of Minnesota, U.S.A.
- Robertson, D.M., Schladow, S.G. and Patterson, J.C. (1991)
"Interacting bubble plumes: the effect on aerator design", Environmental Hydraulics, 1, 167-172.
- Schladow, S.G. (1991)
"A design methodology for bubble plume destratification systems", Environmental Hydraulics, 1, 173-178.
- Schladow, S.G. and Patterson, J.C. (1991)
"Bubble plumes and mixing efficiency in a stratified reservoir", Proceedings of the International Hydrology and Water Resources Symposium, Perth, Australia, 274-279.
- Schladow, S.G. (1992)
"Bubble plume dynamics in a stratified medium and the implications for water quality amelioration in lakes", Water Resources Research, 28(2), 313-321.
- Thirion, C. and Chutter, F.M. (1993)
"The use of artificial aeration in Inanda Dam as a management tool for the control of eutrophication and its effects", Hydrological Research Institute Report No. N U200/04/DPQ/0693, Department of Water Affairs and Forestry, Pretoria, South Africa.
- United States Army Corp of Engineers (1984)
"Shore protection manual", Coastal Engineering Research Centre, Volume I, Chapter 3, Sections IV and V, pp 3-24 to 3-54.
- Walmsley, R.D. and Bruwer, C.A. (1980)
"Water transparency characteristics of South African impoundments", Journal of the Limnological Society of South Africa, 6(2), 69-76.

CHAPTER 3 **CE-QUAL-W2 APPLICATIONS**

Contents List

| | Page: |
|---|--------------|
| 3.1 INTRODUCTION | 3.1 |
| 3.1.1 Reservoir applications | 3.1 |
| 3.1.2 Model description | 3.2 |
| 3.1.3 References | 3.5 |
| 3.2 APPLICATION OF CE-QUAL-W2 TO SIMULATE THE WATER QUALITY AND HYDRODYNAMIC BEHAVIOUR OF INANDA DAM. | 3.6 |
| 3.2.1 Introduction | 3.6 |
| 3.2.2 Model configuration | 3.10 |
| 3.2.3 Model calibration | 3.12 |
| 3.2.4 Model application and scenario evaluation | 3.20 |
| 3.2.5 Conclusions | 3.36 |
| 3.2.6 Recommendations | 3.37 |
| 3.2.7 References | 3.39 |
| 3.3 APPLICATION OF CE-QUAL-W2 TO SIMULATE THE SALINITY AND HYDRODYNAMICS OF THE VAAL BARRAGE. | 3.43 |
| 3.3.1 Introduction | 3.43 |
| 3.3.2 Model input | 3.45 |
| 3.3.3 Model configuration | 3.46 |
| 3.3.4 Model calibration | 3.47 |
| 3.3.5 Salinity characteristics during the freshening release | 3.49 |
| 3.3.6 Description of scenarios | 3.54 |
| 3.3.7 Results of scenario testing | 3.54 |
| 3.3.8 Conclusions | 3.62 |
| 3.3.9 Recommendations | 3.63 |
| 3.3.10 References | 3.63 |
| 3.4 APPLICATION OF CE-QUAL-W2 USING THE ROODEPLAAT DAM DATA SET TO EVALUATE THE SIMULATION OF THERMAL AND CHEMICAL STRATIFICATION. | 3.65 |
| 3.4.1 Introduction | 3.65 |
| 3.4.2 Data compilation | 3.67 |
| 3.4.3 Model application and calibration | 3.73 |
| 3.4.4 Results and conclusions | 3.85 |
| 3.4.5 Recommendations | 3.87 |
| 3.4.6 References | 3.88 |
| 3.5 APPLICATION OF CE-QUAL-W2 IN THE ESTIMATION OF THE WATER QUALITY OF A PROPOSED RESERVOIR ON THE OLIFANTS RIVER AT ROOIPOORT. | 3.89 |
| 3.5.1 Introduction | 3.89 |
| 3.5.2 Compilation of data set | 3.90 |
| 3.5.3 Model configuration | 3.92 |
| 3.5.4 Results | 3.94 |
| 3.5.5 Conclusions | 3.98 |
| 3.5.6 Acknowledgment | 3.101 |
| 3.5.7 References | 3.102 |
| 3.6 APPLICATION OF CE-QUAL-W2 TO LAING DAM TO EVALUATE THE MANAGEMENT IMPLICATIONS OF DIVERSIONS FROM WRIGGLESWADE DAM. | 3.103 |
| 3.6.1 Introduction | 3.103 |
| 3.6.2 Input data compilation | 3.104 |
| 3.6.3 Model verification | 3.106 |
| 3.6.4 Wriggleswade diversion scenarios | 3.114 |
| 3.6.5 Conclusions | 3.119 |
| 3.6.6 References | 3.121 |

CHAPTER 3

APPLICATION OF *CE-QUAL-W2*

GENERAL INTRODUCTION

by
A J Bath

3.1 BACKGROUND

This chapter describes the application and testing of *CE-QUAL-W2* using the data sets for five water bodies. This section provides an overview of the applications and the model.

3.1.1 Reservoir applications

Five applications were undertaken to demonstrate the use of *CE-QUAL-W2* to provide information for the management of water quality. The applications are summarized below:

- **Inanda Dam (Section 3.2):** The reservoir experiences extended periods of stratification, sediment release of contaminants, and high algal growth. These factors have affected the fitness for use of the reservoir. The nutrient/algal interactions of Inanda Dam are simulated to provide information on: drawoff depth, sediment interactions, reservoir draw-down, reservoir hydrodynamics, and the phosphorus regime of the reservoir.
- **Vaal Barrage (Section 3.3):** The salinity of the water body is governed to a large extent by saline tributary inflows and low salinity releases from the Vaal Dam. The hydrodynamic and salinity behaviour of the Barrage was simulated to provide information on the influence of freshening releases, optimization of releases, and diversion canal options.
- **Roodeplaat Dam (Section 3.4):** The reservoir shows pronounced thermal and chemical stratification for almost nine months each year. The model was used to simulate the thermal stratification and dissolved oxygen regime of Roodeplaat. These results were compared with the output from *DYRESM*, described in Chapter 2, and also used to assess the calibration requirements of the model.
- **Rooipoort Dam (Section 3.5):** A reservoir was proposed on the Olifants River at Rooipoort to supply potable water to Pietersburg, in the Northern Province. The model was used to provide preliminary information on the thermal stratification, hydrodynamic response, and salinity gradients within the reservoir. The information provided by the model was used to identify key water quality issues which include: location of the offtake tower, drawoff depth, water treatment process design, and management of the upstream catchment.

- **Laing Dam (Section 3.6):** During periods of low flow, Laing Dam receives drainage of high salinity from point and nonpoint sources. This gives rise to an elevated salinity in the reservoir. A simulation was performed to determine the influence of low salinity transfers from the Kubusi River catchment on the receiving water quality behaviour of Laing Dam.

3.1.2 Model description

Model Overview *CE-QUAL-W2* is a two-dimensional (2-D), laterally averaged, hydrodynamic and water quality simulation model. The model is based on the assumption that the water body is homogenous across the lateral width. Therefore, the model is best suited for relatively long and narrow water bodies that show water quality gradients in the longitudinal and vertical directions. The model has been developed for use on rivers, lakes, reservoirs and estuaries.

Model Background The original version of the model was known as *LARM* (Laterally Averaged Reservoir Model) which was developed in 1975 by Edinger and Buchak. The first application of the model was on a reservoir with a single main branch. Modifications to the model allowed for multiple branches and the ability to handle estuarine boundary conditions. The revised version of the model was known as *GLVHT* (Generalised Longitudinal-Vertical Hydrodynamics and Transport model). Water quality simulation capabilities were added by the Water Quality Modelling Group at the US Army Engineer Waterways Experimental Station in Vicksburg, Mississippi and was known as *CE-QUAL-W2* Version 1.

Considerable modifications were made to the model to improve the structure of the code and decrease the data storage requirements. These modifications resulted in Version 2 of the model. The latest enhancements to the model include: dynamic adjustment of the timestep, selective withdrawal algorithm, higher order transport scheme, and improved volume balance and mass balance algorithms (Cole, 1993; Cole and Buchak, 1993).

Model Capabilities In summary these include the following:

- The hydrodynamic routines predict the water surface elevations, velocities and temperatures.
- The water quality algorithms allow the simulation of up to 21 constituents in addition to water temperature. These include nutrient/algal interactions and sediment behaviour. Section 3.2 describes the simulation of the eutrophication response of Inanda Dam and Section 3.3 describes the simulation of salinity in the Vaal Barrage.
- The model has been modified so that simulations can be run over extended time periods. The application of the model using the Rooipoort Dam data set was configured using nearly five years of data to examine long-term trends in the salinity response of the reservoir.

- The ability of the model to simulate upstream and downstream head boundary conditions allows the use of the model for estuaries, or reservoirs in which the inflow volumes are unknown.
- The branching algorithm allows the model to be used in reservoirs which have a complex layout such as dendritic reservoirs, or estuaries with multiple freshwater inflows. Section 3.3 describes the use of the model to simulate multiple inflows and outflows using the data set for the Vaal Barrage application. The selective withdrawal algorithm calculates the vertical extent of the withdrawal zone based on outflow velocity and water density.
- The water body may be configured using segments of unequal length and layers of unequal thickness. The model adjusts the location of the surface layer and upstream segment to account for a rising or falling water level. This feature was important in the Laing Dam application where the reservoir showed variable water level during the simulation period.
- The model uses a variable timestep algorithm which ensures numerical stability.
- The control file allows the user to specify the format of the output produced by the model. Görgens *et al.* (1993) describe the development of the post-processor (POST2) which is used in this chapter to produce graphical and animated presentation of the model output.

Model Limitations In summary these include the following

- The lateral averaging assumes that the lateral variations in water velocity, water temperature and constituents are negligible. In a large wide water body this assumption may limit the applicability of the model. The applications described in the following sections include water bodies which are comparatively long and narrow.
- The water quality algorithms used in the model are simplifications of the processes taking place within aquatic systems. Only one algal compartment is simulated and thus algal succession can not be accommodated. The model does not include the influence of zooplankton in the cycling of nutrients and grazing of phytoplankton. The present version of the model does not model the processes and kinetics of the reservoir bottom sediments. This has most influence when the simulation extends over many years.
- The availability of input data is not a limitation of the model. However, it is often the limiting factor in the application of the model where insufficient data are available for calibration and verification.

Model Enhancements: It has been recognised that internal recycling of nutrients in a reservoir plays a major role in water quality. Therefore the latest enhancements being made to the model include refinement of the process descriptions. This will incorporate a fully predictive sediment compartment which it is hoped to eliminate the need to specify the Sediment Oxygen Demand term (SOD) and nutrient fluxes (Cole, 1995).

Model Hardware Requirements The minimum configuration is an 80386 or 80486 personal computer equipped with a mathematical co-processor. The model requires a minimum of four megabytes of memory with between ten and fifteen megabytes of hard disk space. The applications described in the following sections were carried out using a 80486 DX2 (66 Megahertz) with 8 Megabytes of memory and 120 Megabytes of hard disk space.

Model Software Requirements Using the model on a personal computer (PC) operating under DOS, the user requires a 32 bit FORTRAN compiler with a DOS extender that will use the PC's protected mode. The model was compiled using the Lahey FORTRAN F77L3 compiler with DOS extension and optimized for use on a 80486 PC.

Model and Data Availability *CE-QUAL-W2* is freely available from the Environmental Laboratory, US Army Corps of Engineers, Waterways Experimental Station, Vicksburg, MS, United States. The model is provided with a user manual, example data sets, and pre-processor (Cole, 1993). The data sets used as part of this study are held at the offices of Ninham Shand Consulting Engineers, Cape Town, South Africa.

Demonstration data files *CE-QUAL-W2* is provided with a number of demonstration data files, these include the following:

- **Degray Lake** is a reservoir with a single branch configuration and the model is used to simulate and demonstrate the full water quality capabilities.
- **JST Dam** is situated on the Savannah River between Georgia and South Carolina. The model is used to examine the influence of pump storage on the water quality response of the reservoir.
- **Thames River Estuary** is situated on the East Coast of the United States and the model is used to simulate temperature, salinity, water flow velocities, and water surface elevations of the estuary. The model is used to analyze the release of compensation releases on the water quality of the estuary.
- **Cumberland River** near Nashville is modelled to demonstrate the simulation of BOD and dissolved oxygen.

3.1.3 References

Cole, T.M. (1993)

Personal communication, Environmental Laboratory, US Army Corps of Engineers, Waterways Experimental Station, Vicksburg, MS.

Cole, T.M. (1995)

Personal communication, Environmental Laboratory, US Army Corps of Engineers, Waterways Experimental Station, Vicksburg, MS.

Cole, T.M. & Buchak, E.M. (1993)

CE-QUAL-W2: A two-dimensional, laterally averaged, hydrodynamic and water quality model. User Manual, Environmental Laboratory, US Army Corps of Engineers, Waterways Experimental Station, Vicksburg, MS, Instruction report number ITL-93, September 1993.

Görgens, A.H.M., Bath, A.J., Venter, A., de Smidt, K. & Marais, G.v.R. (1993)

Applicability of hydrodynamic reservoir models for water quality management in stratified water bodies in South Africa, Report by Ninham Shand Inc. and the University of Cape Town to the Water Research Commission, Pretoria. Report number 304/1/93.

SECTION 3.2
APPLICATION OF CE-QUAL-W2 TO SIMULATE
THE WATER QUALITY AND HYDRODYNAMIC BEHAVIOUR
OF INANDA DAM.

by
A J Bath

3.2.1 INTRODUCTION

Reservoir description Inanda Dam is located on the lower reaches of the Mgeni River in the KwaZulu-Natal Province, 25 km from the centre of Durban, at a latitude of 29°41'S, longitude of 30°52'E, and elevation at FSL of 148 masl. The dam wall was completed in March 1989 and the reservoir reached full supply level for the first time in February 1990. The reservoir has a full supply capacity of 251 million m³, surface area of 1463 hectare, and mean water residence time of one year. The reservoir is located in a steep sided sinuous river valley and is ±18 km long, ±900 metre wide, and has a mean depth of 17.4 metre. Near the dam wall, the reservoir has a maximum depth of 55 metre (Hudson *et al.*, 1993).

The reservoir was built to increase the yield of the lower Mgeni River system and provide water to Durban. Water is released from Inanda Dam and abstracted from the Mgeni River 20 km downstream at the Clermont Pump station and transferred to the Wiggins water works. Releases are also made from Inanda Dam to manage the Mgeni River Estuary (Tollow, 1991).

The Inanda Dam site is situated downstream of both Nagle Dam and the confluence of the Msunduze River. The Msunduze River drains the population centres of Pietermaritzburg and Edendale, a large informal population, and significant agricultural and industrial development (Hudson *et al.*, 1993). In addition, about 18 million m³ per year of treated wastewater enters Inanda Dam from the Darvill Works which discharges into the Msunduze River.

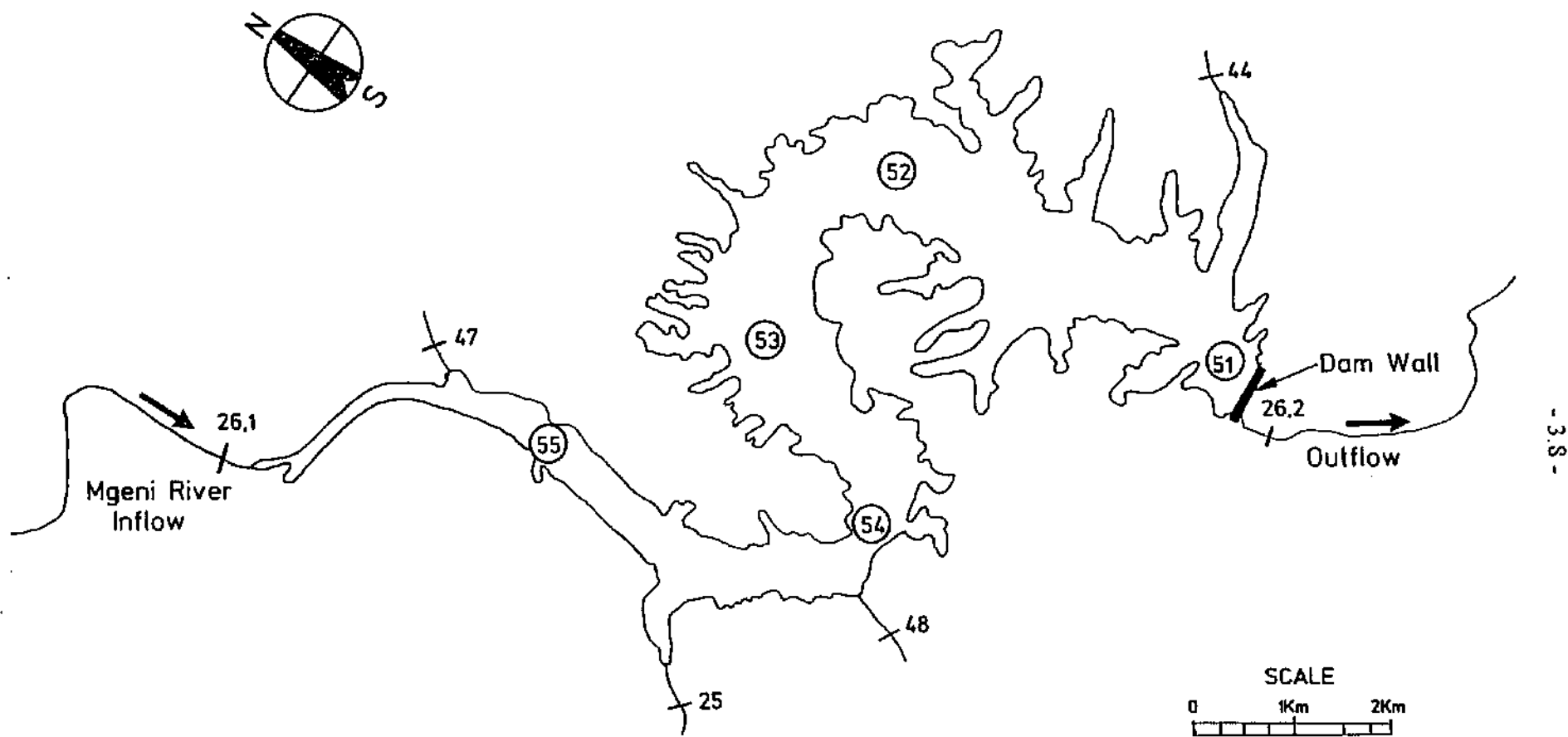
Prior to construction of the reservoir, it was cautioned that the reservoir morphology and location (downstream of the greater Pietermaritzburg area) could give rise to water quality problems associated with stratification and eutrophication (Bruwer, 1979; UW, 1989). In response to this caution, a multi-level outlet structure was incorporated in the design of the dam wall (UW, 1992a). Nine outlets were situated at 3 metre intervals from a depth of 4.5 to 28.5 metre below full supply level. A scour release valve was located at a depth of 30 metre.

Over the past four years, the reservoir has showed a number of water quality problems, including: (1) development of abundant algal biomass, (2) anaerobic hypolimnion, and (3) release of metals and nutrients from the bottom sediments.

Inanda Dam water quality data base The reservoir has been monitored routinely by Umgeni Water since the reservoir construction was completed in 1989. Figure 3.2.1 shows the location of the water quality monitoring points in the reservoir as well as the monitoring points on the inflowing rivers (Point 26.1) and side streams (ie Point 48). In Inanda Dam, water samples were collected from the main water body at five sampling points, see Figure 3.2.1. At present, only three of the original points are monitored. At these points, water samples are collected from the surface and bottom, and an integrated depth sample collected from the top 5 metres of water. Water samples are collected on a weekly basis. The water samples are analyzed for about 20 constituents including: algal count, chlorophyll-a, secchi depth, suspended solids, TDS, alkalinity, nitrate, ammonia, phosphate, total phosphorus, organic carbon, BOD, DO, *E.coli* and total plate counts. Temperature and dissolved oxygen depth profiles are measured at 2 metre intervals at each of the five sampling points in the reservoir (UW, 1993). The side streams are sampled at the points shown in Figure 3.2.1. The Mgeni River is the main inflow to Inanda Dam, and water samples are collected at Point 26.1 (Figure 3.2.1).

Water quality of Inanda Dam Analysis of the measured water quality data for Inanda Dam shows:

- Stratification occurs each summer, beginning around September.
- Maximum stratification is attained at the end of December, with a temperature gradient of about 10 to 12°C between the surface and bottom layers. Limited vertical mixing is evident during stratification, except during discrete storm inflows which cause a temporary (and localised) disruption of the vertical temperature profile.
- The thermocline occurs at a depth of between 10 and 14 metre, with a temperature differential (of the thermocline) of around 5°C.
- During stratification, an oxycline develops at a depth of around 6 to 12 metre and the hypolimnion becomes anaerobic. Therefore, at full supply level, in excess of 44 percent of the storage volume may become anaerobic.
- Under anaerobic conditions, the reservoir sediments release both metals (iron and manganese) and ammonia.
- In the surface layer during the summer, algal growth is pronounced with dominance of the blue-green alga *Microcystis spp.* (UW, 1990; UW, 1993).
- During the summer, super-saturation of dissolved oxygen occurs in the epilimnion associated with algal growth (UW, 1992a and 1993).
- Isothermal conditions occur from May, with rapid cooling of the surface layers bringing about vertical mixing and over-turn.
- During isothermal periods, oxygenated water is mixed into the lower layers. However, the high sediment oxygen demand results in a vertical gradient between the surface and bottom waters (UW, 1993; Görgens *et al.*, 1993).



Location map of Inanda Dam with water quality monitoring points.

Figure 3.2.1

- During periods of high water inflow, oxygenated river water penetrates into the hypolimnion and metalimnion of the reservoir. Similar observations have been made in reservoirs located in the US, and are termed *metalimnetic oxygenation minima* (Cole & Hannan, 1993; Cole, 1993 and 1994).
- As a result of the reservoir being some 18 km long at full supply level, considerable longitudinal gradients are evident in the concentration of various constituents. In response, the algal growth is greatest near the inflow of the Mgeni River (being the major source of nutrients) (Hudson *et al.*, 1993).
- Water quality problems have manifested themselves with taste and odour problems, suspended sediment, dissolved metals, nutrients and algae (Hudson *et al.*, 1993).

Water quality management and study objectives To manage the water quality of Inanda Dam, two approaches are possible. Firstly, the control of contaminant sources derived from the upstream catchment, and secondly the *in-situ* management of the reservoir.

Since reducing the contaminant load from the upstream catchment is comparatively complex and difficult to achieve in the short term (UW, 1992a), various *in-situ* methods have been considered to obtain a short term improvement in water quality. Possible methods include: chemical dosing to kill algae, active management of the reservoir, flushing the dam after the first flood, selective abstraction depth to avoid water of poor quality, and scouring anaerobic bottom water and destratification (UW, 1992a; UW, 1992b). Chapter 2 describes the use of the model *DYRESM* to examine destratification options for Inanda Dam. This section describes the configuration, calibration and application of *CE-QUAL-W2* to provide information on:

- **Optimum abstraction (drawoff) depth** to avoid algae in the surface layers, and/or nutrient/metal-laden water in the middle and lower layers.
- The influence of **reservoir draw-down** on the stratification and water quality response of the reservoir. Future operating conditions may result in the reservoir being kept at a reduced water storage level.
- Influence of **reservoir sediments** on the quality of the epilimnion and hypolimnion.
- Influence of reducing the **phosphorus loading** entering the reservoir, and response of the algal biomass at the dam wall basin.
- Role of **hydrodynamic mixing** and density currents during periods of high runoff on the

water quality response of the reservoir.

- Influence of **hypolimnetic releases** and scours on the water quality in the dam wall basin.

The water quality variables of interest investigated as part of this simulation include: water temperature, dissolved oxygen, algal biomass, suspended solids, phosphorus, nitrogen, and iron.

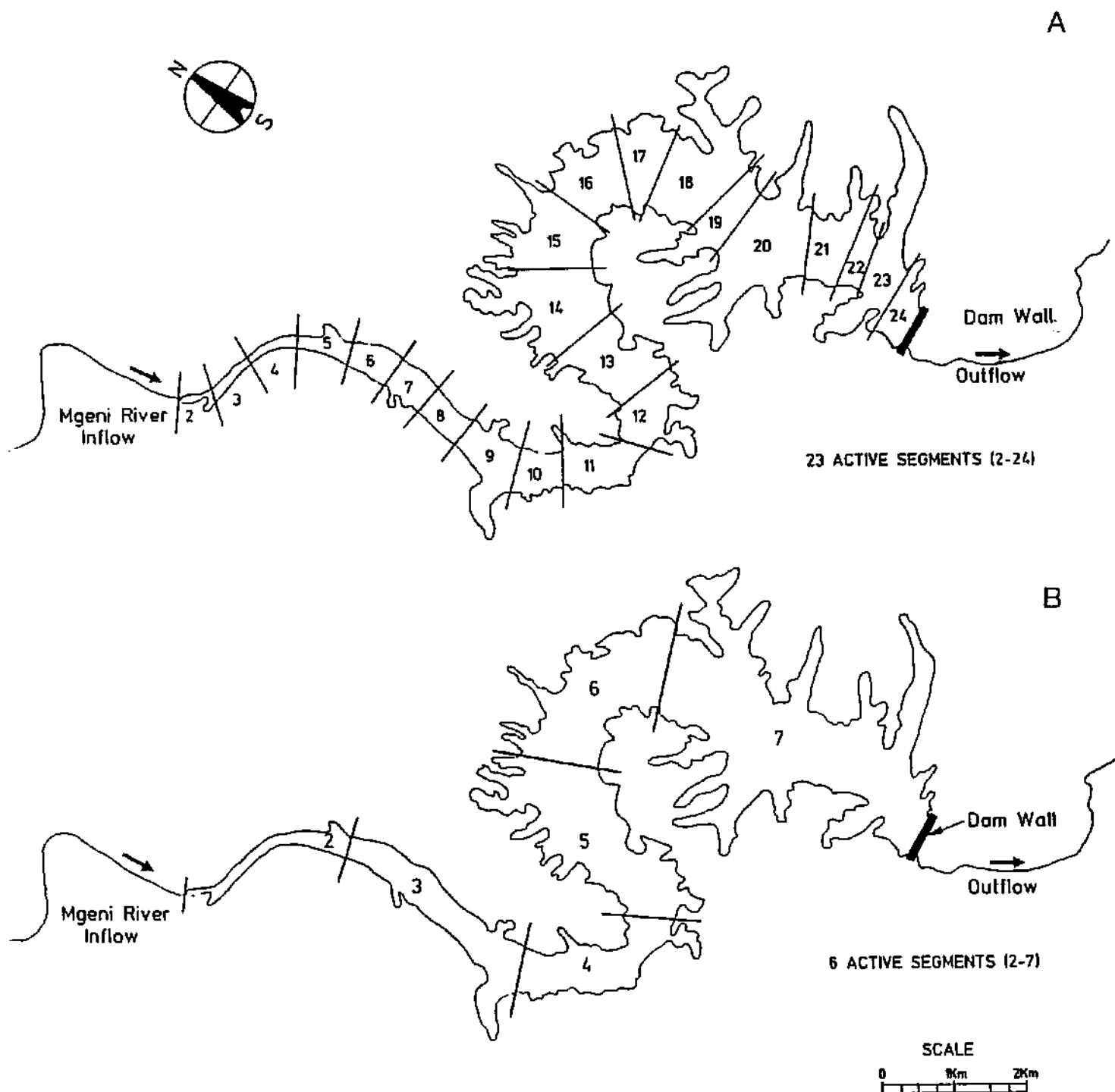
3.2.2 MODEL CONFIGURATION

Görgens *et al.* (1993) reported a model configuration for Inanda Dam with over 400 active cells which had a run-time exceeding 200 minutes (for a simulation period of 360 days). Simulations undertaken to calibrate the model were found to become excessively long. One of the objectives was to reduce the run-time and yet maintain the predictive capabilities of the model. In this regard, two model configurations were tested: (1) a configuration using 23 segments and 25 layers, and (2) a configuration using 6 segments and 13 layers, see Figure 3.2.2.

The following data sources were used in the physical configuration of the model: (1) topographic maps (scales 1:10 000 and 1:50 000), (2) hydrographic survey data (DWAF, 1990), and (3) volume/area elevation tables (DWAF, 1990).

23 Segment configuration The physical layout of the reservoir was modelled using a single branch (Segments 2 to 23), with 25 layers (2 metre deep), with two outflows, one withdrawal, and no tributary inflows to the reservoir. Figure 3.2.2 (Inset A) shows the reservoir divided longitudinally into 23 segments. Where possible, the segment boundaries coincided with the profile cross-sections used in the hydrographic survey. At each of the 23 segments, the reservoir widths were calculated at 2 metre increments from the bottom to full supply level. The length and orientation of each of the 23 segments was determined. The bathymetric data were then collated into a single spread sheet for each of the 23 segments. To verify the bathymetric data, the storage volume of the reservoir was calculated and compared with hydrographic survey data. A close agreement was found between the bathymetric (computed) data and the hydrographic survey (measured) data.

6 Segment configuration The physical layout of the reservoir was modelled using a single branch (Segments 2 to 7), with 13 layers (4 metre deep), with two outflows, one withdrawal, and no tributary inflows to the reservoir. The bathymetric data compiled above was used to determine the storage depth relationship for the 6 segment configuration. Figure 3.2.2 (Inset B) shows the configuration using six segments.



Inset A: 23 segment configuration. Note: Segments 1 and 25 are upstream and downstream boundary segments. Inset B: 6 segment configuration. Note: Segments 1 and 8 are upstream and downstream boundary segments.

Figure 3.2.2

Starting conditions The water quality starting conditions are specified in the control file as well as in the vertical and longitudinal profile files. These data include:

- The starting and ending dates of the simulation period. A simulation period of 365 days was chosen to calibrate the model.
- Reservoir water elevation.
- Initial water temperature and quality data. A longitudinal profile file was used to set the starting conditions in each of the active cells at the start of the simulation (1 January 1990).

In Görgens *et al.* (1993), it was reported that the tributary inflows appear to have a minor influence on the water quality of Inanda compared with the Mgeni River inflow. In this application, the tributary inflows are excluded from the simulation, therefore the main inflow comprises the Mgeni River. For the Mgeni River inflow, the water temperature, mean daily river discharge, and chemical composition are input to the model on a daily basis.

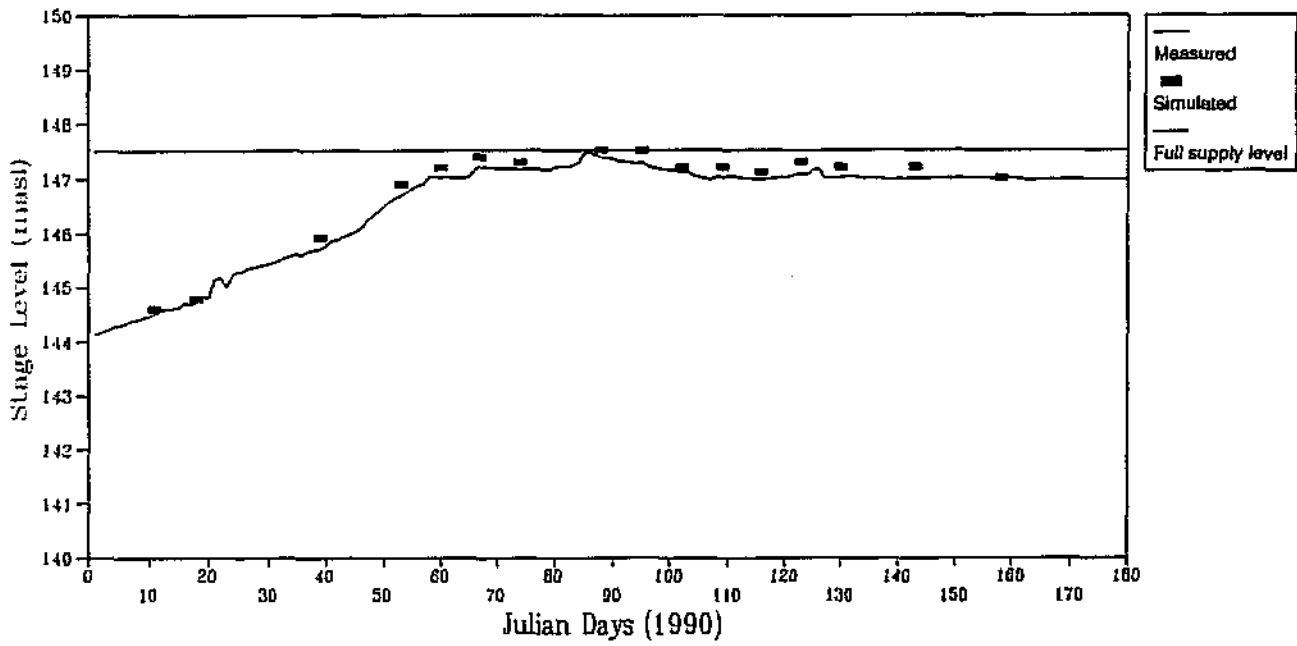
The meteorological input to the model includes: air and dew point temperature, wind speed and direction, and cloud cover. These data were measured at the weather station at Mount Edgecomb, 10 km from Inanda Dam and obtained from the Weather Bureau in digital form.

3.2.3 MODEL CALIBRATION

The model uses 60 rate coefficients to simulate the water quality processes taking place within a water body. As a starting point, values of the coefficients were taken from the Inanda Dam simulation described by Görgens *et al.* (1993). The main components of the calibration procedure are described below.

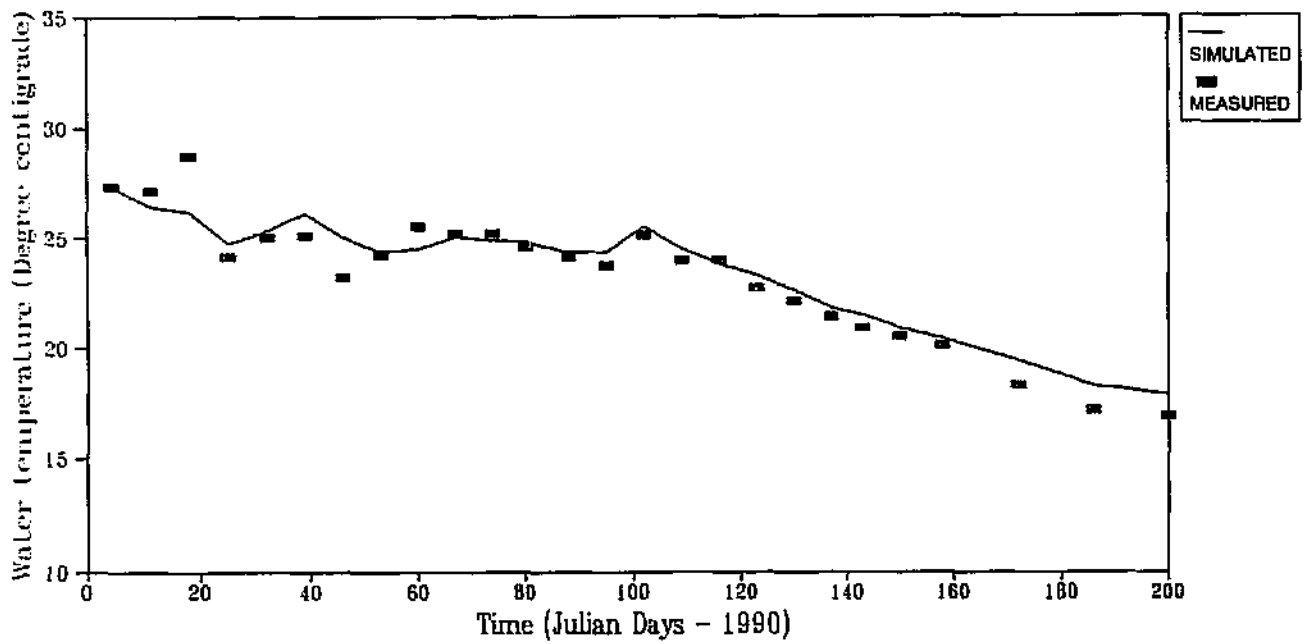
- **Model configuration** Figure 3.2.3 shows the 2-D plots for the 23 and 6 segment configurations. Preliminary calibration runs showed that the 23 segment configuration had a run-time of about 120 minutes to simulate a period of 365 days. In comparison, the 6 segment configuration had a run-time of 35 minutes using the same simulation period. Comparison of the dissolved oxygen and water temperature profile data showed that both configurations of the model provided comparable results. Therefore, based on run-time, the 6 segment configuration was used to calibrate and test the model.
- **Water Budget** The simulation of the water budget is evaluated by comparing the simulated and measured water elevations. During the simulation period, the reservoir started at 83 percent full and within a period of 60 days the reservoir reached maximum operating level. Figure 3.2.4 shows the measured and simulated water surface elevation.





Simulated and measured water elevations.

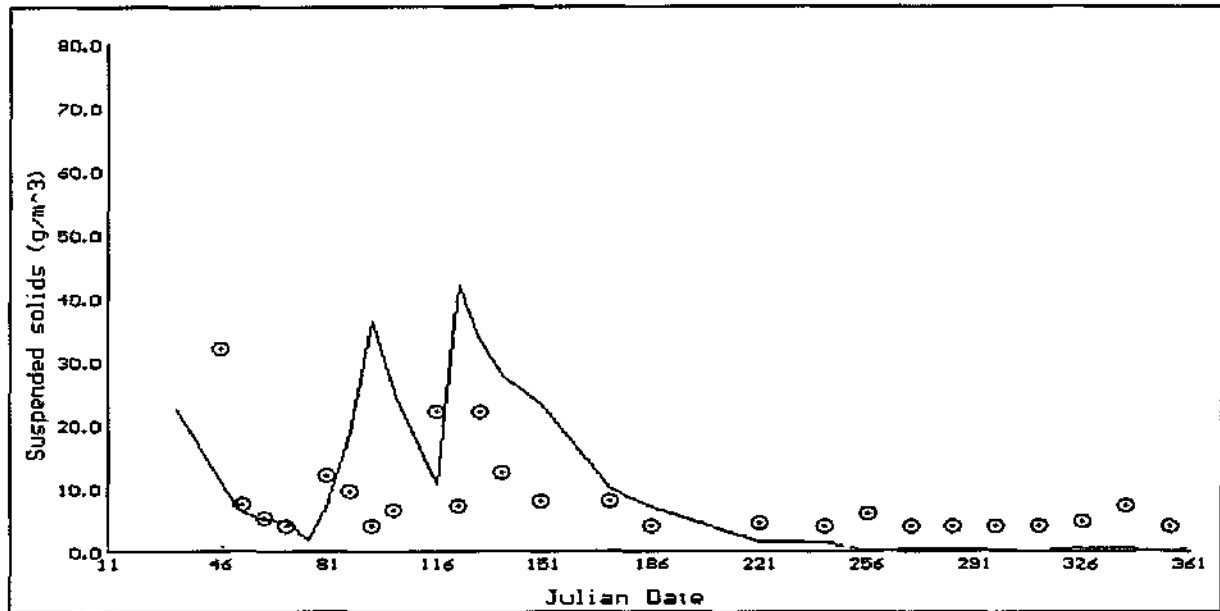
Figure 3.2.4



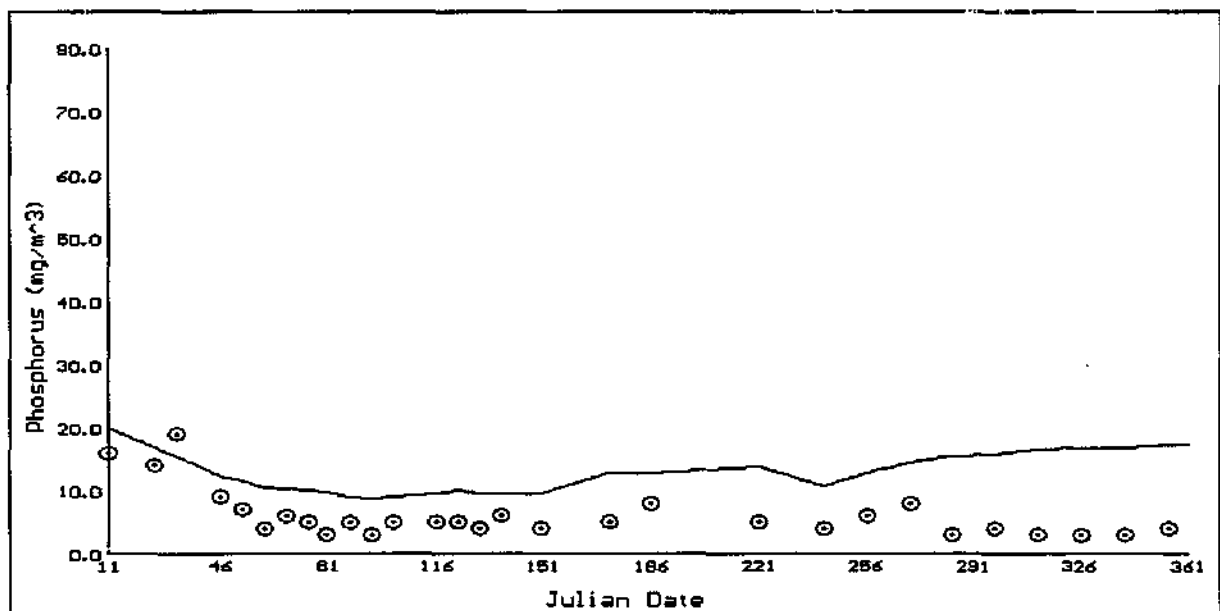
Simulated and measured surface water temperature.

Figure 3.2.5

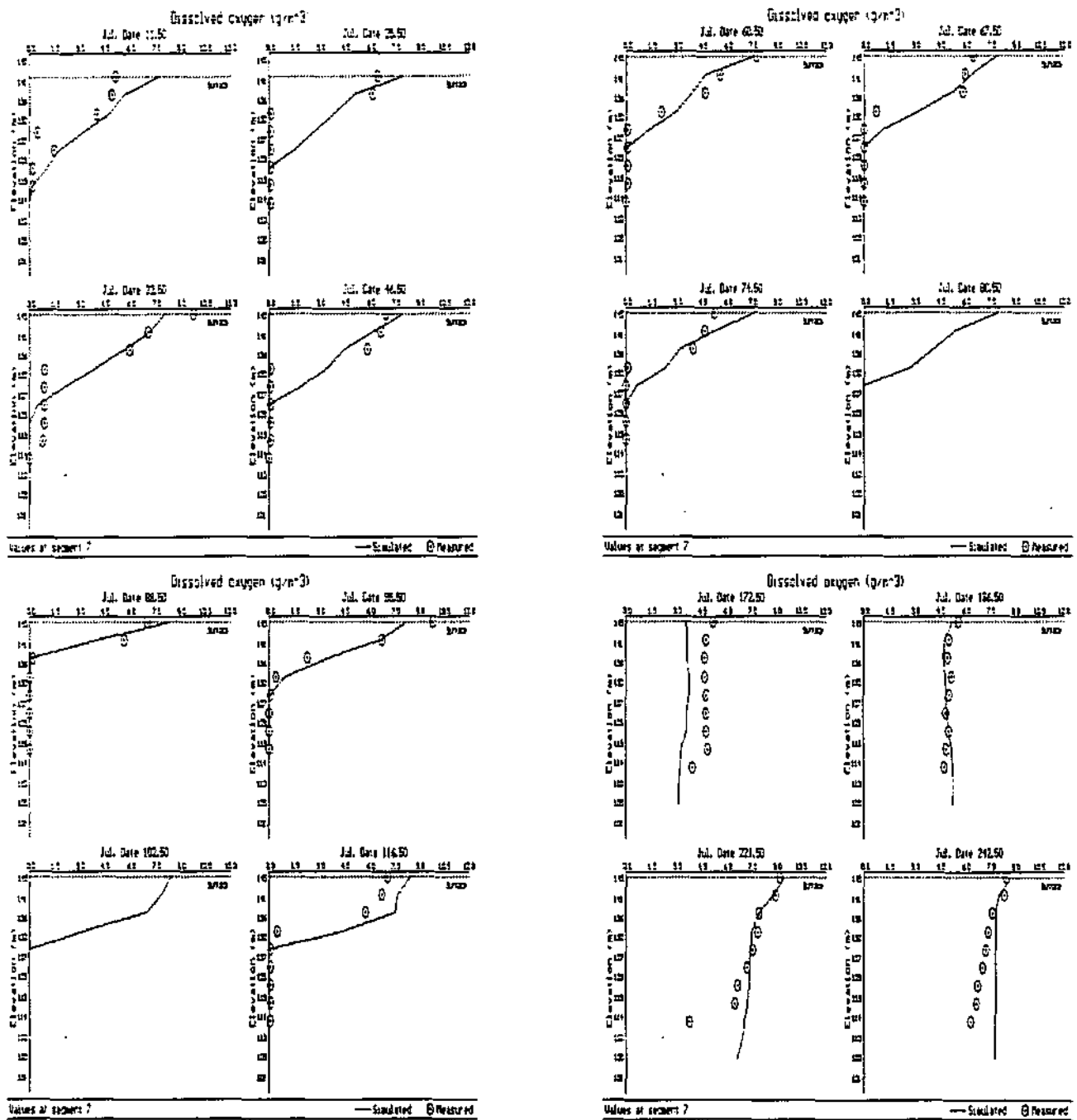
- **Water Temperature** The most acceptable agreement between the measured and simulated water temperature profiles was achieved using a Wind Sheltering Coefficient of 0.9. Figure 3.2.5 shows the simulated and measured surface water temperature data, at the dam wall basin.
- **Suspended solids** The suspended solids settling rate is defined by the term SSETL. Figure 3.2.6 shows the simulated and measured suspended solids data using a settling rate of 0.6 m/day.
- **Hypolimnetic phosphorus** The phosphorus (P) concentration in the hypolimnion is governed by: (1) influx of P from the inflowing river, (2) uptake by algae, (3) release from sediments under anaerobic conditions, and (4) binding of P onto inorganic suspended solids and sedimentation. The partition coefficient for phosphorus, PARTP, accounts for the binding of P onto suspended sediment particles. Repeated simulations showed that although the suspended solids concentration was comparatively high, there was minimal adsorption of P. The term PARTP was therefore given a value of zero. Comparison of the measured and simulated P concentration data showed that the reservoir sediments appear to release minimal quantities of P into the overlying water column during anaerobic periods. Therefore the term PO4REL, accounting for the sediment release of P, was set at a value of zero. Figure 3.2.7 shows the simulated and measured P concentration in the hypolimnion.
- **Dissolved oxygen** The oxygen demand of the reservoir sediments is modelled using the term SOD (sediment oxygen demand). Simulations showed the value of the SOD was 1.1 mgO₂/m²/day, which reflects a high oxygen demand imposed by the sediments. Figure 3.2.8 shows the simulated and measured DO profiles for selected simulation dates, and Figure 3.2.9 shows the 2-D plots for selected days during the simulation period. In the Appendix, Figures 3.2.26 and 3.2.27 show the vertical profile plots and 2-D plots for simulated and measured DO.
- **Surface phosphorus and algal biomass** In the surface waters of the reservoir, the phosphorus concentration is influenced by adsorption onto suspended particles and uptake by algae. As *Microcystis* is the dominant algal genus during the simulation period, the algal growth rate coefficients were taken from literature values (Görgens *et al.*, 1993). Model runs were performed to obtain a satisfactory simulation of the phosphorus and algal biomass in the upper layers of the reservoir. Figure 3.2.10 shows the simulated and measured phosphate concentration, and Figure 3.2.11 shows the simulated and measured algal biomass at the dam wall basin. The second peak in the algal biomass during the




Simulated and measured suspended solids concentration (Note: Simulated data presented as a line and measured data as symbols). Figure 3.2.6

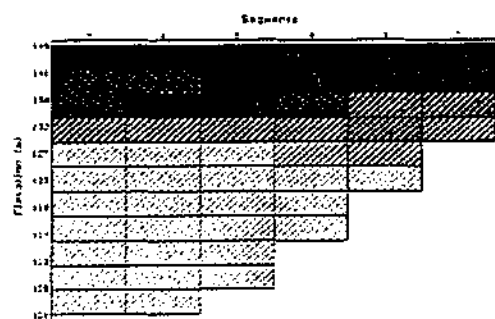


Simulated and measured hypolimnion phosphorus concentration (Note: Simulated data shown as a line and measured data as symbols). Figure 3.2.7

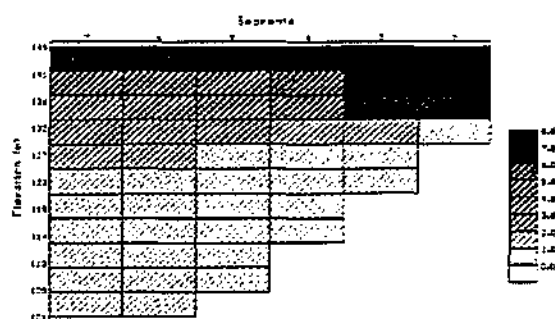


 Simulated and measured dissolved oxygen profiles for the dam wall basin of Inanda.
Figure 3.2.8

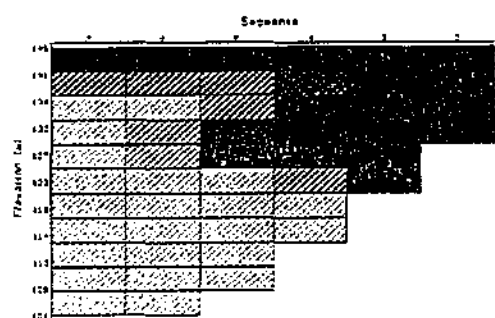
Julian Day 11



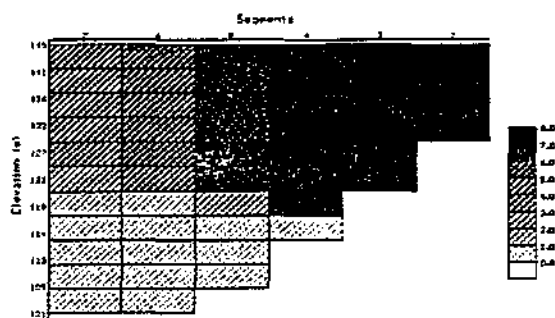
Julian Day 46



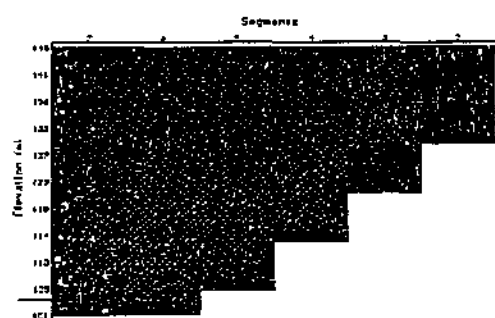
Julian Day 80



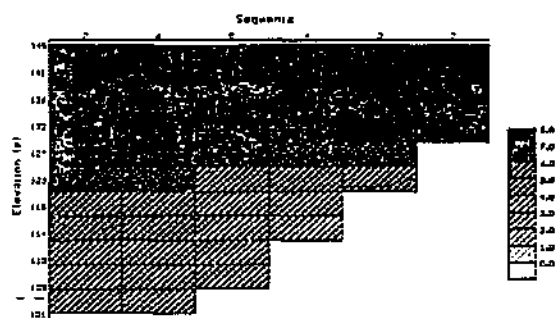
Julian Day 150



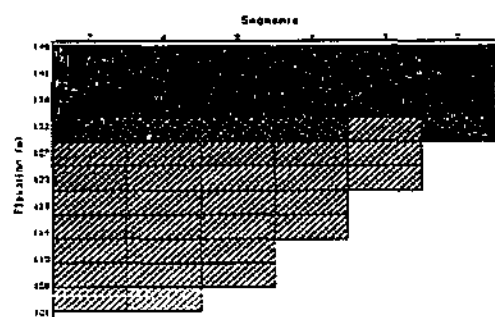
Julian Day 172



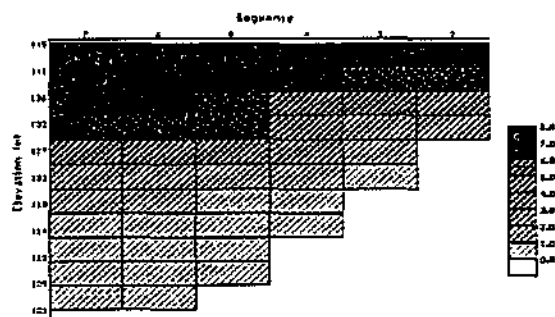
Julian Day 270

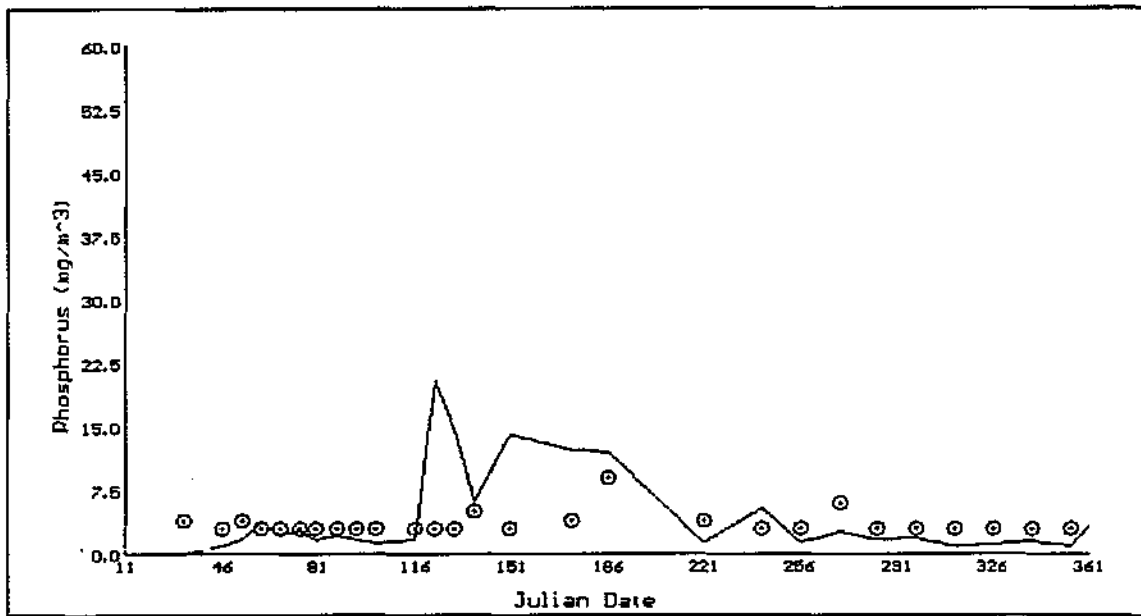


Julian Day 298

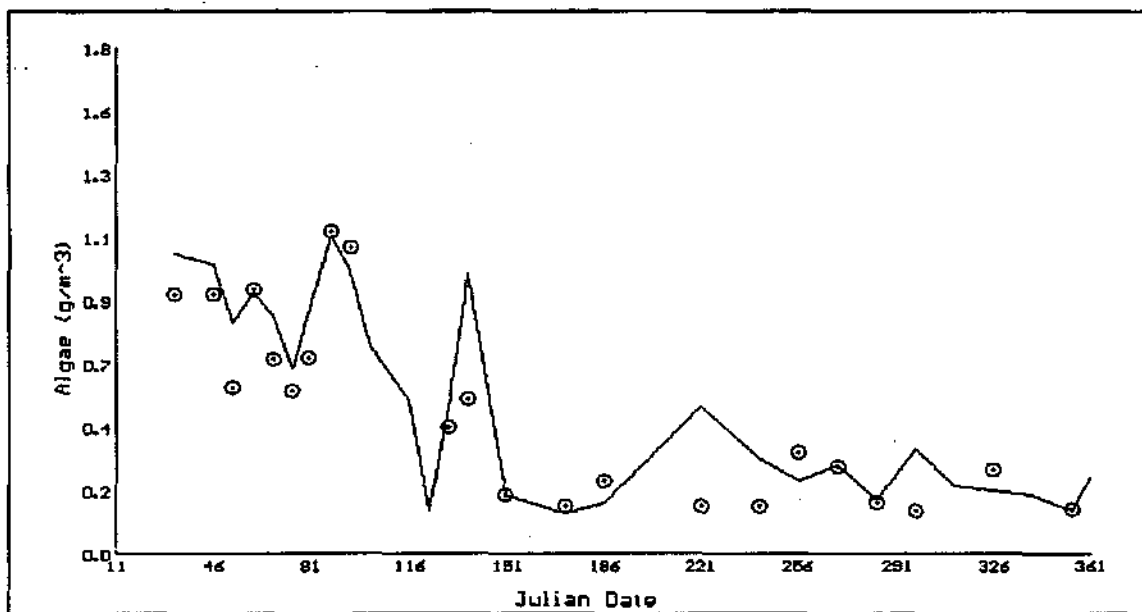


Julian Day 340





Simulated and measured surface phosphorus concentration (Note: Simulated data are shown as a line and measured data as a symbol). Figure 3.2.10



Simulated and measured algal biomass. (Note: Simulated data shown as a line and measured data as a symbol). Figure 3.2.11

middle of the calibration period (day 80 to 120) was caused by an increase in the phosphorus concentration caused by the influx of river inflow into the metalimnion of the reservoir. At the dam wall basin, phosphorus is introduced into the epilimnion by upward mixing from the metalimnion. The model simulations show that the algal growth is limited by the availability of phosphorus and light, as well as by water temperature during the winter months.

- **Nitrogen** Figure 3.2.12 shows the simulated and measured ammonia and nitrate concentrations. The simulation used literature values for the rate coefficients. The release of ammonia from the reservoir sediments was found to be $0.1 \text{ mg/m}^2/\text{day}$.
- **Iron** Preliminary calibration was achieved to simulate the iron concentration in the hypolimnion. The release of iron from the reservoir sediments was simulated using the term FEREL, which was found to have a value of $1 \text{ mg/m}^2/\text{day}$ after calibration. Figure 3.2.13 shows the depth/time distribution of iron in the dam wall basin.

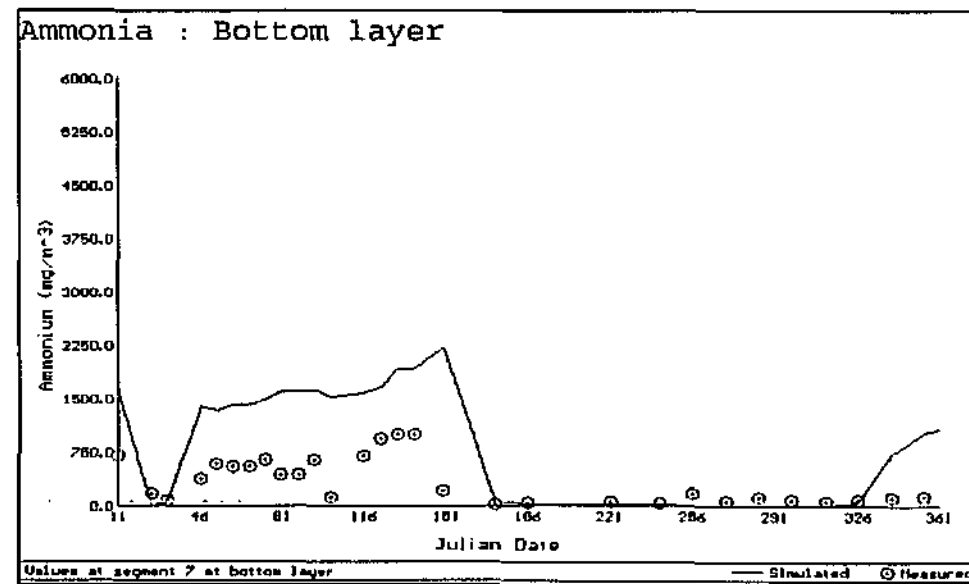
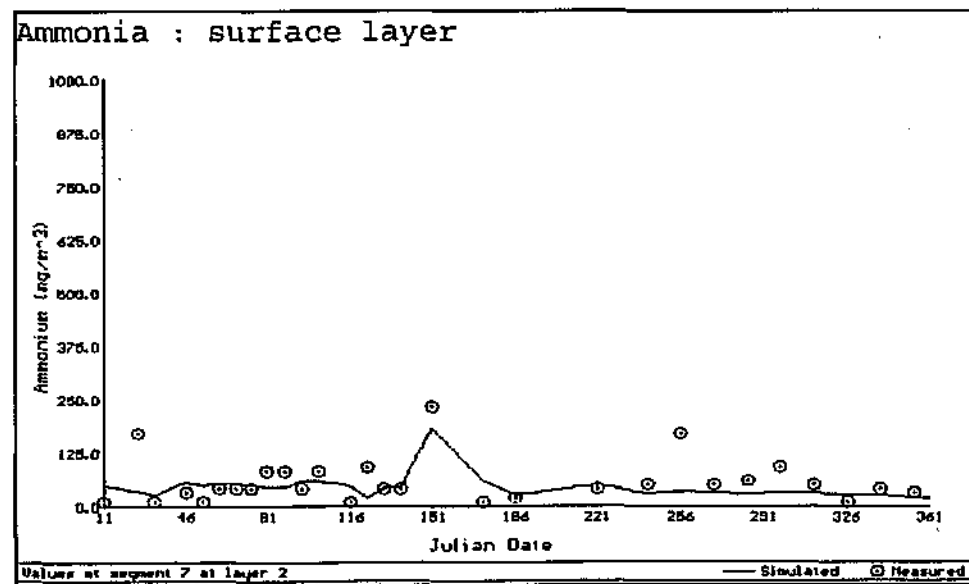
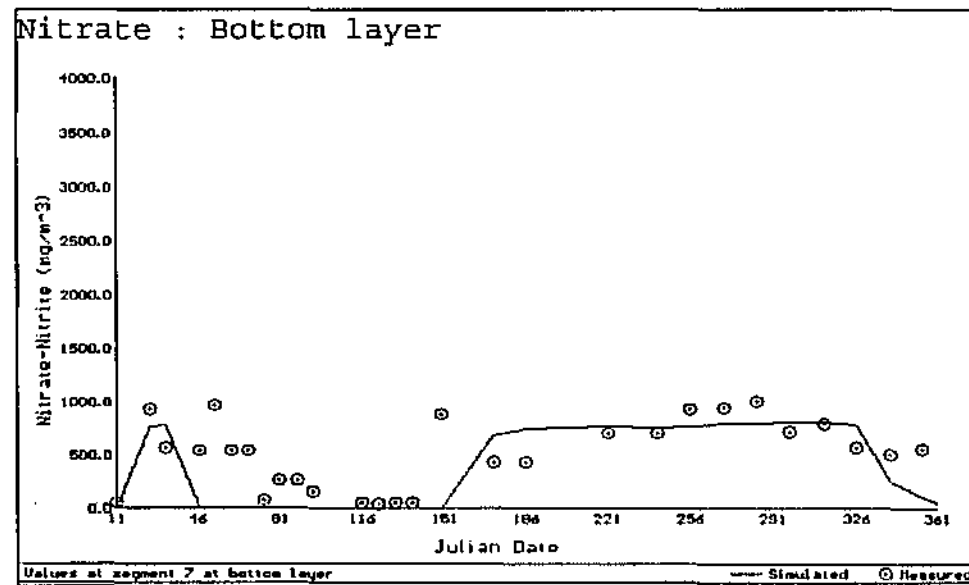
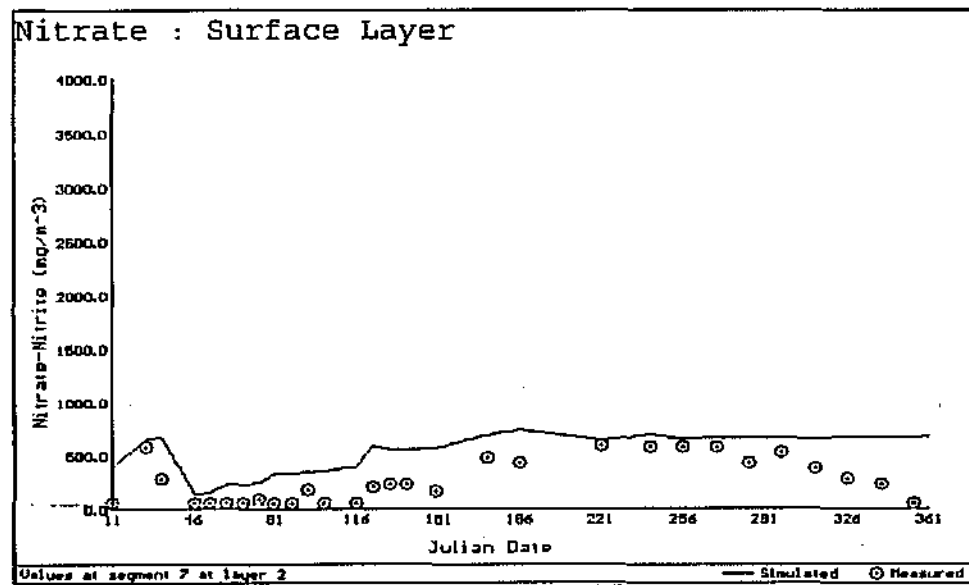
3.2.4 MODEL APPLICATION AND SCENARIO EVALUATION

Optimum abstraction depth A multi-level offtake structure has been incorporated in the design of the dam wall with nine outlets at depth intervals of 3 metre from full supply level. The existing sampling of Inanda Dam includes a surface, depth integrated and bottom sample. Therefore there is sufficient information to determine the depth of drawoff to avoid water of poor quality in the surface, middle or bottom layers (UW, 1993).

Graphical output from the model is used to select the optimum depth of drawoff so that the water contains (1) a minimum concentration of algae and (2) maximum concentration of oxygen thereby avoiding the anaerobic bottom waters containing elevated concentrations of metals and nutrients.

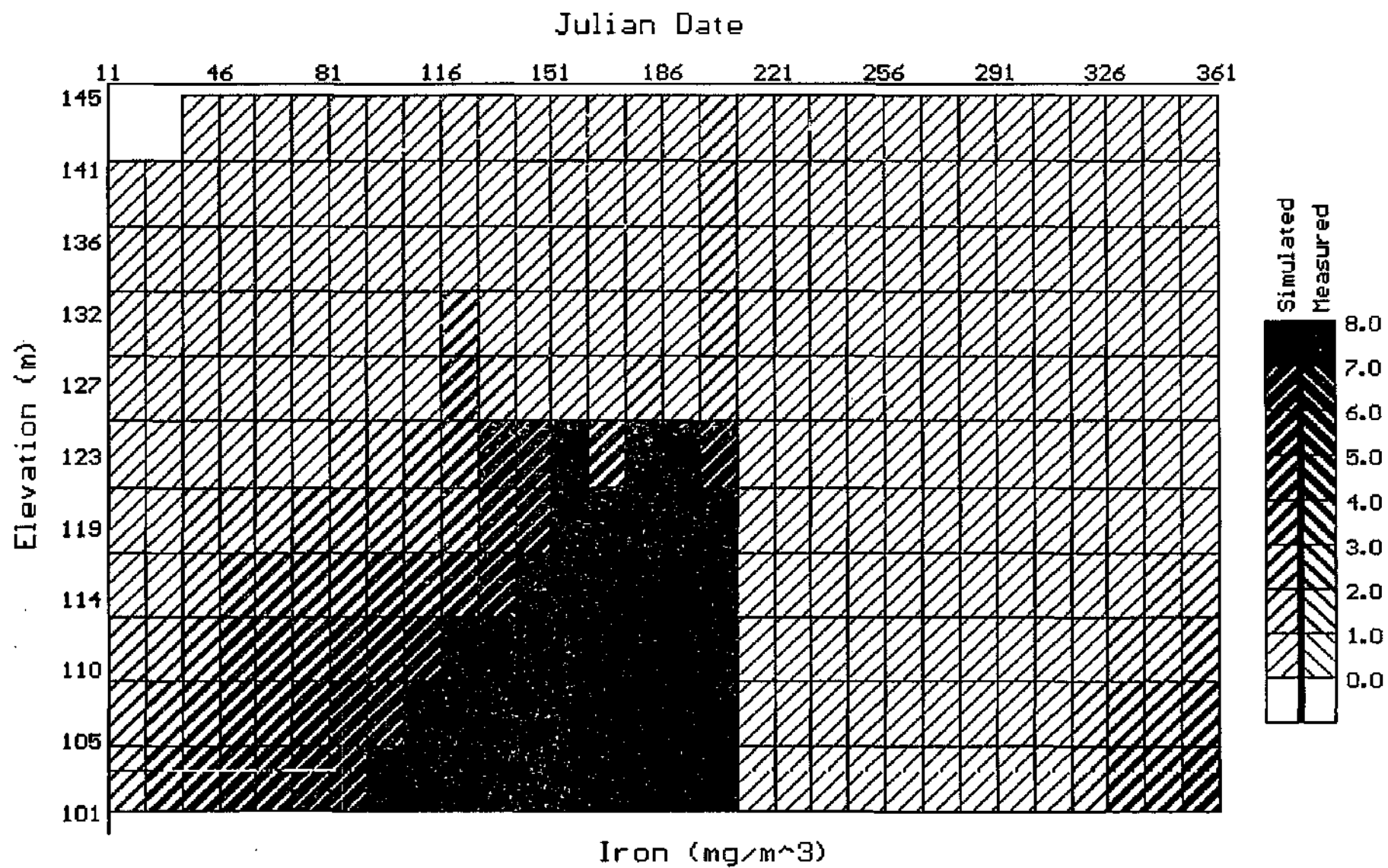
Depth-time (isopleth) plots were produced for algae, ammonia, and dissolved oxygen, see Figures 3.2.14 to 3.2.16. By superimposing the isopleth plots, an estimate was made of the drawoff level.

To avoid the algae in the upper layers, the optimum drawoff was found to be at least 8 metre from the surface. To avoid the anaerobic waters containing elevated concentrations of ammonia, metals and dissolved organic substances, the drawoff had to be less than 18 metre from the water surface. Wind induced currents however influence the vertical position of the oxycline, see Figure 3.2.9. Under such conditions, the deepest drawoff level should be about 14 metre from the surface to account for the variability in vertical elevation in the oxycline. During the winter (mixed period), the abstraction depth is of less concern because of the mixing throughout the vertical profile of the water column.



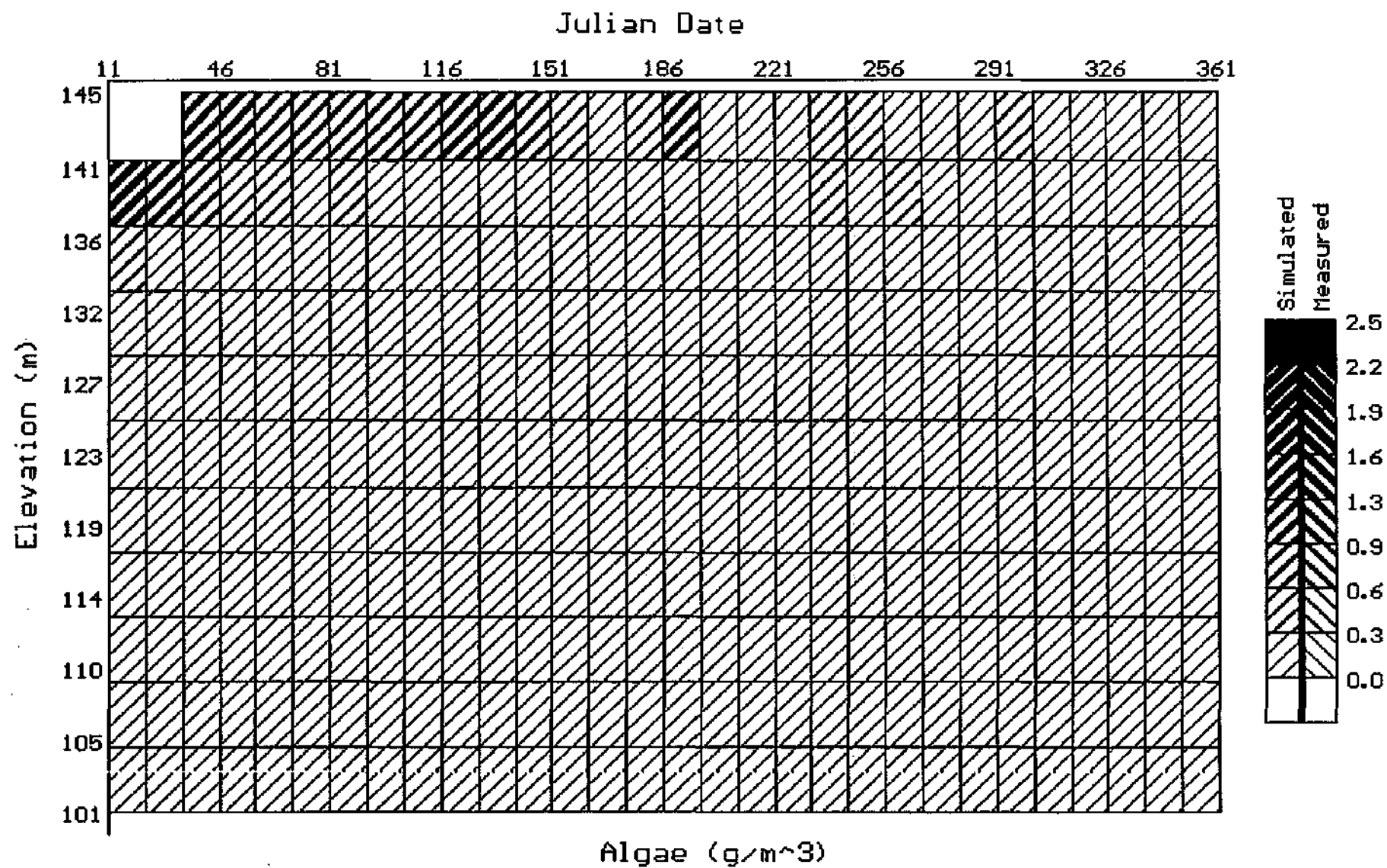
Simulated and measured ammonia and nitrate concentration in the surface layer and hypolimnion.

Figure 3.2.12



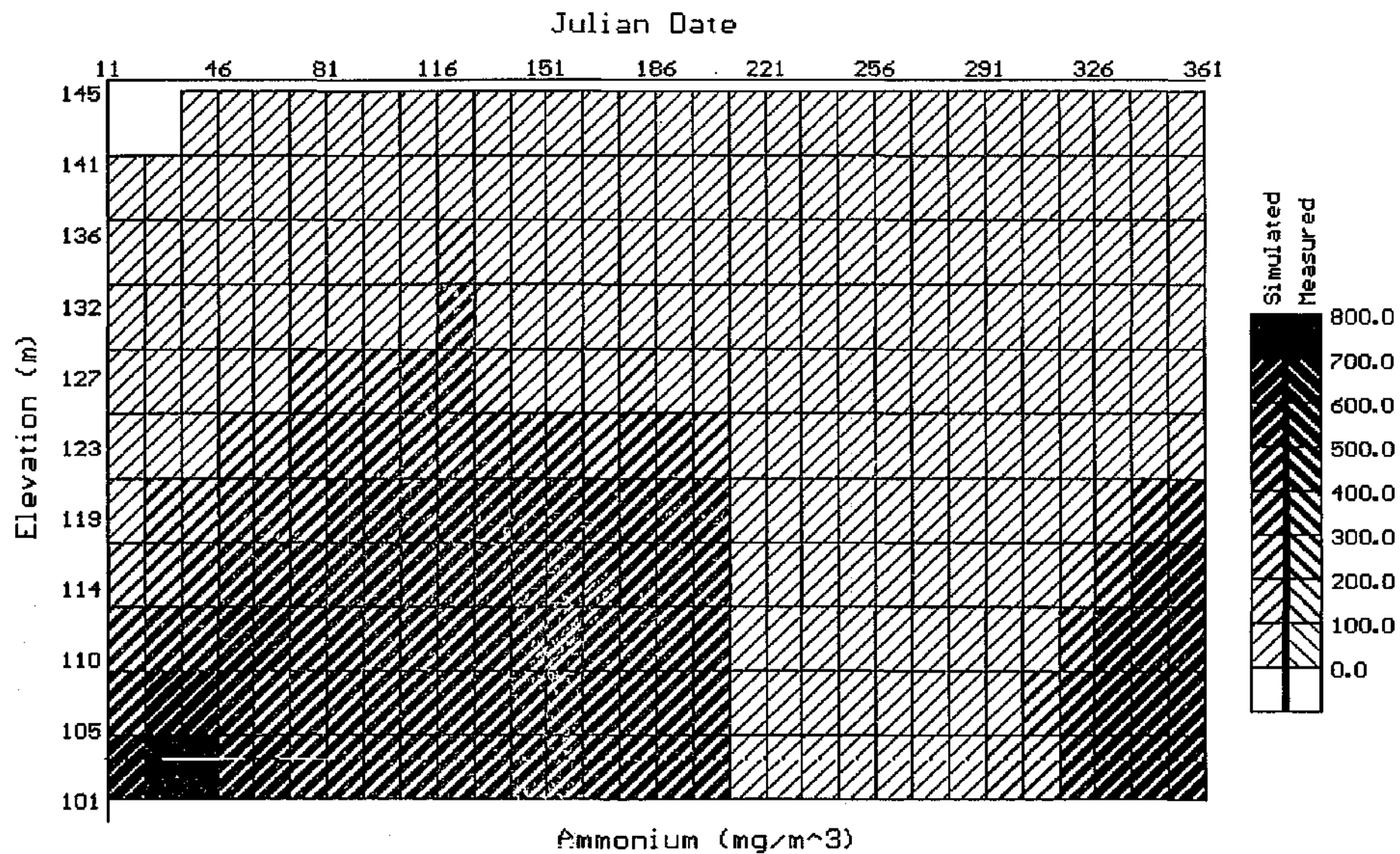
Isopleth (depth vs time) plot: Iron concentration at the dam wall.

Figure 3.2.13

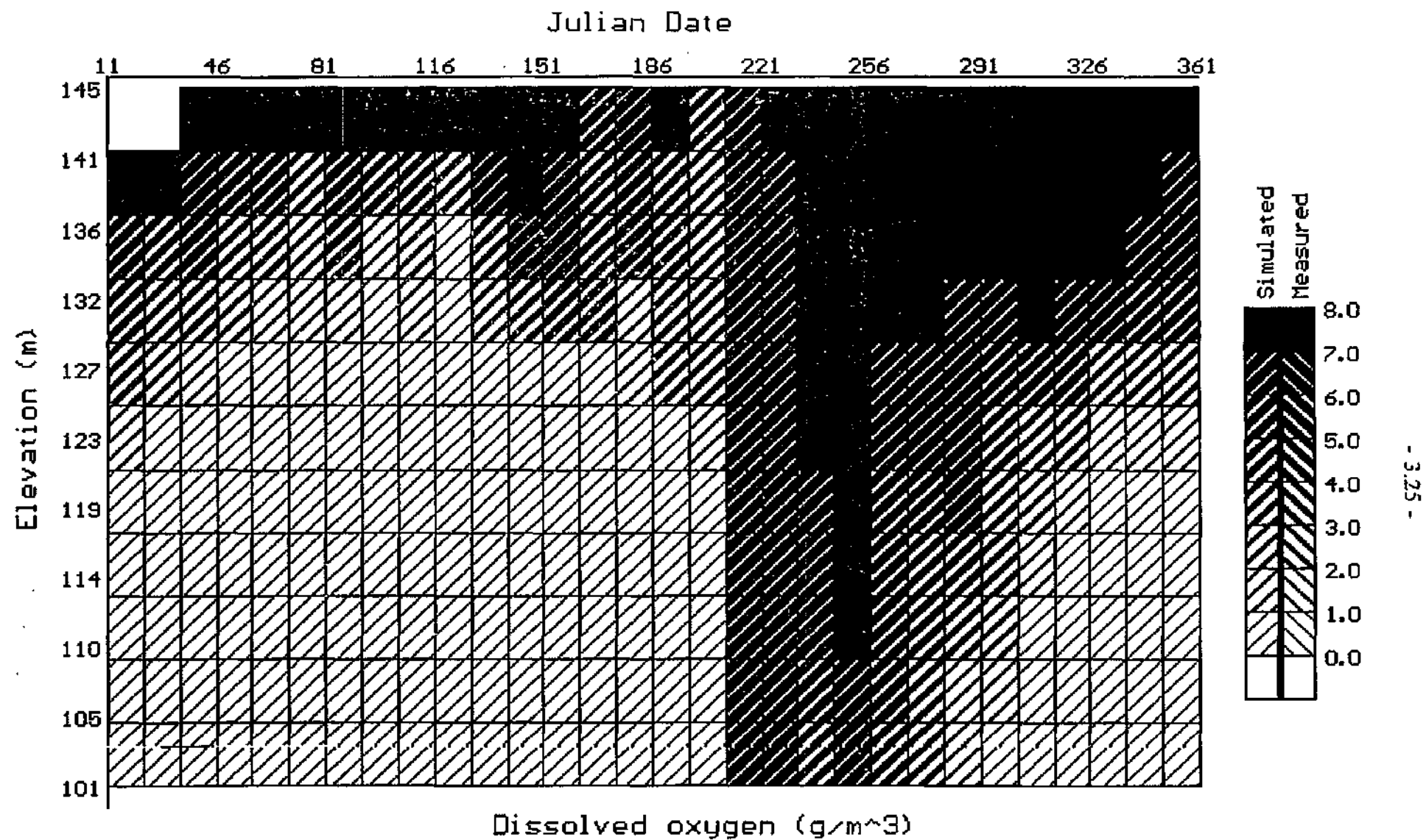


Isopleth (depth vs time) plot: Algal biomass at the dam wall

Figure 3.2.14



Isopleth (depth vs time) plot: Ammonia concentration at the dam wall Figure 3.2.15



Isopleth (depth vs time) plot: dissolved oxygen at dam wall

Figure 3.2.16

Role of reservoir sediments During the calibration of the model, it was observed that the reservoir sediments exerted a high demand for oxygen which caused the development of an extensive anaerobic hypolimnion. During anaerobic conditions, the sediments released iron and ammonia into the hypolimnion. For the period January to December 1990, minimal phosphorus was seen to be released from the sediments and the primary input of P into the reservoir was from the Mgeni River.

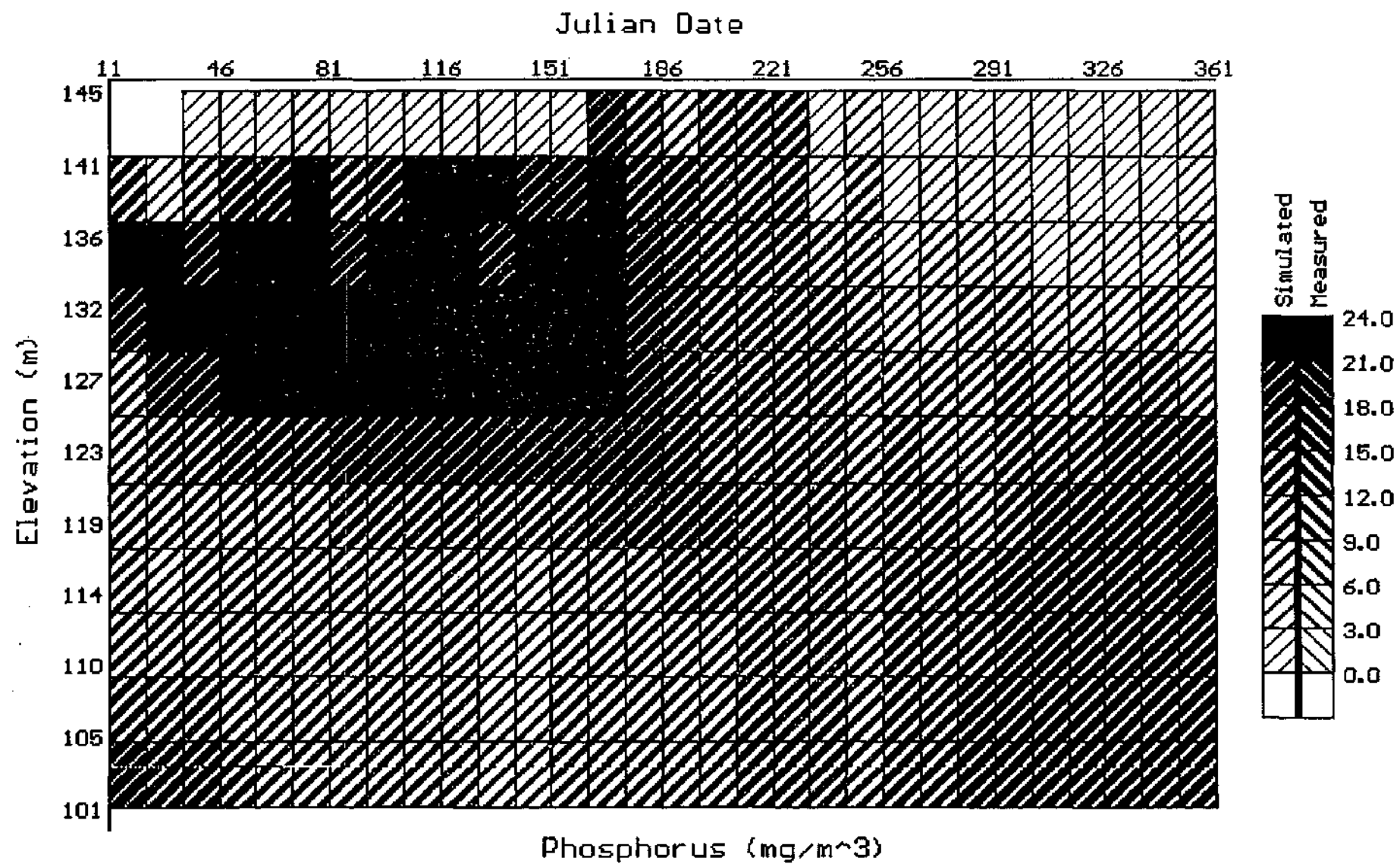
Hudson *et al.* (1993) report that Inanda Dam behaves as a "sink" for phosphorus. Phosphorus is seen to either undergo adsorption onto suspended matter and sedimentation onto the bottom sediments, or uptake by algae. Under the current conditions, the reservoir sediments are accumulating phosphorus and release minimal quantities of P back into the water column. Under suitable (reducing) conditions however it is possible for the P to be released back into the overlying water column.

Silberbauer (1981) investigated the release of phosphorus from the bottom sediments of Roodeplaat, Hartbeespoort and Bloemhof Dams using laboratory based analytical methods. Phosphorus sediment release rates ranged from 1 to 6 mg P/m²/day for the dam wall basins of Roodeplaat and Hartbeespoort Dams. Similar information on the sediment P release characteristics of Inanda Dam were not available. Therefore, a trial simulation was performed to determine the general response of increased P release from the sediments on the algal biomass. A comparatively low sediment phosphate release rate of 0.05 mg/m²/day was used in the simulation.

Figure 3.2.17 shows the P isopleth plot with no release from the sediments, and Figure 3.2.18 shows the influence of sediment release of P. During the first part of the simulation period, the P released from the sediments had a minor influence on the surface layers because of the limited vertical mixing of P into the epilimnion during stratification. At the onset of overturn, the algal biomass increased (by two-fold) in response to the abundant supply of phosphorus from the deeper layers.

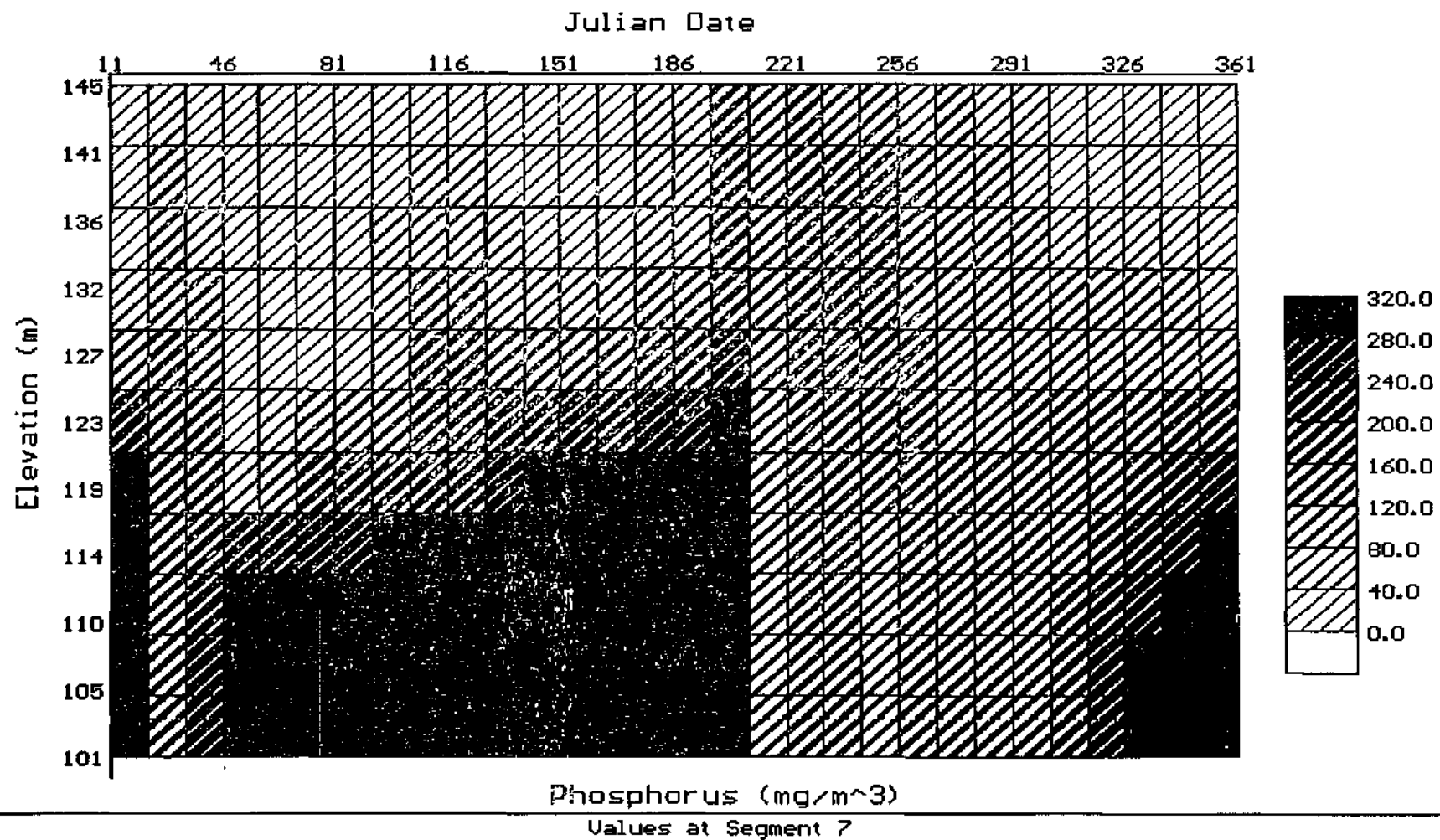
The simulation results show:

- The release of P from the sediments brings about a noticeable accumulation of P in the hypolimnion during periods of stratification, see Figure 3.2.18, which does not have a direct influence on the epilimnion concentrations except during overturn.
- The P budget of Inanda Dam is governed by the input from the Mgeni River.



Isopleth (depth vs time) plot: phosphorus concentration at the dam wall. Figure 3.2.17

TITLE : BRNCH:1 SEGS:8 LAY:13 TRIB:0 OUT:2 AGROW:4 ASATUR:18 ASETL:1 AHSP:008
 AHSN:05 EXH20.25 EXINOR:01 SSETL:6 NH3DK:2 PARTN:0 PARTP:0 SOD1:1 CHZ60
 NH4REL:1 EXOR6.5 DETOK:03 DSETL:6 FESETL:1 FEREL:1 COLDK:4 P04REL=.05
 Model run at Oct 12, 1994 15:33:22



- 3.28 -



Isopleth (depth vs time) plots: phosphorus concentration with sediment release
 of 0.05 mg/m²/day.

Figure 3.2.18

- A considerable increase in algal growth will occur if P is released from sediments. Under such conditions, hypolimnetic aeration may play an important role in controlling the release of P (and other constituents) from the sediments. At present, the simulation shows that hypolimnetic aeration may have minimal influence on the overall nutrient regime of Inanda.
- Routine monitoring of P in the hypolimnion should be implemented to detect changes in the sediment release characteristics.

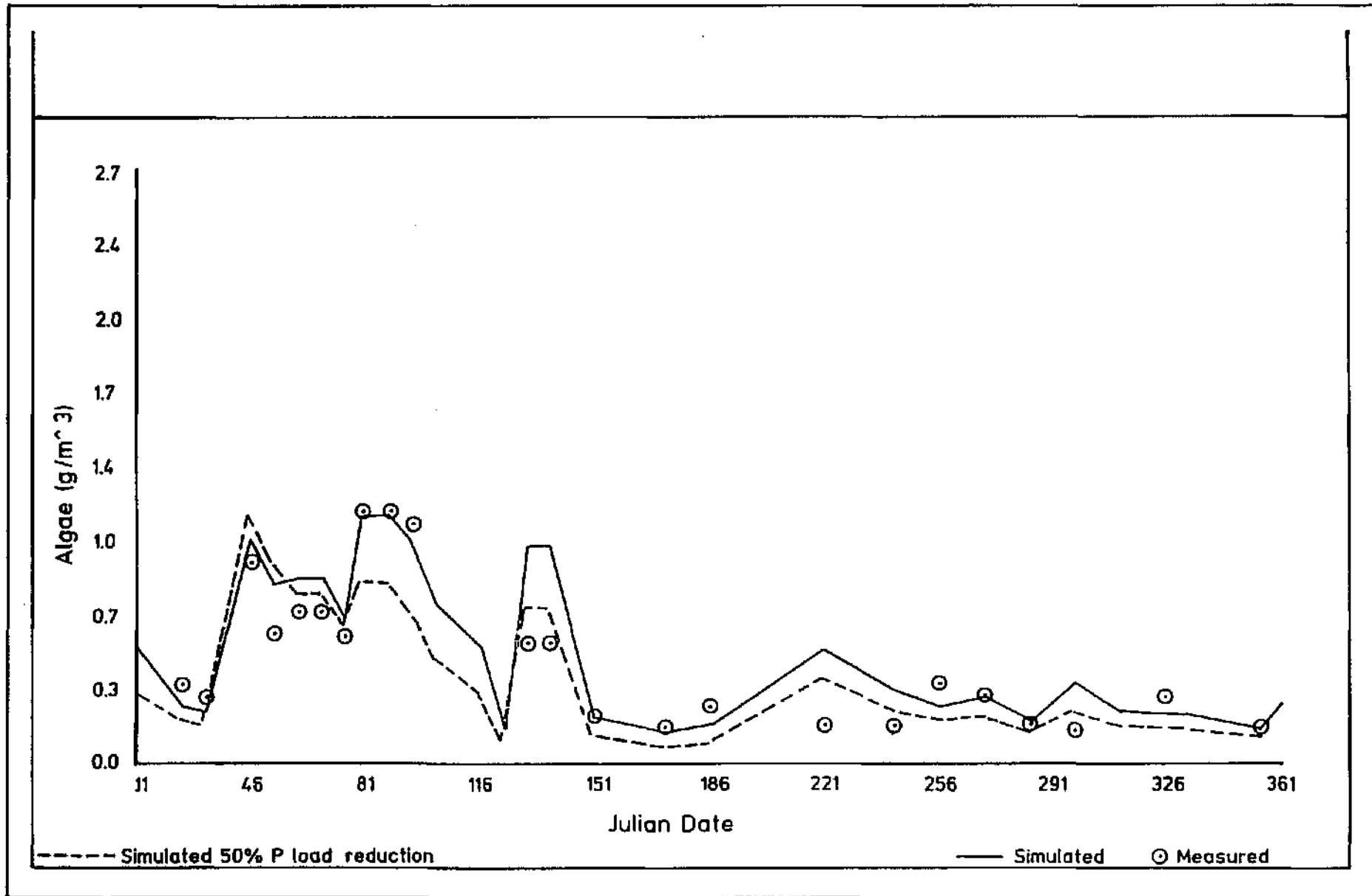
Phosphorus Dynamics As discussed above, the growth of the algal biomass at the dam wall is largely governed by the P load derived from the Mgeni River. However, the simulation results also show that the longitudinal and vertical distribution of P within Inanda is influenced by bio-chemical processes and density mixing characteristics of the inflowing water.

The phosphorus isopleth plot for the dam wall basin (Figure 3.2.17) shows high P concentrations were transported into (1) the hypolimnion during the beginning of the simulation period, and (2) the metalimnion during the latter part of the summer period (Julian Day 46 to 150). In response to the vertical gradients in P concentration, the algal biomass shows the highest growth during the latter part of the summer period when the inflows penetrate into the metalimnion, in closer proximity to the algae.

During periods of low inflow (discharge < 10 cumec), the P in the Mgeni River water undergoes rapid sedimentation and uptake by the algal biomass in the upper reaches of Inanda. This was observed during the end of the simulation period, when the low inflow and low delivery of P limited algal growth in the dam wall basin, see Figures 3.2.17 and 3.2.19.

As an example, the model was used to examine the influence of reducing the phosphorus input loading on the algal biomass. A simulation was performed where the P input loading of the Mgeni River was reduced by 50 percent, representing a considerable reduction in the loading rate to Inanda. Figure 3.2.19 shows the influence on the algal biomass at the dam wall basin. The P load reduction brings about (1) a comparatively rapid response by the algae in the dam wall basin, and (2) only a marginal decrease in the overall algal biomass. The largest reduction in algal biomass was simulated during the high inflow periods (Julian day 81 to 90, and 120 to 135).

The model was configured to determine which variables limited algal growth during the simulation period. The model results show that in the metalimnion and hypolimnion, light was the limiting factor. In the surface layer, both phosphorus and light limited algal growth. During the simulation period, nitrogen did not limit algal growth.



Algal biomass at the dam wall basin, with normal and reduced phosphorus loading.

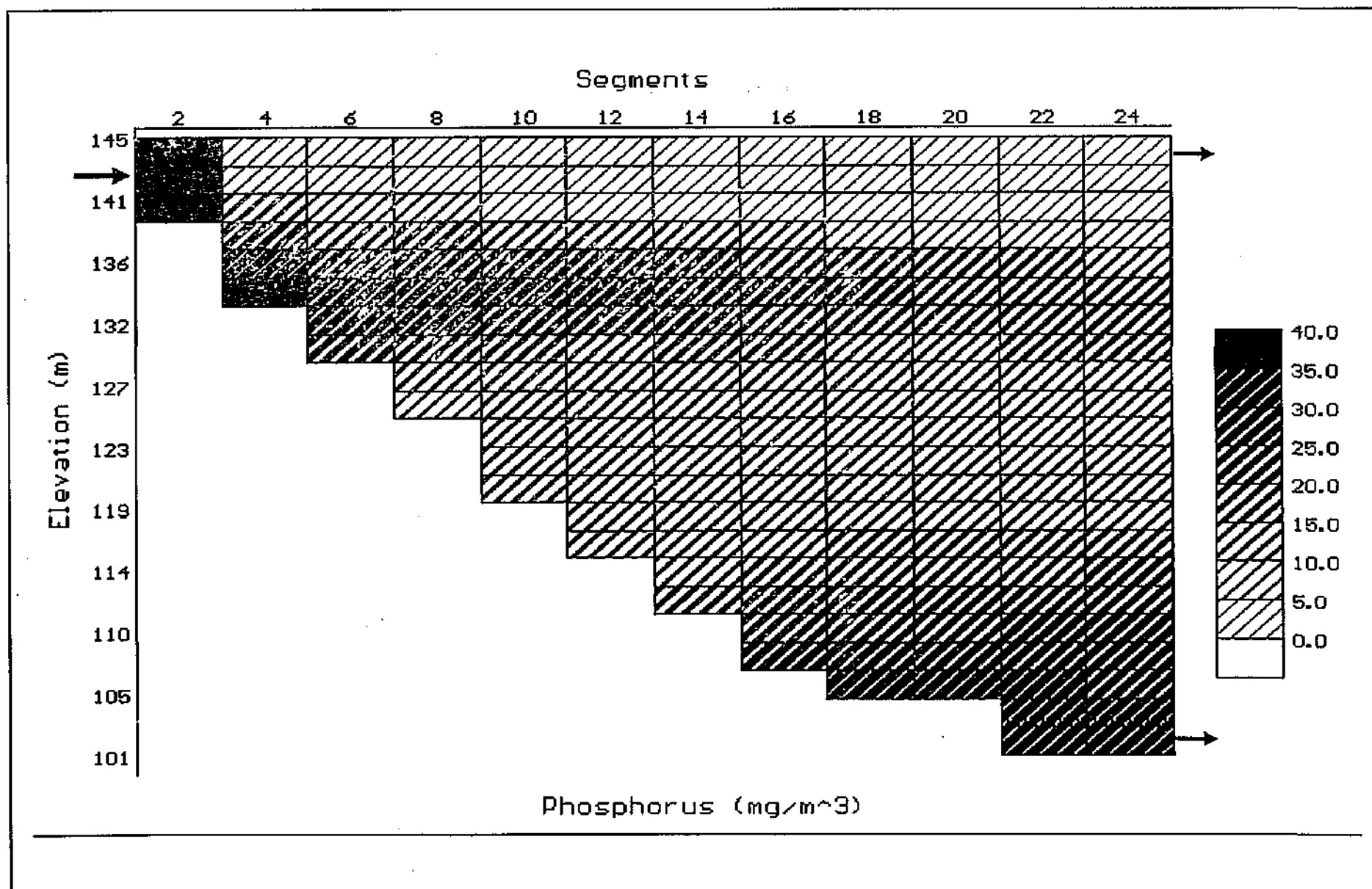
Figure 3.2.19

Hydrodynamic mixing Inanda Dam is characterised by longitudinal and vertical gradients in water quality. Longitudinal gradients are generally brought about by sedimentation and biotic uptake of phosphorus and vertical gradients by depth penetration and stratified flow, see Figure 3.2.20. However, during periods of high inflow the route of the flood waters is governed by the momentum of the inflow, and density of both the inflow and receiving water body. Figures 3.2.21 and 3.2.22 show the flow paths taken during two inflow periods. On Julian Day 88, the flood waters (with discharge of 82 cumec) penetrated into the bottom of the reservoir and pushed aerated river water along the bottom of the reservoir. On Julian Day 123, the flood waters (with discharge of 27 cumec) penetrated into the metalimnion, thereby increasing the concentration of oxygen in the metalimnion. Using a longer simulation period, it would be of interest to see whether the mixing patterns in the simulation period (for 1990) are repeated in subsequent years, and identify the factors which govern the mixing characteristics.

Reservoir draw-down A simulation was performed to estimate the influence of reduced operating level on the water quality of Inanda. The simulation was performed whereby the reservoir water level was maintained 11 metre below full supply capacity by reducing the storage volume at the beginning of the simulation period. Analysis of the time series and isopleth plots showed that the algal biomass and phosphorus response were both unaffected by the reduced operating level. Some improvement in the dissolved oxygen concentration of the reservoir was noted. This may be attributed to increased vertical mixing of oxygenated water (associated with wind action) into the lower layers, giving a deeper oxycline. The vertical mixing was however not sufficient to introduce enough oxygen into the bottom layers to bring about major reduction in the ammonia and iron concentrations.

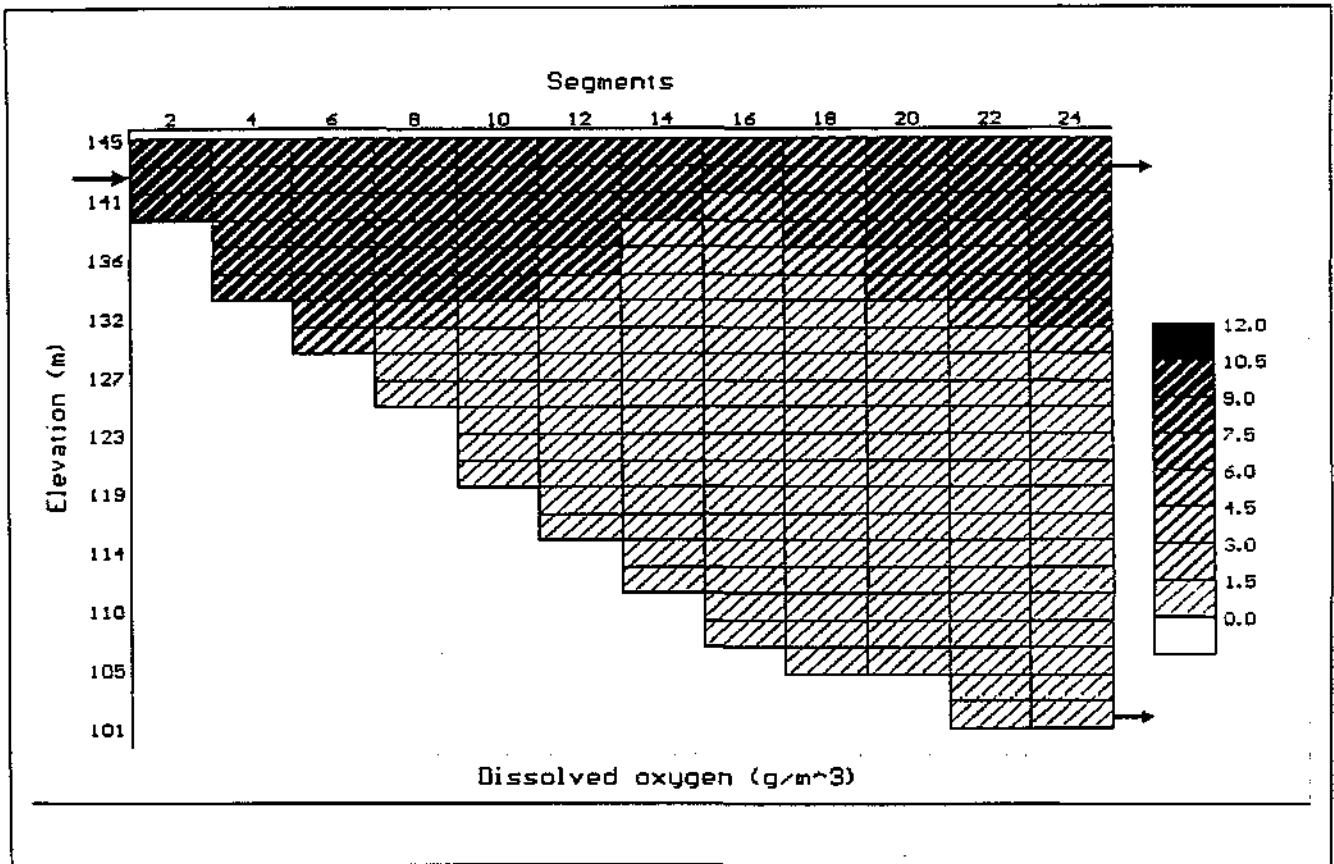
Hypolimnetic releases A simulation was performed to determine the influence of releasing water from the hypolimnion from the scour outlet on water quality characteristics of Inanda. Analysis of the model output showed that in the surface layers, the algal biomass and phosphorus was largely unaffected by the releases. However, in the metalimnion and hypolimnion, a considerable change was observed in the water quality patterns.

On Julian Day 80, the inflowing river water (with discharge of 40 cumec) was entrained along the water body through the bottom layers, see Figure 3.2.23. The entrainment pattern was repeated during each of the major inflows in the summer period. Figure 3.2.24 shows the dissolved oxygen isopleth plot showing the entrainment of storm water resulting in elevated DO concentrations in the hypolimnion. The presence of oxygen in the lower layers was however sufficient to reduce the release of ammonia and iron from the sediments, see Figure 3.2.25.



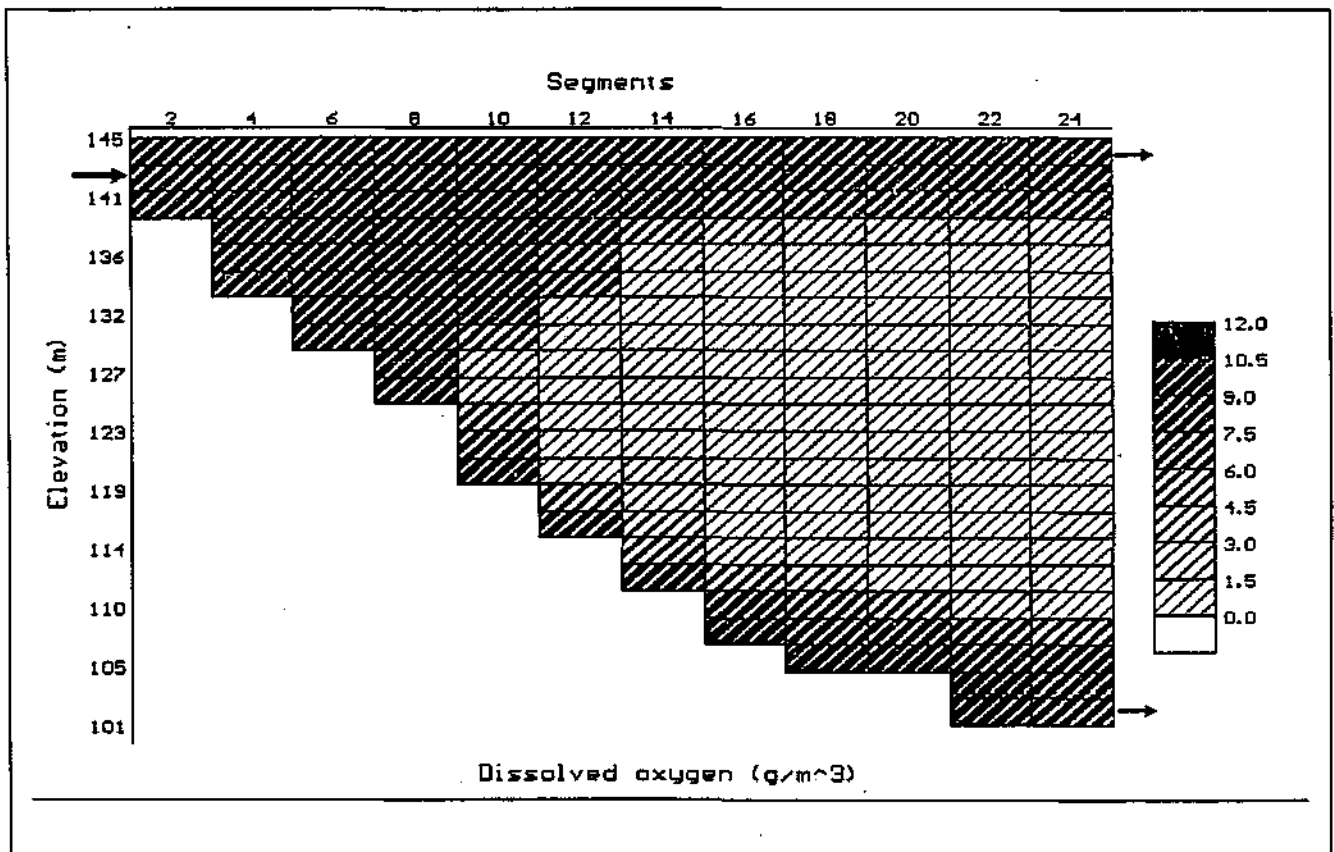
2-D plots showing the distribution of phosphorus with vertical and longitudinal concentration gradients.

Figure 3.2.20



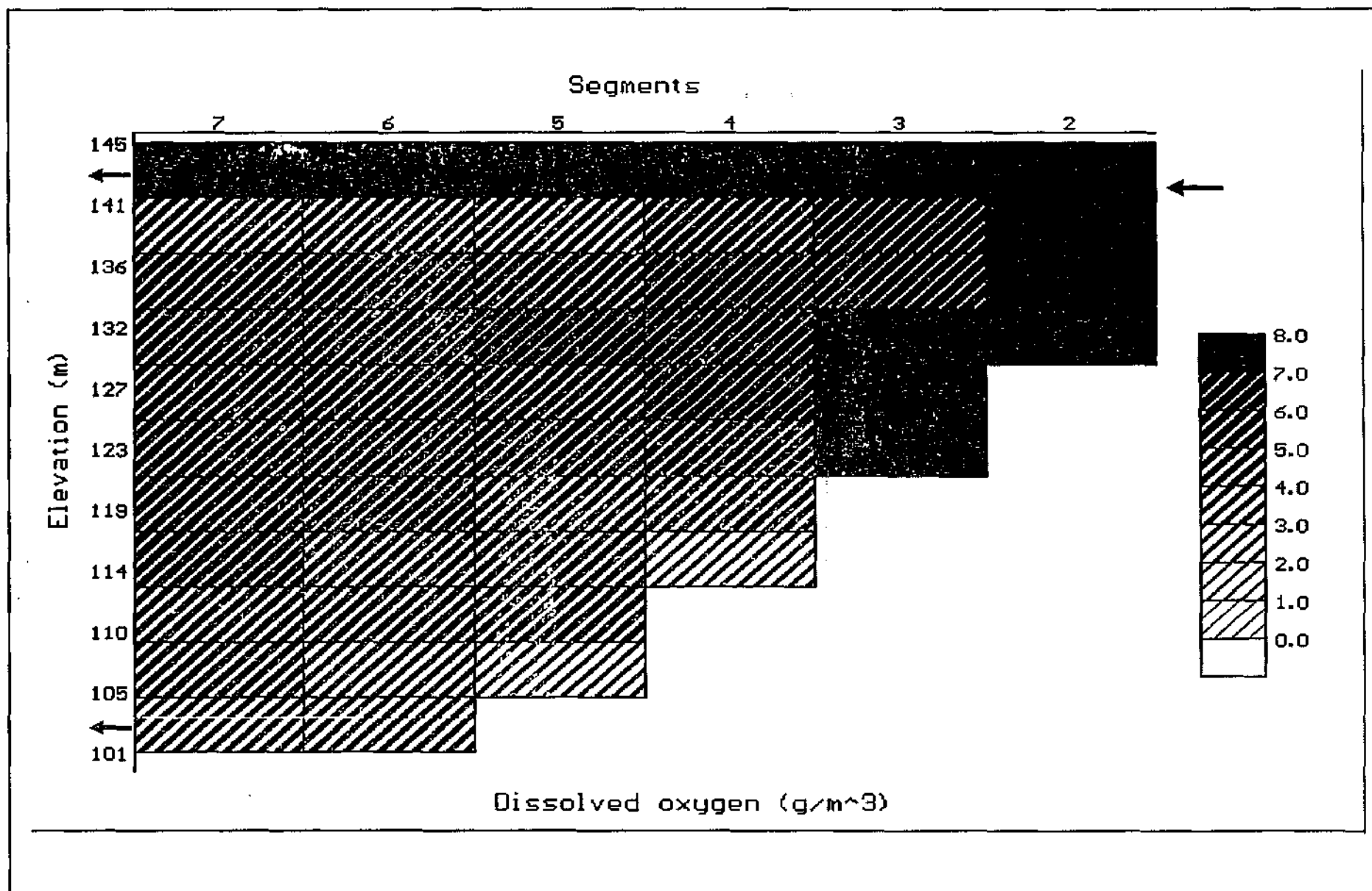
2-D plot showing the penetration of flood waters into the metalimnion of Inanda Dam: Julian Day 123.

Figure 3.2.21



2-D plot showing the penetration of flood waters into the hypolimnion of Inanda Dam: Julian Day 88

Figure 3.2.22

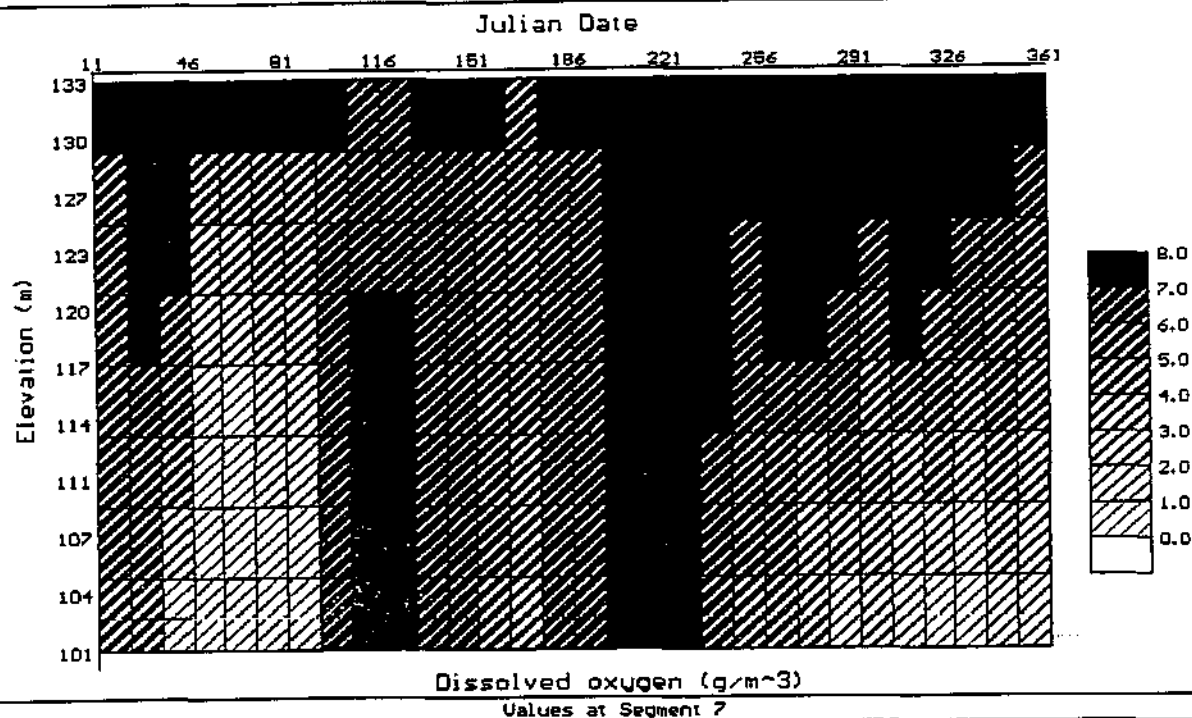


Influence of scour release entrainment on the dissolved oxygen concentration:
Julian Day 116.

Figure 3.2.23

POST PROCESSOR

TITLE : BRNCH:1 SEGS:8 LAY:13 TRIB:0 OUT:2 AGROW:4 ASATUR:18 ASETL:1 AHSP:008
 AHSN:05 EXH20.25 EXINOR:01 SSETL:6 NH3DK:2 PARTN:0 PARTP:0 S001:1 CHZ60
 NH4REL:1 EXORG:5 DETDK:03 DSETL:6 FESETL:1 FEREL:1 COLDK:4 P04REL:0.0
 Model run at Oct 16, 1994 11:21:20



©Ninham Shand Inc (RSA)

Version 2.0

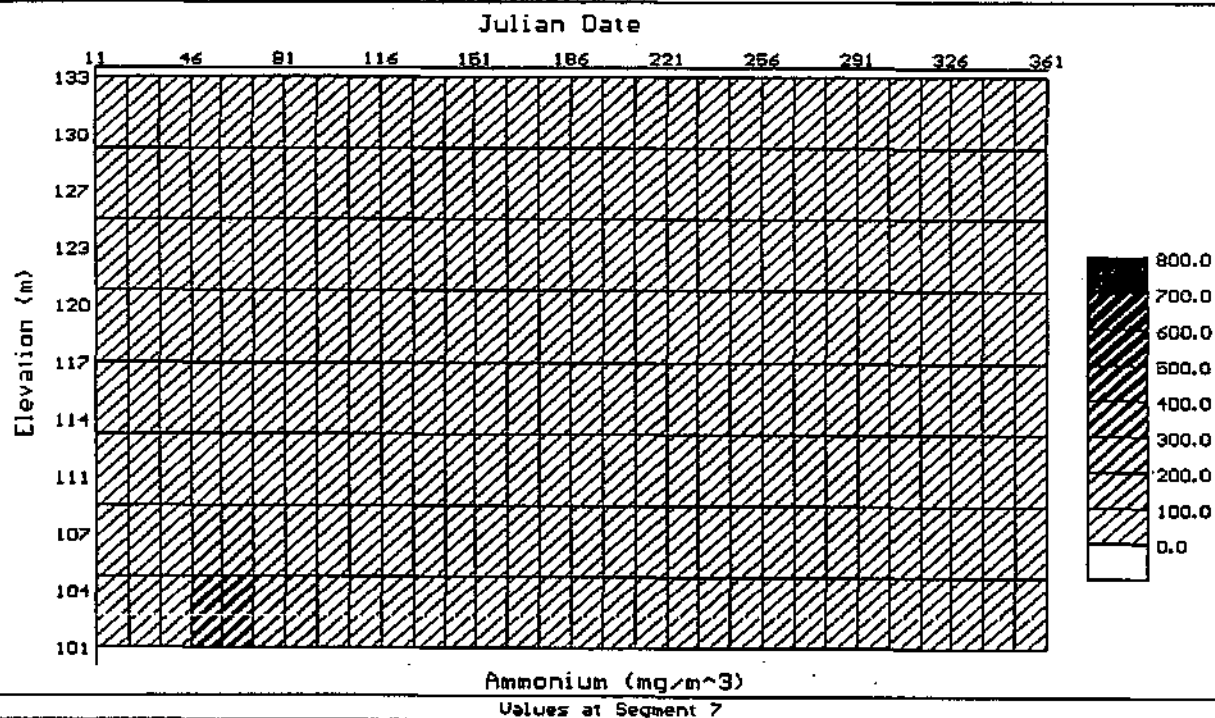


Isopleth plot: dissolved oxygen with scour releases causing entrainment of water during high inflow period.

Figure 3.2.24

POST PROCESSOR

TITLE : BRNCH:1 SEGS:8 LAY:13 TRIB:0 OUT:2 AGROW:4 ASATUR:18 ASETL:1 AHSP:008
 AHSN:05 EXH20.25 EXINOR:01 SSETL:6 NH3DK:2 PARTN:0 PARTP:0 S001:1 CHZ60
 NH4REL:1 EXORG:5 DETDK:03 DSETL:6 FESETL:1 FEREL:1 COLDK:4 P04REL:0.0
 Model run at Oct 16, 1994 11:21:20



©Ninham Shand Inc (RSA)

Version 2.0



Isopleth plot: ammonia with releases from the hypolimnion.

Figure 3.2.25

The entrainment of flood waters causes a marked change in selected constituent concentrations. It was noted that to gain the best improvement in water quality, the releases must coincide with the inflow periods to achieve maximum entrainment within the water body. This operating strategy is however constrained by two factors: (1) the discharge rate of the bottom release, (2) the volume of water which is available for release, and (3) the timing of the releases so that they coincide with the peak inflow into Inanda Dam.

3.2.5 CONCLUSIONS

- Three physical factors are seen to have a direct influence on the water quality of Inanda, namely the quality and discharge of the inflow, morphology of the reservoir basin, and sediment/water interactions. In response, the reservoir has: pronounced stratification, high algal growth, an anaerobic hypolimnion, and release of constituents from the bottom sediments. These factors are expected to have a direct influence on the treatment of water for potable use.
- The model was calibrated using the Inanda Dam data set collected by Umgeni Water. To reduce the run-time of the model, a reduced segment configuration was developed and found to give acceptable results.
- The model was used to provide information on: drawoff depth, sediment interactions, P loading control, mixing conditions, reservoir draw-down, and hypolimnetic releases. It is concluded that a longer simulation period (extending over at least two years) is more suited to evaluate the management options.
- The two-dimensional simulation capability of the model provides detailed information on the movement and process interactions taking place within Inanda. The reservoir exhibits steep vertical and longitudinal gradients in water quality. Detailed testing of *CE-QUAL-W2* in the United States shows that the model is ideally suited to simulate the water quality in reservoirs with longitudinal and vertical gradients. For example, the simulation of metalimnetic deoxygenation using a 2-D model (such as *CE-QUAL-W2*) is achieved through the simulation of the momentum delivered by the inflowing river water. A 1-D model which is unable to simulate the momentum component, requires manipulation of the model to adequately simulate the vertical profile of DO (Cole, 1995).
- The preliminary simulation results show that a reduction in algal biomass may be achieved using: selective drawoff depth, and P loading control (in the upstream catchment). No single

management option was found to provide a complete improvement in water quality of Inanda . It was determined that aeration of the hypolimnion will have minimal beneficial influence on the phosphorus regime and algal biomass. However, complete destratification could have some benefits in reducing the phosphorus concentration in the hypolimnion and also increase the mixed depth thereby decreasing algal growth.

- The reservoir sediments have an important influence on the water quality of the hypolimnion , giving rise to anaerobic conditions and the release of contaminants. The phosphorus budget of Inanda is dominated by the Mgeni River, with the sediments having a negligible influence. Future changes in the P sediment release characteristics are shown to have a potentially important influence on algal growth. In this regard routine monitoring will be required to ascertain the nutrient release characteristics under reducing conditions.
- The model shows that the entrainment of flood waters through the length of Inanda introduces aerated water into the hypolimnion thereby improving the water quality.
- The model is used to identify the algal limiting factors in Inanda. In the metalimnion and hypolimnion light is growth limiting, in the epilimnion both phosphorus and light are growth limiting. This shows that management of algae should focus on the phosphorus budget of Inanda.

3.2.6 RECOMMENDATIONS

Role in decision support system for Inanda Dam The applications described above show the general capabilities of hydrodynamic modelling in the management of Inanda Dam. Further model applications should be carried out to:

- Define operating rules and management options for the control of water quality.
- Identify reservoir processes and sediment interactions. This information will play a vital role in the formulation of a water quality management plan for the lower Mgeni River catchment .

An extended simulation period (greater than one year) should be used to examine

- The influence of P control options on controlling algal growth.
- The hydrodynamic mixing patterns to optimize draw-off level, and operation of releases.

- The influence of sediment release of P on algal growth, and determine the implications for management of the reservoir.

Water Quality Monitoring of Inanda Dam The monitoring program implemented by Umgeni Water provides an extensive data set for the modelling of Inanda Dam. Additional monitoring should include:

- Routine monitoring and analysis to examine the P release potential of the bottom sediments to detect changes in the release characteristics of the sediments.
- In the dam wall basin, collection of water samples at regular intervals throughout the depth profile for the constituents: algal biomass (and species), phosphorus, suspended sediment, ammonia, iron and manganese. This information will assist the operation of the multi-level drawoff.

Reservoir Management During high runoff, test releases should be made from the scour valve to determine the feasibility of entraining flood waters into the hypolimnion of the dam wall basin. At such time, monitoring should be undertaken at the three in-dam points to determine the influence of the flood waters on the dissolved oxygen, iron, ammonia and phosphorus regime of Inanda Dam.

3.2.7 REFERENCES

Bruwer, C.A. (1979)

Socio-economic cost of eutrophication, Internal report of the Department of Water Affairs and Forestry, Pretoria.

Cole, T.M. (1993)

Personal communication. US Army Engineer, Waterways Experimental Station, Vicksburg, Mississippi, USA.

Cole, T.M. & Hannan, H.H. (1993)

Dissolved oxygen dynamics, In Reservoir Limnology, Ecological Perspectives, p.71-107.

Cole, T.M. (1994)

User guide to *CE-QUAL-W2*, Instruction report, US Army Engineer, Waterways Experimental Station, Vicksburg, Mississippi, USA.

Cole, T.M. (1995)

Personal communication. US Army Engineer, Waterways Experimental Station, Vicksburg, Mississippi, USA.

DWAF (1990)

Capacity determination: Inanda Dam, Directorate of Survey Services, Department of Water Affairs and Forestry, Pretoria, Report Number U200_04.

Görgens, A.H.M., Bath, A.J., Venter, A., de Smidt, K. & Marais, G.v.R. (1993)

Applicability of hydrodynamic reservoir models for water quality management in stratified water bodies in South Africa, Report to Water Research Commission, Pretoria, number 304/1/93.

Hudson, N., Furness, H., & Boucher, K. (1993)

Water quality of Inanda Dam - some indicators for the management of a raw water reservoir, Water quality department, Umgeni Water, Report number WQP 4/93.

Silberbauer, M. (1981)

The release of phosphate from the bottom sediments of Roodeplaat, Hartbeespoort, and Bloemhof Dams, Contributions by the Department of Water Affairs, Forestry and Environmental Conservation to the Congress of the Limnological Society of Southern Africa, Rhodes University, Grahamstown, 4 to 9 July, 1980. Technical Report number 114, Department of Water Affairs and Forestry, Pretoria.

Tollow, A.J. (1991)

Durban's newest water resource - Inanda Dam, Journal of the Institute of Water and Environmental Management, 5, 519-528.

UW (1989)

Water quality in the Inanda Dam system, Water quality department, Umgeni Water, Report number WQ 2/89.

UW (1990)

Preliminary assessment of Inanda Dam water quality for the period March 1989 to February 1990, Water quality section, Umgeni Water, Report number WQP 4/90.

UW (1992a)

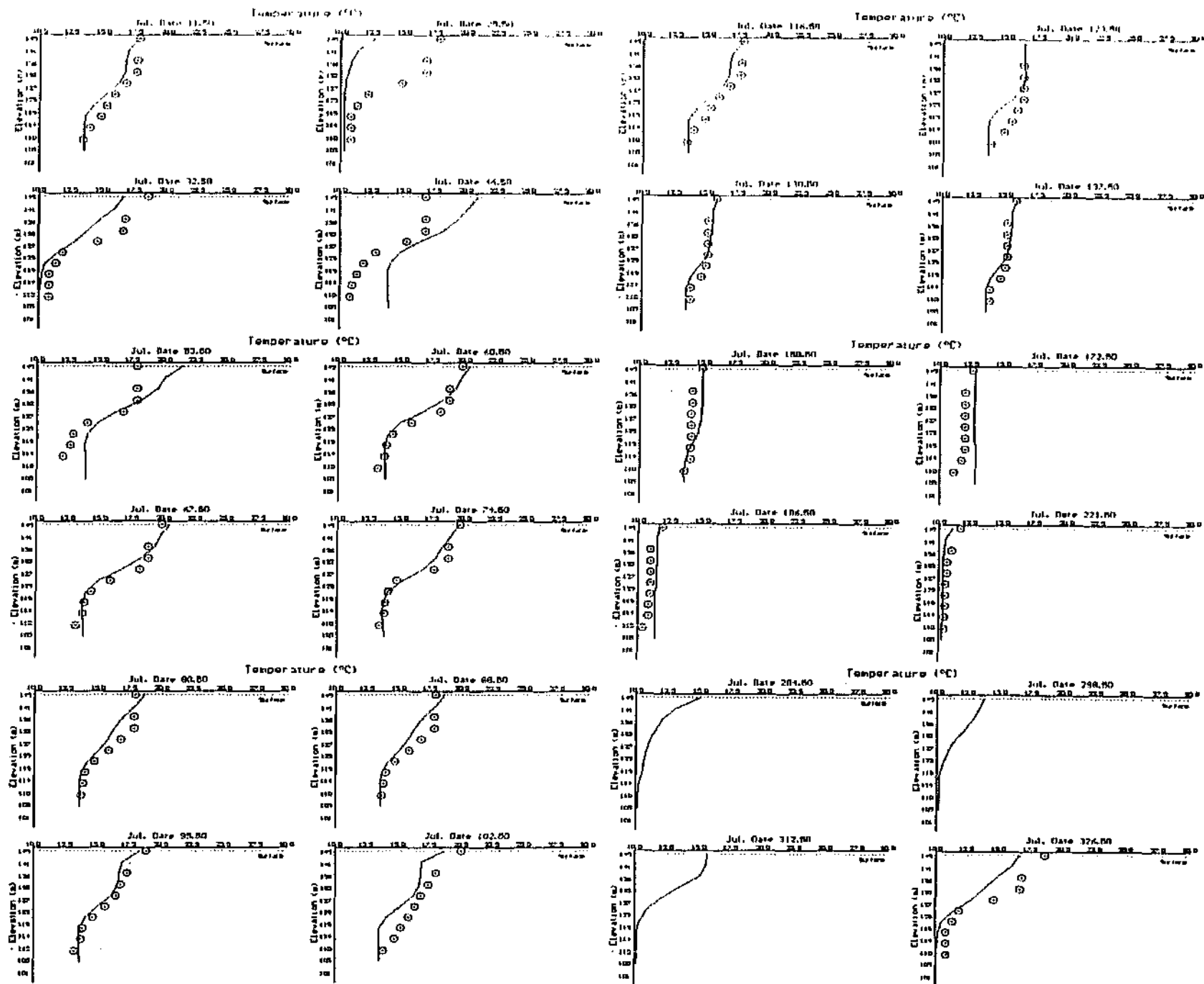
Impact of artificial destratification by aeration on Inanda Dam, Natal, South Africa, Water quality department, Umgeni Water, Report number WQP 6/92.

UW (1992b)

Management strategies for impoundments supply Umgeni Water suggested by temperature and dissolved oxygen data, Water quality section, Umgeni Water, Report number WQP 2/92.

UW (1993)

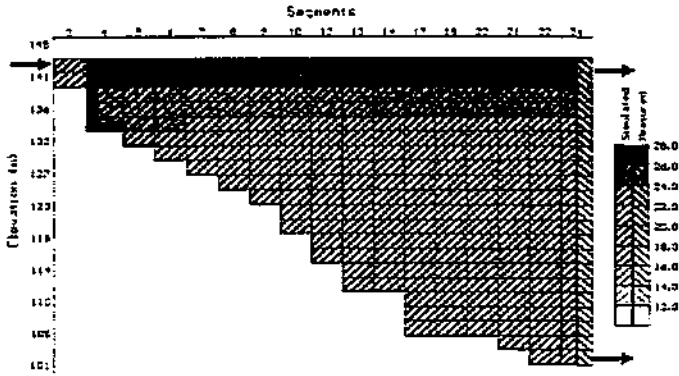
Raw water quality of Inanda Dam: implications for treatment facilities and sludge handling at Wiggins Water Works, Water quality planning section, Umgeni Water, Report number WQP 2/93.



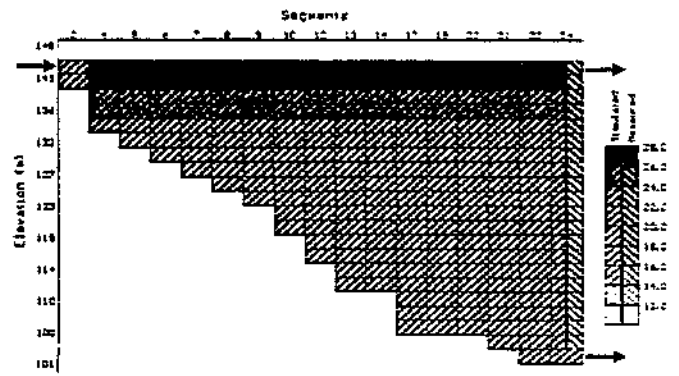
Simulated and measured water temperature: vertical profiles.

Figure 3.2.26

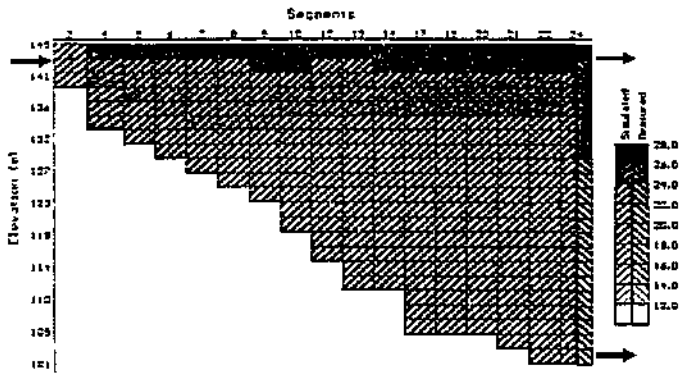
Julian Day 4



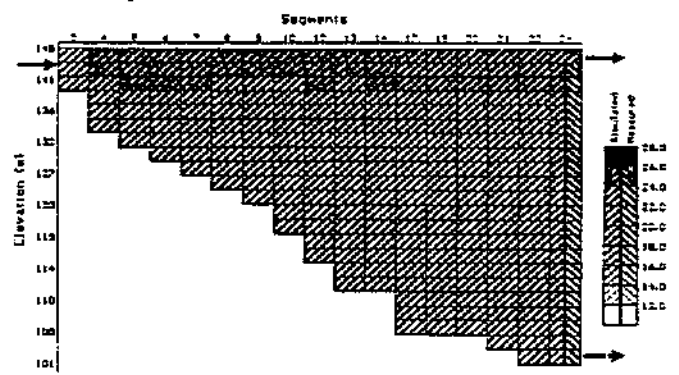
Julian Day 25



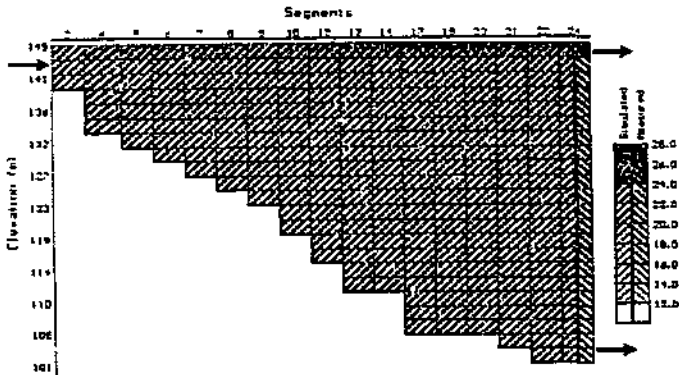
Julian Day 60



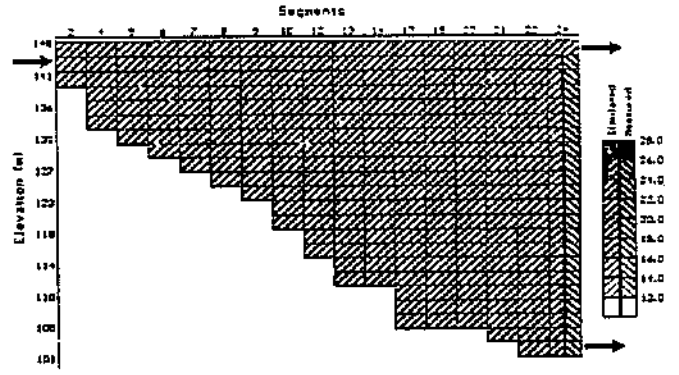
Julian Day 80



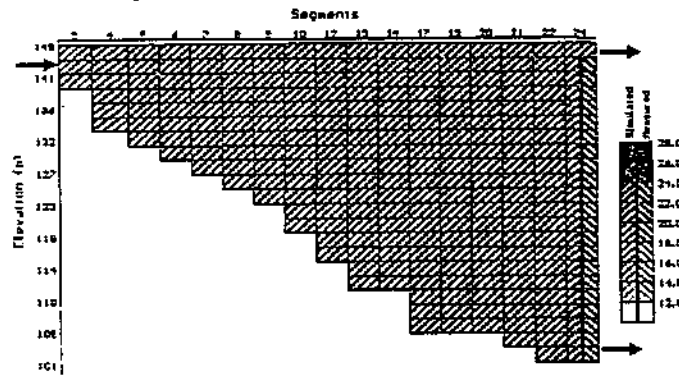
Julian Day 116



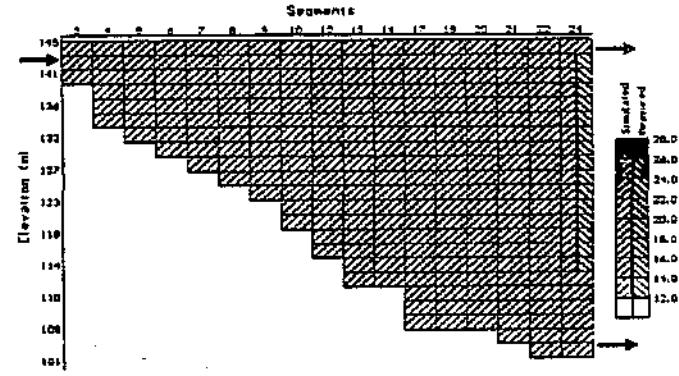
Julian Day 150



Julian Day 172



Julian Day 200



SECTION 3.3

APPLICATION OF CE-QUAL-W2 TO SIMULATE THE SALINITY AND HYDRODYNAMICS OF THE VAAL BARRAGE

by

A J Bath & A H M Görgens

3.3.1 INTRODUCTION

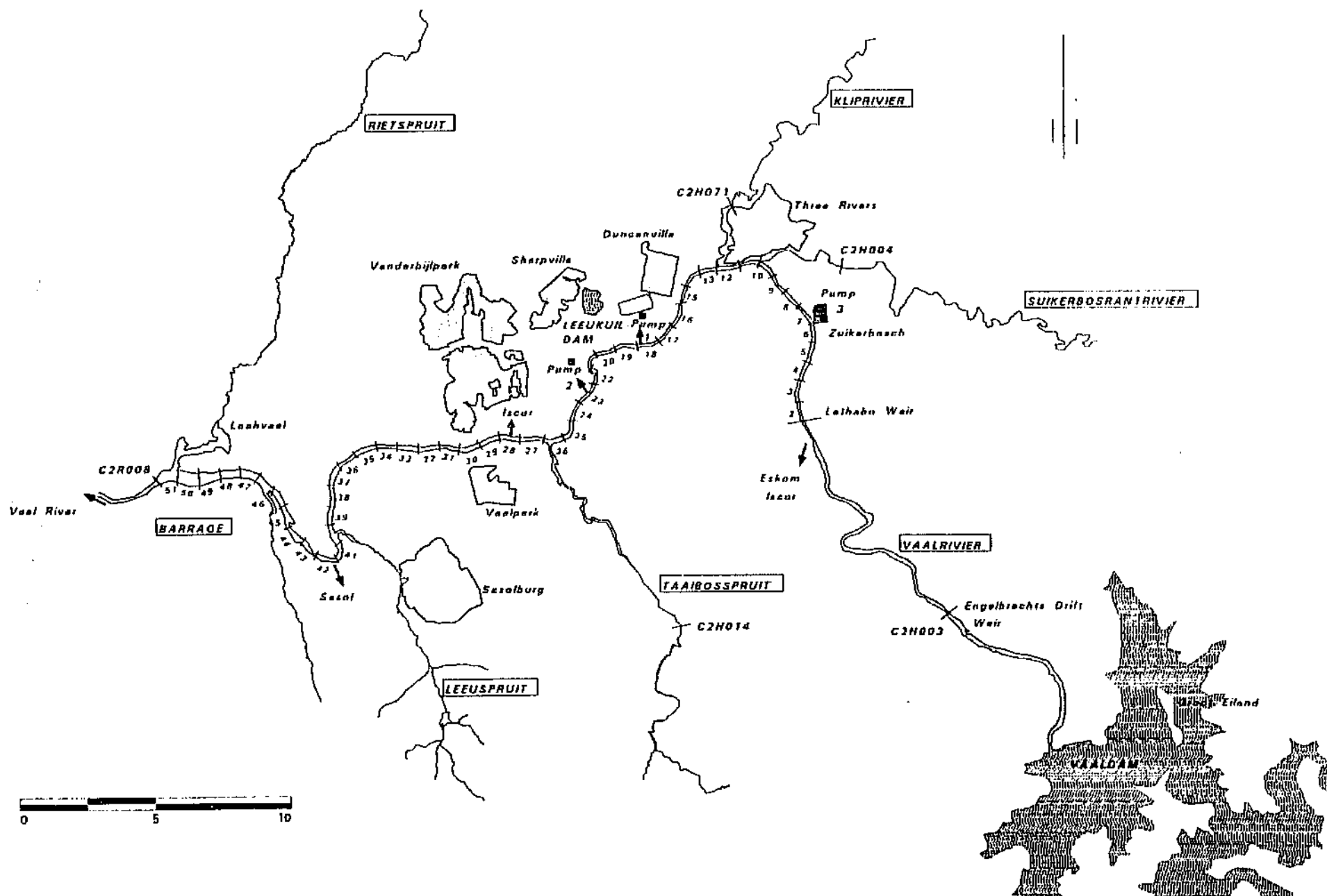
Study area The Vaal Barrage was constructed in 1922 to tap the water resources of the Vaal River. In 1938, the Vaal Dam was built upstream of the Barrage to augment the supply from the Vaal (see Figure 3.3.1). The Barrage is a riverine lake approximately 50 km long, ± 150 metre wide, and ± 6 metre deep. The Vaal Barrage and Dam serve as a bulk supply point for RW, Vereeniging Municipality, as well as local industries. It is estimated that at least one third of the water supplied to the Gauteng Region¹ is derived from this source (Herold & Triebel, 1990). Figure 3.3.1 shows the points of abstraction used by RW, ISCOR and ESKOM.

The Barrage receives inflow from the Klip River, Suikerbosrand River, Taaibosspruit, Leeuspruit and Rietspruit. At the upstream end, releases are made from the Vaal Dam. The Klip River is the largest inflow (between 6 to 10 cumec) and input of dissolved solids to the Barrage. The Klip River receives runoff from urban, industrial and mining areas (DWAf 1986; Jones *et al.* 1988), in addition to treated wastewater from the south of Johannesburg (van Vliet & Nel 1986).

In 1949, Rand Water (RW) curtailed further expansion of the Vaal River intakes at Vereeniging in favour of new intakes at Zuikerbosch, located upstream of the Klip and Suikerbosrand Rivers (see Figure 3.3.1). This was done to prevent the abstraction of high salinity water discharged into the Barrage by the Klip River. Unfortunately, the abstraction at the Zuikerbosch intakes caused a reversal in the flow of the Barrage and saline water was abstracted. In 1969, a pipeline was commissioned to draw low salinity water directly from the Vaal Dam, followed in 1983 by the construction of the Vaal Dam-Zuikerbosch canal.

Water quality operation The Barrage was operated using a *300 mg/l TDS blending option*. Rand Water extracted from three points along the Barrage (see Figure 3.3.1) This water was then blended with treated water from the Vaal Dam to supply a final water with TDS of 300 mg/l. An important feature of the Vaal Barrage was that the offtakes used by Eskom, SASOL, and Rand Water at Zuikerbosch experienced reversed flow in the Barrage and abstracted higher salinity water derived from the Klip River. This problem of reversed flow was overcome through the construction of

¹ The region is formerly known as Pretoria Witswatersrand Vereeniging (PWV) Region.



Location map of the Vaal Barrage showing the main tributaries, abstractions and gauging weirs.

Figure 3.3.1

Lethabo Weir which prevents the backward migration of high salinity water to the offtake points. Under the operating rules of the *300 mg/l blending option*, releases from the Vaal Dam are kept to a minimum and users along the middle Vaal River experience water quality problems as the TDS concentration may occasionally exceed 800 mg/l.

Complaints from users led to an investigation into revising the operating rules. This resulted in the formulation of a new management approach the *600 mg/l dilution option*. This option allows calculated amounts of water to be released from the Vaal Dam to dilute the TDS in the Barrage to below 600 mg/l. Rand Water would then abstract an amount from the Barrage equal to the return flow from the Klip, Suikerbosrand and Riet Rivers. Additional water would be drawn from the Vaal Dam. Calculations showed that this option would provide Rand Water with a TDS concentration of around 300 mg/l, and the water released from the Barrage would be lower in salinity than using the *300 mg/l blending option* (and thus benefit users in the middle Vaal River). This operating rule however places further demands on the water resources of the system, particularly when Bloemhof Dam is at full storage level. Also, pumping costs are increased for Zuikerbosch treatment works.

Unfortunately, the Zuikerbosch abstraction point is positioned so that most of the water released from Vaal Dam could be intercepted and not available to dilute the rest of the Barrage. As an interim measure, it was decided that Rand Water would meet most of its water demand from the Vaal Dam (with a TDS of 150 mg/l).

During July and August of 1990, the *600 mg/l dilution option* was implemented on a trial basis. During this period, monitoring was carried out by the Institute for Water Quality Studies (IWQS) and RW. This data set was used to configure and calibrate CE-QUAL-W2. The model was then used to assess the factors influencing the hydrosalinity and mixing behaviour of the Barrage.

3.3.2 MODEL INPUT

Görgens *et al.* (1993) give a detailed description of the formulation of the input files. In summary, the files contain the following: daily meteorology, daily inflow and withdrawal discharge, daily tributary and effluent water quality, river channel hydrographic survey information (bathymetry), and water quality boundary conditions.

Selection of simulation period The simulation period extended over a period of 137 days, beginning 1 July and ending on 17 November 1990. The period was selected to overlap the duration of the release from Vaal Dam, thereby allowing:

- The simulated conditions in the Vaal Barrage to reach an equilibrium condition before the

release was made on 21 July 1990, and

- the Vaal Barrage sufficient time to reach a final equilibrium after the release had passed through the water body to determine the duration of the mixing process within the water body.

Data Sources Meteorological data include wind speed and direction, solar radiation, dew point temperature, air temperature, and cloud cover. These data were obtained from the Weather Bureau who have measuring points adjacent to the Barrage at Vereeniging and Vanderbijlpark. The water temperature of the Barrage was measured by IWQS and RW. Tributary flow and withdrawal data were obtained from DWAF and RW. These data were processed to determine runoff from ungauged areas and verify the volume balance for the Barrage. Water quality data were obtained from the monitoring exercise of the Barrage carried out by the IWQS and RW. Daily time sequences were created using methods developed by Görgens *et al.* (1993).

The boundary condition data provide the model with the starting conditions of the Vaal Barrage and include water temperature, and electrical conductivity (EC). Field data were used to assess the predictive ability of the model to simulate the quality of the Barrage. The data included grab samples and vertical profiles (obtained by RW and IWQS) for: conductivity, TDS, turbidity, dissolved oxygen, major ions, and selected nutrients.

3.3.3 MODEL CONFIGURATION

Prior to calibration, the model configuration entails the formatting of input data files, compilation of executable code, followed by installation and testing on the personal computer. The model, *CE-QUAL-W2*, has been developed to provide a detailed representation of a water body using a variety of branches, tributaries, segment layouts and withdrawals. However, the complexity of the model representation (ie number of segments, layers and cells) has a direct influence on the run-time of the model. Below a maximum of 400 active cells (equivalent to 50 segments and 8 layers), the run-time of the model was found to be suitable for testing scenarios (Bath & Timm, 1993; Görgens *et al.*, 1993). Above 400 active cells, the run-times were found to become excessively long and restrict the interactive use of the model to test scenarios. The configuration described below gave a run-time of 22 minutes, using a 80486 DX2-66 processor, and a simulation period of 137 days.

Branch layout The Vaal Barrage was configured using a single branch subdivided into a series of vertical segments and horizontal layers. Figure 3.3.1 shows the segment boundaries with their associated tributary inflows and abstractions. Loch Vaal is treated as a tributary inflow.

Segment layout The distance along the Vaal Barrage between Lethabo Weir and the barrage wall is about 52 km. The 52 km river reach² between the upstream (Lethabo Weir) and the downstream boundary (the Barrage) was divided into 52 segments, each with a length of 1 km, see Figure 3.3.1.

Layer configuration The water body was further divided into horizontal layers at 1 metre intervals giving a maximum number of 13 layers at the deepest part of the Barrage. Information provided by the Regional Office of the DWAF was used to identify each of the main points of withdrawal from the Barrage, see Figure 3.3.1. The bathymetric data set was derived from the survey of the Barrage performed by the Department of Water Affairs (DWAF, 1978) and updated using ortho-photos and supplementary monitoring information.

3.3.4 MODEL CALIBRATION

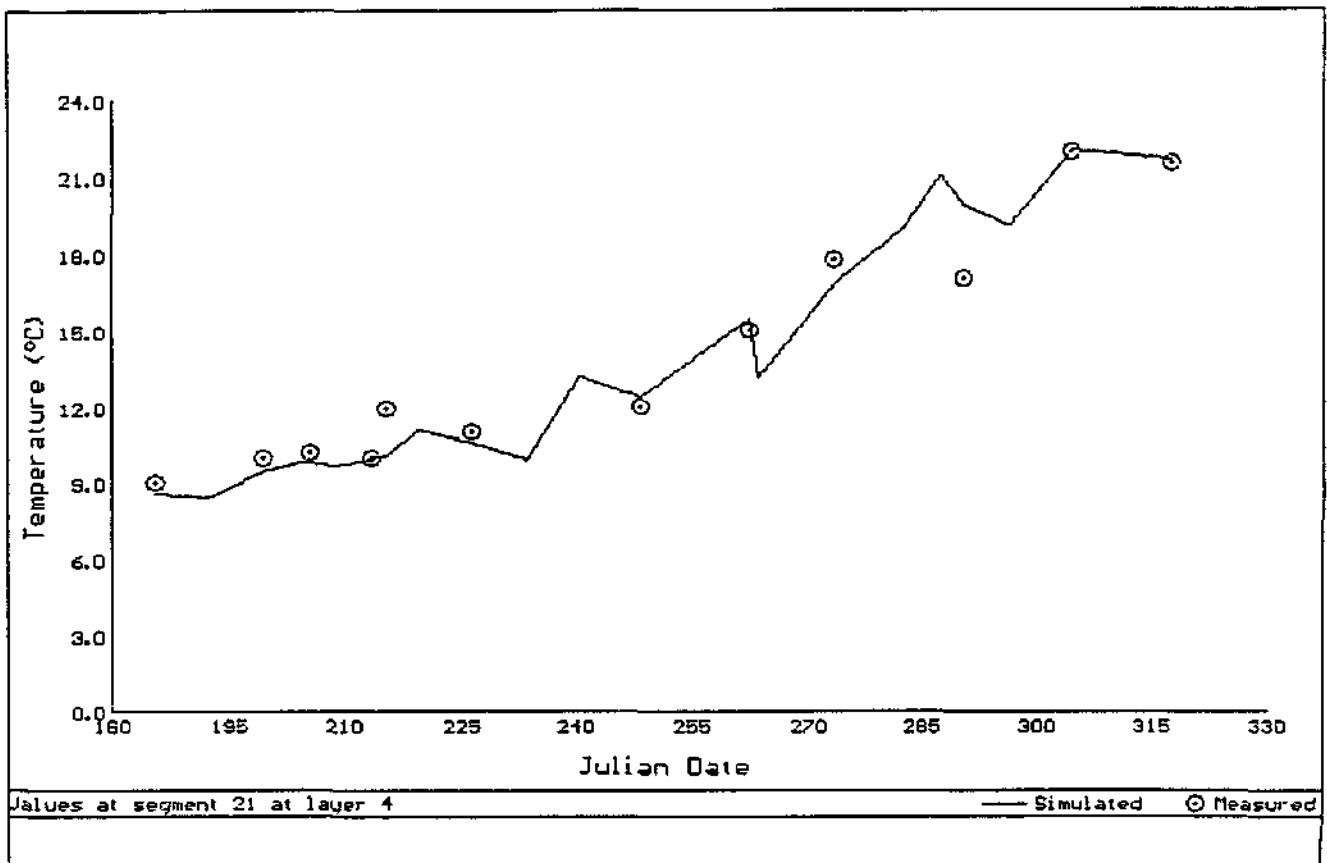
Calibration of the model essentially deals with three components: heat exchange, volume balance and water quality simulation.

Heat Exchange The heat exchange of the water body is simulated using a physically based description of the governing processes. The Roodeplaat Dam application (Section 3.4) shows the model is primarily dependent on the accuracy of the meteorological data and the Wind Sheltering Coefficient (WSC) serves only as a means of compensating for local conditions and factors which reduce the wind exposure, such as trees or buildings. Figure 3.3.2 shows the simulated and measured surface water temperature of the Barrage at Segment 21, near RW pump 2. In Figure 3.3.2, the simulated noon-day water temperature is plotted for selected days showing the general pattern over the simulation period. A number of model runs were performed to determine the influence of the Wind Sheltering Coefficient on the surface temperatures and mixing conditions. The default value (of 0.9) was found to provide the most acceptable agreement between the simulated and measured water temperature.

Volume Balance A volume balance calculation was performed to verify the inflow and outflow hydrograph data. This showed that some of the flow gauging structures were unreliable. A complete revision was made of the flow data and volume balance of the water body. Görgens *et al.* (1993) describe the methods used in the calculation of the volume balance. Figure 3.3.3 shows the measured and simulated water surface elevation data for the Barrage over the simulation period of 137 days using the tributary inflow hydrographs and inflow hydrograph shown in Figures 3.3.4 and 3.3.5. The model provides an acceptable simulation of the volume

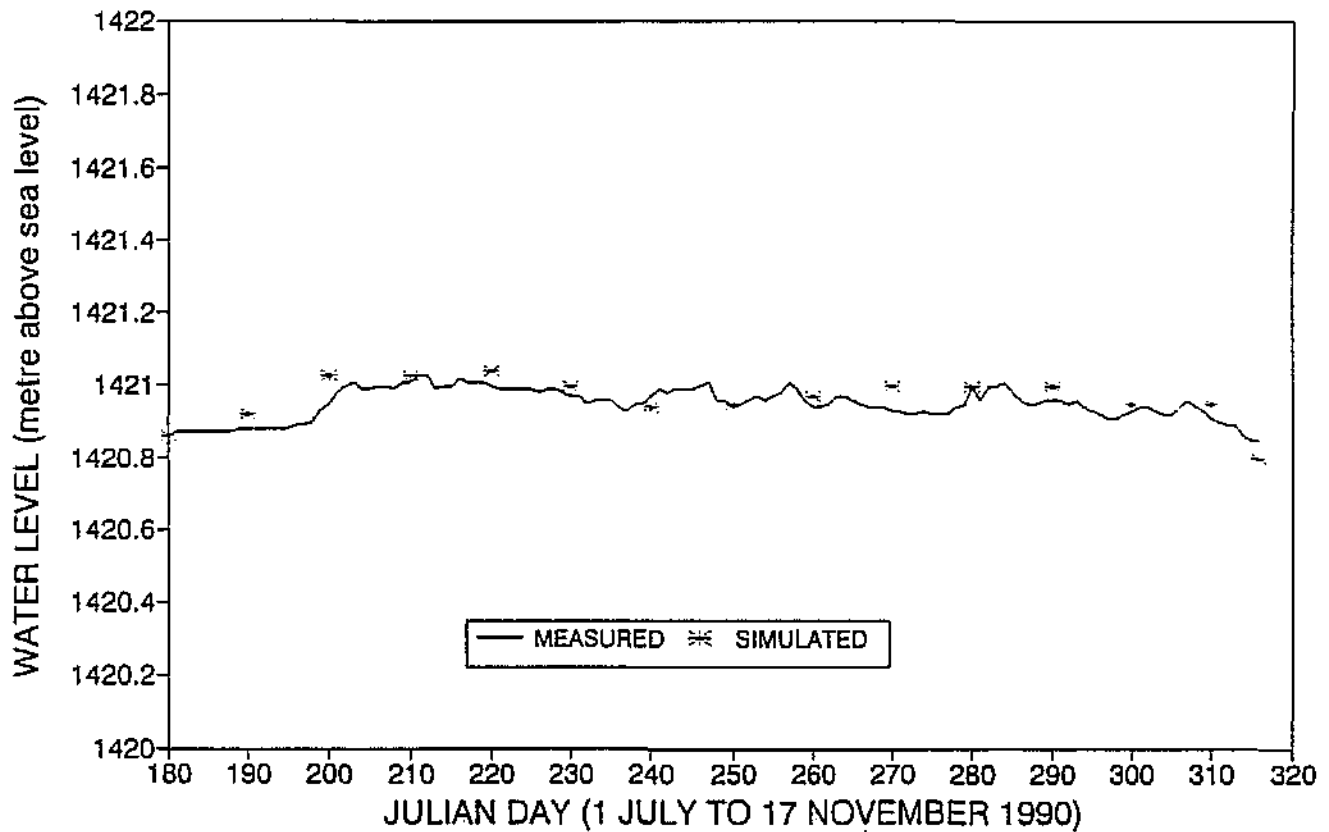
² Studies undertaken by IWQS report a channel length of 50.5 km

- 3.48 -



Simulated and measured surface water temperature.

Figure 3.3.2



Simulated and measured water elevation.

Figure 3.3.3

balance taking account of the comparatively complex set of inflows, outflows, releases and withdrawals (many of which are not measured on a continuous basis).

Salinity (conductivity) For graphical purposes, the 600 mg/l dilution option is equated for the purposes of this study to be a conductivity of 90 mS/ms. In practice, DWAF use a field reading of 85 mS/m for operational purposes. This conductivity is referred to as the *operational guide*.

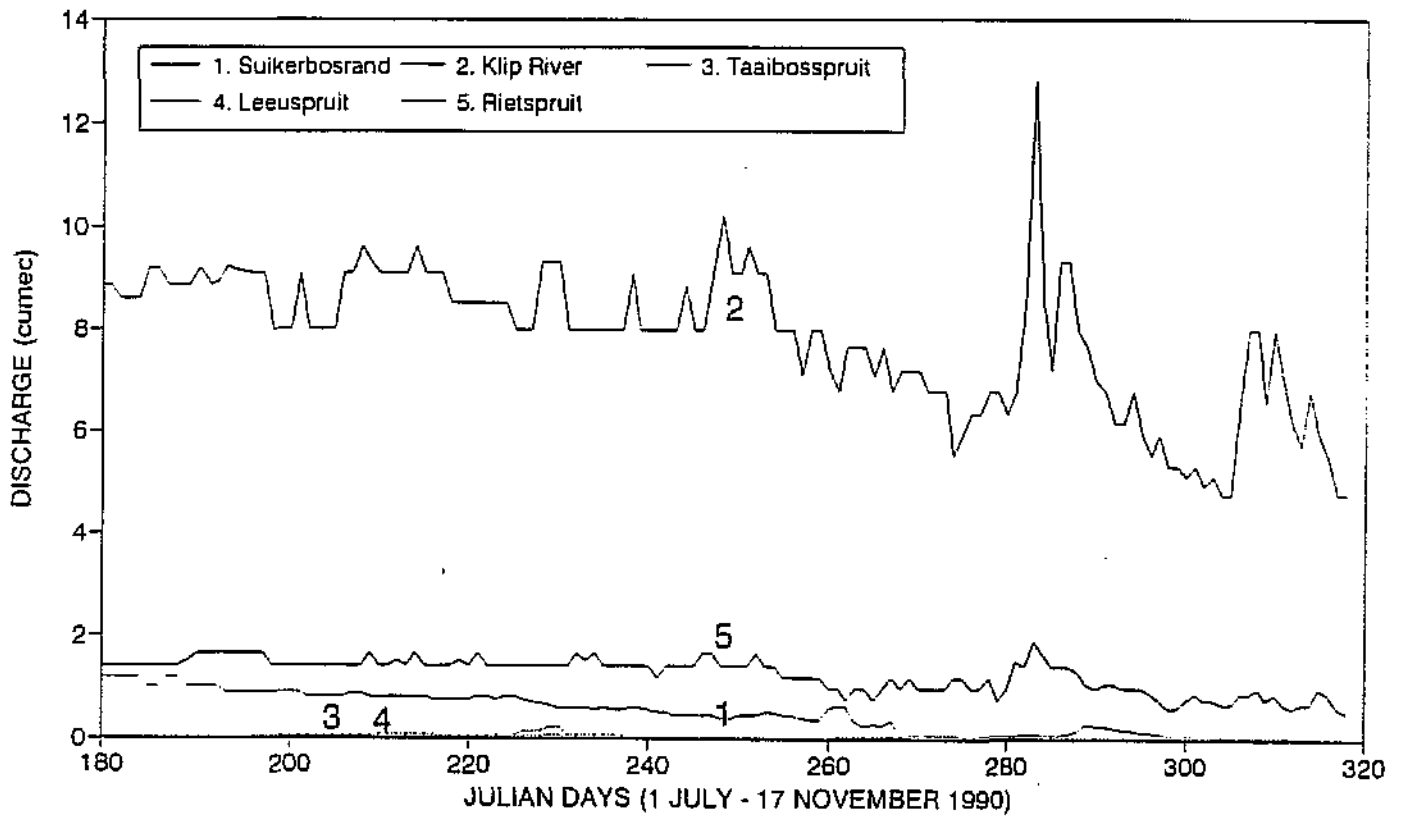
Figure 3.3.6 shows the simulated and measured electrical conductivity at eight Segments along the length of the Barrage. Segment 5 is located at Zuikerbosch close to the inflow, and Segment 45 is in the lower reaches close to Loch Vaal. Figure 3.3.6 shows the model provides an acceptable simulation of the conductivity during the release period. Analysis of the measured conductivity data showed that some variation in conductivity occurred across the width of the Barrage, particularly near the tributary inflow points. The model assumes the water body is laterally averaged which accounts for the discrepancies between the simulated and measured conductivities, see Figure 3.3.6.

3.3.5 SALINITY CHARACTERISTICS DURING THE FRESHENING RELEASE

Figure 3.3.6 shows that the freshening release brings about an abrupt reduction in the conductivity of the Barrage and complies with the operational guide.

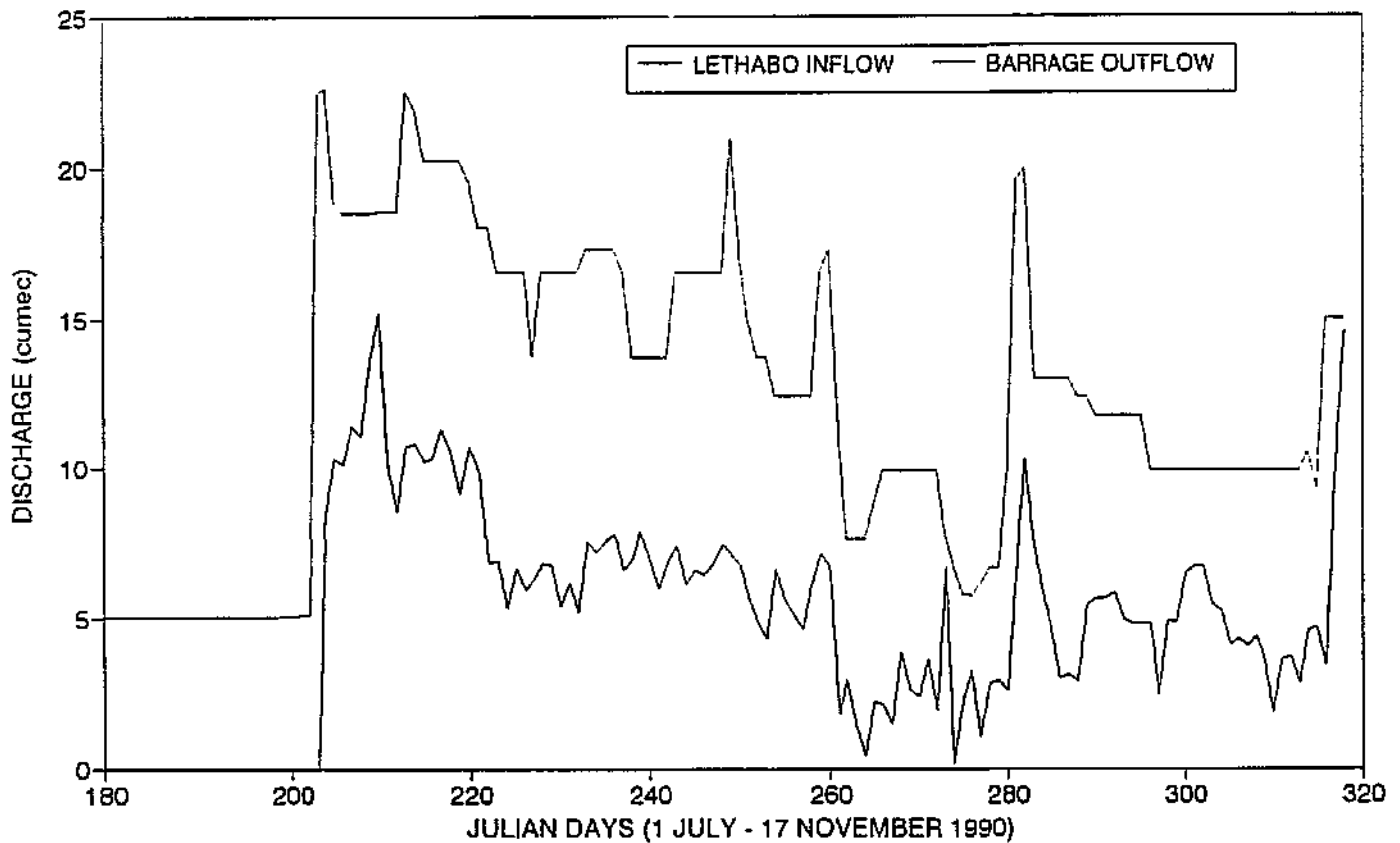
Figure 3.3.7 shows the two-dimensional (2-D) representation of the conductivity during the release period.

- (1) **Day 199:** prior to the release taking place, the conductivity of the Barrage was dominated by the release of saline water from the Klip River, entering the Barrage at Segment 12.
- (2) A saline plume (with EC > 110 mS/m) discharged from the Klip River, moved upstream and downstream of the tributary inflow point caused by abstraction at the Zuikerbosch Intakes drawing water upstream. The plume extended over a distance of almost 14 km, from Lethabo Weir to Segment 15 (near Duncanville).
- (3) **Day 204:** The first part of the freshening release flowed into the upstream Segments 2 and 3. The saline water progressed along the bottom of the Barrage.
- (4) **Day 205:** At the beginning of the freshening release, movement of the high salinity plume along the Barrage, and introduction of saline water from the Klip River produced two saline plumes.



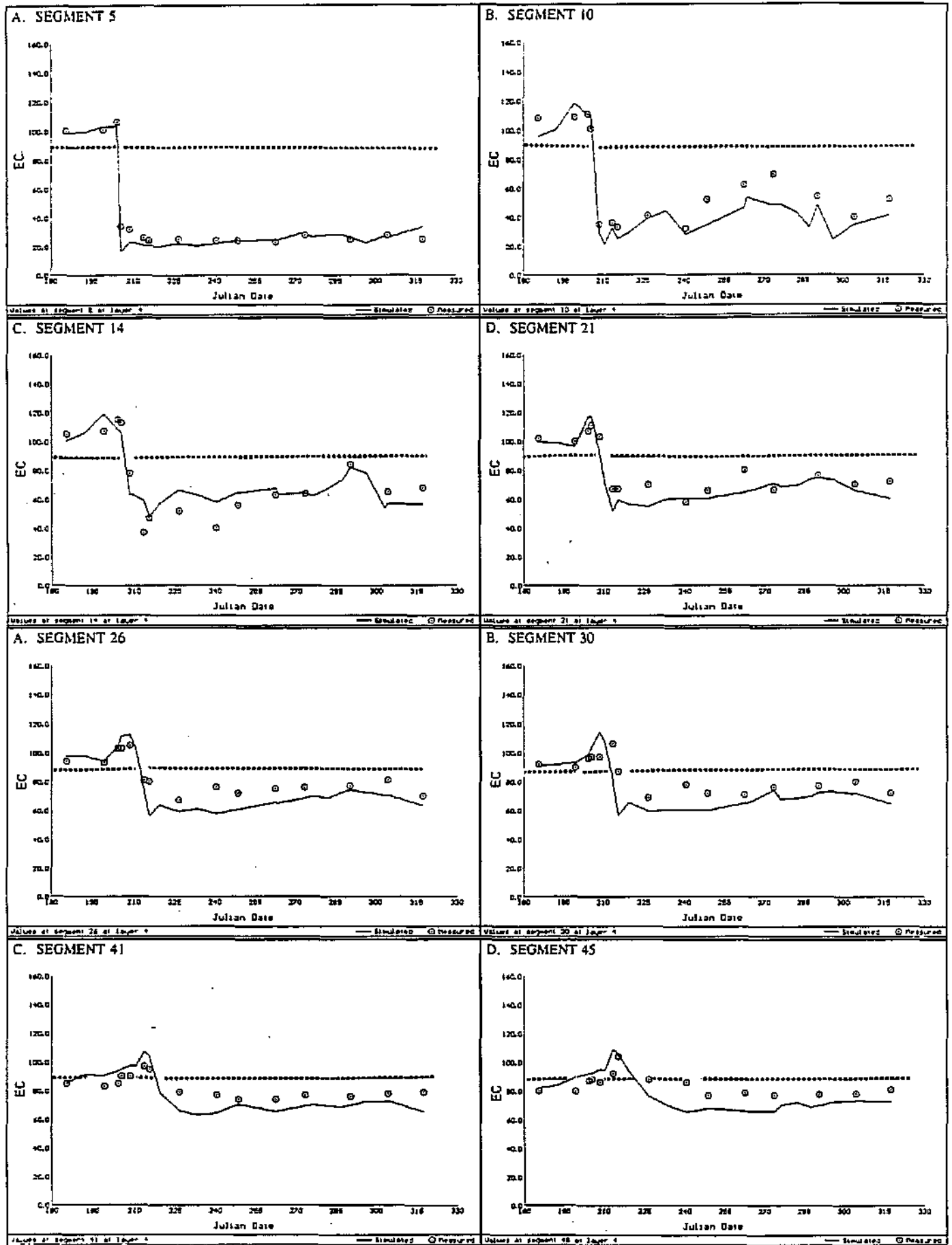
Measured tributary inflows to the Barrage

Figure 3.3.4



Measured Barrage inflow at Lethabo Weir and spillage from the Vaal Barrage.

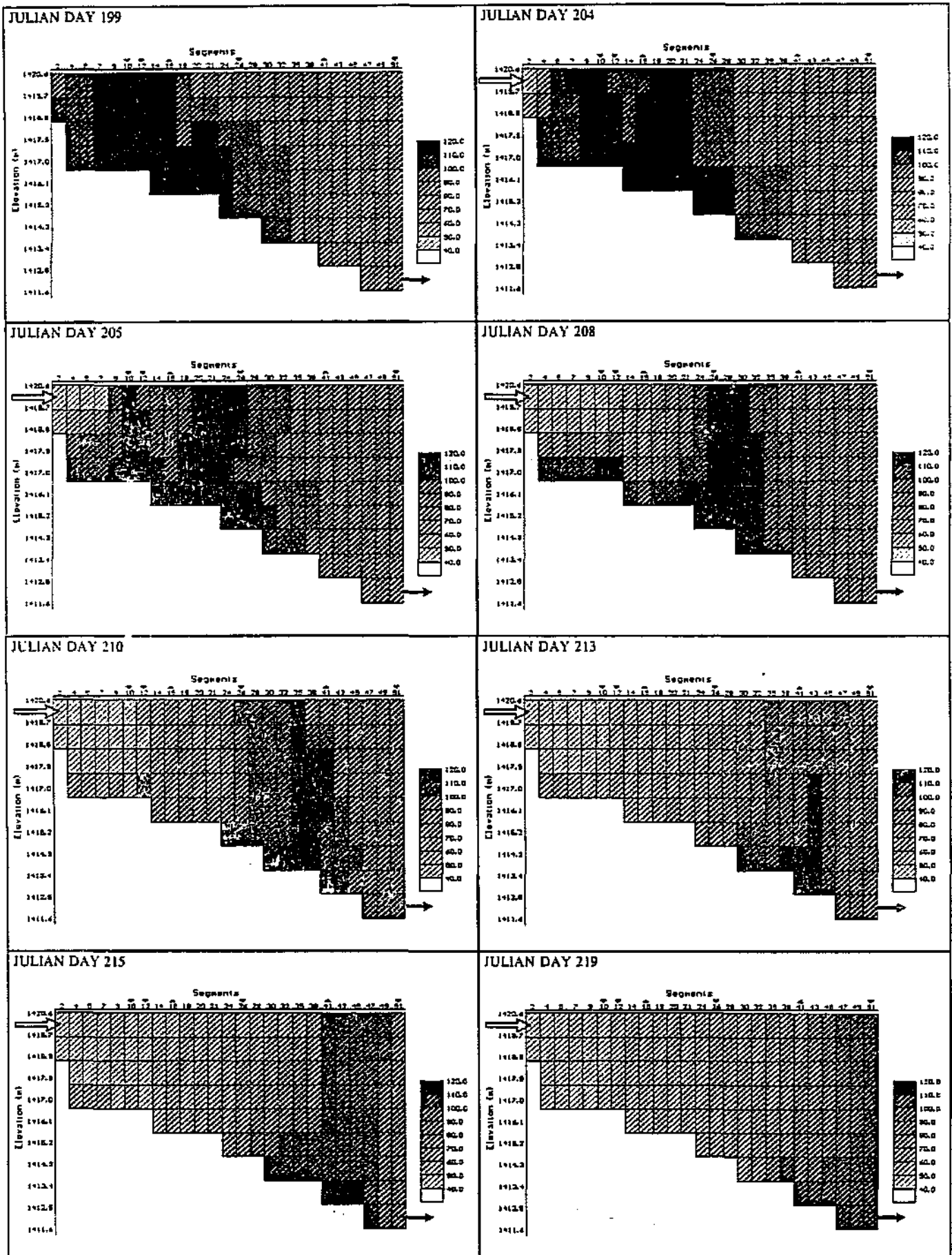
Figure 3.3.5



Measured and simulated EC for segments along the length of the Barrage.

Figure 3.3.6

- 3.52 -



2-D plot of the simulated electrical conductivity (EC) of the Vaal Barrage during the release period (Day 204 onward). Figure 3.3.7

- (5) **Day 208:** the release water reduced the surface conductivity to below 40 mS/m. Higher salinity water in Segments 2 to 12 remained in the bottom layers. This feature was thought to be caused by a submerged weir at the boundary of Segment 13 which restricted the flow of saline water. The model was configured with a weir at Segment 13. Subsequent simulations were carried out to determine the influence on the conductivity of the Barrage by removing the weir. The results showed that the weir had little influence on the conductivity of the upper reaches. The salinity pattern was caused by (1) the comparatively high flow (± 8 cumec) of the Klip River which caused a localised downward and lateral movement of water, and (2) localised reversed flow caused by wind action.
- (6) As the release continued, the saline plume moved along the length of the Barrage and at Day 208 was situated at Segments 24 to 32.
- (7) **Day 210:** The release from Vaal Dam (of 12 cumec) resulted in vertical mixing in the upper segments (2 to 12). The saline had moved between Segments 35 and 41.
- (8) **Day 213:** The saline plume passed into the lower layers of the Barrage, and then dispersed.
- (9) **Day 215:** The release water dominated the conductivity of the upper and middle reaches of the Barrage (Segments 2 to 30). In the lower reaches, wind action increased mixing which dissipated the saline plume.
- (10) **Day 219:** The release water had nearly reached the lower segment of the Barrage and plunged into the deeper layers.
- (11) **Day 226:** The release water finally reached the Barrage at Segment 51.
- (12) **Day 233:** Increased wind velocities brought about vertical and longitudinal mixing of the waterbody.
- (13) **Day 240:** Vertical and longitudinal gradients were not evident and the Barrage was comparatively mixed with lower salinity water distributed evenly throughout the water body.

The Vaal Barrage shows a number of different mixing and salinity characteristics. Prior to the release, there is flow reversal caused by the abstraction of water at the Zuikerbosch Intakes. At the beginning of the release, the comparatively high discharge from the Vaal Dam passes over the top of the saline water in the Barrage, with minimal mixing into the lower layers. This was brought

about by *density and momentum factors*. The saline water from the Klip River creates a plume of high salinity water in the upper reaches of the Barrage. During the release, this plume, passes along the length of the Barrage with minimal mixing into surrounding water thereby showing a *plug flow response*. The Klip, Suikerbosrand and Rietspruit Rivers contain comparatively high salinity water and discharge into the lower layers of the Barrage (*density stratification response*). Once the release water approaches the lower reaches of the Barrage, the lower salinity water plunges into the deeper layers, showing an *inverse density stratification response*. During the latter part of the release, wind action results in the *vertical mixing* of the Barrage. Figure 3.3.8 shows the horizontal and vertical velocity (vector) plots for selected simulation dates. During day 233, the prevailing wind creates circulation currents in the lower reaches which mix the contents of the Barrage.

3.3.6 DESCRIPTION OF SCENARIOS

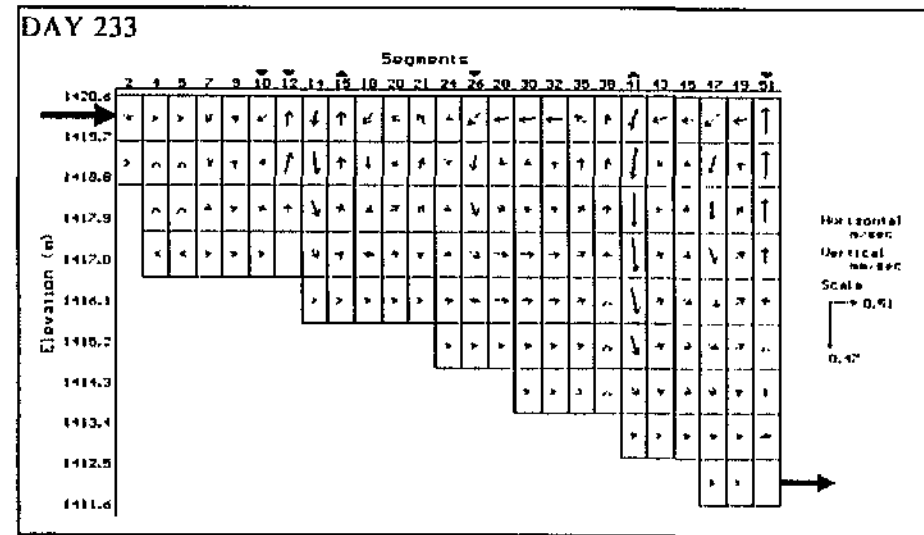
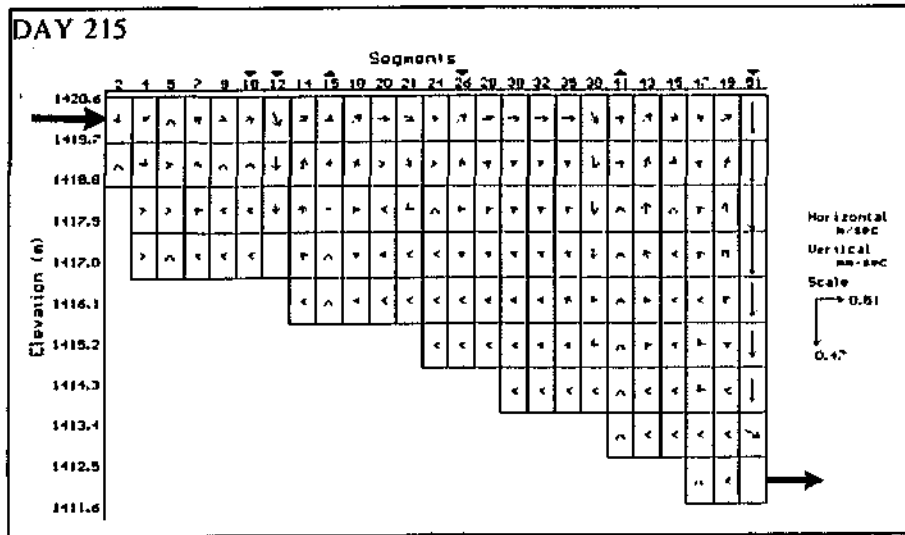
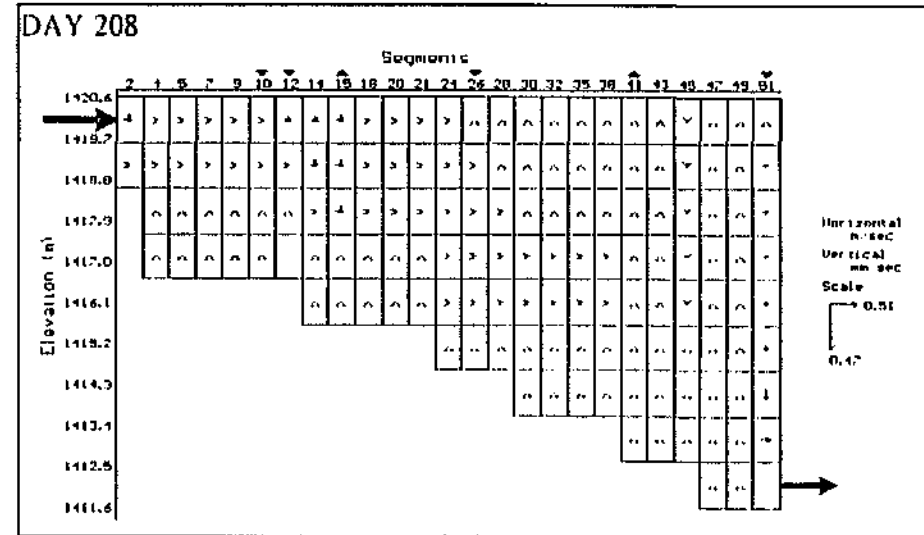
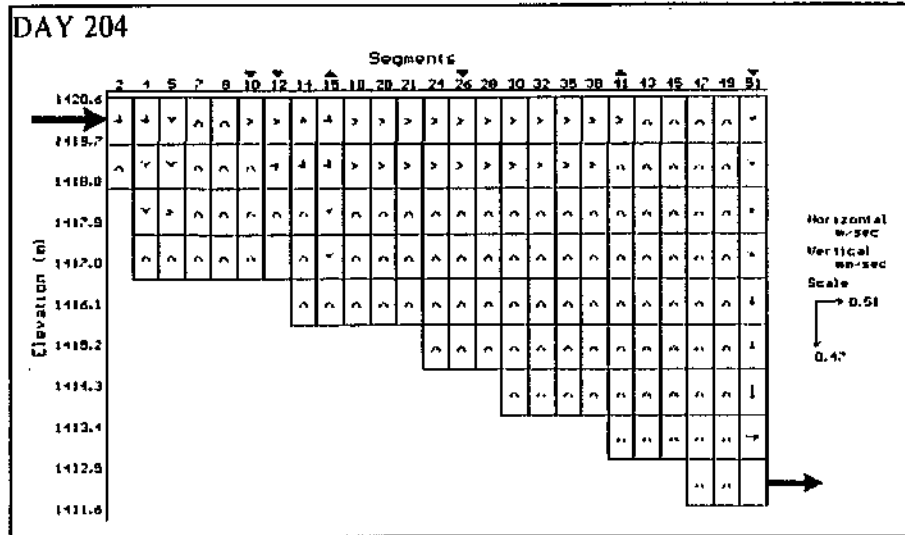
Scenario 1: Reduced freshening release from Vaal Dam The salinity of the Vaal Barrage and middle reaches of the Vaal River may be managed using releases of low salinity water from the Vaal Dam. *CE-QUAL-W2* is used to investigate the influence of reducing the volume of the freshening release on the salinity (conductivity) gradients within the Barrage.

Scenario 2: Blending Option of 500 mg/l When the TDS concentration exceeds 600 mg/l, low salinity releases may be made from the Vaal Dam to freshen the contents of the Barrage. *CE-QUAL-W2* is used to determine the increased volume of water required to achieve a more stringent TDS *operational guide* of 500 mg/l (given the same inflows).

Scenario 3: Diversion Canal When a freshening release is made from Vaal Dam it is possible for the Zuikerbosch Intakes to abstract the release water which is intended to reduce the salinity in the Vaal River. A diversion canal is being considered which transfers low salinity water from Lethabo Weir (downstream of Vaal Dam) into the Barrage, bypassing the Zuikerbosch Intakes. Two hypothetical canal configurations are evaluated.

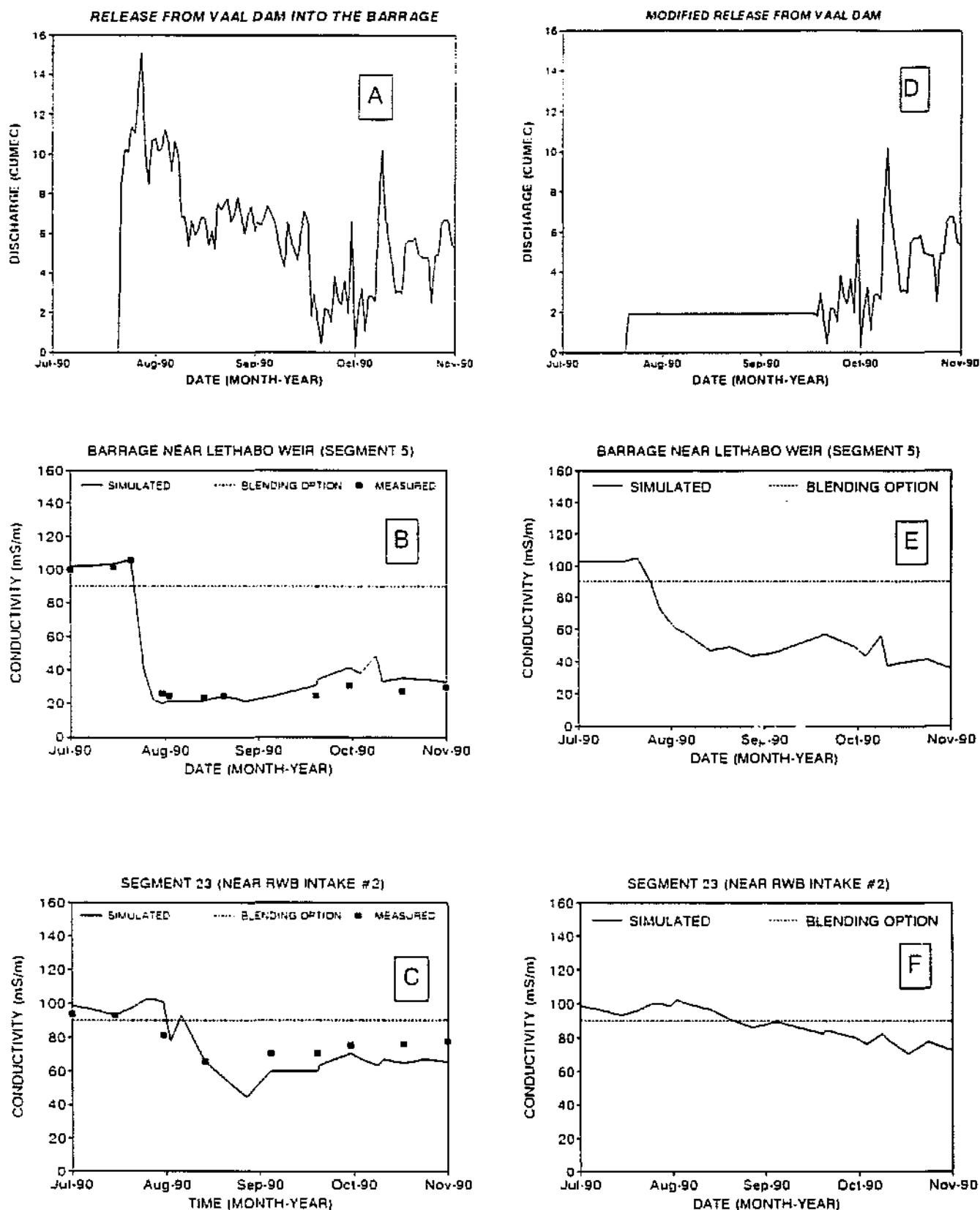
3.3.7 RESULTS OF SCENARIO TESTING

Scenario 1: Reduced freshening release from Vaal Dam - impact on salinity behaviour of the Barrage. Section 3.3.5 shows the water quality of both the Vaal Barrage and downstream Vaal River may be managed using freshening releases from the Vaal Dam. Figure 3.3.9 (Inset A) shows the measured release hydrograph from Vaal Dam. Insets B and C show the simulated and measured conductivity in the upper reaches of the Barrage near Lethabo Weir (Segment 5) and in the middle reaches near RW intake at Vanderbijlpark (± 28 km downstream of Lethabo Weir).



2-D plots of the vertical and horizontal movement of water in the Vaal Barrage.

Figure 3.3.8



Insets A, B and C showing the hydrograph and EC during the release period. Insets D, E and F showing the modified release hydrograph and simulated EC response of the Barrage.

Figure 3.3.9

The release causes an abrupt change in the salinity of the upper reaches and a more gradual change in the middle reaches.

Insets E and F (in Figure 3.3.9) show the influence of reducing the freshening release from Vaal Dam on the conductivity of the Barrage. The release hydrograph shown in Inset A was reduced to one quarter of its original volume, see Inset D. In the upper section, near Lethabo Weir, the reduced release still causes a marked reduction in conductivity. In the middle section, the release caused a small reduction in conductivity, taking the Barrage barely below a conductivity of 90 mS/m. The reduced release caused the conductivity of the Barrage to go below 90 mS/m about one month later than the full release, but in turn reduced the volume of water which had to be released from the Vaal Dam.

A number of simulations were performed to examine the influence of reduced release hydrographs on the conductivity of the Barrage. Figure 3.3.10 shows the results of the different simulations. The model was configured using:

- (1) the original (**full**) release, serving as a baseline to assess the other simulations.
- (2) 50 percent reduction in the original release hydrograph (shown on Figure 3.3.10 as **-50%**).
- (3) 75 percent reduction in the release (shown as **-75%**).
- (4) no freshening release from the Vaal Dam (shown as: **no release**).

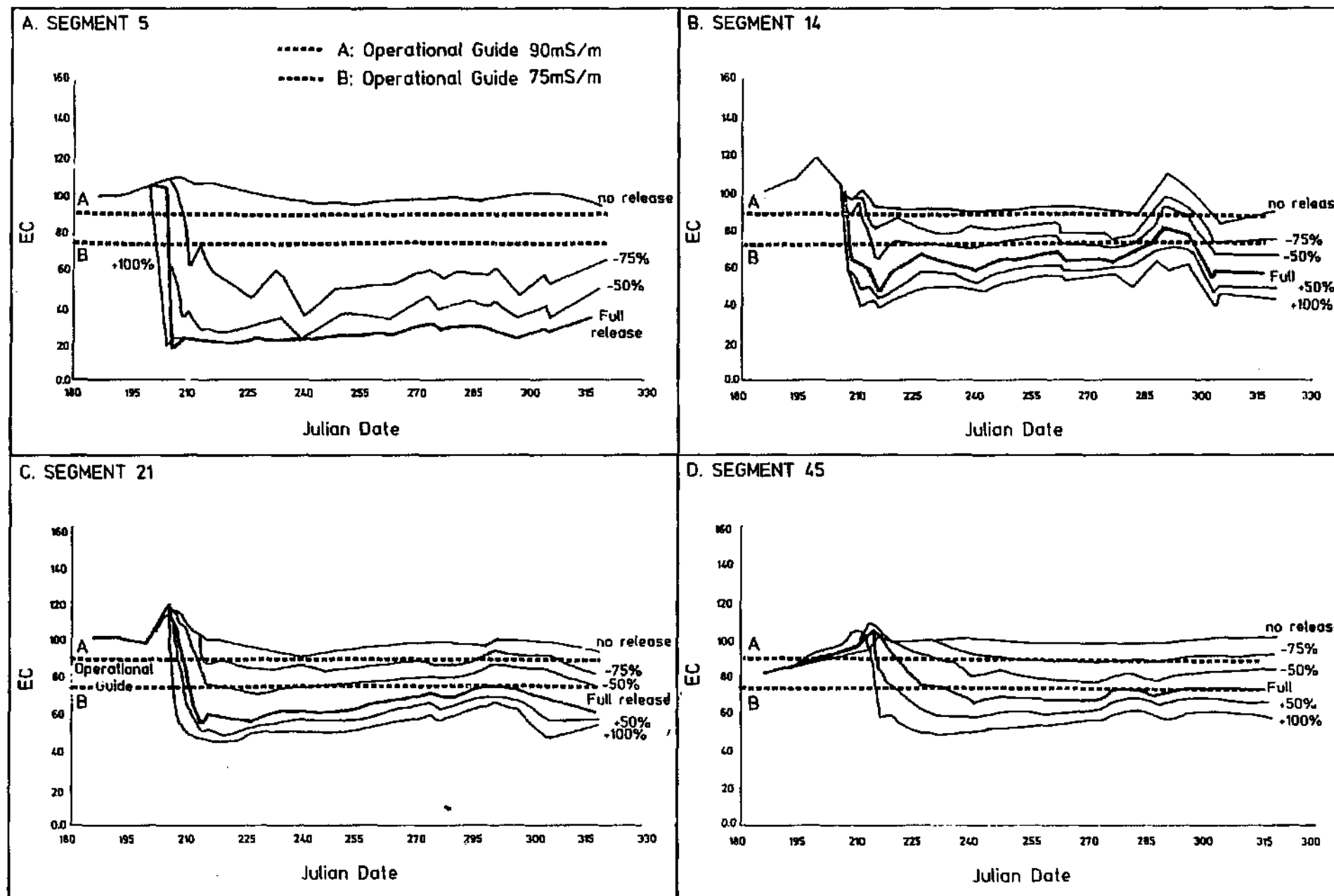
In the upper reaches (Segment 5), when no release was made from Vaal Dam, the conductivity remains between 90 and 100 mS/m over the full simulation period. The other releases keep the conductivity below 90 mS/m.

In the middle reaches (Segments 14 and 21), the 50% release is sufficient to reduce the conductivity to below 90 mS/m. The release reduced by 75% is however insufficient to keep the conductivity below 90 mS/m for the full period. When no release is made, the conductivity remains above 90 mS/m. In the lower reaches (Segment 45), the 50% release is sufficient to keep the conductivity below 90 mS/m.

Scenario 2: Blending option - 500 mg/l

The model is used to examine the increased volume of Vaal Dam which could be required to attain an *operational guide* of 500 mg/l (estimated to be a conductivity of 75 mS/m). Figure 3.3.10 shows the simulations where increased releases are made from Vaal Dam. The simulations include:

- (1) the original (**full**) release.
- (2) 50 percent increase in the original release (shown as **+50%**).
- (3) 100 percent increase in the original release (shown as **+100%**).



Simulated EC response of the Barrage to reduced releases (zero, 75% and 50% reduction), and increased releases (50% and 100%).

Figure 3.3.10

In the upper reaches (Segment 5), no improvement in the conductivity is achieved by using either a 50 or 100 percent increase in the release volume. During the release period the conductivity remains well below the *operational guide* of 75 mS/m. Analysis of the 2-D plots showed the 100% increase in release brings about a near instantaneous scour of the saline water in the bottom layers of Segments 2 to 12. In the middle reaches (Segment 14 and 21), the increased releases maintain the conductivity below the *operational guide*. In the lower reaches (Segment 45), the increased release has an almost immediate influence on the conductivity, which stays well below the 75 mS/m guide.

Scenario 3: Diversion canal

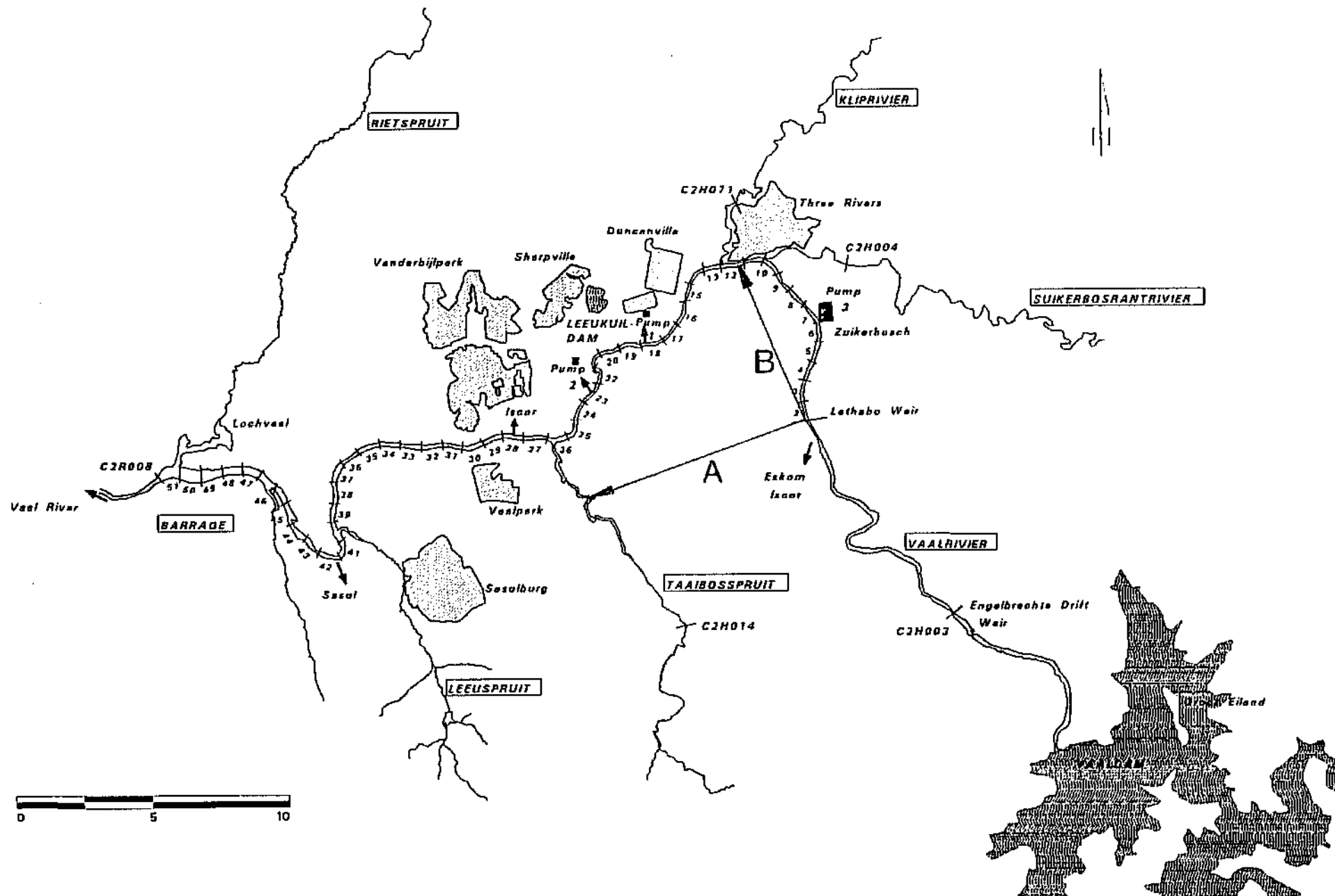
The model is configured to examine the salinity behaviour of the Barrage brought about by the diversion of some of the freshening releases into the middle reaches of the water body. Such an option would require the construction of a canal which conveys water from Lethabo Weir to a specific point in the Barrage. Such an option is being considered because it would allow freshening releases from the Vaal Dam to by-pass the intakes of Zuikerbosch. This would in turn result in Zuikerbosch intake abstracting a greater portion of the tributary inflow, thereby improving the abstraction of saline tributary inflow.

The model is configured to examine:

- (1) the salinity response of the Barrage,
- (2) possible water quality benefits for downstream users, and
- (3) identify an optimum canal outlet point.

Figure 3.3.11 shows the two diversion canal options evaluated using the model. Canal A is 20 km long and transfers water from Lethabo Weir to the Taaibosspruit which then flows into the Barrage at Segment 26. Canal B is 14 km long and transfers water from Lethabo Weir to the Barrage at the confluence with the Klip River at Segment 12. For Canal A and B, three maximum diversion rates are tested (2, 4 and 8 cumec). It should be noted that a canal with a maximum diversion of 8 cumec was not a practical design option, but included in the simulation for comparison purposes.

Figure 3.3.12 shows the conductivity at Segments 5, 14, 21 and 45 with (1) normal release (via Lethabo), (2) short and long canal options (with 4 cumec maximum diversion) and (3) long canal option with 8 cumec maximum diversion. In the upper reaches (Segment 5), the diversion canals cause the conductivity to increase, this would allow the Zuikerbosch Intakes to abstract a large portion of the Klip River (saline) inflow. In the lower reaches, all three canal options have minimal influence on the conductivity when compared with the normal release.

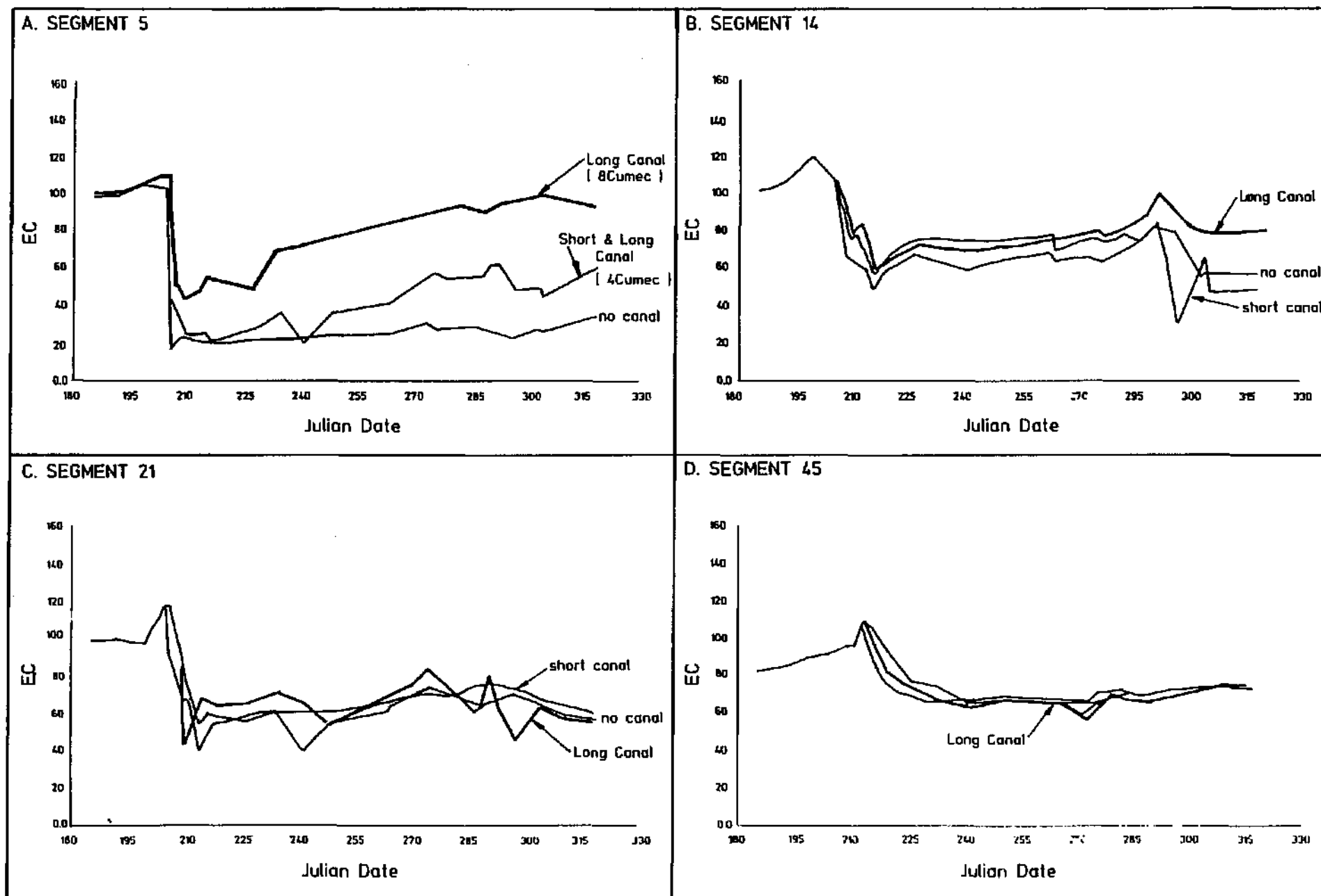


- 3.60 -



Location map showing the two hypothetical diversion canal options investigated using CE-QUAL-W2.

Figure 3.3.11



Simulated EC response of the Barrage to the diversion canal options. Normal release, Canal option A (20 km long) with maximum transfer of 8 cumeC, and Canal option B (14 km long) with maximum transfer of 4 cumeC.

Figure 3.3.12

The simulation shows that:

- (1) The diversion canal increases the conductivity in the upper reaches near Zuikerbosch.
- (2) The canal option could allow improved abstraction of saline tributary water by Zuikerbosch.
- (3) There will be no appreciable difference in the salinity of the water released from the Barrage to downstream users unless the intakes and diversion canal are operated so that a large volume of the saline tributary inflow is abstracted at Zuikerbosch.
- (4) There is little difference in overall response between the long and short canal option. The long canal option would however improve abstraction of the tributary inflows by discharging the freshening release as far as possible downstream of the Zuikerbosch intakes.

3.3.8 CONCLUSIONS

Calibration During the freshening release, abrupt changes in conductivity were measured within the water body. The simulation shows that intricate mixing processes occur in the Barrage. Governing processes identified include density stratification, plug flow, momentum effects, flow reversal, and wind mixing. The available data set was sufficient to allow detailed calibration at a number of points along the water body. The model provides an acceptable simulation of the conductivity, heat exchange and volume balance of the Barrage. Comparison of the simulated and measured conductivity data shows that the Barrage is not always laterally averaged, giving rise to localised discrepancies between the simulated and measured data (at the segments near the Klip River inflow).

Information for operational management of water quality The simulation shows that the salinity of the Vaal Barrage can be managed using releases of low salinity water from the Vaal Dam. The study confirms that such releases from Vaal Dam are capable of maintaining a TDS concentration of 600 mg/l. However, it is shown that the release should be optimized so that the minimum Vaal Dam water is used to achieve the necessary TDS concentration at selected points in the Barrage. It is also shown that increased freshening releases could be made from the Vaal dam to achieve a TDS concentration of 500 mg/l TDS in the Barrage but at the cost of using increased volumes of water from the Vaal Dam.

The simulation performed to evaluate the diversion canal showed that to achieve maximum benefit to the users downstream of the Barrage, the diversion canal and Zuikerbosch Intakes would require

joint operation to maximize the reuse of the saline tributary inflow from the Klip River.

3.3.9 RECOMMENDATIONS

Decision support role *CE-QUAL-W2*, now configured and tested using the data set for the Vaal Barrage, can play a valuable decision support function in providing information on:

1. The development, testing and fine tuning of operating rules. The model could be used to evaluate and test a number of dilution options. This information could then be used to develop a decision support system for (1) scheduling and control of dilution releases from Vaal Dam, and (2) determining the fate and transport of other water quality constituents, such as phosphorus.
2. The feasibility of constructing a diversion canal. Such a study will require detailed information on: the location of the canal outlet, maximum flow rate, salinity response of the Barrage, selection of operation rules, and water quality benefits for downstream users. Some of these issues were briefly addressed as part of this study.

Water quality monitoring The data set used in this study was adequate to calibrate the model for salinity simulations. However, the simulation of the algal and phosphorus dynamics of the Barrage requires information on the suspended solids concentration of the inflowing tributaries and Barrage. Unfortunately, insufficient data were available to calibrate the model adequately for suspended solids and phosphorus.

To meet the primary input requirements of the model, monitoring of the Barrage should include:

- Inflows: TDS, EC, phosphate, total phosphorus, suspended solids, nitrate, ammonia, E.coli, water temperature, dissolved oxygen and discharge (flow rate)
- Barrage: the above constituents plus chlorophyll-a, secchi depth and water level. Vertical profiles of water temperature, EC, and dissolved oxygen.

3.3.10 REFERENCES

Bath, A.J. & Timm, T.D. (1993)

Water quality investigation of Fika Patso and Swartwater Dams, Proceedings of the ICOLD 18th congress, Durban.

TABLE 2.4.6 : DETAILS OF COMBINATION SCENARIO

| Design Details | Destratification (Scenario 2A from Table 2.4.4) | Maintenance (Scenario 4B from Table 2.4.5) |
|--------------------------------------|---|--|
| Q_b (l/s) | 8.49 | 3.34 |
| Q_i (l/s) | 314 | 157 |
| N_i | 37 | 47 |
| Spacing (m) | 9.2 | 9.2 |
| Length (m) | 340 | 432 |
| Level of stratification based on | 'strong' | 'weak' |
| Plumes | independent | independent |
| Case | second peak case | second peak case |
| Bubbler operation time (Julian days) | 80353 - 81012 (26 days) (18 December 1980 - 12 January 1981) | 81013 - 82096 (449 days) (13 January 1981 - 6 April 1982) |

Note: No bubbler operates for the period 80107-80352 (246 days)
 * $0.2 \times$ height of rise (46m)

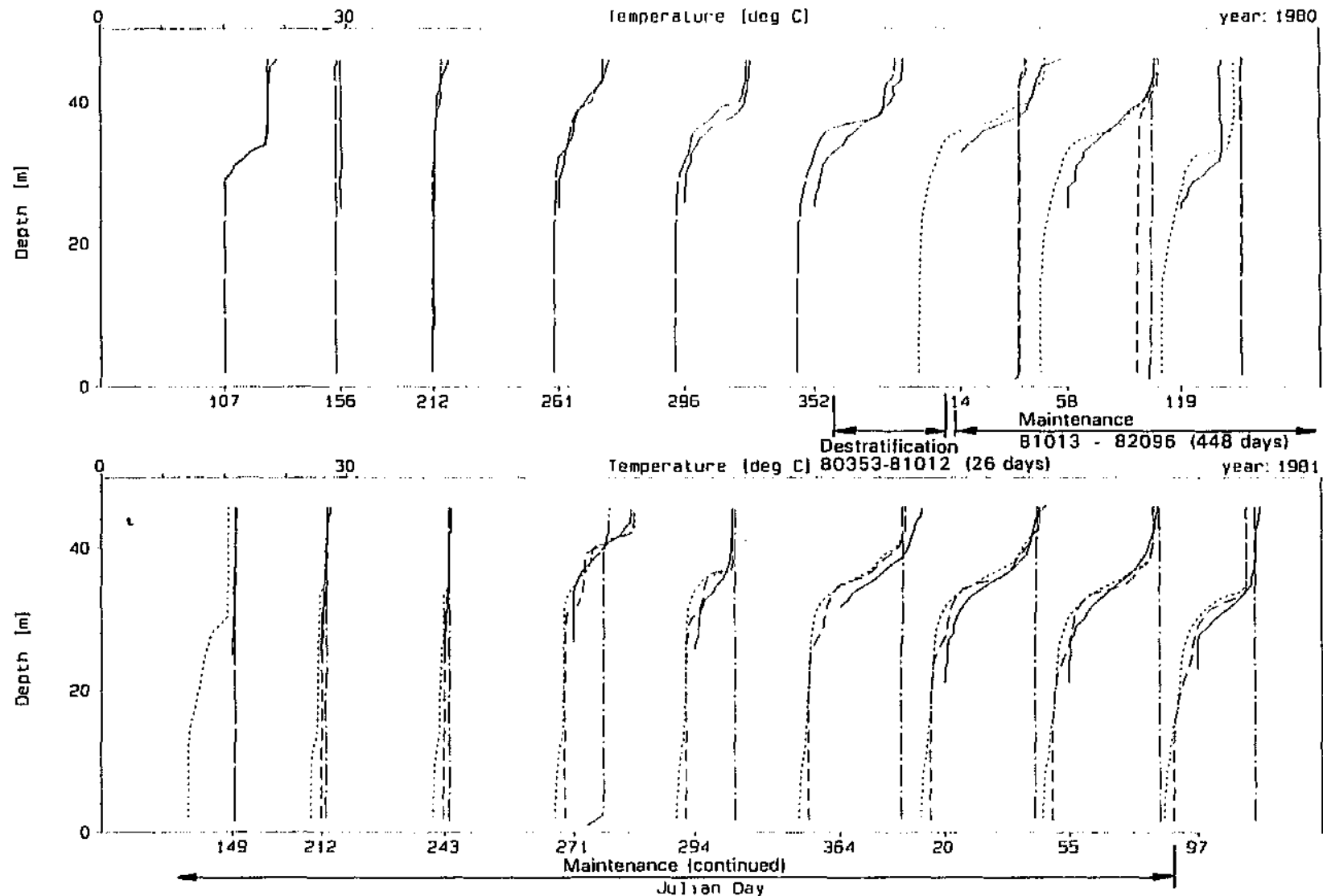
Figure 2.4.17 shows the results of this combination plotted against the results of a simulation with the destratification portion only (case 2A). During the period from 80353 to 81012 when the destratification bubbler operates for both cases, the reservoir is destratified. This is evident from the difference in profiles on Julian days 80353 and 81014. From Julian day 81013, the combination scenario has the maintenance bubbler operating, while the other scenario shown on the figure has no bubbler operating. This difference shows a minor effect until Julian day 81271 when the reservoir begins to stratify again in September 1981. From this date onwards, the maintenance bubbler maintains a mixed reservoir, while the scenario with no bubbler operating stratifies to almost the same extent as the completely 'unbubbled' scenario.

Figure 2.4.18 shows the results of the combination plotted against the results of a simulation with the maintenance scenario (case 4B) operating for the entire period. The case with the maintenance bubbler operating from Julian day 80107 prevents the onset of stratification evident in the 'unbubbled' scenarios at Julian day 80261. It also achieves a greater degree of destratification at Julian day 80014 than the destratification scenario was able to achieve during the 26 days it operated in the combination scenario.

DYPLOT10 : DYRESM-10

Dam : Rondeplaat Dam

Plot Date : 25 Oct 94, 15:51



Profile Legend: — Observed - - - Simulated . . . Bub 2A - . - Comb-2A&4B



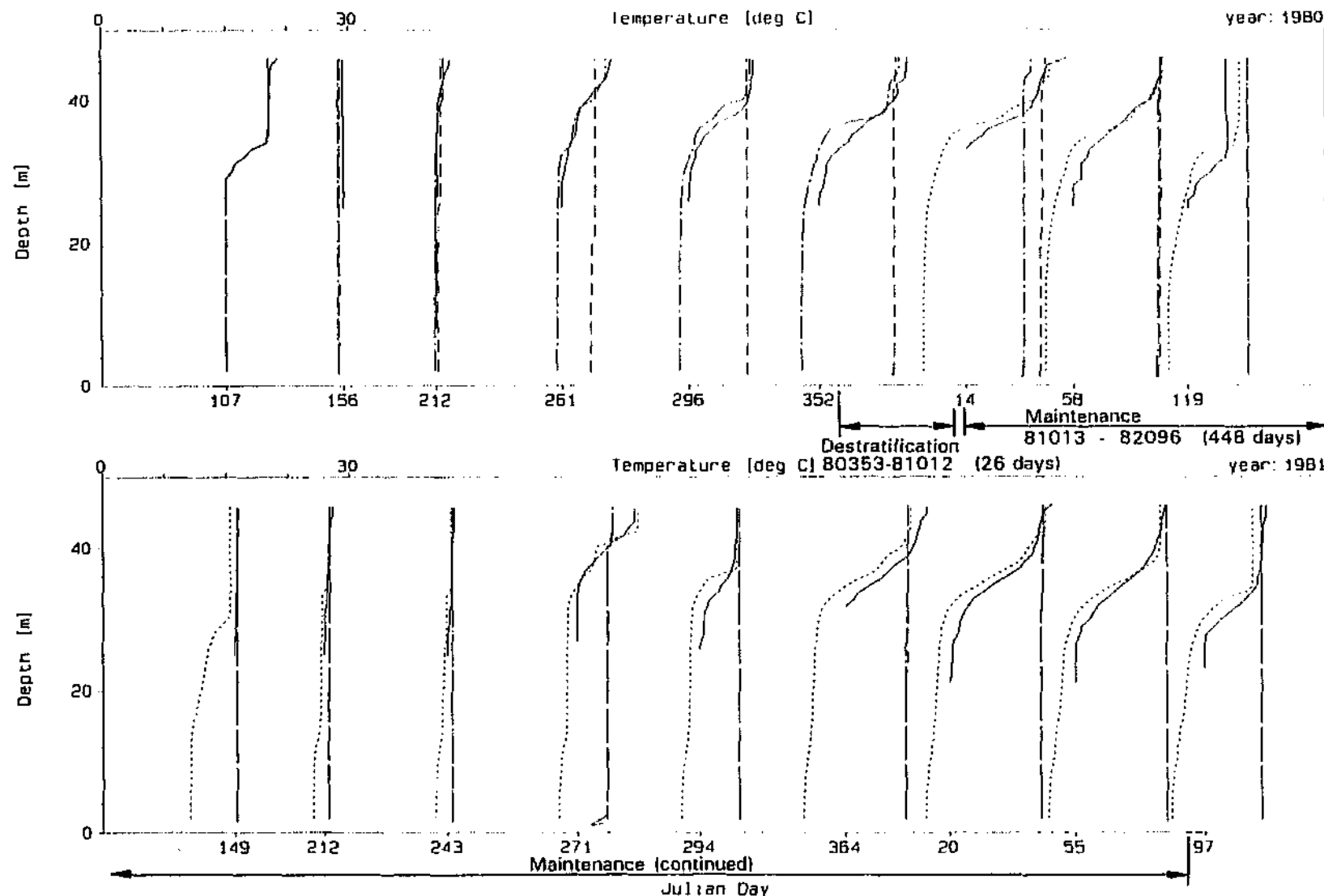
Comparison of the combined bubbler run (2A&4B) with the destratification run only (2A)

Figure 2.4.17

DY PLOT 10 : DYRESM-10

Dam : Roo deplaat Dam

Plot Date : 25 Oct 94, 15:52



Comparison of the combined bubbler run (2A&4B) with the maintenance run only (4B)

Figure 2.4.18

Bubbler system operational costs

Using the same costs as detailed in Section 2.3.5, the electricity costs for the combination scenario would be as follows:

Destratification:

$$26 \text{ days} \times 2 \text{ compressors} = R286,54 + R184,54 \times (26 \times 2 - 1) = R9\ 700$$

Maintenance:

Monthly electricity cost with bubbler operating full time:

$$30 \text{ days} \times 1 \text{ compressor} = R286,54 + R184,54 \times 29 = R5\ 640$$

If the maintenance bubbler is kept operating on a continuous basis for seven months of the year, this would amount to approximately R40 000. If such a bubbler operation resulted in a significant improvement in water quality, significant savings in treatment costs could result. These may far exceed destratification costs (Quibell, 1994). In comparison with the cost of this continuous bubbler operation, intermittent bubbler operation between 1°C and 3°C (Bubbler scenario 4C) would result in an annual cost of approximately R12 000, based on the bubbler operating for 57 days from September to March. Intermittent operation between 2°C and 4°C (Bubbler scenario 4D) would result in an annual cost of approximately R10 000, based on the bubbler operating for 48 days from September to March.

2.4.4 Bubbler Plume Destratification - Conclusions

The bubbler scenario that was most effective at destratification is the design based on the strongly stratified profile, second peak case, with independent plumes (scenario 2A and C). The most successful maintenance scenario was the design based on the weak stratification, second peak (scenario 4). Independent plumes was the preferred option if the bubbler length was practical at that spacing. Optimisation of the bubbler operation requires obtaining a balance between operating time (cost), mechanical efficiency and effectiveness at breaking down the stratification. The advantage of combining two different bubbler designs to deal separately with destratification and maintenance was demonstrated.

SECTION 2.5

DYPLOT : *DYRESM* OUTPUT VISUALISATION SOFTWARE

by

K O de Smidt and A J Greyling

Due to the difficulty of obtaining high quality, high resolution plots via both the one- and two-dimensional *DYRESM* models' plotting facility, and in line with the recommendation in the *DYRESM* chapter of Görgens *et al.* (1993), the DYPLOT program which is capable of viewing and plotting reservoir profiles was converted and enhanced to be able to read directly from the latest *DYRESM* version's output files.

Other enhancements undertaken during the course of this research project include the following:

- 1) The ability to display up to seven profile datasets on a single plot.
- 2) Flexibility in the number of Julian days, profile temperature range, depth range and starting profile.
- 3) The option of specifying the profile interval to display, eg. matching Julian days or regular weekly profiles extracted from daily profile data.
- 4) Automatic, customisable and storable profile legends.
- 5) The ability to display inflow and inflow temperature timeseries along with reservoir profiles correctly spaced relative to time.
- 6) Tabular output of any simulated or observed profile.
- 7) Report ready laser printer plot output.
- 8) Automatically stored parameter file.

It is envisaged that further enhancements to the software should include the ability to plot isoline information, timeseries of outflow and bubbler configuration, air flow rate and mechanical efficiency along with reservoir profiles correctly spaced relative to time. The inclusion of an interface to the WATERMARQUE graphical data visualisation software developed by the DWAF IWQS, would also further enhance the post-processing capabilities of the *DYRESM* models.

The profile plots displayed in the above sections of this report were produced using the latest version of the DYPLOT software, which has now been renamed DYPLOT1D.

Significant progress was also made on a version of DYPLOT to easily view and produce laser printer plots of the two-dimensional *DYRESM-2D* output. The 2D plots displayed in Section 2.2.3 of this report were produced using the latest version of this software, which is now called DYPLOT2D. Features incorporated in DYPLOT2D include:

- 1) The ability to display up to two 2D output datasets for comparison purposes. The datasets may either both be simulated data or one may be observed profiles at several sites along the length of the reservoir.
- 2) The option of animating up to two 2D output datasets in order to enhance the visualisation capabilities of the program and the resultant increased understanding of the hydrodynamic and destratification processes at work within the reservoir.

SECTION 2.6

CONCLUSIONS : *DYRESM* APPLICATIONS

2.6.1 Simulation capabilities and the role of data

- (i) It has been shown that the *DYRESM-1D* reservoir simulation model is capable of acceptably accurate one-dimensional hydrodynamic simulation of typical South African impoundments with relatively minor, plausible adjustment to the available hydrometeorological datasets (usually to the wind data).
- (ii) The quasi two-dimensional *DYRESM-2D* model is capable of simulating the hydrodynamics of a South African hydrodynamically two-dimensional reservoir with reasonable accuracy, given its current limitations. At present, however, the model has certain aspects that are either disabled or do not function correctly. These include the inability to record bubbler efficiencies, the inability to specify interacting bubble plumes and the disabling of particular aspects of the inflow downflow stack, which in turn prevents visualisation of the migration and insertion into the water body of underflows. The *DYRESM-2D* model may also be optimistic with respect to the degree and efficiency of longitudinal mixing when compared with the observed data for Inanda Dam. This observation may indicate that the longitudinal mixing initiated by a physical bubbler system in Inanda Dam may not be quite as successful as indicated by the model simulations.
- (iii) The *DYRESM-2D* model enhances the user and decision maker's capability to conceptualise and visualise the two-dimensional hydrodynamic and destratification processes at work within a reservoir.
- (iv) Since *DYRESM* is a physical process based model it does not require fundamental calibration and therefore, each adjustment made to the input data and parameters to obtain a better fit between the simulated and observed profiles must be justifiable and must represent a possible scenario or encompass feasible data measurement, extrapolation or translation anomalies.

- (v) The necessity of regular, accurate and representative measurement of the various aspects of inflow, outflow, meteorological and observed field profile data has again been highlighted.
- (vi) The sensitivity of the models to wind data indicates the necessity of instituting and maintaining a suitable wind measuring network and database for all dams that are likely to require hydrodynamic analysis in the future.
- (vii) The development and enhancement of the DYLOT1D and DYLOT2D *DYRESM* post-processing software has enhanced the user and decision maker's capability to conceptualise and visualise the one- and two-dimensional hydrodynamic and destratification processes at work within a reservoir.

2.6.2 Destratification modelling : General

- (i) The bubble plume destratification modelling results show that the use of the bubbler routine within *DYRESM* allows the evaluation of existing bubbler systems and the design and optimisation of feasible systems for the destratification and hydrodynamic management of typical South African reservoirs.
- (ii) There is a need for two aerators to be included in the design of a bubbler system, viz. a destratification and a maintenance aerator. The point at which the bubbler operation should be changed from using the destratification aerator to the maintenance aerator should be based on the optimisation of mechanical efficiency. This strategy results in the maximisation of bubbler effectiveness at maintaining mixed conditions, while minimising operational costs.
- (iii) Bubbler designs based on the second efficiency peak are more efficient and effective overall at both destratification and maintenance, due to the changing degree of stratification experienced during bubbler operation. First efficiency peak designs do however show an initial short period of higher efficiency/effectiveness during the breakdown of strong stratification.
- (iv) Independent plumes were found to be more effective than interacting plumes. Ensuring independent plumes sometimes results in impractical aerator lengths, in which case interacting plumes should be used.

- (v) Intermittent bubbler operation results in significant savings in operational cost. Due to a decrease in effectiveness associated with intermittent bubbler operation, an appropriate intermittent operation scenario needs to be determined for each specific dam in order to avoid unacceptable stratification during the height of summer.

2.6.3 Destratification modelling : Specific reservoirs

- (i) Reservoir depth was found to influence the effectiveness of bubbler designs. In the case of Hartbeespoort Dam the full dam case required higher air flow rates per source to achieve destratification, and a higher total air flow rate for adequate maintenance, than for the drawn down dam case.
- (ii) Preliminary comparison of *DYRESM-1D* and *DYRESM-2D* simulations of Inanda Dam showed that the profiles describing the quasi two-dimensional simulation better approximated the observed profiles when compared with the one-dimensional simulation. The preliminary theoretical bubbler design is capable of destratifying a strongly stratified Inanda Dam over a three to four week period in a hydrodynamically two-dimensional environment. Prevention of the onset of stratification at the beginning of spring and maintenance of mixed conditions throughout the summer season is also theoretically possible in the hydrodynamically two-dimensional Inanda Dam.
- (iii) The most significant and most probable causes of the failure of the previous two attempts to destratify and prevent the stratification of Inanda Dam are twofold. Firstly, the wrong number of bubble plume sources and hence the air flow rate per source was used for the desired destratification or stratification prevention objective associated with each attempt. In the case of the revised design the total design air flow rate was also insufficient to efficiently destratify the water body in the available time before natural overturn. Secondly, the aerator layout prevented the forming of proper bubble plumes due to large, erratic bubbles in the original design, and the aerator nozzle hydraulics in the revised design would have resulted in as little as one third of the design air flow rate being achieved. The use of *state of the art* bubbler design (Schladow, 1991) in combination with optimisation by hydrodynamic simulation and the practical realisation of design parameters in the field, are clearly indispensable in the successful implementation of a bubble plume destratification system.

- (iv) The bubble plume aerator designs for destratification and maintenance of mixed conditions for Inanda, Hartbeespoort and Roodeplaat Dams, as determined by the reconnaissance level research performed during this study, are presented in Table 2.6.1 (The Hartbeespoort Dam designs are based on the hypothetical full dam case). It can be seen that in general two 157 l/s compressors (typical compressor suitable for this application) are required for both destratification and maintenance of mixed conditions, with the exception of the destratification of Inanda Dam which requires three compressors and the maintenance of mixed conditions in Roodeplaat Dam which requires only one compressor. Estimated energy operating costs vary between approximately R40 000 and R80 000 per summer for the prevention of the onset of stratification. As shown in the case of Roodeplaat Dam, intermittent bubbler operation results in significant savings in operational cost. However, due to a decrease in effectiveness associated with intermittent bubbler operation, a scenario between continuous and 1-3°C operation is required in order to avoid unacceptable stratification during the height of summer.

TABLE 2.6.1: COMPARISON OF BUBBLER DESIGNS

| RESERVOIR | INANDA | HARTBEESPOORT* | ROODEPLAAT | | |
|--|------------|----------------|------------|---------------|---------------|
| DESTRATIFICATION | | | | | |
| Reference No | 7 | 6D & E | 2A | | |
| Design level of stratification (°C/m) | 0,131 | 0,500 | 0,289 | | |
| No of compressors | 3 | 2 | 2 | | |
| Total air flow rate (l/s) | 471 | 314 | 314 | | |
| Air flow rate per source (l/s) | 15,19 | 2,53 | 8,49 | | |
| Aerator length (m) | 250 | 744 | 340 | | |
| No of days of operation required | 29 | 21 | 26 | | |
| Estimated energy cost | R12 800 | R7 900 | R9 700 | | |
| MAINTENANCE | | | | | |
| Reference No | 9 | 2D | 4B | | |
| Design level of stratification (°C/m) | 0,050 | 0,160 | 0,101 | | |
| No of compressors | 2 | 2 | 1 | | |
| Total air flow rate (l/s) | 314 | 314 | 157 | | |
| Air flow rate per source (l/s) | 1,00 | 0,50 | 3,34 | | |
| Aerator length (m) | 628 | 628 | 432 | | |
| Type of operation | Continuous | Continuous | Continuous | Between 1-3°C | Between 2-4°C |
| No of days of operation required (Sep-Mar) | 212 | 212 | 212 | 57 | 48 |
| Estimated monthly energy cost | R8 500 | R11 200 | R5 640 | varies | varies |
| Estimated energy cost (Sep-Mar) | R59 500 | R78 400 | R40 000 | R12 000 | R10 000 |

* Based on hypothetical full dam case

SECTION 2.7

RECOMMENDATIONS : *DYRESM* APPLICATIONS

In order for continued success in hydrodynamic reservoir modelling the following general and *DYRESM* specific recommendations are made :

- 2.7.1 Since the wind speed is of major significance in both of the *DYRESM* models and other hydrodynamic models, careful attention should be given to the placement of wind measuring stations where possible. Periods of wind measurement should be undertaken at a height of 10 metres in order to validate the conversion of wind measured at other heights. Similarly, over water wind speeds should be measured where possible and compared with that measured over land, so that these locational effects may be quantified. It is also recommended that further research be undertaken into the over land to over water and height conversion of wind speeds. Daily wind speed and direction measuring stations and their corresponding databases should be instituted and maintained for all dams that are likely to require hydrodynamic analysis in the future. Moreover, the recorded data should be stored in a digital form that would simplify the extraction of data required by hydrodynamic reservoir models. Preferably more than one wind measurement station should be located at representative sites as close as possible to the water body and a height of 10 m.
- 2.7.2 As far as possible, when hydrometeorological data sets are prepared for the purposes of hydrodynamic modelling, a base set which consists of unadjusted measured field data should be constructed before specific data sets are developed by adjustments such as factoring, conversions, etc. This will allow data sets to be easily transferred which will result in maximum and most accurate use of such data, which are costly to collect and process.
- 2.7.3 When adjustment of measured field data is required, eg. due to locational effects, seasonal effects should be taken into account. This is particularly true for the case of wind speed where seasonal predominant wind direction can result in non-representative wind speed being applied to the water body. Seasonal effects may equally well apply to the adjustment of other hydrometeorological data.

- 2.7.4 The field measurement of profile data should be undertaken at several representative points within water bodies likely to require hydrodynamic analysis. The measurement of profiles should be done from the water surface to the dam bottom, at regular intervals, under all circumstances and Secchi disk depth measurements should always be performed.
- 2.7.5 The current version of *DYRESM* should be implemented on a dataset for a reservoir with a significant salinity component in order to test this aspect of the model's capabilities.
- 2.7.6 Further investigation into the relationship between total dissolved salts (TDS in mg/l) and NaCl concentration (ppm) is required in order that the density function within the model can be amended for South African conditions, ie. to use TDS in place of NaCl concentration.
- 2.7.7 The quasi two-dimensional *DYRESM-2D* model should be re-applied to Inanda Dam once the problems associated with the inflow downflow stack and the use of interacting bubble plumes have been addressed.
- 2.7.8 Further bubble plume destratification field experiments should be undertaken by the Department of Water Affairs and Forestry using refined designs based on the *state of the art* bubbler design methodology and theoretical and simulation research presented in this report and that of Görgens *et al.* (1993). These prototype destratification/stratification prevention attempts would provide a clearer understanding of the potential of bubble plume destratification as a management tool in South African reservoirs than that obtained from the previous attempts undertaken at Inanda Dam.
- 2.7.9 The DY PLOT programs which are capable of producing, viewing and plotting both profiles and two-dimensional model output data should be enhanced to be able to display isoline plots and additional timeseries information, such as bubbler configuration, air flow rate and mechanical efficiency along with reservoir profiles correctly spaced relative to time.
- 2.7.10 Further research using the *DYRESM-WQ* model which incorporates the simulation of the water quality components of a reservoir should be undertaken using South African datasets, when the model becomes available. Apart from the benefit of the

availability of an additional tool for the prediction of the biological and chemical aspects of water quality, which has been shown by the Centre for Water Research to give good results, the use of *DYRESM-WQ* would enable an investigation of the effects of the use of bubble plume destratification on the biological and chemical components of reservoir water quality in South Africa.

2.7.11 The following general rules should be applied when a bubble plume destratification system design is undertaken:

- i) The 2nd efficiency peak associated with the forming of 2 whole plumes should be aimed for in most cases.
- ii) If possible the aerator layout should ensure independent bubble plumes by spacing the sources at a distance of at least 20% of the full supply level depth of the reservoir.
- iii) Although designs should be undertaken for a reservoir depth measured from full supply level, other reservoir depths should be taken into account when performing the design.
- iv) Maximum operating efficiency and effectiveness, both during destratification and maintenance of mixed conditions, should be strived for in the design and operation of a bubbler system.
- v) The minimisation of energy requirements should be integral to the design process in order to ensure minimum operating costs. This is achieved by ensuring maximum operating efficiency and effectiveness, while using the minimum number of compressors required and intermittent bubbler operation if appropriate.
- vi) A design should combine the ability to operate effectively as both a strong destratification dismantling system and a prevention system capable of maintaining the reservoir in a mixed state efficiently. This requires the design of two aerator lines in most cases.

The use of *state of the art* bubbler design (Schladow, 1991) in combination with optimisation by hydrodynamic simulation and the practical realisation of design parameters in the field, are indispensable in the successful implementation of a bubble plume destratification system.

SECTION 2.8

REFERENCES : *DYRESM* APPLICATIONS

- Centre for Water Research, (1992)
"DYRESM 1D user's manual, Ver. 6.75.2 DW", University of Western Australia, Nedlands, Australia.
- Centre for Water Research, (1992)
"2D *DYRESM* supplement to the 1D *DYRESM* user's manual (6.75.2 DW)", University of Western Australia, Nedlands, Australia.
- Daugherty, R.L. and Franzini, J.B. (1981)
"Fluid mechanics with engineering applications", 7th Edition, McGraw Hill, London, 259-261.
- Department of Water Affairs and Forestry (1990)
"Inanda Dam : Capacity Determination", Directorate of Survey Services, Report No. U200-04, Pretoria, South Africa.
- Department of Water Affairs and Forestry (1992)
"Crocodile River (Western Transvaal) Catchment Study : Hydrology of the Upper Crocodile River Sub-system", Report by Stewart, Sviridov & Oliver in association with BKS Inc. to DWA&F (Project Planning), Report No. P A200/00/1492 (Volume 1), Pretoria, South Africa.
- Görgens, A.H.M., Bath, A.J., Venter, A., de Smidt, K. and Marais, G.v.R. (1993)
"The applicability of hydrodynamic reservoir models for water quality management of stratified water bodies in South Africa", Report by Ninham Shand Inc. and the University of Cape Town to the Water Research Commission, Report No. 304/1/93, Pretoria, South Africa, ISBN 1 86845 004 X.
- Hocking, G.C. and Patterson, J.C. (1991)
"Quasi-two-dimensional reservoir simulation model", ASCE Journal of Environmental Engineering, 117(5), 595-613.
- Howard, J.R. (1994)
Umgeni Water, Pietermaritzburg, South Africa, Personal communication.
- Imberger, J., Patterson, J.C., Hebbert, R. and Loh, I. (1978)
"Dynamics of reservoir of medium size", ASCE Journal of Hydraulic Engineering, 104(HY5), 725-743.
- Imberger, J., Patterson, J.C. (1981)
"A dynamic reservoir simulation model - *DYRESM* : 5", Transport Models for Inland and Coastal Waters, Academic Press, New York, 310-361.

- National Institute for Water Research (1985)
"The Limnology of Hartbeespoort Dam", South African National Scientific Programmes Report No. 110, CSIR, Pretoria, South Africa.
- Patterson, J.C. and Imberger, J. (1989)
"Simulation of bubble plume destratification systems in reservoirs", Aquatic Sciences, 51(1), 3-18.
- Patterson, J.C. (1995)
Centre for Water Research, University of Western Australia, Nedlands, Perth, Western Australia, Personal communication.
- Quibell, G. (1994)
Institute for Water Quality Studies, Department of Water Affairs and Forestry, Pretoria, South Africa, Personal communication.
- Riley, M. J. (1988)
"User's manual for the dynamic lake water quality simulation program 'MINLAKE'", St. Anthony Falls Hydraulic Laboratory, University of Minnesota, U.S.A.
- Robertson, D.M., Schladow, S.G. and Patterson, J.C. (1991)
"Interacting bubble plumes: the effect on aerator design", Environmental Hydraulics, 1, 167-172.
- Schladow, S.G. (1991)
"A design methodology for bubble plume destratification systems", Environmental Hydraulics, 1, 173-178.
- Schladow, S.G. and Patterson, J.C. (1991)
"Bubble plumes and mixing efficiency in a stratified reservoir", Proceedings of the International Hydrology and Water Resources Symposium, Perth, Australia, 274-279.
- Schladow, S.G. (1992)
"Bubble plume dynamics in a stratified medium and the implications for water quality amelioration in lakes", Water Resources Research, 28(2), 313-321.
- Thirion, C. and Chutter, F.M. (1993)
"The use of artificial aeration in Inanda Dam as a management tool for the control of eutrophication and its effects", Hydrological Research Institute Report No. N U200/04/DPQ/0693, Department of Water Affairs and Forestry, Pretoria, South Africa.
- United States Army Corp of Engineers (1984)
"Shore protection manual", Coastal Engineering Research Centre, Volume I, Chapter 3, Sections IV and V, pp 3-24 to 3-54.
- Walmsley, R.D. and Bruwer, C.A. (1980)
"Water transparency characteristics of South African impoundments", Journal of the Limnological Society of South Africa, 6(2), 69-76.

CHAPTER 3
CE-QUAL-W2 APPLICATIONS
Contents List

| | Page: |
|---|-------|
| 3.1 INTRODUCTION | 3.1 |
| 3.1.1 Reservoir applications | 3.1 |
| 3.1.2 Model description | 3.2 |
| 3.1.3 References | 3.5 |
| 3.2 APPLICATION OF <i>CE-QUAL-W2</i> TO SIMULATE THE WATER QUALITY AND HYDRODYNAMIC BEHAVIOUR OF INANDA DAM. | 3.6 |
| 3.2.1 Introduction | 3.6 |
| 3.2.2 Model configuration | 3.10 |
| 3.2.3 Model calibration | 3.12 |
| 3.2.4 Model application and scenario evaluation | 3.20 |
| 3.2.5 Conclusions | 3.36 |
| 3.2.6 Recommendations | 3.37 |
| 3.2.7 References | 3.39 |
| 3.3 APPLICATION OF <i>CE-QUAL-W2</i> TO SIMULATE THE SALINITY AND HYDRODYNAMICS OF THE VAAL BARRAGE. | 3.43 |
| 3.3.1 Introduction | 3.43 |
| 3.3.2 Model input | 3.45 |
| 3.3.3 Model configuration | 3.46 |
| 3.3.4 Model calibration | 3.47 |
| 3.3.5 Salinity characteristics during the freshening release | 3.49 |
| 3.3.6 Description of scenarios | 3.54 |
| 3.3.7 Results of scenario testing | 3.54 |
| 3.3.8 Conclusions | 3.62 |
| 3.3.9 Recommendations | 3.63 |
| 3.3.10 References | 3.63 |
| 3.4 APPLICATION OF <i>CE-QUAL-W2</i> USING THE ROODEPLAAT DAM DATA SET TO EVALUATE THE SIMULATION OF THERMAL AND CHEMICAL STRATIFICATION. | 3.65 |
| 3.4.1 Introduction | 3.65 |
| 3.4.2 Data compilation | 3.67 |
| 3.4.3 Model application and calibration | 3.73 |
| 3.4.4 Results and conclusions | 3.85 |
| 3.4.5 Recommendations | 3.87 |
| 3.4.6 References | 3.88 |
| 3.5 APPLICATION OF <i>CE-QUAL-W2</i> IN THE ESTIMATION OF THE WATER QUALITY OF A PROPOSED RESERVOIR ON THE OLIFANTS RIVER AT ROOIPOORT. | 3.89 |
| 3.5.1 Introduction | 3.89 |
| 3.5.2 Compilation of data set | 3.90 |
| 3.5.3 Model configuration | 3.92 |
| 3.5.4 Results | 3.94 |
| 3.5.5 Conclusions | 3.98 |
| 3.5.6 Acknowledgment | 3.101 |
| 3.5.7 References | 3.102 |
| 3.6 APPLICATION OF <i>CE-QUAL-W2</i> TO LAING DAM TO EVALUATE THE MANAGEMENT IMPLICATIONS OF DIVERSIONS FROM WRIGGLESWADE DAM. | 3.103 |
| 3.6.1 Introduction | 3.103 |
| 3.6.2 Input data compilation | 3.104 |
| 3.6.3 Model verification | 3.106 |
| 3.6.4 Wriggleswade diversion scenarios | 3.114 |
| 3.6.5 Conclusions | 3.119 |
| 3.6.6 References | 3.121 |

CHAPTER 3
APPLICATION OF *CE-QUAL-W2*
GENERAL INTRODUCTION

by
A J Bath

3.1 BACKGROUND

This chapter describes the application and testing of *CE-QUAL-W2* using the data sets for five water bodies. This section provides an overview of the applications and the model.

3.1.1 Reservoir applications

Five applications were undertaken to demonstrate the use of *CE-QUAL-W2* to provide information for the management of water quality. The applications are summarized below:

- **Inanda Dam (Section 3.2):** The reservoir experiences extended periods of stratification, sediment release of contaminants, and high algal growth. These factors have affected the fitness for use of the reservoir. The nutrient/algal interactions of Inanda Dam are simulated to provide information on: drawoff depth, sediment interactions, reservoir draw-down, reservoir hydrodynamics, and the phosphorus regime of the reservoir.
- **Vaal Barrage (Section 3.3):** The salinity of the water body is governed to a large extent by saline tributary inflows and low salinity releases from the Vaal Dam. The hydrodynamic and salinity behaviour of the Barrage was simulated to provide information on the influence of freshening releases, optimization of releases, and diversion canal options.
- **Roodeplaats Dam (Section 3.4):** The reservoir shows pronounced thermal and chemical stratification for almost nine months each year. The model was used to simulate the thermal stratification and dissolved oxygen regime of Roodeplaats. These results were compared with the output from *DYRESM*, described in Chapter 2, and also used to assess the calibration requirements of the model.
- **Rooipoort Dam (Section 3.5):** A reservoir was proposed on the Olifants River at Rooipoort to supply potable water to Pietersburg, in the Northern Province. The model was used to provide preliminary information on the thermal stratification, hydrodynamic response, and salinity gradients within the reservoir. The information provided by the model was used to identify key water quality issues which include: location of the offtake tower, drawoff depth, water treatment process design, and management of the upstream catchment.

- **Laing Dam (Section 3.6):** During periods of low flow, Laing Dam receives drainage of high salinity from point and nonpoint sources. This gives rise to an elevated salinity in the reservoir. A simulation was performed to determine the influence of low salinity transfers from the Kubusi River catchment on the receiving water quality behaviour of Laing Dam.

3.1.2 Model description

Model Overview *CE-QUAL-W2* is a two-dimensional (2-D), laterally averaged, hydrodynamic and water quality simulation model. The model is based on the assumption that the water body is homogenous across the lateral width. Therefore, the model is best suited for relatively long and narrow water bodies that show water quality gradients in the longitudinal and vertical directions. The model has been developed for use on rivers, lakes, reservoirs and estuaries.

Model Background The original version of the model was known as *LARM* (Laterally Averaged Reservoir Model) which was developed in 1975 by Edinger and Buchak. The first application of the model was on a reservoir with a single main branch. Modifications to the model allowed for multiple branches and the ability to handle estuarine boundary conditions. The revised version of the model was known as *GLVHT* (Generalised Longitudinal-Vertical Hydrodynamics and Transport model). Water quality simulation capabilities were added by the Water Quality Modelling Group at the US Army Engineer Waterways Experimental Station in Vicksburg, Mississippi and was known as *CE-QUAL-W2* Version 1.

Considerable modifications were made to the model to improve the structure of the code and decrease the data storage requirements. These modifications resulted in Version 2 of the model. The latest enhancements to the model include: dynamic adjustment of the timestep, selective withdrawal algorithm, higher order transport scheme, and improved volume balance and mass balance algorithms (Cole, 1993; Cole and Buchak, 1993).

Model Capabilities In summary these include the following:

- The hydrodynamic routines predict the water surface elevations, velocities and temperatures.
- The water quality algorithms allow the simulation of up to 21 constituents in addition to water temperature. These include nutrient/algal interactions and sediment behaviour. Section 3.2 describes the simulation of the eutrophication response of Inanda Dam and Section 3.3 describes the simulation of salinity in the Vaal Barrage.
- The model has been modified so that simulations can be run over extended time periods. The application of the model using the Rooipoort Dam data set was configured using nearly five years of data to examine long-term trends in the salinity response of the reservoir.

- The ability of the model to simulate upstream and downstream head boundary conditions allows the use of the model for estuaries, or reservoirs in which the inflow volumes are unknown.
- The branching algorithm allows the model to be used in reservoirs which have a complex layout such as dendritic reservoirs, or estuaries with multiple freshwater inflows. Section 3.3 describes the use of the model to simulate multiple inflows and outflows using the data set for the Vaal Barrage application. The selective withdrawal algorithm calculates the vertical extent of the withdrawal zone based on outflow velocity and water density.
- The water body may be configured using segments of unequal length and layers of unequal thickness. The model adjusts the location of the surface layer and upstream segment to account for a rising or falling water level. This feature was important in the Laing Dam application where the reservoir showed variable water level during the simulation period.
- The model uses a variable timestep algorithm which ensures numerical stability.
- The control file allows the user to specify the format of the output produced by the model. Görgens *et al.* (1993) describe the development of the post-processor (POST2) which is used in this chapter to produce graphical and animated presentation of the model output.

Model Limitations In summary these include the following

- The lateral averaging assumes that the lateral variations in water velocity, water temperature and constituents are negligible. In a large wide water body this assumption may limit the applicability of the model. The applications described in the following sections include water bodies which are comparatively long and narrow.
- The water quality algorithms used in the model are simplifications of the processes taking place within aquatic systems. Only one algal compartment is simulated and thus algal succession can not be accommodated. The model does not include the influence of zooplankton in the cycling of nutrients and grazing of phytoplankton. The present version of the model does not model the processes and kinetics of the reservoir bottom sediments. This has most influence when the simulation extends over many years.
- The availability of input data is not a limitation of the model. However, it is often the limiting factor in the application of the model where insufficient data are available for calibration and verification.

Model Enhancements: It has been recognised that internal recycling of nutrients in a reservoir plays a major role in water quality. Therefore the latest enhancements being made to the model include refinement of the process descriptions. This will incorporate a fully predictive sediment compartment which it is hoped to eliminate the need to specify the Sediment Oxygen Demand term (SOD) and nutrient fluxes (Cole, 1995).

Model Hardware Requirements The minimum configuration is an 80386 or 80486 personal computer equipped with a mathematical co-processor. The model requires a minimum of four megabytes of memory with between ten and fifteen megabytes of hard disk space. The applications described in the following sections were carried out using a 80486 DX2 (66 Megahertz) with 8 Megabytes of memory and 120 Megabytes of hard disk space.

Model Software Requirements Using the model on a personal computer (PC) operating under DOS, the user requires a 32 bit FORTRAN compiler with a DOS extender that will use the PC's protected mode. The model was compiled using the Lahey FORTRAN F77L3 compiler with DOS extension and optimized for use on a 80486 PC.

Model and Data Availability *CE-QUAL-W2* is freely available from the Environmental Laboratory, US Army Corps of Engineers, Waterways Experimental Station, Vicksburg, MS, United States. The model is provided with a user manual, example data sets, and pre-processor (Cole, 1993). The data sets used as part of this study are held at the offices of Ninham Shand Consulting Engineers, Cape Town, South Africa.

Demonstration data files *CE-QUAL-W2* is provided with a number of demonstration data files, these include the following:

- **Degray Lake** is a reservoir with a single branch configuration and the model is used to simulate and demonstrate the full water quality capabilities.
- **JST Dam** is situated on the Savannah River between Georgia and South Carolina. The model is used to examine the influence of pump storage on the water quality response of the reservoir.
- **Thames River Estuary** is situated on the East Coast of the United States and the model is used to simulate temperature, salinity, water flow velocities, and water surface elevations of the estuary. The model is used to analyze the release of compensation releases on the water quality of the estuary.
- **Cumberland River** near Nashville is modelled to demonstrate the simulation of BOD and dissolved oxygen.

3.1.3 References

Cole, T.M. (1993)

Personal communication, Environmental Laboratory, US Army Corps of Engineers, Waterways Experimental Station, Vicksburg, MS.

Cole, T.M. (1995)

Personal communication, Environmental Laboratory, US Army Corps of Engineers, Waterways Experimental Station, Vicksburg, MS.

Cole, T.M. & Buchak, E.M. (1993)

CE-QUAL-W2: A two-dimensional, laterally averaged, hydrodynamic and water quality model. User Manual, Environmental Laboratory, US Army Corps of Engineers, Waterways Experimental Station, Vicksburg, MS, Instruction report number ITL-93, September 1993.

Görgens, A.H.M., Bath, A.J., Venter, A., de Smidt, K. & Marais, G.v.R. (1993)

Applicability of hydrodynamic reservoir models for water quality management in stratified water bodies in South Africa, Report by Ninham Shand Inc. and the University of Cape Town to the Water Research Commission, Pretoria. Report number 304/1/93.

SECTION 3.2

APPLICATION OF *CE-QUAL-W2* TO SIMULATE THE WATER QUALITY AND HYDRODYNAMIC BEHAVIOUR OF INANDA DAM.

by
A J Bath

3.2.1 INTRODUCTION

Reservoir description Inanda Dam is located on the lower reaches of the Mgeni River in the KwaZulu-Natal Province, 25 km from the centre of Durban, at a latitude of 29°41'S, longitude of 30°52'E, and elevation at FSL of 148 masl. The dam wall was completed in March 1989 and the reservoir reached full supply level for the first time in February 1990. The reservoir has a full supply capacity of 251 million m³, surface area of 1463 hectare, and mean water residence time of one year. The reservoir is located in a steep sided sinuous river valley and is ± 18 km long, ± 900 metre wide, and has a mean depth of 17.4 metre. Near the dam wall, the reservoir has a maximum depth of 55 metre (Hudson *et al.*, 1993).

The reservoir was built to increase the yield of the lower Mgeni River system and provide water to Durban. Water is released from Inanda Dam and abstracted from the Mgeni River 20 km downstream at the Clermont Pump station and transferred to the Wiggins water works. Releases are also made from Inanda Dam to manage the Mgeni River Estuary (Tollow, 1991).

The Inanda Dam site is situated downstream of both Nagle Dam and the confluence of the Msunduze River. The Msunduze River drains the population centres of Pietermaritzburg and Edendale, a large informal population, and significant agricultural and industrial development (Hudson *et al.*, 1993). In addition, about 18 million m³ per year of treated wastewater enters Inanda Dam from the Darvill Works which discharges into the Msunduze River.

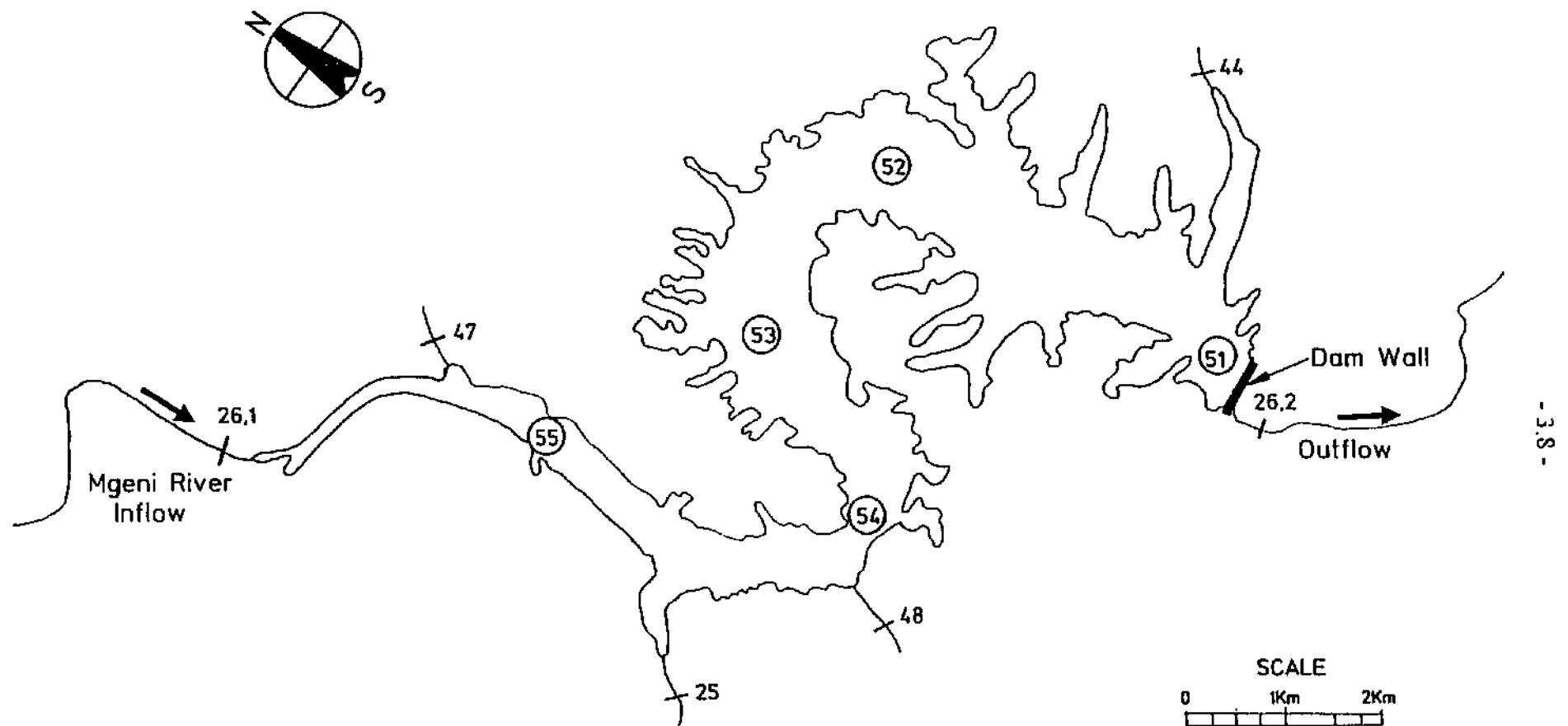
Prior to construction of the reservoir, it was cautioned that the reservoir morphology and location (downstream of the greater Pietermaritzburg area) could give rise to water quality problems associated with stratification and eutrophication (Bruwer, 1979; UW, 1989). In response to this caution, a multi-level outlet structure was incorporated in the design of the dam wall (UW, 1992a). Nine outlets were situated at 3 metre intervals from a depth of 4.5 to 28.5 metre below full supply level. A scour release valve was located at a depth of 30 metre.

Over the past four years, the reservoir has showed a number of water quality problems, including: (1) development of abundant algal biomass, (2) anaerobic hypolimnion, and (3) release of metals and nutrients from the bottom sediments.

Inanda Dam water quality data base The reservoir has been monitored routinely by Umgeni Water since the reservoir construction was completed in 1989. Figure 3.2.1 shows the location of the water quality monitoring points in the reservoir as well as the monitoring points on the inflowing rivers (Point 26.1) and side streams (ie Point 48). In Inanda Dam, water samples were collected from the main water body at five sampling points, see Figure 3.2.1. At present, only three of the original points are monitored. At these points, water samples are collected from the surface and bottom, and an integrated depth sample collected from the top 5 metres of water. Water samples are collected on a weekly basis. The water samples are analyzed for about 20 constituents including: algal count, chlorophyll-a, secchi depth, suspended solids, TDS, alkalinity, nitrate, ammonia, phosphate, total phosphorus, organic carbon, BOD, DO, *E.coli* and total plate counts. Temperature and dissolved oxygen depth profiles are measured at 2 metre intervals at each of the five sampling points in the reservoir (UW, 1993). The side streams are sampled at the points shown in Figure 3.2.1. The Mgeni River is the main inflow to Inanda Dam, and water samples are collected at Point 26.1 (Figure 3.2.1).

Water quality of Inanda Dam Analysis of the measured water quality data for Inanda Dam shows:

- Stratification occurs each summer, beginning around September.
- Maximum stratification is attained at the end of December, with a temperature gradient of about 10 to 12°C between the surface and bottom layers. Limited vertical mixing is evident during stratification, except during discrete storm inflows which cause a temporary (and localised) disruption of the vertical temperature profile.
- The thermocline occurs at a depth of between 10 and 14 metre, with a temperature differential (of the thermocline) of around 5°C.
- During stratification, an oxycline develops at a depth of around 6 to 12 metre and the hypolimnion becomes anaerobic. Therefore, at full supply level, in excess of 44 percent of the storage volume may become anaerobic.
- Under anaerobic conditions, the reservoir sediments release both metals (iron and manganese) and ammonia.
- In the surface layer during the summer, algal growth is pronounced with dominance of the blue-green alga *Microcystis spp.* (UW, 1990; UW, 1993).
- During the summer, super-saturation of dissolved oxygen occurs in the epilimnion associated with algal growth (UW, 1992a and 1993).
- Isothermal conditions occur from May, with rapid cooling of the surface layers bringing about vertical mixing and over-turn.
- During isothermal periods, oxygenated water is mixed into the lower layers. However, the high sediment oxygen demand results in a vertical gradient between the surface and bottom waters (UW, 1993; Görgens *et al.*, 1993).



Location map of Inanda Dam with water quality monitoring points.

Figure 3.2.1

- During periods of high water inflow, oxygenated river water penetrates into the hypolimnion and metalimnion of the reservoir. Similar observations have been made in reservoirs located in the US, and are termed *metalimnetic oxygenation minima* (Cole & Hannan, 1993; Cole, 1993 and 1994).
- As a result of the reservoir being some 18 km long at full supply level, considerable longitudinal gradients are evident in the concentration of various constituents. In response, the algal growth is greatest near the inflow of the Mgeni River (being the major source of nutrients) (Hudson *et al.*, 1993).
- Water quality problems have manifested themselves with taste and odour problems, suspended sediment, dissolved metals, nutrients and algae (Hudson *et al.*, 1993).

Water quality management and study objectives To manage the water quality of Inanda Dam, two approaches are possible. Firstly, the control of contaminant sources derived from the upstream catchment, and secondly the *in-situ* management of the reservoir.

Since reducing the contaminant load from the upstream catchment is comparatively complex and difficult to achieve in the short term (UW, 1992a), various *in-situ* methods have been considered to obtain a short term improvement in water quality. Possible methods include: chemical dosing to kill algae, active management of the reservoir, flushing the dam after the first flood, selective abstraction depth to avoid water of poor quality, and scouring anaerobic bottom water and destratification (UW, 1992a; UW, 1992b). Chapter 2 describes the use of the model *DYRESM* to examine destratification options for Inanda Dam. This section describes the configuration, calibration and application of *CE-QUAL-W2* to provide information on:

- **Optimum abstraction (drawoff) depth** to avoid algae in the surface layers, and/or nutrient/metal-laden water in the middle and lower layers.
- The influence of **reservoir draw-down** on the stratification and water quality response of the reservoir. Future operating conditions may result in the reservoir being kept at a reduced water storage level.
- Influence of **reservoir sediments** on the quality of the epilimnion and hypolimnion.
- Influence of reducing the **phosphorus loading** entering the reservoir, and response of the algal biomass at the dam wall basin.
- Role of **hydrodynamic mixing and density currents** during periods of high runoff on the

water quality response of the reservoir.

- Influence of **hypolimnetic releases** and scours on the water quality in the dam wall basin.

The water quality variables of interest investigated as part of this simulation include: water temperature, dissolved oxygen, algal biomass, suspended solids, phosphorus, nitrogen, and iron.

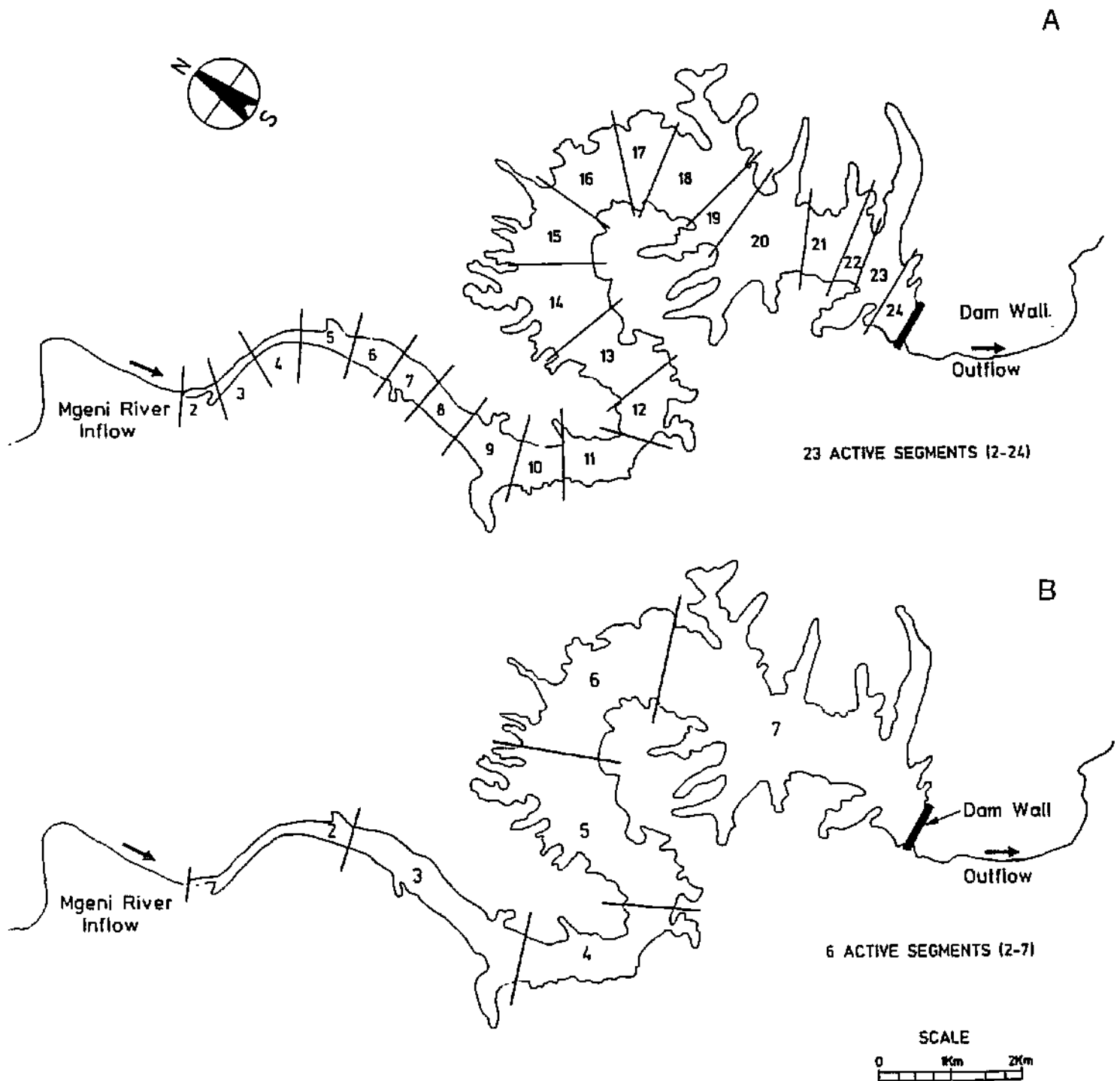
3.2.2 MODEL CONFIGURATION

Görgens *et al.* (1993) reported a model configuration for Inanda Dam with over 400 active cells which had a run-time exceeding 200 minutes (for a simulation period of 360 days). Simulations undertaken to calibrate the model were found to become excessively long. One of the objectives was to reduce the run-time and yet maintain the predictive capabilities of the model. In this regard, two model configurations were tested: (1) a configuration using 23 segments and 25 layers, and (2) a configuration using 6 segments and 13 layers, see Figure 3.2.2.

The following data sources were used in the physical configuration of the model: (1) topographic maps (scales 1:10 000 and 1:50 000), (2) hydrographic survey data (DWAF, 1990), and (3) volume/area elevation tables (DWAF, 1990).

23 Segment configuration The physical layout of the reservoir was modelled using a single branch (Segments 2 to 23), with 25 layers (2 metre deep), with two outflows, one withdrawal, and no tributary inflows to the reservoir. Figure 3.2.2 (Inset A) shows the reservoir divided longitudinally into 23 segments. Where possible, the segment boundaries coincided with the profile cross-sections used in the hydrographic survey. At each of the 23 segments, the reservoir widths were calculated at 2 metre increments from the bottom to full supply level. The length and orientation of each of the 23 segments was determined. The bathymetric data were then collated into a single spread sheet for each of the 23 segments. To verify the bathymetric data, the storage volume of the reservoir was calculated and compared with hydrographic survey data. A close agreement was found between the bathymetric (computed) data and the hydrographic survey (measured) data.

6 Segment configuration The physical layout of the reservoir was modelled using a single branch (Segments 2 to 7), with 13 layers (4 metre deep), with two outflows, one withdrawal, and no tributary inflows to the reservoir. The bathymetric data compiled above was used to determine the storage depth relationship for the 6 segment configuration. Figure 3.2.2 (Inset B) shows the configuration using six segments.



Inset A: 23 segment configuration. Note: Segments 1 and 25 are upstream and downstream boundary segments. Inset B: 6 segment configuration. Note: Segments 1 and 8 are upstream and downstream boundary segments.

Figure 3.2.2

Starting conditions The water quality starting conditions are specified in the control file as well as in the vertical and longitudinal profile files. These data include:

- The starting and ending dates of the simulation period. A simulation period of 365 days was chosen to calibrate the model.
- Reservoir water elevation.
- Initial water temperature and quality data. A longitudinal profile file was used to set the starting conditions in each of the active cells at the start of the simulation (1 January 1990).

In Görgens *et al.* (1993), it was reported that the tributary inflows appear to have a minor influence on the water quality of Inanda compared with the Mgeni River inflow. In this application, the tributary inflows are excluded from the simulation, therefore the main inflow comprises the Mgeni River. For the Mgeni River inflow, the water temperature, mean daily river discharge, and chemical composition are input to the model on a daily basis.

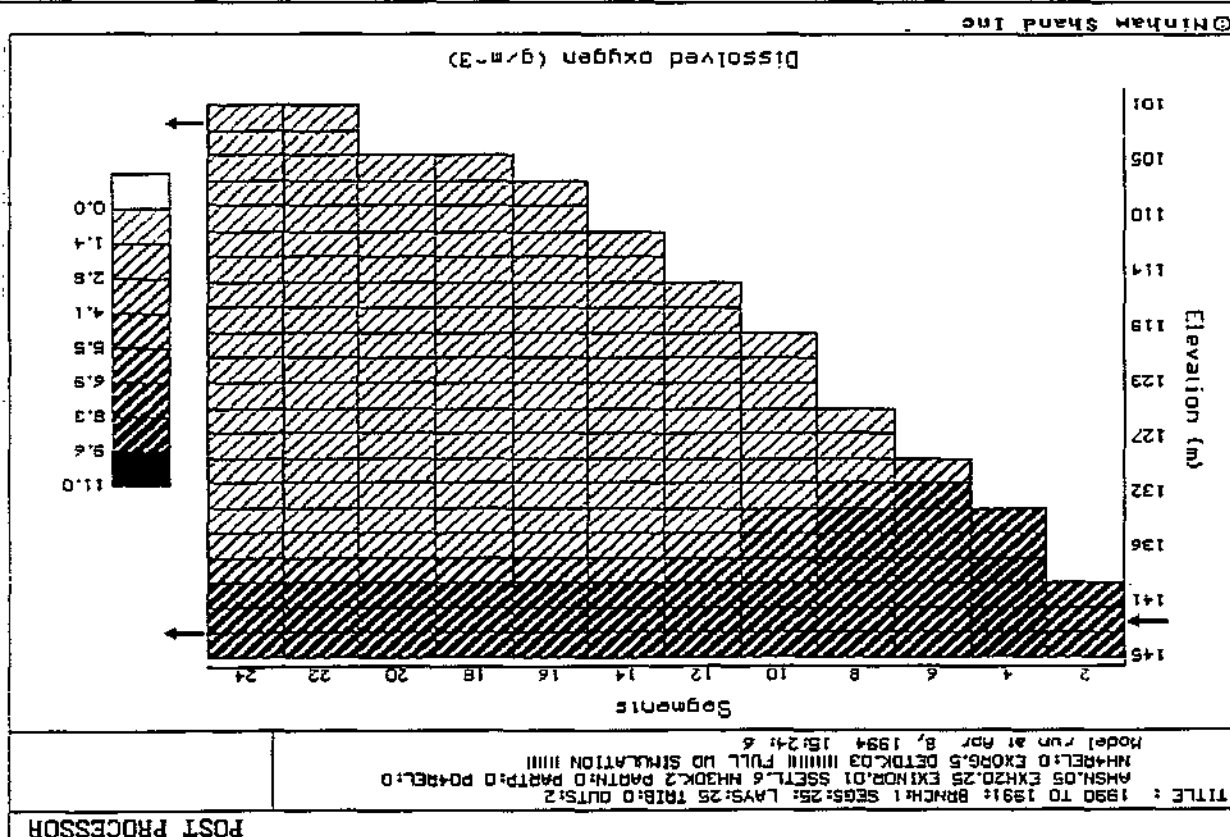
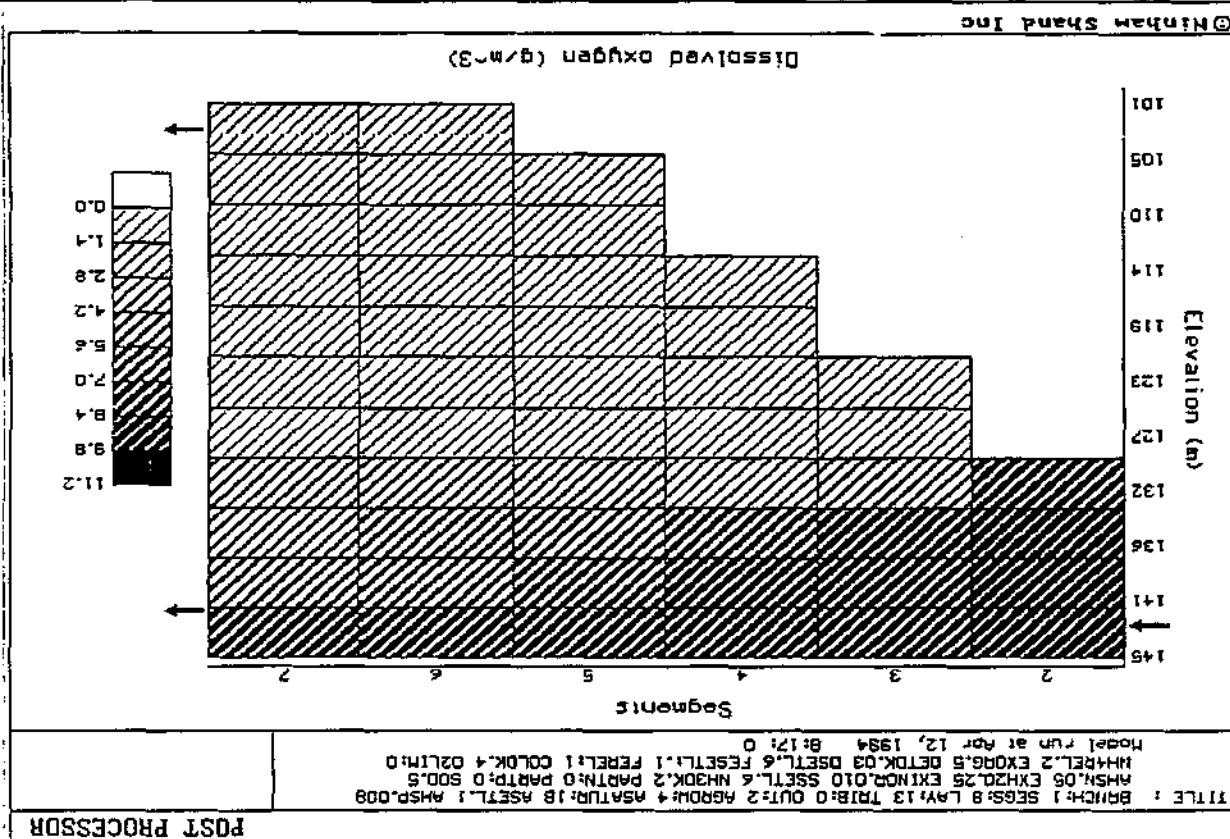
The meteorological input to the model includes: air and dew point temperature, wind speed and direction, and cloud cover. These data were measured at the weather station at Mount Edgecomb, 10 km from Inanda Dam and obtained from the Weather Bureau in digital form.

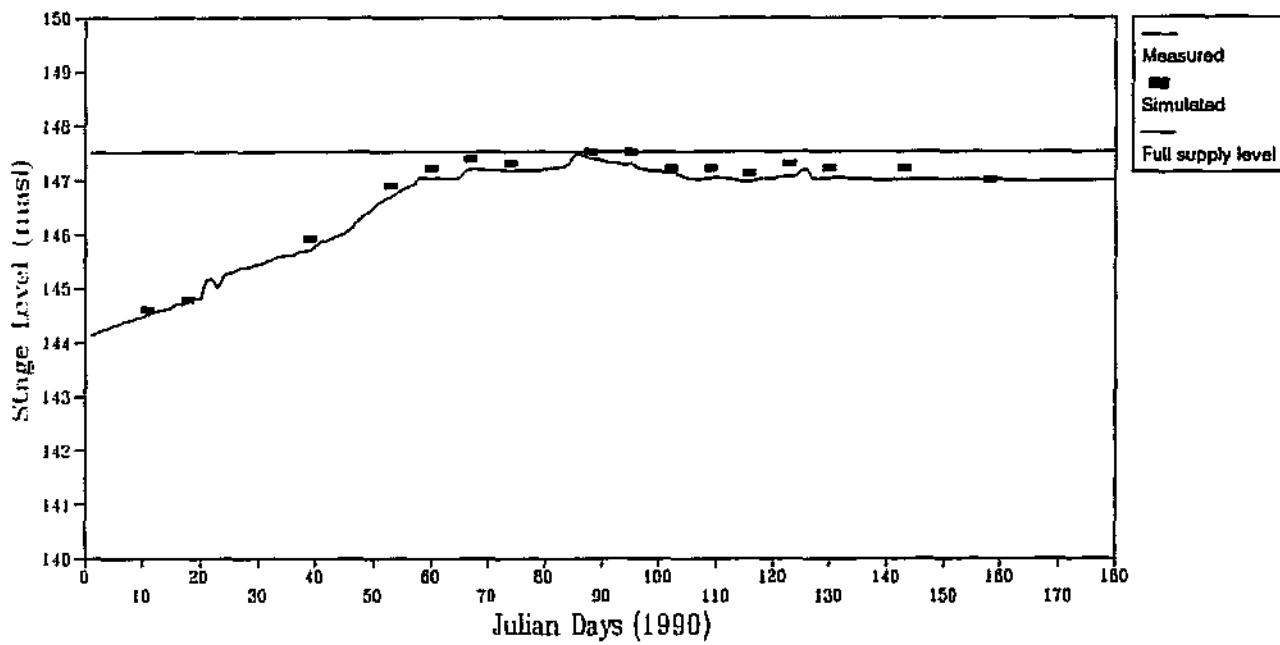
3.2.3 MODEL CALIBRATION

The model uses 60 rate coefficients to simulate the water quality processes taking place within a water body. As a starting point, values of the coefficients were taken from the Inanda Dam simulation described by Görgens *et al.* (1993). The main components of the calibration procedure are described below.

- **Model configuration** Figure 3.2.3 shows the 2-D plots for the 23 and 6 segment configurations. Preliminary calibration runs showed that the 23 segment configuration had a run-time of about 120 minutes to simulate a period of 365 days. In comparison, the 6 segment configuration had a run-time of 35 minutes using the same simulation period. Comparison of the dissolved oxygen and water temperature profile data showed that both configurations of the model provided comparable results. Therefore, based on run-time, the 6 segment configuration was used to calibrate and test the model.
- **Water Budget** The simulation of the water budget is evaluated by comparing the simulated and measured water elevations. During the simulation period, the reservoir started at 83 percent full and within a period of 60 days the reservoir reached maximum operating level. Figure 3.2.4 shows the measured and simulated water surface elevation.

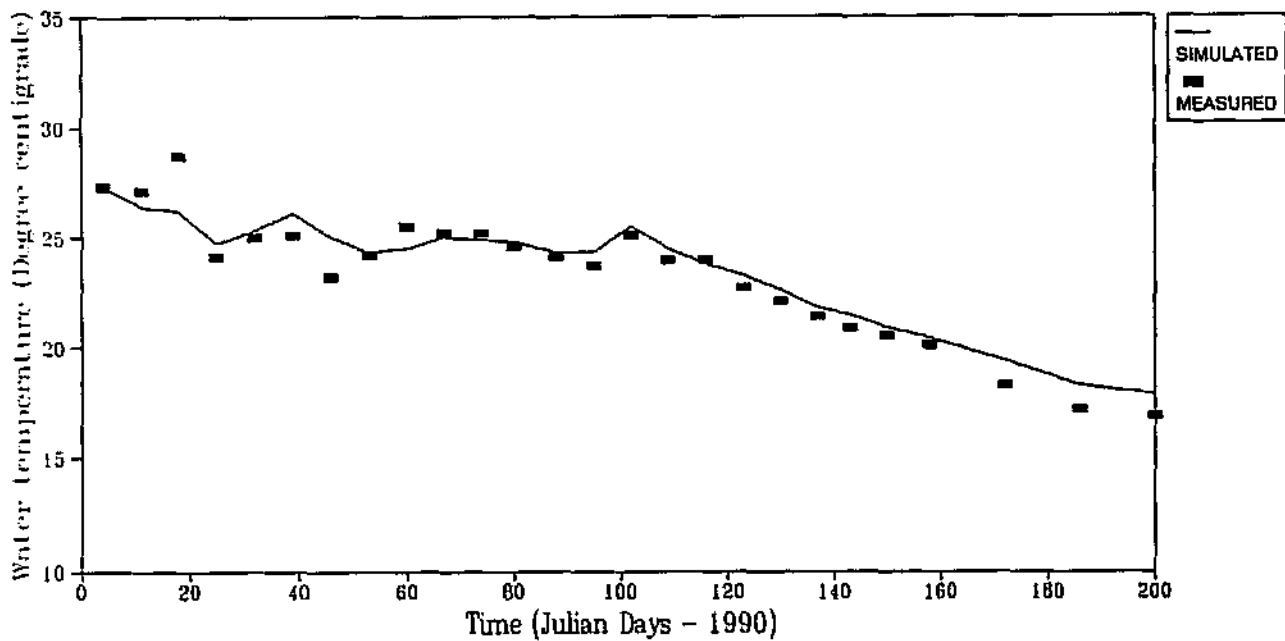
Two dimensional plots for the 23 and 6 segment reservoir configurations. Figure 3.13





Simulated and measured water elevations.

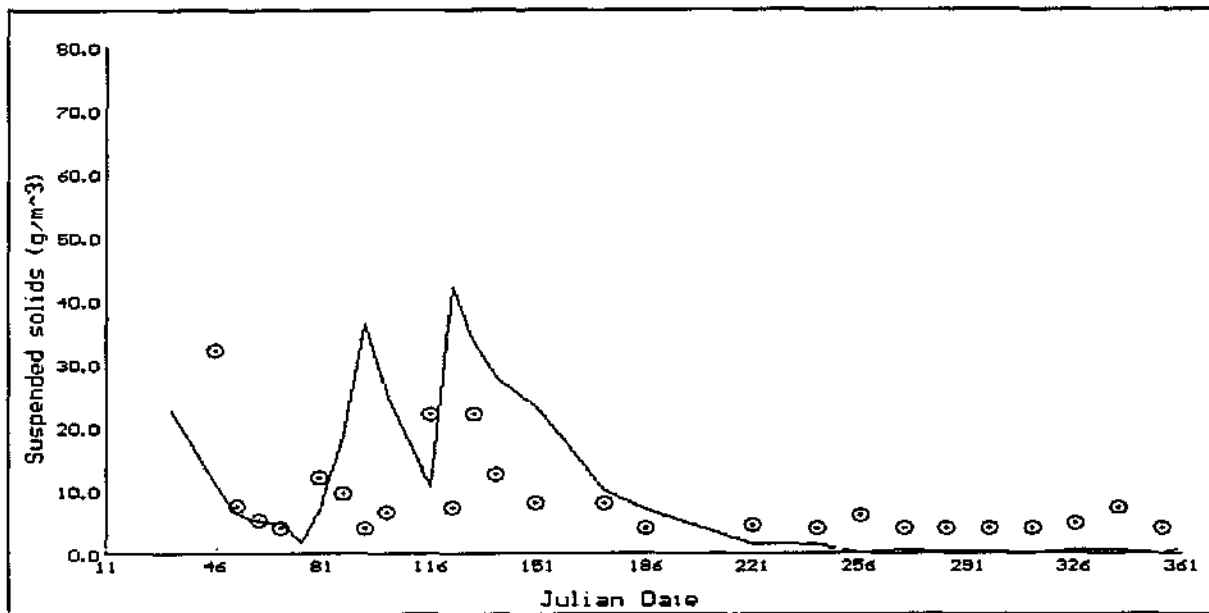
Figure 3.2.4



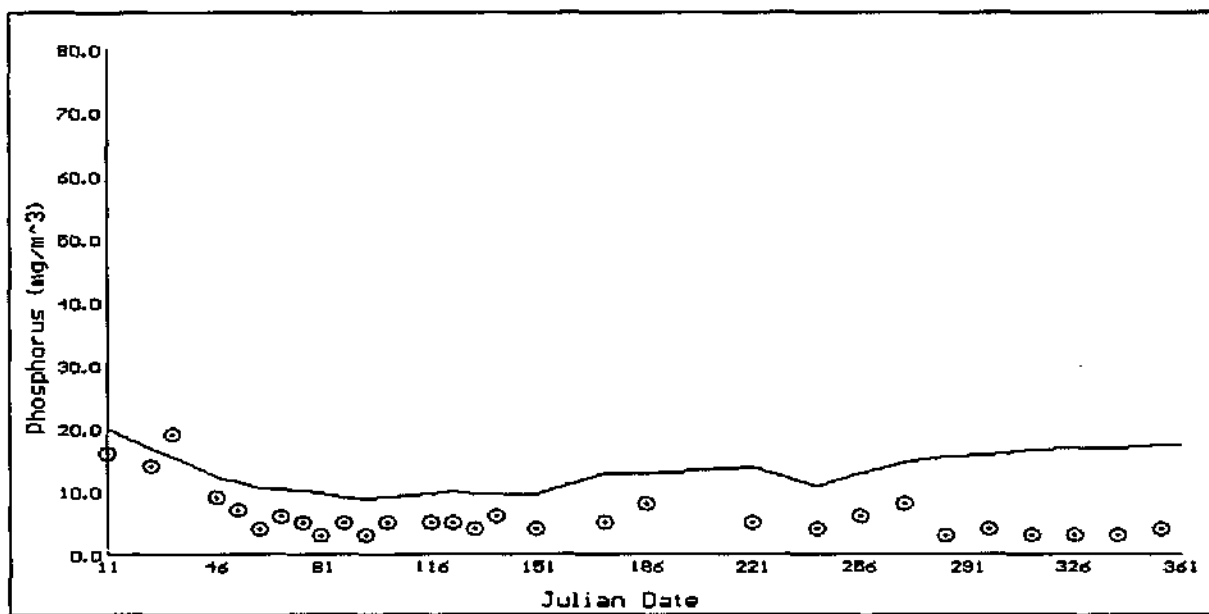
Simulated and measured surface water temperature.

Figure 3.2.5

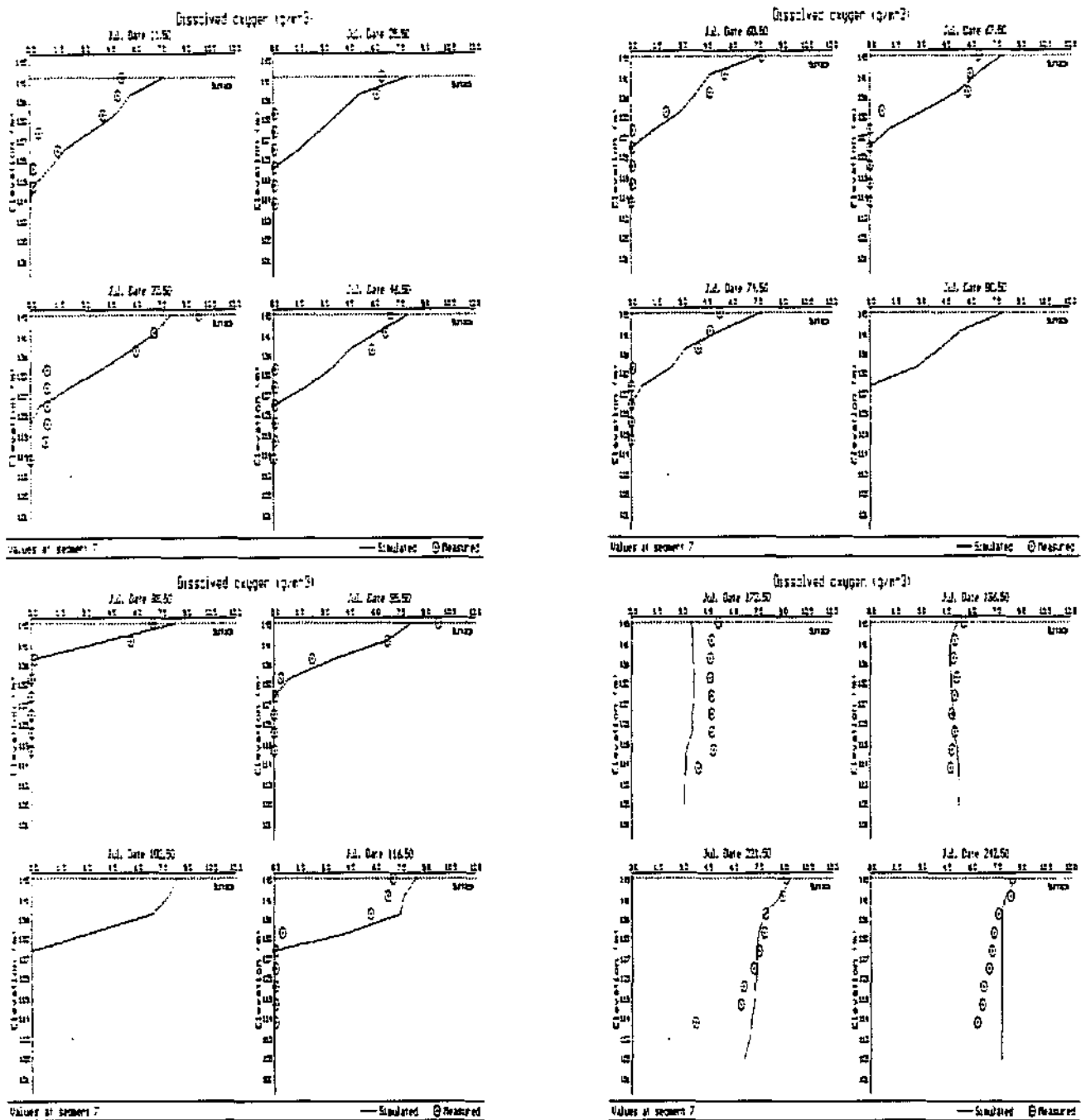
- **Water Temperature** The most acceptable agreement between the measured and simulated water temperature profiles was achieved using a Wind Sheltering Coefficient of 0.9. Figure 3.2.5 shows the simulated and measured surface water temperature data, at the dam wall basin.
- **Suspended solids** The suspended solids settling rate is defined by the term SSETL. Figure 3.2.6 shows the simulated and measured suspended solids data using a settling rate of 0.6 m/day.
- **Hypolimnetic phosphorus** The phosphorus (P) concentration in the hypolimnion is governed by: (1) influx of P from the inflowing river, (2) uptake by algae, (3) release from sediments under anaerobic conditions, and (4) binding of P onto inorganic suspended solids and sedimentation. The partition coefficient for phosphorus, PARTP, accounts for the binding of P onto suspended sediment particles. Repeated simulations showed that although the suspended solids concentration was comparatively high, there was minimal adsorption of P. The term PARTP was therefore given a value of zero. Comparison of the measured and simulated P concentration data showed that the reservoir sediments appear to release minimal quantities of P into the overlying water column during anaerobic periods. Therefore the term PO4REL, accounting for the sediment release of P, was set at a value of zero. Figure 3.2.7 shows the simulated and measured P concentration in the hypolimnion.
- **Dissolved oxygen** The oxygen demand of the reservoir sediments is modelled using the term SOD (sediment oxygen demand). Simulations showed the value of the SOD was 1.1 mgO₂/m²/day, which reflects a high oxygen demand imposed by the sediments. Figure 3.2.8 shows the simulated and measured DO profiles for selected simulation dates, and Figure 3.2.9 shows the 2-D plots for selected days during the simulation period. In the Appendix, Figures 3.2.26 and 3.2.27 show the vertical profile plots and 2-D plots for simulated and measured DO.
- **Surface phosphorus and algal biomass** In the surface waters of the reservoir, the phosphorus concentration is influenced by adsorption onto suspended particles and uptake by algae. As *Microcystis* is the dominant algal genus during the simulation period, the algal growth rate coefficients were taken from literature values (Görgens *et al.*, 1993). Model runs were performed to obtain a satisfactory simulation of the phosphorus and algal biomass in the upper layers of the reservoir. Figure 3.2.10 shows the simulated and measured phosphate concentration, and Figure 3.2.11 shows the simulated and measured algal biomass at the dam wall basin. The second peak in the algal biomass during the



Simulated and measured suspended solids concentration (Note: Simulated data presented as a line and measured data as symbols).
Figure 3.2.6



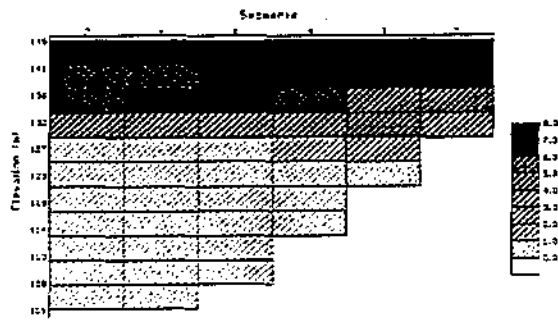
Simulated and measured hypolimnion phosphorus concentration (Note: Simulated data shown as a line and measured data as symbols).
Figure 3.2.7



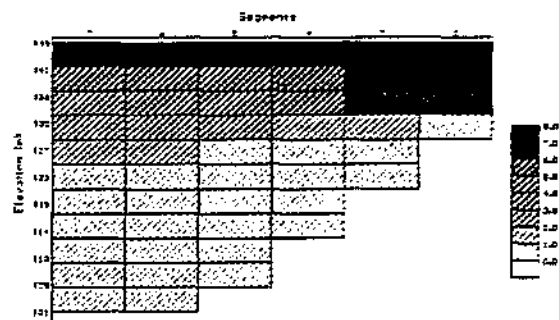
Simulated and measured dissolved oxygen profiles for the dam wall basin of Inanda.

Figure 3.2.8

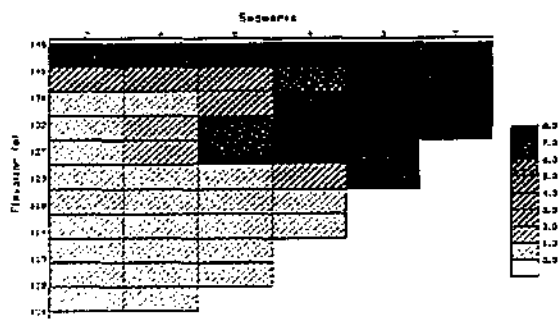
Julian Day 11



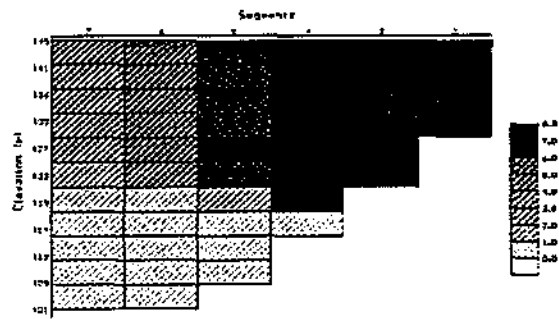
Julian Day 46



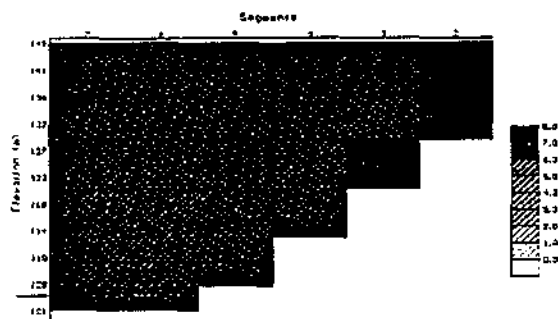
Julian Day 80



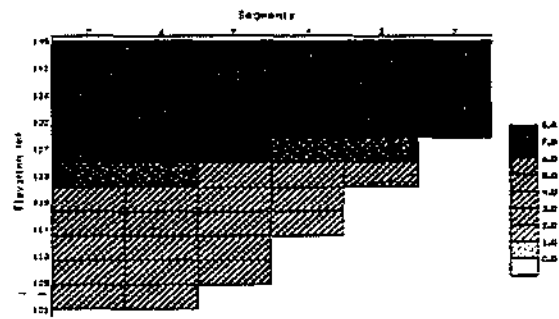
Julian Day 150



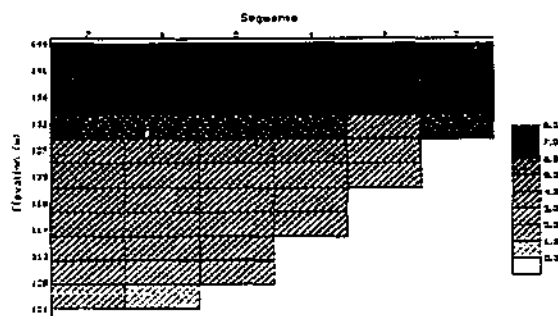
Julian Day 172



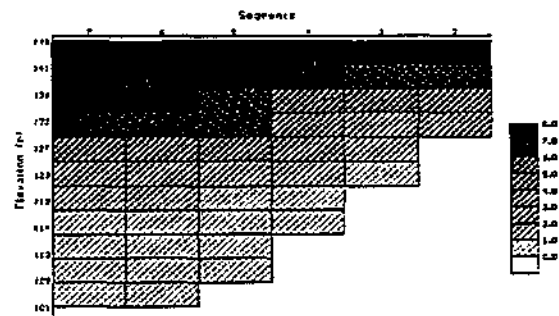
Julian Day 270

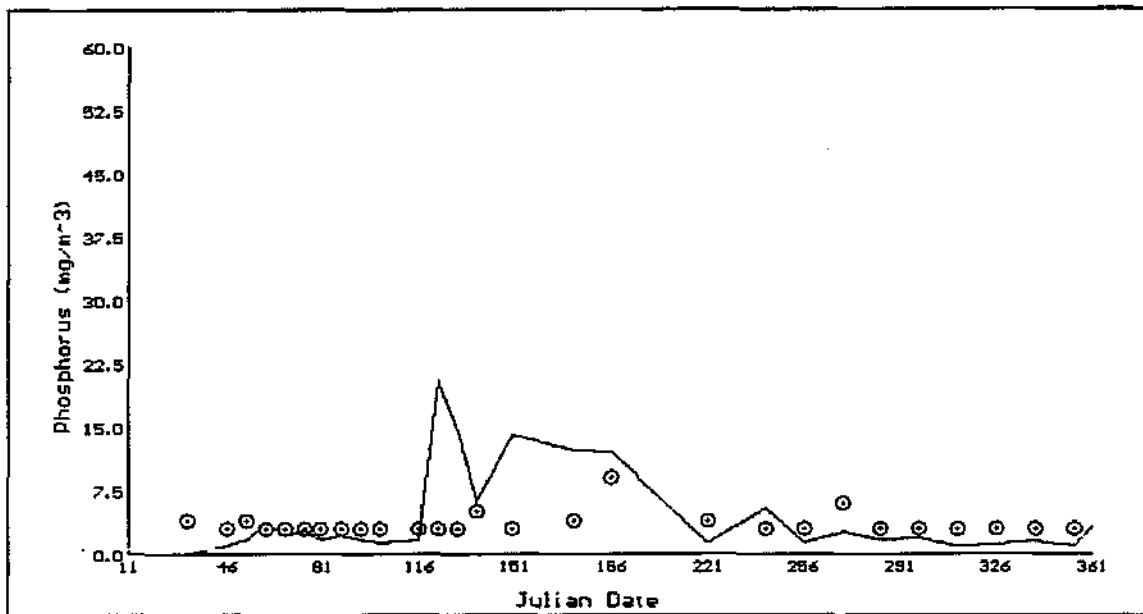


Julian Day 298

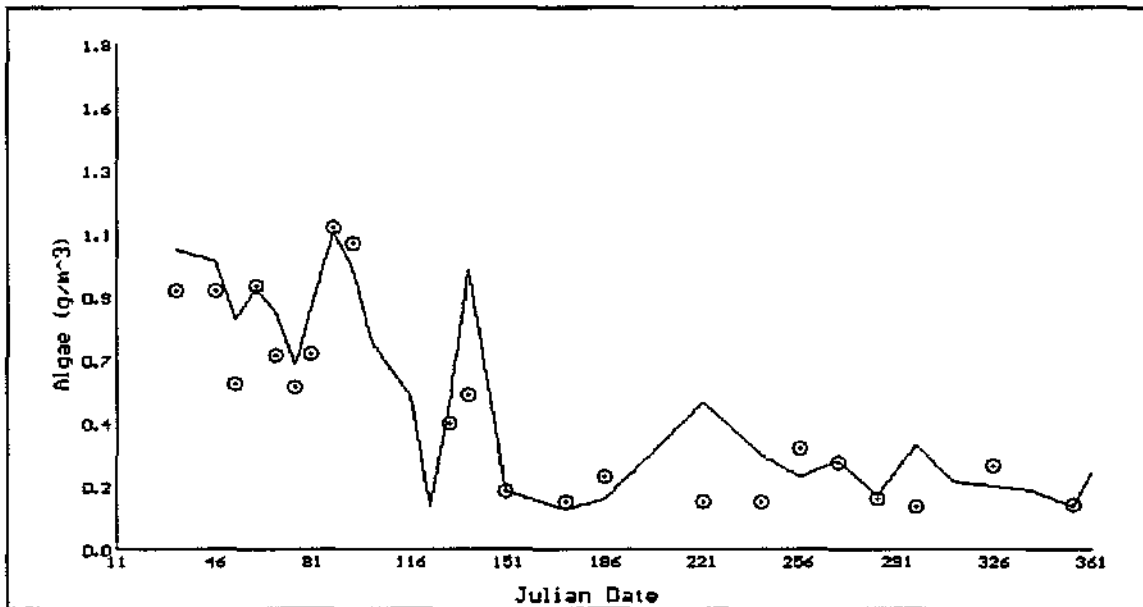


Julian Day 340





Simulated and measured surface phosphorus concentration (Note: Simulated data are shown as a line and measured data as a symbol). Figure 3.2.10



Simulated and measured algal biomass. (Note: Simulated data shown as a line and measured data as a symbol). Figure 3.2.11

middle of the calibration period (day 80 to 120) was caused by an increase in the phosphorus concentration caused by the influx of river inflow into the metalimnion of the reservoir. At the dam wall basin, phosphorus is introduced into the epilimnion by upward mixing from the metalimnion. The model simulations show that the algal growth is limited by the availability of phosphorus and light, as well as by water temperature during the winter months.

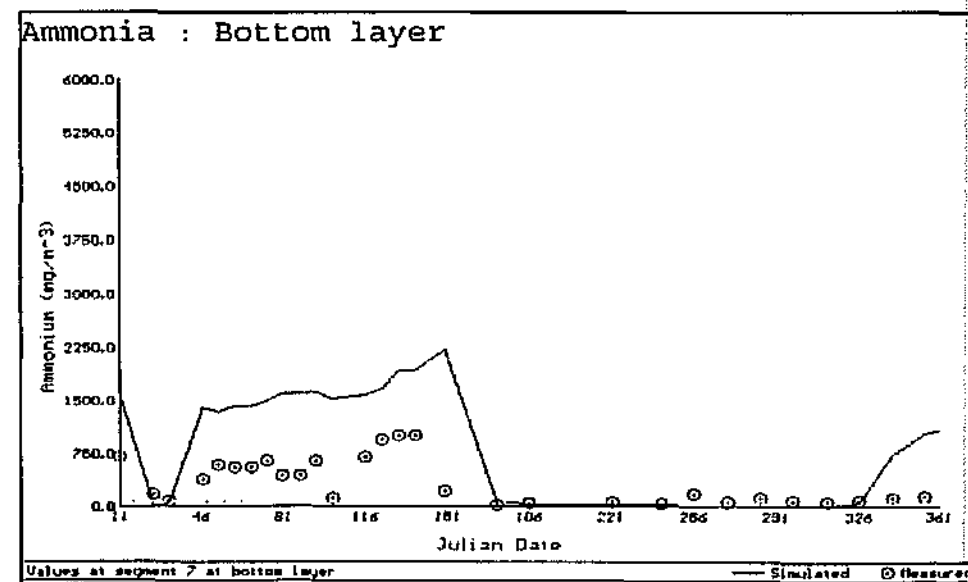
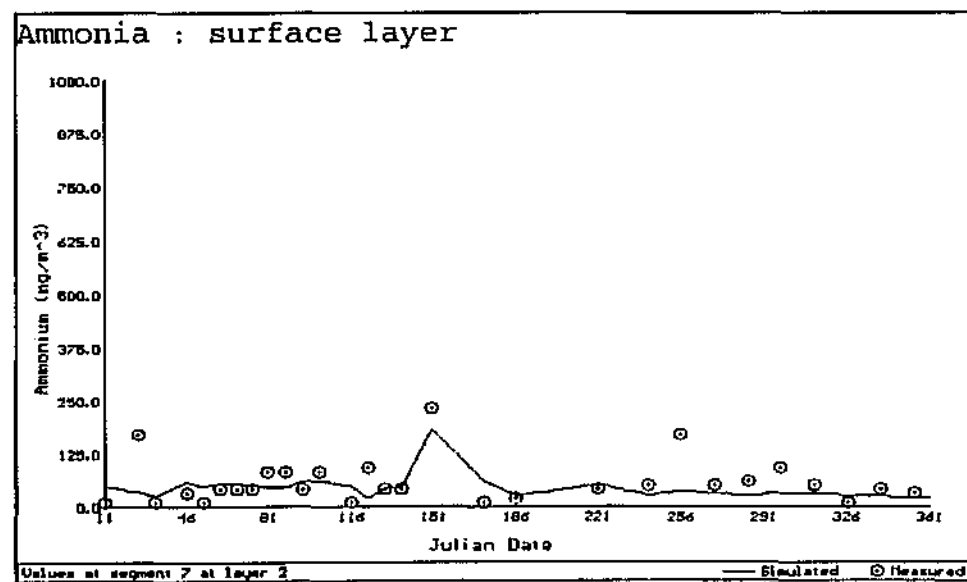
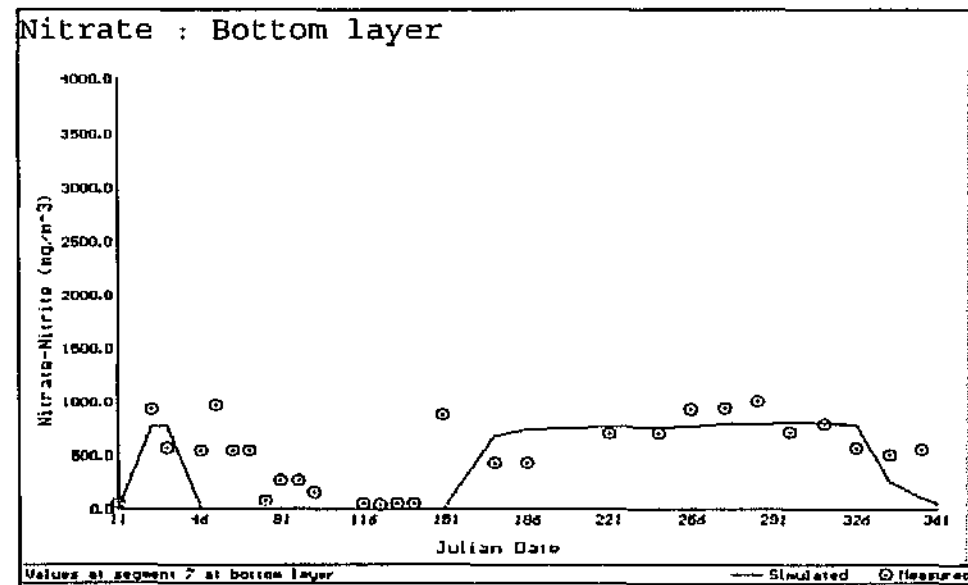
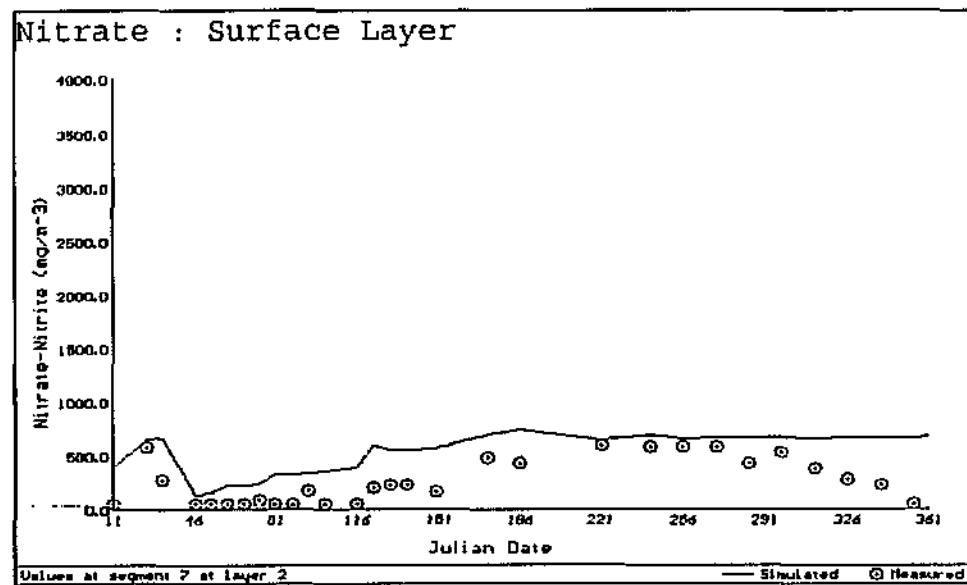
- **Nitrogen** Figure 3.2.12 shows the simulated and measured ammonia and nitrate concentrations. The simulation used literature values for the rate coefficients. The release of ammonia from the reservoir sediments was found to be 0.1 mg/m²/day.
- **Iron** Preliminary calibration was achieved to simulate the iron concentration in the hypolimnion. The release of iron from the reservoir sediments was simulated using the term FEREL, which was found to have a value of 1 mg/m²/day after calibration. Figure 3.2.13 shows the depth/time distribution of iron in the dam wall basin.

3.2.4 MODEL APPLICATION AND SCENARIO EVALUATION

Optimum abstraction depth A multi-level offtake structure has been incorporated in the design of the dam wall with nine outlets at depth intervals of 3 metre from full supply level. The existing sampling of Inanda Dam includes a surface, depth integrated and bottom sample. Therefore there is sufficient information to determine the depth of drawoff to avoid water of poor quality in the surface, middle or bottom layers (UW, 1993).

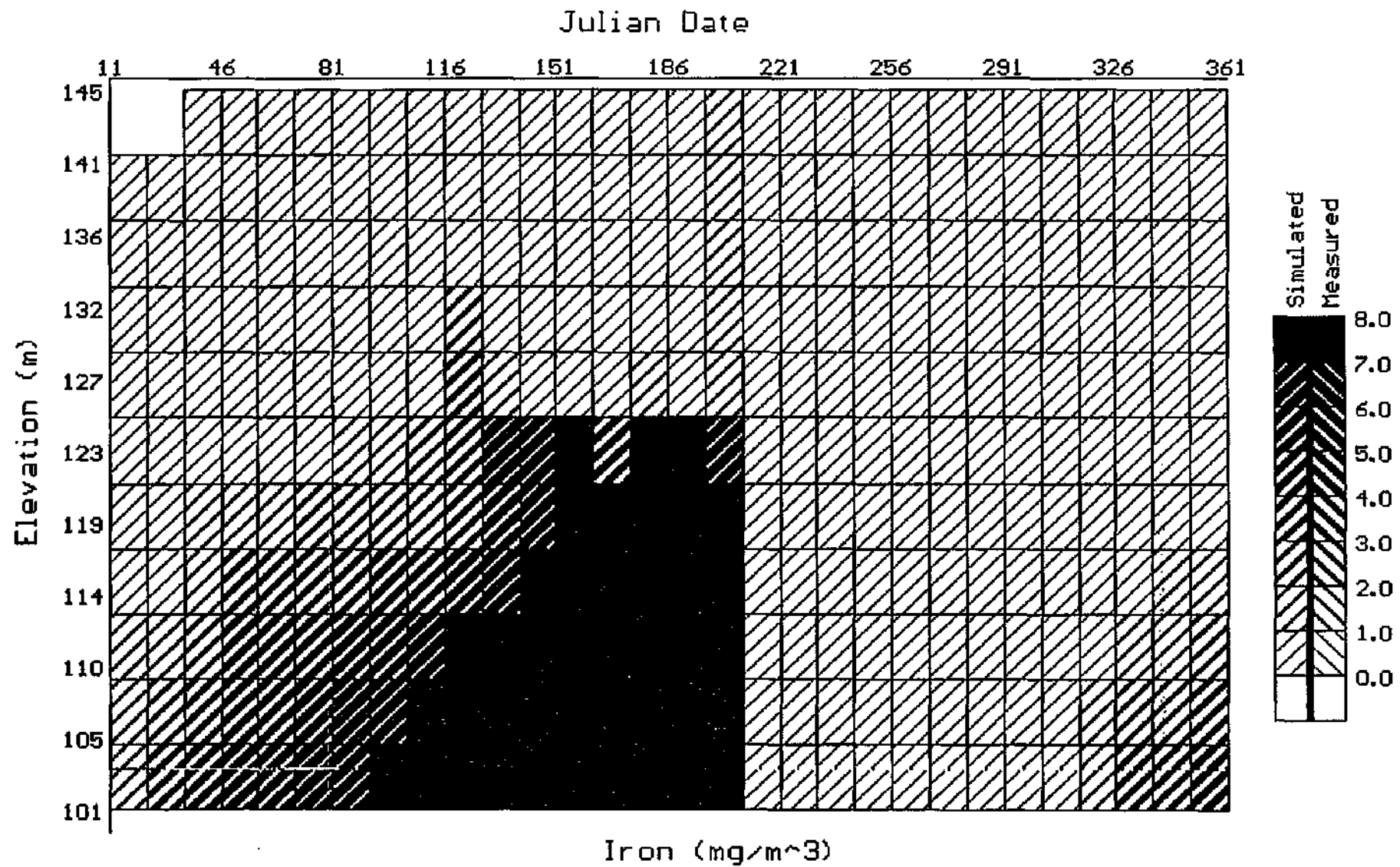
Graphical output from the model is used to select the optimum depth of drawoff so that the water contains (1) a minimum concentration of algae and (2) maximum concentration of oxygen thereby avoiding the anaerobic bottom waters containing elevated concentrations of metals and nutrients.

Depth-time (isopleth) plots were produced for algae, ammonia, and dissolved oxygen, see Figures 3.2.14 to 3.2.16. By superimposing the isopleth plots, an estimate was made of the drawoff level. To avoid the algae in the upper layers, the optimum drawoff was found to be at least 8 metre from the surface. To avoid the anaerobic waters containing elevated concentrations of ammonia, metals and dissolved organic substances, the drawoff had to be less than 18 metre from the water surface. Wind induced currents however influence the vertical position of the oxycline, see Figure 3.2.9. Under such conditions, the deepest drawoff level should be about 14 metre from the surface to account for the variability in vertical elevation in the oxycline. During the winter (mixed period), the abstraction depth is of less concern because of the mixing throughout the vertical profile of the water column.



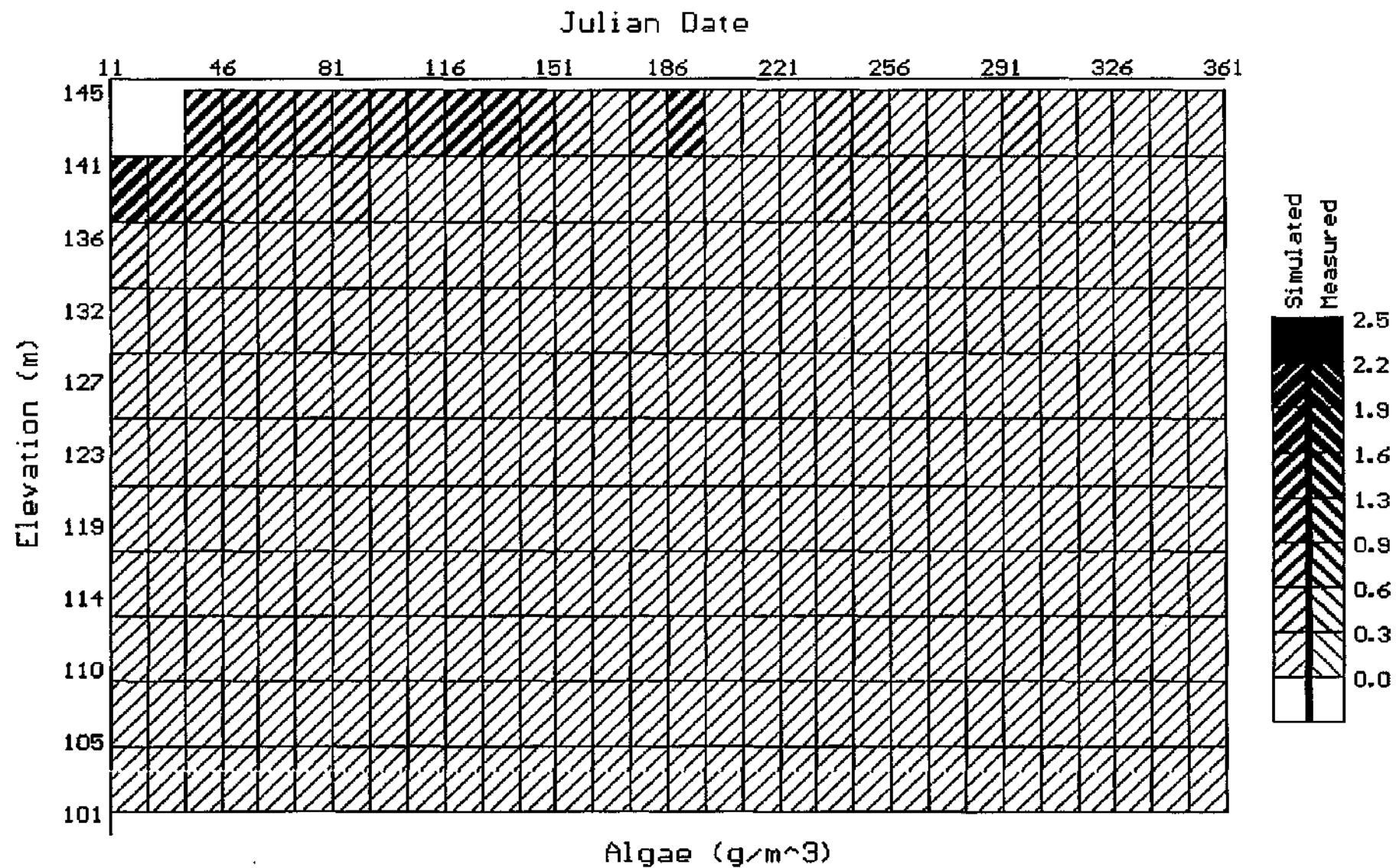
Simulated and measured ammonia and nitrate concentration in the surface layer and hypolimnion.

Figure 3.2.12



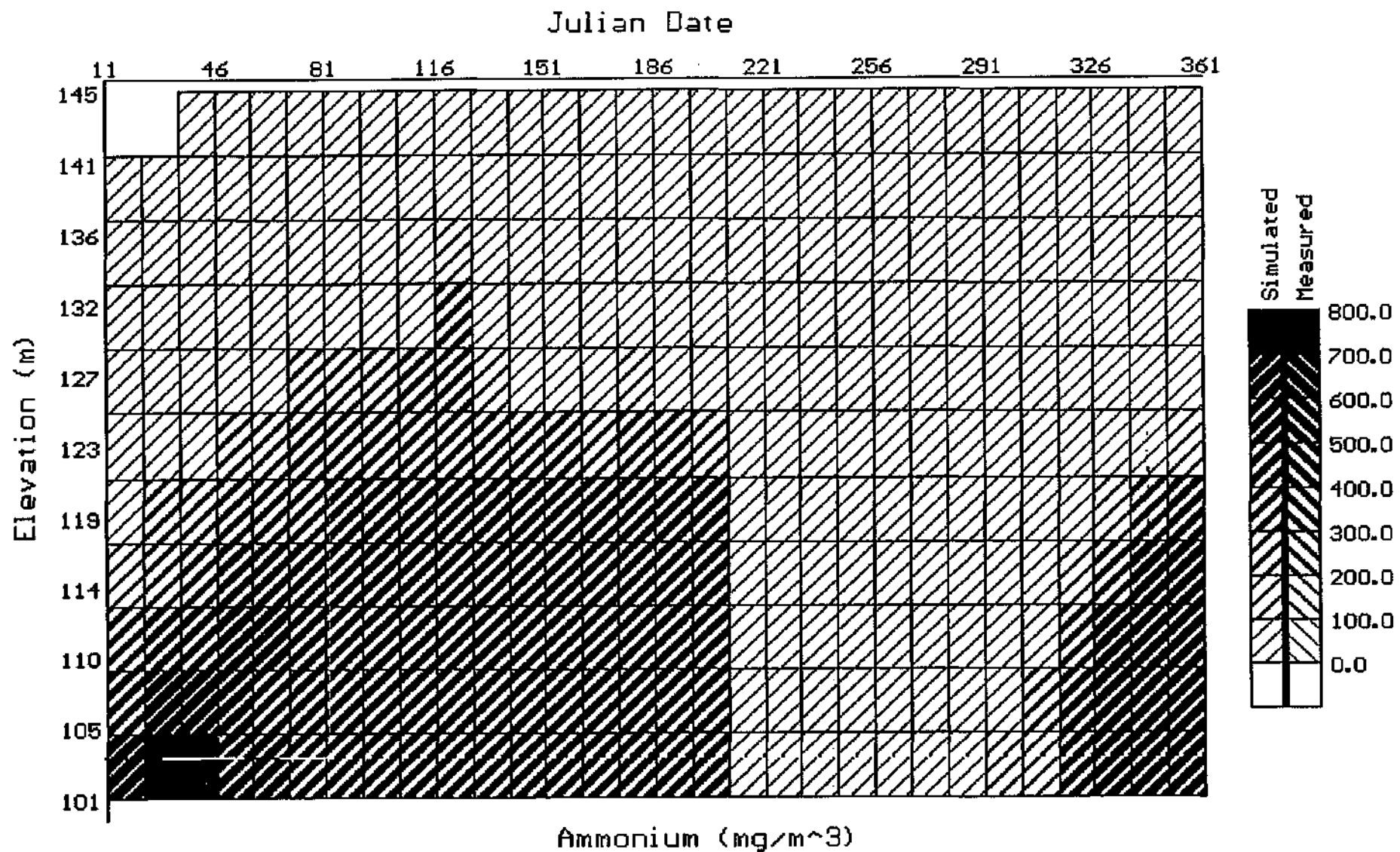
Isopleth (depth vs time) plot: Iron concentration at the dam wall.

Figure 3.2.13

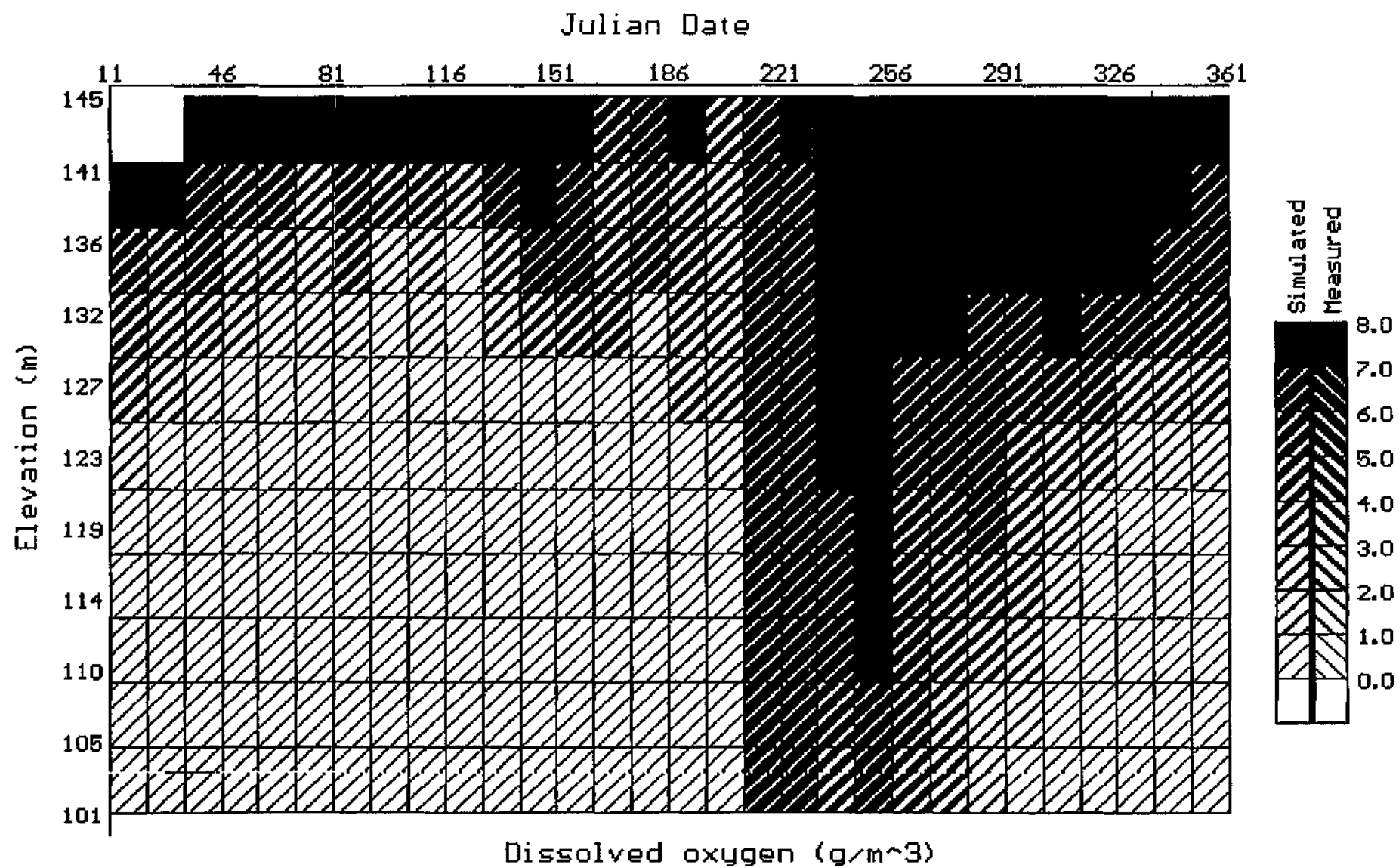


Isopleth (depth vs time) plot: Algal biomass at the dam wall

Figure 3.2.14



Isopleth (depth vs time) plot: Ammonia concentration at the dam wall Figure 3.2.15



Isopleth (depth vs time) plot: dissolved oxygen at dam wall

Figure 3.2.16

Role of reservoir sediments During the calibration of the model, it was observed that the reservoir sediments exerted a high demand for oxygen which caused the development of an extensive anaerobic hypolimnion. During anaerobic conditions, the sediments released iron and ammonia into the hypolimnion. For the period January to December 1990, minimal phosphorus was seen to be released from the sediments and the primary input of P into the reservoir was from the Mgeni River.

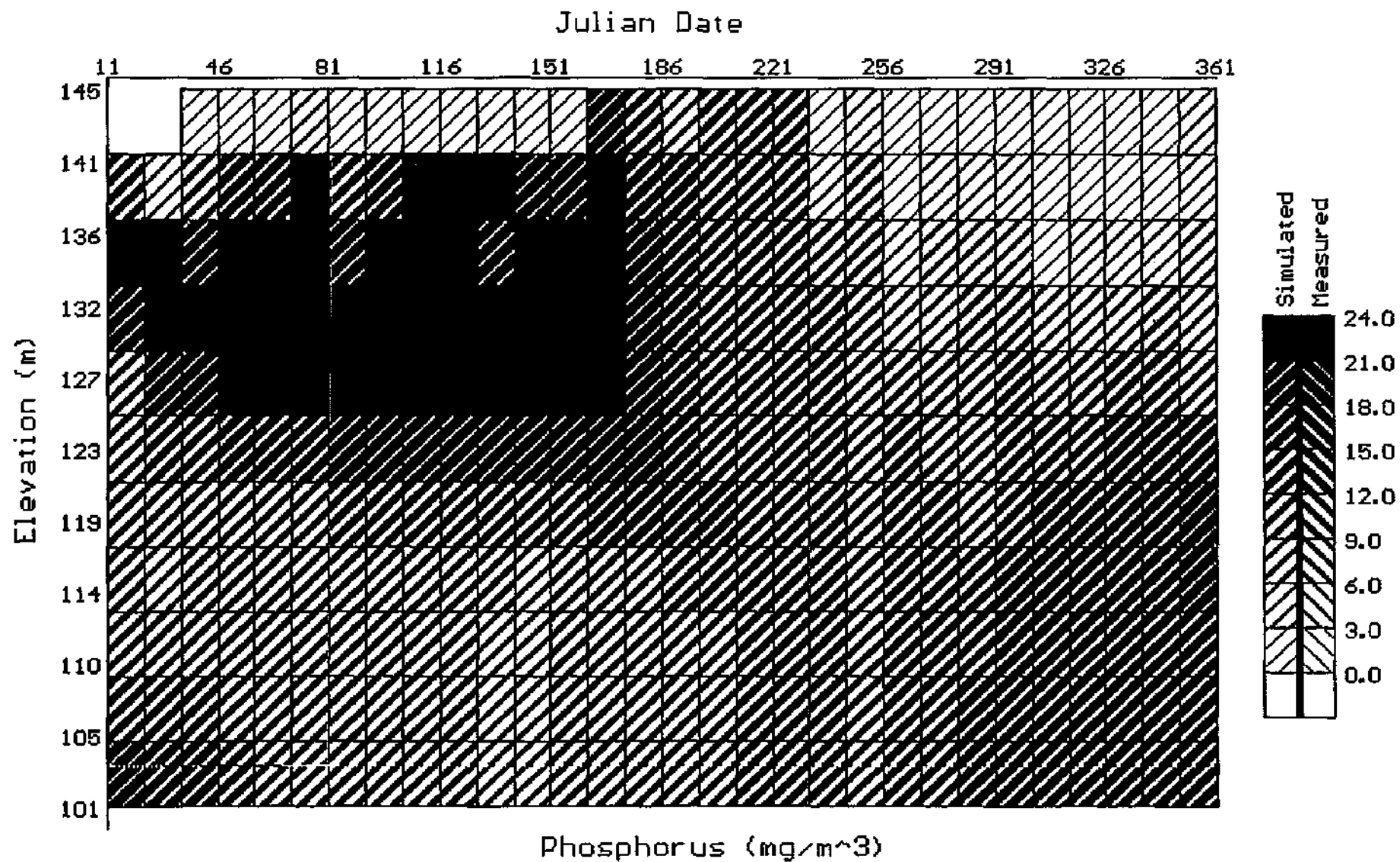
Hudson *et al.* (1993) report that Inanda Dam behaves as a "sink" for phosphorus. Phosphorus is seen to either undergo adsorption onto suspended matter and sedimentation onto the bottom sediments, or uptake by algae. Under the current conditions, the reservoir sediments are accumulating phosphorus and release minimal quantities of P back into the water column. Under suitable (reducing) conditions however it is possible for the P to be released back into the overlying water column.

Silberbauer (1981) investigated the release of phosphorus from the bottom sediments of Roodeplaat, Hartbeespoort and Bloemhof Dams using laboratory based analytical methods. Phosphorus sediment release rates ranged from 1 to 6 mg P/m²/day for the dam wall basins of Roodeplaat and Hartbeespoort Dams. Similar information on the sediment P release characteristics of Inanda Dam were not available. Therefore, a trial simulation was performed to determine the general response of increased P release from the sediments on the algal biomass. A comparatively low sediment phosphate release rate of 0.05 mg/m²/day was used in the simulation.

Figure 3.2.17 shows the P isopleth plot with no release from the sediments, and Figure 3.2.18 shows the influence of sediment release of P. During the first part of the simulation period, the P released from the sediments had a minor influence on the surface layers because of the limited vertical mixing of P into the epilimnion during stratification. At the onset of overturn, the algal biomass increased (by two-fold) in response to the abundant supply of phosphorus from the deeper layers.

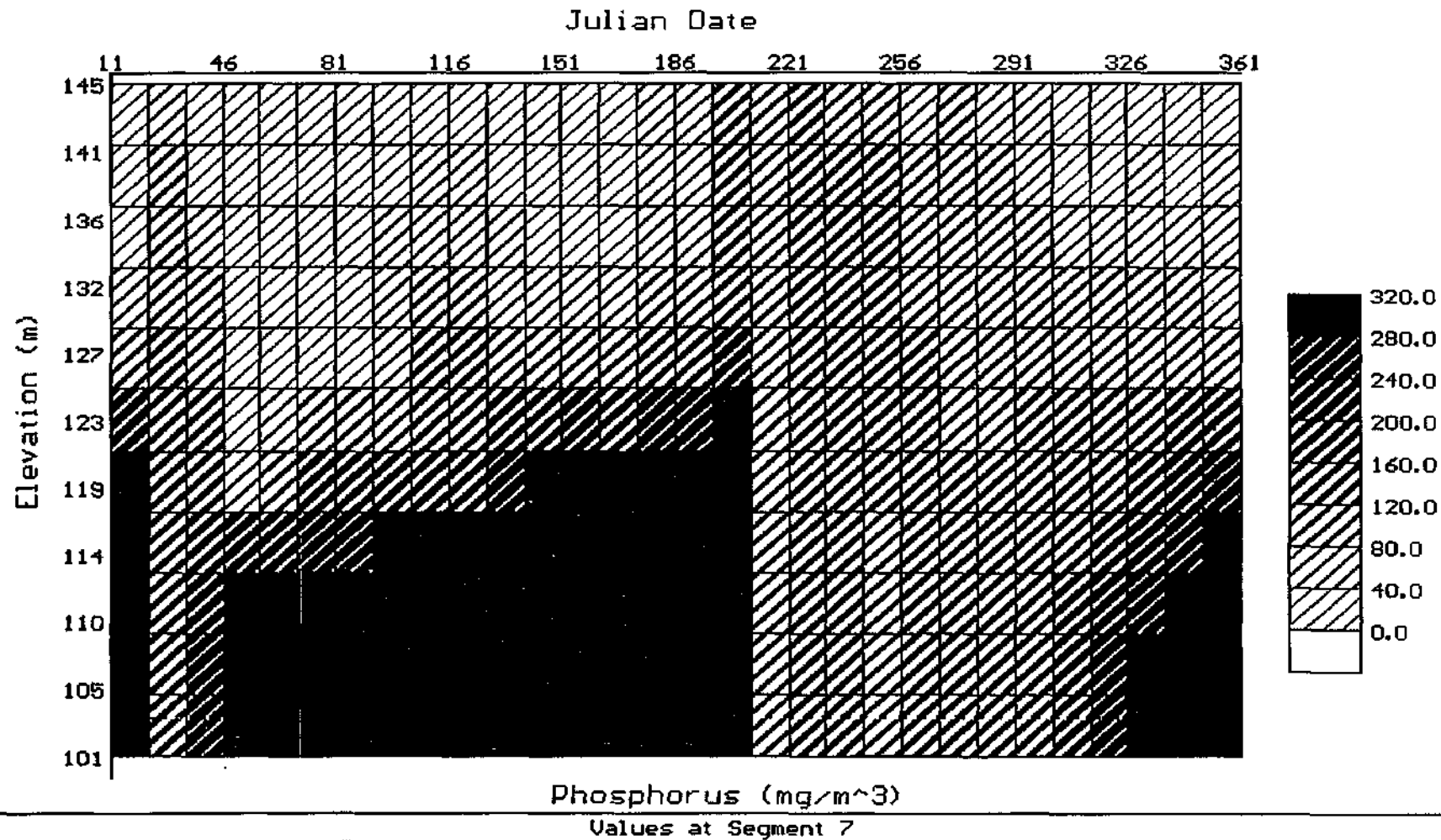
The simulation results show:

- The release of P from the sediments brings about a noticeable accumulation of P in the hypolimnion during periods of stratification, see Figure 3.2.18, which does not have a direct influence on the epilimnion concentrations except during overturn.
- The P budget of Inanda Dam is governed by the input from the Mgeni River.



Isopleth (depth vs time) plot: phosphorus concentration at the dam wall. Figure 3.2.17

TITLE : BRNCH:1 SEGS:8 LAY:13 TRIB:0 OUT:2 AGROW:4 ASATUR:18 ASETL.1 AHSP.008
 AHSN.05 EXH20.25 EXINOR.01 SSETL.6 NH3DK.2 PARTN:0 PARTP.0 SOD1.1 CHZ60
 NH4REL.1 EXORG.5 DETDK.03 DSETL.6 FESETL.1 FEREL:1 COLDK.4 P04REL=.05
 Model run at Oct 12, 1994 15:33:22



Isopleth (depth vs time) plots: phosphorus concentration with sediment release
 of 0.05 mg/m²/day.

Figure 3.2.18

- A considerable increase in algal growth will occur if P is released from sediments. Under such conditions, hypolimnetic aeration may play an important role in controlling the release of P (and other constituents) from the sediments. At present, the simulation shows that hypolimnetic aeration may have minimal influence on the overall nutrient regime of Inanda.
- Routine monitoring of P in the hypolimnion should be implemented to detect changes in the sediment release characteristics.

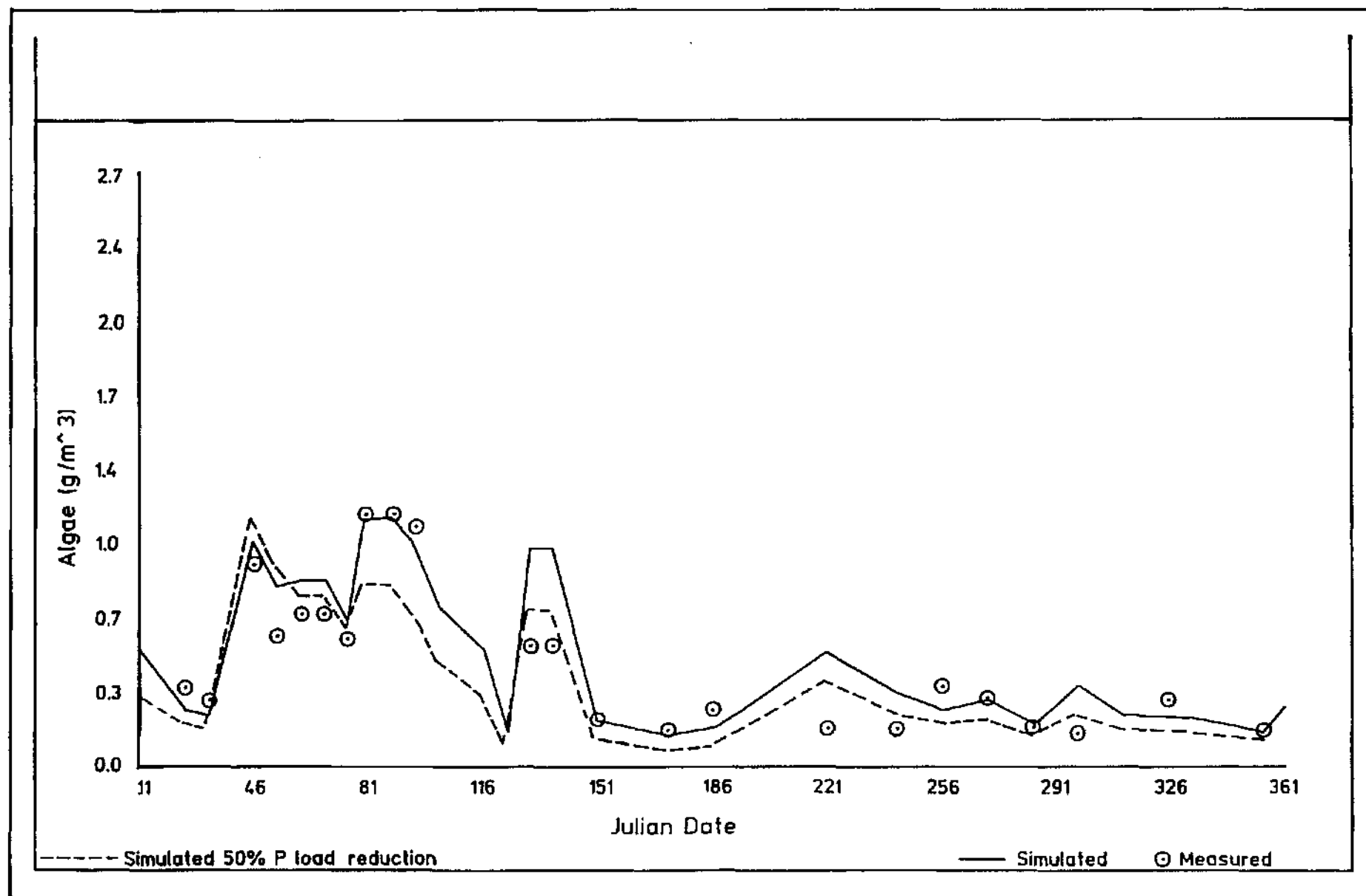
Phosphorus Dynamics As discussed above, the growth of the algal biomass at the dam wall is largely governed by the P load derived from the Mgeni River. However, the simulation results also show that the longitudinal and vertical distribution of P within Inanda is influenced by bio-chemical processes and density mixing characteristics of the inflowing water.

The phosphorus isopleth plot for the dam wall basin (Figure 3.2.17) shows high P concentrations were transported into (1) the hypolimnion during the beginning of the simulation period, and (2) the metalimnion during the latter part of the summer period (Julian Day 46 to 150). In response to the vertical gradients in P concentration, the algal biomass shows the highest growth during the latter part of the summer period when the inflows penetrate into the metalimnion, in closer proximity to the algae.

During periods of low inflow (discharge < 10 cumec), the P in the Mgeni River water undergoes rapid sedimentation and uptake by the algal biomass in the upper reaches of Inanda. This was observed during the end of the simulation period, when the low inflow and low delivery of P limited algal growth in the dam wall basin, see Figures 3.2.17 and 3.2.19.

As an example, the model was used to examine the influence of reducing the phosphorus input loading on the algal biomass. A simulation was performed where the P input loading of the Mgeni River was reduced by 50 percent, representing a considerable reduction in the loading rate to Inanda. Figure 3.2.19 shows the influence on the algal biomass at the dam wall basin. The P load reduction brings about (1) a comparatively rapid response by the algae in the dam wall basin, and (2) only a marginal decrease in the overall algal biomass. The largest reduction in algal biomass was simulated during the high inflow periods (Julian day 81 to 90, and 120 to 135).

The model was configured to determine which variables limited algal growth during the simulation period. The model results show that in the metalimnion and hypolimnion, light was the limiting factor. In the surface layer, both phosphorus and light limited algal growth. During the simulation period, nitrogen did not limit algal growth.



Algal biomass at the dam wall basin, with normal and reduced phosphorus loading.

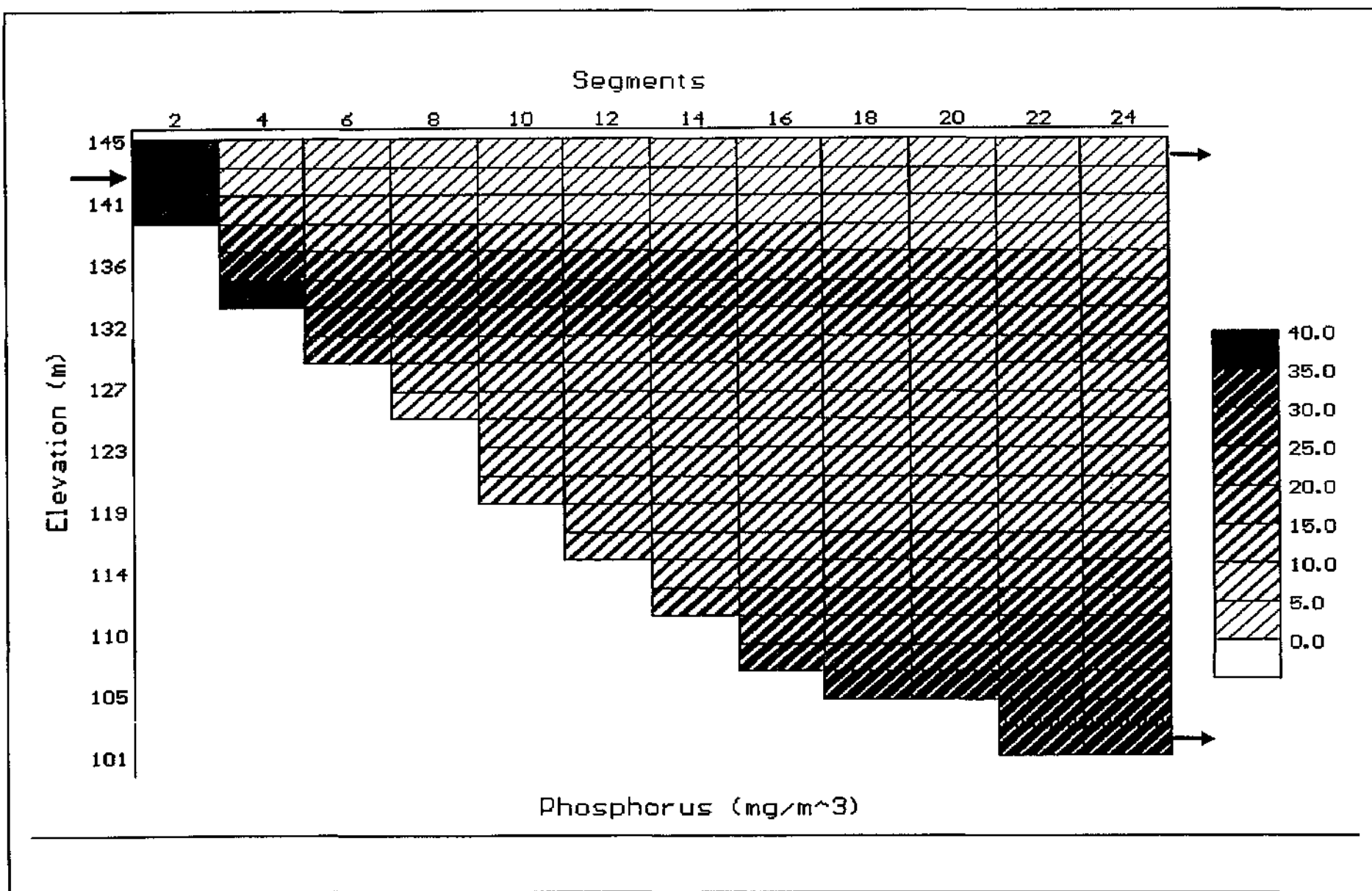
Figure 3.2.19

Hydrodynamic mixing Inanda Dam is characterised by longitudinal and vertical gradients in water quality. Longitudinal gradients are generally brought about by sedimentation and biotic uptake of phosphorus and vertical gradients by depth penetration and stratified flow, see Figure 3.2.20. However, during periods of high inflow the route of the flood waters is governed by the momentum of the inflow, and density of both the inflow and receiving water body. Figures 3.2.21 and 3.2.22 show the flow paths taken during two inflow periods. On Julian Day 88, the flood waters (with discharge of 82 cumec) penetrated into the bottom of the reservoir and pushed aerated river water along the bottom of the reservoir. On Julian Day 123, the flood waters (with discharge of 27 cumec) penetrated into the metalimnion, thereby increasing the concentration of oxygen in the metalimnion. Using a longer simulation period, it would be of interest to see whether the mixing patterns in the simulation period (for 1990) are repeated in subsequent years, and identify the factors which govern the mixing characteristics.

Reservoir draw-down A simulation was performed to estimate the influence of reduced operating level on the water quality of Inanda. The simulation was performed whereby the reservoir water level was maintained 11 metre below full supply capacity by reducing the storage volume at the beginning of the simulation period. Analysis of the time series and isopleth plots showed that the algal biomass and phosphorus response were both unaffected by the reduced operating level. Some improvement in the dissolved oxygen concentration of the reservoir was noted. This may be attributed to increased vertical mixing of oxygenated water (associated with wind action) into the lower layers, giving a deeper oxycline. The vertical mixing was however not sufficient to introduce enough oxygen into the bottom layers to bring about major reduction in the ammonia and iron concentrations.

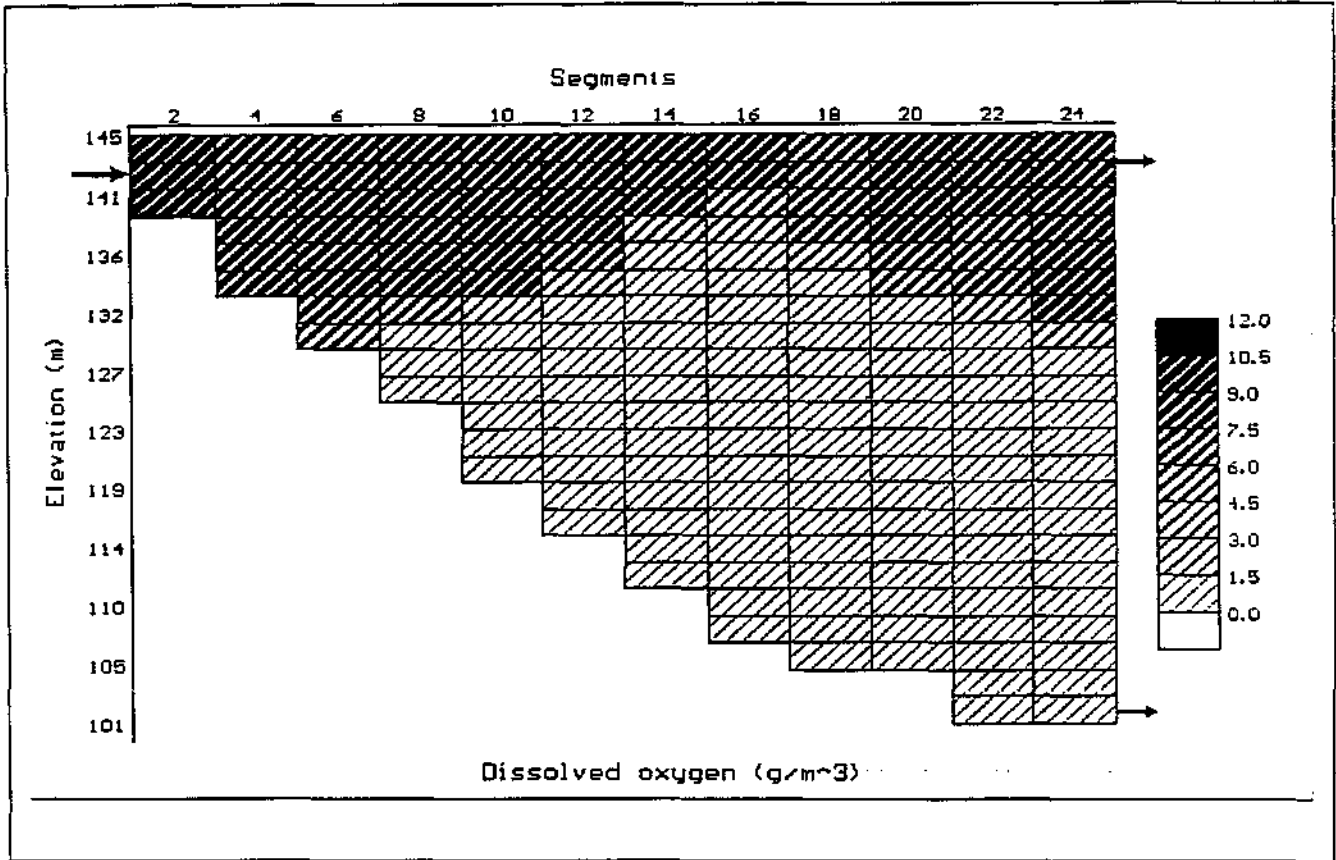
Hypolimnetic releases A simulation was performed to determine the influence of releasing water from the hypolimnion from the scour outlet on water quality characteristics of Inanda. Analysis of the model output showed that in the surface layers, the algal biomass and phosphorus was largely unaffected by the releases. However, in the metalimnion and hypolimnion, a considerable change was observed in the water quality patterns.

On Julian Day 80, the inflowing river water (with discharge of 40 cumec) was entrained along the water body through the bottom layers, see Figure 3.2.23. The entrainment pattern was repeated during each of the major inflows in the summer period. Figure 3.2.24 shows the dissolved oxygen isopleth plot showing the entrainment of storm water resulting in elevated DO concentrations in the hypolimnion. The presence of oxygen in the lower layers was however sufficient to reduce the release of ammonia and iron from the sediments, see Figure 3.2.25.



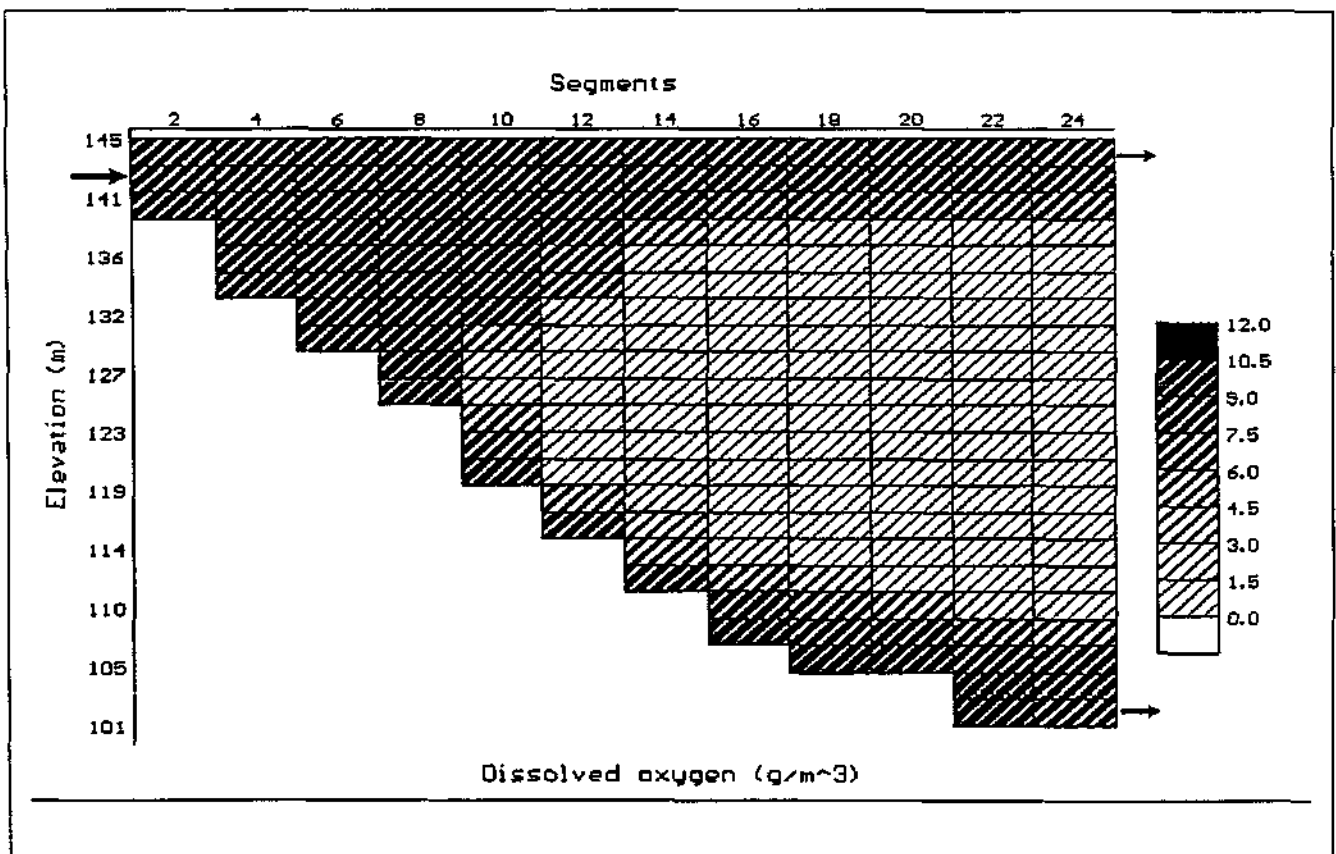
2-D plots showing the distribution of phosphorus with vertical and longitudinal concentration gradients.

Figure 3.2.20



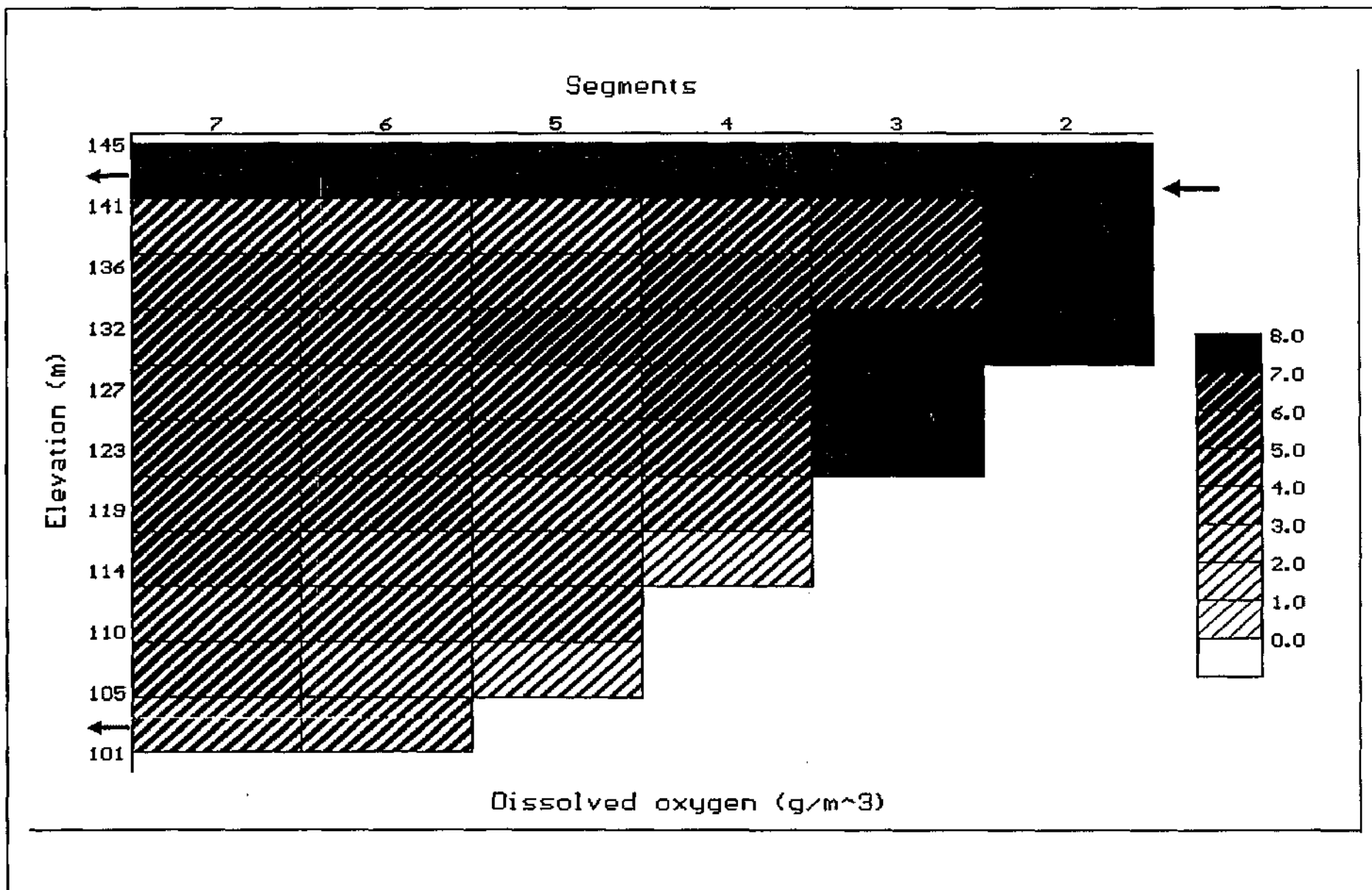
2-D plot showing the penetration of flood waters into the metalimnion of Inanda Dam: Julian Day 123.

Figure 3.2.21



2-D plot showing the penetration of flood waters into the hypolimnion of Inanda Dam: Julian Day 88.

Figure 3.2.22



- 3.34 -

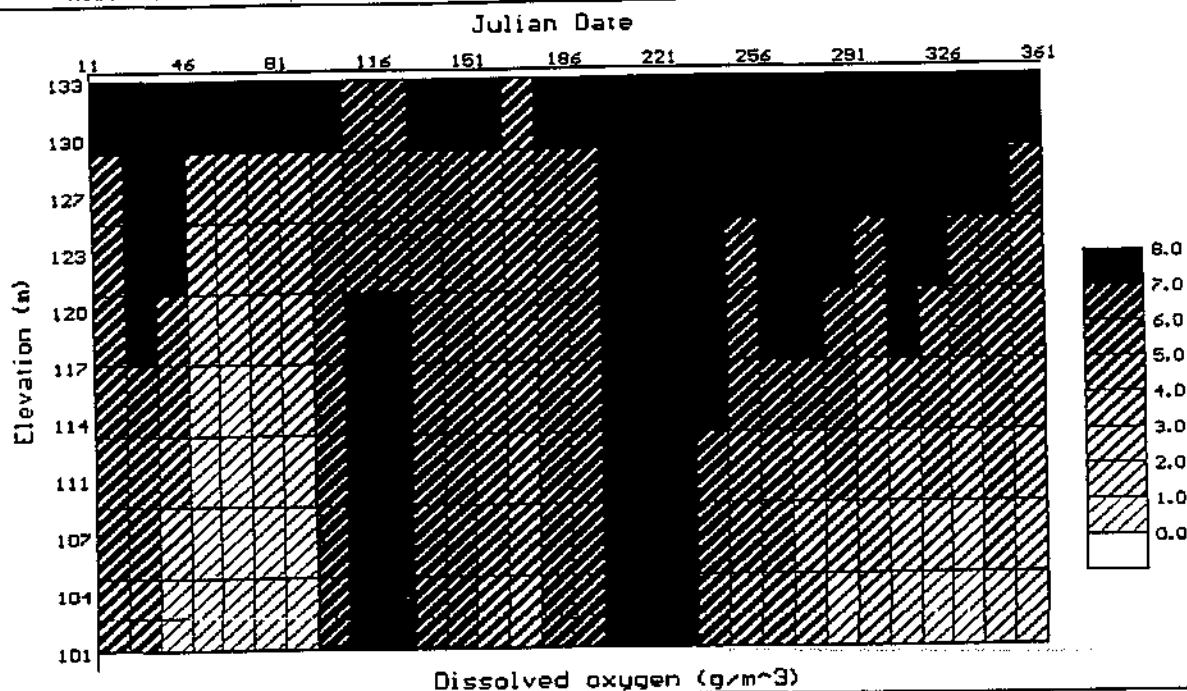


Influence of scour release entrainment on the dissolved oxygen concentration:
Julian Day 116.

Figure 3.2.23

POST PROCESSOR

TITLE : BRNCH:1 SEGS:8 LAY:13 TRIB:0 OUT:2 AGRW:4 ASATUR:18 ASETL:1 AHSP:008
 AHSN:05 EXH20:25 EXINOR:01 SSETL:6 NH3DK:2 PARTN:0 PARTP:0 SOD1:1 CHZ60
 NH4REL:1 EXORG:5 DETDK:03 DSETL:6 FESETL:1 FEREL:1 COLDK:4 PO4REL:0.0
 Model run at Oct 16, 1994 11:21:20



©Ninham Shand Inc (RSA)

Version 2.0

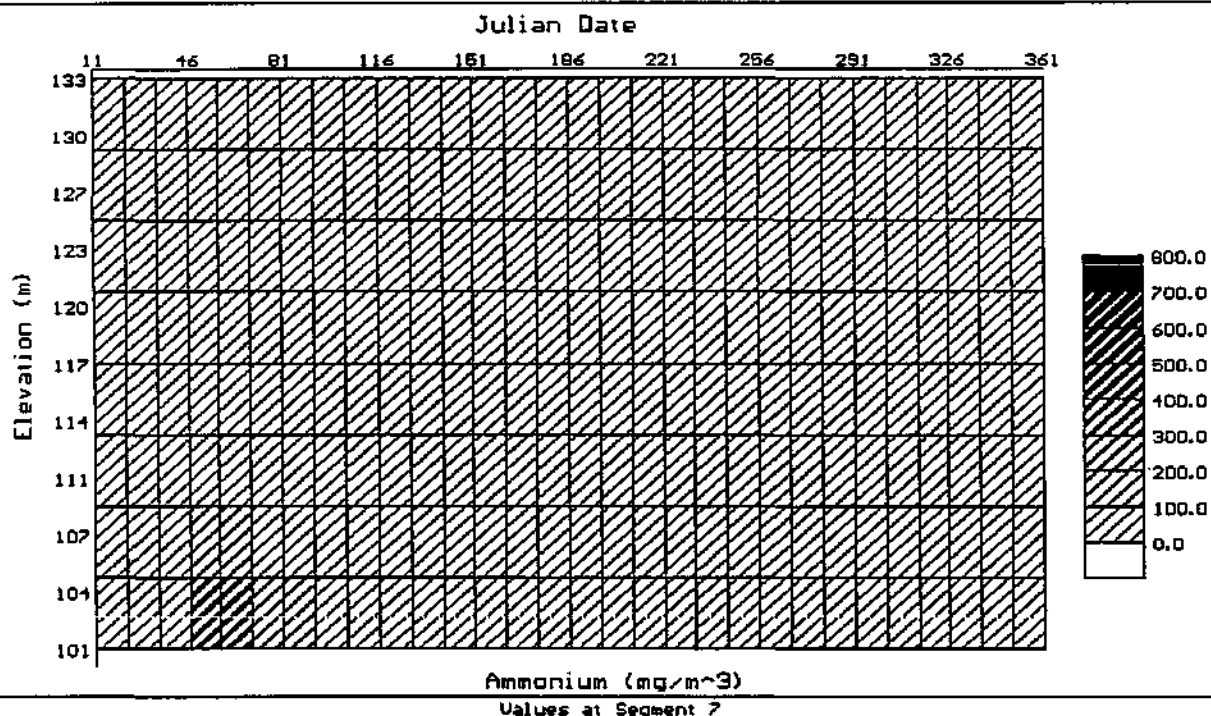


Isopleth plot: dissolved oxygen with scour releases causing entrainment of water during high inflow period.

Figure 3.2.24

POST PROCESSOR

TITLE : BRNCH:1 SEGS:8 LAY:13 TRIB:0 OUT:2 AGRW:4 ASATUR:18 ASETL:1 AHSP:008
 AHSN:05 EXH20:25 EXINOR:01 SSETL:6 NH3DK:2 PARTN:0 PARTP:0 SOD1:1 CHZ60
 NH4REL:1 EXORG:5 DETDK:03 DSETL:6 FESETL:1 FEREL:1 COLDK:4 PO4REL:0.0
 Model run at Oct 16, 1994 11:21:20



©Ninham Shand Inc (RSA)

Version 2.0



Isopleth plot: ammonia with releases from the hypolimnion.

Figure 3.2.25

The entrainment of flood waters causes a marked change in selected constituent concentrations. It was noted that to gain the best improvement in water quality, the releases must coincide with the inflow periods to achieve maximum entrainment within the water body. This operating strategy is however constrained by two factors: (1) the discharge rate of the bottom release, (2) the volume of water which is available for release, and (3) the timing of the releases so that they coincide with the peak inflow into Inanda Dam.

3.2.5 CONCLUSIONS

- Three physical factors are seen to have a direct influence on the water quality of Inanda, namely the quality and discharge of the inflow, morphology of the reservoir basin, and sediment/water interactions. In response, the reservoir has: pronounced stratification, high algal growth, an anaerobic hypolimnion, and release of constituents from the bottom sediments. These factors are expected to have a direct influence on the treatment of water for potable use.
- The model was calibrated using the Inanda Dam data set collected by Umgeni Water. To reduce the run-time of the model, a reduced segment configuration was developed and found to give acceptable results.
- The model was used to provide information on: drawoff depth, sediment interactions, P loading control, mixing conditions, reservoir draw-down, and hypolimnetic releases. It is concluded that a longer simulation period (extending over at least two years) is more suited to evaluate the management options.
- The two-dimensional simulation capability of the model provides detailed information on the movement and process interactions taking place within Inanda. The reservoir exhibits steep vertical and longitudinal gradients in water quality. Detailed testing of *CE-QUAL-W2* in the United States shows that the model is ideally suited to simulate the water quality in reservoirs with longitudinal and vertical gradients. For example, the simulation of metalimnetic deoxygenation using a 2-D model (such as *CE-QUAL-W2*) is achieved through the simulation of the momentum delivered by the inflowing river water. A 1-D model which is unable to simulate the momentum component, requires manipulation of the model to adequately simulate the vertical profile of DO (Cole, 1995).
- The preliminary simulation results show that a reduction in algal biomass may be achieved using: selective drawoff depth, and P loading control (in the upstream catchment). No single

management option was found to provide a complete improvement in water quality of Inanda . It was determined that aeration of the hypolimnion will have minimal beneficial influence on the phosphorus regime and algal biomass. However, complete destratification could have some benefits in reducing the phosphorus concentration in the hypolimnion and also increase the mixed depth thereby decreasing algal growth.

- The reservoir sediments have an important influence on the water quality of the hypolimnion , giving rise to anaerobic conditions and the release of contaminants. The phosphorus budget of Inanda is dominated by the Mgeni River, with the sediments having a negligible influence . Future changes in the P sediment release characteristics are shown to have a potentially important influence on algal growth. In this regard routine monitoring will be required to ascertain the nutrient release characteristics under reducing conditions.
- The model shows that the entrainment of flood waters through the length of Inanda introduces aerated water into the hypolimnion thereby improving the water quality.
- The model is used to identify the algal limiting factors in Inanda. In the metalimnion and hypolimnion light is growth limiting, in the epilimnion both phosphorus and light are growth limiting. This shows that management of algae should focus on the phosphorus budget of Inanda.

3.2.6 RECOMMENDATIONS

Role in decision support system for Inanda Dam The applications described above show the general capabilities of hydrodynamic modelling in the management of Inanda Dam. Further model applications should be carried out to:

- Define operating rules and management options for the control of water quality.
- Identify reservoir processes and sediment interactions. This information will play a vital role in the formulation of a water quality management plan for the lower Mgeni River catchment.

An extended simulation period (greater than one year) should be used to examine

- The influence of P control options on controlling algal growth.
- The hydrodynamic mixing patterns to optimize draw-off level, and operation of releases.

- The influence of sediment release of P on algal growth, and determine the implications for management of the reservoir.

Water Quality Monitoring of Inanda Dam The monitoring program implemented by Umgeni Water provides an extensive data set for the modelling of Inanda Dam. Additional monitoring should include:

- Routine monitoring and analysis to examine the P release potential of the bottom sediments to detect changes in the release characteristics of the sediments.
- In the dam wall basin, collection of water samples at regular intervals throughout the depth profile for the constituents: algal biomass (and species), phosphorus, suspended sediment, ammonia, iron and manganese. This information will assist the operation of the multi-level drawoff.

Reservoir Management During high runoff, test releases should be made from the scour valve to determine the feasibility of entraining flood waters into the hypolimnion of the dam wall basin. At such time, monitoring should be undertaken at the three in-dam points to determine the influence of the flood waters on the dissolved oxygen, iron, ammonia and phosphorus regime of Inanda Dam.

3.2.7 REFERENCES

Bruwer, C.A. (1979)

Socio-economic cost of eutrophication, Internal report of the Department of Water Affairs and Forestry, Pretoria.

Cole, T.M. (1993)

Personal communication. US Army Engineer, Waterways Experimental Station, Vicksburg, Mississippi, USA.

Cole, T.M. & Hannan, H.H. (1993)

Dissolved oxygen dynamics, In Reservoir Limnology, Ecological Perspectives, p.71-107.

Cole, T.M. (1994)

User guide to *CE-QUAL-W2*, Instruction report, US Army Engineer, Waterways Experimental Station, Vicksburg, Mississippi, USA.

Cole, T.M. (1995)

Personal communication. US Army Engineer, Waterways Experimental Station, Vicksburg, Mississippi, USA.

DWAF (1990)

Capacity determination: Inanda Dam, Directorate of Survey Services, Department of Water Affairs and Forestry, Pretoria, Report Number U200_04.

Görgens, A.H.M., Bath, A.J., Venter, A., de Smidt, K. & Marais, G.v.R. (1993)

Applicability of hydrodynamic reservoir models for water quality management in stratified water bodies in South Africa, Report to Water Research Commission, Pretoria, number 304/1/93.

Hudson, N., Furness, H., & Boucher, K. (1993)

Water quality of Inanda Dam - some indicators for the management of a raw water reservoir, Water quality department, Umgeni Water, Report number WQP 4/93.

Silberbauer, M. (1981)

The release of phosphate from the bottom sediments of Roodeplaat, Hartbeespoort, and Bloemhof Dams, Contributions by the Department of Water Affairs, Forestry and Environmental Conservation to the Congress of the Limnological Society of Southern Africa, Rhodes University, Grahamstown, 4 to 9 July, 1980. Technical Report number 114, Department of Water Affairs and Forestry, Pretoria.

Tollow, A.J. (1991)

Durban's newest water resource - Inanda Dam, Journal of the Institute of Water and Environmental Management, 5, 519-528.

UW (1989)

Water quality in the Inanda Dam system, Water quality department, Umgeni Water, Report number WQ 2/89.

UW (1990)

Preliminary assessment of Inanda Dam water quality for the period March 1989 to February 1990, Water quality section, Umgeni Water, Report number WQP 4/90.

UW (1992a)

Impact of artificial destratification by aeration on Inanda Dam, Natal, South Africa, Water quality department, Umgeni Water, Report number WQP 6/92.

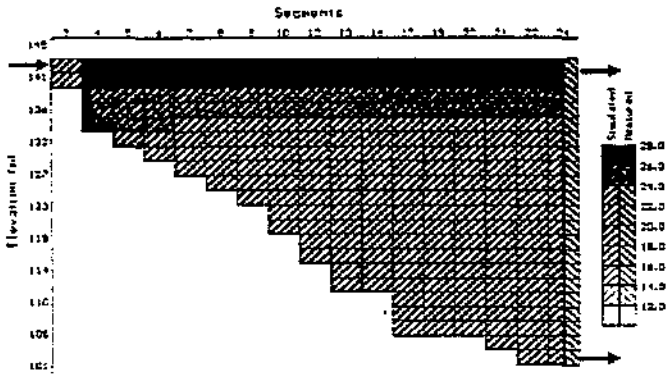
UW (1992b)

Management strategies for impoundments supply Umgeni Water suggested by temperature and dissolved oxygen data, Water quality section, Umgeni Water, Report number WQP 2/92.

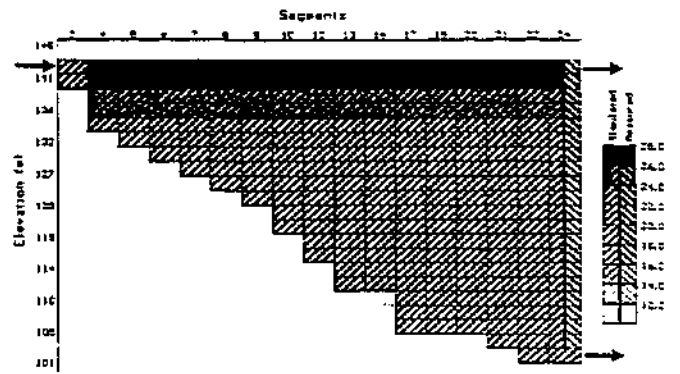
UW (1993)

Raw water quality of Inanda Dam: implications for treatment facilities and sludge handling at Wiggins Water Works, Water quality planning section, Umgeni Water, Report number WQP 2/93.

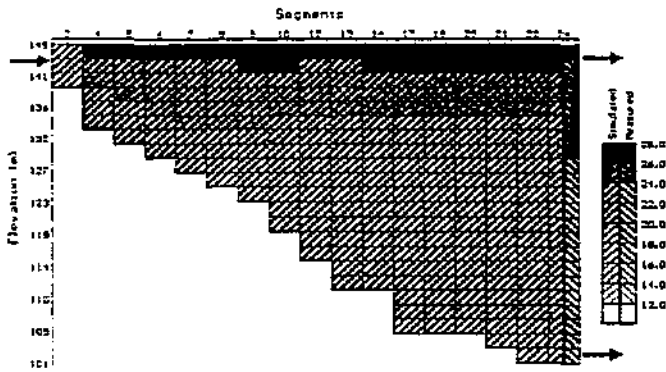
Julian Day 4



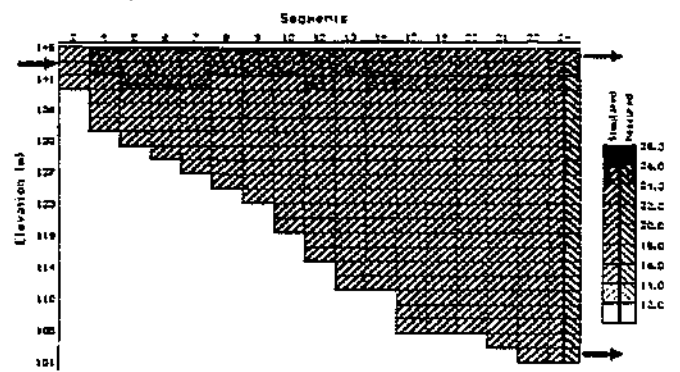
Julian Day 25



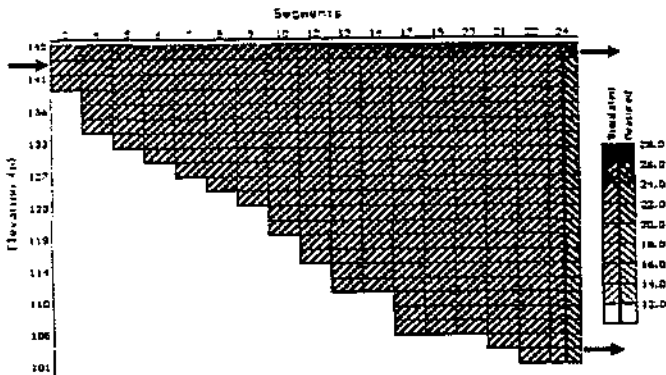
Julian Day 60



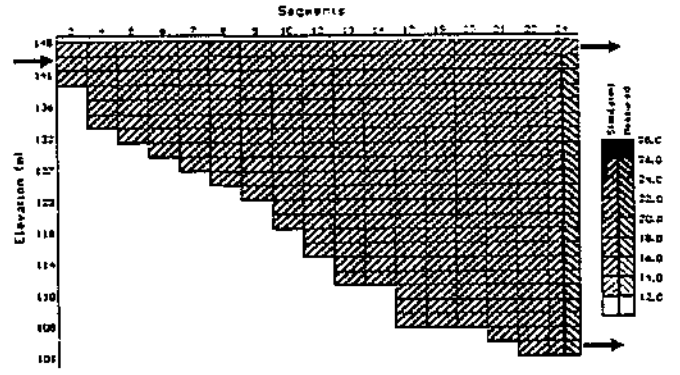
Julian Day 80



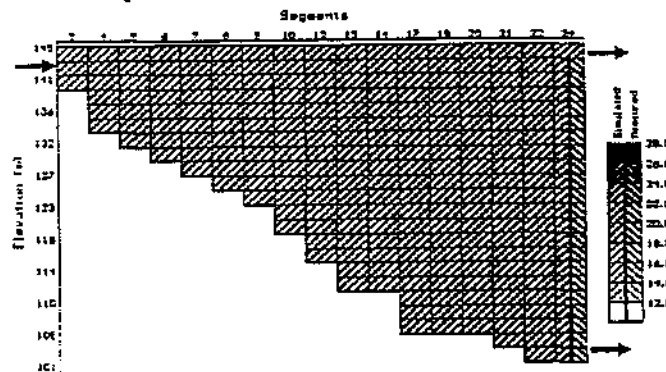
Julian Day 116



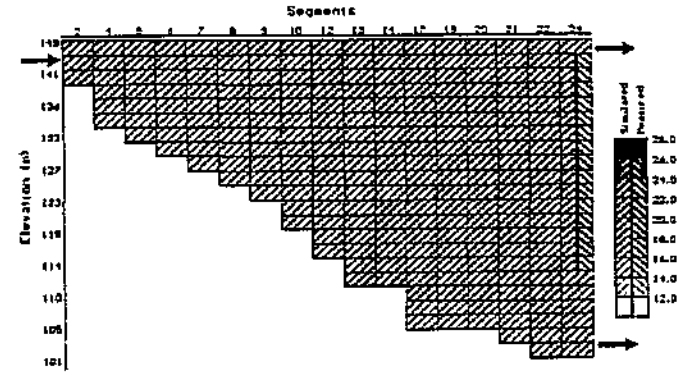
Julian Day 150



Julian Day 172



Julian Day 200



SECTION 3.3

APPLICATION OF *CE-QUAL-W2* TO SIMULATE THE SALINITY AND HYDRODYNAMICS OF THE VAAL BARRAGE

by

A J Bath & A H M Görgens

3.3.1 INTRODUCTION

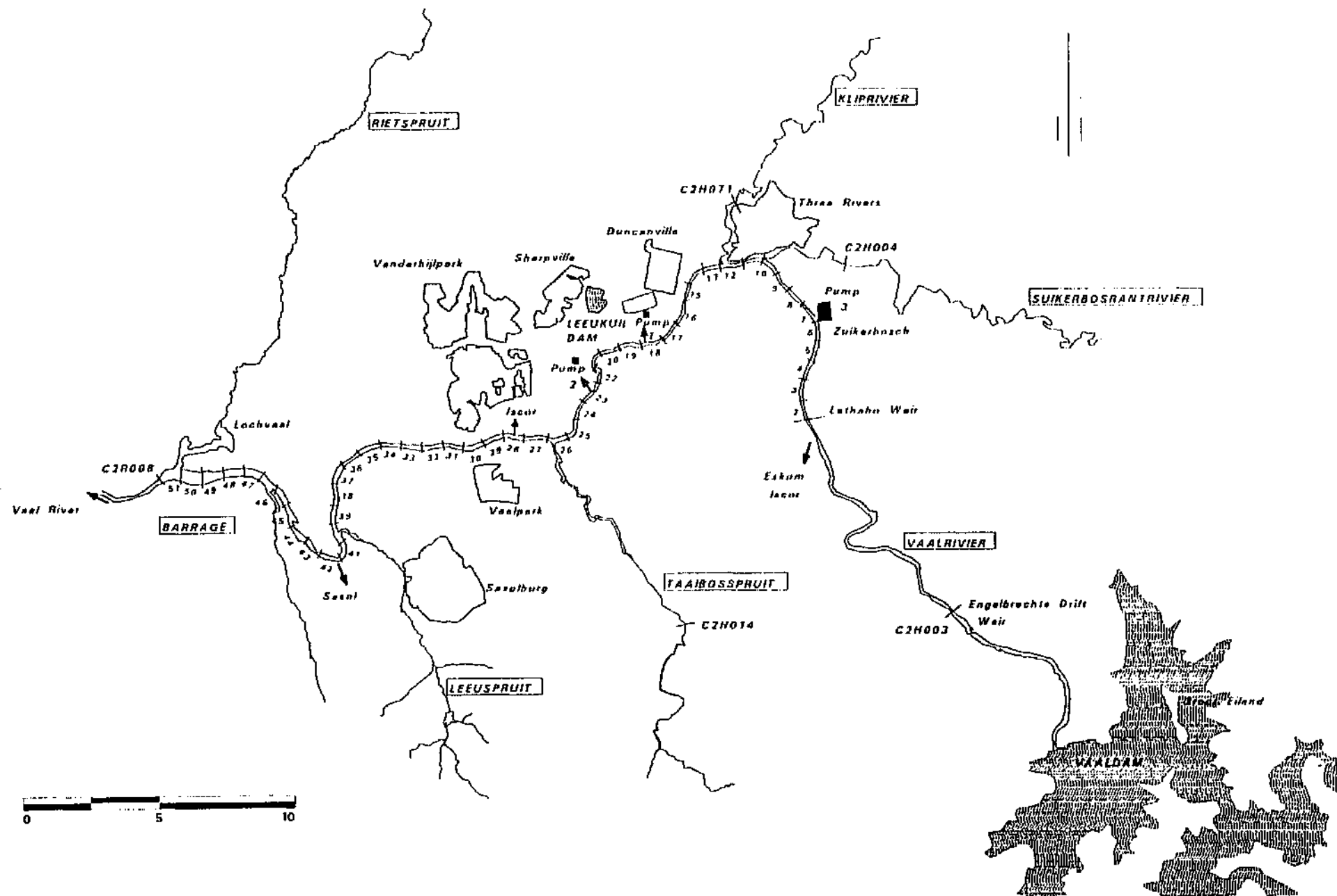
Study area The Vaal Barrage was constructed in 1922 to tap the water resources of the Vaal River. In 1938, the Vaal Dam was built upstream of the Barrage to augment the supply from the Vaal (see Figure 3.3.1). The Barrage is a riverine lake approximately 50 km long, ± 150 metre wide, and ± 6 metre deep. The Vaal Barrage and Dam serve as a bulk supply point for RW, Vereeniging Municipality, as well as local industries. It is estimated that at least one third of the water supplied to the Gauteng Region¹ is derived from this source (Herold & Triebel, 1990). Figure 3.3.1 shows the points of abstraction used by RW, ISCOR and ESKOM.

The Barrage receives inflow from the Klip River, Suikerbosrand River, Taaibosspuit, Leeuspruit and Rietspruit. At the upstream end, releases are made from the Vaal Dam. The Klip River is the largest inflow (between 6 to 10 cumec) and input of dissolved solids to the Barrage. The Klip River receives runoff from urban, industrial and mining areas (DWAf 1986; Jones *et al.* 1988), in addition to treated wastewater from the south of Johannesburg (van Vliet & Nel 1986).

In 1949, Rand Water (RW) curtailed further expansion of the Vaal River intakes at Vereeniging in favour of new intakes at Zuikerbosch, located upstream of the Klip and Suikerbosrand Rivers (see Figure 3.3.1). This was done to prevent the abstraction of high salinity water discharged into the Barrage by the Klip River. Unfortunately, the abstraction at the Zuikerbosch intakes caused a reversal in the flow of the Barrage and saline water was abstracted. In 1969, a pipeline was commissioned to draw low salinity water directly from the Vaal Dam, followed in 1983 by the construction of the Vaal Dam-Zuikerbosch canal.

Water quality operation The Barrage was operated using a *300 mg/l TDS blending option*. Rand Water extracted from three points along the Barrage (see Figure 3.3.1) This water was then blended with treated water from the Vaal Dam to supply a final water with TDS of 300 mg/l. An important feature of the Vaal Barrage was that the offtakes used by Eskom, SASOL, and Rand Water at Zuikerbosch experienced reversed flow in the Barrage and abstracted higher salinity water derived from the Klip River. This problem of reversed flow was overcome through the construction of

¹ The region is formerly known as Pretoria Witswatersrand Vereeniging (PWV) Region.



Location map of the Vaal Barrage showing the main tributaries, abstractions and gauging weirs.

Figure 3.3.1

Lethabo Weir which prevents the backward migration of high salinity water to the offtake points. Under the operating rules of the *300 mg/l blending option*, releases from the Vaal Dam are kept to a minimum and users along the middle Vaal River experience water quality problems as the TDS concentration may occasionally exceed 800 mg/l.

Complaints from users led to an investigation into revising the operating rules. This resulted in the formulation of a new management approach the *600 mg/l dilution option*. This option allows calculated amounts of water to be released from the Vaal Dam to dilute the TDS in the Barrage to below 600 mg/l. Rand Water would then abstract an amount from the Barrage equal to the return flow from the Klip, Suikerbosrand and Riet Rivers. Additional water would be drawn from the Vaal Dam. Calculations showed that this option would provide Rand Water with a TDS concentration of around 300 mg/l, and the water released from the Barrage would be lower in salinity than using the *300 mg/l blending option* (and thus benefit users in the middle Vaal River). This operating rule however places further demands on the water resources of the system, particularly when Bloemhof Dam is at full storage level. Also, pumping costs are increased for Zuikerbosch treatment works.

Unfortunately, the Zuikerbosch abstraction point is positioned so that most of the water released from Vaal Dam could be intercepted and not available to dilute the rest of the Barrage. As an interim measure, it was decided that Rand Water would meet most of its water demand from the Vaal Dam (with a TDS of 150 mg/l).

During July and August of 1990, the *600 mg/l dilution option* was implemented on a trial basis. During this period, monitoring was carried out by the Institute for Water Quality Studies (IWQS) and RW. This data set was used to configure and calibrate CE-QUAL-W2. The model was then used to assess the factors influencing the hydrosalinity and mixing behaviour of the Barrage.

3.3.2 MODEL INPUT

Görgens *et al.* (1993) give a detailed description of the formulation of the input files. In summary, the files contain the following: daily meteorology, daily inflow and withdrawal discharge, daily tributary and effluent water quality, river channel hydrographic survey information (bathymetry), and water quality boundary conditions.

Selection of simulation period The simulation period extended over a period of 137 days, beginning 1 July and ending on 17 November 1990. The period was selected to overlap the duration of the release from Vaal Dam, thereby allowing:

- The simulated conditions in the Vaal Barrage to reach an equilibrium condition before the

release was made on 21 July 1990, and

- the Vaal Barrage sufficient time to reach a final equilibrium after the release had passed through the water body to determine the duration of the mixing process within the water body.

Data Sources Meteorological data include wind speed and direction, solar radiation, dew point temperature, air temperature, and cloud cover. These data were obtained from the Weather Bureau who have measuring points adjacent to the Barrage at Vereeniging and Vanderbijlpark. The water temperature of the Barrage was measured by IWQS and RW. Tributary flow and withdrawal data were obtained from DWAF and RW. These data were processed to determine runoff from ungauged areas and verify the volume balance for the Barrage. Water quality data were obtained from the monitoring exercise of the Barrage carried out by the IWQS and RW. Daily time sequences were created using methods developed by Görgens *et al.* (1993).

The boundary condition data provide the model with the starting conditions of the Vaal Barrage and include water temperature, and electrical conductivity (EC). Field data were used to assess the predictive ability of the model to simulate the quality of the Barrage. The data included grab samples and vertical profiles (obtained by RW and IWQS) for: conductivity, TDS, turbidity, dissolved oxygen, major ions, and selected nutrients.

3.3.3 MODEL CONFIGURATION

Prior to calibration, the model configuration entails the formatting of input data files, compilation of executable code, followed by installation and testing on the personal computer. The model, *CE-QUAL-W2*, has been developed to provide a detailed representation of a water body using a variety of branches, tributaries, segment layouts and withdrawals. However, the complexity of the model representation (ie number of segments, layers and cells) has a direct influence on the run-time of the model. Below a maximum of 400 active cells (equivalent to 50 segments and 8 layers), the run-time of the model was found to be suitable for testing scenarios (Bath & Timm, 1993; Görgens *et al.*, 1993). Above 400 active cells, the run-times were found to become excessively long and restrict the interactive use of the model to test scenarios. The configuration described below gave a run-time of 22 minutes, using a 80486 DX2-66 processor, and a simulation period of 137 days.

Branch layout The Vaal Barrage was configured using a single branch subdivided into a series of vertical segments and horizontal layers. Figure 3.3.1 shows the segment boundaries with their associated tributary inflows and abstractions. Loch Vaal is treated as a tributary inflow.

Segment layout The distance along the Vaal Barrage between Lethabo Weir and the barrage wall is about 52 km. The 52 km river reach² between the upstream (Lethabo Weir) and the downstream boundary (the Barrage) was divided into 52 segments, each with a length of 1 km, see Figure 3.3.1.

Layer configuration The water body was further divided into horizontal layers at 1 metre intervals giving a maximum number of 13 layers at the deepest part of the Barrage. Information provided by the Regional Office of the DWAF was used to identify each of the main points of withdrawal from the Barrage, see Figure 3.3.1. The bathymetric data set was derived from the survey of the Barrage performed by the Department of Water Affairs (DWAF, 1978) and updated using ortho-photos and supplementary monitoring information.

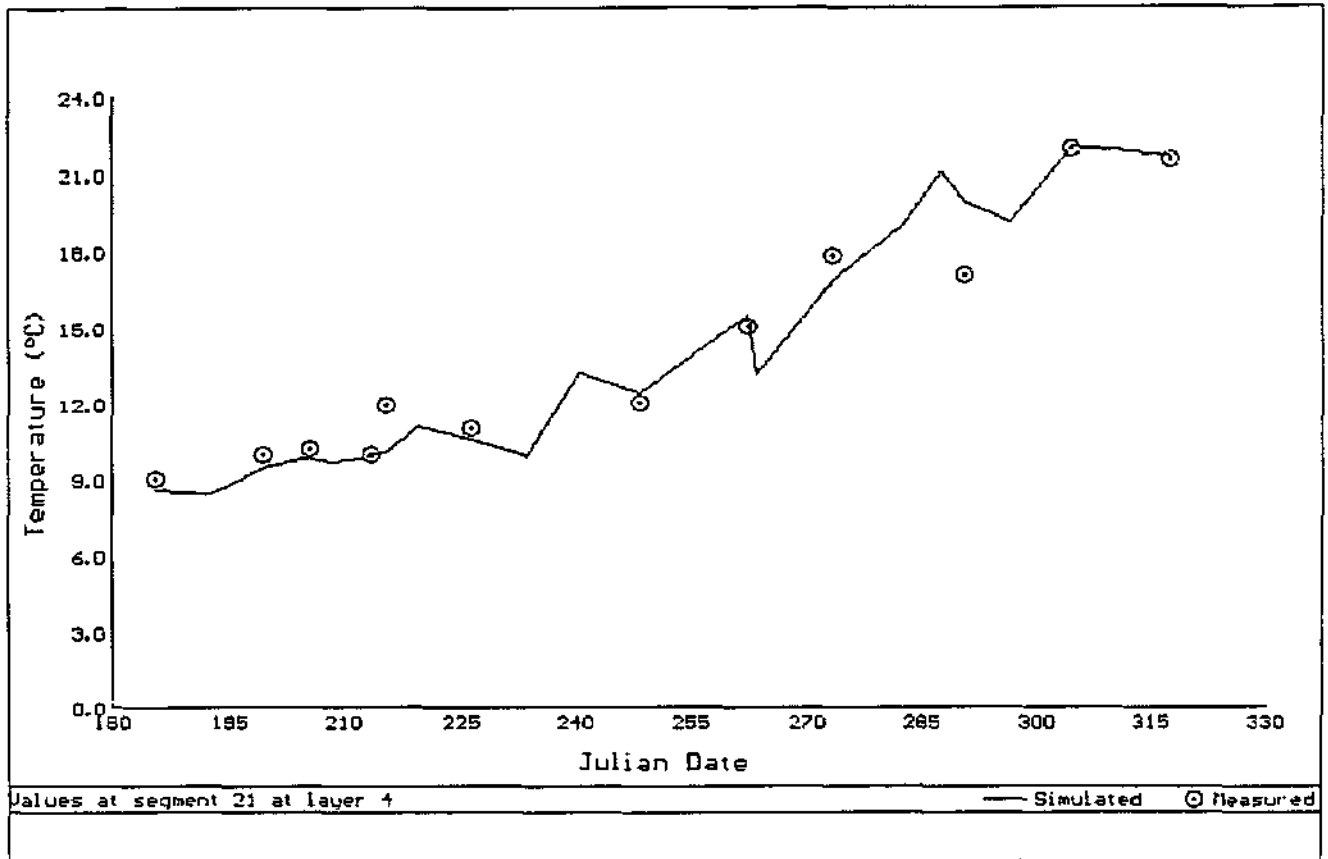
3.3.4 MODEL CALIBRATION

Calibration of the model essentially deals with three components: heat exchange, volume balance and water quality simulation.

Heat Exchange The heat exchange of the water body is simulated using a physically based description of the governing processes. The Roodeplaat Dam application (Section 3.4) shows the model is primarily dependent on the accuracy of the meteorological data and the Wind Sheltering Coefficient (WSC) serves only as a means of compensating for local conditions and factors which reduce the wind exposure, such as trees or buildings. Figure 3.3.2 shows the simulated and measured surface water temperature of the Barrage at Segment 21, near RW pump 2. In Figure 3.3.2, the simulated noon-day water temperature is plotted for selected days showing the general pattern over the simulation period. A number of model runs were performed to determine the influence of the Wind Sheltering Coefficient on the surface temperatures and mixing conditions. The default value (of 0.9) was found to provide the most acceptable agreement between the simulated and measured water temperature.

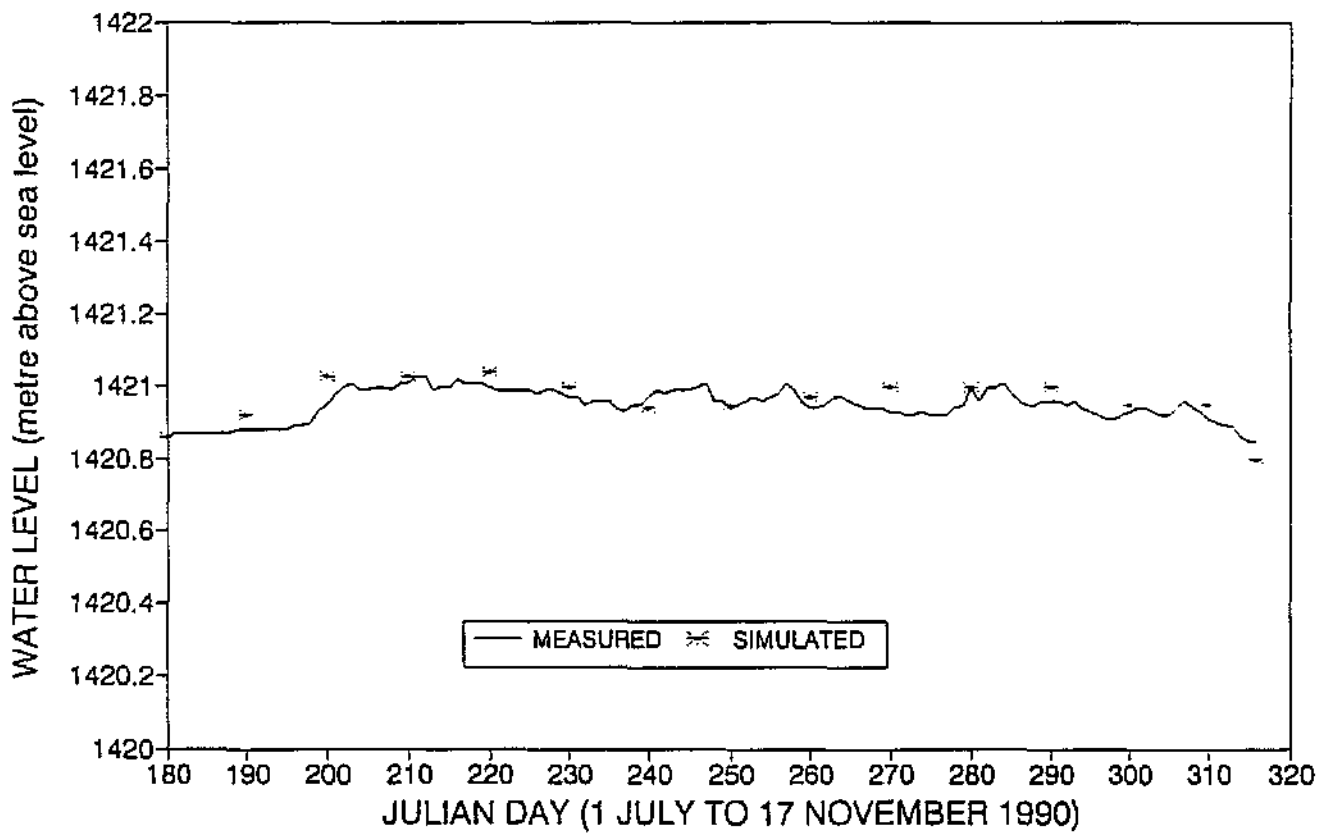
Volume Balance A volume balance calculation was performed to verify the inflow and outflow hydrograph data. This showed that some of the flow gauging structures were unreliable. A complete revision was made of the flow data and volume balance of the water body. Görgens *et al.* (1993) describe the methods used in the calculation of the volume balance. Figure 3.3.3 shows the measured and simulated water surface elevation data for the Barrage over the simulation period of 137 days using the tributary inflow hydrographs and inflow hydrograph shown in Figures 3.3.4 and 3.3.5. The model provides an acceptable simulation of the volume

² Studies undertaken by IWQS report a channel length of 50.5 km



Simulated and measured surface water temperature.

Figure 3.3.2



Simulated and measured water elevation.

Figure 3.3.3

balance taking account of the comparatively complex set of inflows, outflows, releases and withdrawals (many of which are not measured on a continuous basis).

Salinity (conductivity) For graphical purposes, the 600 mg/l dilution option is equated for the purposes of this study to be a conductivity of 90 mS/ms. In practice, DWAF use a field reading of 85 mS/m for operational purposes. This conductivity is referred to as the *operational guide*.

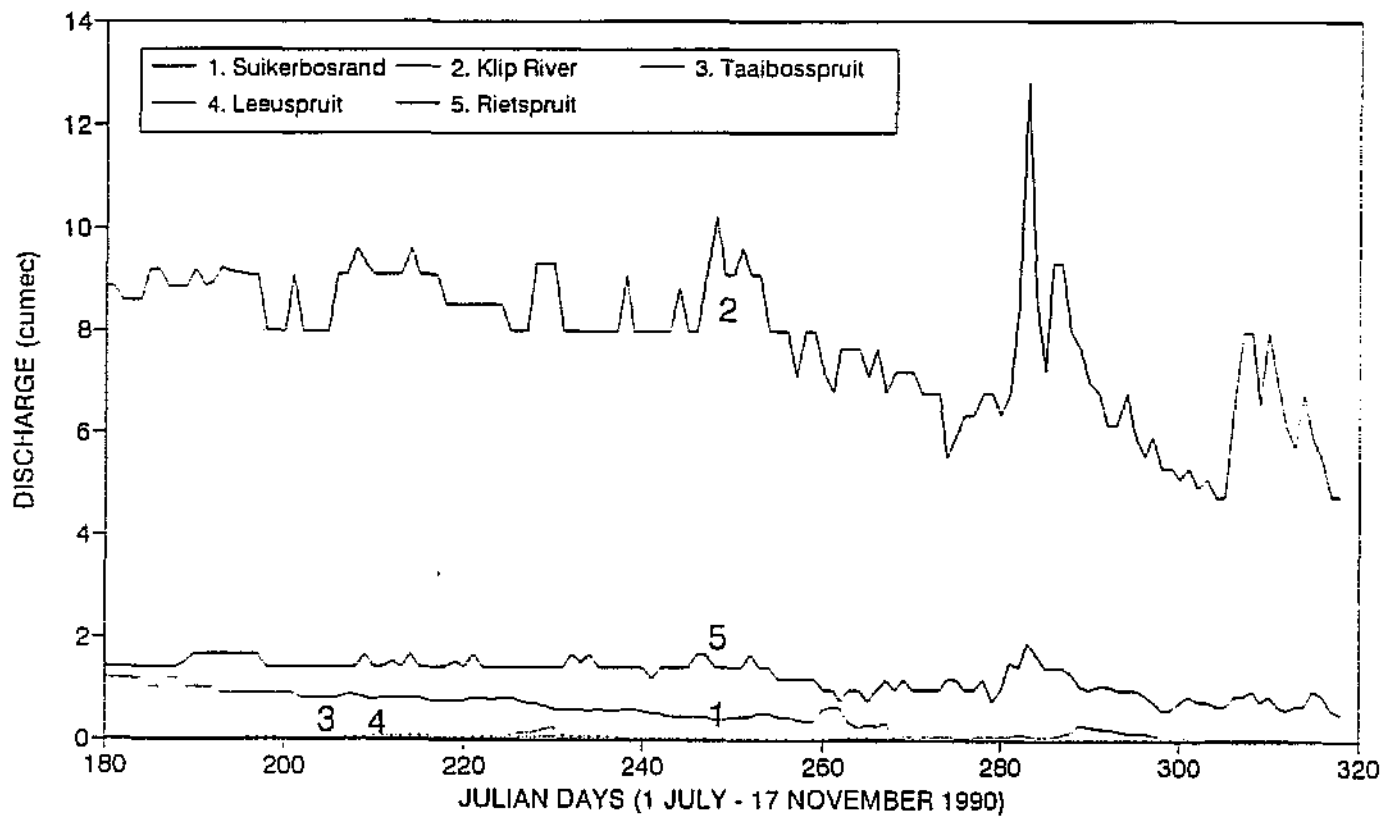
Figure 3.3.6 shows the simulated and measured electrical conductivity at eight Segments along the length of the Barrage. Segment 5 is located at Zuikerbosch close to the inflow, and Segment 45 is in the lower reaches close to Loch Vaal. Figure 3.3.6 shows the model provides an acceptable simulation of the conductivity during the release period. Analysis of the measured conductivity data showed that some variation in conductivity occurred across the width of the Barrage, particularly near the tributary inflow points. The model assumes the water body is laterally averaged which accounts for the discrepancies between the simulated and measured conductivities, see Figure 3.3.6.

3.3.5 SALINITY CHARACTERISTICS DURING THE FRESHENING RELEASE

Figure 3.3.6 shows that the freshening release brings about an abrupt reduction in the conductivity of the Barrage and complies with the operational guide.

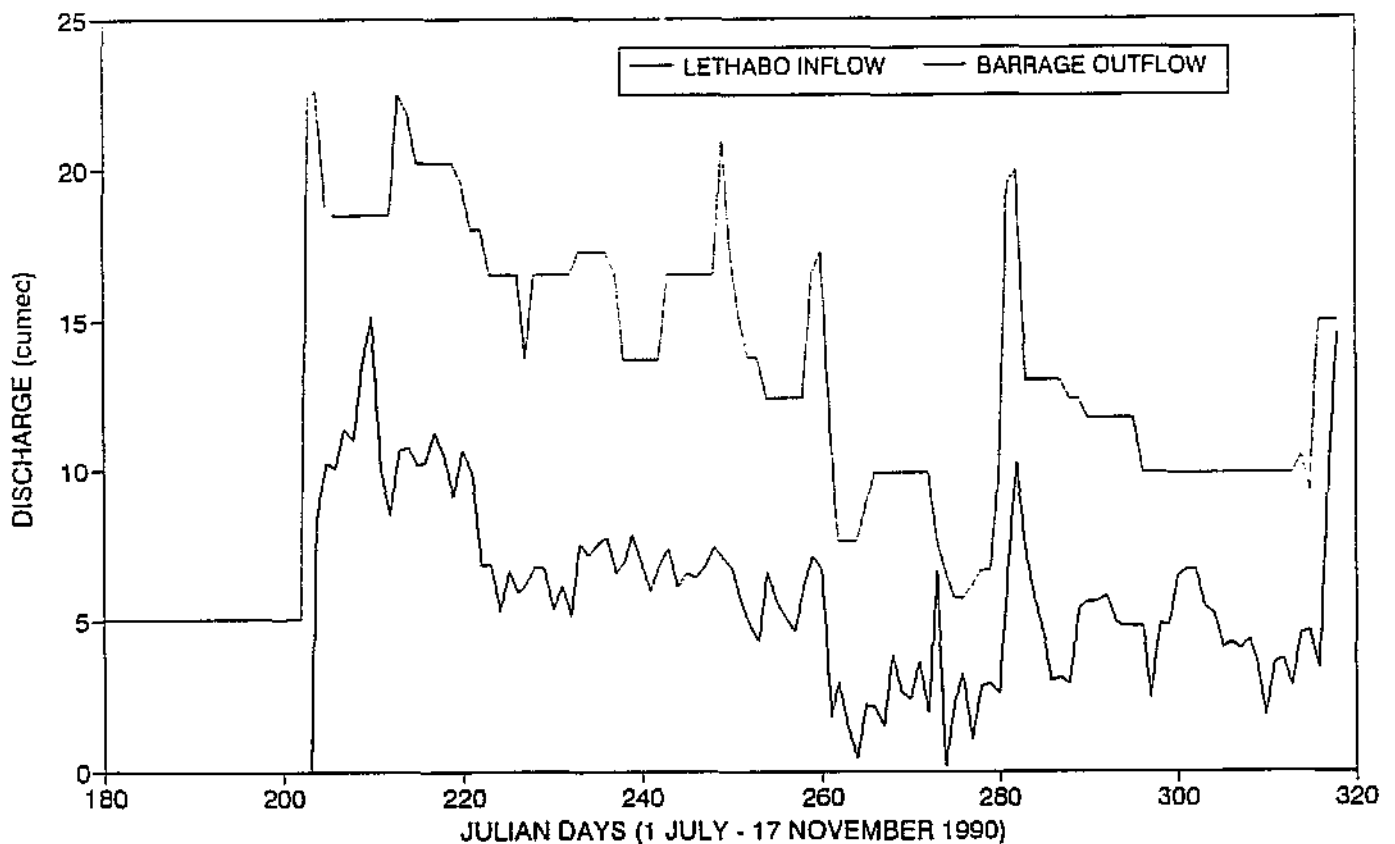
Figure 3.3.7 shows the two-dimensional (2-D) representation of the conductivity during the release period.

- (1) **Day 199:** prior to the release taking place, the conductivity of the Barrage was dominated by the release of saline water from the Klip River, entering the Barrage at Segment 12.
- (2) A saline plume (with EC > 110 mS/m) discharged from the Klip River, moved upstream and downstream of the tributary inflow point caused by abstraction at the Zuikerbosch Intakes drawing water upstream. The plume extended over a distance of almost 14 km, from Lethabo Weir to Segment 15 (near Duncanville).
- (3) **Day 204:** The first part of the freshening release flowed into the upstream Segments 2 and 3. The saline water progressed along the bottom of the Barrage.
- (4) **Day 205:** At the beginning of the freshening release, movement of the high salinity plume along the Barrage, and introduction of saline water from the Klip River produced two saline plumes.



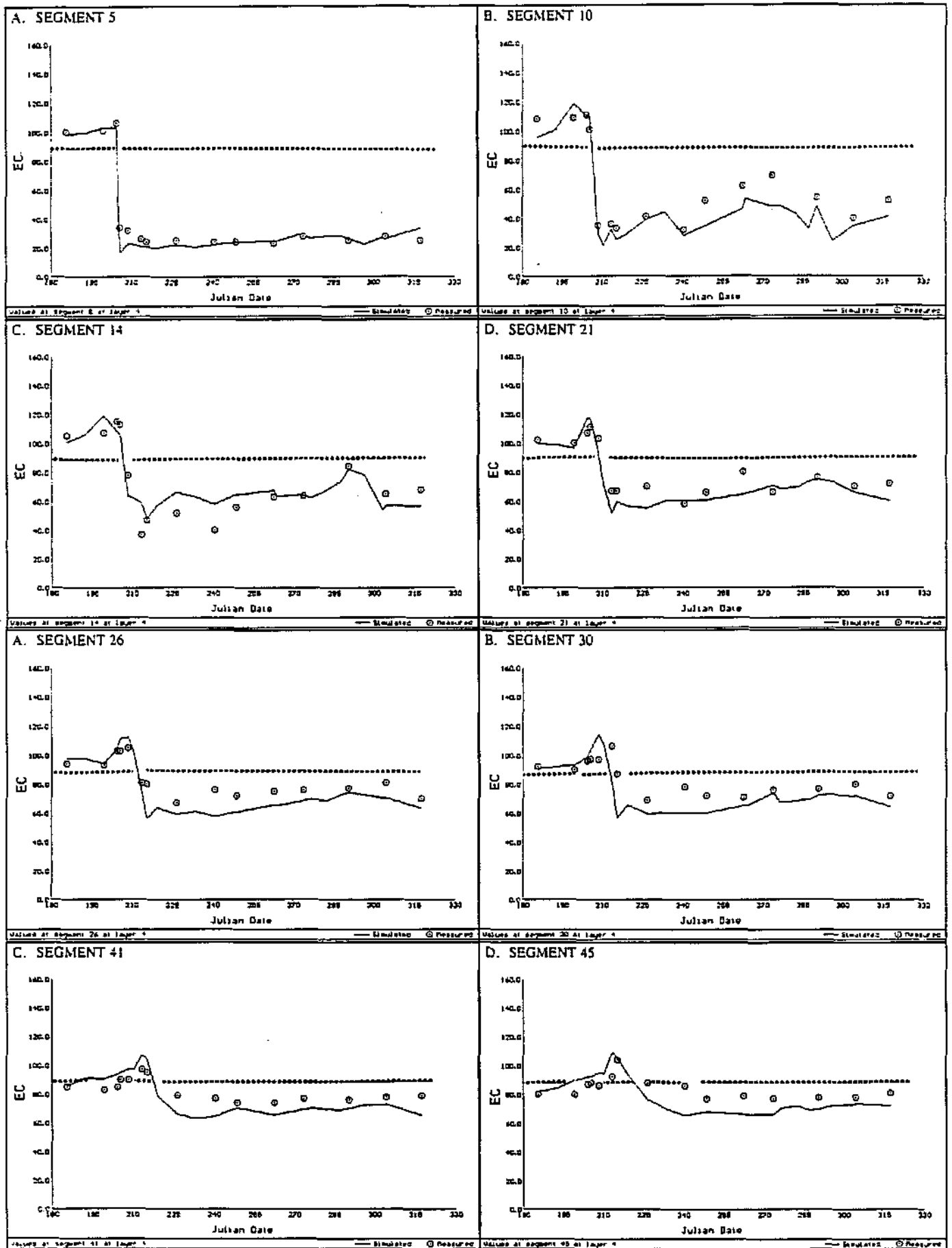
Measured tributary inflows to the Barrage

Figure 3.3.4



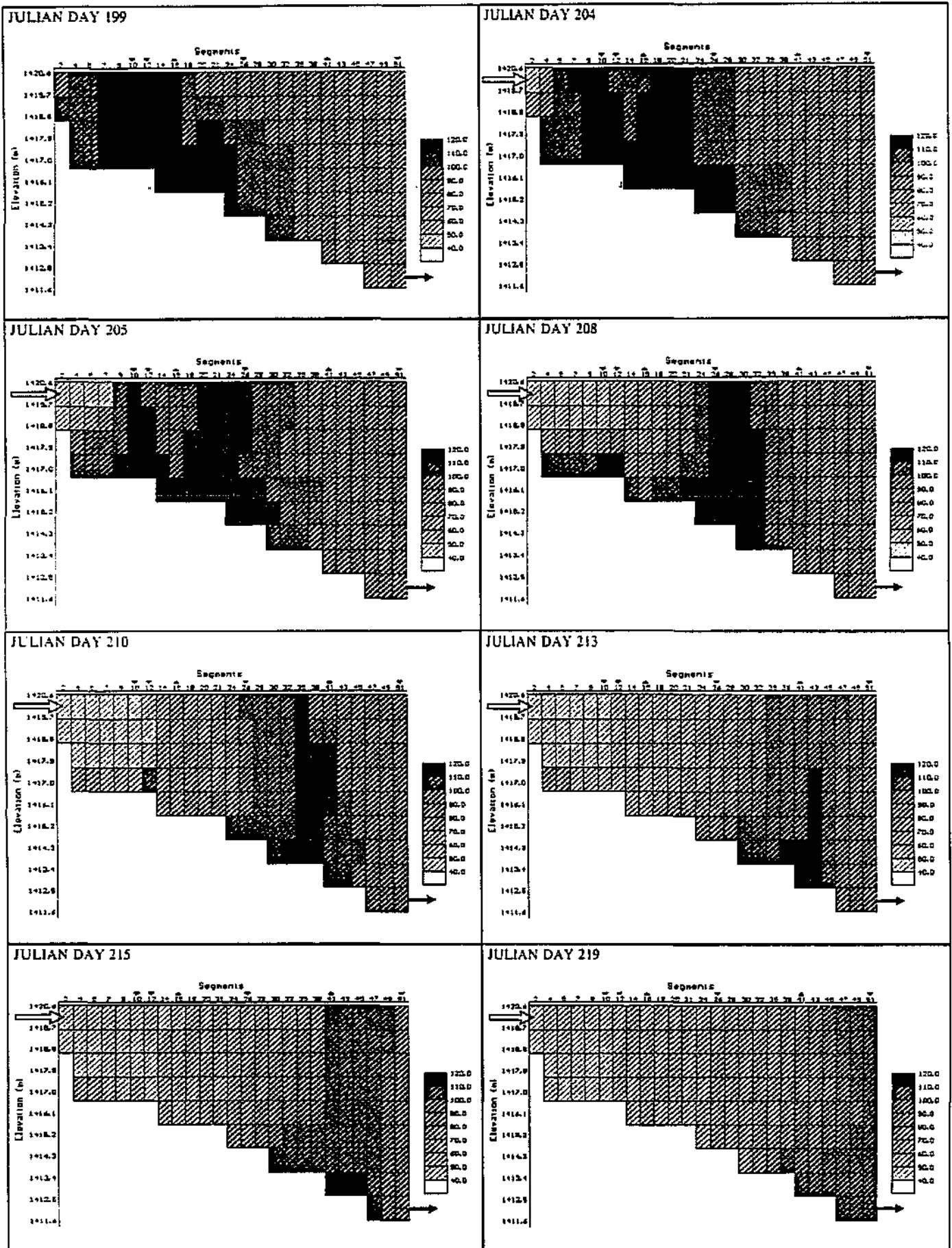
Measured Barrage inflow at Lethabo Weir and spillage from the Vaal Barrage.

Figure 3.3.5



Measured and simulated EC for segments along the length of the Barrage.

Figure 3.3.6



2-D plot of the simulated electrical conductivity (EC) of the Vaal Barrage during the release period (Day 204 onward). Figure 3.3.7

- (5) **Day 208:** the release water reduced the surface conductivity to below 40 mS/m. Higher salinity water in Segments 2 to 12 remained in the bottom layers. This feature was thought to be caused by a submerged weir at the boundary of Segment 13 which restricted the flow of saline water. The model was configured with a weir at Segment 13. Subsequent simulations were carried out to determine the influence on the conductivity of the Barrage by removing the weir. The results showed that the weir had little influence on the conductivity of the upper reaches. The salinity pattern was caused by (1) the comparatively high flow (± 8 cumec) of the Klip River which caused a localised downward and lateral movement of water, and (2) localised reversed flow caused by wind action.
- (6) As the release continued, the saline plume moved along the length of the Barrage and at Day 208 was situated at Segments 24 to 32.
- (7) **Day 210:** The release from Vaal Dam (of 12 cumec) resulted in vertical mixing in the upper segments (2 to 12). The saline had moved between Segments 35 and 41.
- (8) **Day 213:** The saline plume passed into the lower layers of the Barrage, and then dispersed.
- (9) **Day 215:** The release water dominated the conductivity of the upper and middle reaches of the Barrage (Segments 2 to 30). In the lower reaches, wind action increased mixing which dissipated the saline plume.
- (10) **Day 219:** The release water had nearly reached the lower segment of the Barrage and plunged into the deeper layers.
- (11) **Day 226:** The release water finally reached the Barrage at Segment 51.
- (12) **Day 233:** Increased wind velocities brought about vertical and longitudinal mixing of the waterbody.
- (13) **Day 240:** Vertical and longitudinal gradients were not evident and the Barrage was comparatively mixed with lower salinity water distributed evenly throughout the water body.

The Vaal Barrage shows a number of different mixing and salinity characteristics. Prior to the release, there is flow reversal caused by the abstraction of water at the Zuikerbosch Intakes. At the beginning of the release, the comparatively high discharge from the Vaal Dam passes over the top of the saline water in the Barrage, with minimal mixing into the lower layers. This was brought

about by *density and momentum factors*. The saline water from the Klip River creates a plume of high salinity water in the upper reaches of the Barrage. During the release, this plume, passes along the length of the Barrage with minimal mixing into surrounding water thereby showing a *plug flow response*. The Klip, Suikerbosrand and Rietspruit Rivers contain comparatively high salinity water and discharge into the lower layers of the Barrage (*density stratification response*). Once the release water approaches the lower reaches of the Barrage, the lower salinity water plunges into the deeper layers, showing an *inverse density stratification response*. During the latter part of the release, wind action results in the *vertical mixing* of the Barrage. Figure 3.3.8 shows the horizontal and vertical velocity (vector) plots for selected simulation dates. During day 233, the prevailing wind creates circulation currents in the lower reaches which mix the contents of the Barrage.

3.3.6 DESCRIPTION OF SCENARIOS

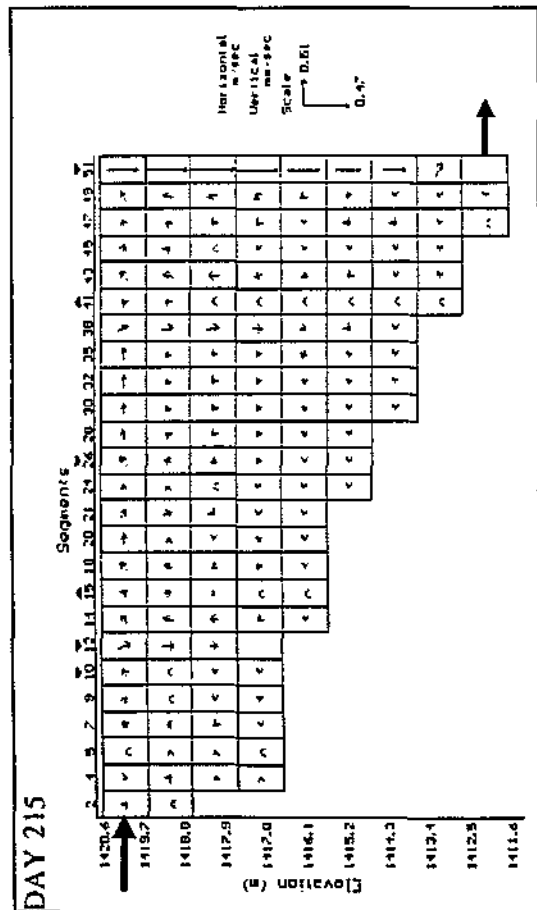
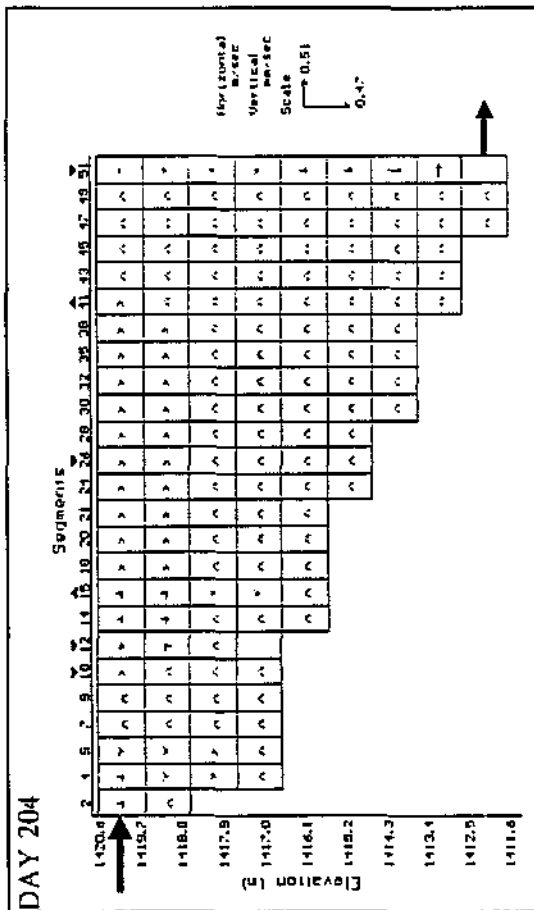
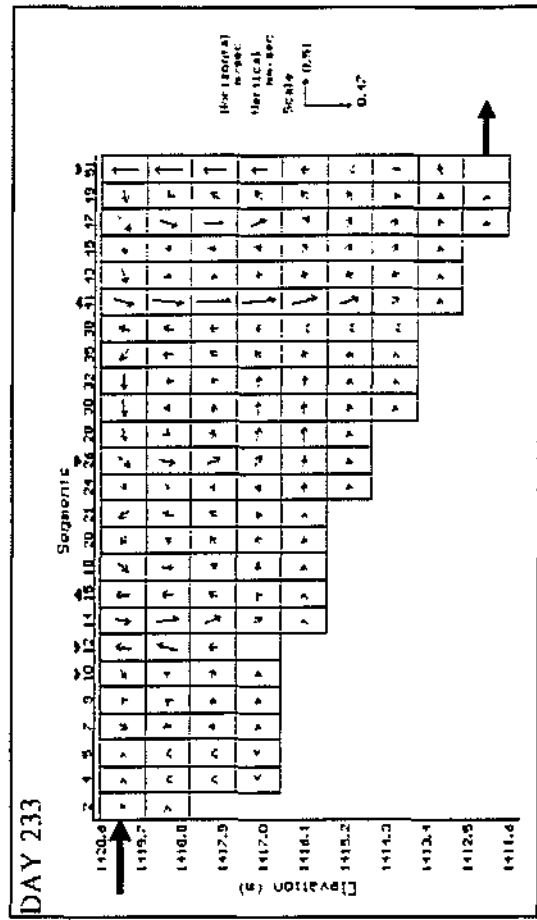
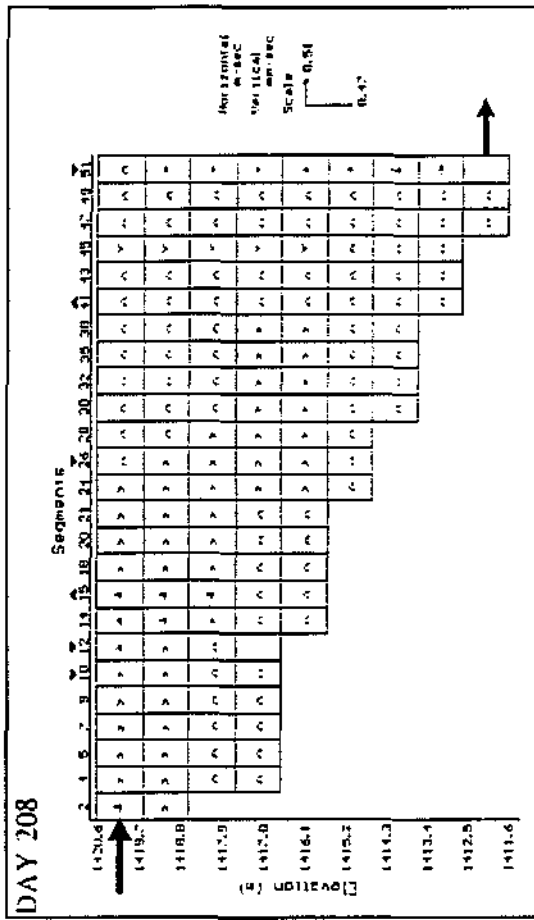
Scenario 1: Reduced freshening release from Vaal Dam The salinity of the Vaal Barrage and middle reaches of the Vaal River may be managed using releases of low salinity water from the Vaal Dam. *CE-QUAL-W2* is used to investigate the influence of reducing the volume of the freshening release on the salinity (conductivity) gradients within the Barrage.

Scenario 2: Blending Option of 500 mg/l When the TDS concentration exceeds 600 mg/l, low salinity releases may be made from the Vaal Dam to freshen the contents of the Barrage. *CE-QUAL-W2* is used to determine the increased volume of water required to achieve a more stringent TDS *operational guide* of 500 mg/l (given the same inflows).

Scenario 3: Diversion Canal When a freshening release is made from Vaal Dam it is possible for the Zuikerbosch Intakes to abstract the release water which is intended to reduce the salinity in the Vaal River. A diversion canal is being considered which transfers low salinity water from Lethabo Weir (downstream of Vaal Dam) into the Barrage, bypassing the Zuikerbosch Intakes. Two hypothetical canal configurations are evaluated.

3.3.7 RESULTS OF SCENARIO TESTING

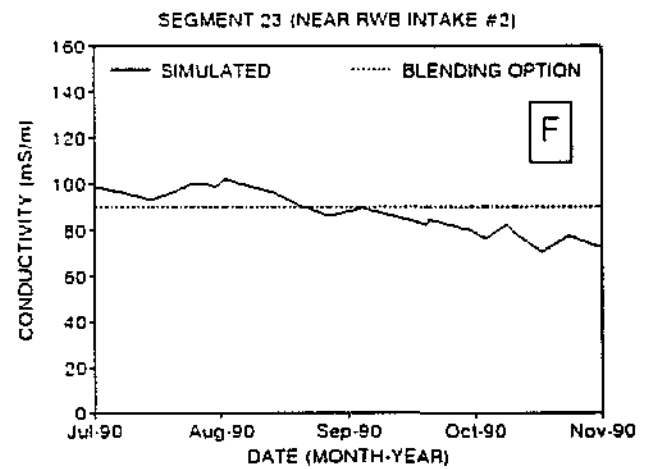
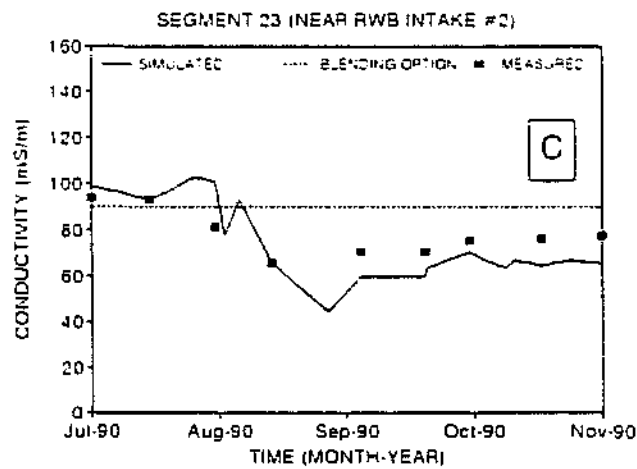
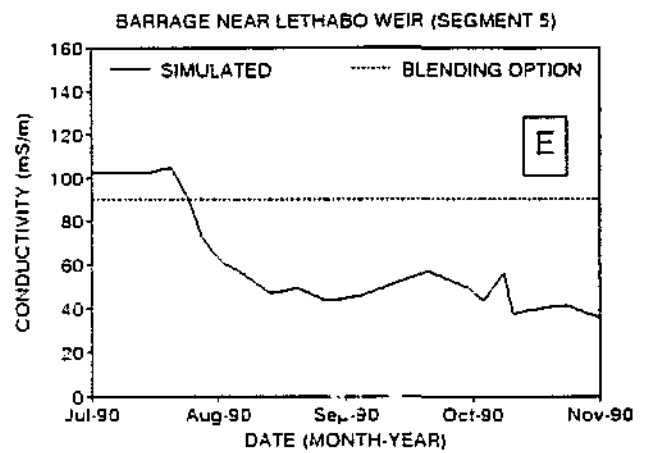
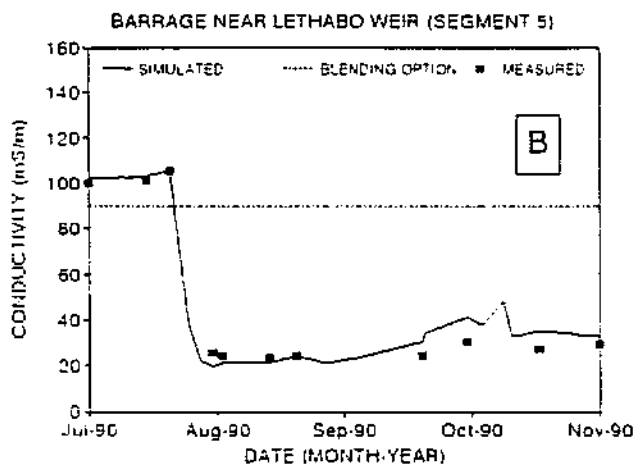
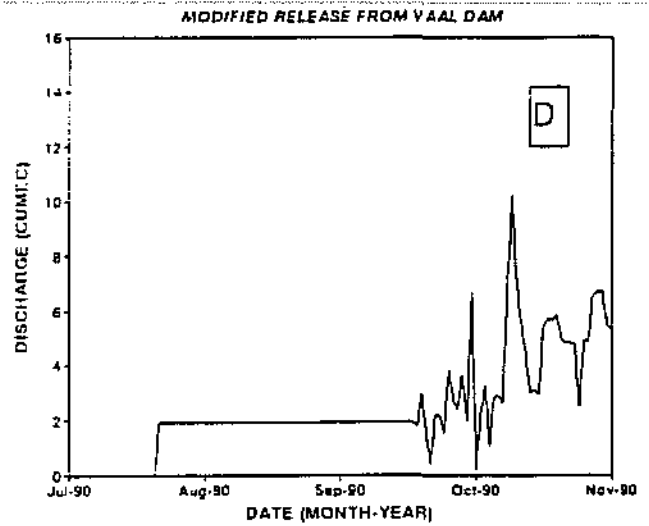
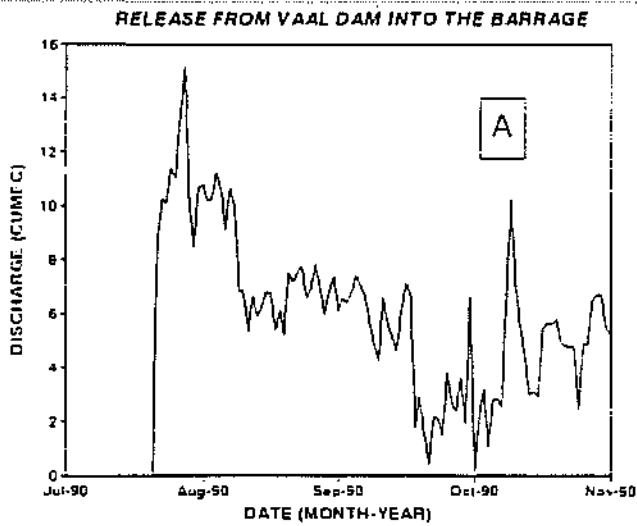
Scenario 1: Reduced freshening release from Vaal Dam - impact on salinity behaviour of the Barrage. Section 3.3.5 shows the water quality of both the Vaal Barrage and downstream Vaal River may be managed using freshening releases from the Vaal Dam. Figure 3.3.9 (Inset A) shows the measured release hydrograph from Vaal Dam. Insets B and C show the simulated and measured conductivity in the upper reaches of the Barrage near Lethabo Weir (Segment 5) and in the middle reaches near RW intake at Vanderbijlpark (± 28 km downstream of Lethabo Weir).



2-D plots of the vertical and horizontal movement of water in the Vaal Barrage.



Figure 3.3.8



Insets A, B and C showing the hydrograph and EC during the release period. Insets D, E and F showing the modified release hydrograph and simulated EC response of the Barrage.

Figure 3.3.9

The release causes an abrupt change in the salinity of the upper reaches and a more gradual change in the middle reaches.

Insets E and F (in Figure 3.3.9) show the influence of reducing the freshening release from Vaal Dam on the conductivity of the Barrage. The release hydrograph shown in Inset A was reduced to one quarter of its original volume, see Inset D. In the upper section, near Lethabo Weir, the reduced release still causes a marked reduction in conductivity. In the middle section, the release caused a small reduction in conductivity, taking the Barrage barely below a conductivity of 90 mS/m. The reduced release caused the conductivity of the Barrage to go below 90 mS/m about one month later than the full release, but in turn reduced the volume of water which had to be released from the Vaal Dam.

A number of simulations were performed to examine the influence of reduced release hydrographs on the conductivity of the Barrage. Figure 3.3.10 shows the results of the different simulations. The model was configured using:

- (1) the original (**full**) release, serving as a baseline to assess the other simulations.
- (2) 50 percent reduction in the original release hydrograph (shown on Figure 3.3.10 as **-50%**).
- (3) 75 percent reduction in the release (shown as **-75%**).
- (4) no freshening release from the Vaal Dam (shown as: **no release**).

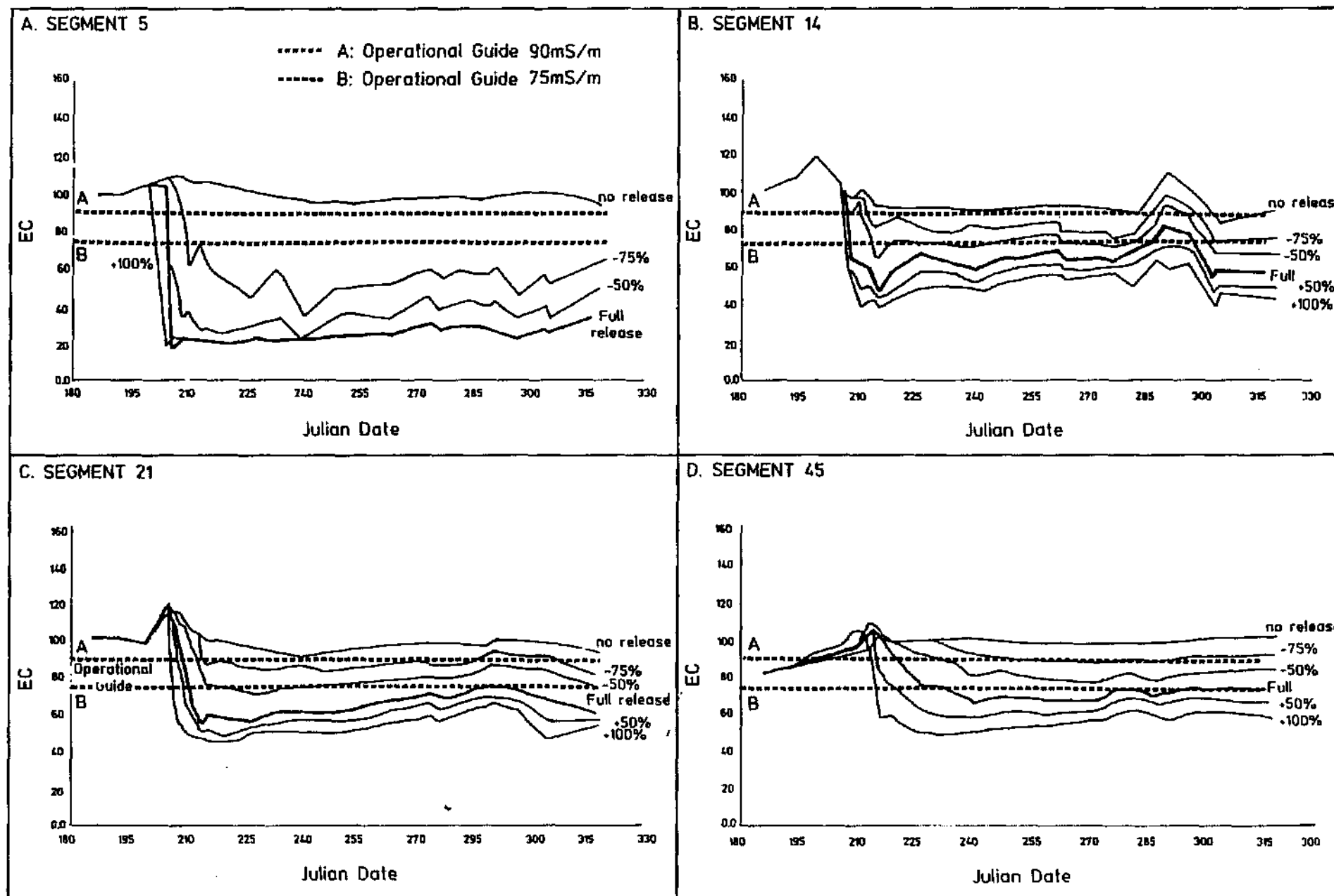
In the upper reaches (Segment 5), when no release was made from Vaal Dam, the conductivity remains between 90 and 100 mS/m over the full simulation period. The other releases keep the conductivity below 90 mS/m.

In the middle reaches (Segments 14 and 21), the 50% release is sufficient to reduce the conductivity to below 90 mS/m. The release reduced by 75% is however insufficient to keep the conductivity below 90 mS/m for the full period. When no release is made, the conductivity remains above 90 mS/m. In the lower reaches (Segment 45), the 50% release is sufficient to keep the conductivity below 90 mS/m.

Scenario 2: Blending option - 500 mg/l

The model is used to examine the increased volume of Vaal Dam which could be required to attain an *operational guide* of 500 mg/l (estimated to be a conductivity of 75 mS/m). Figure 3.3.10 shows the simulations where increased releases are made from Vaal Dam. The simulations include:

- (1) the original (**full**) release.
- (2) 50 percent increase in the original release (shown as **+50%**).
- (3) 100 percent increase in the original release (shown as **+100%**).



Simulated EC response of the Barrage to reduced releases (zero, 75% and 50% reduction), and increased releases (50% and 100%).

Figure 3.3.10

In the upper reaches (Segment 5), no improvement in the conductivity is achieved by using either a 50 or 100 percent increase in the release volume. During the release period the conductivity remains well below the *operational guide* of 75 mS/m. Analysis of the 2-D plots showed the 100% increase in release brings about a near instantaneous scour of the saline water in the bottom layers of Segments 2 to 12. In the middle reaches (Segment 14 and 21), the increased releases maintain the conductivity below the *operational guide*. In the lower reaches (Segment 45), the increased release has an almost immediate influence on the conductivity, which stays well below the 75 mS/m guide.

Scenario 3: Diversion canal

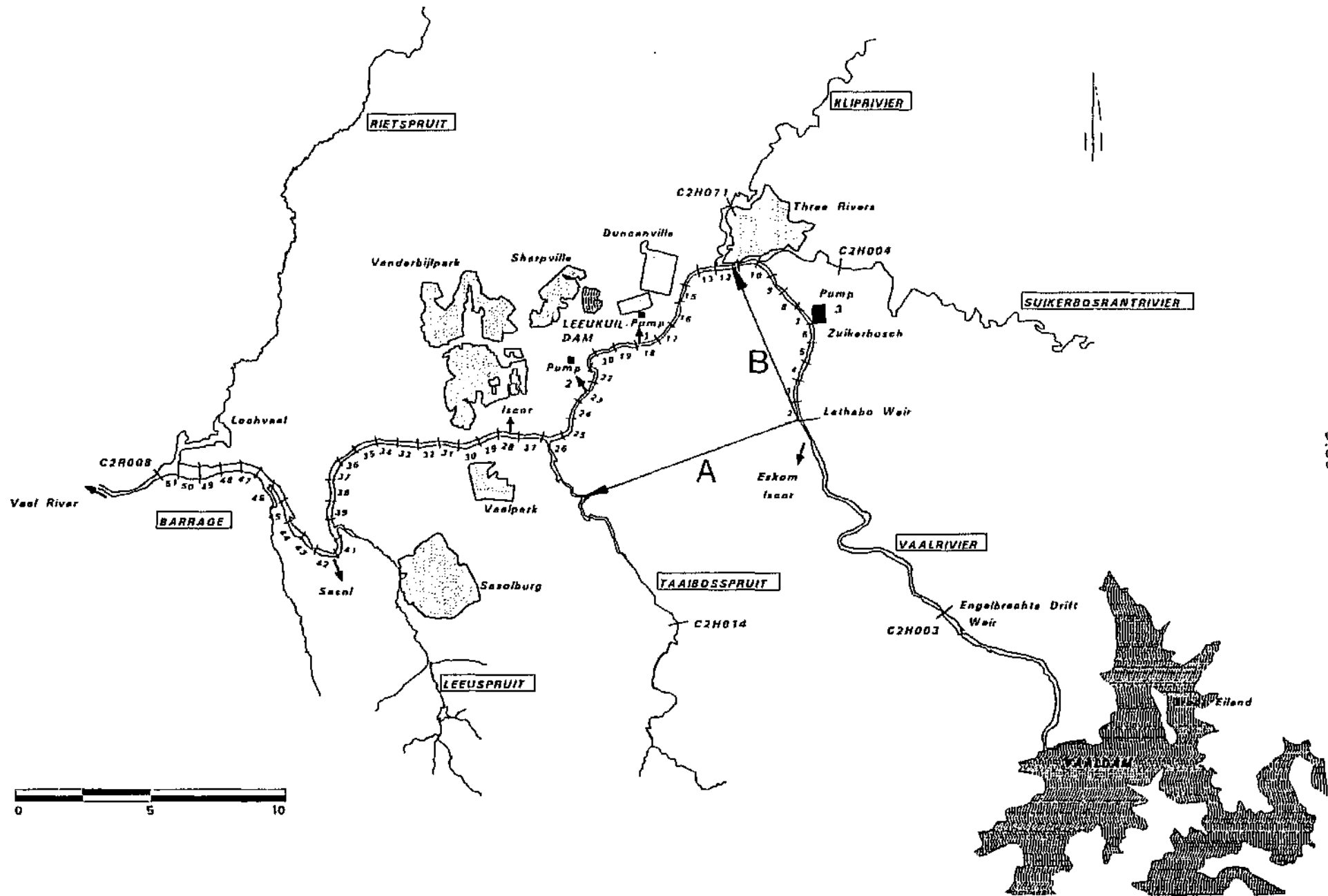
The model is configured to examine the salinity behaviour of the Barrage brought about by the diversion of some of the freshening releases into the middle reaches of the water body. Such an option would require the construction of a canal which conveys water from Lethabo Weir to a specific point in the Barrage. Such an option is being considered because it would allow freshening releases from the Vaal Dam to by-pass the intakes of Zuikerbosch. This would in turn result in Zuikerbosch intake abstracting a greater portion of the tributary inflow, thereby improving the abstraction of saline tributary inflow.

The model is configured to examine:

- (1) the salinity response of the Barrage,
- (2) possible water quality benefits for downstream users, and
- (3) identify an optimum canal outlet point.

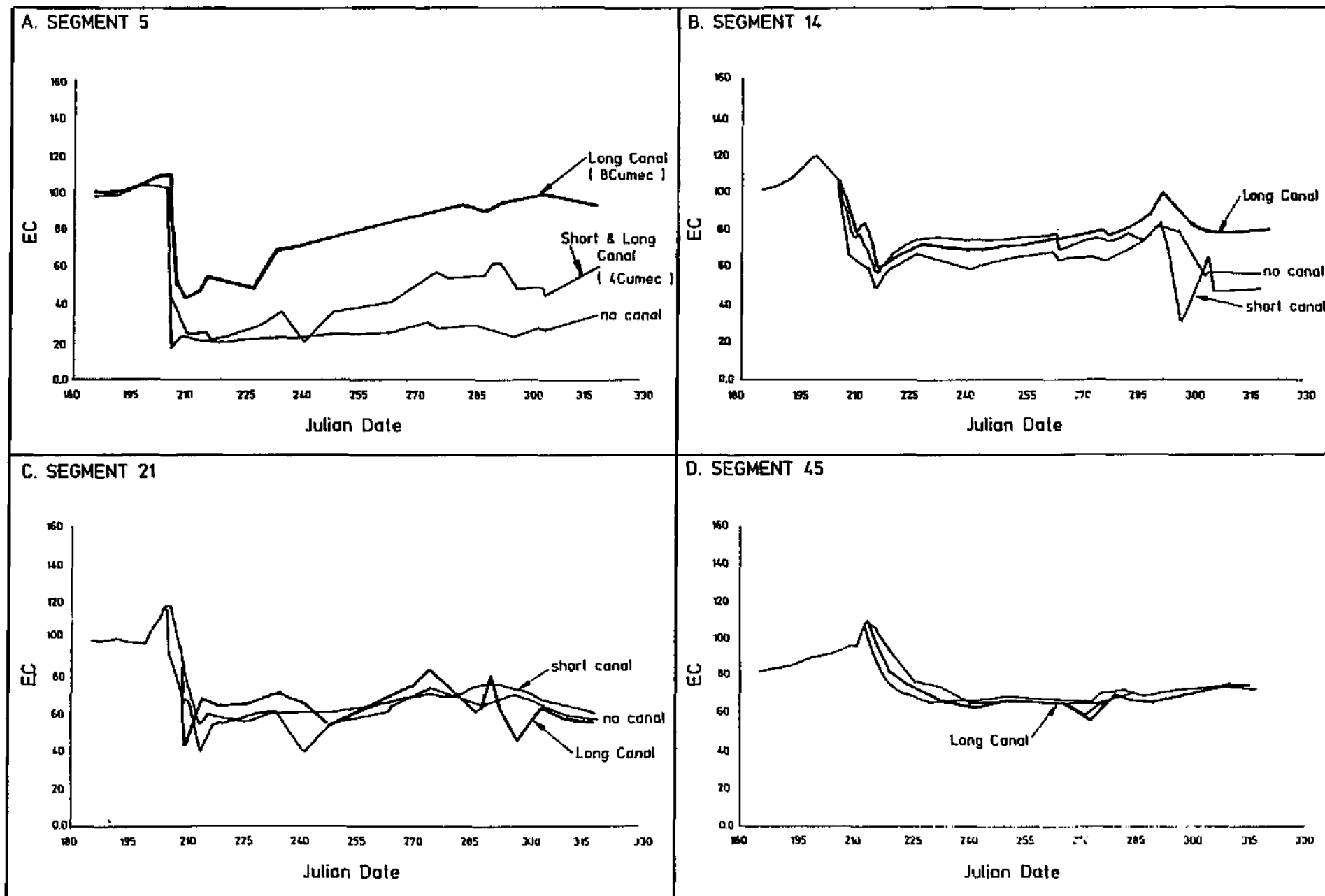
Figure 3.3.11 shows the two diversion canal options evaluated using the model. Canal A is 20 km long and transfers water from Lethabo Weir to the Taaibosspruit which then flows into the Barrage at Segment 26. Canal B is 14 km long and transfers water from Lethabo Weir to the Barrage at the confluence with the Klip River at Segment 12. For Canal A and B, three maximum diversion rates are tested (2, 4 and 8 cumec). It should be noted that a canal with a maximum diversion of 8 cumec was not a practical design option, but included in the simulation for comparison purposes.

Figure 3.3.12 shows the conductivity at Segments 5, 14, 21 and 45 with (1) normal release (via Lethabo), (2) short and long canal options (with 4 cumec maximum diversion) and (3) long canal option with 8 cumec maximum diversion. In the upper reaches (Segment 5), the diversion canals cause the conductivity to increase, this would allow the Zuikerbosch Intakes to abstract a large portion of the Klip River (saline) inflow. In the lower reaches, all three canal options have minimal influence on the conductivity when compared with the normal release.



Location map showing the two hypothetical diversion canal options investigated using CE-QUAL-W2.

Figure 3.3.11



Simulated EC response of the Barrage to the diversion canal options. Normal release, Canal option A (20 km long) with maximum transfer of 8 cumec, and Canal option B (14 km long) with maximum transfer of 4 cumec.

Figure 3.3.12

The simulation shows that:

- (1) The diversion canal increases the conductivity in the upper reaches near Zuikerbosch.
- (2) The canal option could allow improved abstraction of saline tributary water by Zuikerbosch.
- (3) There will be no appreciable difference in the salinity of the water released from the Barrage to downstream users unless the intakes and diversion canal are operated so that a large volume of the saline tributary inflow is abstracted at Zuikerbosch.
- (4) There is little difference in overall response between the long and short canal option. The long canal option would however improve abstraction of the tributary inflows by discharging the freshening release as far as possible downstream of the Zuikerbosch intakes.

3.3.8 CONCLUSIONS

Calibration During the freshening release, abrupt changes in conductivity were measured within the water body. The simulation shows that intricate mixing processes occur in the Barrage. Governing processes identified include density stratification, plug flow, momentum effects, flow reversal, and wind mixing. The available data set was sufficient to allow detailed calibration at a number of points along the water body. The model provides an acceptable simulation of the conductivity, heat exchange and volume balance of the Barrage. Comparison of the simulated and measured conductivity data shows that the Barrage is not always laterally averaged, giving rise to localised discrepancies between the simulated and measured data (at the segments near the Klip River inflow).

Information for operational management of water quality The simulation shows that the salinity of the Vaal Barrage can be managed using releases of low salinity water from the Vaal Dam. The study confirms that such releases from Vaal Dam are capable of maintaining a TDS concentration of 600 mg/l. However, it is shown that the release should be optimized so that the minimum Vaal Dam water is used to achieve the necessary TDS concentration at selected points in the Barrage. It is also shown that increased freshening releases could be made from the Vaal dam to achieve a TDS concentration of 500 mg/l TDS in the Barrage but at the cost of using increased volumes of water from the Vaal Dam.

The simulation performed to evaluate the diversion canal showed that to achieve maximum benefit to the users downstream of the Barrage, the diversion canal and Zuikerbosch Intakes would require

joint operation to maximize the reuse of the saline tributary inflow from the Klip River.

3.3.9 RECOMMENDATIONS

Decision support role *CE-QUAL-W2*, now configured and tested using the data set for the Vaal Barrage, can play a valuable decision support function in providing information on:

1. The development, testing and fine tuning of operating rules. The model could be used to evaluate and test a number of dilution options. This information could then be used to develop a decision support system for (1) scheduling and control of dilution releases from Vaal Dam, and (2) determining the fate and transport of other water quality constituents, such as phosphorus.
2. The feasibility of constructing a diversion canal. Such a study will require detailed information on: the location of the canal outlet, maximum flow rate, salinity response of the Barrage, selection of operation rules, and water quality benefits for downstream users. Some of these issues were briefly addressed as part of this study.

Water quality monitoring The data set used in this study was adequate to calibrate the model for salinity simulations. However, the simulation of the algal and phosphorus dynamics of the Barrage requires information on the suspended solids concentration of the inflowing tributaries and Barrage. Unfortunately, insufficient data were available to calibrate the model adequately for suspended solids and phosphorus.

To meet the primary input requirements of the model, monitoring of the Barrage should include:

- Inflows: TDS, EC, phosphate, total phosphorus, suspended solids, nitrate, ammonia, E.coli, water temperature, dissolved oxygen and discharge (flow rate)
- Barrage: the above constituents plus chlorophyll-a, secchi depth and water level. Vertical profiles of water temperature, EC, and dissolved oxygen.

3.3.10 REFERENCES

Bath, A.J. & Timm, T.D. (1993)

Water quality investigation of Fika Patso and Swartwater Dams, Proceedings of the ICOLD 18th congress, Durban.

| KEY TO JULIAN DAYS | | | | | | | | | | | | | |
|--------------------|-------------|---------|----------|--------|--------|---------|---------|---------|---------|-----------|---------|----------|----------|
| Month | | January | February | March | April | May | June | July | August | September | October | November | December |
| Season | | summer | | autumn | | | winter | | | spring | | | summer |
| Julian day | Normal year | 1-31 | 32-59 | 60-90 | 91-120 | 121-151 | 152-181 | 182-212 | 213-243 | 244-273 | 274-304 | 305-334 | 335-365 |
| | Leap year | 1-31 | 32-60 | 61-91 | 92-121 | 122-152 | 153-182 | 183-213 | 214-244 | 245-274 | 275-305 | 306-335 | 336-366 |